SHS 2017

XIV INTERNATIONAL SYMPOSIUM ON SELF-PROPAGATING HIGH TEMPERATURE SYNTHESIS

Book of Abstracts

SEPTEMBER 25-28, 2017
TBILISI, GEORGIA

ORGANIZERS

GEORGIAN NATIONAL ACADEMY OF SCIENCES

LEPL - FERDINAND TAVADZE METALLURGY AND MATERIALS SCIENCE INSTITUTE

INSTITUTE OF STRUCTURAL MACROKINETICS AND MATERIALS SCIENCE RUSSIAN ACADEMY OF SCIENCES

SPONSOR

GEORGIAN MANGANESE

ISBN 978-9941-426-8

CONFERENCE COMMITTEES

SYMPOSIUM CHAIRMAN:
Giorgi Tavadze (Georgia)

SYMPOSIUM CO - CHAIRMAN:
Mikhail Alymov (Russia)

INTERNATIONAL COORDINATORS:
George Oniashvili (Georgia)
Vladimir Sanin (Russia)

LOCAL ORGANIZING COMMITTEE:
G. Tavadze (Georgia)
G. Oniashvili (Georgia)
A. Gachechiladze (Georgia)
Z. Aslamazashvili (Georgia)
G. Zakharov (Georgia)
G. Mikaberidze (Georgia)
T. Badzoshvili (Georgia)
A. Todadze (Georgia)
P. Khojashvili(Georgia)
N. Abashidze (Georgia)
E. Chichashvili(Georgia)

PROGRAM COMMITTEE:
J. Khantadze (Georgia) – Chairman
G. Oniashvili (Georgia)
V. Yukhvid (Russia)
E. Levashov (Russia)
A. Mukasyan (USA)
A. Rogachev (Russia)
A. Sytschev (Russia)
V. Sanin (Russia)
A. Gachechiladze (Georgia)
Z. Aslamazashvili (Georgia)
G. Zakharov (Georgia)
O. Likhanova (Russia)
Yu. Scheck (Russia)

INTERNATIONAL ADVISORY BOARD:
I.P. Borovinskaya (Russia) (Honorary member)
I. Agote (Spain)
M. Alymov (Russia)
A. Amosov (Russia)
J. Aruna (India)
F. Bernard (France)
V. Borodulya (Belarus)
G. Cao (Italy)
C. C. Ge (China)
B. Derin (Turkey)
E. Dreizin (USA)
M. Filonov (Russia)
E. Gutmanas (Israel)
O. Ivasishin (Ukraine)
S. Kharatyan (Armenia)
E. Levashov (Russia)
J. Lis (Poland)
Y. Maksimov (Russia)
Z. Mansurov (Kazakhstan)
K. Martirosyan (USA)
A. Mukasyan (USA)
O. Odawara (Japan)
G. Oniashvili (Georgia)
J. Puszynski (USA)
M. Rodriguez (Spain)
A. Rogachev (Russia)
V. Sanin (Russia)
A. Sytschev (Russia)
G. Tavadze (Georgia)
A. Tsivadze (Russia)
N. N. Thadhani (USA)
P. Vincenzini (Italy)
D. Vrel (France)
T. Weihs (USA)
G. Xanthopoulou (Greece)
O. Yucel (Turkey)
X. H. Zhang (China)

PLENARY TALKS:

D. Shechtman

QUASI-PERIODIC MATERIALS – A PARADIGM SHIFT IN CRYSTALLOGRAPHY

Technion, Haifa, Israel and ; ISU, Ames, Iowa, USA

G.Tavadze

SUCCESSES AND WAYS OF DEVELOPMENT OF SHS IN GEORGIA

LEPL - Ferdinand Tavadze Metallurgy And Materials Science Institute

M.I. Alymov

ISMAN: PRESENT STATE AND PERSPECTIVES

Institute of Structural Macrokinetics and Materials Science, Russian Academy of Sciences, Chernogolovka, Moscow, 142432 Russia

I.P. Borovinskaya[1], A.S. Mukasyan[2]

FIFTY YEARS OF DISCOVERY: HISTORY AND FUTURE

[1] *1 Institute of Structural Macrokinetics and Materials Science, RAS, Chernogolovka 142432, Russia*

[2] *Department of Chemical & Biomolecular Engineering, and §Nuclear Science Laboratory, Department of Physics, University of Notre, Dame, Notre Dame, Indiana 46556, United States*

Orest Ivasishin

HYDROGEN APPROACH IN POWDER METALLURGY OF Ti AND Zr BASED ALLOYS

G.V. Kurdyumov Institute for Metal Physics

CONTENT

SELF-PROPAGATING HIGH TEMPERATURE SYNTHESIS OF BORONCONTAINING COMPOSITION MATERIALS

R.G. Abdulkarimova*[1], K.Kamunur[1], A.J. Seidualieva[2], Z.A. Mansurov[2]

[1]Al-Farabi Kazakh National University, 050040, Almaty, 71 al-Farabi av., Kazakhstan
[2]The Institute of Combustion Problems, 050012, Almaty, 172 Bogenbai Batyr Str., Kazakhstan
*abdulkarimovaroza@mail.ru

INTRODUCTION

Development of new composition ceramic materials with a unique set of properties and simultaneously a high level of physic-chemical properties is the most important and actual task of modern materials science. Often it is impossible to solve this problem within the framework of notions on equilibrium states and it is necessary to use new approaches and methods of synthesis of a special class of composition ceramic materials [1].

One of such methods is self propagating high temperature synthesis (SHS) and its combination with mechanical activation (MA). SHS technologies are energy effective as they allow producing new substances and materials including powder and bulk ceramic materials in one technological cycle.

The aim of this investigation is self propagating high temperature synthesis (SHS) of composition materials with a wide range of phase compositions using borate ore of Inder deposite of the Republic of Kazakhstan. The ores of Inder deposite are represented mainly by asharite, hydroboracite and ulexite [2]. The average content of B_2O_3 in Inder ores makes up 15-27.5%. In relation to the fact that borate ore of Inder deposite is distinguished by a considerable content of gypsum, the initial raw material was concentrated, the maximum content of boron oxide after concentration of ore made up 40 mass.%.

MATERIALS AND METHODS

SH-synthesis was carried out in the systems B_2O_3-Al-MeO, B_2O_3-Mg-MeO (where MeO – are titanium, chromium, zirconium oxides, B_2O_3 in the composition of borate ore).

The samples were prepared from the charge containing aluminium (99% purity), magnesium (99% purity) and borate ore of Inder deposit (the content of boron oxide up to 40%, preliminary mechanical activation was carried out in a high power planetary-centrifugal mill. The prepared samples were burnt at room temperature in air initiating ignition by magnesium. The microstructure and phases composition of synthesized products were investigated using microanalyses-scanning electron microscope (SEM) and XRD.

RESULTS AND DISCUSSION

To produce refractory composition materials, the amount of oxides, borate ore, aluminium and magnesium were varied in the course of experiments and calculated taking into account stoichiometry and possibilities of optimization of magnesium and aluminium content in the initial mixture of components in order to increase reactivity in the reactions of aluminothermal and magnesiumthermal combustion. The effect of SHS medium (air, argon), the preliminary mechanical activation before SH- synthesis on the phase composition of the synthesized materials and macrokinetic characteristics of the combustion process was stated. The study on

the effect of preliminary mechanical activation (MA) of the charge on macrokinetic characteristics of SHS, phase composition and structure of the obtained composites in the systems B_2O_3-Al-MeO, B_2O_3-Mg-MeO with the use of borate ore is of both theoretical and practical application. Synthesis of products under the condition of combustion proceeds supposedly in the following reactions:

$$3ZrSiO_4 + 10Al + 3B_2O_3 \rightarrow 3ZrB_2 + 5Al_2O_3 + 3SiO_2$$

$$3TiO_2 + 3B_2O_3 + 10Al \rightarrow 3TiB_2 + 5Al_2O_3$$

$$Cr_2O_3 + 2B_2O_3 + 6Al \rightarrow 2CrB_2 + 3Al_2O_3$$

The use of preliminary mechanical activation of the charge in a high power planetary mill significantly decreases the temperature of beginning of exothermal interaction of the mixture components, reduces the synthesis time of the final product, and results in a more complete procedure of chemical reactions [3, 4]. Therefore, the powder of the prepared charge was activated for 5-10 minutes before SH-synthesis.

Acceleration of the chemical reaction after mechanical reaction is conditioned by «pumping» of additional (excessive) energy into the reacting substances, the energy accumulating in the formed structural defects. Excessive energy reduces the activation barrier of the chemical reaction. The effect of excessive energy on the reaction rate is a kinetic factor of acceleration of a chemical reaction [5]. The effect of MA on the yield of SHS products on the example of Cr2O3 –B_2O_3- Al system is shown in table 1.

Formation of the phase and chemical composition, crystalline structure and microstructure of SHS products is a complex interrelated process.

Investigation of these processes under the conditions of SHS is very important as the structure determines the properties of materials.

Table 1. Combustion products of Cr_2O_3 –B_2O_3- Al

Cr_2O_3-B_2O_3 nAl	Activation time. min	Content, %								
		CrB	CrB_2	Cr_2B	Cr_5B_3	CrB_6	SiO_2	Na (AlO_2)	Al_5BO_9	Al_2O_3
30%	5	11.5	2.6	2.6		2.5	2.6	13.9	17.5	45.9
30%	7	13.3		2.6	4.2	3.6	2.4	5.4	5.3	63.1
30%	10	12.9	2.2	2.0	2.2	2.6	2.3	7.4	3.5	64.8
35%	5	17.4	-	-	-	-	1.4	-	-	81.3
35%	7	16.5	5.6	2.9	3.5	3.3	2.1	-	-	66.1
35%	10	20.3	2.4	-	-	-	1.3	-	-	76.0

Figure 1 presents electron-microscopic images of SHS products on the basis of $ZrSiO_4$ + Al + B_2O_3 (borate ore) system.

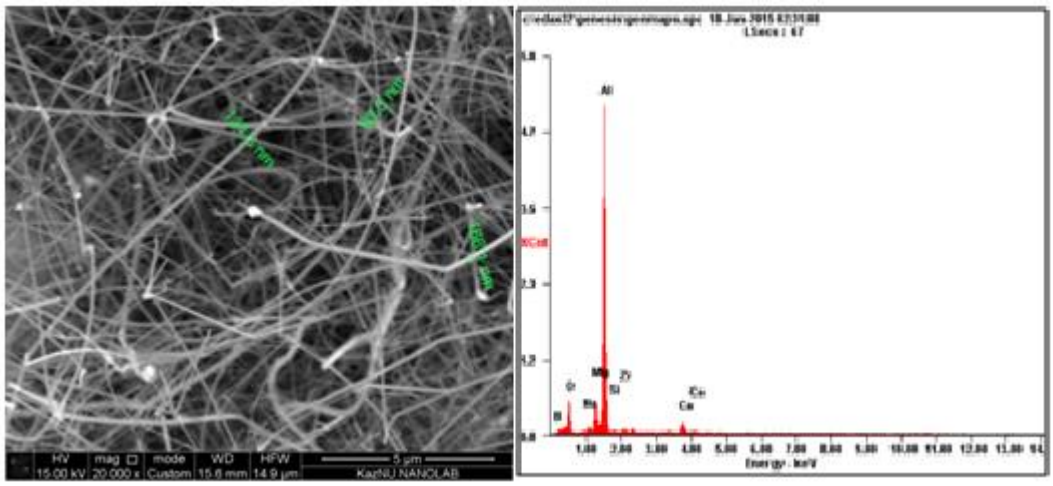

Figure 1 - The microstructure and elemental analysis (SEM, EDAX) of SHS products of the system $ZrSiO_4$ + Al + B_2O_3(in borate ore)

CONCLUSIONS

The possibility of using borates of Inder deposite of RK as a boron containing component for production of composition materials by the method of self propagating high temperature synthesis was shown.

The effect of preliminary MA on microkinetic characteristics of SHS process, the yield of SHS products and microstructure of the obtained materials is stated.

Formation of submicron crystals of titanium, chromium borides and fibrous nanosize crystals of zirconium diboride in the matrix of aluminium oxide is stated.

REFERENCES

[1] A.E.Sytschev, A.G.Merzhanov, Chemistry advances, 73 (2), 2004, pp. 157-170.

[2] Natural resources of Inder and their use, ed.by M.D.Diyarov, D.A. Kalicheva, S.V. Mescheryakov, Nauka, Alma-Ata, 1981, p.102

[3] Fundamental bases of mechanical activation, mechano-synthesis and mechano-chemical technologies, ed. by E.G. Avakumov. – Novosibirsk: Nauka, 2009, 342 p.

[4] D.S.Raimkhanova, R.G.Abdulkarimova, Z.A.Mansurov, Journal of Materials Science and Chemical Engineering, 2, 2014, p.66-69.

[5] V.V. Boldyrev, Material science forum, 1996,Vol. 225, p. 511-520.

PROCESSING TECHNOLOGY OF LASER WELDING OF COMBUSTION CHAMBER ELEMENTS RECEIVED BY METHOD OF SELECTIVE LASER MELTING

A.V. Agapovichev *, V.G. Smelov, A.V. Sotov, R.R. Kyarimov

[1] Samara University, Samara, Moskovskoye shosse 34, 443086, Russia
* agapovichev5@mail.ru

Recently the significant growth in use of the additive technologies by production of figurine details is observed [1]. One of the directions of an additive technologies is the technology of the selective laser melting (SLM). The SLM technology allows to make products and details of the irregular shape, in short terms, practically without use of the industrial equipment at the expense of what the cycle of production of products [2] is considerably reduced.

In SLM technology the high power laser for melting thin layer of powder according to a 3D model is used [3]. The SLM method is a perspective method for manufacture of details from materials which processing by traditional methods is difficult, is limited to larger expenses and is not always possible.

The combustion chamber of an aircraft gas-turbine engine (GTE) is the composite and responsible node on which perfection degree the main characteristics of all engine, its reliability and a resource in many respects depend. The combustion chamber (CC) of aircraft GTE can have various form of a flowing part and design realization. The greatest distribution wasgained by combustors of three main schemes: tubular, tubular - ring and ring.

METHODS OF RESEARCH AND EQUIPMENT

Manufacture of CC was supposed to be made on the SLM 280HL equipment. Equipment has the construction chamber dimension of 280x280x350 mm and is equipped with the 400 W fiber laser. Because dimensions of CC appeared more camera of creation of the SLM 280HL equipment, was made the decision to divide CC into several sectors, and to make them separately, assembly of sectors of CC to carry out argon and laser welding.

For processing of a weld procedure of the details made by SLM exemplars were made of metal refractory chromium-nickel powder of the squared VV751P brand in accordance with GOST 6996-66.

Welding of plates was end-to-end carried out on parting lines, and also with use of adding material in the form of a metal wire of the X15H60 brand. When welding with an overlap, plates were imposed at each other with shift on 10 mm.

RESULTS OF RESEARCHES

For laser welding of plates the optimum modes of a laser emission beforehand were chosen. Welding was carried out in a pulsed operation.

Results of mechanical tests on stretching of the welded exemplars made by SLM technology are presented in table 1 in comparison with properties of a whole exemplar.

Table 1 - Data of tests of the flat exemplars received by the SLM method

Type of welding	№ sample	Ultimate strength, MPa	Tension set, ε_t %	Type of a welded joint	Note
Laser welding	L-1.1	947	7,4	end-to-end	-
	L-1.2	1003	8,3	end-to-end	-
	L-1.3	982	7,1	end-to-end	-
	L-1.4	276	1,2	overlap	cracks under seams
	L-1.5	860	3,7	overlap	-
	L-1.6	674	2,2	overlap	-
Argon welding	A-1.1	525	1,9	end-to-end	-
	A-1.2	551	2,1	end-to-end	-
	A-1.3	476	1,6	end-to-end	-
	A-1.4	550	2,3	overlap	-
	A-1.5	585	2,6	overlap	-
	A-1.6	273	1,4	overlap	seam only on the one hand
VV751P	5	1112	14,43	-	whole

From test data it is visible that mechanical characteristics of exemplars after laser welding are end-to-end close to the mechanical characteristics of exemplars made of the material VV751P by SLM technology. Ultimate strength is model welded end-to-end by argon welding practically twice to time yield to ultimate strength of the exemplars welded end-to-end by laser welding.

After laser welding end-to-end, this type of welding at assembly of sectors of CC allows to recommend high values of indexes of durability and plasticity of exemplars.

For the purpose of studying of a microstructure of a zone of welding, fractographic studies with use of a method of a raster submicroscopy were executed. For studying of border between an original material and welded material the card of distribution of chemical elements in the field of a micromicrosection (figure 1) was received.

From the figure 1 it is visible that border "an original material – welding" clear, is available a metallic binding (the figure 1, a). At an original material, there are defects in the form of lack of welding. In the field of welding "an original material – welding" is observed small chemical heterogeneity. In the field of welding "an original material – welding" the transitional layer is absent. The transition zone has clearly defined boundaries.

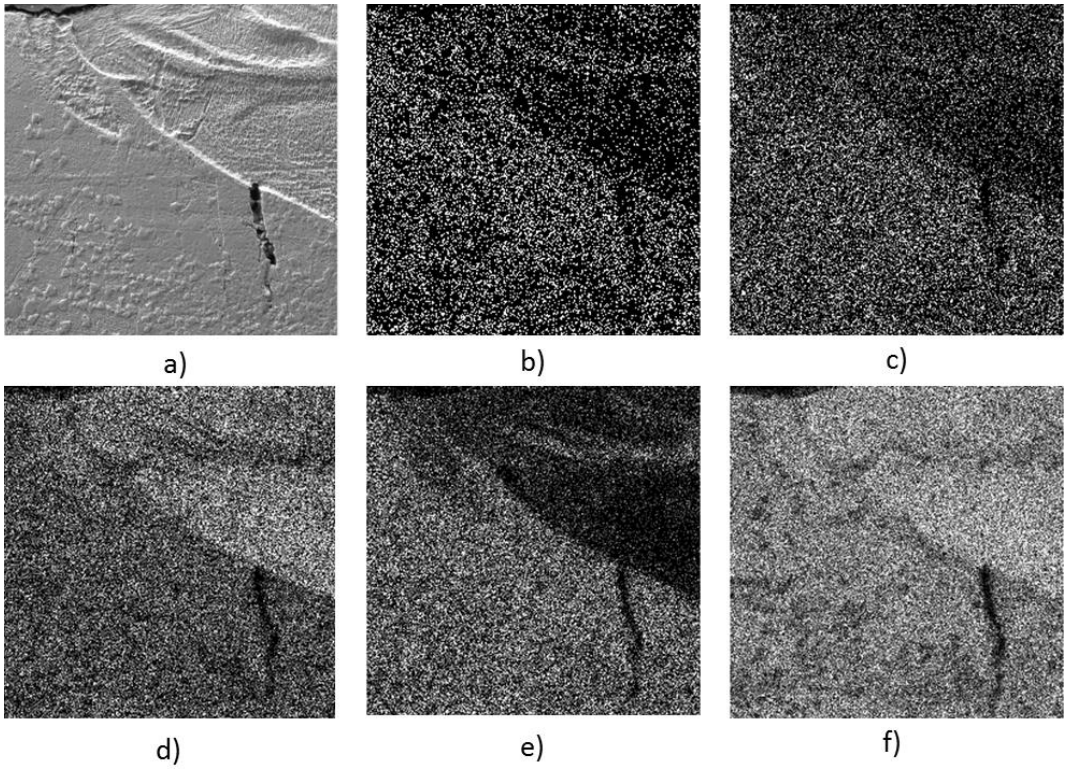

a) Electronic image of a microsection (x500); b) distribution of Al; c) distribution of Ti; d) distribution of Cr; e) distribution of Co; f) distribution of Ni

Figure 2 - Card of distribution of chemical elements

CONCLUSION

1. The weld procedure of the details made by SLM is fulfilled.
2. The optimum modes of laser welding of the details made by SLM of a high-temperature alloy of VV751P are selected.
3. Mechanical characteristics of the exemplars welded end-to-end and with an overlap are investigated. After laser welding end-to-end, this type of welding at assembly of sectors of CC allows to recommend high values of indexes of durability and plasticity of exemplars.
4. Further researches will be directed to researches of the modes of laser welding on a transitional layer to the "original material-welding" areas and on mechanical characteristics of exemplars.

REFERENCES

[1] A.V. Agapovichev, A.V. Balaykin, V.G. Smelov Production technology of the internal combustion engine crankcase using additive technologies // Modern Applied Science. 2015. V. 9, Iss. 4. P. 335-343.

[2] D.D. Gu, W. Meiners, K. Wissenbach, R. Poprawe Laser additive manufacturing of metallic components: Materials, processes and mechanisms. International Materials Reviews.-2012 № 57 (3) P. 133-164.

[3] R.A. Vdovin, V.G. Smelov Elaboration of a casting defects prediction technique via use of computer-aided design systems. International Journal of Engineering and Technology (IJET). Vol 6 No 5 Oct-Nov 2014, pp. 2269-2275.

[4] V.Sh. Sufiiarov, A.A. Popovich, E.V. Borisov, I.A. Polozov 2015 Selective laser melting of heat-resistant nickel alloy J. Tsvetnye Metally Vol. 1, pp. 79-84.

SELF PROPAGATING HIGH -TEMPERATURE SYNTHESIS OF MULTICOMPONENT CARBOHYDRIDES IN THE Ti-Nb-V-C-H SYSTEM

N.N. Aghajanyan *, S.K. Dolukhanyan, and O.P. Ter-Galstyan

Nalbandyan Institute of Chemical Physics, NAS 5/2 P. Sevak Str., Yerevan, 0014, Armenia
*seda@ichph.sci.am

Refractory metal-like compounds, in particular carbides of transition metals, being multi-purpose materials, occupy a special place in a number of technology branches. The study of multicomponent implantation phases is of great interest, as each of the element, introduced into the crystal structure creates a new dimension in the solid state. Such approach can radically change the physico-chemical properties of the materials. Earlier we studied the combustion processes in Ti-Nb-W-C-H and Ti-Nb-Cr-C-H systems, defined the main parameters of formation of multicomponent single-phase products [1-3].

The present work is directed to the investigation of the combustion process in the Ti-Nb-V-C-H system. The batches of the variable composition $xTi + (1-x)(Nb + V) + yC$, $[0.3 \le x \le 0.9, 0.5 \le y \le 0.9]$ were burned in argon and hydrogen environment. The obtained samples were studied by chemical and X-ray analyses. The hydrogen and carbon contents were evaluated by pyrolysis at temperatures 350-1100°C; X-ray analysis was performed on diffractometer DRON-0.5 using CuK_α radiation. The crystal phases were identified using the ASTM card indexes. The roles of composition of the initial batch (the ratio of taken components), and of hydrogen in the formed in combustion front end products, were studied. Table 1. shows the results of the experiments carried out in the Ar and H_2 atmospheres.

It was shown that in the entire range of changes of metal/carbon ratio, carbides and carbohydrides with cubic fcc lattice formed. As can be seen from the Table, at combustion of a number of compositions, complete dissolution of the intermediate phases occurred, and single-phase multicomponent carbides and carbohydrides formed. In carbohydrides, the hydrogen content ranged from 0.11 to 0.96 wt. %. This amount is sufficient to disperse them to 20 μm. Usually, for the dispersion of high-melting metals and their compounds, in powder metallurgy the disintegrating action of hydrogen is used. It was found that the compositions with low titanium content $Ti_{0.3} + Nb_{0.35} + V_{0.35} + C_{0.5\text{-}0.9}$ did burn neither in argon nor in hydrogen. Actually, titanium starts and leads the combustion reaction; niobium and vanadium are involved in the combustion later.

Table 1 - Characteristics of combustion products in Ti–Nb–V–C–H system

Charge	gas	Phase composition	TiC a, Å	C, wt. %	H_2, wt. %
$Ti_{0.9}+Nb_{0.05}+V_{0.05}+C_{0.5}$	Ar	TiC	4.310	10.49	-
$Ti_{0.9}+Nb_{0.05}+V_{0.05}+C_{0.5}$	H_2	TiC	4.310	10.51	0.83
$Ti_{0.9}+Nb_{0.05}+V_{0.05}+C_{0.6}$	Ar	TiC	4.315	12.45	-
$Ti_{0.9}+Nb_{0.05}+V_{0.05}+C_{0.6}$	H_2	TiC	4.319	12,44	0,49
$Ti_{0.9}+Nb_{0.05}+V_{0.05}+C_{0.7}$	Ar	TiC	4.325	13.73	-
$Ti_{0.9}+Nb_{0.05}+V_{0.05}+C_{0.7}$	H_2	TiC	4.323	14.24	0.49
$Ti_{0.9}+Nb_{0.05}+V_{0.05}+C_{0.9}$	Ar	TiC	4.323	16.00	-

$Ti_{0.9}+Nb_{0.05}+V_{0.05}+C_{0.9}$	H_2	TiC	4.332	16.98	0.25
$Ti_{0.7}+Nb_{0.15}+V_{0.15}+C_{0.5}$	Ar	TiC+NbC+VC	4.322	10.23	-
$Ti_{0.7}+Nb_{0.15}+V_{0.15}+C_{0.5}$	H_2	TiC	4.324	9.81	0.96
$Ti_{0.7}+Nb_{0.15}+V_{0.15}+C_{0.6}$	Ar	TiC	4.325	12.35	-
$Ti_{0.7}+Nb_{0.15}+V_{0.15}+C_{0.6}$	H_2	TiC	4.327	12.13	0.49
$Ti_{0.7}+Nb_{0.15}+V_{0.15}+C_{0.7}$	Ar	TiC	4.320	13.24	-
$Ti_{0.7}+Nb_{0.15}+V_{0.15}+C_{0.7}$	H_2	TiC+NbC tr.	4.319	12.66	0.4
$Ti_{0.7}+Nb_{0.15}+V_{0.15}+C_{0.9}$	Ar	TiC+NbC	4.327	15.96	-
$Ti_{0.7}+Nb_{0.15}+V_{0.15}+C_{0.9}$	H_2	TiC+NbC	4.327	16.27	0.35
$Ti_{0.5}+Nb_{0.25}+V_{0.25}+C_{0.5}$	Ar	TiC+NbC tr.	4.323	9.73	-
$Ti_{0.5}+Nb_{0.25}+V_{0.25}+C_{0.5}$	H_2	TiC+NbC tr.	4.335	9.78	0.89
$Ti_{0.5}+Nb_{0.25}+V_{0.25}+C_{0.6}$	Ar	$TiC+NbC+Nb_2C$	4.335	10.24	-
$Ti_{0.5}+Nb_{0.25}+V_{0.25}+C_{0.6}$	H_2	TiC	4.329	11.20	0.33
$Ti_{0.5}+Nb_{0.25}+V_{0.25}+C_{0.7}$	Ar	TiC+NbC tr.	4.318	11.88	-
$Ti_{0.5}+Nb_{0.25}+V_{0.25}+C_{0.7}$	H_2	TiC+NbC	4.319	11.64	0.33
$Ti_{0.5}+Nb_{0.25}+V_{0.25}+C_{0.9}$	Ar	TiC+NbC	4.319	14.38	-
$Ti_{0.5}+Nb_{0.25}+V_{0.25}+C_{0.9}$	H_2	TiC+NbC	4.324	14.47	0.11

Figure 1. shows the diffractograms of $Ti_{0.5}Nb_{0.25}V_{0.25}C_{0.6}$ carbide and $Ti_{0.5}Nb_{0.25}V_{0.25}C_{0.64}H_{0.22}$ carbohydride. As can be seen from this Figure, the synthesized in argon carbide is multiphase (Fig. 1a). When the batch of the same composition is burned in hydrogen, single-phase carbohydride is formed (Fig. 1b). These results prove the homogenizing role of hydrogen, previously found in work [1].

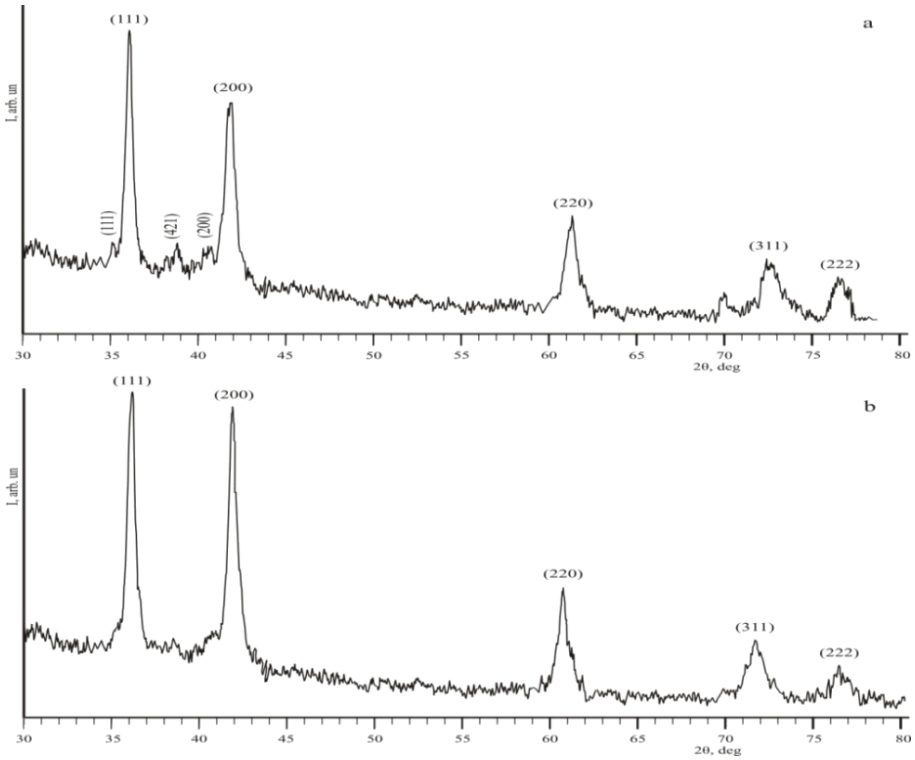

Fig. 1 - Diffraction patterns of combustion products: (a) $Ti_{0.5}Nb_{0.25}V_{0.25}C_{0.6}$ (combustion in Ar) and (b) $Ti_{0.5}Nb_{0.25}V_{0.25}C_{0.64}H_{0.22}$ (combustion in H_2).

Table 2. shows the X-ray densities of the single-phase carbides and carbohydrides formed in the Ti-Nb-V-C-H system. These densities were calculated using the ratio $\rho = P/V$, where P and V are the weight the volume of a single cell, respectively. $P = MN/N_{Av}$, where M is the molecular weight, N for the fcc lattice is 4 atoms per cell.

It is known that carbon in the fcc lattice occupied the octahedral pores of the crystal lattice [4]. Based on the data presented in Table 2, one can say that for identical metal ratios, the X-ray density in carbides increases with the carbon content increasing. In non-stoichiometric carbides, some of the octahedral pores are free and can be occupied with any atoms. Therefore, during combustion in hydrogen, for example, of the composition $Ti_{0.5}+Nb_{0.25}+V_{0.25}+C_{0.6}$, the hydrogen atoms implant into the vacant octahedral pores of the fcc lattice and formed the $Ti_{0.5}Nb_{0.25}V_{0.25}C_{0.64}H_{0.22}$ carbohydride with high X-ray density.

Let's note that the increasing of the niobium and vanadium concentrations leaded to the more essential (by 15.28%) increasing in the X-ray density from 4.708 g/cm^3 to 5.557 g/cm^3.

Thus, by the SHS method single-phase carbides and carbohydrides based on titanium, niobium, vanadium, carbon and hydrogen were obtained. In the entire range of changes of metal/carbon ratio, carbohydrides with cubic fcc lattice formed always, even at low carbon concentration. The influence of the concentration of components on the X-ray density is manifested.

Table 2 - X-ray density of Ti–Nb–V - based carbides and carbohydrides

Compound	Crystal lattice parameter, Å	Volume of unit cell, Å^3	Molecular mass, g	X-ray density g/cm^3
$Ti_{0.9}Nb_{0.05}V_{0.05}C_{0.6}$	4.315	80.342	57.49	4.750
$Ti_{0.9}Nb_{0.05}V_{0.05}C_{0.6}H_{0.29}$	4.319	80.566	57.78	4.763
$Ti_{0.9}Nb_{0.05}V_{0.05}C_{0.67}$	4.325	80.90	58.33	4.788
$Ti_{0.9}Nb_{0.05}V_{0.05}C_{0.68}$	4.329	81.127	58.45	4.785
$Ti_{0.9}Nb_{0.05}V_{0.05}C_{0.8}$	4.323	80.79	59.89	4.923
$Ti_{0.9}Nb_{0.05}V_{0.05}C_{0.84}$	4.323	80.790	60.37	4.963
$Ti_{0.9}Nb_{0.05}V_{0.05}C_{0.5}H_{0.47}$	4.310	80.06	56.76	4.708
$Ti_{0.9}Nb_{0.05}V_{0.05}C_{0.71}H_{0.29}$	4.323	80.790	59.10	4.858
$Ti_{0.7}Nb_{0.15}V_{0.15}C_{0.64}$	4.325	80.902	62.79	5.154
$Ti_{0.7}Nb_{0.15}V_{0.15}C_{0.64}H_{0.77}$	4.327	81.014	63.56	5.21
$Ti_{0.7}Nb_{0.15}V_{0.15}C_{0.7}$	4.320	80.622	63.51	5.232
$Ti_{0.7}Nb_{0.15}V_{0.15}C_{0.51}H_{0.6}$	4.324	80.850	61.83	5.079
$Ti_{0.5}Nb_{0.25}V_{0.25}C_{0.64}H_{0.22}$	4.329	81.127	67.88	5.557

REFERENCES

[1] N. N. Aghajanyan, S. K. Dolukhanyan, Investigation of combustion in Ti-Nb-W-C-H system and synthesis of complex carbohydrides. International Journal of Self-Propagating High-Temperature Synthesis, vol. 21, no.1, 2012, p. 7.

[2] N. N. Aghajanyan, S. K. Dolukhanyan, N. L. Mnatsakanyan, Synthesis of Ti-Nb-Cr-C-H carbohydrides in the combustion mode. Abstract of XII Int. Symposium on Self-Propagating High-Temperature Synthesis (SHS-2013), 21-24 October, Texas, USA, 2013, p. 68.

[3] N.N. Aghajanyan, S.K. Dolukhanyan, and N. L. Mnatsakanyan, Combustion synthesis of Ti-Nb-Cr-C-H carbohydrides. International Journal of Self-Propagating High-Temperature Synthesis, vol. 23, no. 2, 2014, p. 118.

[4] I.S. Latergaus, V.T. Em, I. Karimov, D.B. Khvatinskaya, and S. K. Dolukhanyan, Neutronographic Investigation of Cubic Titanium Carbohydrides with Deficient Nonmetal Sublattice, Neorganic Materials, vol. 20, no. 10, 1984, p. 1648.

ISMAN: PRESENT STATE AND PERSPECTIVES

M.I. Alymov

Institute of Structural Macrokinetics and Materials Science, Russian Academy of Sciences,
Chernogolovka, Moscow, 142432 Russia
*alymov@ism.ac.ru

Institute of Structural Macrokinetics and Materials Science, Russian Academy of Sciences (acronym ISMAN, founded in 1987) is currently engaged in basic and applied research on the physical chemistry of combustion and explosion, high temperature–high pressure transformations of matter, and on some aspects of modern materials science.

A prominent scientist, academician Alexander Merzhanov, was the founding father and the first ISMAN director. It was him who developed the thermal theory of combustion and explosion in condensed media and suggested many original methods for investigating non-isothermal kinetics. He had investigated the mechanisms of numerous high-temperature physicochemical transformations in solid–solid and solid–gas systems and gave birth to a number of new lines of research, such as structural macrokinetics, self-propagating high-temperature synthesis (SHS), solid-flame combustion, infiltration-mediated combustion, non-linear dynamics of combustion processes, and patterning of combustion products.

Presently, ISMAN is a leading institution in the field of modern SHS research and development. To date, the number of SHS-produced compounds and materials (ceramics, cermets, intermetallics) is countless. The pioneering works by Merzhanov, Borovinskaya, and their coworkers have been widely recognized and their numerous scholars and followers can be found in many countries all over the world: in Russia, CIS countries, China, Japan, Georgia, India, France, Germany, Italy, Greece, etc.

Currently, the basic and applied studies are conducted at ISMAN along the following lines of research:

– general and structural macrokinetics of combustion and explosion processes
– self-propagating high-temperature synthesis
– synthesis and modification of materials by high dynamic pressure
– controlling combustion/explosion processes
– chemical energetics
– materials science
– theoretical backgrounds for designing new materials (structural, functional, cutting) and coatings

For over the past years, ISMAN has proven to be a firmly united team of persons who really love their job and demonstrate allegiance to macrokinetic approach in their theoretical and experimental every-day work. The institute brought up a pleiad of outstanding research workers active in the field of combustion science and engineering.

The research is executed at the expense of a grant of Russian Science Foundation (project No. 16-13-00013).

SHS OF ULTRAFINE AND NANOSIZED POWDER OF ALUMINUM NITRIDE USING SODIUM AZIDE AND HALIDE SALT $(NH_4)_3AlF_6$

Yu.V. Titova, A.P. Amosov*, D.A. Maidan, A.V. Sholomova, A.V. Bolotskaya

Samara State Technical University, 244, Molodogvardeiskaya str.,443100 Samara, Russia
* egundor@yandex.ru

Highly dispersed (nanosized and ultrafine) aluminum nitride powder is of great interest in various industries, including production of substrates for microelectronic components, heat-absorbing materials for light-emitting diode devices, and high-power electronic equipment, because AlN has exceptional thermal, mechanical, dielectric and optical properties. Highly dispersed aluminum nitride powder is difficult to obtain by ordinary mechanical grinding; therefore, numerous chemical and physicochemical technologies have been developed for their production, such as direct nitriding, plasma chemical synthesis, carbothermal synthesis, chemical vapor deposition, aluminum wire explosion, etc. However, due to high energy consumption, complicated equipment, high cost of raw materials, most of these methods are not used for the production of nanosized and ultrafine powder of aluminum nitride. Currently on the market are, for example, nanopowders of aluminum nitride obtained by energy-intensive technology of plasma-chemical synthesis with expensive and complex equipment, which cost approximately 2000 Euro per 1 kg [1].

In this regard, undoubted interest represents the technology of self-propagating high-temperature synthesis (SHS), characterized by low energy consumption, simple compact equipment, possibility of using cheap raw materials. To solve the problem of obtaining AlN nanopowder by resource-saving technologies of SHS, it is promising to use such option as azide technology of SHS, denoted as SHS-Az and since 1970 is being developed in Samara State Technical University [2]. The technology of SHS-Az is based on the use of sodium azide NaN_3 as a solid nitriding agent and halide salts. The SHS-Az process produces large quantities of vaporous and gaseous reaction products, which in turn loosen up the reagents, making it difficult to merge the original particles of the products of synthesis, allowing you to keep them in nanosized state. As a result of the synthesis, a sintered AlN is not formed, as in furnace technology or in classical SHS, but a loose powdery target product is formed. Sodium, released during the thermal decomposition of sodium azide, intensively reduces the oxide film covering the particles of aluminum powder, and simultaneously reacts with the halides with the formation of neutral salts, most of which are soluble in water and subsequently washed from the desired product. From this point of view, the choice falls on the ion of fluorine taking into account the greatest activity of the halogen ion and the formation of water-soluble salt NaF.

In the coarse of chemical reactions, radical of halide salt NH^{4+} in complex with sodium azide forms ammonia NH_3, which is more active than molecular nitrogen in nitriding, as well as hydrogen which together with sodium favours to the reduction of the oxide film on the surface of particles of the initial powder of aluminum. Therefore, among the inorganic halide salts, which can be used in the SHS-Az systems (AlF_3, Na_3AlF_6, K_3AlF_6, $(NH_4)_3AlF_6$), a complex halide salt of the element to be nitrided (Al) - ammonium hexafluoroaluminate $(NH_4)_3AlF_6$ – deserves the most attention. However, this salt has been not used until now in the process of SHS-Az to obtain highly dispersed powder of aluminum nitride.

Halide salts Na_3AlF_6 and AlF_3 were used previously to study the process of obtaining ultrafine powder of aluminum nitride by azide technology of SHS [2, 3]. The equations of the studied reactions of SHS-Az are as follows:

$$AlF_3 + 3NaN_3 + nAl + = (1 + n)AlN + 3NaF + (1/2)\ (8 – n)/N_2; \quad (1)$$

$$Na_3AlF_6 + 3NaN_3 + nAl = (1 + n)AlN + 6NaF + (1/2)(8 – n)N_2, \quad (2)$$

where n = 0, 2, 4, 6, 8 is the number of moles of the energy additive of aluminum. A value of 8 moles is stoichiometric when the gaseous nitrogen is not evolved.

It turned out that the AlN powder is synthesized in nanosized form only in the "halide-sodium azide" systems, that is, in the absence of energy addition of aluminium powder in the starting mixture of powders, when n = 0. However, in this case, the washed products of combustion contain a large amount (approximately one third by weight) of the water-insoluble impurity of Na_3AlF_6 salt. For example, in the case of the starting mixture "AlF_3+$3NaN_3$", the washed products SHS-Az consist of two phases: AlN – 64% and Na_3AlF_6 – 36 %. These products represent the whiskers of AlN with a diameter of 50-100 nm covered with Na_3AlF_6. Similar results were obtained for the starting system "Na_3AlF_6 + $3NaN_3$". When adding aluminum powder in the initial powder mixture, the combustion temperature and burning rate increase, the impurity content of Na_3AlF_6 in the combustion products decreases, but the size of the synthesized particles of AlN increases significantly and reaches almost 1 μm at n = 8. For example, in the case of the starting mixture "AlF_3+$3NaN_3$+8Al", the composition of the washed products of combustion is AlN – 83.5 %, Na_3AlF_6 – 16.5 %, and the synthesized AlN particles represent fibers and strips with a size of 500-1000 nm. In the case of the starting mixture "Na_3AlF_6+$3NaN_3$+8Al", the washed products consist of AlN – 88.2 %, Na_3AlF_6 – 10.2 %, Al – 1.6 %.

The aim of this work was to study the possibility of synthesis of ultrafine and nanosized powder of aluminum nitride with the use of sodium azide and halide salt $(NH_4)_3AlF_6$. For this study, the following chemical reactions were selected:

$$(NH_4)_3AlF_6 + 6NaN_3 = AlN + 6NaF + 6H_2 + 10N_2, \quad (3)$$

$$(NH_4)_3AlF_6 + 6NaN_3 + 10Al = 11AlN + 6NaF + 6H_2 + 5N_2, \quad (4)$$

$$(NH_4)_3AlF_6 + 6NaN_3 + 20Al = 21AlN + 6NaF + 6H_2. \quad (5)$$

The phase composition of the synthesized products was determined by X-ray diffractometer ARL X TRA (Thermo Scientific). Shooting X-ray spectra was performed using Cu-radiation with continuous scanning in the range of angles $2\theta = 20°\div80°$ at a speed of 2 deg/min. The obtained spectra were processed using a special software package WinXRD. Quantitative phase analysis was carried out by full-profile analysis (Rietveld method) using the software PDXL 1.8.1.0 and the crystallographic open database (COD). The results of X-ray phase analysis of the products are given in Table 1.

Table 1 - The ratio of the phases in the washed products of combustion

№	Starting mixture	Composition of combustion products, mass. %	
		AlN	Na_3AlF_6
3	$(NH_4)_3AlF_6 + 6NaN_3$	39.0	61.0
4	$(NH_4)_3AlF_6 + 6NaN_3 + 10Al$	80.5	19.5
5	$(NH_4)_3AlF_6 + 6NaN_3 + 20Al$	95.0	5.0

It is seen that the content of water-insoluble impurity Na_3AlF_6 decreases from 61% to 5% with the introduction of the energy additive of Al powder up to 20%.

Study of surface topography and morphology of powder particles was carried out on scanning electron microscope JSM-6390A (Jeol) with the attachment Jeol JED-2200. The results are presented in Figure 1.

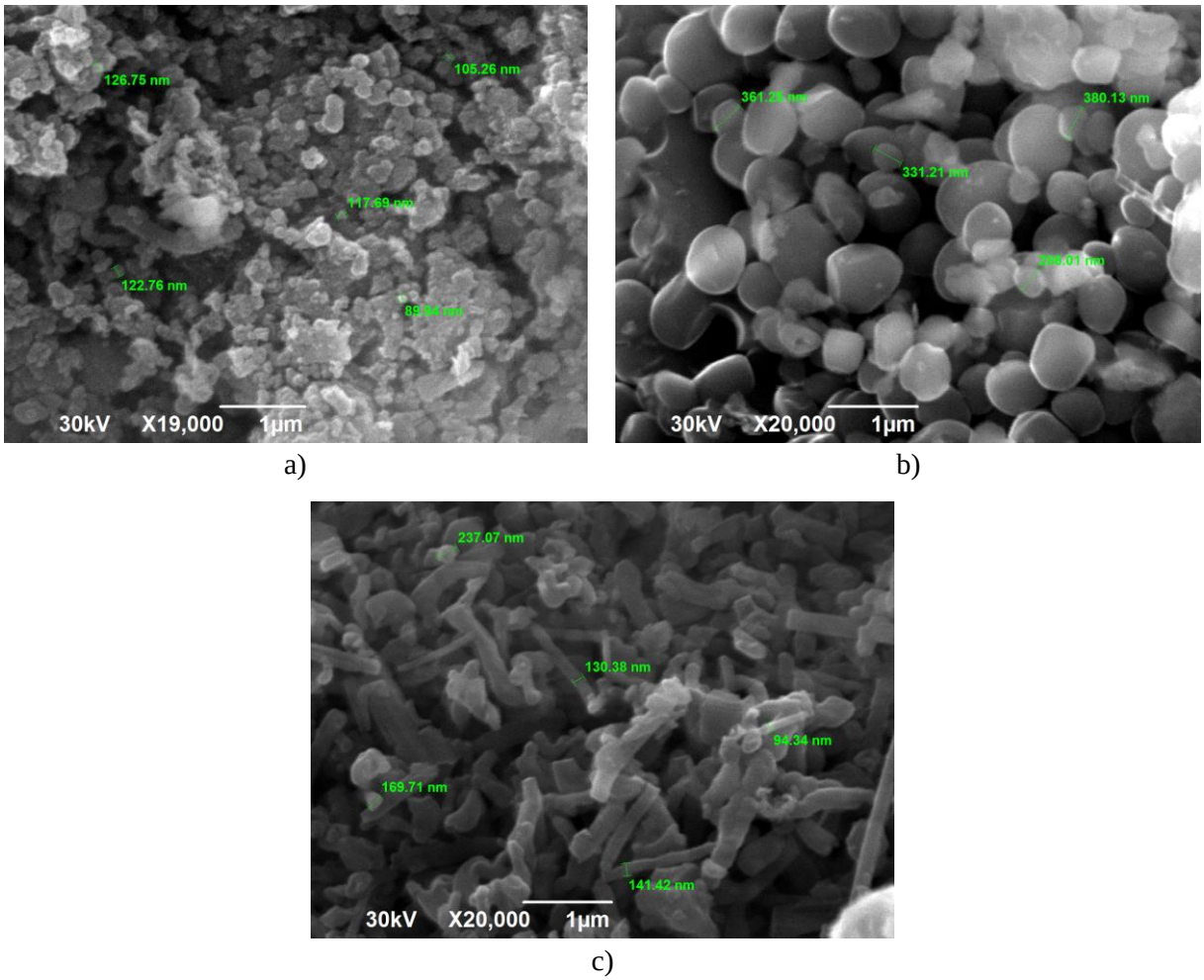

a) b)

c)

Figure 1 - The morphology and size of particles of combustion products of mixtures:
a) «$(NH_4)_3AlF_6 + 6NaN_3$»; b) «$(NH_4)_3AlF_6 + 6NaN_3 + 10Al$»; c) «$(NH_4)_3AlF_6 + 6NaN_3 + 20Al$»

Analyzing the photo presented on Figure 1 and considering the results of XRD, it can be concluded that changing the ratio of the starting components changes not only the content of the target phase AlN, but also the size and morphology of powder particles of aluminum nitride. In

the absence of the energy additive of Al powder, the combustion product represents equiaxed agglomerates of nanoparticles with a size of about 100 nm. When the content of Al in the mixture is 10 mol, AlN represents ultrafine particles of spherical shape with a diameter of 200-400 nm. With increasing Al content up to 20 moles, aluminum nitride is synthesized in the form of ultrafine fibers with a diameter of 100-300 nm and length up to 3 μm. This is due to the increase of temperature and burning rate of mixtures with increasing Al content.

Thus, the use of halide salt $(NH_4)_3AlF_6$ in azide SHS allows us to obtain highly dispersed (nanosized and ultrafine) powder of aluminum nitride with a purity of up to 95%, which is significantly better than in the case of salts of AlF_3 and Na_3AlF_6 (83.5 and 88.2% correspondingly).

The work is executed at financial support of RFBR under the project No. 16-08-00826.

REFERENCES

[1] http://www.plasmachem.com/download/PlasmaChem-General_Catalogue_Nanomaterials.pdf

[2] G.V. Bichurov, Nitride Ceramics: Combustion Synthesis, Properties, and Applications, ed. by A.A. Gromov and L.N. Chukhlomina, Wiley–VCH, Weinheim, 2015, p. 229.

[3] A. P. Amosov, Yu. V. Titova, D. A. Maidan and A. V. Sholomova, Rus. J. Inorg. Chem., 61, 2016, pp. 1225–1234.

STUDY OF INTRODUCTION OF ALN NANOPOWDER OF SHS-AZ BRAND INTO ALUMINUM MELT FOR EX-SITU PREPARATION OF COMPOSITES AL-(1-10%)ALN

A.P. Amosov[1]*, Yu.V. Titova[1], D.A. Maidan[1], A.A. Kuzina[2],
I.Yu. Timoshkin[1], A.V. Sholomova[1], A.V. Bolotskaya[1]

[1]Samara State Technical University, 244, Molodogvardeiskaya str.,443100 Samara, Russia
[2]Samara National Research University, 34, Moskovskoe shosse, 443086 Samara, Russia
* egundor@yandex.ru

Having low weight, nanocomposites of Al-AlN possess increased physico-mechanical properties, including high temperatures up to 400-550°C, which makes them very attractive for use in automotive, aerospace and semiconductor technology [1]. However, due to the long duration and high energy consumption, expensive and complex equipment, low efficiency of existing methods of solid-phase powder metallurgy and liquid-phase metallurgical processes of fabrication of Al-AlN nanocomposites, there are still no mastered industrial technologies of these nanocomposites.

The introduction in production of the aluminum matrix composites, reinforced with AlN particles, is hampered by some unsolved technological and economic problems. For example, the introduction and uniform distribution of nanopowders in the melt of aluminium is a big problem compared to larger powders, as the particles of nanopowders are easy to stick together into agglomerates, they are poorly wetted by liquid metal. Solid-phase methods of powder metallurgy have such disadvantages as a noticeable residual porosity, low adhesion of the matrix with the nanoparticles, the high cost of production. In-situ fabrication of the composite Al-AlN by blowing the melt with nitrogen requires a lot of hours maintaining the melt at a high temperature, which significantly increases the power consumption of the fabrication process. Finally, the AlN nanopowders, which are available for ex-situ production of reinforced aluminum alloys, have a very high cost: approximately 2000 Euro per 1 kg AlN of plasma-chemical synthesis [1].

A significant contribution to the solution of these problems can make the use of simple energy-saving powder technology on the base a process of self-propagating high-temperature synthesis (SHS). To solve the problem of obtaining nanopowder AlN by resource-saving SHS technology, it is promising to use such option as azide technology of SHS, denoted as SHS-Az and based on the use of sodium azide NaN_3 as a solid nitriding agent and halide salts [3]. A cost evaluation of SHS-Az nanopowders shows that because of the simplicity of the technology and equipment they can be 2-3 times cheaper than similar nanopowders of plasma-chemical synthesis.

To obtain highly dispersed powder of aluminum nitride by azide technology of SHS, halide salts AlF_3 and Na_3AlF_6 were used [3, 4]. The combustion process was supposed to take place in accordance with the reactions

$$AlF_3 + 3NaN_3 = AlN + 3NaF + 4N_2; Na_3AlF_6 + 3NaN_3 = AlN + 6NaF + 4N_2.$$

A by-product of NaF is highly soluble in water, so a pure powder of aluminum nitride should be obtained after the water washing. But in reality, it turned out that the washed products of

combustion contain a large amount (approximately one third by weight) of water-insoluble impurity of Na_3AlF_6 salt. For example, in the case of the starting mixture "AlF_3+3NaN_3", the washed products of SHS-Az consist of two phases: AlN – 65 % and Na_3AlF_6 – 35 %. These products represent the whiskers of AlN with a diameter of 50-100 nm covered with Na_3AlF_6. Similar results were obtained for the starting system "Na_3AlF_6 + 3NaN_3". But this by-product is a typical Na_3AlF_6 flux "cryolite" for refining and modification of molten aluminum alloys, and can facilitate the introduction of nanopowder AlN into the aluminum melt. In this regard, the AlN nanopowder of SHS-Az brand was not cleared from the by-product Na_3AlF_6, and was mixed along with it in the melt of Al or Al alloy to obtain ex-situ the nanocomposite Al-AlN [5, 6].

The AlN nanopowder has a low bulk density (1800-2000 kg/m^3), which makes it hard to dip into the aluminum melt with higher density 2300 kg/m^3; the particles of nanopowder are poorly wetted by molten aluminum, they stick together into agglomerates and are oxidized on the surface of the melt; therefore, direct mixing of the powdery AlN in a bulk form in the aluminum melt does not lead to success. Several methods are known to introduce AlN nanopowder into the aluminum melt in the form of pellets, pressed from a mixture of nanopowder AlN (1.5-5% wt.) with the aluminum powder, or in the form of aluminum cartridge filled with AlN nanopowder, previously cladded with Al and Cu; but these methods do not allow you to introduce AlN in amounts more than 0.05-0.1 % weight of the melt; whereby the composites Al-AlN, obtained in this manner, should be regarded as modified aluminum alloys more likely than as reinforced aluminum matrix composites [6]. Therefore, it is of undoubted interest to study simple methods of introduction of relatively cheap SHS-Az AlN nanopowder in Al melt to obtain ex-situ by the liquid-phase technology the nanocomposites Al-AlN with AlN content of more than 0.1% wt.

A method of introduction using nanopowdery master alloy was investigated in [5]. The washed product of SHS-Az was mixed with powder of copper, subjected to mechanical activation and pressed into the briquette of nanopowdery master alloy of composition Cu-4%(AlN+35%Na_3AlF_6). Copper was selected as a powder carrier having regard to its high density (8200 kg/m^3) compared to Al and good solubility in it. The briquette weighing 2.5 g was completely dissolved in the melt of aluminum A7 of weight 198 g at a temperature of 850°C and allowed us to introduce the reinforcing particles of AlN into Al to form a cast composite alloy of design composition Al-2% Cu-0.035%AlN. X-ray phase analysis of the cast sample showed the presence of lines of Al, Al_4Cu_9, Cu and AlN in the composition of the alloy, which indicates an assimilation of AlN powder by Al melt, but the lack of lines of Na_3AlF_6, i.e. the salt had played the role of a flux in the Al melt, but had not entered into the composition of the solidified alloy. With increasing content of nanopowder mixture AlN+35%Na_3AlF_6 in the briquette over 4%, the briquette ceased to dissolve completely in the Al melt, so attempts to obtain a composite alloy with AlN content more than 0.035% have not been successful with this method.

Another method of introducing AlN nanoparticles of SHS-Az brand into the melt of aluminum-magnesium alloy AlMg6 in the form of the composite master alloy, obtained by fusing the flux carnallite $KCl{\cdot}MgCl_2$ together with nanopowder mixture (AlN+35%Na_3AlF_6), was proposed in [6]. A crucible heated to 400°C was filled with powder of flux carnallite. After melting, the flux was overheated up to 800 °C and with constant stirring was charged with AlN-35%Na_3AlF_6 in the ratio 8:2 = flux : AlN-35%Na_3AlF_6 so that the melt remained always in a liquid or pasty state. After introducing all of the nanopowder, the melt was put in graphite molds in the form of

pieces of the composite master alloy. Alloy AlMg6 was alloyed with these pieces of the composite master alloy at the rate of 0.1 % AlN or 1.0% AlN. The introduction of the composite master alloy "carnallite - AlN-35%Na_3AlF_6" into AlMg6 melt were carried out at a melt temperature 720-730 °C, held for 5 minutes and poured into a metal mold to obtain a rod of a composite AlMg6-AlN with a diameter of 22 mm and a length of 170 mm. By this means a nanocomposite with a matrix of aluminum-magnesium alloy AlMg6 containing up to 1% of reinforcing phase of AlN nanopowder was obtained. By the same procedure, the pieces of the composite master alloy "carnallite - AlN-35%Na_3AlF_6" with a content of 30% AlN were prepared, which were introduced in the melt of aluminum A7 with the aim of obtaining nanocomposite Al-5%AlN. However, the assimilation of this composite master alloy in the melt during stirring and aging did not occur, the composite master alloy was almost entirely left on the stirrer and the walls of the crucible when the melt was poured out from the crucible. Cast nanocomposite Al-5%AlN could not be obtained in this way.
We also analyzed the method of introducing 5% nanopowder AlN into the solid-liquid molten alloy AlCu5 by mixing at a temperature of 630-670 °C and aging for 10 min to obtain a homogeneous consistency. However, after heating the melt to a liquid state, the nanopowder began to emerge and settle on the walls of the crucible. Cast nanocomposite with 5%AlN could not be obtained in this way too.

Finally, an attempt was made to prepare cast nanocomposite of Al-10%AlN by heating the sample of nanopowder mixture AlN-35%Na_3AlF_6 at the bottom of the crucible to 900 °C for 15 min, followed by filling the crucible with the melt of aluminum A7 heated to 850 °C. After aging for 5 min, the melt was poured out from the crucible, but the powder mixture was almost entirely left on the walls of the crucible.

Thus, ex-situ obtaining the cast aluminum matrix discretely reinforced composite with a high content (1-10%) of reinforcing phase of AlN nanopowder remains an unsolved problem and requires further research.

The work is executed at financial support of RFBR under the project No. 16-08-00826.

REFERENCES

[1] C. Borgonovo, D. Apelian, M.M. Makhlouf, JOM, 63, 2011, pp. 57-64.
[2] http://www.plasmachem.com/download/PlasmaChem-General_Catalogue_Nanomaterials.pdf
[3] G.V. Bichurov, Nitride Ceramics: Combustion Synthesis, Properties, and Applications, ed. by A.A. Gromov and L.N. Chukhlomina, Wiley–VCH, Weinheim, 2015, p. 229.
[4] A. P. Amosov, Yu. V. Titova, D. A. Maidan and A. V. Sholomova, Rus. J. Inorg. Chem., 61, 2016, pp. 1225–1234.
[5] Y.V. Titova, A.V. Sholomova, A.A. Kuzina, D.A. Maidan and A.P. Amosov, IOP Conf. Series: Materials Science and Engineering, 156, 2016, 012037.
[6] A.P. Amosov, Y.V. Titova, I.Y. Timoshkin, A.A. Kuzina, Key Engineering Materials, 684, 2016, pp. 302-309.

INTERACTION OF MOLTEN METALS WITH POROUS SKELETON OF Ti_3SiC_2 MAX-PHASE IN SHS CONDITIONS

E. I. Latukhin, A. P. Amosov*, A. M. Ryabov, A. Y. Illarionov, V. A. Novikov

Samara State Technical University, 244, Molodogvardeiskaya str.,443100 Samara, Russia
* egundor@yandex.ru

Skeleton ceramic-metal composites consist of two interpenetrating continuous skeletons: refractory ceramics and metal (alloy). The development of such composites is of great interest, since the rigid ceramic skeleton can provide improved wear resistance and heat resistance [1]. There is a traditional two-stage method of producing the skeleton composites, when the first ceramic powders are sintered to obtain a porous ceramic skeleton and then the skeleton is impregnated (infiltrated) with the metal melt. Two-stage technology requires a lot of energy and expensive equipment to obtain a ceramic skeleton and molten metal. In this connection, it is noteworthy to study the possibility of applying single-stage technology of self-propagating high-temperature synthesis (SHS), which do not require large expenditures of electric energy for sintering ceramic porous skeleton and melting metal. Such one-step technology of SHS-pressing was first successfully applied for obtaining functionally graded materials with high physical-mechanical properties, when the porous SHS-skeleton made of titanium carbide was impregnated with the melt of nickel [2].

Skeletons made of conventional binary refractory compounds (aluminium oxide Al_2O_3, silicon carbide SiC or titanium carbide TiC) are in most common use, but they have a relatively low strength due to their brittleness. Therefore, in recent years, considerable attention be given to a new kind of ternary refractory compounds – MAX-phases, which combine the advantages of refractory ceramics with the ductility of metals, so they are not so brittle. Energy saving SHS method is promising also for the synthesis of MAX-phases which are mostly produced by long reaction sintering of powders under high-temperature heating.

The application of SHS-pressing method was investigated in [3] to obtain aluminum-ceramic skeleton composites based on MAX-phase of Ti_2AlC. Such composites are attractive due to their low specific weight, but cannot provide the particularly high hardness, wear resistance and strength. To solve such problems, the impregnation of ceramic skeleton should be performed not with the aluminum melt but with a melt of other, more strong and refractory metals: Ni, Cr, Ti, Fe. In this connection, it is necessary to investigate the interaction of melts of these metals with porous skeletons of MAX-phases in terms of SHS process. The results of these studies are presented in this work.

First the possibility was considered [4] to apply the SHS method for obtaining the composite material consisting of a porous skeleton of MAX-phase of titanium silicon carbide (Ti_3SiC_2) impregnated with nickel. To synthesize Ti_3SiC_2, the SHS charge was used representing the initial mixture of powders of titanium, silicon and carbon (soot) 3Ti+1,25Si+2C. Nickel for impregnation of Ti_3SiC_2 skeleton was introduced in three variants: the first - with the addition of nickel powder to the initial powder mixture (SHS charge), the second – in the form of briquette, pressed from nickel powder, between two briquettes pressed from SHS charge, and the third - similar to the second variant, but with the paper barrier layers between the briquettes of nickel and SHS charge, and with the application of pressure after the combustion of the charge. The combustion process was carried out in the filling of dried river sand at a depth of 15-20 mm.

Using X-ray diffraction, scanning electron microscopy and energy dispersive analysis, it is established that in all three variants, the presence of a melt of nickel prevents the formation of MAX-phase Ti_3SiC_2, reducing its amount or destroying it completely. Nickel, even in small quantities, introduced into the charge before synthesis, reduced formation of MAX-phase Ti_3SiC_2 and the size of its plates, and the large amount of nickel led to a complete lack of MAX-phase after synthesis. In the second and third variants, the molten nickel was formed near the area of the synthesis of porous MAX-phase and partially impregnated it, leading to the formation of intermetallic phase, preventing the formation of MAX-phase or destroy it in the field of impregnation. This can be explained by the high chemical activity of the liquid phase of nickel with respect to titanium at elevated temperatures, leading to the formation of intermetallic compounds of nickel-titanium instead of the MAX-phase. Thus, the attempts to produce skeleton composite Ti_3SiC_2-Ni have failed in all three investigated variants of SHS conditions.

Further the possibility of impregnation of the MAX-phase with nickel in the second variant was investigated, when adding silicon powder to nickel powder in the preparation of pressed briquette placed between the briquettes of SHS charge for the synthesis of the MAX-phase Ti_3SiC_2. Nickel with silicon gives low-melting compound NiSi, which is melted at a temperature 964-966°C, which is much less than the melting temperature of nickel 1455°C. The addition of silicon to the briquette of nickel in the amount of 20 wt.% of nickel allowed us to melt a larger quantity of nickel, reduce its chemical activity with respect to titanium and impregnate the lower porous layer of MAX-phase fully. X-ray phase analysis of the synthesized samples showed the presence of MAX-phase Ti_3SiC_2, as well as phases of titanium carbide, titanium disilicide and pure nickel. Thus, it was possible to produce the skeleton ceramic-metal composite material based on MAX-phase Ti_3SiC_2 and nickel.
Similarly, adding titanium powder to nickel powder in the preparation of pressed briquette placed between the briquettes of SHS charge in the second variant facilitated the impregnation of the skeleton of MAX-phase Ti_3SiC_2.

The investigation of Ti_3SiC_2 samples after impregnation with titanium in the second variant with the briquette, pressed from the titanium powder, showed that the titanium melt wetted the reaction products of SHS, and filled the pores of Ti_3SiC_2 under the action of capillary forces and gravity. The distribution of the titanium melt at the interface with Ti_3SiC_2 skeleton was uniform. Molten titanium was distributed between the upper and lower Ti_3SiC_2 briquettes in the ratio 1:3.

The investigations of the interaction of melts of chromium with a porous skeleton of MAX-phase Ti_3SiC_2 in the process of its synthesis and after synthesis were performed. It is established that, as in the case of the introduction of nickel, the chromium introduction both into the initial powder mixture and as a molten metal into the products of synthesis, prevents the formation of MAX-phase, reducing its amount or destroying it. This can also be explained by the high reactivity of the melt of chromium at elevated temperatures. But if the main reaction products of interaction of nickel with MAX-phase are intermetallic compounds, the main phase among the products of the reaction the interaction of the melt of chromium with the skeleton of MAX-phase is titanium carbide. Thus, chromium may be present both in pure form, and enter into the composition of titanium carbide forming a solid solution. In addition, the chromium atoms may introduce into the crystal lattice of MAX-phase, forming an ordered solid solution on the basis of its crystal lattice.

With the introduction of 10 wt.% of iron powder into the initial mixture of powders for the synthesis of Ti_3SiC_2, the phase composition of the reaction products has considerably changed. Using X-ray phase analysis of the obtained material, it was determined that it consists of TiC, Ti_3SiC_2, $TiFeSi_2$. With increasing amounts of introduced iron, the amount of Ti_3SiC_2 in the final product decreases up to its complete disappearance. Thus, the interaction of porous MAX-phase Ti_3SiC_2 with the molten iron during the combustion process leads to the destruction of the MAX-phase.

When placing a briquette from iron powder between the two briquettes of the charge 3Ti+1,25 Si+2C, the iron was melted at the expense of heat evolved during the synthesis of Ti3SiC2, but the molten iron did not wet and not impregnate the Ti_3SiC_2 skeleton and was squeezed out from a clearance between layers of Ti_3SiC_2 during the application of pressure. The result was substantially changed when the silicon powder in an amount of 5 wt.% of iron or the carbon powder in an amount of 4% was added to the briquette from iron powder. In both cases, the melt of iron was absorbed by upper and lower Ti_3SiC_2 briquettes, that is, the melt of iron with these additions already wetted products of SHS and filled the pores of Ti_3SiC_2 briquettes under the action of capillary forces and gravity. As this took place, the upper briquette absorbed about 25% of the melt and the lower about 75%. The distribution of a melt of iron at the interface with Ti_3SiC_2 skeleton was uniform when adding the silicon to iron, but the iron was localized at the site of initiation of SHS reaction, that is, ignition of the charge, when adding the carbon to iron. Thus, in conditions of SHS, the skeleton composite Ti_3SiC_2-Fe can be produced using iron alloys Fe-Si and Fe-C.

The work is executed at financial support of RFBR under the project No. 16-08-00867.

REFERENCES

[1] J. Liu, J. Binner, R. Higginson, Wear, 276-277, 2012, pp. 94-104.

[2] A.N. Pityulin, Yu.V. Bogatov, A.S., Inter. Journal of SHS, 1, 1992, pp. 111-118.

[3] A.F. Fedotov, A.P. Amosov, E.I. Latukhin, V.A. Novikov, Rus. Journal of Non-Ferr. Met., 57, 2016, pp. 33-40.

[4] E.I. Latukhin, A.P. Amosov, D.V. Borisov, A.M. Ryabov, V.A. Novikov, A.Yu. Illarionov, Vestnik Samarskogo Gosudastvennogo Tekhnicheskogo Universiteta, Tekhnicheskie Nauki, 53, 2017, pp. 143-152.

MANIFESTATION OF INSTABILITY ARISING DURING SHS SURFACING ON TO TI-SUBSTRATE. NUMERICAL MODEL AND EXPERIMENT

D.E. Andreev*[1], S.A. Rogachev[1], V.I. Yukhvid[1], and K.G. Shkadinskii[1,2]

[1]Institute of Structural Macrokinetics and Materials Science, Chernogolovka, Moscow, 142432 Russia
[2]Institute of Problems of Chemical Physics, Chernogolovka, Moscow, 142432 Russia
*ade@ism.ac.ru

An important parameter in production of layered materials and SHS-surfacing is the profile of contact zone – substrate and deposited coating, the shape of the profile this zone will determine the adhesive strength and other characteristics. Therefore, the detection of instabilities arising during the welding or surfacing phase is an important criterion for obtaining high-quality gradient materials. On the basis of a special mathematical model that takes into account the diffusion interaction, when the melting temperature of the substrate and the deposited metal is reached when organizing the «transverse» propagation regime of the combustion front (side ignition, parameter C_w, Fig. 1) conditions for the appearance of instabilities were obtained and a comparison was made with an adequate experiment organized in the centrifugal force field.

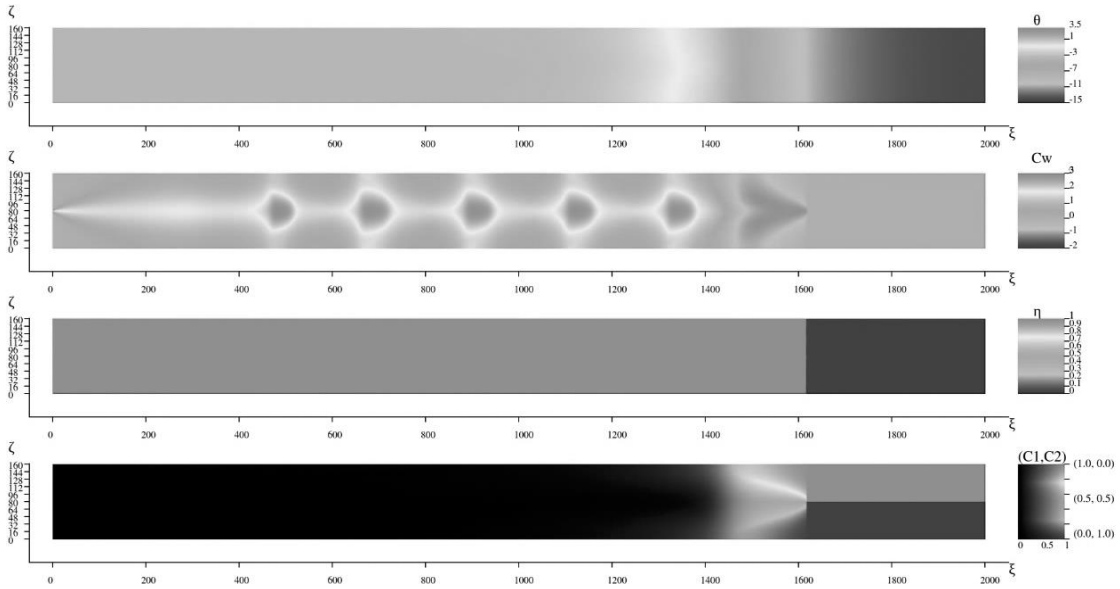

Fig. 1 - Numerical calculation results

A characteristic manifestation of instability revealed by changing the regime of SHS-surfacing on to titanium substrate is the formation of a wave-like profile at the interface of the coating-base contact. The manifestation of this instability is a distinctive feature of the structure of explosion-welded composites along the boundaries of welded seams.

We explored the possibility of centrifugal SHS surfacing in a mode of transversal deposition both experimentally and also by theoretical modeling for a laterally ignited double-layer system used as a model. Overall reaction schemes used in our experiments are given below.

$$NiO + Al \rightarrow Ni_3Al + Al_2O_3 \quad (1)$$

$$NiO + MoO_3 + Al + C \rightarrow Ni_3Al + Mo_2C + Al_2O_3 \quad (2)$$

Experiments on SHS surfacing of Ti were conducted in graphite cartridges placed in a centrifugal machine as described elsewhere [1], with the only difference that ignition was done at the side sample surface within the zone of contact between Ti substrate and green mixture.
The coatings deposited through reaction (1) showed better results as concerning both their practical implementation and perspectives for subsequent more detailed investigation. The front instability arising during combustion was found to result in formation of the wavy structure within the transition zone, which is known to facilitate strong joining between the coating and substrate material, just as it happens during explosive welding of dissimilar metals [2].

This work was supported by the Russian Foundation for Basic Research (project no. 15-03-01986).

REFERENCES

[1] V.N. Sanin, D.M. Ikornikov, D.E. Andreev, V.I. Yukhvid, B. Derin, O. Yücel, Int. J. Self-Propag. High-Temp. Synth, 24(3), 2015, pp. 161-170.

[2] B. Crossland, Explosive Welding of Metals and Its Application, (Oxford Univ. Press, Oxford, 1982).

MICROSTRUCTURE PECULIARITIES OF METAL-CERAMIC MATERIALS OF TI-Cr-C SYSTEM BY SHS-COMPACTION

Z.Aslamazashvili, G.Zakharov, G.Oniashvili, G.Urushadze, G.Mikaberidze, G.Tavadze, M.Chikhradze

LEPL - Ferdinand Tavadze Metallurgy And Materials Science Institute

The progress of science and technique is in direct connection with the application of specific new metal-ceramic and composite materials, which can work/resist at high temperature and aggressive media[1]. Majority of the materials in the mentions class represent the prospective materials for application in modern machine building, airspace, chemical and metallurgical industry and nuclear fields. Although the it must be mentioned, that the wide application of application metal-ceramic materials is restricted due to the absence of effective technologies for the production of such materials. In this point it is very important to orientate industry onto development and realization of resource-saving, environmentally friendly technologies [1].

The metal-ceramic materials consist of hard-melting wear-resistant frame and metal joiner. In ISMAN there are elaborated different classical materials by SHS-compaction method, in particular, СТИМ-1/В3 and СТИМ-3Б. They consist of two phases, wear-resistant frame and metal joiner. In СТИМ-1/В3 material the were-resistant frame is on the base of solid solutions of TiC and TiB_2, and the metal joiner is Cupper. In СТИМ-3Б the wear-resistant frame is the oversaturated solid solution of Cr_3C_2 in TiC, and the metal joiner in Nickel. On the base of the last product were elaborated new material СТИМ-3В, which differs from the СТИМ-3Б. In particular the chasm of new material contains steel Х18Н15, instead of Nickel. This steel have to have better wetting ability with the grains titanium-Chromium solid solution [3].

The study of the regularities of synthesis gives possibility to make conclusions about some peculiarities of the process. During the different stages of the process we have heating zone, zone of actual chemical reaction, reaction finishing zone and zone of final formation of the product. The investigation of the structure of final product will show the full knowledge about the phase formation mechanisms.

Namely it is important to have knowledge about the sequence order of formation from initial components to the final product. It enables to determine the optimal content of initial chasm and technological parameters, as well as to predict the exploitation properties of final product.
In the heating zone the sizes of metal particles are in the range of 10-40 micron, and there is no avidance of melting or any other interaction.

So called “paused fronts” methodology was used to study the phase formation mechanisms for the materials in Ti-Cr-C-Х18Н15 system. In the initial- heating zone the grain size is in the ranges of 10-40 microns, and there are no evidences of particle melting or any interaction.

The melting and capillary flow of metal particles, Titanium and steel Х18Н15, starts at the heating zone 180-200 micron distance away from the synthesis front. In this zone may be underlined two different type of structure with different particle sizes. In the first type of structure the particle sizes of Ti, Cr and Х18Н15 are several microns. These particles are partly melted, but bat their capillary flow has not started and therefore they maintain initial form. The second type of structure is formed in the area of capillary flow of metals and the particle sizes are less than 1 micron.

In the zone of active chemical interaction there is interaction between titanium and carbon. It is most predicted that the formation of target product is realized by mixing up carbon in melted metal solution and then crystallization of carbide grains in the whole volume of the sample fig.3. The fact that the majority of chromium particles are not fully melted in this zone and converted in ultrafine structure, gives us possibility to predict that crisstalized carbide grains is mostly based on TiC_x content with the small content of chromium.

In reaction finishing zone, 200-250 micron distance away from the synthesis front (fig.1 a), practically all titanium and steel are in the ultrafine grained structure, while chromium is partly in ultrafine grained structure, partly as melted metal condition. The whole conversion of chromium in the ultrafine grained mode takes place later, ongoing by diffusion mechanism. In this case $(Ti,Cr)C_x$ phase is formed, which creates whole carbide frame. The vacancies between the $(Ti,Cr)C_x$ phase grains are filled with metal joiner, which is steel based alloy, mixed with Titanium, chromium and nickel.

In the zone of formation of final structure (crystallization zone), the grain sizes of $(Ti,Cr)C_x$ carbides increases, which forms by uniting ultra dispersed grains and crystallization from liquid phase.

On fig.1 b is shown the microstructure of this material.

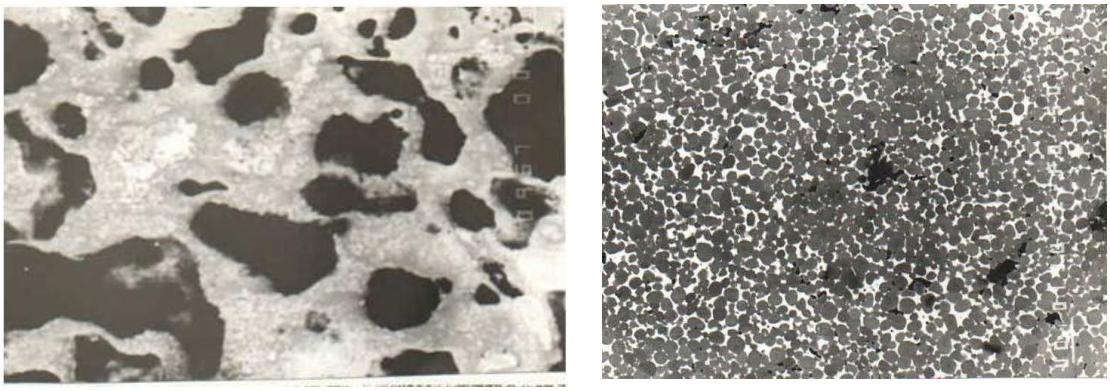

a b

Fig.1. - Microstructure of material obtained in Ti-Cr-C-X18H15 system a) In reaction finishing zone, 200-250 micron distance away from the synthesis front; b) after compaction

For the investigation of the samples were used local X-ray analyzer, and was established, that three phases are formed during the synthesis of material by SHS method in Ti-Cr-C-X18H15 system. These phases are: Phase I is Titanium-Chromium carbide $(Ti,Cr_x)C_y$, Phase II is Carbide on the base of chromium, which also contains iron and chromium, and Phase III - alloy of the metals, which contains iron, nickel, chromium and titanium.

The first phase is shown as round-shaped graines and the second and the third phases are located in it. The content of the phases depends on the content of X18H15 in the initial chasm. These relationships are presented on fig.2.

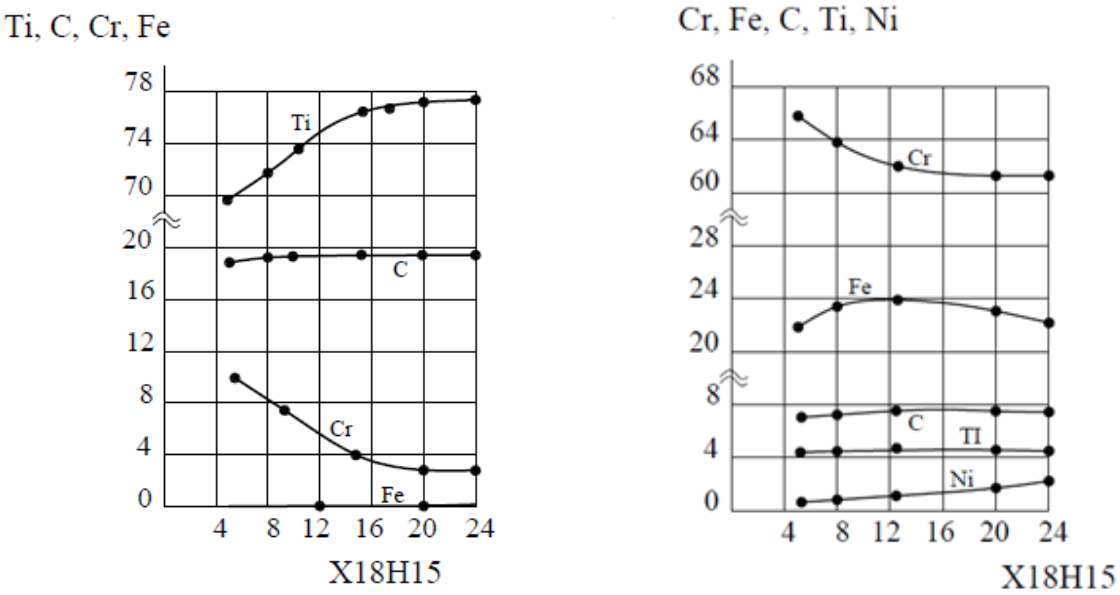

Fig.2. - Variation of phase contentents depending on the quantity of steel X18H15 in initial chasm (in wt %): a) Phase I; b) Phase II

When increasing the content of steel X18H15 in chasm, there is decreasing the chromium content in The phase I, while there is no changes in the content of carbon - 19 % (wt) and iron-1 %(wt). In Phase II we have the enrichment with Chromium and iron. When the content of steel X18H15 is 8 %(wt) and more there is formation of complicated iron-chromium carbide $Cr_{16}Fe_7C_6$, mixed with low content of titanium (4%wt) and nickel (2%wt). The Phase II content in the metal-ceramic material is 14-17%(wt). The Phase III in addition to iron may contain chromium 20%(wt) and titanium 17%(wt). When the content of steel X18H15 in chasm is 20% and more, the Phase III corresponds to , but the phase content in material does not exceed 4-5% (wt).

One of the main properties of hard alloys is the oxidation resistance at high temperatures. The materials with such properties can be successfully used for the production of stamps, die hole, cutting tools, and etc.

The investigations showed that the microstructure of СТИМ-3В differs from the microstructure of other metal-ceramic hard-alloy material. Therefore it is predicted that this material may have improved properties, in particular oxidation and were resistant properties.

Chromium carbides Cr_3C_2 and $Cr_{23}C_6$ are oxidation resistant materials and are resistant up to 1100^0C [4,5].

Metal-Ceramic material СТИМ-3В elaborated in Ti-Cr-C-X18H15 system, because of the different phase composition, in particular, Phase I is graines of $(Ti,Cr_x)C_y$ and containes Cr_3C_2, the Phase II is $Cr_{23}C_6$, where part of chromium atomes are replaced with iron atoms, and has

role of joiner in the $Cr_xFe_{23-x}C_6$ based metal-ceramic materil, surrounds the titanium-chromium graines of Phase I and protects from the oxidation.

In Table 1 is presented oxidation properties at 1000^0C in atmosphare of the material СТИМ-3В elaborated in Ti-Cr-C-X18H15 system and other СТИМ materials widely spread in industry.

Table.1

Alloy	porosity %	Increase in weight mg/cm^2; 5 hr	Oxidation mg/cm$^{2/}$g	Increase in weight mg/cm^2; 10 hr	Increase in weight mg/cm^2; 50 hr
СТИМ-3В -5%	2,8	6,34	1,2687	6,34	6,34
СТИМ-3В -8%	0,9	1,8	0,35	1,8	1,8
СТИМ-3В -10%	0,7	1,4	0,28	1,4	1,4
СТИМ-3В -12%	0,75	1,5	0,3	1,5	1,5
СТИМ-3В -15%	0,78	1,6	0,32	1,6	1,6
СТИМ-3В -18%	0,82	1,9	0,38	1,9	1,9
СТИМ-3В -20%	0,95	2,2	0,40	2,2	2,2
СТИМ-3В -25%	1,35	2,6	0,52	3,2	3,8
СТИМ-3В -10%	0,7	3,92	0,65	4,1	4,7
СТИМ-1В/3	0,8	7,81	1,3	8,1	8,5
СТИМ-3В А	0,85	795	0,93	8,2	8,8
СТИМ-3В -4	0,6	10,43	1,738	12,0	12,4
СТИМ-3В -5	0,5	22,22	3,7	48,6	53,7
Ti-Cr-C-Fe	0,8	3,18	0,53	3,3	4,0
Ti-Cr-C-Co	0,8	4,1	0,82	5,5	6,1
TiC : Cr_3C_2 =8 : 1	5,2	9,54	1,908	11,8	12,2
TiC : Cr_3C_2 =6 : 1	5,5	8,48	1,696	11,2	11,8
TiC : Cr_3C_2 =4 : 1	5,8	7,19	1,438	10,8	11,3
$TiC_{0,7}$	3,5	11,81	2,9625	12,5	13,2
$TiC_{0,98}$	5,4	10,5	2,1	12,2	12,9
ВК-8	1	179,7			
Т5К10	1	141,75		Whole material rusted	
ТН-20					

It can be concluded that the study of the microstructure of the material enables to determine the areas of potential application of the materials. It is also possible to make conclusions about the exploitation properties of those materials in extreme condtions.

REFERENCE

[1] “СВС-Керамика: Синтез, Технология, Применение” И.П. Боровинская, д-р хим. наук, Наука- производству. 2001, №10 (42).

[2] G.Oniashvili, Z. Aslamazashvili, G.Zakharov, G.Tavadze, M.Chikhradze, T. Dzigrashili, A.Berner SHS of Fine-Grained Ceramics Containing Carbides, Nitrdes and Borides International Journal on SHS, Vol.22, No.4, 2013

[3] З.Г.Асламазфшвили, А.Г.Мержанов, Г.Ш.Ониашвили, Ф.Н.Тавадзе и др. Разработка, получение и свойства окалиностойкого инструментального сплава СТИМ-3В. Препринт Черноголовка 1985

[4] Г.В.Самсонов, И.М.Виницкий. Тугоплавкие соединения. Справочник. – М.: Металлургия, 1976. – 557 с.

[5] Р.Киффер, Ф.Бенезовский. Твердые материали. - М.: Металлургия, 1968 – 383 с., ил.

PECULIARITIES OF MICROSTRUCTURE OF CERAMIC MATERIALS IN OBTAINED IN TI-B-C-N SYSTEM BY SHS

Z.Aslamazashvili, G.Zakharov, G.Oniashvili, N.Aslamazashvili, G.Mikaberidze, M.Chikhradze, G.Tavadze

LEPL - Ferdinand Tavadze Metallurgy And Materials Science Institute

One of the main goal of the work was to elaborate ceramic materials which could work under high intensity loadings and at the same time not to use deficit, expensive, limited raw materials and complicated technologies [1,2]. In case of reaching the set goal, our product will be cheap and production friendly from the technological and economical point of view. Therefore, at this stage we plan to elaborate materials, which will be obtained by comparably easy Self Propagating High-temperature Synthesis (SHS)-Compaction method in combustion mode and not in thermal explosion mode, which itself requires additional energy expenses.

The knowledge of regularity of transformation of initial components into a final product allows identifying not only the optimal composition and the technological parameters for obtaining the materials, but also we can forecast exploitation properties of these materials [3].

By means of compression of synthesized hot SHS product, the most significant is to select optimal technology parameters. These parameters are time and pressure.

In result of a correct selection of these characteristics the authors obtained in the Ti-B-N-Me and Ti-B-N-C-Me systems compact, practically non-porous materials, the porosity - 0,4% and 1,2% respectively, hardness - 91,0-91,5 HRA and 92,0-92,5HRA respectively, density - 4.3-4,4 g/cm^3 and 4,5-4,7 g/cm^3 respectively.

These materials resist once-only (single) dynamic impact possessing energy 18000-20000 joules, with the weight of manufactures 68-65 kg/m^2 (6,8-6,5 g/cm^2).

The fundamental research of microstructure and content showed (Fig.1) that the material obtained in Ti-B-N-Me system consists of two types of grains: pillar, needle type and round, sphere type. The chemical microanalysis made by electrical probe, showed that the pillar (needle) type grains belong to phase based on TiB_2, while round (sphere) type grains belong to phase based on TiN (Fig.1, Table 1).

Table 1

Result Type	Weight %					
Spectrum Label	Spectrum 8	Spectrum 9	Spectrum 10	Spectrum 11	Spectrum 12	Spectrum 13
B	1.96	5.24	22.37	17.01	0.95	2.30
C	4.03	2.52	3.98	3.36	5.42	6.67
N	5.26	1.88	0.00	0.00	9.20	12.10
O	0.63	2.26	0.00	0.00	1.37	2.06
Si		0.16				
Ti	88.12	87.51	73.65	79.63	83.07	76.86
Cu		0.43				
Total	100.00	100.00	100.00	100.00	100.00	100.00

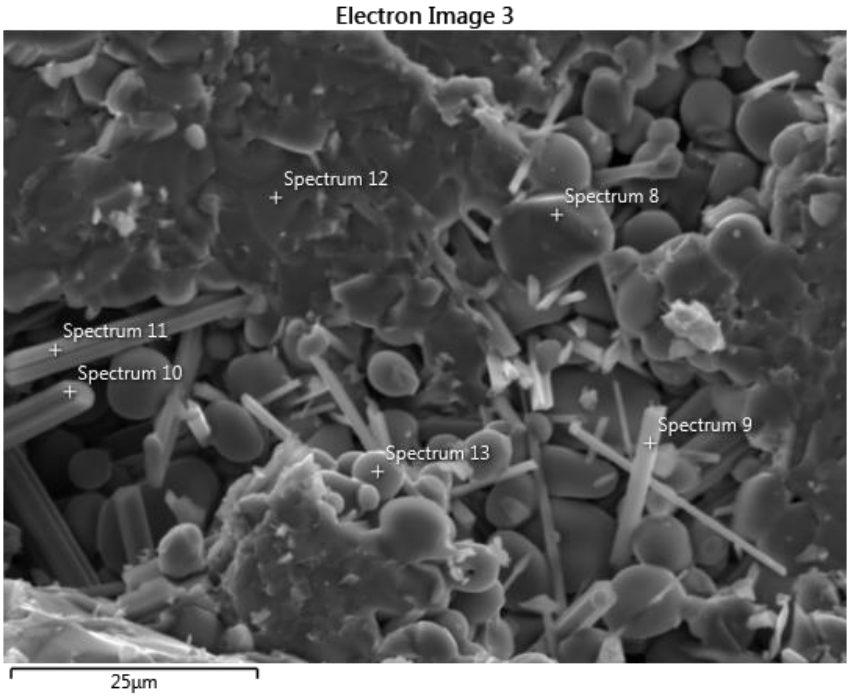

Fig.1. - Microstructure of material obtained in Ti-B-N-Me system, with the micro analysis of relevant points.

The fundamental research of microstructure and content showed (Fig.2) that the material obtained in Ti-B-N-Me system consists of two types of grains: pillar, needle type and round, sphere type. The chemical microanalysis made by electrical probe, showed that the pillar (needle) type grains belong to phase based on TiB_2, while round (sphere) type grains belong to phase based on TiCN (Fig.2, Table 2)

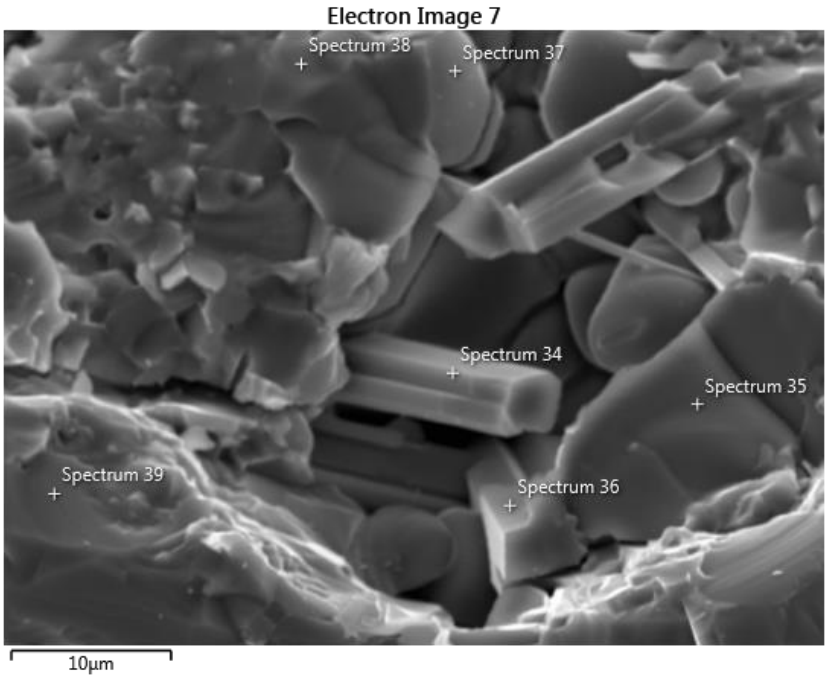

Fig.2. - Microstructure of material obtained in Ti-B-N-C-Me system, with the relevant points.

Table 2

Result Type	Weight %					
Spectrum Label	Spectrum 39	Spectrum 34	Spectrum 35	Spectrum 36	Spectrum 37	Spectrum 38
B		25.10		22.65		
C	9.26	11.16	9.20	11.42	7.08	7.91
N	13.08		12.64		10.75	14.46
Ti	77.66	63.26	78.16	65.92	82.17	77.63
Cu		0.48				
Total	100.00	100.00	100.00	100.00	100.00	100.00

The microstructure looks quite fine-dispersive, especially one direction of pillar and round type grains on the base of TiB_2 phase, where size is several hundred nanometers.

According to author's opinion, the resistance of materials against high dynamic loadings and shocks, which are obtained by SHS in Ti-B-N-Me and Ti-B-N-C-Me systems, can be explained by some peculiarities of microstructure. These peculiarities stipulate the accumulation of high energies and increase the resistance of those materials.

It can be predicted that when destructive energy penetrates in the product, prepared from the presented SHS material, initially crashes the pillar type grains. These grains are characterized with higher hardness, than the sphere-type grains based on TiN and TiCN phases. These phases itself are characterized with higher viscosity and plasticity than the grains of TiB_2 phase. During crashing of pillar-type grains, some destruction energy is accumulated, though the distruction of TiN and TiCN phases is not observed at first stage. As a result the distribution of cracks and the crashing of material is delayed, which itself increases the resistance and lifetime of the material. It can be concluded, that the study of microstructure enables to determine the potential areas of application of discussed materials and make conclusions about exploitation properties of those materilas for working in extreme conditions.

REFERENCES

[1] "СВС-Керамика: Синтез, Технология, Применение" И.П. Боровинская, д-р хим. наук, Наука- производству. 2001, №10 (42).

[2] G.Oniashvili, Z.Aslamazashvili, G.Zakharov Effect of Titanium-Aluminum Ratio on the Thermal Explosion Processing of TiAl-$TiB_{0.6}$ Layered Composites Materials and Manufacturing Processes, 26:9 pp 1157-1163, 2011.

[3] G.Sh.Oniashvili, Z.G.Aslamazashvili, G.V.Zakharov, G.F.Tavadze, M.N.Chikhradze, T.A. Dzigrashvili, A.Berner. SHS of Fine-Grained Ceramics Containing Carbides,Nitrides, and Borides ISSN 1061-3862,International Journal of Self-Propagaiting High-Temperature Synthesis, 2013,Vol.22,No 4, pp. 185-188.

THE MECHANISM OF $WO_3(MoO_3)$ & CuO COREDUCTION BY COMBINED Mg/C REDUCER AT NON ISOTHERMAL CONDITIONS

Sofiya Aydinyan*[1,3], Suren Kharatyan[1,2]

[1] A.B. Nalbandyan Institute of Chemical Physics NAS RA, 0014, 5/2, P.Sevak str., Yerevan, Armenia
[2]Yerevan State University, 0025, 1, A. Manukyan str., Yerevan, Armenia
[3]Tallinn University of Technology, Ehitajate 5, 19086, Tallinn, Estonia
*sofiya.aydinyan25@gmail.com

During last two decades, an increased interest has been paid to the so-called pseudoalloys based on Cu–refractory metal system (such as Cu-W, Cu-Mo). Their unique properties and multiple functionalities make them ideal for numerous high-tech applications. A number of novel technologies have been developed to enhance Cu-W(Mo) composite densification ability by using finer precursors, such as homogeneously mixed molybdenum and copper oxides/salts. In our previous works [1,2] for the manufacturing of Cu-W(Mo) composite powders it was suggested to apply a new, simple approach based on coreduction of oxides/salts with Mg-C combined reducer in combustion process by applying reactions' coupling approach [3]. The use of such reducing mixture as a strategy to control the reaction temperature in a wide range, allows to synthesize target materials in a controllable combustion mode. On the other hand, the use of salts ($CuMoO_4$ and $CuWO_4$) as precursors has privileges because both metals are chemically bonded in the same crystalline structure and the formation of more homogeneous composite is supposed.

It was revealed that introducing of even small amount of carbon into the MoO_3-CuO-Mg mixture brings in controversial change of combustion parameters (T_c, U_c) (see Fig. 1). Moreover, similar to MoO_3-Mg-C ternary system, in the range of sharp decline of combustion velocity (more than 10 times) the combustion temperatures remain virtually at the same level. In order to clarify such behaviour, in this work the mechanism of joint reduction of W(Mo) and Cu from oxide and salt precursors at non isothermal conditions was studied. It should be noted that it is highly challenging to *in situ* monitor and reveal the detailed mechanism of the combustion reaction due to its high velocity. To solve this issue one of the approaches is modeling the process at "soft" conditions using the methods of thermal analisis combined with XRD analysis of intermediate and final products. Two various instruments were used: DTA/TG analyser with heating rates up to 20 ^{o}/min and High-speed temperature scaner (HSTS) with heating rates up to 10000 ^{o}/min. This approach provides an enhanced opportunity to reveal the stepwise nature of complex reactions in the systems under study.

It was shown that at heating the $MoO_3(WO_3)$-CuO-Mg-C mixture, the whole process involves several phenomena: interaction between oxides with salt formation, high-exothermic reactions occurring directly between oxides and magnesium, as well as low-exothermic carbothermal reactions. It has been demonstrated that in the presence of only magnesium as a reducer salt-formation process takes place and complicates the magnesiothermal reduction of oxides. In contrast to magnesium, the addition of carbon in to the oxides' mixtures prevents the formation of $CuMoO_4$ ($CuWO_4$), because the carbothermal reduction of oxides starts earlier and occurs faster, than the salt-formation process. As a conclusion one may state that the simultaneous reduction of oxides proceeds more easily by carbon than by magnesium. And finally, only due to such pathway of reduction reactions becomes possible the combined and complete reduction

of oxides at relatively low temperatures by Mg/C reducing mixture. At that the reduction of the oxides mixture under consideration firstly begins with carbothermal reduction of copper and partially of Mo (from MoO_3 to MoO_2), followed by magnesiothermic reduction of tungsten/molybdenum oxide.

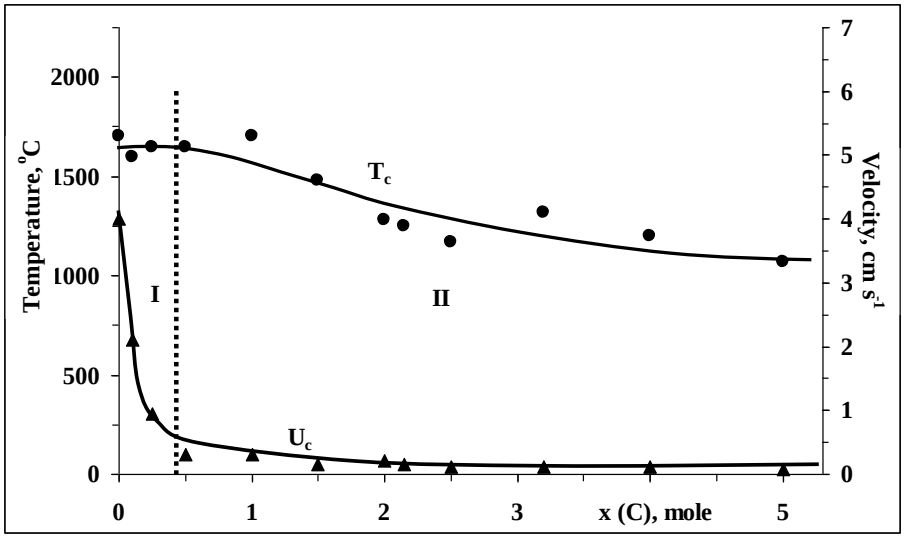

Fig. 1 - Combustion parameters behaviour (U_c, T_c) against carbon amount (x, mole)

In parallel with thermographic studies, copper wedge experiments were performed, which have also shown, that the reduction process starts with low exothermic reaction (carbothermal reduction) and then continued with high-exothermic one (reduction by magnesium). Such behaviour of reaction system under study conforms to the model for proceeding of two sequential exothermic reactions being spatially separated (so-called splitting mode). At that combustion velocity is determined by the first - low temperature stage, i.e. slow carbothermal reaction, while combustion temperature is determined by the overall enthalpy of the process. Taking into account the results of copper wedge experiments, that the first stage of reduction of both oxides is carbothermal reaction (e.g. MoO_3 to MoO_2), a series of experiments were performed by replacing MoO_3 with MoO_2 to confirm the suggested mechanism of reduction reaction. The phenomena of combustion parameters' quite different behaviour caused by carbon addition was not observe during the combustion of MoO_2-Mg-C mixture and combustion parameters decrease gradually. It is also evident that the introduction of carbon dramatically reduces the combustion velocity due to the low-temperature MoO_3-C interaction, proceeding in the frontal part of combustion wave.

In summary, taking into account the results of: (i) combustion experiments for binary, ternary and quaternary systems, (ii) molybdenum dioxide model experiments, (iii) copper wedge experiments, (iv) thermal analysis results, (v) detailed XRD analyses, the interaction scheme in the quaternary MoO_3-CuO-Mg-C system can be presented by the following main stages:

I - low-temperature stage
$CuO + C \rightarrow Cu + CO(CO_2)$ & $MoO_3 + C \rightarrow MoO_2 + CO(CO_2)$;

II - high-temperature stage
$MoO_2 + Mg \rightarrow Mo + MgO$

At insufficient amount of magnesium, the reaction may proceed by the following way:
$MoO_2 + MgO \rightarrow MoO_2 \cdot MgO$

While at excess amount of carbon the following reactions take place:
$MoO_2 + C \rightarrow Mo\ (Mo_2C) + CO(CO_2)$ and $Mo + C \rightarrow Mo_2C$.

In conclusion, it was shown that in the reaction's coupling process carbon influences not only on the thermal regime, products phase and microstructure characteristics, but also on the reaction mechanism. The detailed investigation of combustion thermograms and phase composition of quenched products from different areas of combustion wave asserted that carbothermal reduction preceded the magnesiothermal one, as a result of which a sharp decreasing of combustion velocity occurs. The latter allows to perform preparation of Cu-W(Mo) composite powders at mild and controlled conditions.

REFERENCES

[1] S.V. Aydinyan, H.V. Kirakosyan, S.L. Kharatyan, Int. J. Ref. Met. & Hard Mater., 54, (2016) 455-463.
[2] H.V. Kirakosyan, S.V. Aydinyan, S.L. Kharatyan, Int. J. SHS, 25(4), (2016) 215-223.
[3] S.L. Kharatyan, A.G. Merzhanov, Int. J. SHS, 21(1) (2012) 59-73.

MECHANOCHEMICAL TREATMENT OF METALLIC POWDERS AND PECULIARITIES OF SH-SYNTHESIS OF COMPOSITION SYSTEMS WITH THEIR PARTICIPATION

N.N. Mofa, B.S. Sadykov, A.Ye. Bakkara, Z.A. Mansurov

al-Farabi Kazakh National University, Institute of combustion problems, Bogenbai batyr str., 172, Almaty, Kazakhstan
bakkara_ayagoz@mail.ru

Self propagating high temperature synthesis (SHS) is an effective energy- and resource saving method for production of cermet composition systems [1]. Thermokinetic characteristics of SHS process depend on the composition, structure and state of the reagents being used. To increase the energy characteristics of condensed systems, different methods of their preparation are used. Mechanochemical treatment (MCT) is a simple and effective method for changing the physic-chemical properties and reactivity of different solid bodies including, metallic powders [2]. In the process of mechanochemical treatment, there takes place dispersion of powders and the increase in chemical activity of particles on account of the increase in their defectiveness and the increase in the reaction surface as a result of the decrease in particle sizes [3].

This work deals with the effect of the obtained by mechanochemical treatment submicron nanostructured particles of Al and Mg on combustion of a thermite mixture where submicron particles of silicon oxide were used as an oxidizer. Mechanochemical treatment (MCT) of powders was carried out in a centrifugal planetary mill CPM “Pulverisette 5” with acceleration of motion of grinding balls equal to 40 g. Mechanochemical grinding of metallic particles of Al of the brand PA4 and Mg of the brand MPF 3 was performed with graphite additives the presence of which facilitates the dispersion process and there takes place chemical modification of the surface of metallic particles providing conservation of the activated state of aluminum and magnesium particles and preventing their oxidation in air. In the course of MCT, the time of treatment and the amount of carbon modifier were varied.

EDX analysis of the elemental composition of aluminum powder after MCT with graphite showed the decrease in the content of oxygen, this indicating reduction of the oxide film by graphite on the surface of aluminum particles. Aluminum and magnesium are quite soft and ductile metals, therefore, as a result of mechanochemical treatment they acquire the form of thin plates (Figure 1). Evaluation of distribution of particles by sizes after MCT, carried out on “Malvern 3600 E” showed that with the increase in the content of graphite in the system up to 15-20% after grinding the main mass of aluminum powder has a linear size of particles less than 5 μm with the thickness less than 1 μm. The linear size of magnesium particles after MCT with graphite makes up less than 150 μm.

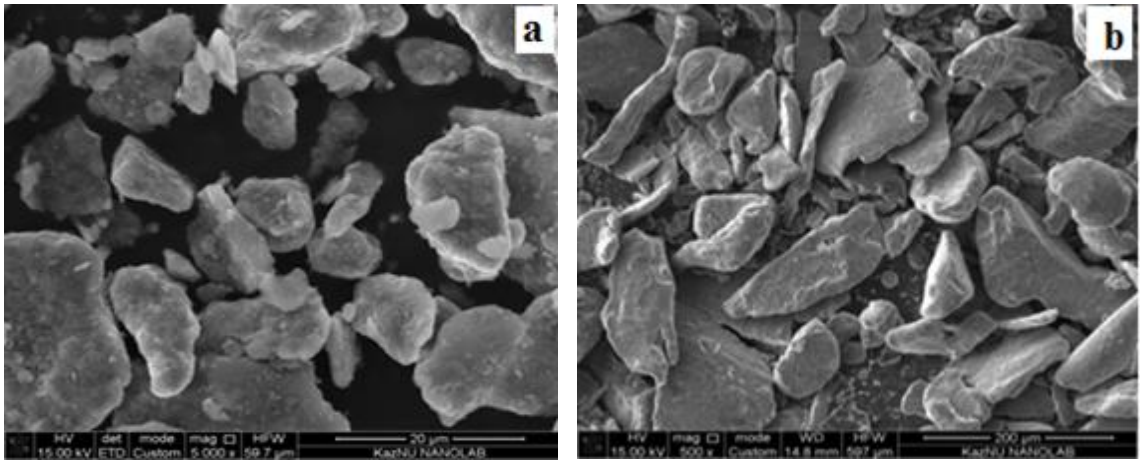

Figure 1 - SEM images of Al-C composite (a) and Mg-C (b) after 20 minutes of MCT

To evaluate the structural peculiarities of metallic particles after MCT, the sizes of crystallites in the obtained Me-C were studied by the XRD method. The obtained metallic powders after MCT are nanostructured particles with the size of crystallites less than 100 nm. The optimum time of treatment of composites makes up 20 min. The obtained under such conditions Me-C composites have a high activity and resistance to external influences at long-term storage.

The effect of submicron nanostructured particles of Al and Mg obtained by the method of mechanochemical treatment on the combustion process of thermite mixtures where silicon oxide was used as an oxidizer at the stoichiometric ratio of the components was studied. Combustion under the conditions of SHS was carried out in a muffle furnace at the pre-determined temperature of 900ºC for the composition with aluminum particles and at 650 ºC – for the samples with magnesium.

The combustion temperature in the process of synthesis was measured with the help of a pyrometric thermometer of the brand "Raytek Raynger 3i".

Combustion thermograms were built according to the results of the measured temperature indices. From the obtained thermograms it follows that, when using the mixture Al PA4-C as a fuel after MCT, the induction ignition period of the samples significantly decreases and the maximum temperature of combustion increases (Figure 2a). The results showed that the sample [(Al PA4 95%+C 5%)+SiO_2] has the maximum temperature of combustion (~1532 ºC). Introduction of carbon into the composition and the increase in its content in the mixture composition resulted in the decrease in the strength of the synthesized sample (from 100 to 1 MPa). This is due to the increase in the amount of gaseous products leading to the porosity of the sample. The main phases of combustion products of thermite mixtures with activated aluminum are aluminum oxides and reduced silicon, i.e. there takes place complete conversion of the initial reagents.

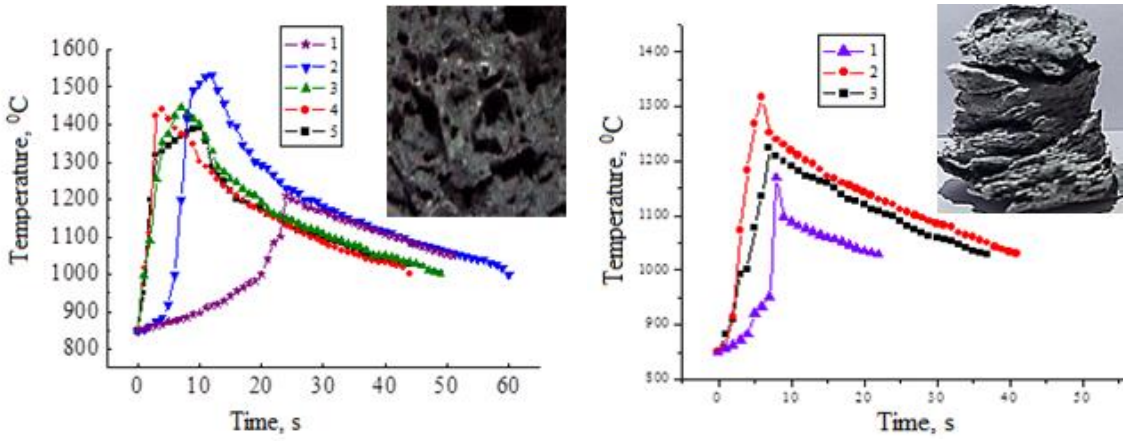

a: 1 − [Al+SiO_2], 2 − [(Al 95%+C 5%)+SiO_2], 3 − [(Al 90%+C 10%)+SiO_2], 4 − [(Al 85%+C 15%)+SiO_2], 5 − [(Al 80%+C 20%)+SiO_2]

b: 1 − [Mg+SiO_2], 2 − [(Mg 85%+C 15%)+SiO_2], 3 − [(Mg 75%+C 25%)+SiO_2]

Figure 2 - Combustion thermograms and appearance of the synthesized sample of the systems with Al PA4 (a) and with magnesium (b)

The thermite mixtures with Mg-C composite at a stoichiometric ratio of the components (Mg–44%), (SiO_2–56%) also showed that after MCT of Mg-C mixture the induction period of ignition decreases and the combustion temperature of the system increases (Figure 2b). The sample [(Mg 85%+C 15%)+SiO_2] has the maximum temperature of combustion (~ 1318 ºC). The products of technological combustion of thermite mixtures based on Mg-C composites have a low index of strength characteristics due to disturbance of sample continuity as a result of layer-by-layer combustion and formation of gaseous products of synthesis in a great amount.

Thus, the results of combustion of thermite mixtures in which aluminum and magnesium were used as a fuel component after MCT in the presence of graphite showed the efficiency of this method for increasing thermo-kinetic characteristics of the composition process and a more complete conversion of the used reagents. Also, the conditions for preparation of the combustible material and the combustion process under which formation of gaseous products of synthesis in a great volume is possible were determined [4]. The latter fact is of great importance, when using the obtained nanostructured Me-C composites in the composition of combustible systems designed for, e.g., gas generators or the swelling and production of porous systems of definite purposes.

REFERENCES

[1] Physico-chemical and technological grounds of self propagating high temperature synthesis, ed.by E.A. Levashov, A.S. Rogachev, V.I. Yukhwid, I.P. Borovinskaya, – M.: Binom, 1999, 176 p.

[2] Fundamental foundations of mechanical activation, mechanosynthesis and mechanochemical technologies ed.by E.G. Avakumova, - Novosibirsk: Nauka, 2009. 342 p.

[3] Z.A. Mansurov, N.N. Mofa, B.S. Sadykov, Zh.Zh. Sabaev, A.Ye. Bakkara, Engineering and physical journal. V. 89, №1. 2016, P. 1-8.

[4] N.N. Mofa, B.S. Sadykov, A.Ye. Bakkara, Z.A. Mansurov, Moscow. – Space challenge of the XXIth century. The Publ. House of the Institute of Chem. physics. V.5, 2016, P. 173-177.

SHS IN NiAl NANOFOILS: AN ATOMISTIC-SCALE DESCRIPTION

F. Baras*, V. Turlo, O. Politano

ICB, CNRS-University of Bourgogne Franche-Comté, France
* mailto:fbaras@u-bourgogne.fr

Self-propagating reactions are typical of reactive multilayer nanofoils [1]. Nanofoils - also called nanometric metallic multilayers - are composed of thin layers of metals stacked together and can be produced in the form of a coating or a freestanding foil. After being triggered at one edge of the sample, the reaction propagates along the sample without any further energy supply and produces a glowing front. The reaction is associated with phase transformations and accompanied by heat release. The most obvious features of the reactions which occur in nanofoils are the relatively low ignition temperature and the high velocity propagation of the reaction, up to tens of meters per second [2]. Among the numerous nanofoils of interest, the Ni-Al system is a particular object of study, both experimentally and theoretically.

In order to control the reactive process, the emphasis has been on the structure of the combustion front and its relation to the resultant microstructure. An important issue is to understand the elemental mechanisms responsible for the heating and nucleation and growth of new phases. To this end, we have adopted an atomistic-scale description [3] that does not presuppose any mechanism. In this talk, we will show that it is possible to simulate the propagtion of a front and obtain the microstructure/combustion wave relation, in a direct way.

The possibility of a stationary self-sustaining reactive wave while varying the initial temperature (from 300 to 800 K) and stoichiometry (from 0.35 to 0.77 of Ni mole fraction) was investigated [4,5]. The main features of the wave propagation were obtained: temperature profile, combustion temperature, and velocity of the front. The products of the reaction, and their microstructure along the sample after the passage of the front were described. After the formation of a melted alloy Ni-Al at high temperatures, the crystallization of an intermetallic compound B2-NiAl was observed. Two formation mechanisms of B2-NiAl were identified: dissolution-precipation and rapid crystallization from melts. We will show that the microstructure differs widely according to the stoichiometry and initial temperature. In the case of dissolution-precipitation, the crystallographic orientation of the Ni/Al interfaces influences the kinetic and microstructure during the subsequent grain formation. Besides nucleation and growth at interfaces, several new processes were identified, such as the merging of two grains with similar orientation, the separation of one grain into two grains, the rotation of a grain during coalescence, Ostwald ripening associated with the disappearance of small grains and, finally, crystallization from melt [6].

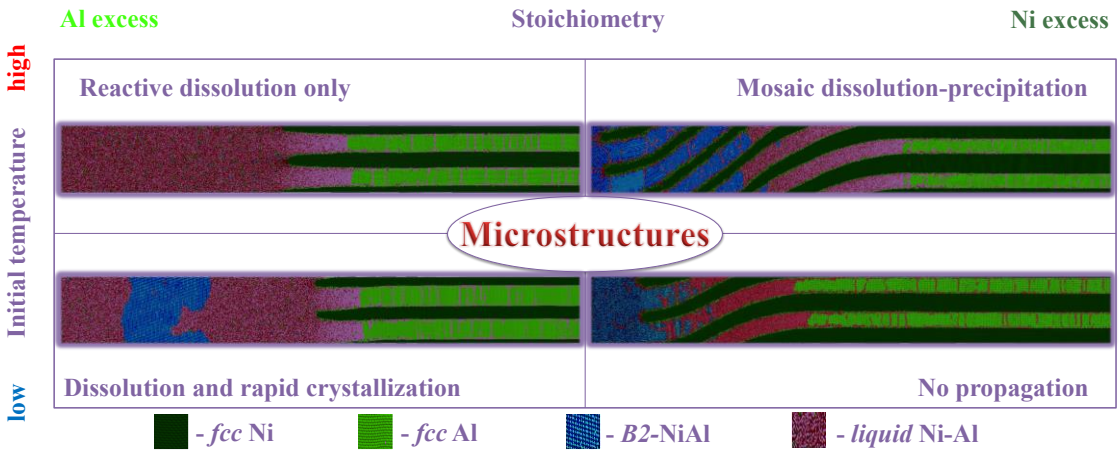

REFERENCES

[1] T.P. Weihs, Handbook of Thin Film Process Technology, D. A. Glocker and S. I. Shah Eds., IOP Publishing, Bristol (1998).

[2] A.S. Rogachev, Russ. Chem. Rev. 77 (2008) 21-37.

[3] F. Baras, O. Politano, Phys. Rev. B. 84, 024113 (2011).

[4] O. Politano, F. Baras, J. Alloy Compd 652 (2015) 2529.

[5] V.Turlo, O. Politano, F. Baras, J. Alloys Comp. 708 (2017) 989-998.

[6] V.Turlo, O. Politano, F. Baras, J. Appl. Phys. 121 (2017) 055304.

PRODUCTION OF TiB_2-B_4C-TiC COMPOSITE POWDER MIXTURES VIA SHS

Kağan Benzeşik[1], Mehmet Buğdaycı[1, 2], Ahmet Turan[2], Onuralp Yücel[1]

[1]Istanbul Technical University, Metallurgy and Materials Engineering, Maslak, Istanbul, 34469, Turkey
[2]Yalova University, Chemical and Process Engineering Department, Yalova, 77100, Turkey
benzesik@itu.edu.tr, mbugdayci@itu.edu.tr, yucel@itu.edu.tr

There are many production methods for the synthesis of advanced composite ceramics such as carbothermic reduction, synthesis from elements, gas phase reactions and self-propagating high-temperature synthesis (SHS). SHS is a combustion synthesis process which presents some advantages such as high quality of production, low cost, low processing temperatures, low energy requirement, very short processing time and simple operation. This method allows synthesizing advanced materials such as ceramics (e.g. ZrB_2, TiB_2, B_4C, Si_3N_4); abrasives, cutting tools and polishing powders (e.g. TiC, cemented carbides); resistive heating elements (e.g. $MoSi_2$), shape-memory alloys (e.g. TiNi); high-temperature structural alloys (e.g. nickel aluminides); master alloys (e.g. AlTiB); neutron attenuators (e.g. refractory metal hydrides) as well as conventional metals and their alloys. In a SHS process, the ignition begins the combustion and it propagates throughout the reactant mixture yielding the desired product. However, the disadvantages of the process such as unreacted products due to undesirable reaction rates needs to be overcome by changing some parameters such as ignition temperature, particle size, additive, atmosphere etc.

Titanium-diboride (TiB_2) is an important transition metal boride with its unique properties such as high strength, hardness, durability, melting point, wear resistance, thermal conductivity and low electric resistivity. Boron Carbide (B_4C) is one of the hardest materials known, ranking third behind diamond and cubic boron nitride. It is the hardest material produced in tonnage quantities. TiB_2 and B_4C are are being used in various industrial areas from space technology to nuclear industry owing to combination of their unique properties. Present study was conducted in two main stages: Self-propagating high-temperature synthesis (SHS) reactions and leaching. TiO_2, Carbon black, B_2O_3 were used as starting materials to produce TiB_2-B_4C-TiC powders by SHS. Also magnesium powder is used as the reductant. The metal oxide powders have over 97% purity and 150 µm average grain sizes. In addition, the adiabatic temperatures were calculated for each system by using FactSage 6.2 Termochemistry simulation software.

Eleven mixtures were prepared at different rates (from 100% TiB_2 - 0% B_4C to 0% TiB_2 - 100% B_4C). The reaction mixtures were mixed thoroughly 15 minutes in a turbula mixer and powder mixtures (approximately 100 g) were charged into Cu crucible and compacted. W (tungsten) wire was placed at the top of copper crucible and the reaction realized by passing current through the wire. After initiation, a highly exothermic reaction became in a self-sustaining mode and propagated throughout the SHS mixture. The obtained SHS products were discharged from the crucible after cooling. After the SHS process optimum leaching parameters were determined. Leaching was performed at 80 ºC for 1 hour. The solid-liquid ratio was 1/5 and 20 grams of solid mixture were used for each leaching process. The samples were characterized by using Atomic Absorption Spectrometer, X-Ray Diffraction, X-Ray Fluorescence, Scanning Electron Microscope and EDS techniques.

REFERENCES

[1] O. Yücel, F.C. Sahin, A. Tekin, "The Preparation of Ferroboron and Ferrovanadium by Aluminathermic Reduction," High Temperature materials and Processes, 15 (1-2) (1996) 103–106.

[2] A.G. Merzhanov, "Self-propagating High-temperature Synthesis (SHS)," (ISMAN, Russia, 2002).

[3] I.P. Borovinskaya, "Chemical Classes of the SHS Processes and Materials," Pure and Applied Chemistry, 64 (1992) 919-940.

[4] V.I. Yukhvid, "Modifications of SHS Processes," Pure and Applied Chemistry, 64 (1992) 977-988.

[5] Z. A. Munir, U. Anselmi-Tamburini, Materials Science Reports, 3 (1989) 277-365.

[6] O. Yücel, F. Ç. Şahin, High Temperature Materials and Processes, 20 (2) (2011) 137-142.

FUNCTIONAL METAL-KERAMIC COATINGS: STRUCTURE AND OPERATING PROPERTIES

L.I. Markashova[1], G.M. Grigorenko[1], Yu.N. Tyurin[1], O.M. Berdnikova*[1], O.V. Kolisnichenko[1], E.P. Titkov[1], E.V. Polovetskyi[1], O.S. Kushnarova[1]

[1] Paton Welding Institute of the NAS of Ukraine, Kazimira Malevicha str, 11, 03650, Kyiv, Ukraine
* omberdnikova@gmail.com

One of the most widespread and at the same time perspective way to improve operation properties and durability of products is deposition of various functional coatings on their surfaces using different spraying technologies [1 - 4].

At the E.O. Paton Electric Welding Institute of the NAS of Ukraine the technology and equipment for cumulative-detonation spraying (CDS) were developed by which high-quality coatings are obtained with high materials utilization factor and productivity [5 - 6]. The demanded direction for application of cumulative-detonation method is spraying of powders of different systems: Ni-Cr-Si; WC-Co-Cr; Cr_3C_2-NiCr; Cr_3C_2-TaC-NiCr; Al_2O_3-Ti / Al; $ZrSiO_4$, etc. Such coatings possess high strength and corrosion resistance, hardness and high wear resistance.

The aim of the present work was to study the phase and structural features of metal-ceramic coatings from based on zirconium ceramics ($ZrSiO_4$) powder obtained by CDS and to assess their effect on the mechanical properties and crack resistance of the coatings.

The investigations of structural-phase state of coatings (micro-hardness, volume fraction of pores, phase composition, distribution of dispersed phases, character of grain, sub-grain and dislocation structures, etc.) were carried out at all the structural levels using comprehensive methodological approach including optical metallography (Versamet-2; Leco-M400), analytical scanning electron microscopy (Philips SEM-515), X-ray structural phase analysis (DRON-UM1), as well as transmission micro diffraction electron microscopy (JEM-200CX, company JEOL=with accelerating voltage of 200kV).

Two groups of coatings were produced with the thickness up to 300 μm (№1 – on titanium substrate, №2 – on aluminum substrate with an underlayer Co-Cr-Al-Y). The investigations using the method of optical metallography showed that the porosity of such coatings doesn't exceed 2...3%. Using X-ray diffraction phase analysis of the produced coatings, it was revealed the formation of coatings of identical phase composition (ZrO_2, SiO_2 and residual $ZrSiO_4$) at approximately equal in content of the forming phase components (61…64%, 33% and 3…6%). However, in the coatings No.2 the integrated microhardness is by 24% increased (from 5270-7360 to 7100-8560 MPa) with a decrease in the size of the grain structure by a factor of 1.2.
Features of fine structure of coatings and its parameters such as: changes in density and character of dislocation density in different structural components, character of the forming substructure, its parameters, diameter of particles of phase precipitations and effective distances between the forming phases, were determined by electron-microscopic studies on the lumen.
In the coatings No.2 the size of particles of nano-size phase excretions (ZrO_2) of (20...100 nm) in 10% decreases in the surface layers of coatings as compared to coatings No.1. The distance between the forming dispersed phases is almost identical (10…50 nm), which characterizes the uniform distribution of the forming phases in the volume fraction in the matrix. The dislocation

density at the outer surface of coatings is $(5…9)\times10^{9}cm^{-2}$ (№1) and $6\times10^{9}…10^{10}cm^{-2}$ (№2):. At the same time in the coatings near to boundary the dislocation density is $(2…4)\times10^{10}cm^{-2}$ (№1) and $(4…6)\times10^{9}cm^{-2}$ (№2).

The executed complex of experimental investigations at all the structural levels allowed to carry out analytical evaluations of the (differentiated) contribution of different structural and phase factors and parameters (Figure 1), formed in the coatings, in change of strength characteristics and to determine the structural factors influencing the on character and distribution of local inner stresses, which are the potential sources of incipience of cracks [7 - 9].

At that, the following were taken into account: the resistance of metal lattice to the movement of free dislocations (friction stress of lattice or Peierls-Nabarro stress); the hardening of solid solution by alloying elements and impurities (solid solution hardening); the hardening due to changes in grain and sub-grain size (dependences of Hall-Petch, grain boundary and substructure hardening); dislocation hardening, caused by interaction between dislocations; the hardening, caused by dispersed particles according to Orowan (dispersion hardening).

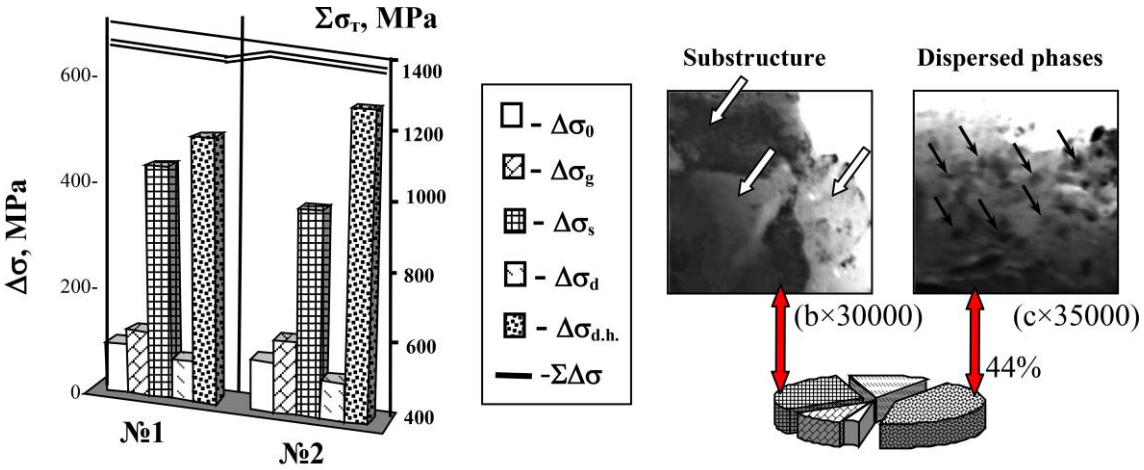

Figure 1. Histograms (a) show the differentiated contribution of grain ($\Delta\sigma_G$), substructure ($\Delta\sigma_S$), dispersion ($\Delta\sigma_{d.h.}$) and dislocation ($\Delta\sigma_d$) hardening to changes in integrated values $\Sigma\Delta\sigma_T$ in the material of coatings sprayed using different modes: №1 – Ti substrate, №2 – Al substrate and contribution of phase formations disperse particles (b, c) to overall level $\Sigma\Delta\sigma_T$ (d).

We have shown that the integral value of the hardening for coatings is 1390 MPa (No. 1) and 1330MPa (No. 2) (Figure 1, a). In both cases, the maximum contribution (up to 36…44%, Figure 1, d). to the total hardening value is made by hardening the coating matrix with dispersed nano-size particles of phase excretions (Orovan dispersion hardening): 498 MPa (coating No. 1) and 587 MPa (coating No. 2) (Figure 1, a, c). The contribution of subgrain hardening is 450 and 400 MPa, respectively (Figure 1, a, b).

Calculation-analytical techniques of determination of the level of local inner stresses allowed evaluating the crack resistance of coatings considering the character of dislocation structure [10 - 12]. It is quite clearly revealed during examination of fine structure on the lumen using the methods of ion thinning of fine foils. From the analysis of different approaches to determination of mechanisms of incipience of cracks and fracture of materials the evaluation was chosen

basing namely on the dislocation theory of crystal solid bodies, which associates the processes of formation of local inner stresses with incipience and rearrangement of dislocation structure [10].

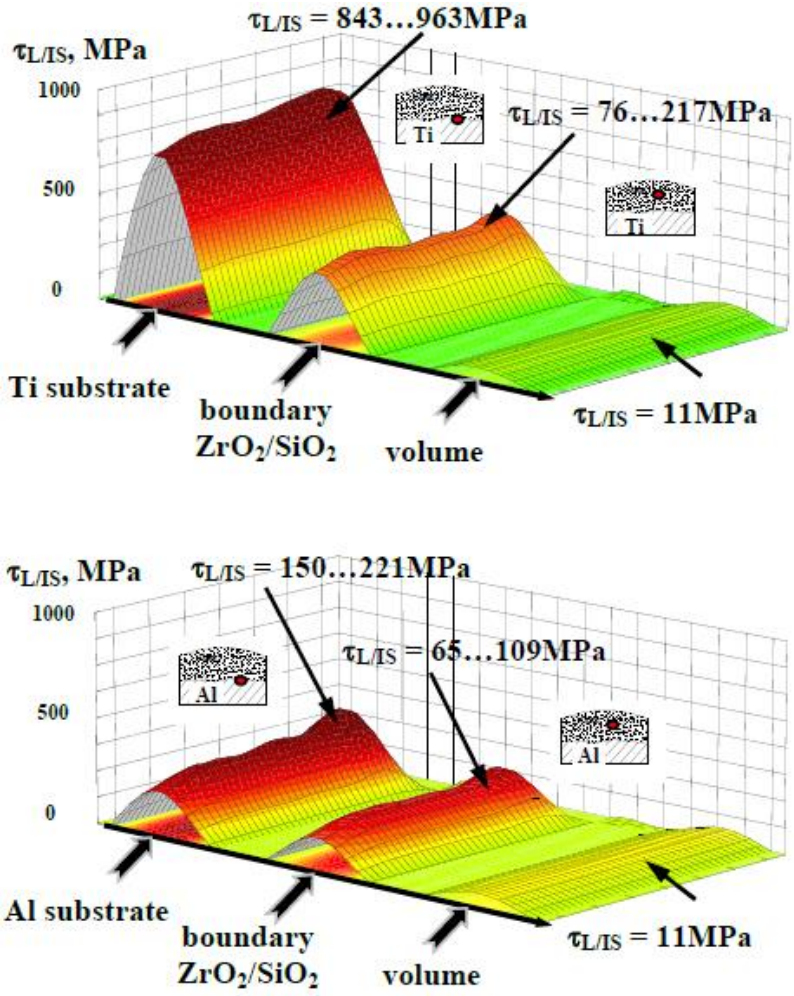

Figure 2 - Distribution of local inner stresses ($\tau_{L/IS}$) in the material of coatings and substrate: a – coating №1 (Ti substrate), b - coating №2 (Al substrate).

We have revealed that in all the investigated modes of cumulative-detonation spraying of coatings a low level of local inner stresses is observed (Figure 2). The maximum of local inner stresses are formed in the coating-substrate interface (coating No. 1, Figure 2, a.). Here their level does not exceed 963 MPa (or 0.22· from the theoretical level of material shear strength). It provides producing the high-quality coatings with high crack resistance.

As a result of comprehensive investigations of metal-ceramic coatings ($ZrSiO_4$), sprayed using multi-chamber detonation spraying at different structural levels (grain, subgrain, dislocation), it was revealed that the most significant contribution to the properties of strength and crack resistance of investigated coatings is made by: dispersion of grain and sub-grain structures; uniform distribution of the forming hardening phases of dispersed sizes in the absence of extended and dense dislocation clusters - potential areas of incipience of cracks.

REFERENCES

[1] A. L. Borisova and Yu. S. Borisov, Powder Metallurgy and Met. Cer., 47 (1-2), 2008, pp. 80-92.

[2] Gas Thermal Spraying of Composite Powders. Ya. Kulik, Yu. S. Borisov, A. S. Mnushin and M. D. Nikitin. Mashinostroenie, Leningrad, 1985, p.199.

[3] Plasma Powder Coatings. Yu. S. Borisov and A. L. Borisova. Kiev, Tekhnika, 1986, p.223.

[4] Detonation Coatings in Mechanical Engineering. S. S. Bartenev, Yu. P. Fedko and A. I. Grigorov. Mashinostroenie, Leningrad, 1982, p.214.

[5] Yu. Tyurin, A. Pogrebnjak and O. Kolisnichenko. PSE, 7, 2009, pp. 39.

[6] Yu. Tyurin, A. Pogrebnyak, O. Kolisnichenko, et al. The hardening technology, 5, 2009, pp. 27-33.

[7] L. Markashova, V. Poznyakov, E. Berdnikova, et al. Mater. Sci., 47, 2012, p. 799.

[8] L. Markashova, V. Poznyakov, E. Berdnikova, et al. The Paton Welding J., 6, 2014, pp.22-28.

[9] L. Markashova, A. Poklyatsky and O. Kushnaryova. The Paton Welding J., 6, 2016, pp.80-85.

[10] Structural Levels of Deformation of Solids. V. E. Panin, V. A. Likhachov and Yu. V.Griyatva. Nauka, Novosibirsk, 1985, p. 251.

[11] H. Conrad, Acta Metall., 11, 1963, pp. 75–77.

[12] A. N. Stroh, Proc. of the Roy. Soc. A. 223 (1154), 1954, pp. 404-415.

COMPREHENSIVE CHEMICAL AND STRUCTURAL CHARACTERIZATION OF COMPOSITE MATERIALS PRODUCED BY SHS WITH THE HELP OF MODERN MICROSCOPY TECHNIQUES

A. Berner[*1], G. Oniashvili[2], G. Tavadze[2] , Z.Aslamazashvili[2], G.Zakharov[2]

[1] Dept. of Materials Sci. & Eng., Technion – Israeli Institute of Technology, Technion City, Haifa 32000, Israel

[2] Ferdinand. Tavadze Institute of Metallurgy and Materials Science,10 E.Mindelistr,Tbilisi 0111, Georgia

* berner@technion.ac.il

Development of technology for producing new hard materials based on carbides-nitrides-borides composite ceramics is a subject of much current interest. Chemical and structural characterization of produced materials at macro- and micro-scale is very important for understanding processes of their formation and optimization of their mechanical properties. Phase composition of produced composite materials is studied as a rule by X-ray Diffraction Techniques (XRD), which make it possible to obtain a basic macro information on samples. Chemical characterization of such materials at micrometer scale is performed as a rule by a combination of Scanning Electron Microscopy (SEM) and Energy Dispersive Spectroscopy (EDS) techniques. EDS faces essential problems connected, first of all, to small sizes (micron and sub-micron) of structural constituents, which can be smaller than the characteristic size of X-ray excited volume. This leads to considerable inaccuracy in results of EDS. An additional problem decreasing accuracy of chemical analysis of such specimens is a presence of all light elements (B, C, N and O) together. At present, determination of light elements by EDS is not specified well even for cases when the analyst has not restrictions in sizes of analyzed particles. One more difficulty is a possible overlap of characteristic X-ray peaks of metals with peaks of light elements. The classic example is the known strong overlap of Ti Lα and N Kα characteristic peaks. Taking into account that carbon is most frequently contained in surface contaminations and presence of oxygen can be often explained by partial surface oxidation one can conclude that EDS analysis of such specimens is extremely difficult and ambiguous. In the present article, we will demonstrate a way to override the indicated difficulties with the help of combination of two analytical techniques in SEM, namely EDS and Electron Back Scatter Diffraction (EBSD).

The current study was carried out on two specimens produced by SHS. Specimens presented a Ti-B-N composite on different substrates. Powders of boron nitride and titanium were used as initial materials. The process flow included weighting and mixing initial powders with functional additives, mechanical milling and preliminary pressing followed by synthesis by SHS compacting proceeded in combustion mode. In the process of the synthesis, active atoms of nitrogen originated from decomposition of boron nitride are released and interact with melted titanium. As a result, formation of titanium borides and titanium nitrides took place. For microscopy study pieces of specimens were cut from the produced samples using a diamond wheel and mounted in an epoxy resin. They were then grounded on silicon carbide papers and polished with fine diamond suspensions. Finishing of sample preparation was done with 50 nm colloidal alumina.

XRD patterns measured from Ti-B-N side of the specimens showed the presence of the following phases: TiB phase (orthorhombic, space group 62), $TiN_{0.5}$ (or Ti_2N) phase (cubic,

space group 225), TiB_2 phase (hexagonal, space group 191) and a small amount of Ti(B) phase (hexagonal, space group 194). Typical SEM images in back scattered electrons (BSE) measured far from the interface (a) and close to the interface (b) are shown in Fig.1.

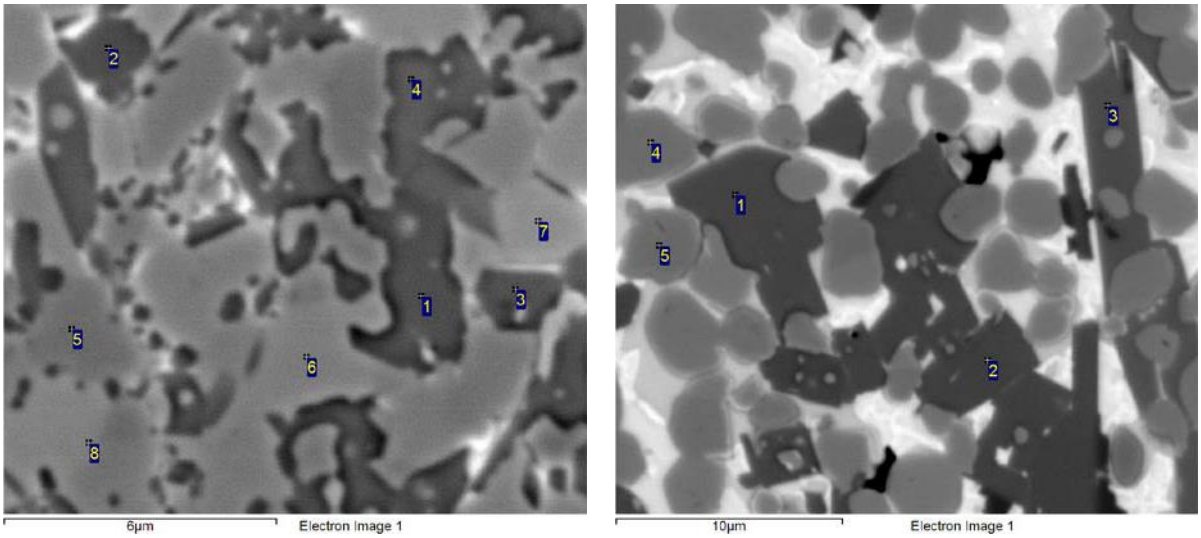

(a) (b)

Fig. 1 - BSE images measured from Ti-B-N side of the studied specimens: numbers indicate points where EDS spectra were collected from.

Analysis of EDS spectra collected from points marked by numbers in the images showed the following: compositions measured from points 1-4 in Fig.1 (a) correspond to that of TiB phase and measured from points 5-8 are close to that of Ti_2N phase (see, Table 1).

Table 1 - Results of EDS analysis in atomic percents of regions marked by numbers 1-8 in Fig. 1 (a)

Spectrum	B	Ti
1	55.9	44.1
2	57.3	42.7
3	53.1	46.9
4	55.3	44.7
Mean	55.4	44.6
Std. deviation	1.7	1.7

Spectrum	N	Ti
5	24.4	75.6
6	35.2	64.8
7	33.0	67.0
8	32.3	67.7
Mean	31.2	68.8
Std. deviation	4.7	4.7

Correspondingly, compositions measured from points 1-3 in Fig.1 (b) correspond to that of TiB_2 phase and measured from points 4-5 are close to that of Ti_2N phase. To confirm these results EBSD mapping was performed. EBSD diffraction patterns were collected from four different areas on the surface of the studied specimen with a typical step between map points 50-130 nm. It was found an excellent correlation between results of EDS and EBSD. Results of EBSD are summarized in Table 2. No preferred orientation for grains of revealed phases was found.

Table 2 - Phase distribution and grain size measured by EBSD

Site	Surface fraction, %			Mean grain size, μm
	$TiN_{0.5}$ (Ti_2N)	TiB	TiB_2	
1 (far from the interface)	62.9	23.3	13.8	1.4
2 (far from the interface)	75.1	13.5	11.3	1.8
3 (far from the interface)	67.8	19.0	13.2	2.0
4 (near the interface)	47.2	10.0	42.7	2.8

More representative information on the studied samples can be obtained by a combination of SEM, EDS, EBSD with layer-by-layer ion etching of surface layers followed by 3D-volume reconstruction. The region on the specimen surface selected for 3D reconstruction is shown in Fig.2 (a). Fig.2 (b) demonstrates a tilted view from the same region separated from the sample by ion etching before starting layer-by-layer etching. The ion etching was done with a step of 50 nm in depth. After removal of each 50 nm thick layer, SEM imaging and EDS mapping were carried out. 3D reconstruction of SEM images and element distributions was performed.

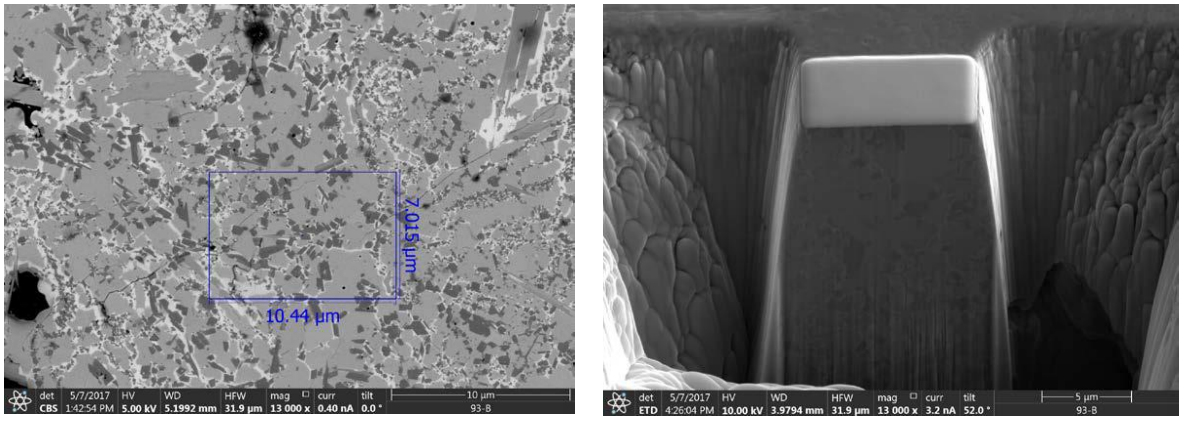

Fig. 2 - Region on the surface selected for 3D reconstruction (a) and the same region tilted at 52° and separated from the rest of the sample by ion etching (b)

THERMODYNAMIC MODELLING OF MAGNESIUM, STRONTIUM AND CALCIUM VIA VACUUM METALLOTHERMIC PROCESSES

M.Bugdayci*[1,2], K.C. Tasyurek[1], O.Yucel[1]

[1]Metallurgical and Materials Engineering Department, Faculty of Chemical and Metallurgical Engineering, Istanbul Technical University, 34469, Maslak, Istanbul, Turkey
[2]Chemical and Process Engineering Department, Faculty of Engineering, Yalova University, 77100, Yalova, Turkey
* mbugdayci@itu.edu.tr

In order to produce metallic Mg, Sr and Ca, vacuum metallothermic process is a valuable alternative method. For this process temperature, reductants and pressure conditions are very important parameters. This paper is a contribution to the theory and quantitative understanding of the processes for the production of Magnesium, Strontium and Calcium metals by metallothermic process. In the present study, effect of reductant type was investigated. Thermodynamic simulation of system were made by Fact Sage 6.4 program. Different reductants effects such as Si, FeSi, Al, CaC_2 were investigated on the understanding production conditions of Magnesium metal from calcined magnesite and calcined dolomite minimum reduction temperatures and probable products were determined via Fact Sage. Products predictions calculated for different atmospheric conditions. Figure1. presents MgO reduction conditons for different reductants.

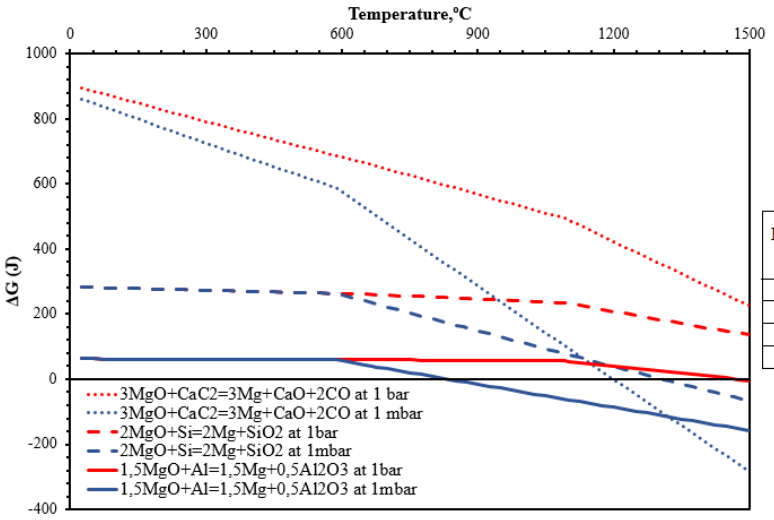

Reductant Type	Minimum Reduction Temperature, °C			
	MgO		Calcined Dolomite	
	1 bar	1 mbar	1 bar	1 mbar
Si	2143	1325	2489	1318
Al	1475	850	1427	842
FeSi	1789	1155	1870	1098
CaC_2	1847	1200	1828	1191

Figure1- The change of gibbs free energies for the reactions between MgO and Si-CaC2-Al under 1 bar and 1 mbar reaction pressures

In the second simulation set, aluminothermic SrO reduction was invastigated. In this stage Al used as main reductant and effect of functional additives such as BaO and CaO were exemined for different temperatures and vacuum conditions. Finally reduction temperatures and probable phases are determined. Figure 2. Shows SrO reduction conditions for different reductants.

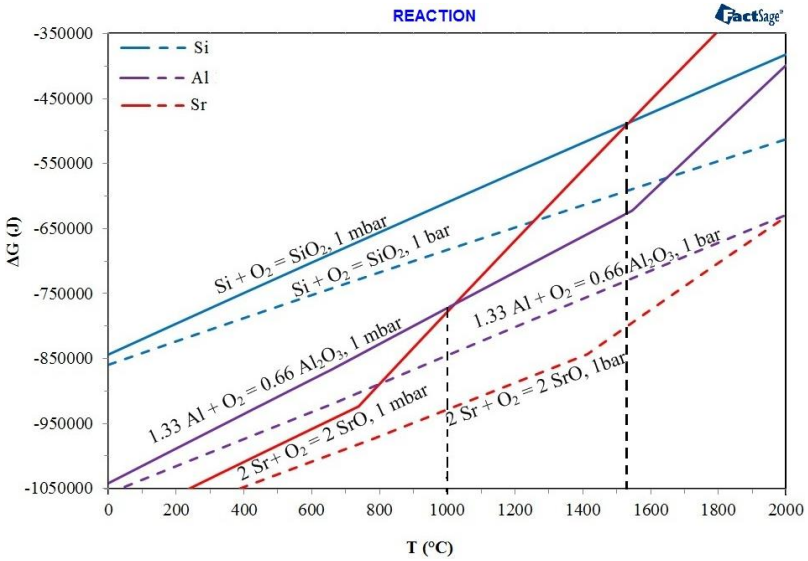

Figure 2 - SrO reduction with Si and Al

In the final prediction set, aluminothermic CaO reduction was invastigated via Factsage 6.4 soft ware. In this process also minimum reduction temperatures and probable products were determined by Fact Sage 6.4 database. Figure 3. presents probable phases of CaO reductions.

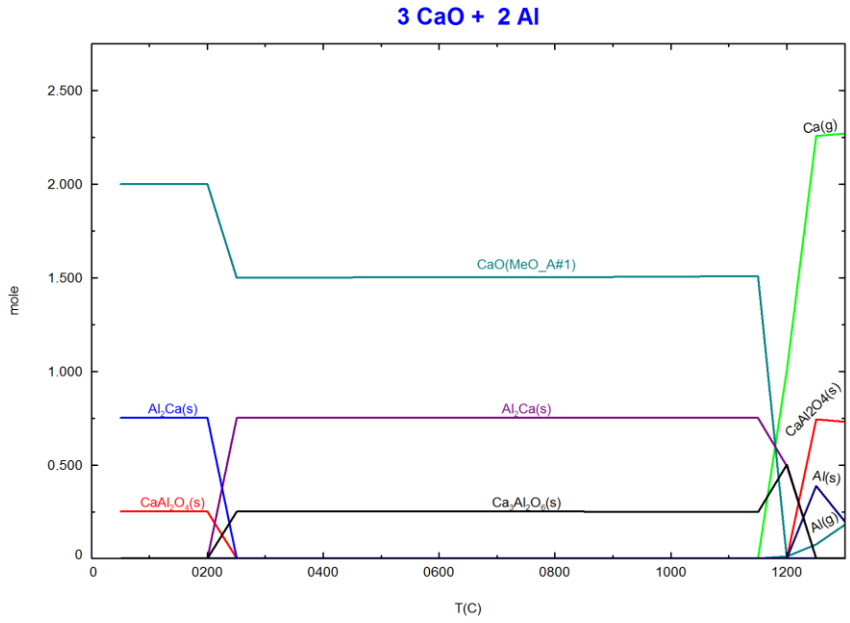

Figure 2.CaO reduction with Al

REFERENCES

[1] M. Bugdayci, A. Turan, M.Alkan and O. Yucel, High Temp. Mater. Proc., 37(1) (2017) 185–193.

[2] Fact Sage 6.4 database.

SYNTHESIS AND ADIABATIC EXPLOSIVE COMPACTION OF Ti-Al-B-C POWDERS

M. Chikhradze*[1,3], G.Oniashvili[2], G.Tavadze[2], G.Mikaberidze[2], F.D.S Marquis[3]

[1]F. Tavadze Institute of Metallurgy and Materials Science,10 E.Mindelistr,Tbilisi 0111, Georgia
[2] San Diego State University, 5500 Campanile Drive San Diego, CA 92182-8010,USA
[3] Georgian Technical University, 75 Kostava Str., Tbilisi 0175, Georgia
* cmike@ymail.com

ABSTRACT

Recent developments of modern materials science has increased the interest towards the bulk (energetic/energy) materials and the technologies for their production. The unique properties which are typical for the composites fabricated in Ti-Al-B-C systems makes them attractive for aerospace, power engineering, machine and chemical and other practical applications. Besides, Aluminum matrix composites (AMCs) have great potential as structural materials again due to their excellent physical, mechanical and tribological properties [1-4]. Because of good combination of thermal conductivity and dimensional stability AMCs are found to be potential materials for electronic packaging/application. The methodology and technology for the fabrication of bulk materials from ultrafine grained powders of Ti-Al-B-C system are described in this abstract. It includes preliminary results of theoretical and experimental investigation for selection of powder compositions and determination of thermodynamic conditions for blend preparation, as well as optimal technological parameters for mechanical alloying and adiabatic compaction.

According to the phase diagrams in binary and ternary system the composites/intermetallics may be obtained with wide spectrum of phase composition, in crystalline and amorphous (brittle and ductile) structures. Depending on the composition and structure, the synthesized composites may have different specific properties. The potential of the system for development of new structural/composite materials in different thermodynamic conditions is very attractive.
Fine grained composite materials of Ti-Al-B-C system, prepared in the form of micromechanical blends, solid solutions and intermetallic compounds are of great practical interest because of improved mechanical properties in comparison with coarse grain material (>1 μm) [5-6].

The crystalline coarse Ti, Al, C powders and amorphous B were used as precursors, and blends with different compositions of Ti-Al-B-C and Ti-Al-C were prepared. Preliminary determinations/selections of blend compositions were made on the basis of phase diagrams.

Precursors were classified by vibratory sieves within the particle size ranges: (-0,063, + 0) mm; (-0.16, + 0.063) mm; (-0.315, + 0.16) mm; and +0.315mm. The powders were weighed and mixed to produce the blend.

The powders were mixed according the selected ratios of components to produce the blend.

For Mechanical alloying (MA) the high energetic “Fritsch” Planetary premium line ball mill was used. The mill was equipped with Zirconium Oxide jars and balls. Ratio ball to powder by mass was 5:1. The time of the processing was varied from 1 to 5 hours. Rotation speed of the jars were 500 rpm. The SEM picture of the 3Ti/2Al/1C blends obtained upon MA in Ball mill are shown in Fig. 1.

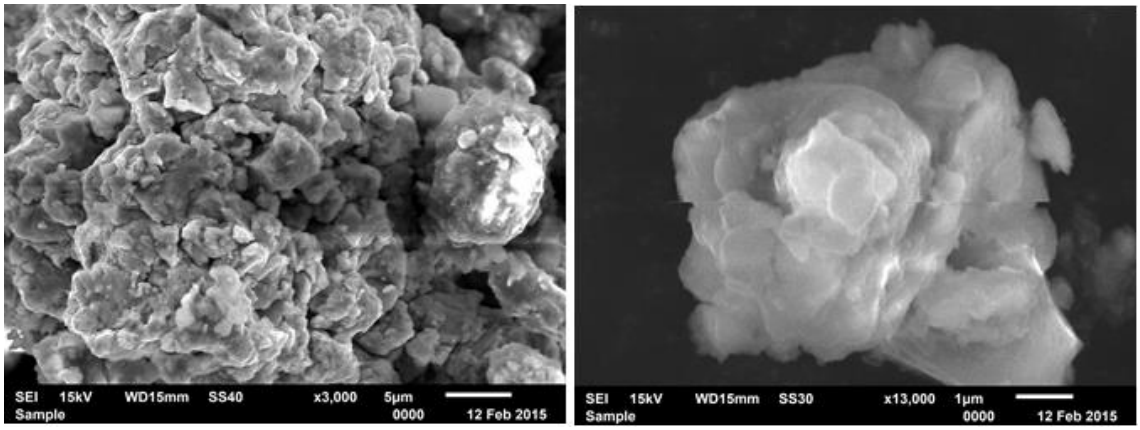

Fig. 1 - SEM picture of the Ti-Al-C blend. Processing time - 5 hours

The optimal technological regimes of blend preparation were determined experimentally.

Consolidation of the samples was performed in two stages. The powder blend was loaded in the carbon steel tube container and at the first stage the pre-densification of the mixtures was performed under static press loading (intensity of loading P=500-1000 kg/cm^2). Cylindrical container/tube was closed from the both sides.

A card box was filled with the powdered explosive and placed around the cylindrical powder container. The experiments were performed at room temperature. The shock wave pressure was varied in the range of 3-20 GPa. The explosive was detonated by electrical detonator. The explosive compaction schemes are shown in (Fig. 2).

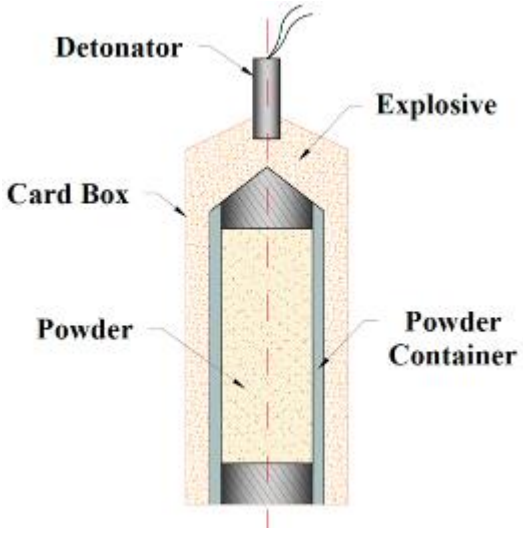

Fig. 2 - Scheme of explosive compaction setups

The motivation was derived from preliminary works showing that the explosive consolidation (EC) of metal-ceramic compositions is not only feasible but can produce materials of almost theoretical densities [7-8]. It was clear that the preliminary ball milling (due to fragmentation, mechanical alloying and critical reduction of particles sizes) should significantly increase the sintering ability of the blend and improve the compacting process and mechanical alloying of selected powder compositions. The major advantages of EC for bulk nanomaterials production

are realization of high pressure, short processing time, and super high cooling rate (adiabatic cooling).

The bulk compacts were recovered in different shapes and prepared for investigations. The density of specimens was determined (cut from different part of samples) by the Archimedean method. The microstructure was studied by SEM. As a result :

- The effective technology/regimes for obtaining nanopowders and nanocomposites in Ti-Al-B-C composition has been elaborated;
- Rational technology for fabrication of bulk amorphous and nanostructured materials by shock wave induced syntheses has been selected.

.**REFERENCES**

[1] Mania, M. Dabrowski et all, Some application of TiAl Micropowders Produced by Self-Propagating High Temperature syntheses, International Journal of Self-Propagating High-Temperature Synthesis. 2003 vol. 12 no. 3 s. 159–164.

[2] E. A. Levashov, B. R. Senatulin et all, Peculiarities of the Functionally Graded Targets in Combustion Wave of the SHS-System with Working Layer Ti-Si-B, Ti-Si-C, Ti-B-N, Ti-Al-B, Ti-C, Book of Abstracts. IV Int. Symposium on SHS, Technion, Haifa, Israel, Feb. 17-21, 2002, p. 35.

[3] A.G.Merzhanov, A.N.Pityulin. Self-Propagating High-Temperature Synthesis in Production of Functionally Graded Materials. Proceedings of 3 rd Int. Symp. on FGM, Lausanne, Switzerland, pp.87-94 (1995).

[4] A.N.Pityulin, A.E.Sytschev, A.S.Rogachev, A.G.Merzhanov. One-Stage Production of Functionally Graded Materials of the Metal-Hard Alloy Type by SHS Compaction. Proceedings of 3 rd Int. Simp. on FGM, Lausanne, Switzerland, pp. 101-108 (1995).

[5] Z. H. Zhang, B. Q. Han, Syntheses of Nanocrystalline Aluminum Matrix Composites Reinforced With in Situ Devitrified Al-Ni-La Amorphous Particles, University of California Postprints, Paper 39, 2006.

[6] J. Hebeisen, P. Tylus, D. Zick, D. K. Mukhopadhyay, K. Brand, C. Suryanarayana, F. H. Froes, "Hot Isostatic Pressing of Nanostructured γ-TiAl Powders", Metals and Materials, Vol. 2. No. 2 (1996) pp. 71-74.

[7] L.J.Kecskes, R.H.Woodman, N. Chikhradze A.Peikrishvili Processing of Aluminum Nickelides by Hot Explosive Consolidation, International Journal of Self-Propagating High-Temperature Synthesis Volume 13, #1, 2004.

[8] N. Chikhradze, K. Staudhammer, F. Marquis, M. Chikhradze, Explosive Compaction of Me-Boron Containing Composite Powders, Proceeding of Powder Metallurgy World Congress & Exhibition, PM2005, Prague, Czech Republic, V.3, pp. 163-173, 2005.

EFFECT OF ADDITION OF EXCESS SILICON ON SHS SYNTHESIS OF Ti_3SiC_2 MAX PHASES POWDERS

L. Chlubny[1], J. Lis[1], P. Borowiak[1], K. Chabior[1], K. Kozak[1], A. Misztal[1]

[1] AGH-University of Science and Technology, Faculty of Materials Science and Ceramics, Department of Ceramics and Refractories , al.Mickiewicza 30, 30-059, Krakow, Poland
*leszek@agh.edu.pl

In the Ti-Si-C system, among materials such as carbides or intermetallics, exists group of interesting ternary and quaternary materials called MAX-phases, H-phases, Hägg-phases, Novotny-phases or thermodynamically stable nanolaminates. These materials are characterised by heterodesmic layer structure and have a $M_{n+1}AX_n$ stoichiometry, where M is an early transition metal, A is an element of A groups (mostly IIIA or IVA) and X is carbon and/or nitrogen. Their specific structure consisting of covalent and metallic chemical bonds strongly influence their semi-ductile features locating them on the boundary between metals and ceramics [1, 2, 3]. This fact may lead to many potential applications, for example as a part of ceramic armour.

The Self-propagating High-temperature Synthesis (SHS) with local ignition system was applied for obtaining active precursors powders of Ti_3SiC_2. Basing on the previous researches on synthesis MAX phase materials in Ti-Al-C-N system it is known that stoichiometry and amount of excess reactant plays crucial role during the synthesis and may influence the final phase composition of final product [4, 5, 7, 8]. The reactions were conducted in argon atmosphere according to the reaction:

$$3Ti + Si_{1+x} + 2C \rightarrow Ti_3SiC_2 \quad (1)$$

where x varies from 0.1 to 1.

The XRD analysis method was used to determine influence of excess aluminium on phase composition of the synthesised materials. The basis of quantitative and qualitative phase analysis were data from ICCD. Amounts of the respective phases were calculated by the Rietveld analysis [9]. Observations of the powders morphology were done by FEI Europe Company Nova Nano SEM 200 scanning electron microscope. The example of the best results of the synthesis where x was equal 0.8 is presented on Figure 1.

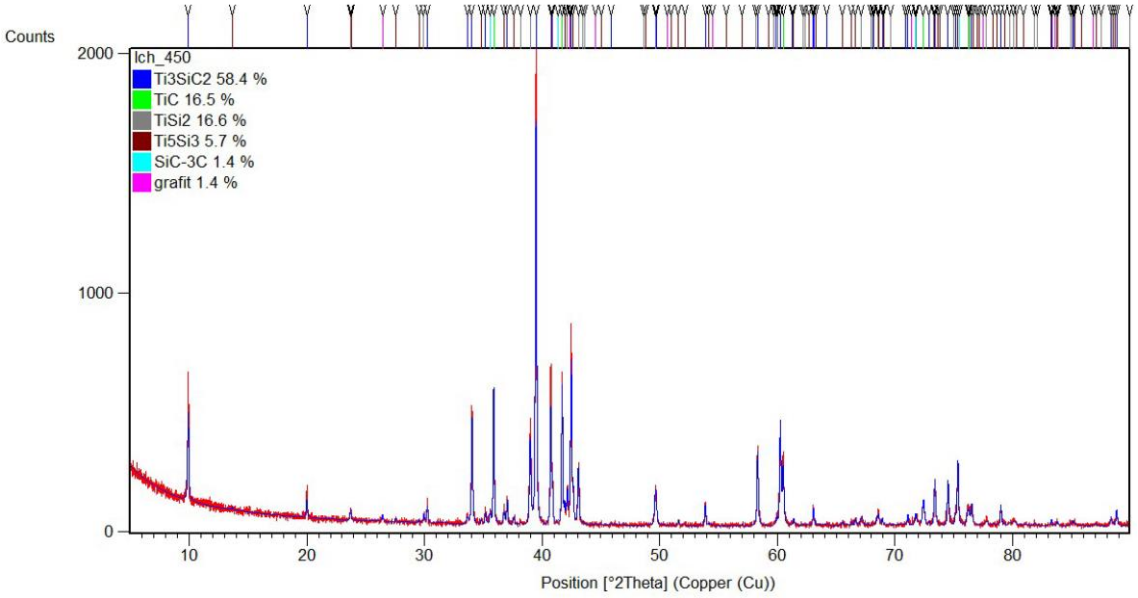

Fig.1 - The XRD pattern of synthesized Ti3SiC2 powder with 80% of excess Si

The SHS synthesis seems to be effective method for manufacturing of sinterable powders of Ti_3SiC_2 MAX phases materials. It was proved that the excess amount of silicon during SHS process has important role in formation of ternary phase in the final product. The best powders were destined for further pressureless sintering and hot pressing process in order to manufacture dense, single phase polycrystalline materials.

REFERENCES

[1] M.W. Barsoum, Prog Solid St. Chem., 28, (2000), 201-281.

[2] M.W. Barsoum "MAX Phases: Properties of Machinable Ternary Carbides and Nitrides", Wiley, 2013.

[3] M. Radovic, M.W. Barsoum, Am. Cer. Soc. Bull., 92 [3], (2013), 20-27.

[4] J. Lis, R. Pampuch, L. Stobierski, Int. J. Self-Propag. High-Temp. Synth., 1, , 401 (1992).

[5] L. Chlubny, M.M. Bucko, J. Lis, Adv. Sci. Tech., 45, (2006), p 1047-1051.

[6] L. Chlubny, J. Lis, M.M. Bućko, Ceram. Eng. Sci. Proc., Vol.34, 10, (2013), 265-271.

[7] L. Chlubny, J. Lis , Ceram. Trans., Vol. 240, (2013), 79-86.

[8] L. Chlubny, J. Lis, M.M. Bucko: Influence of Nitrogen Pressure on SHS Synthesis of Ti_2AlN Powders, Developments in Strategic Ceramic Materials, (2015), 251-260.

[9] H. M. Rietveld: J. Appl. Cryst. 2 (1969) p. 65-71.

COMBUSTION SYNTHESIS OF h-BN AND ITS APPLICATIONS IN HIGH THERMAL CONDUCTIVITY POLYMER COMPOSITES

Shyan-Lung Chung [1,2,*] and Jeng-Shung Lin [2]

[1] Advanced Optoelectronic Technology Center, National Cheng Kung University, Tainan 70101, Taiwan
[2] Department of Chemical Engineering, National Cheng Kung University, Tainan 70101, Taiwan;
* slchung@mail.ncku.edu.tw

Hexagonal boron nitride (h-BN) possesses many desirable properties such as high thermal conductivity, high electrical resistivity, chemical and thermal stability and excellent lubrication. Recently, we have developed a combustion synthesis method for the synthesis of h-BN powder, which is characterized by low energy consumption, fast reactions, simple processing and low production cost. One of the interesting applications of h-BN is the manufacturing of high thermal conductivity polymer (e.g. epoxy resin) composites where h-BN is used as a filler. In this application, the interface between h-BN particles and epoxy resin presents a major thermal barrier in the heat conduction of composites. Different synthesis methods may produce h-BN particles with different surface properties, affecting the thermal conduction resistance and thus resulting in different thermal conductivity. Besides, a h-BN powder with a low production cost can significantly boost the practical applications of h-BN/epoxy resin composite materials. We therefore investigate in this work the thermal conductivity of epoxy resin composites filled with h-BN powders synthesized by our newly developed combustion synthesis method. The mixing of the composite constituents was carried out by either a dry method (involving no use of solvent) for low filler loadings or a solvent method (using acetone as solvent) for higher filler loadings. It was found that surface treatment of the h-BN particles using the silane 3-glycidoxypropyltrimethoxysilane (GPTMS) increases the thermal conductivity of the resultant composites in a lesser amount compared to the values reported by other studies. This was explained by the fact that the combustion synthesized h-BN particles contain less –OH or active sites on the surface, thus adsorbing less amounts of GPTMS. However, the thermal conductivity of the composites filled with the combustion synthesized h-BN was found to be comparable to that with commercially available h-BN reported in other studies. The thermal conductivity of the composites was found to be higher when larger h-BN particles were used. The thermal conductivity was also found to increase with increasing filler content to a maximum and then begin to decrease with further increases in this content. In addition to the effect of higher porosity at higher filler contents, more horizontally oriented h-BN particles formed at higher filler loadings (perhaps due to pressing during formation of the composites) were suggested to be a factor causing this decrease of the thermal conductivity. The measured thermal conductivities were compared to theoretical predictions based on the Nielsen and Lewis theory. The theoretical predictions were found to be lower than the experimental values at low filler contents (< 60 vol %) and became increasing higher than the experimental values at high filler contents (> 60 vol %).

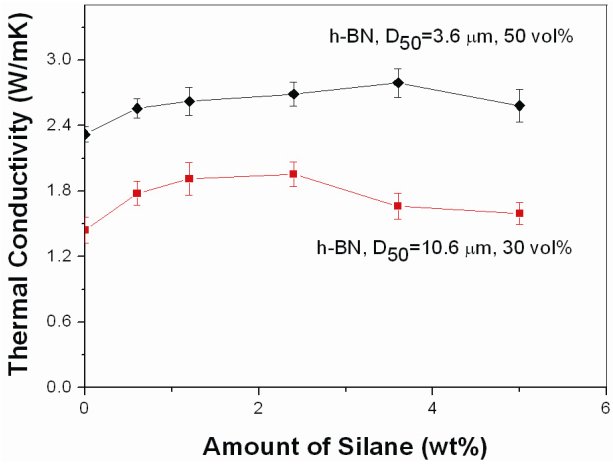

Figure 1 - Effect of the amount of GPTMS used in surface treatment of h-BN on the thermal conductivity of the composites.

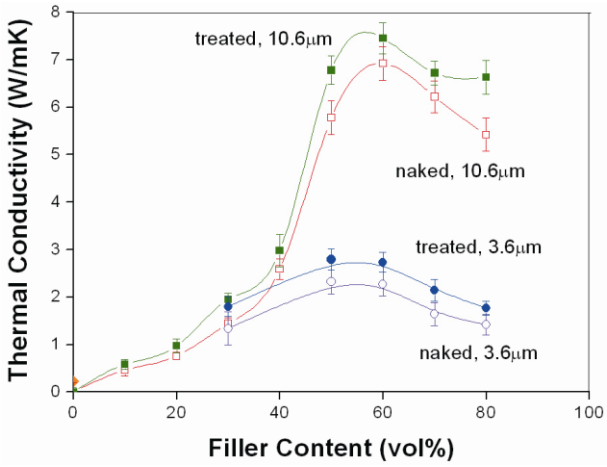

Figure 2 - Effects of surface treatment, h-BN particle size and filler content on thermal conductivity of composites.

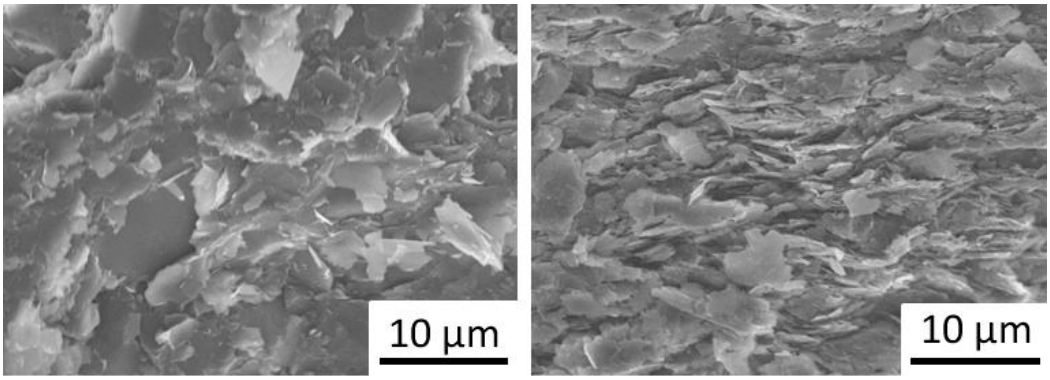

Figure 3 - SEM photographs of the fractured surfaces of the composites with filler contents of (a) 50 vol % and (b) 70 vol % (both composites were filled with 3.6 μm h-BN particles with 3.6 wt% GPTMS treatment).

REFERENCES

[1] S.Y. Wu,; Y.L. Huang,; C.C.M. Ma,; S.M. Yuen,; C.C. Teng and S.Y. Yang, Comps. Part A 42, 2011, pp. 1573–1583.

[2] Y. Nagai and G.C. Lai, J. Ceram. Soc. Jpn. 105, 1997, pp. 197–200.

[3] K. Hirao,; K. Watari,; H. Hayashi and M. Kitayama, MRS Bull. 26, 2001, pp. 451–455.

[4] G.H. Hsiue,; W.J. Wang and F.C. Chang, J. Appl. Polym. Sci. 73, 1997, pp. 1231–1238.

[5] S.V. Levchik and E.D. Weil, Polym. Int. 53, 2004, pp. 1901–1929.

EFFECT OF ALUMINUM NANOPOWDERS ELECTRON BEAM IRRADIATION ON SHS WITHIN THE SILICON OXIDE - ALUMINUM SYSTEM

E.E. Dilmukhambetov *[1], V.N. Yermolaev[1], S.M. Fomenko[2], Z.T. Turganov[2]

[1]Kazakh National Agrarian University, 8 Abay ave., Almaty Kazakhstan
[2] The Institute of Combustion Problems, Almaty, 172 Bogenbai Batyr Str., Kazakhstan
*esen.dil@yandex.ru

Currently application of metal nanopowders as an active additive at manufacturing of new materials is considered to be a perspective trend in the composite materials technology. Application of metal nanopowders can promote decrease of the synthesis process initiation temperature, intensification of the solid-phase combustion, and homogeneous distribution of products in the final material [1].

Preliminary activation of initial powders is a necessary technological operation during production of numerous metal-composite and metal-oxide materials. In this respect, the metals nanopowders subject to the electron beam irradiation are thought to be promising for the production of new composite and refractory materials. At present there are available only indirect data testifying to the irradiation effect on the nanopowders accompanied by the thermal effects caused by their higher chemical activity, however macrokinetic peculiarities of the solid-phase combustion with participation of the irradiation activated nanopowders are not known yet [2].

The purpose of the study is to identify effects of the aluminum nanopowders electron beam irradiation on the temperature and rate characteristics of the aluminathermal silicon oxide combustion in the SHS regime.

Aluminum nanopowders with the particle size 90-110 nm and industrial aluminum powder with the particle size not less than 60 μm have been used as a reducing agent. The nanopowder contents ranged from 0 up to 10 % mass so that the general aluminum contents remains constant and corresponds to stoichiometry of complete silicon oxide reduction.

Combustion temperatures in the SHS regime have been determined using a Raitek 3I infra-red radiation pyrometer. The combustion wave velocity has been measured using the thermocouple technique by means of the digital signal processing device connected to the PC.

To carry out the SHS process, samples have been fabricated in the form of 4 cm high and 2 cm diameter pressed cylinders.

The electron beam irradiation of the metal powders has been carried out using the linear electron accelerator ELU-6 of the al-Farabi Kazakh National University.

Radiographic measurements have been carried out using x-ray diffractometer X'Petro PRO with a CuK_{α} copper source. Accuracy of calculating the interplane distances in crystal substances equals 0.001Å.

Picture 1 demonstrates the roentgenogram of the aluminum nanopowder subject to 10 Mrad electron beam irradiation.

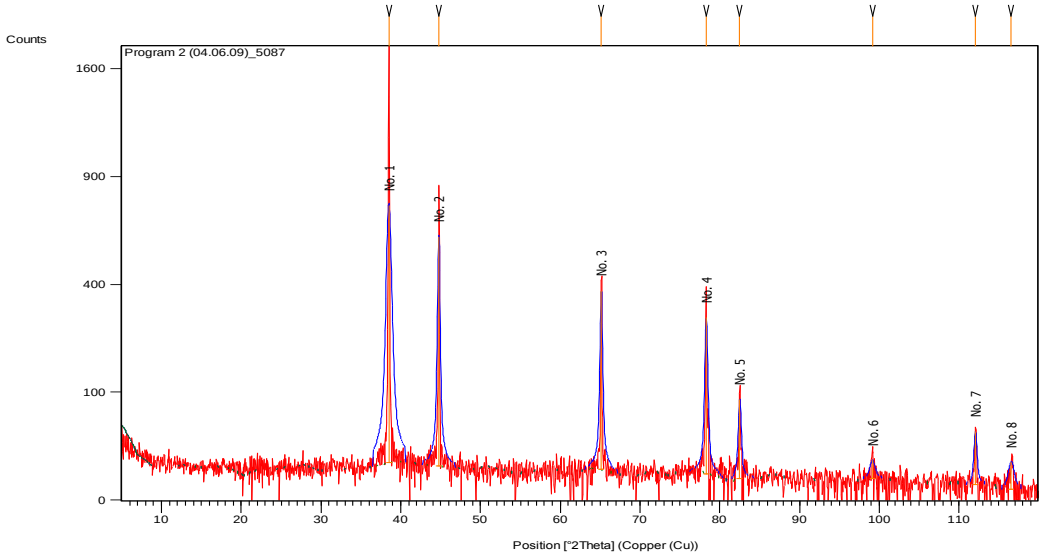

Picture 1 - Roentgenogram of the aluminum nanopowder following its 10 Mrad irradiation

Decoding of the aluminum nanopowder roentgenograms at various electron beam irradiation doses is given in Table 1 along with the reference interplane distances [3].

Table 1 - Interplane distances in Al nanopowders

No	(n k l)	d, A°[3]	Irradiation dosage, Mrad			
			0	5	10	15
1	(1 1 1)	2.336	2.336	2.336	2.33	2.334
2	(2 0 0)	2.023	2.022	2.023	2.023	2.216
3	(2 2 0)	1.430	1.430	1.431	1.431	1.430
4	(3 1 1)	1.219	1.220	1.220	1.22	1.23
5	(2 2 2)	1.168	1.168	1.168	1.168	1.168
6	(4 0 0)	1.011	-	1.013	1.012	1.012
7	(3 3 1)	0.928	-	0.929	0.929	0.928
8	(4 2 0)	0.904	0.905	0.906	0.906	0.907

These results specify that electron beam irradiation of aluminum nanopowders leads to some increase of certain interplane distances. This is well manifested in (4 2 0) and (3 1 1) planes. The key physical effect of the electron beam irradiation with up to 2 MeV energy on solid bodies consists of atoms ionization without radical change in their lattice position. In this case electrostatic pushing off of the ionized atoms leading to nonequilibrium interatomic and interplane distances increases in the metal lattice.

Picture 2 shows the effect of the aluminum nanopowder irradiation on the combustion rate and temperature at stoichiometric correlation between aluminum and silicon oxide.

The effect of the irradiation dosage on the combustion temperature is noticeably manifested even at insignificant contents of aluminum nanopowder (2 % mass), i.e. the higher is the dose, the higher is the combustion temperature.

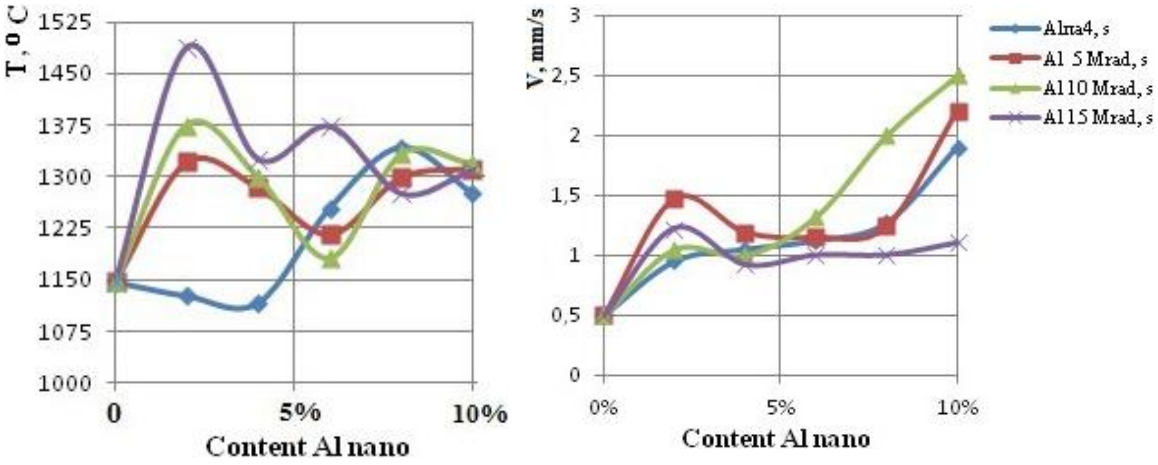

Picture 2 - Silicon oxide combustion temperatures and rates in the presence of irradiated aluminum nanopowder

At the nanopowder contents 8-10 % mass, combustion temperatures demonstrate their slight dependence on the irradiation dosage and stay around 1300^0C. At the same time combustion rates demonstrate weak dependence both on the temperature and the irradiation dosage within 2-8 % mass of the nanopowder content. Absence of any correlation between temperature and combustion rates testifies to complex nature of chemical processes occurring in the combustion wave. One can assume that the basic chemical reactions of silicon oxide reduction take place in a liquid phase of the aluminum melt with low activation energies thus leading to independence of a combustion rate on the temperature.

Therefore, obtained study results allow for the following conclusions:

- radiation treatment of aluminum nanopowders leads to appreciable change in the interplane distances, in particular (3 1 1) and (4 2 0);

- irradiated aluminum nanopowder as an additive to the exothermal aluminum-silicon oxide system effectively initiates the SHS process and increases the temperature and velocity characteristics.

REFERENCES

[1] A.V. Sychev, A.G. Merzhanov Self-Propagating High-Temperature Synthesis of Nanomaterials. Chemistry Achievements, 2004. Vol.73, No 2, pages 157-170;

[2] Sh. Xu Bing, T. Shunichiro, Behavior and Bonding Mechanisms of Aluminum Nanoparticles by Electron Beam Irradiation. Nanostructured Materials. 1999 Vol.12, pages 915-918;

[3] Chemical Database Service CrystMet http://cds. dl.ac.uk ./cds /datasets/ crys/ mdf/llmdf.html

SUPERCONDUCTING CHARACTERISTICS OF SWCNT DOPED MgB_2 OBTAINED BY COMBUSTION SYNTHESIS

S. Tolendiuly*[1], S.M. Fomenko[2], Ch. Dannangoda[3], Z.A. Mansurov[2], K.S. Martirosyan[3]

[1] Al-Farabi Kazakh National University, 71 al-Farabi Ave., 050040,Almaty, Republic of Kazakhstan
[2]Insitute of Combustion Problems, 172 Bogenbay Batyr str., 480012,Almaty, Republic of Kazakhstan
[3]Department of Physics, University of Texas Rio Grande Valley, Brownsville, TX 78520, USA
* sanat_tolendiuly@mail.ru

The highest critical transition temperature (Tc) among all the intermetallic superconductorswas discovered for MgB_2that has changed the previous approaches to the theory of superconductivity because the Tc limits in metallic superconductors had been believed to be ~ 30 K, which is predicted by the Bardeen-Cooper-Schrieffer (BCS) theory [1]. Magnesium diboride MgB_2 BCS-type superconductors (SCs) are widely used in sensors, electric power applications and electronic devices. In fact, their critical temperature is ~39 K,$T_c$is lower than in traditional cuprate SCs, their upper critical field H_{2c} is actually higher while an operating temperature of ~30 K is relatively easy to reach using liquid hydrogen or cryocoolers. The absence of weak links in the matrix (no intergranular obstacles impede current flow) as well as a strong coupling between grains makes MgB_2 very useful in technological applications [2].The possible enhancement of the critical temperature and the improvement of the existing high levels of transport current are important research area for development of this material. On the other hand, the low density of the pure compound and the relative scarcity of pinning centers, actually reduce the sustainable current density in high magnetic fields. The metal-like structure of MgB_2 at room temperature makes it ideal for applications in engineering contexts unlike the cuprate SCs, which exhibits a non-metallic behavior at room temperature. The latter fact limits the technological applications of cuprate due to difficulties associatedwith the material processing [3].

In order to increase the values of the two parameters T_c and J_c, the introduction of controlled amounts of doping agents is an interesting procedure: in past experiments, the critical superconducting field was observed to rise but the critical temperature remained idle [4].An increase of T_c induced by doping MgB_2 was only reported in the high field case of nano-C doped MgB_2. Conversely, it was found that the critical current could be increased through doping.Different types of pinning centers can be introduced, e.g. grain boundaries, point defects as well as impurities and lattice variations brought on by doping. In order to make the formation of pinning centers effective to increase Jc, they should exhibit sizes as large as the coherence length that in the MgB_2 it is valued in the range of 2 - 10 nm [5].Since grain boundaries also act as pinning centers, the decreasing grain dimensions improve the critical current.Beside the pinning centers, the densification of the compound in general enhances the superconducting state. For MgB_2 in particular, good results in J_c enhancement have been obtained by the use of doping agents. Different elements have been used so far, spanning from rare-earths to magnetic elements as well as silicon [6 - 8]. The best results are obtained when carbon substitutes boron. Carbon is an electron donor that can influence the Fermi surface of the MgB_2 lattice. The result is a significant enhancement of H_{2c} and J_c through enhanced interabang scattering [4].

This paper describes the study of the superconducting parameters of magnesium diboride doped with SWCNT, acting as an electron donor. In particular, scope of this work is to clarify the

influence of SWCNT doping agent on the critical current density Jc. Solid state reaction technique has been used to obtain consolidated MgB_2 bulk samples. The samples were prepared as follow, magnesium (100-200 μm), boron (1-5 μm) powders and SWCNT (1.1 nm in diameter and 20-30 nm in length) in the composition Mg + 2B+ X_{SWCNT} = MgB_2+ X_{SWCNT}(where, X=0.3 wt. %, 0.5 wt. %, 0.7 wt. %, 1 wt. %, 5 wt. %,), have been ignited under argon at 2.5 MPa in High Pressure Chamber (HPC) in Figure 1.

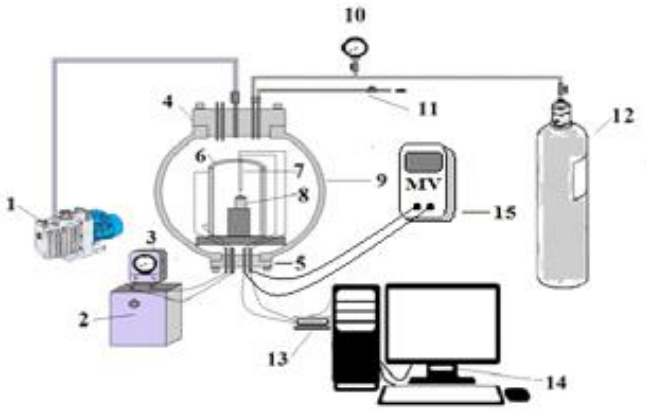

Figure 1 - Schematic diagram of the high-pressure chamber: (1 - vacuum pump, 2 - transformer 3 - ammeter, 4 - the top cover of the reactor, 5 - the bottom cover of the reactor, 6 - tubular heating furnace 7 - thermocouple 8 - sample 9 - the case of the reactor, 10 - gauge 11 - intake and exhaust valves, 12 - nitrogen cylinder 13 - the data acquisition system LTR-U-1, 14 - computer 15 - multimeter).

Self-sustainable combustion was initiated at temperature T = 600 – 650°C. After combustion the samples were structurally characterized by X-ray diffraction (XRD) using Dron– 4 diffractometer (operating with a Cu-Kα radiation source). The AC magnetic measurements were carried out on a Physical Property Measurement System (Quantum Design, USA). Complex magnetic susceptibility data were collected as a function of temperature by applying a static field (varying from 1.5 to 9.0T).X-ray patterns recorded for the SWCNT doped samples are reported in Table1.

Table 1 - The results of XRD for system Mg-2B-SWCNT

Mixture	The results of XRD, wt. %			
	MgB_2	MgB_4	MgO	Mg
Undoped MgB_2	94.2	-	5.8	-
MgB_2 + 0.3 wt%SWCNT	90.8	3.7	4.6	0.9
MgB_2 + 0.5 wt% SWCNT	94.9	1.2	3.4	0.5
MgB_2 + 0.7 wt% SWCNT	93.4	2.2	3.9	0.6
MgB_2 + 1 wt% SWCNT	94.7	1.6	3.3	0.4
MgB_2 + 5 wt% SWCNT	90.5	3.6	5.9	-

XRD patterns show all the peaks inherent (Table - 1) to MgB_2 in all samples. Some MgO,MgB_4impurity phases were detected by the XRD analysis. There was some unreacted metallic magnesium. The presence of SWCNT in samples was observed by Raman spectroscopy in Figure 2. According to this analysis, SWCNT was presented in amorphous

form, which matches peak 1560 cm^{-1} (good related with literature data [9]). That is why XRD analysis did not observe them.

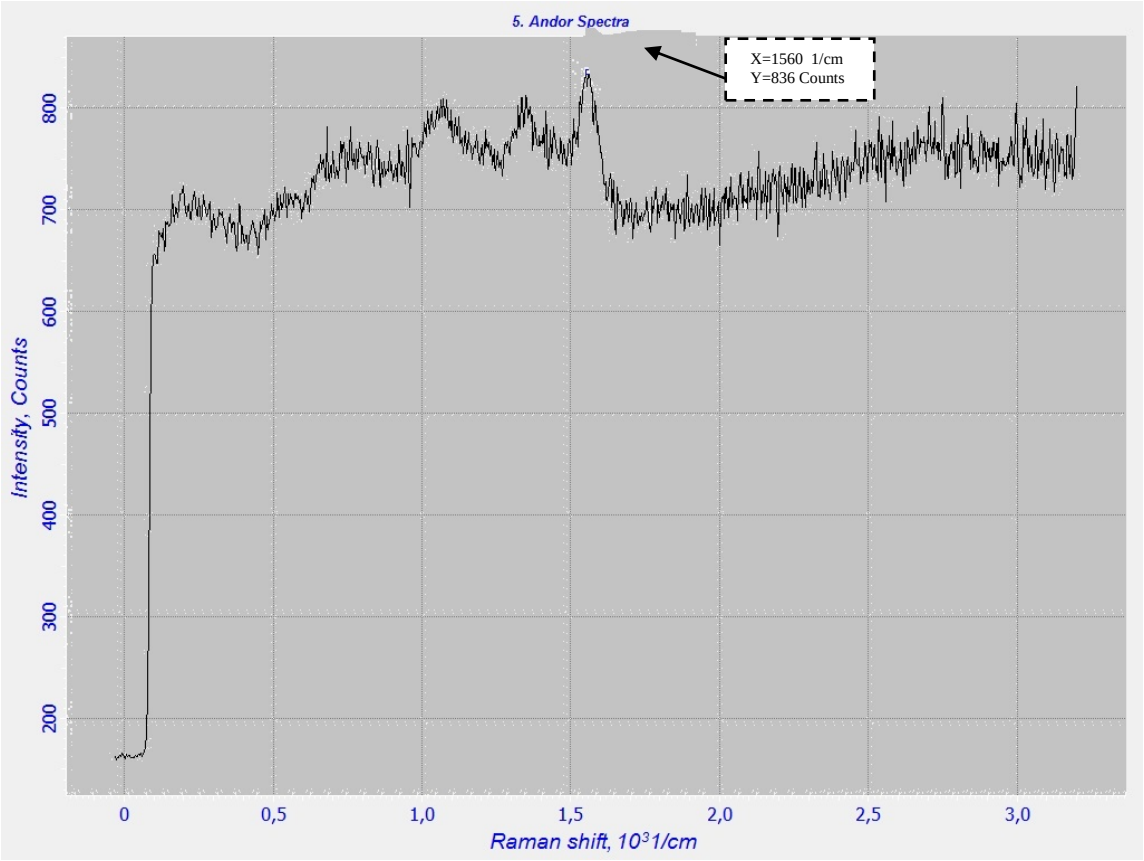

Figure 2 - Raman spectrum of sample with SWCNT

As a result of measurements of the temperature dependences of the magnetic moment of the system Mg-2B-SWCNTwas observed a decrease in the magnetic moment of the samples at a temperature in the range 38 <T <50 K, which is preceded by a sharp response of the magnetic moment in the diamagnetic state at T = 39.5 K. The findings suggest that the origin of the superconducting phase in the Mg-2B-SWCNT system samples at a temperature Tc = 39.5 K. We are also the second main superconducting characteristic was calculated as the limit of the current density (Jc). Bean's equation was used to calculate the Jc values: Jc = 30 * ΔM / d, where Jc - critical current density in A/cm^2, ΔM - difference between the bottom and top of the magnetization of the magnetic hysteresis. d - the average particle size.The calculated data is presented in Table 2.

Table 2 - The results of the critical temperature and current density for system Mg-B-SWCNT

#	Name	Critical temperature, Tc, K	Critical current density Jc, A/cm2	
			In self-field	External magnetic field, 2T
1	Undoped MgB2	39.7	2.0*108	0.8*107
2	Mg-B+0.3 wt. %SWCNT	39,5	3.3*108	1.7*107
3	Mg-B+0.5 wt. %SWCNT	39,4	3.2*108	1.6*107
4	Mg-B+0.7 wt. %SWCNT	39,4	2.6*108	0.7*107
5	Mg-B+1.0 wt. %SWCNT	39,5	2.4*108	0.7*107
6	Mg-B+5.0 wt. %SWCNT	39,4	0.6*108	0.4*107

The results indicate in the Table 2, doping does not considerably effect on the critical transition temperature (T_c), which is extremely constant for all obtained samples. It is found that the critical current density (J_c) depending on the particle content in magnesium diboride SWCNT varies over a wide range of values. According to current density estimation, the most optimal dose doping of SWCNT, which achieves the highest J_c, at the range of 0.3 - 0.5 wt.%. The SWCNT generated increased the amount of pinning centers in samples which acting as barrier to locomotion of magnetic force line in lattice structure.

REFERENCES

[1] J. Bardeen, L. Cooper, J.R. Schrieffer, Physical Review, 106 (1), 1957, pp. 162–164.
[2] R.G. Chandrashekar, R.S. Tiwari, Journal of Applied Physics, 8, 2007, p. 101.
[3] C.H. Cheng, Y. Zhao, X.T. Zhu, Physica C: Superconductivity, 386, 2003,pp. 588-592.
[4] J.E.Hirsch, Phys. Lett.A, 282(6), 2001, pp. 392-398.
[5] J.E. Hirsch and F. Marsiglio, Phys. Rev. B, 64(14), 2001, 144532.
[6] V.A. Ivanov, M. Broek and F.M. Peeters, Solid State Commun., 120, 2001, pp. 53-57.
[7] J. Hlinka, I. Gregora, J. Pokorny, Phys. Rev. B, 64(14), 2001, 140503.
[8] A.F. Goncharov, V.V. Struzhkin, E. Gregoryanz, Phys. Rev. B, 64(10), 2001, 100509.
[9] M. S. Dresselhaus and et al., Physics Reports, 409(2), 2005, pp. 47-99.

SHS- METALLURGY OF ALUMINUMOXINITRIDES FOR TRANSPARENT CERAMICS PRODUCTION

V.A. Gorshkov*[1], P.A. Miloserdov[1], V.I.Yukhvid[1] and E.G. Grigoriev[2]

[1]Institute of Structural Macrokinetics and Materials Science RAS, Academician Osipyan str., 8, Chernogolovka, Moscow Region, 142432, Russia
[2]NationalResearchNuclearUniversityMePhI, Kashirskoe sh., 8, Moscow, 115409, Russia.
* gorsh@ism.ac.ru

Design of high-strengthtransparent ALON ceramics is one of the promising directions for the new materials production. Traditionally the ceramics is obtained by powder metallurgy [1]. In [2–4] the possibility for synthesis of cast ALONs from CrO_3/Al/AlN and Fe_2O_3/Al/AlN mixtures by SHS-metallurgy wasshown. This work aimed at investigation of syntheses parameters, microstructure and composition of cast aluminum oxinitrides as function of components rate in MoO_3/Al/AlN initial mixture. Optimal conditions for obtaining the most stable phase Al_5O_6N were determined as well as grinding regime. The obtained powders are used for Spark Plasma Sintering (SPS) [5].

EXPERIMENTAL

Molybdenum (VI) oxide, aluminum nitride, and aluminum (ASD - 1 brand) were used as raw materials. Initial mixture (mass 100 and 3000 gm) was burned in quartz or graphite forms (d=20–100 mm, the layer height = 50–250 mm) in SHS-reactors (volume3, 5 and 20 liters) under nitrogen initial pressure 5 MPa. The products were analyzed by XRD and EDS.

RESULTS AND DISCUSSION

Green mixtures (in wt. %) were prepared according to the following reaction scheme:
$(MoO_3 + 3Al) + 10\%\ AlN \rightarrow Al_2O_3–AlN + MoAl$. As the combustion temperature in all experiments exceeded melting points of the products (Mo_xAl_y and Al_5O_6N), the process of separation took place. Mo_xAl_y lowered and Al_5O_6N formed the upper ingot that was powdered (to 150 μm) and sintered by SPS. In the experiments, the following optimal conditions of sintering were determined: Tc = 1850°C, delay time 10 min, heating rate 100°C/s,cooling rate50°C/s, external pressure 40 MPA. Under these conditions we prepared samples of sintered aluminum oxinitrides with density (3.61±0.01) g/cm3, mean micro hardness (18.2±0.1) GPa, bending strength (261±13)MPa. Their phase composition corresponded the initial powder composition.

CONCLUSIONS

The results of the work show that initial pressure and components proportion (α) are the main parameters affecting microstructure and phase composition of the product. Optimal conditions were determined for SPS where high-strength compact ceramics with specified microstructure and phase composition of initial powders can be produced.

REFERENCES

[1] McCauley J.W., Patel P., Chen M., Gilde G., Strassburger E., Paliwal B., Ramesh K.T., Dandecar D.P. AlON: A brief history of its emergence and evolution. Journal of the European Ceramic Society, 2009, no.29, pp. 223–236.

[2] S. L. Sylyakov, V. A. Gorshkov, V. I. Yukhvid, T. I. Ignatyeva. Chemical physics, 2013, v. 32, 7, pp 49–53.

[3] Silyakov S.L., Gorshkov V.A., Yukhvid V.I. Effect of nitrogen pressure and aluminum content in a Fe2O3/Al mixture on combustion and chemical composition of combustion products. Combustion, Explosion, and Shock Waves, 2012, Vol. 48, no.4, pp. 428–431.

[4] Gorshkov V.A, Tarasov A.G., Yuhvid V.I. Autowave synthesis of cast aluminum oxynitrides with a high nitrogen content. Russian Journal of Physical Chemistry B, 2010, v. 4, no. 2 pp. 304–307.

[5] Olevskii E.A., Aleksandrova E.V., Ilyina A.M., Novoselov A.N., Pelve K.Yu. ,Grigoryev E.G. Electro consolidation of powder materials. I. Method so flow- and high-tension consolidation. Physic sand chemistry of materials treatment, 2013, no. 2, pp. 53–64.

The work was financially supported by the Russian Science Foundation (grant no. 16-08-00499).

QUASI-STEADY MODES OF FILTRATION COMBUSTION WITH HEAT LOSSES

V.V. Grachev

Institute of Structural Macrokinetics and Materials Sciences RAS, Academician Osipyan str., 8, Chernogolovka, Moscow Region, 142432, Russia
grachev@ism.ac.ru

Filtration combustion is widely applied in processes of self-propagating high-temperature synthesis. In this case an exothermic reaction takes place in porous medium between the solid reagent and gaseous oxidant which is consumed and a solid product is formed. The gas consumption in the reaction front causes a pressure gradient which drives natural filtration of oxidant through a porous substance towards the reaction front. The development of modern macrokinetic theory of filtration combustion started with the analysis of adiabatic quasi-steady modes for case when all sample boundaries are closed to the gas penetration except one, which is open to exchange with a large bath of gas so that the pressure is that of the bath at that end [1]. The reaction is initiated at the opposite end of the sample. It was shown that two modes are possible, with complete and incomplete conversion. Heat losses effect for quasi-steady modes was formulated (without details or computations) in [2]: at the modes of complete conversion the combustion extinction is observed in accordance with the theory of flame propagation limits [3], but in the case of incomplete conversion heat losses do not lead to extinction. This conclusion was repeated in several subsequent reviews. In that theoretical analysis the initial gas content in pores was not taken into account (this assumption simplified solution of the problem).

The aim of the present work is to revise the effect of heat losses on the basis of a generalized mathematical model with heat losses through the side surface and with account of the initial gas content in the sample pores. If the sample length much more than the characteristic scale of the filtration zone, the combustion wave propagation at the initial sample part (far from the open end of the sample) is only possible due to the gas in pores. In this case, the approximate analysis of the steady modes with heat losses shows that the combustion limit exists for both modes, with complete and incomplete conversion [4]. Fig. 1 shows a relationship between initial gas pressure p_0 and critical value of heat losses coefficient α_{cr} which defines the domain of existence ('combustion peninsula') for steady wave propagation in the presence of heat losses. Maximum of α_{cr} corresponds to the stoichiometric pressure. At high heat losses combustion is impossible, while at lower ones combustion is possible only within some certain range of p_0. The lower limit (left branch in Fig. 1) arises due to deficiency of gaseous reagent (incomplete conversion mode) while the upper one (right branch in Fig. 1 – the mode of complete conversion), due to the excess of gaseous reagent which begins to act as a heat-absorbing diluent.

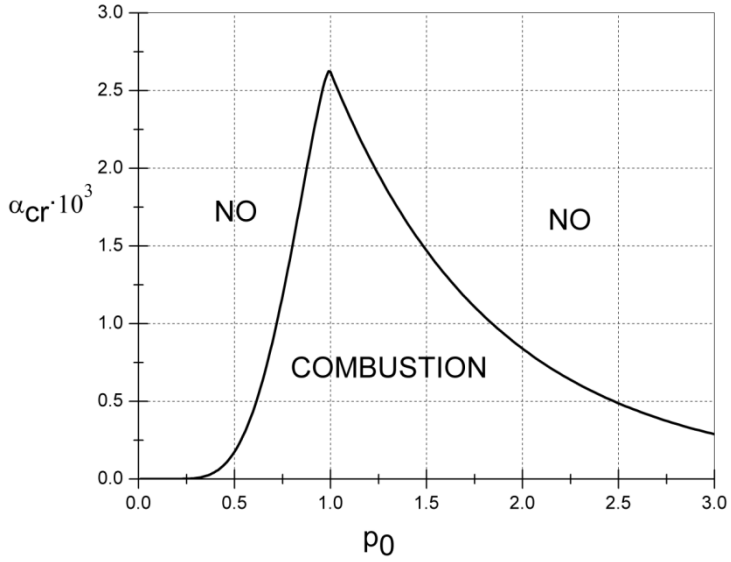

Fig. 1 - Combustion peninsula for a steady wave in the presence of heat losses.

The results of analytical solution for quasi-steady combustion modes are presented in the Fig.2 showing the dependence (CD_i curve) of critical value of parameter R (that defines a combustion mode) on heat losses coefficient α for three initial gas pressures p_0. At a given level of heat losses (α), combustion is only possible for $R < R_{cr}(\alpha)$. The range of combustion mode with incomplete conversion is under the BCD_i curves. Transition from incomplete to complete conversion takes place on the curve *BC*. Horizontal straight line *AC* corresponds to the combustion extinction at the modes of complete conversion in accordance with the theory of flame propagation limits [3] - ultimate decrease of combustion temperature is one characteristic interval, and the combustion velocity is $\sqrt{e}$ times lower. The dashed curve close to CD_1 (p_0 = 0.1) corresponds to the boundary of incomplete conversion mode within limits of low initial pressure (this border approaches asymptotically to the abscissa axis). With an increase in p_0, the CD_i curves at large *R* approach not to the abscissa axis but to some horizontal asymptote such as FD_3 (in case of p_0 = 0.7). Position of such asymptotes is defined by critical value of α for the steady combustion sustained only by the gas reactant initially located in the sample pores [4] (see Fig.1). The larger p_0, the higher is position of the respective asymptote.

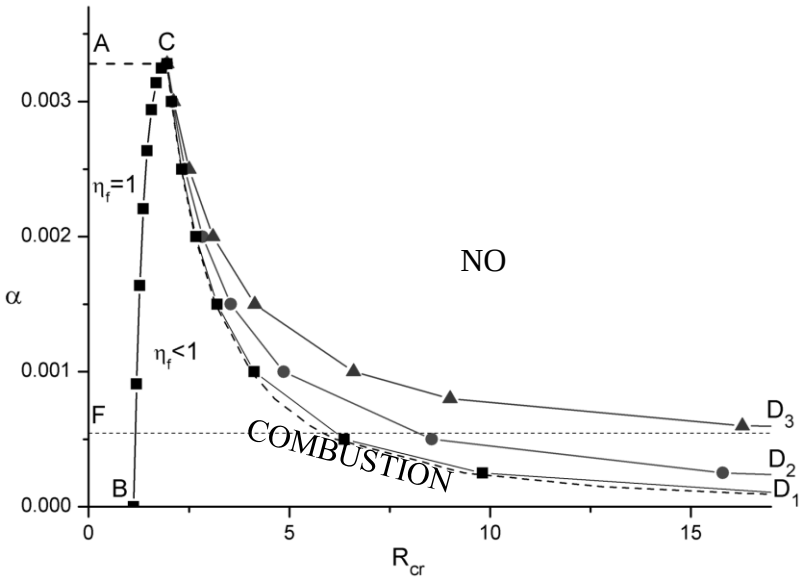

Fig. 2 - Combustion peninsula for a quasi-steady wave in the presence of heat losses.

At high values of *R* (to the right from the point C abscissa at Fig. 2) the increase of heat losses leads to combustion extinction under the mode of incomplete conversion at border of CD_i. Therefore, in the common case the corresponding line of ACDi restricts the region of the combustion modes for the preset value of the initial pressure. In the region of parameters above the line, the combustion is impossible because of too high heat losses.

The results of the theoretical analysis are in good agreement with experimental observations. The value of *R* parameter is directly proportional to the distance from the combustion front to the open end through which gas is supplied. Existence of the critical value of R_{cr} means that there is a critical distance from the combustion front to the open end of the sample. If the distance is longer than the critical value, the combustion wave propagation is impossible because of the extinction at heat losses under the mode of incomplete conversion; it was observed experimentally [5, 6].

REFERENCES

[1] A.P. Aldushin, A.G. Merzhanov, and B.I. Khaikin, Dokl. Phys. Chem., 1974, vol. 215, no. 3, pp. 295–298.

[2] A.P. Aldushin, B.S. Seplyarskii, Theory of Filtration Combustion of Porous Metal Samples, Preprint, Inst. Chem. Phys., Chernogolovka, 1977, p.32.

[3] Zeldovich Ya.B., Theory of propagation limit for slow flame. Zhurnal eksperimentalnoy i teoreticheskoy fiziki (Journal of experimental and theoretical physics), 1941, 11(1), 159-169.

[4] Grachev, V.V., Theory of propagation limits for infiltration-mediated combustion in the absence of external gas supply, Int. J. SHS, 2013, vol. 22, no. 1, pp.1–4.

[5] Pityulin, A., Ph.D. Thesis, Branch of the Institute of Chemical Physics, Chernogolovka, 1980, 150 p.

[6] Mei L., Li J.-T., Synthesis of AlN–SiC solid solution through nitriding combustion of Al–C–Si3N4 in air. Acta Materialia, 2008, 56, 3543–3549.

SYNTHESIS AND DECOMPOSITION OF MAX PHASE Ti_2AlN IN THE MODE OF FILTRATION COMBUSTION

A.A. Kondakov, A.V. Linde, I.A. Studenikin, V.V. Grachev*

Institute of Structural Macrokinetics and Materials Sciences RAS, Academician Osipyan str., 8, Chernogolovka, Moscow Region, 142432, Russia
* grachev@ism.ac.ru

The ternary system titanium–aluminum–nitrogen is of great interest from the scientific point of view as well as from the viewpoint of practical application of the obtained combustion products. The scientific interest consists in experimental investigation of filtration combustion regularities of the system in which several simultaneous competitive reactions are possible. In addition to two parallel gas–solid reactions such as titanium–nitrogen and aluminum–nitrogen with formation of nitrides, the reaction between solid reagents titanium–aluminum with formation of intermetallic compounds is possible. These compounds can react with nitrogen. Besides, the formation of ternary compounds titanium–aluminum–nitrogen is possible too. Some of these compounds belong to MAX phases which are of great interest for different research groups in last decade [1].

The principal possibility of MAX phase Ti_2AlN synthesis by filtration combustion was shown earlier [2]. But its content in the combustion product was less 50% wt. It is known that MAX phase decomposes at temperature higher than 1400°C [3]. Respectively to prevent MAX phase decomposition it is necessary to decrease combustion temperature lower than the temperature interval of MAX phase decomposition. The standard procedure of temperature decreasing in SHS processes is an addition of combustion products into the initial mixture. As our aim was an increasing of MAX phase content in final product, then according to simple logic it should be added into the initial mixture.

Due to Ti_2AlN powder is commercially unpurchaseable an attempt was made to obtain it by vacuum sintering. As a result of performed researches [4] the sintering parameters were defined and 500-g sintered sample was obtained. According to XRD-analysis the obtained sample was a monophase product (100% Ti_2AlN). The product micrographs (Fig. 1) demonstrate its nanolaminate structure. Prepared from obtained sample Ti_2AlN powder was used further as a component of the initial mixtures.

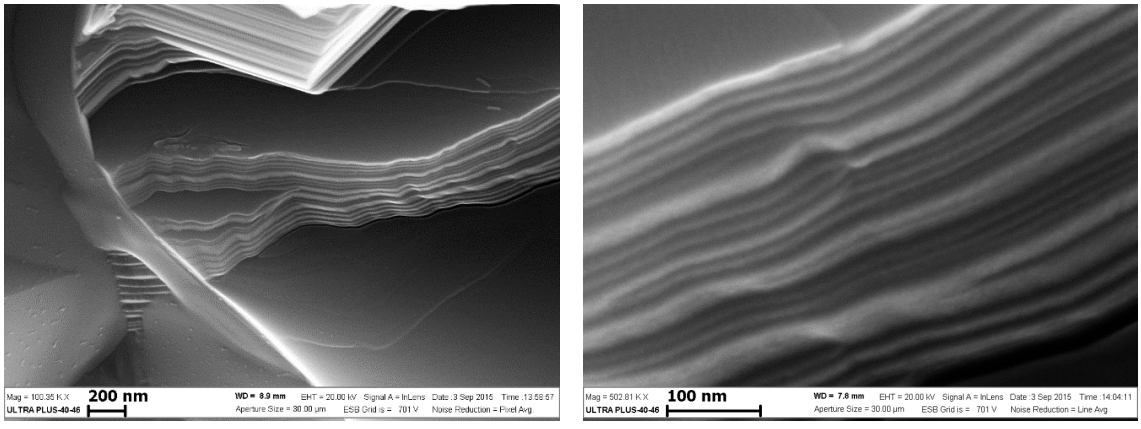

Fig.1 - Fracture surface of obtained MAX phase Ti_2AlN.

The experiments for combustion in the gaseous nitrogen under pressure 0.1 MPa were carried out for two initial mixtures $2Ti+Al+xTi_2AlN$ with MAX phase containing 50 and 75% wt. respectively. XRD-analysis of obtained combustion products showed full absence of MAX phase in the phase compositions of the products i.e. a full decomposition of MAX phase had occurred at the combustion. On the one hand this may be explained by the next fact. For samples with 50% wt. MAX phase content in the initial mixture the process maximal temperature (indicated by thermocouple) was T_{max}=1580°C and exceeded the start temperature of MAX phase decomposition. On the other hand for samples with 75% wt. MAX phase content in the initial mixture the measured temperatures did not exceed 1300°C. It follows the decomposition temperature of MAX phase in the gaseous nitrogen is lower than in vacuum. As MAX phase content in the initial mixture was rather high, a hypothesis about possible nitriding reaction of Ti_2AlN at combustion mode arose.

To test this hypothesis we carried out experiments for combustion of Ti_2AlN samples in the gaseous nitrogen. The samples presented 16x16 mm rectangular blocks with 28 mm height. They were cut out from Ti_2AlN preform obtained by sintering in vacuum. The experiments were carried out at several values of nitrogen pressure, the self-sustaining combustion was observed at pressure 1 MPa and 0.3 MPa. In the last case the combustion mode was unsteady with a lot of moving hot spots. At nitrogen pressure 0.1 MPa after burning of igniting pellet (titanium and boron mixture) the combustion of sample was not observed. XRD-analysis of products after combustion at nitrogen pressure 1 MPa showed the presence only nitride phases 74% wt. TiN and 26 % wt. AlN. The products obtained by combustion under the nitrogen pressure 0.3 MPa besides nitride phases (76% wt. TiN and 21 % wt. AlN) contained a little amount 3% wt. of the intermetallic $TiAl_3$. Fig. 2 demonstrates microstructure of obtained product. Comparison of the micrographs on Fig.1 and Fig.2 shows qualitative change of the initial material microstructure from nano-laminate to micro-composite structure with fibrous inclusions. EDS microanalysis (INCA Energy 350 XT, Oxford Instruments) showed, the micro-agglomerates consist mainly from titanium nitride, but the fibrous inclusions are whiskers and fibers of aluminum nitride.

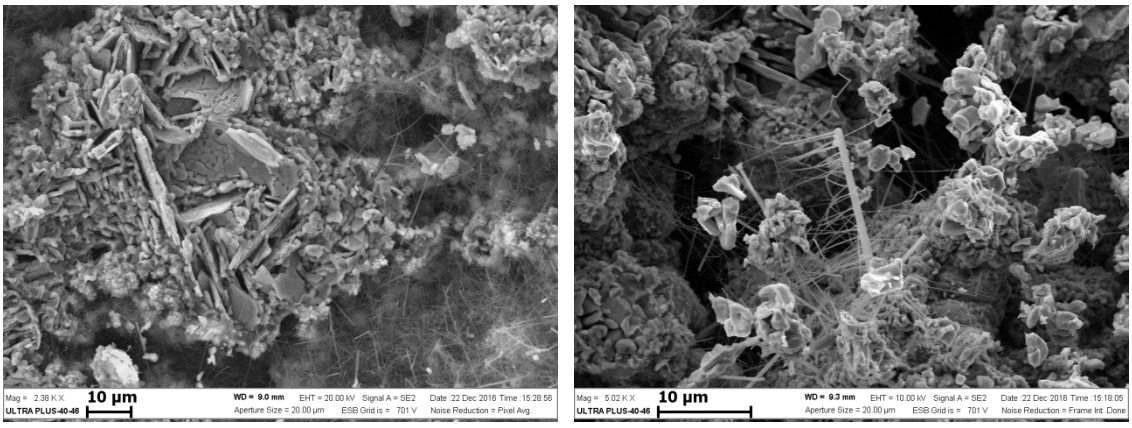

Fig.2 - Microstructure of Ti_2AlN decomposition combustion product.

So in this experimental work the decomposition of MAX phase Ti_2AlN in the gaseous nitrogen at the mode of self-propagating reaction wave with formation of titanium and aluminum nitrides

has been observed in the first time. This result has a particular importance for the operation of Ti_2AlN-based material at high temperature in the nitrogen-containing medium.

REFERENCES

[1] M.W. Barsoum, MAX Phases: Properties of Machinable Ternary Carbides and Nitrides, Wiley-VCH Verlag GmbH, Germany, 2013. 437 p.

[2] A. A. Kondakov, V. V. Grachev. Modes of Filtration Combustion of Titanium-Aluminum –Nitrogen ternary system, Proceedings of the Third Conference on Filtration Combustion, Chernogolovka, Russia, 18-21 June 2013, pp. 35-38.

[3] I.M. Low, W.K. Pang, S.J. Kennedy, R.I. Smith. High-temperature thermal stability of Ti2AlN and Ti4AlN3: A comparative diffraction study. Journal of the European Ceramic Society, 31 (2011), pp. 159–166.

[4] A. A. Kondakov, I. A. Studenikin, A. V. Linde, N. A. Kondakova, and V. V. Grachev. MAX phase Ti_2AlN by sintering in vacuum. In book: EPNM2016/ Explosive Production of New Materials: Science, Technology, Business, and Innovations. [Edited by A.A. Deribas, Yu.B. Scheck and R. L. Mendes] — Coimbra, Portugal, 2016. pp.76-78.

DENSE IN SITU CERAMIC AND INTERMETALLIC MATRIX COMPOSITES *VIA* PRESSURE ASSITED THERMAL EXPLOSION MODE OF SHS: FROM BASIC RESEARCH TO FABRICATION OF STRUCTURAL PARTS

E.Y. Gutmanas and I. Gotman

Technion – Israel Institute of Technology, Haifa, 32000, Israel

Over the last decade a gradual shift from the basic to applied research has lead to the development of a number of unconventional SHS processes that allow simultaneous synthesis and consolidation of the inherently porous combustion products. Pressure assisted thermal explosion (TE) mode of SHS results in dense products in cases when the heat evolved during TE and pressure applied are sufficient for consolidation. Reactive Forging (RF) SHS/TE-based method has been developed: in RF, a self-sustained reaction is ignited in a reagent blend by rapid heat transfer from preheated press rams, and a moderate uni-axial pressure is applied while a sufficient amount of a liquid or very soft phase is present in the combustion product. Combined with the developed Short Distance Infiltration (SDI) approach, RF provides conditions for fabrication of interpenetrating phase *in situ* composites with binary (Al_2O_3, TiB_2, TiC) or ternary ($MgAl_2O_4$, Ti_3SiC_2, Ti_3AlC_2, Ti_2AlC) ceramic matrices, as well as well as intermetallic-ceramic and metal-ceramic composites (MgB_2-Mg, Mg_2Si-Mg, Ti/Nb-Al_2O_3, TiNi-Al_2O_3, NiAl-Al_2O_3). Compared to traditional melt infiltration, SDI has the advantage of the considerably shorter infiltration distances (μm vs. mm/cm). SDI is based on the presence of low melting phases in the powder blend. Rapid heating of compacts above T_m followed by application of pressure results in squeezing the liquid phase into the pores which promotes SHS reactions and consolidation and results in dense products with fine homogeneous microstructures. The RF-SDI approach has also been successful in fabrication ceramic matrix-diamond grinding wheels, parts from machinable ternary ceramics and light armor tiles. RF approach can be used also for production of 3-D porous structures by diluting the blend with non-reacting spacers that can be easily dissolved after SHS processing.

Nanostructuring of powder blends results in lower ignition temperatures, T_{ig}, and can be used for ignition of high T_{ig} blends and thus for fabrication of two component materials and structures. RF approach employing exothermic inserts and "chemical furnace" approach be can be also used for consolidation of refractory materials and composites.

Simultaneous synthesis and consolidation of reaction products employing pressure assisted SHS is a "green", cost effective and thus perspective fabrication route of structural parts.

COMBUSTION SYNTHESIS OF NOVEL NANOCARBONS VIA PROCESSING OF MAGNESIUM-CONTAINING COMPOSITIONS

A. Huczko*[1], A. Dąbrowska[1], M. Fronczak[1], M. Bystrzejewski[1], D. P. Subedi[2], B. P. Kafle[2], R. Bhatta[2], P. Subedi[2], A. Poudel[2]

[1] Department of Chemistry, Warsaw University, Warsaw, 1 Pasteur str., 02-093, Poland
[2] School of Science, Kathmandu University, Dhulikhel, Kavre,Nepal
* ahuczko@chem.uw.edu.pl

Self-propagating high-temperature synthesis (SHS) or combustion synthesis (CS) is practiced all over the world for the production of advanced and novel materials [1]. The CS process has several advantages over the conventional synthesis approaches these being (i) generation of high temperatures, (ii) short duration of highly exothermic reactions, and (iii) processing under conditions usually far from equilibrium. It makes use of chemical reactions involving redox compounds and redox mixtures. Huczko et al. [2] reported fast combustion synthesis and characterization of YAG:Ce^{3+} garnet nanopowders. Magnesium-thermal CS has been specifically an efficient technique for manufacturing a number of compounds and elements for years [3]. Novel nanocarbons have been efficiently produced following the 'bottom-up' approach via the condensation of carbon gas [4]. The combustion temperatures in case of magnesium-driven reduction are well above 2000 K. Thus, graphitization conditions may prevail during the process resulting in formation of carbon nanotubes, encapsulates and graphene-related nanostructures. Dyjak et al. [5] produced hierarchical, nanoporous graphenic materials through an instant, self-sustaining magnesiothermic reduction of oxalic acid. The extended studies carried out in recent years in the Laboratory of Nanomaterials Physics and Chemistry (Department of Chemistry, Warsaw University) have shown that different carbon- and oxygen-containing compounds are efficiently reduced with magnesium. The high temperatures of magnesium-driven reduction of carbon-bearing oxidants (carbon oxides, oxalates, etc.) along with extremely short duration of combustion (usually below 1 sec) result in almost total atomization of reactants paving the way towards condensation of carbon gas resulting in formation of graphene-related and porous carbon nanostructures with many potential application (sorbents, supercapacitors) [6-8].

The aim of this work was to extend those experimentation into converting carbon-containing ammonium oxalate ($(NH_4)_2C_2O_4$) and acetate ($NH_4CH_3CO_2$) into 3D graphene-related nanocarbons following the reaction schemes

$$5\ Mg + (NH_4)_2C_2O_4{\cdot}H_2O \rightarrow 2\ C + 5\ MgO + 2\ NH_3 + 2\ H_2$$

$$2\ Mg + NH_4CH_3CO_2 \rightarrow 2\ C + 2\ MgO + NH_3 + 2\ H_2$$

Comparing to the previously reported Mg-driven reduction of Mg/Ca oxalates [6] one could expect here much more vigorous evolution of gaseous products resulting in the expanded internal morphology of final porous nanocarbons. The exploratory study was also carried out to test the adsorption properties of the produced material.

All combustions were carried out (after ohmic ignition) in the high-pressure stainless-steel reactor following the protocol outlined elsewhere [9] and using the stoichiometric ratio of the solid starting reactants. The runs were performed under neutral atmosphere (Ar). After the

combustion the reactor was cooled down while the puffy and greyish/blackish solid product was collected. Both the raw and purified (leaching with 3M HCl solution at 90 ^{o}C for 30 min.) products were analyzed (XRD, SEM, TGA and Raman spectroscopy). The adsorption performance was tested via the removal of 4-chlorophenol from water. The combustions were accompanied by a high pressure increase which results from the evolution of hot gaseous reactants. Table 1 presents the operational parameters of all runs (O: oxalate; A: acetate).

Table 1 - Operational parameters of all combustions

Run #	Green composition	Initial pressure, at	Peak pressure, at	Mass of starting reactants, g	Mass of raw product, g	Mass of purified product, g*	Solid carbon yield, %*
O-1	Mg/O = 5/1	1	30	11,12	5,55	0,27	8,5
O-2	as above	1	32	11,96	6,20		
O-3	as above	1	35	11,56	5,93		
A-1	Mg/A = 2/1	1	18	11,74	6,94	5,14	90,0
A-2	as above	1	17	6,49	3,90		
A-3	as above	1	18	11,63	6,65		

*cumulative (for 3 runs each)

From the data presented in Table 1 and the reaction equation the mass balance was carried out to estimate the conversion of starting carbon (in O and A salts) into solid carbon (in a purified product). This varied between 8,5% (for oxalate) and 90,0 % (for acetate). Such a huge difference suggests quite different combustion mechanisms: in case of oxalate reduction the high temperature of Mg oxidation initiates efficient gasification of carbon elemental while for the acetate the process seems to be dominated by thermal pyrolysis of the salt with soot formation. The water vapor (hydrated oxalate reduction) can also efficiently etch and gasify the formed carbon elemental thus decreasing its content in the purified product.

The XRD spectra of the selected products for the raw and purified material are shown in Fig. 1.

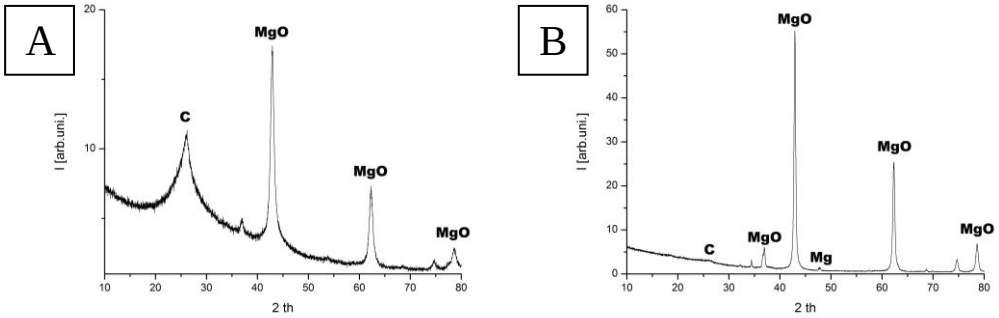

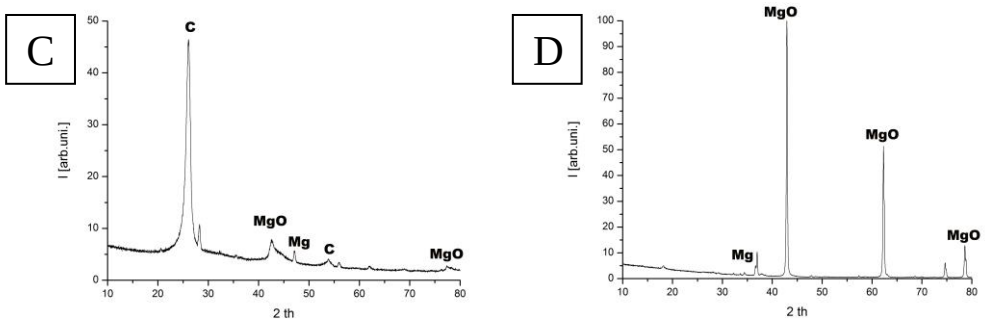

Fig. 1 - XRD spectra of raw and purified products. A: run A-1, purified product; B: run A-1, raw product; C: run O-1, purified product; D: run O-1, raw product

The results confirm the deep transformation of the reactants into the sought products, with the total disappearance of the starting salts in the raw products which are dominated by MgO, along the presence of some unreacted Mg. The purified product is dominated by turbostratic carbon with much better graphitization obtained for an oxalate reduction. Surprisingly, the purified product also contains some residual MgO and Mg which, presumably, were not leached in the acid during purification and plausibly remained encapsulated in protective carbon coatings.

Figure 2 shows the representative SEM images of the reactants.

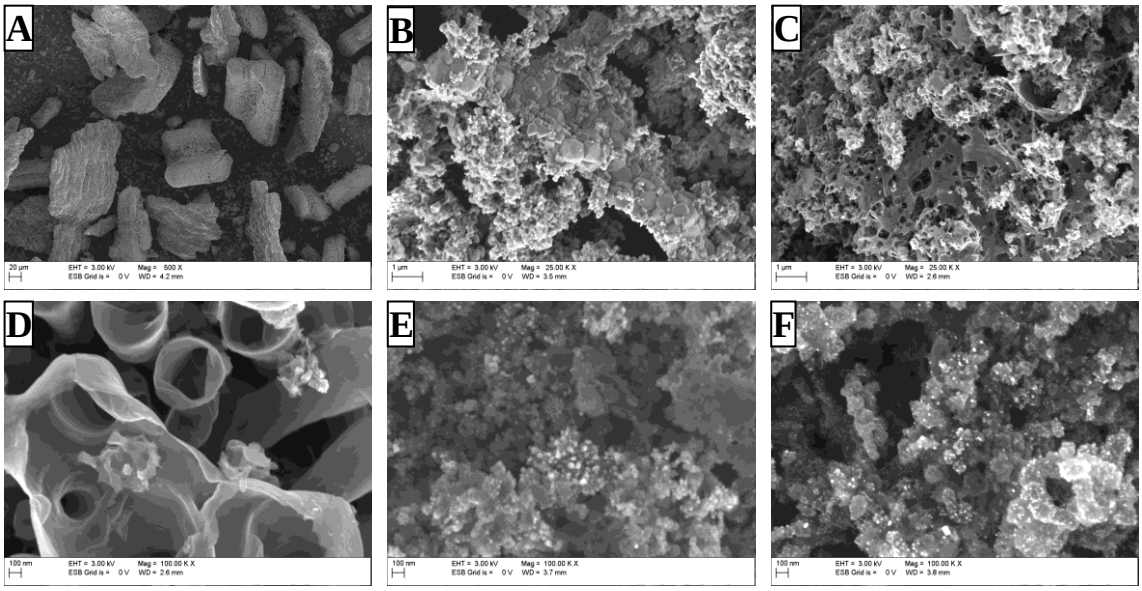

Fig.2 - Representative SEM images of the reactants. A: starting mixture Mg/O; B: run O-1, raw product; C: run O-1, purified product; D: run O-1, purified product; E: run A-1, raw product; F: run A-1, purified product

The green composition of Mg and salts is a non-homogeneous mixture of metal microcrystallies and agglomerates of salt nanocrystallites. The morphology of product (oxalate processing) is completely different just confirming the total conversion of reactants. The raw product contains mostly cubic nano- and micro-crystallites of carbon-coated MgO particles (ca 50-200 nm in diameter) with some un-reacted round-shaped Mg particles. The purified product is dominated by petal-like 3D graphene material forming both a kind of a 'Swiss cheese' carbon matrix and

hollow carbon nanospheres, clearly resulting from the acid etching of MgO/Mg. In case of acetate reduction the product contain mostly MgO and soot nanoparticles.

The adsorption properties were investigated via the removal of 4-chlorophenol from water for the carbon material obtained (run A-1), both for a pristine and KOH-activated product. It can be seen (Fig. 3) that the maximum adsorption capacity for the case of pristine material does not exceed 75 mg/g, whilst after activation this value rises up to 225 mg/g.

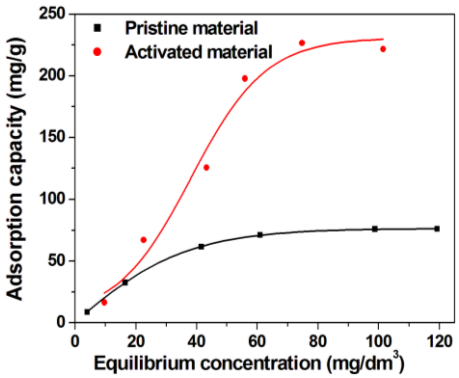

Fig. 3 - Adsorption isotherms for the carbon material obtained from $NH_4CH_3CO_2$

Thus, the uptake of 4-chlorophenol onto the activated sample is comparable to the uptakes determined for the activated carbon [10] and higher than onto the other carbon nanomaterials [10].

REFERENCES

[1] Self-Propagating High-Temperature Synthesis of Materials, ed. By A.A. Borisov, L. De Luca and A. Merzhanov, Taylor & Francis, New York, 2002, p. 189.

[2] A. Huczko, M. Kurcz, P. Baranowski, M. Bystrzejewski, A. Bhattarai, S. Dyjak, R. Bhatta, B. Pokhrel, B.P. Kafle, Phys. Status Solidi B, 250, 2013, p. 2702.

[3] S.S. Mamyan and V.I. Vershinnikov, Inter. Journal of SHS, 1, 1992, p. 392.

[4] A. Huczko, A. Dąbrowska and M. Kurcz, Graphene: Synthesis, Characterization, Applications, Warsaw University Publishing House (in Polish), Warsaw, 2016, p. 41.

[5] S. Dyjak, W. Kicinski, M. Norek, A. Huczko, O. Łabędź, S. Budner, M. Polański, Carbon, 96, 2016, p. 937.

[6] A. Huczko, M. Kurcz, A. Dąbrowska, M. Fronczak, M. Bystrzejewski, M. Drozdowski, D.P. Subedi, B.P. Kafle, B.K. Kafle, P. Lamichhane, P. Saren, S.K. Tiwari, ECS J. of Solid State and Technol., 6, 2017, p. M3090.

[7] A. Huczko, M. Kurcz, A. Dąbrowska, M. Bystrzejewski, P. Strachowski, S. Dyjak, R. Bhatta, B. Pokhrel, B.P. Kafle, D. Subedi, Phys. Status Solidi B, 253, 2016, p. 2486.

[8] A. Huczko, O. Łabędź, A. Dąbrowska, M. Kurcz, M. Bystrzejewski, H. Lange, P. Baranowski, L. Stobiński, A. Malolepszy, A. Okotrub, M. Soszyński, Phys. Status Solidi B, 252, 2015, p. 2412.

[9] A. Dąbrowska, S. Belluci, A. Cataldo, F. Micciulla, and A. Huczko, Phys. Status Solidi B, 251, 2014, p. 2599.

[10] P. Strachowski, M. Bystrzejewski, Colloids and Surfaces A, 467, 2015, p.113.

COMBUSTION SYNTHESIS OF GRAPHENE-RELATED COMPOSITE NANOMATERIALS

M. Kurcz*[1], A. Huczko[1]

[1] Warsaw University, Chemistry Department, Pasteura 1, 02-093, Warsaw, Poland
* magdalena.osica@gmail.com

Herein a novel and simple protocol for the fast and autothermal synthesis of graphene-like nanocomposites via the self-sustaining combustion synthesis (SHS) is presented. Two starting redox green compositions $Si/CF_{1,06}$ and Mg_2Si/GO (Graphite Oxide) were tested . The parametric studies in $Si/CF_{1,06}$ system were conducted and the following parameters: kind of atmosphere, pressure, stoichiometry of reactants were investigated in terms of product formation efficiency and its characteristics. Mg_2Si/GO mixture was also combusted and analyzed. The resulting raw and purified graphene-SiC nanofiber composites were analyzed with XRD, SEM and Raman spectroscopy.

Graphene attracts nowadays much attention due to its unusual electronic, magnetic, thermal, lubricant, chemical, optical, and mechanical properties [1] hence it can be widely used in composites [2]. A wet chemistry technique (exfoliation route) via the graphite oxidation (to GO) followed by a GO reduction to reduced graphene oxide (rGO) remains the most popular production technique. This approach is, however, obsolete due to its time-consuming procedure and the use of harmful reactants. Thus, new methods are sought, mostly exploring a 'bottom-up' approach of the formation of nanomaterials [3]. A self-propagating high-temperature synthesis (SHS) [4] is well suited for such approach. The atomization of the starting components (green mixture of a strong reductant and a strong oxidant) is here due to the high temperatures which can easily approach 3000 K (thermite reactions). High temperature and pressure gradients, a short duration of redox 'combustion', and a fast quench of products give way to the formation of novel products (non-stoichiometric, nanosized).

We have shown elsewhere [5,6] that SHS can be harnessed for graphene-like material production. We have also proved [7,8] that combustion synthesis can be efficiently used for SiC nanowires (SiCNWs) production in a simple Si/Teflon® system.

We propose here SHS approach for nanocompositions (graphene-like material/SiCNWs) production. Such nanocomposites can be very attractive for materials science as fillers of polymers improving not only electrical and thermal properties but also mechanical ones [9].

The goal of the research was to test such selected systems that would lead to the formation of composite components (graphene-related and SiCNWs) in a single combustion. Based on our previous experience we put forward two systems $Si/CF_{1,06}$ and Mg_2Si/GO. In the first one we assumed that exothermic reaction between a strong oxidant and a medium reductant (Si) should allow for both chemical (leading to SiCNWs) and thermal reduction of fluorinated carbon (to graphene-like nanomaterial). In the second one two reductants (strong Mg and a weaker Si) and strong oxidant (GO - graphene oxide) were tested which may lead to deep reduction and formation of both graphene-like structures and SiCNWs. The released energy should be, however, lower than in the first system, what may lead to different products/morphologies.

Experimantal Si/$CF_{1,06}$

All thermolyses were carried out in the high-pressure reactor following the procedures described in [6]. Well-mixed reactants were placed in a quartz crucible, with a carbon thread (electrical igniter) immersed inside and reaction was ohmically initiated. All combustions proceeded spontaneously, strong light and high pressure jump (up to 20 atm for low initial pressure and up to 90 atm for high initial pressure) were observed. The following equation describes the chemical transformations in the system:

$$Si + CF_x \rightarrow C + SiF_4 + SiC$$

After the reaction termination, the reactor was cooled down and blackish, puffy solid product was collected, mixed and purified (30 min boiling in 30% KOH to remove unreacted Si and side product - SiO_2), and analyzed.

A wide range of combustion parameters (type of atmosphere, pressure, reactant's stoichiometries) were tested. The combustions are summarized in Table 1. The efficiency of the synthesis was close to 50%. The highest efficiency of solid products (comparing the same pressures) was obtained for an inert gas, both active environments caused reduction in solid products, probably oxygen reacts with carbon towards CO_x. The relations are even stronger with an increase of the pressure. In case of the air, the least amount of SiC and C is produced, however no significant efficiency drop is observed (this due to SiO_2 formation). Comparing amounts of SiC and C one can notice that the presence of an oxygen (active gases), as well as higher pressure, favors SiCNWs formation, therefore the atmosphere together with pressure can control proportions of SiCNWs and graphene-like material in composites. Stoichiometry changes, as expected, influence amount of C and SiC in products, surprisingly either increase or decrease of Si increases total SiC and C formation in compare to stoichiometric reagent mixture.

Sample	Gas	p [atm]	$m_{reagents}$ [g]	$m_{products}$ [g]	Efficiency towards solid products[1]	$m_{for\ purific.}$ [g]	$m_{after\ purific.}$ [g]	% C & SiC in product[2]	% of C in product	% of SiC in product
40%:60%										
Ar_5atm	Ar	5	4,17	1,96	47,06%	0,609	0,342	56,16%	34,42%	21,74%
Ar_50atm	Ar	50	4,39	1,91	43,58%	0,604	0,387	64,07%	26,29%	37,79%
CO_2_5atm	CO_2	5	4,39	2,16	49,20%	0,609	0,300	49,26%	17,73%	31,53%
CO_2_50atm	CO_2	50	4,37	1,96	44,88%	0,611	0,298	48,77%	14,63%	34,14%
Pow_5atm	Pow	5	4,25	2,01	47,42%	0,616	0,306	49,68%	17,74%	31,93%
Pow_50atm	Pow	50	4,21	1,78	42,15%	0,607	0,203	33,44%	2,57%	30,87%
31%:69%										
Ar_5atm	Ar	5	4,01	1,36	33,93%	0,472	0,305	64,62%	50,77%	13,85%
CO_2_5atm	CO_2	5	4,15	1,83	44,13%	0,613	0,368	60,03%	34,90%	25,13%
47%:53%										
Ar_5atm	Ar	5	4,07	1,60	39,36%	0,600	0,344	57,33%	24,84%	32,49%
CO_2_5atm	CO_2	5	4,17	2,29	55,03%	0,600	0,368	61,33%	16,58%	44,75%

[1] efficiency counted as mass of products/ mass of reagents

[2] assuming that solid products after purification contains only pure C and SiC

The amount of C and SiC were calculated after calcination of the purified product in air at 650°C for 3,5h. The residue was only SiC and the difference in masses gave the mass of C.

XRD analysis of raw products (Fig. 1) confirmed the reduction of CF_x to carbon and formation of SiC.. At higher pressures SiC dominate while un-reacted Si is much weaker. The role of active atmosphere in removing carbon material is also confirmed (weaker signals of carbon in Air and CO_2).

SEM analysis (Fig 2) showed both highly exfoliated carbon material and SiCNWs as expected. At higher pressure not only SiCNWs but also SiC nanocrystallites are present. In raw products (air, CO_2) some silica is also visible. Changes in stoichiometry do not have such a strong effect on products as changes of gases, however increasing amount of Si results in higher amount of SiCNWs and crystal formation.

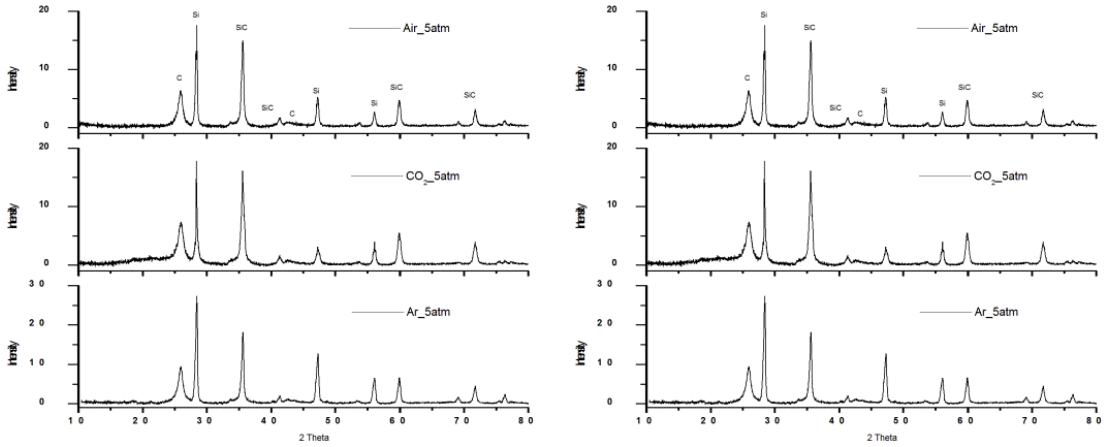

Fig. 1 - XRD spectra of raw and purified product

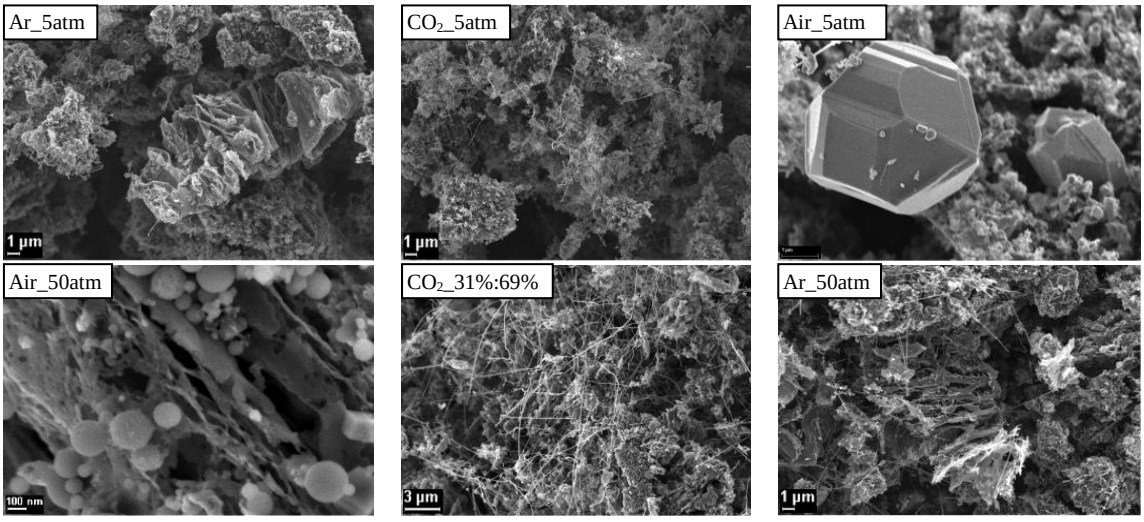

Fig. 2 - SEM images

Structural details of the products were obtained from Raman spectra (Fig 3, Table 2). The spectra are dominated by 2D (band typical for graphene-based structure material), G and D bands. G band in all samples is wider than graphite's and 2D is wider than graphene's its FWHM is about 50 cm^{-1} which is close to turbostratic carbon. The lowest amount of defects is found for the sample produced in Ar (the lowest value of D/G and highest 2D/G); oxygen atmospheres cause depletion of amorphous carbon. Increasing pressure results in higher graphitization in

case of inert gas and increases amount of defects for active atmospheres. Increasing amount of Si (stoichiometry changes) results in increasing amount of defects (data not presented).

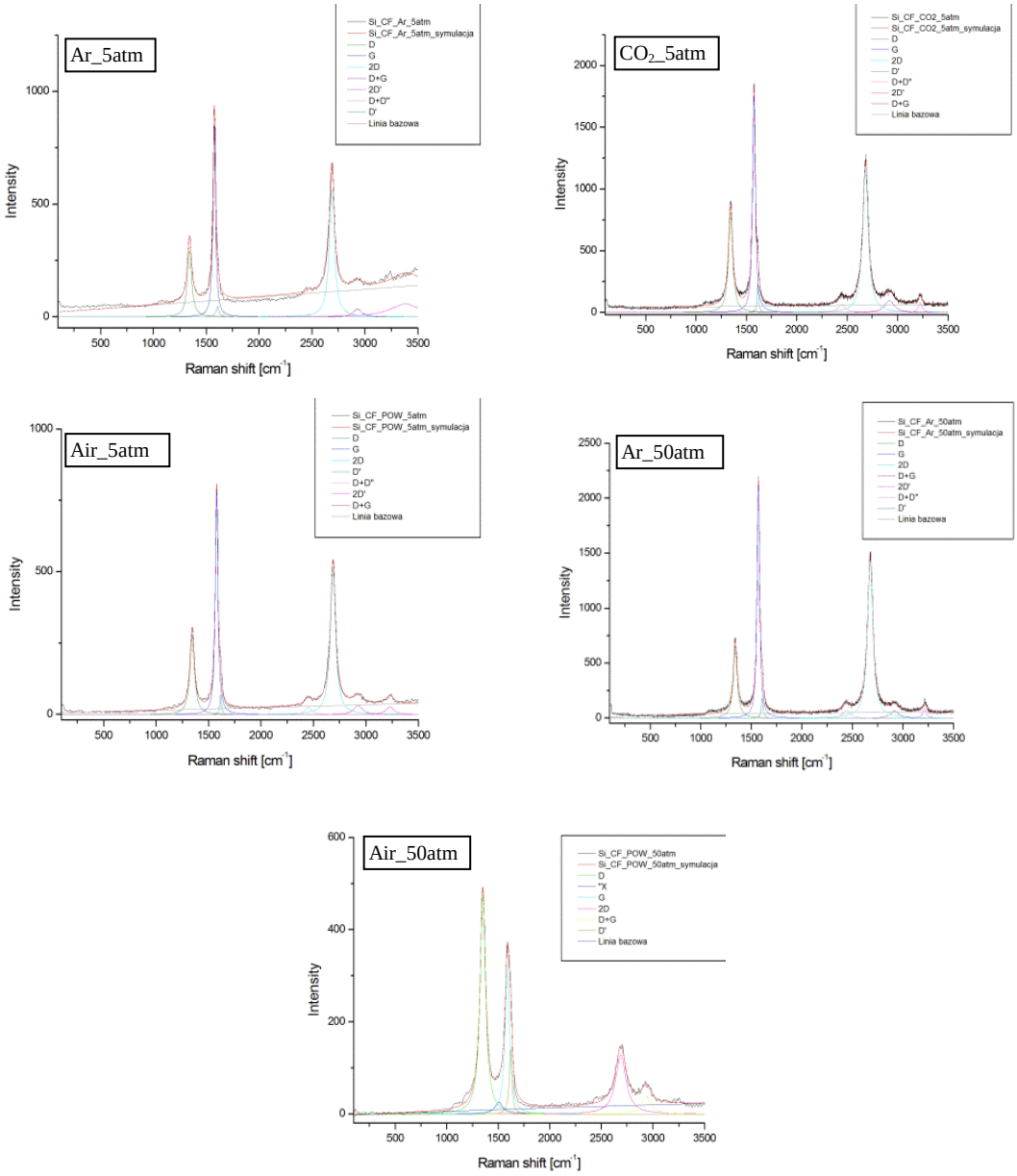

Fig. 3 - Raman spectra

Table 2 - Parameters obtained from Raman spectra

Gas	P [atm]	G [cm^{-1}]	FWHM (G)	2D [cm^{-1}]	FWHM (2D)	D/G	2D/G
Ar	5	1577	29	2690	58	0,58	1,32
CO_2	5	1576	32	2684	64	0,71	1,31
Pow	5	1578	30	2688	60	0,60	1,26
Ar	50	1570	30	2678	63	0,48	1,43
CO_2	50	1579	36	2688	67	0,95	1,19
Pow	50	1588	52	2691	121	1,85	0,25

To sum up, the presence of oxygen favors formation of silica and decrease of carbon, the effect is strengthened at higher pressures, thus the atmosphere controls the products. The pressure increase favors formation of SiC, not only as nanowires but also nanocrystals and it lowers amount of defects at inert atmoshere (it has opposite effect at active atmosphere). Changes in stoichiometry control the amount of SiC and C in product.

Mg_2Si/GO

In the exploratory study we assumed that the reaction follows the following scheme:

$$Mg_2Si + 2\ C_{1.15}O \rightarrow 2\ MgO + SiC + 1{,}30\ C$$

The synthesis was conducted in Ar at 5atm. The efficiency was 89%, what clearly proves formation of gasous products (CO_x?). Contrary to former system the longer heating was required to initiate the combustion this probably due to thermodynamic stability of Mg_2Si. The as produced material was black, fluffy powder. XRD analysis (Fig. 4) confirmed the formation of MgO and SiC, some un-reacted Si as well as unreacted Mg_2Si was also present, however no C was observed.

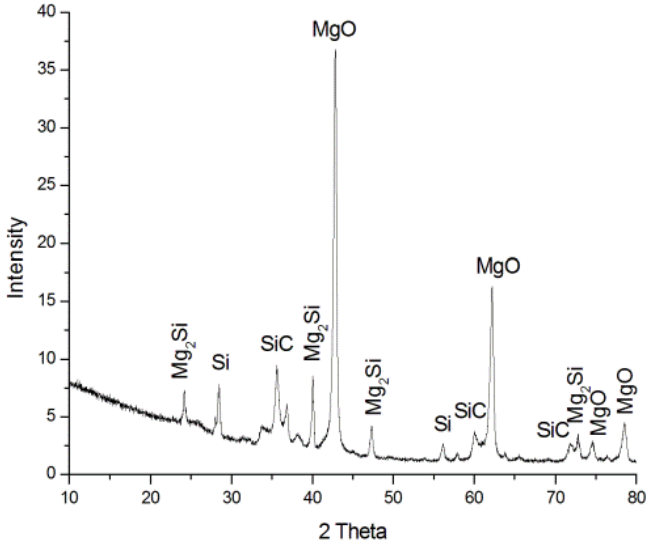

Fig. 3 - XRD spectrum otf the raw product

SEM analysis showed large variety of product's morphologies (Fig. 4). There are not only exfoliated carbon structures (not confirmed by XRD) but also MgO crystals (located between carbon layers) and alongated forms, patel-like carbon, SiCNWs.

To summarize, as a result of thermo-chemical reaction between Mg_2Si and GO highly exfoliated and reduced forms of carbon were produced. The results are encouraging for more in deepth research.

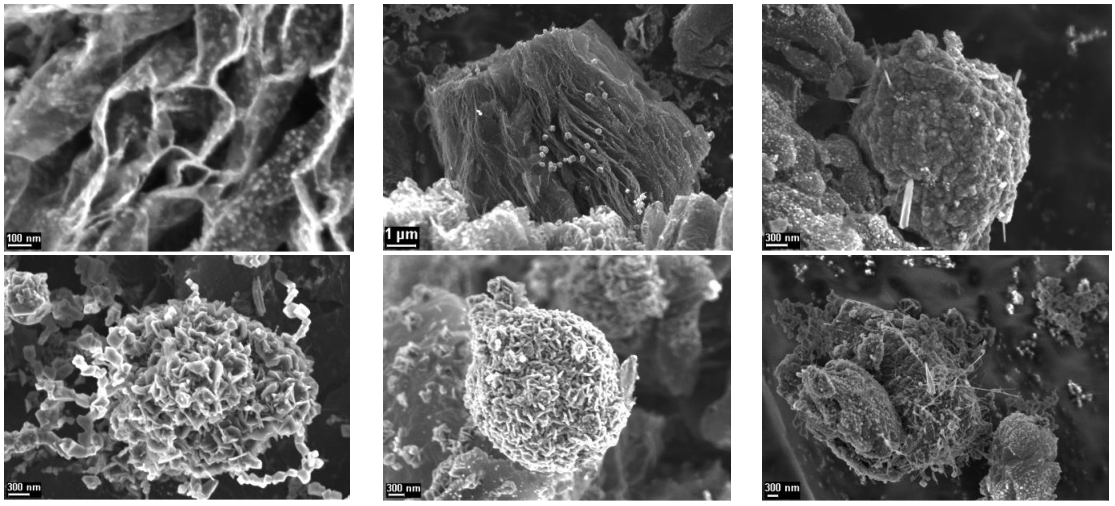

Fig. 4 - SEM images

SHS is proved to be a fast and efficient method for production of nanocomposite materials. Process parameters like combustion atmosphere, pressure and reactants stoichiometry control not only the reaction yield but also the composition and morphology of products.

Acknowledgement. GO was kindly provided by Institute of Electronic Materials Technology, Warsaw

REFERENCES

[1] K.S. Novoselov, V. I. Falko, L. Colombo, P. R. Gellert, M. G. Schwab, and K. Kim, Nature, 490, 2012, 192.

[2] R. L. Zhang, J. Zhang, C. G. Wang, F. H. Li, L. Liu, and H. Z. Cui, ECS J. Solid State Sci. Technol., 5, 2016, M127.

[3] M. Fronczak, P. Fazekas, Z. Karoly, B. Hamankiewicz, M. Bystrzejewski, Chemical Engineering Journal, 322, 2017, 385-396.

[4] G. Merzhanov and I. P. Borovinskaya, Dokl. Chem., 204, 1972, 429.

[5] A. Huczko, M. Kurcz, A. Dąbrowska, M. Fronczak, M. Bystrzejewski, M. Drozdowski, D. P. Subedi, B. P. Kafle, B. K. Kafle, P. Lamichhane, P. Saren and S. K. Tiwari, ECS J. Solid State Sci. Technol., 6, 2017, M3090.

[6] A. Huczko, M. Kurcz, Machines, Technologies, Materials, 6, 2016, 43.

[7] Huczko, M. Osica, A. Rutkowska, M. Bystrzejewski, H. Lange, S. Cudziło, J. Phys. Condens. Matter, 19, 2007, 395022, 2. Huczko, M. Osica, M. Bystrzejewski, H. Lange, S. Cudziło, J. Leis, M. Arulepp, Phys. Status Solidi B, 244, 2007, 3969.

[8] A. Huczko, M. Osica, M. Bystrzejewski, H. Lange, S. Cudziło, J. Leis, M. Arulepp, Phys. Status Solidi B, 244, 2007, 3969

[9] S. Paszkiewicz, I. Taraghi, A. Szymczyk, A. Huczko, M. Kurcz, B. Przybyszewski, R. Stanik, A. Linares, T. A. Ezquerra, Z. Rosłaniec.,, Composite Sci. Technol., 146, 2017, 20.

PREPARATION OF ADVANCED ZrB_2 BASED CERAMICS BY SHS, HOT PRESSING AND SPARK PLASMA SINTERING METHODS

I.V. Iatsyuk[1]*, Yu.S. Pogozhev[1], D.Yu. Kovalev[2], N.A. Kochetov[2], E.A. Levashov[1]

[1] National University of Science and Technology "MISIS", Leninsky prospect, 4, Moscow, 119049, Russia
[2] Institute of Structural Macrokinetics and Materials Science, Russian Academy of Sciences, ul. Academica Osipyana, 8, Chernogolovka, 142432, Russia
* ivansvoy@mail.ru

Zirconium diboride ZrB_2 possesses a complex of unique physical and mechanical properties [1, 2]: high melting point (3245 °C), thermal conductivity (57.9 W / (m · K)), hardness (20-22 GPa), abrasion resistance, and resistance to aggressive environments. Constructional high-temperature ceramics based on ZrB_2, which is capable of long-term operation in an oxidizing environment at temperatures above 1500 °C, has low density and high strength characteristics at elevated temperatures. The use of such materials is promising in engineering industry [3], as well as for protective coatings deposition by PVD technologies [4, 5]. The main disadvantage of ceramics based on ZrB_2 is low crack resistance. To improve the oxidation resistance and strength of ceramics based on ZrB_2, various alloying additives are used, for example $ZrSi_2$, $TaSi_2$, $MoSi_2$ and etc. [6-9]. Prospective methods for obtaining of ZrB_2 based ceramics are hot pressing (HP), spark plasma sintering (SPS) and SHS [7, 10, 11].

In this paper, the kinetics and mechanism of combustion of Zr-Si-B-(C) mixtures, the staging of chemical reactions in the combustion wave during synthesis of ceramics based on ZrB_2 with silicon containing dopants were studied. The experimental dependences of T_c and U_c on T_0 were determined, the values of effective activation energy of combustion process E_{eff} were calculated to be around 170-200 kJ/mol, which is an evidence that the limiting stage is the liquid-phase interaction. The staging of chemical transformations in combustion wave was studied by dynamic XRD. It was found that during the first stage of reaction, ZrB_2 forms from the melt, and then, after insignificant period of time (0.1-0.2 s) silicon containing binder forms due to interaction of molten silicon with other components.

Compact ceramics based on ZrB_2, characterized by high hardness (20-24 GPa) and low residual porosity (less than 1.5%), were manufactured using SHS technology, as well as hybrid technologies of SHS + HP and SHS + SPS. Microstructure and elemental composition of the compact synthesized samples before (cross sections and fractures) and after (fractures) annealing were studied using SEM, EDS and XRD techniques. Figure 1 shows typical microstructures of the compact samples based on ZrB_2 with Si-containing binder, obtained by SHS (Fig. 1a) and by hybrid SHS + HP technology (Fig. 1b).

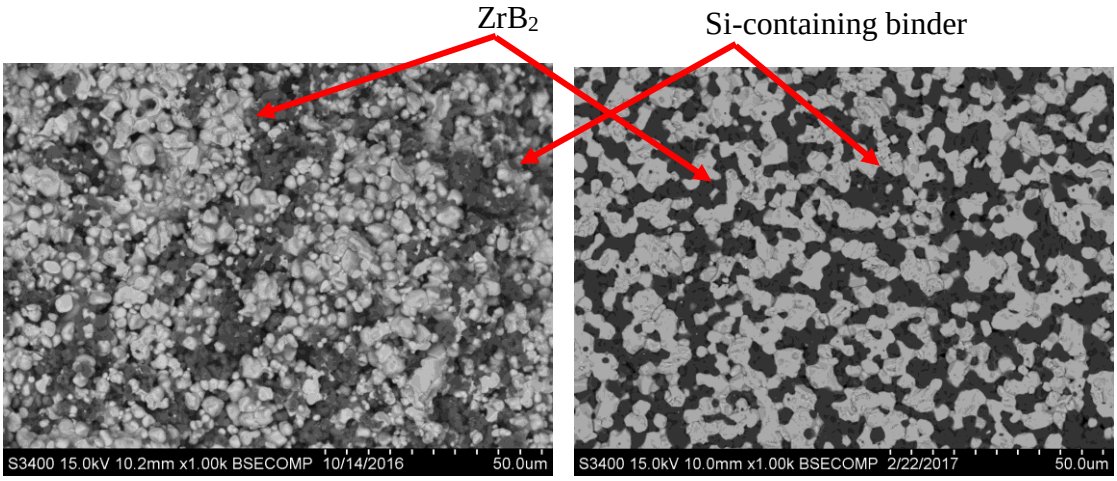

Figure 1 - SEM images of microstructure of the samples based on ZrB_2 with Si-containing binder obtained by (a) force SHS-pressing and (b) by hybrid SHS+HP technology

To study the oxidation resistance compact samples were annealed in air at a temperature of 1200 °C for 30 hours. During the oxidation measurements of the samples mass change were fulfilled ad every 5 hours of the tests. It was shown that during the oxidation of the samples, depending on their composition, a film with thickness of 10-40 μm and consisting of complex oxides SiO_2-ZrO_2-B_2O_3, $ZrSiO_4$ is formed on the surface. This film acts as an effective diffusion barrier reducing the oxidation rate. Oxidation rates were determined from the kinetic curves and were in the range of 0.0055-0.022 mg/(h×cm^2). After annealing for more than 10 hours, the mass loss was observed as a result of the evaporation of B_2O_2 and other gaseous oxides.

This work was carried out with partial financial support from the Ministry of Education and Science of the Russian Federation in the framework of state assignment No.11.1207.2017/ПЧ.

REFERENCES

[1] K.Upadhya, J.-M.Yang, W.P.Hoffman, Materials for ultrahigh temperature structural applications, Am. Ceram. Soc. Bull. 76 (12) (1997) 51–56.

[2] R. Licheri, R.Orrù, C.Musa, G.Cao, Combination of SHS and SPS techniques for fabrication of fully dense ZrB_2–ZrC–SiC composites, Mater. Lett. 62 (2008) 432–435.

[3] E. Wuchina, E. Opila, M. Opeka, W. Fahrenholtz, I. Talmy, UHTCs: Ultra-High Temperature Ceramic Materials for Extreme Environment Applications, Interface. 16 (4) 2007 30 – 36.

[4] Ph. V. Kiryukhantsev-Korneev, A. V. Bondarev, D. V. Shtansky, E. A. Levashov. Structure and properties of nanocomposite Mo—Si—B—(N) coatings, Protection of Metals and Physical Chemistry of Surfaces 51 (2015), 794-802.

[5] Ph.V. Kiryukhantsev-Korneev, J.F. Pierson, K.A. Kuptsov, D.V. Shtansky. Hard Cr–Al–Si–B–(N) coatings deposited by reactive and non-reactive magnetron sputtering of CrAlSiB target, Applied Surface Science 314 (2014) 104–111.

[6] D. Sciti, S.Guicciardi, A.Bellosi, Properties of apressureless-sintered ZrB_2–$MoSi_2$ ceramic composite, J. Am. Ceram. Soc. 7 (2006) 2320–2322.

[7] I.V. Iatsyuk, Yu.S. Pogozhev, E.A. Levashov, A.V. Novikov, N.A. Kochetov, D.Yu. Kovalev, Features of production and high-temperature oxidation of SHS-ceramics based on zirconium boride and zirconium silicide, Izv. vuzov. Poroshk. Metallurgiya i funkts. pokrytiya, 1 (2017) 29–41.

[8] W.W.Wu, G.J.Zhang, Y.M.Kan, P.L.Wang, K.Vanmeense, J.Vleugels, O. Vander Biest, Synthesis and microstructural features of ZrB_2–SiC-based composites by reactive spark plasma sintering and reactive hot pressing, Scr. Mater. 57 (2007) 317–320.

[9] Silvestroni L, Sciti D. Effects of $MoSi_2$ additions on the properties of Hf–and Zr–B_2 composites produced by pressureless sintering. Scripta Mater 2007;57:165–8.

[10] E.A. Levashov, Yu.S. Pogozhev, A.Yu. Potanin, N.A. Kochetov, D.Yu. Kovalev, N.V. Shvyndina, T.A. Sviridova, Self-propagating high-temperature synthesis of advanced ceramics in the Mo–Si–B system: Kinetics and mechanism of combustion and structure formation, Ceram. Intern. 40 (2014) 6541–6552.

[11] Yu.S. Pogozhev, I.V. Iatsyuk, A.Yu. Potanin, E.A. Levashov, A.V. Novikov, N.A. Kochetov, D.Yu. Kovalev, The kinetics and mechanism of combusted Zr-B-Si mixtures and structural features of ceramics based on zirconium boride and silicide, Ceram. Intern., 42 (2016) 16758-1676.

STUDYING HARDNESS WITH SUB-MICRON LATERAL RESOLUTION OF COMPOSITE MATERIALS PRODUCED BY SHS WITH THE HELP OF PICOINDENTOR BUILT IN A HIGH RESOLUTION SCANNING ELECTRON MICROSCOPE

M. Kalina[*1], G. Oniashvili[2], G. Tavadze[2] , Z.Aslamazashvili[2], G.Zakharov[2]

[1] Dept. of Materials Sci. & Eng., Technion – Israeli Institute of Technology, Technion City, Haifa 32000, Israel
[2] Ferdinand. Tavadze Institute of Metallurgy and Materials Science,10 E.Mindelistr,Tbilisi 0111, Georgia
*mkalinar@technion.ac.il

One of important application of SHS technology is a fabrication of armor plates from hard materials based on ceramics-ceramics or metal-ceramics composite materials. Such composite materials should have high mechanical properties with a combination of a low specific density and low prices. Practically, it has been shown that high values of hardness and fracture toughness result in enhanced ability to withstand destroying. However, an exact theory describing a material destroying under ultra-fast dynamic loading does not exist so far. The situation becomes more complicated for composite materials produced by a fast SHS compacting. Different constituents of a composite material may have different mechanical properties and different ratios of thermal expansion. For this reason, some grains can be partially stretched and other grains - partially compressed relative to their equilibrium state. Therefore, the material produced by such a way presents a complex state with alternating stretching and compressing fields of stresses. An experimental study of such state can help to illuminate the nature and mechanism of crack propagation and, finally, provide us with understanding material destroying under the ultra-fast dynamic loading. However, so far mechanical properties of materials could be measured at macro-scale only. A goal of the present paper is to describe novel possibilities for studying hardness with a sub-micrometer lateral resolution through the use of a picoindentor built in a high-resolution scanning electron microscope (HR SEM).

The current study was carried out on a specimen of a T-B-N composite produced by SHS. Powders of boron nitride and titanium were used as initial materials. The process flow included weighting and mixing initial powders with functional additives, mechanical milling and preliminary pressing followed by synthesis by SHS compacting proceeded in combustion mode. In the process of the synthesis, active atoms of nitrogen originated from decomposition of boron nitride are released and interact with melted titanium. As a result, formation of titanium borides and titanium nitrides took place. For microscopy study, a piece of the specimen was cut from the produced sample using a diamond wheel and mounted in an epoxy resin. It was then grounded on a 180-grit silicon carbide paper and polished sequentially with 9 μm, 3 μm and 1 μm water-based diamond suspensions. Finishing of the sample preparation was done with a 50 nm colloidal alumina.

XRD patterns measured from the specimen showed the presence of the following phases: TiB phase (orthorhombic, space group 62), $TiN_{0.5}$ (or Ti_2N) phase (cubic, space group 225) and a small amount of TiB_2 phase (hexagonal, space group 191) and Ti(B) phase (hexagonal, space group 194). Typical SEM image in secondary electrons (SE) aquired from the specimen surface

is shown in Fig.1, where numbers denote grains of Ti_2N and TiB phases found by EDS and EBSD analysis.

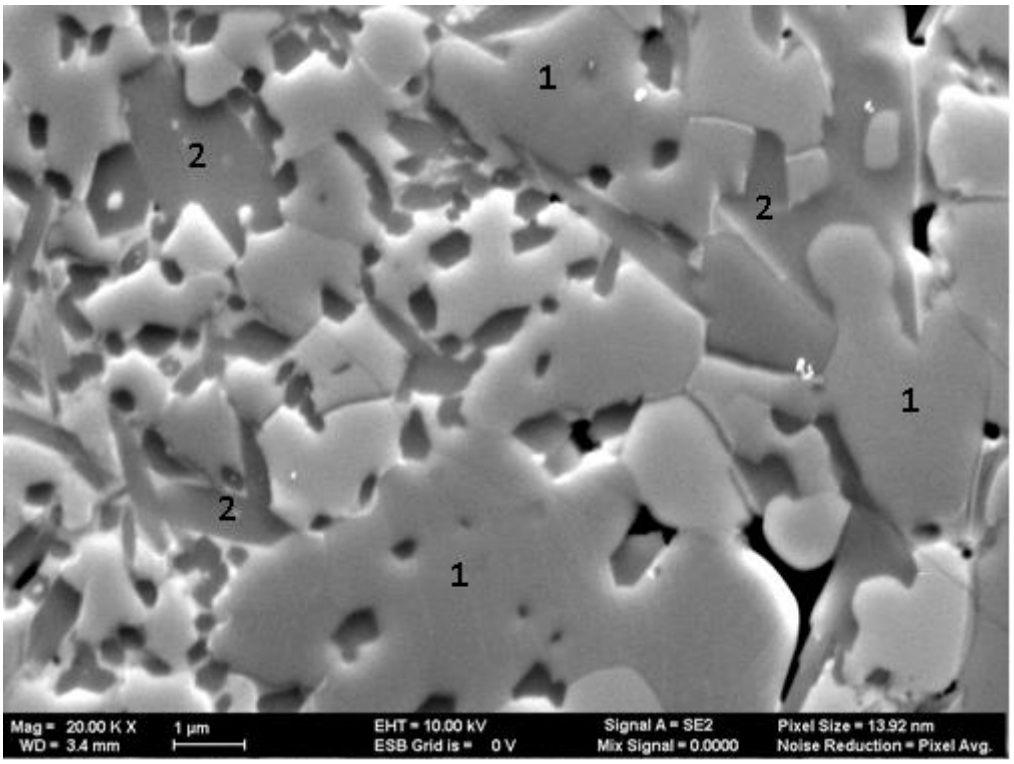

Fig. 1 - SE image measured from Ti-B-N specimen: 1 denotes grains of Ti_2N phase and 2 – grains of TiB phase.

Local measurements of hardness and Young's modulus were performed with the help of a Hysitron PI 85 picoindentor built in a HR SEM ZEISS Ultra Plus. A typical experimental layout is shown in Fig.2. The studied specimen is mounted on a piezo-stage of the picoindentor in such a way that the direction of movement of the picoindentor tip is perpendicular to the specimen surface. The picoindentor on a special holder is loaded in the microscope specimen chamber. To observe the studied surface the holder is tilted at 10°. A point for indentation is selected on the electron image and directed under the tip by pieze stage controls. Fig.3 presents a general view of the tip above the tilted specimen surface. Arrows in Fig.3 denote points, where indentations were done. One can see that all indentations were produced within one grain of Ti_2N phase with sub-micrometer lateral resolution.

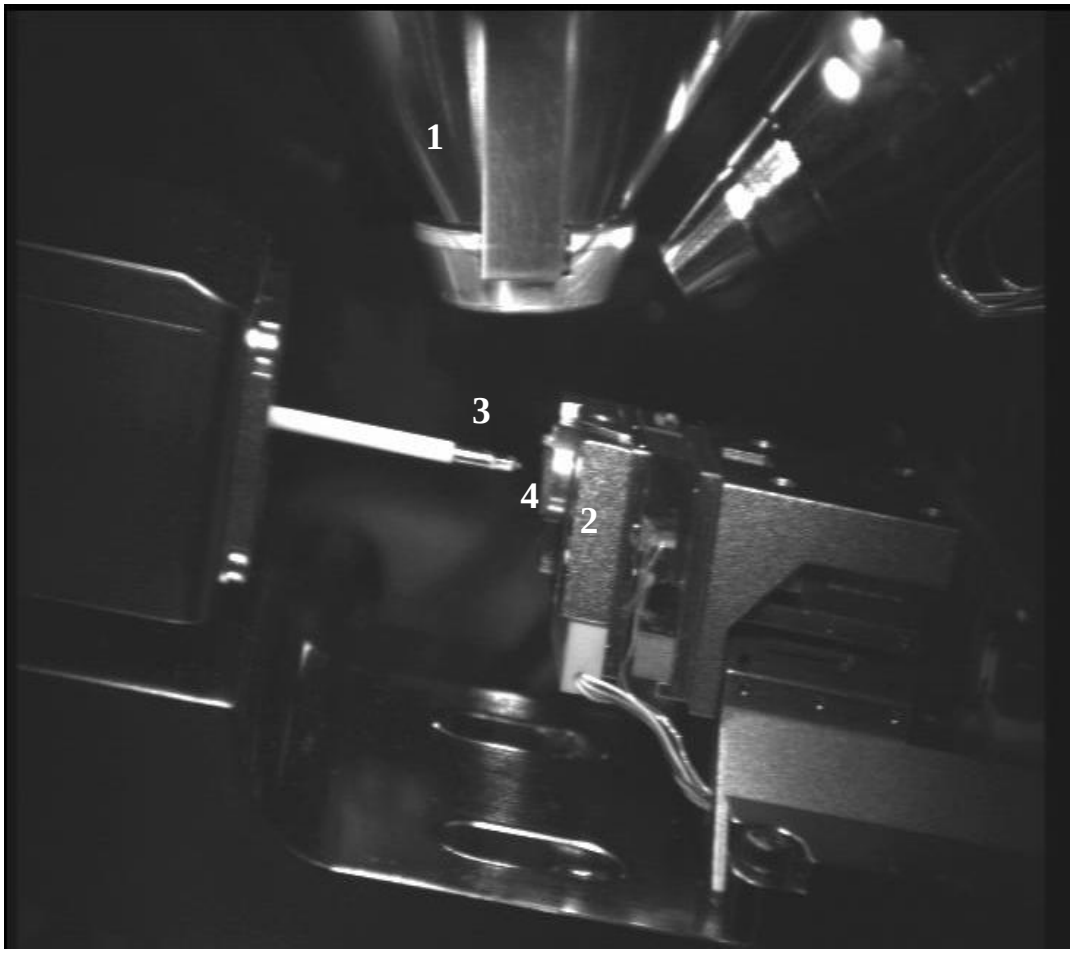

Fig.2: Experimental layout: 1 – electron column, 2 – specimen piezo-stage, 3 – picoindentor tip, 4 – specimen.

A plot of Force (μN) along the ordinate axis versus Displacement (nm) along the abscissa axis measured from one of points in Fig.3 is shown in Fig.4. Data handling of the presented plot makes it possible calculation of hardness (25.92 GPa) and reduced elastic modulus (265.6 GPa). In such a manner, the introduced technique can be used for measurement of mechanical properties of separate constituents of composite materials with a sub-micrometer lateral resolution.

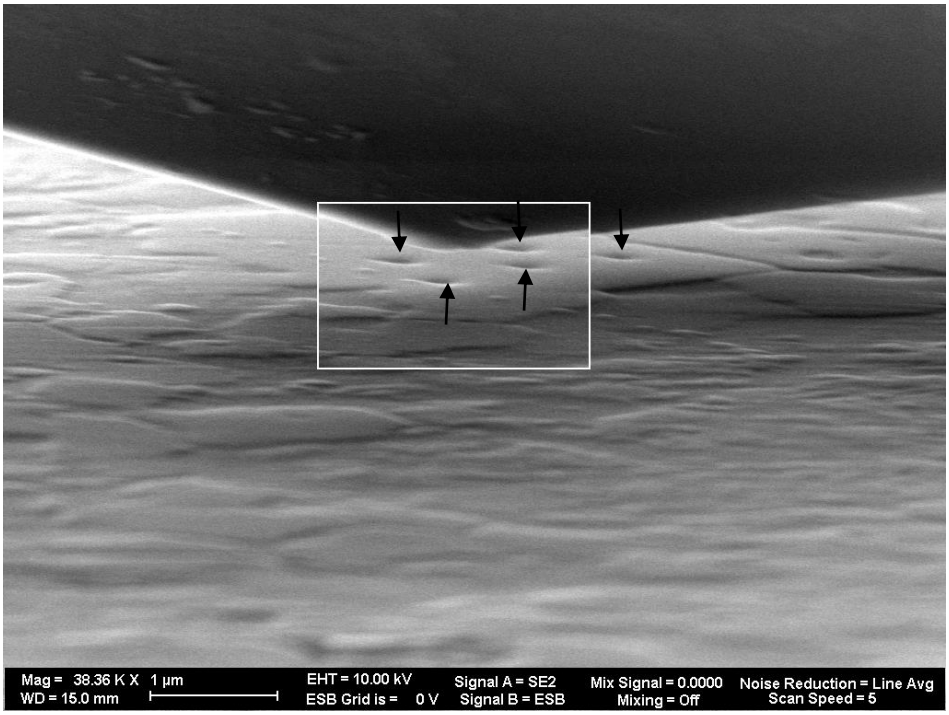

Fig.3: SE image from the specimen surface tilted at 10° with the picoindentor tip above the surface; arrows show points where indentation was done

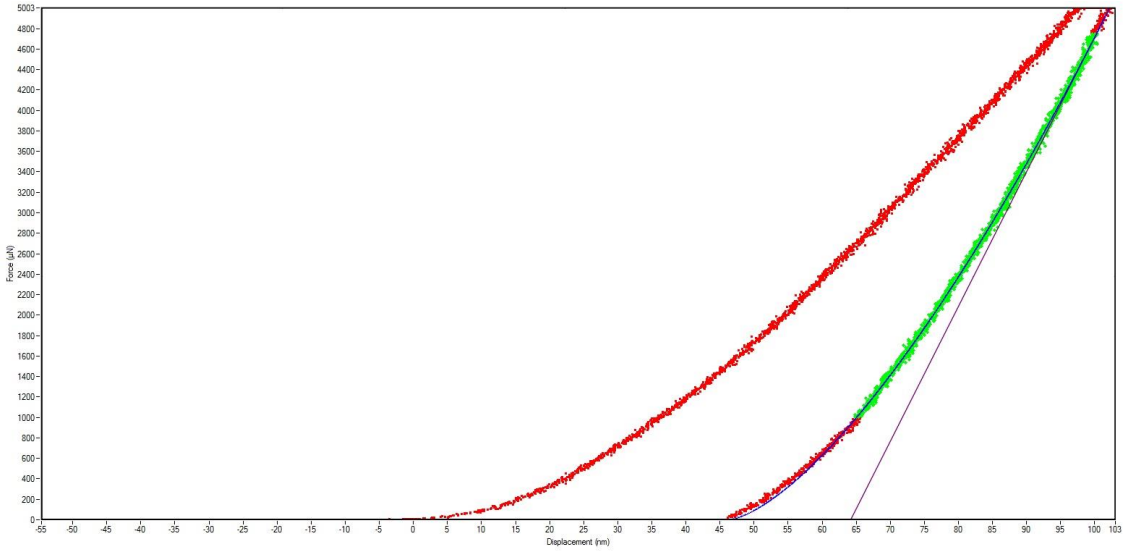

Fig.4: Force (µN) along the ordinate axis versus Displacement (nm) along the abscissa axis

SHS SURFACING OF Ti AND Ta SUBSTRATES

O.K. Kamynina*, S.G. Vadchenko, A.S. Shchukin, I.D. Kovalev

Institute of Structural Macrokinetics and Materials Science, Russian Academy of Sciences, Chernogolovka, Moscow, 142432 Russia
*kuz@ism.ac.ru

A popular trend in modern R & D is the design of materials that combine, two in one, the properties of ceramics and metals, such as hardness, strength, heat resistance, high-temperature strength, wear resistance, and ductility [1]. In this communication, we report on the deposition of multilayer ceramic coatings onto Ti and Ta substrates by the method of SHS surfacing.

Commercial powders of Ti (PTS brand), carbon black (P804T), and Si (d<10 μm, 99.4% pure) were used to prepare Ti + 0.5C; Ti + Si, 5Ti + 3Si, and Ti + 0.65C pellets. The Ti foils 180 and 270 μm thick were used as a substrate. Sandwich-type samples were ignited (under a load of 400 g) in a closed reactor under 1 atm of Ar to yield a strong metal–ceramic joining [2]. In case of Ta substrate (100-μm foil), the tablets had a three-layer structure: (Ti + 0.65C)/(Ti + 2B)/(5Ti + 3Si); these were ignited under a load 3360 g. Combustion products were characterized by SEM, EDS, and XRD.

Combustion products represented graded materials with changing composition and structure. The absence of clearly pronounced transition zones is indicative of good diffusion-assisted intermixing of constituent components. Comparative analysis has shown that the important prerequisites for good joining between ceramic coating and metallic substrate are: (a) the presence of the liquid phase, (b) wettability of a metal, and (c) closeness of combustion temperature to the melting point of a substrate. Due to possibility of varying green composition within wide limits, SHS method opens up new horizons for deposition of multilayer coatings onto metallic substrates.

This work was financially supported by the Russian Foundation for Basic Research (project no. 15-08-04595-a) and conducted by using the set of modern scientific instruments available for multiple accesses at the ISMAN Center of Shared Services.

REFERENCES

[1] G. Erkens, Surf. Coat. Technol., 201, (2007) 4806–4812.
[2] O.K. Kamynina, S.G. Vadchenko, A.S. Shchukin, I.D. Kovalev, Int. J. Self.-Propag. High-Temp. Synth., 25, (2016) 238–242.

PRODUCTION OF FERRO-MOLYBDENUM FROM DOMESTIC RESOURCES VIA METALLOTHERMIC PROCESS

S.Kan[1*], M.Bugdayci[1,2], K.Benzesik[1], O.Yucel[1]

[1]Metallurgical and Materials Engineering Department, Faculty of Chemical and Metallurgical Engineering, Istanbul Technical University, 34469, Maslak, Istanbul, Turkey
[2]Chemical and Process Engineering Department, Faculty of Engineering, Yalova University, 77100, Yalova, Turkey
* kan15@itu.edu.tr

Molybdenum is an alloying element which increases high temperature strength and corrosion resistance. Therefore molybdenum is widely used in stainless steels, high-speed steels and heat resisting steels. Molybdenum is added to steels as ferromolybdenum.

Molybdenum melting point is 2617 °C. Metal's main usage area is alloying element for steel applications. Liquid steel bath has 1565 °C temperature, this value is not enough to melting Molybdenum, so master alloys can be solution for this circumstance. FeMo is master alloy form of Iron and Molybdenum.

In this study ferromolybdenum is produced via SHS method and molybdenum trioxide is used as molybdenum resource. Molybdenite is roasted in rotary kiln under different conditions and sulphur content is reduced to 0.6 %. After roasting process ferromolybdenum is produced via SHS method. Mixture of ferrosilicon and aluminum are used as reductants. The main reactions occur during the process have shown below:

$2/3MoO_3 + FeSi \rightarrow 2/3Mo + Fe + SiO_2$

$2/3MoO_3 + 4/3\ Al \rightarrow 2/3Mo + 2/3Al_2O_3$

$2/3\ Fe_2O_3 + 4/3Al \rightarrow 4/3Fe + 2/3Al_2O_3$

Before the experiments, Thermodynamic software Factsage 6.4 used, in order to simulate the chemical and phase equilibria of arbitrary systems at different temperatures will be determined quantitative and phase compositions for the temperature range. Figure 1. Present probable phases of metallothermic reduction.

Experiments were made by changing the parameters such as reductant aluminum content and ferrosilicon content. FeMo containing Mo 60.5%, Fe 33.69% and Cu 3.12% has produced. Copper content is much higher than FeMo standards. After SHS process, copper content is reduced to under standard limit which is 0.5 % by leaching.

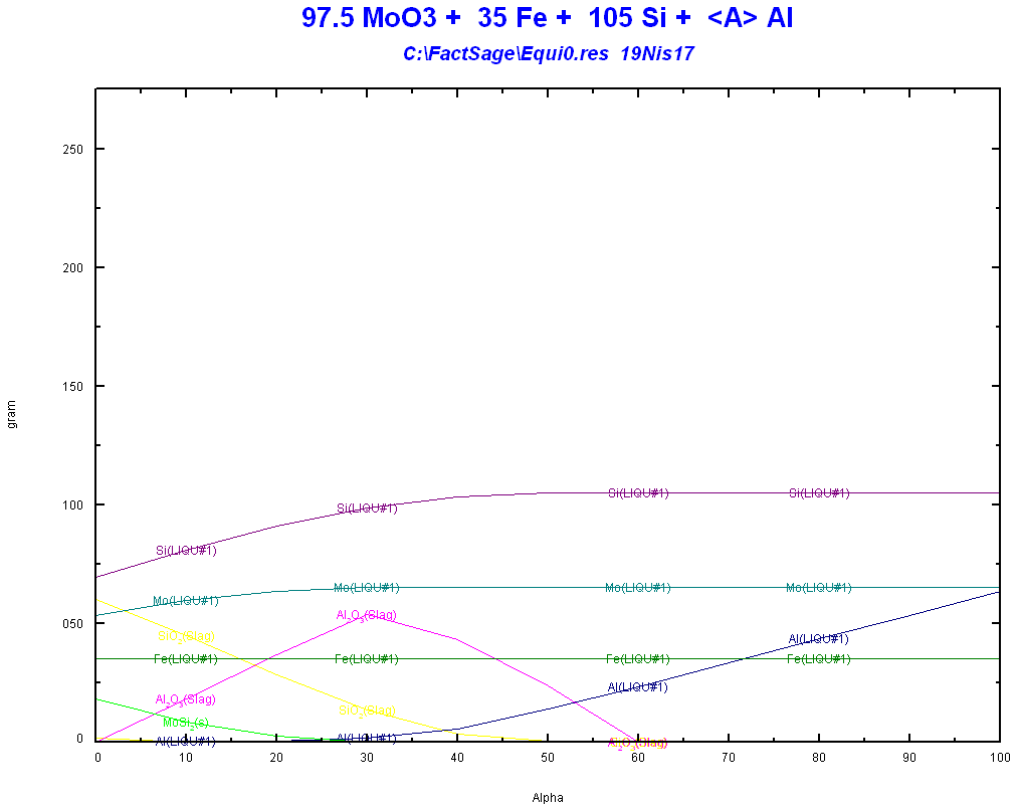

Figure1 - MoO_3 Reduction Conditions

The samples were characterized by using Atomic Absorption Spectrometer, X-Ray Diffraction, X-Ray Fluorescence, Scanning Electron Microscope and EDS techniques.

Self-propagating high temperature synthesis process (SHS) is a combustion synthesis process which presents some benefits such as high quality of production, low cost, low processing temperatures, low energy requirement, very short processing time and simple operation [1, 2].

In a SHS process, the ignition begins the combustion and it propagates throughout the reactant mixture yielding the desired product. However, the disadvantages of the process such as unreacted products due to undesirable reaction rates needs to be overcome by changing some parameters such as ignition temperature, particle size, additive, atmosphere etc. [3, 4].

REFERENCES

[1] O. Yücel, F.C. Sahin, A. Tekin, "The Preparation of Ferroboron and Ferrovanadium by Aluminathermic Reduction," High Temperature materials and Processes, 15 (1-2) (1996) 103–106.

[2] A.G. Merzhanov, "Self-propagating High-temperature Synthesis (SHS)," (ISMAN, Russia, 2002).

[3] I.P. Borovinskaya, "Chemical Classes of the SHS Processes and Materials," Pure and Applied Chemistry, 64 (1992) 919-940.

[4] V.I. Yukhvid, "Modifications of SHS Processes," Pure and Applied Chemistry, 64 (1992) 977-988.

[5] FactSage 6.4 Thermochemical Software for WindowsTM. Thermfact and GTT-Technologies (2016).

CONSIDERING STRUCTURAL HETEROGENEITY IN THE SYNTHESIS OF MATERIALS

G.F. Tavadze, D.V. Khantadze

LEPL - Ferdinand Tavadze Metallurgy And Materials Science Institute

From the structural point of view, inorganic materials are found either in the form of a crystalline, ordered, regular lattice (numerous minerals, metals, alloys, etc.), or in the form of disordered, irregular substances (liquids, amorphous substances, granular materials, etc.).

Building materials (cement, sand, gravel), most agricultural and food products (wheat, rice, granulated sugar, grains, etc.), as well as metallic and nonmetallic powders used in the SHS process, belong to disordered systems and are investigated by a special section of applied mechanics - mechanics of granular media.

The very notion of disorder in principle already implies the existence and order. For the microscopic description of the crystalline body, Bravais lattice models are created, to which the world of crystals obeys.

How to characterize a disordered structure? For atomically disordered systems, for example, liquids, numerous models have been proposed, which basically use two structural concepts: the hypothesis of quasi-crystallinity and Bernal's geometric model. The first allows the presence of atomic configurations with fragments of the crystal structure in liquids. This hypothesis formed the basis for many variants of lattice theories, according to which simple liquids, including liquid metals, retain to a considerable extent the structural characteristics of the short-range order of pre-melting. In particular, it is believed that the structural element of the liquid is the "fuzzy" unit cell of the crystal.

Bernal pointed to a radical difference between the lattice structure and the irregularity and put forward the hypothesis that a dense irregular arrangement of particles in space is characterized by a symmetry of the fifth order, which is forbidden for crystalline bodies [1, 2].

Investigating the regularities of the irregular filling of a three-dimensional space by steel balls (the rigid sphere approximation) and using the mathematical theory of arrangements, a structural model of irregular packing was developed in [3]. The model describes the stacking density, the motifs for constructing the structure and the microscopic characteristics (coordination number, number of unlike contacts, their concentration and fractional dependencies), both atomically disordered and macroscopic disordered systems.

These results are successfully used in estimating the contribution of the size factor to the excess volume, for calculating the isotherms of the surface tension of the metal solution, for excess thermodynamic mixing functions, for ascertaining the causes of their concentration asymmetry, etc. The model has found further development with respect to SHS processes [4].

Powder materials of different physico-chemical nature participate in the SHS process. In this case, every expected process begins at the points of contact of heterogeneous particles. This trivial statement does not require clarification, since in the absence of heterogeneous contacts no process can be expected. Consequently, it can be assumed that the number of heterogeneous contacts will significantly affect the SHS process.

In the present study, it is proposed to use the patterns of statistics of two fractional granular systems to estimate the number of heterogeneous contacts.

In our discussions there is used the simplest pattern of the granular environment according to which initial furnace charge is considered as statistical set metal (Ti, Al, Ni …) and nonmetallic (B, C, Si …) spherical particles of two sizes (*D*>*d*).

If the particles of metal powders *(D)* and nonmetal (*d*) are equal in size *(D = d)*, then when they are mixed, a mono fractional two-component statistical mixture is formed. In this mixture, contacts of three kinds can be observed: the particles contact themselves with similar particles, forming bonds 1-1 and 2-2, and also form heterogeneous contacts 1-2. According to the laws of statistical physics, the entropy of such a chaotic system is:

$$\Delta S = -R(N_1 \ell n N_1 + N_2 \ell n N_2), \qquad (1)$$

the probability of formation of bonds between identical particles is proportional to a numerical share of a component (N_i)

$$\frac{P_{1-1}}{ZN_0} = N_1^2; \quad \frac{P_{2-2}}{ZN_0} = N_2^2, \qquad (2)$$

while the concentration dependence of number of heteronymic contacts (P_{1-2}) is described by a symmetric parabola

$$\frac{P_{1-2}}{ZN_0} = N_1 N_2, \qquad (3)$$

where N_0 is a total number of particles in system, and Z is the coordination number of the particle, which, because of the mono fractionality of the system, is constant throughout the concentration interval. The maximum value of the packing density coefficient for mono fractional granular media is known to reach *K = 0.64.*

When mixing particles of different sizes, however, these regularities do not hold. The difference in the sizes of mixed pairs produces an increase in *K*, a change in the internal structure of the mixture and an increase in the number of dissimilar bonds as compared with mono fractional system [3]. This is easy to understand if we imagine that in an unordered system of identical particles, some of them are replaced in one case by the same number of colored particles of similar size, and in the other by particles of a larger size.. In the first case, the number of "multicolored" or unlabeled contacts can be calculated from formula (3) for ideal mixtures, and in the latter from an empirically established relationship for two fractional systems [3,4]. The number of heteronymic links of i.e. the number of contacts arising between large and small particles is estimated by the formula:

$$\frac{P(N)}{Z_0} = \frac{1}{4} N (1 - N)[\alpha (1-N) + \beta N], \qquad (4)$$

where $\alpha = \left(1 + \frac{D}{d}\right)^2$, $\beta = \left(1 + \frac{d}{D}\right)^2$, D and d is diameters of mixed particles (while $D > d$), and N is share of particles of the bigger size. Function (4) describes a set of asymmetrical parabolic curves whose shift toward the component characterized by a smaller particle size is

more pronounced for higher *D/d* ratios. At significant granulometric difference of the mixed powders (*D*>>*d*) the coefficient β in a formula (4) becomes negligible. One can therefore assume that the number of heteronymic contacts increases in proportion to $\left(\frac{D}{d}\right)^2$.

We will use the scheme [5] in which reactionary mix is considered on the scale of separate particles of powder (fig. 1). Let mix consist of two reagents, spherical particles of *D*>*d*; Stoichiometry of the planned reaction, the quantity and the size of particles is set by the experimenter. We will allocate some area in the neighborhood of a big particle where the ratio of big and small particles is approximately identical (the darkened area in the drawing). In [5] this area is called an elementary reactionary cell.

Since the mixture is statistical, it can be expected that the composition of each elementary reactionary cell will not strongly deviate from the average composition of the mixture. This fact greatly facilitates further research, since it allows, in the replacement of the entire continuum, to investigate its part in the form of a separate cell, and to generalize the result of observations to the entire system.

The exothermic mixture presented in Fig. 1 contains a lot of elementary reactionary cells. In the terminology of an unordered state, elementary reactionary cell is a Voronoi polyhedron that can be thought of in the mind near a large particle.

In the result of studying the statistical properties of Voronoi polyhedra arising in dilute bifractional mixtures and using the mathematical theory of arrangements [6, 7], a formula was proposed in [3] for estimating the coordination number in a system of various spheres

$$Z = \frac{Z_0}{4}\left(\frac{D}{d}+1\right)^2, \qquad (5)$$

where Z_0 is the coordination number of the monofractive (*D* = *d*) mixture. It follows that in irregular mixtures the number of spheres in simultaneous contact with the central one depends strongly on the fractional composition of the mixture (*D* / *d*) and can be estimated according to (5).

The reaction in a mixture with saturated elementary reactionary cell can be initiated by a thermal explosion or in the SHS mode. In the first case, the entire volume, similar to an inert body, is heated by the heat supplied from outside. When a certain temperature (ignition temperature) is reached, the reaction begins, and the initial mixture "burns" in the regime of a thermal explosion due to the increasing self-heating.

Unlike a thermal explosion, in the case of SHS, this process is localized in a micro volume, and accordingly the reaction site is also local. This is why SHS favourably differs from other technologies.

The development of the SHS process is as follows: after the heat pulse is applied, as a rule, by heating the tungsten filament, contact melting begins in elementary reactionary cell at the points of contact of the dissimilar particles to form combustion products (borides, carbides, silicides). The heat evolved during the reaction melts the metal particle and spreads outward, heating the adjacent layers of the charge. The metallic melt, wetting the newly formed solid combustion

products according to the mechanism of capillary spreading [8], penetrates to the next layers of heated but unreacted nonmetal particles and reacts with them. Thus, the combustion wave spontaneously moves along the sample. The presence of the liquid phase improves the contact between the reagents, enhances the processes of heat and mass transfer and, on the whole, intensifies the combustion process

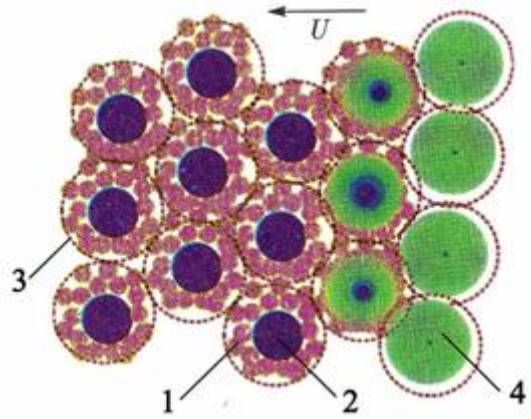

Fig.1 - Schematic structure of reaction mix and combustion wave front according to [5].
1 - and 2 - particles of initial reagents, 3 - elementary reaction cell, 4 - reaction products

From the presented combustion mechanism it follows that the number of heterogeneous contacts arising in the elementary reactionary cell between the metal and nonmetal particles determines the successful development of the synthesis process - the greater the number of unlike contacts or the higher the fractional difference *(D / d)* between the particles of the mixed reagents, the more efficient the synthesis reaction. In this case, it is obvious that the particles of a relatively easily fusible reactant should be larger than the particles of the reagent with a higher melting point.

REFERENCES

[1] Бернал Дж. Д. Геометрический подход к структуре жидкостей. Успехи химии. - 1961, 60, № 10, 1312-I323 с.

[2] Бернал Дж. Д. О структуре жидкости. - В кн.: Рост кристаллов; Доклады 3- го Московского совещания по росту кристаллов. М.: Наука, 1965,с. 149-162.

[3] Хантадзе Д. Структурные модели и свойства металлических расплавов. Тбилиси, «Форма», 2009, 160с.

[4] Giorgi F. Tavadze, Alexander S. Shteinberg. Production of Advanced Materials by Methods of Self-Propagating High-Temperature Synthesis. Springer, 2013, 156p.

[5] Рогачев А.С., Мукасьян А.С. Горение для синтеза материалов: введение в структурную макрокинетику. Москва, ФИЗМАТЛИТ, 2012, 398с.

[6] Toth l.Fejes. Lagerungen in Der Ebene auf der Kugel und im Raum. Springer-Verlag.Berlin- Gottingen-Heidelberg. 1953. Перевод: Тот Ласло Фейеш. Расположение на плоскости, на сфере и в пространстве.- М.: Госиздат физ. мат. литературы, 1958, 364 с.

[7] Барановский Е.П. Упаковки, покрытия, разбиения и некоторые другие расположения в пространствах постоянной кривизны. - В кн.: Алгебра, топология, геометрия. - М.: ВИНИТИ АН СССР, 1969, с.I89-225.

[8] Шкиро В.М., Боровинская И.П. Физика горения и взрыва. 1976, 6, 945-948.

MAX COMPOUNDS BY SHS IN Ti–Al–C–B SYSTEM

E.A. Amosov[1], E.I. Latukhin[1], D.Yu. Kovalev[2], , S.V. Konovalikhin*[2], A.E. Sytschev[2]

[1]Samara State Technical University, Samara, Russia
[2] Institute of Structural Macrokinetics and Materials Science, Russian Academy of Sciences, Chernogolovka, Moscow, 142432 Russia
*ksv17@ism.ac.ru

Due to unique combination o their properties, MAX compounds $M_{n+1}AX_n$—where M is a trabsition metal, A a group IIIA or IVA element, and X = C, N—are thought to be very promising for numerous applications [1–3]. In this communication, we report on the SHS of a MAX phase with X = B from 3Ti + 2Al +2[(1 – *x*)C + *x*B] green powder compacts (*x* = 0.0, 0.15, 0.25, 0.50, 0.75, see Table 1). Combustion reaction was monitored by time resolved X-ray diffraction [4] and its products were characterized by conventional XRD (DRON-3M) with Rietveld refining.

Table 1 - Phase composition of the final product as function of boron content, at.%.

% at. B	Ti_2AlC	Ti_3AlC_2	TiC	TiB_2	$TiAl_3$	C	TiAl
0	28.5	46.3	5.6	-	19.6	-	-
15	10.6	41.1	7.9	6	34.5	>0	-
25	19.6	44.9	1.3	6.2	19.9	8.1	-
50	33.5	10.48	2	10.3	-	5.5	38.2
75	28.8	-	-	20.5	-	11.8	38.9

For $x < 50\%$, the diffraction patterns of products are nearly the same (Fig. 1a) and become different for $x \geq 50\%$ (Fig. 1b). The lattice parameters of Ti_3AlC_2 and Ti_2AlC varied within the limits of experimental spread (Table 2).

According to TRXRD results, combustion of 3Ti–2Al–2C occurs in several stages. At the first stage, predominant is the reaction yielding TiC crystals in the Ti–Al melt. In 5 s behind the wave, TiC dissolves in the melt thus giving rise ti formation of the MAX phases.

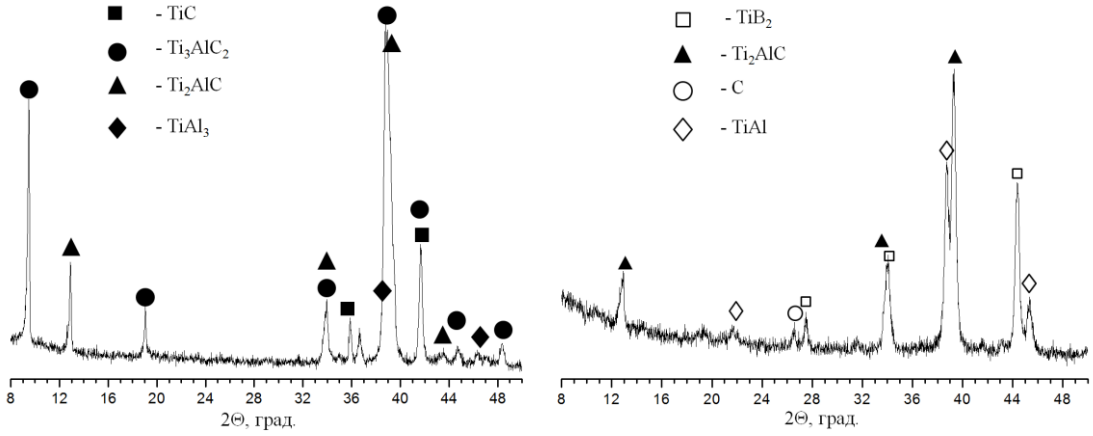

Fig. 1 - XRD patterns of products derived from 3Ti–2Al–2C (a) and 3Ti–2Al–2(0.25C–0.75B) green compacts (b).

Table 2 - Lattice parameters (*a*) of Ti_2AlC and Ti_3AlC_2 as a function of *x*.

x	Ti_3AlC_2	Ti_2AlC
0	3.08(3) 18.6(1)	3.06(4) 13.7(4)
15	3.08(3) 18.6(1)	3.05(8) 13.9(7)
25	3.07(3) 18.5(5)	3.06(6) 13.7(1)
50	3.07(4) 18.5(5)	3.05(7) 13.6(5)
75	– –	3.05(9) 13.7(2)
PDF2 000-52-0875 010-78-3753	3.069 18.501	3.06743 13.6988

We have assumed that the replacement of C atoms by larger B atoms is accompanied by an increase in lattice parameter [5]. Total amount of MAX phases attained a value of 75% while that of TiC, below 6%. An increase in *x* was accompanied by a decrease in the TiC content and appearance of free carbon in products.

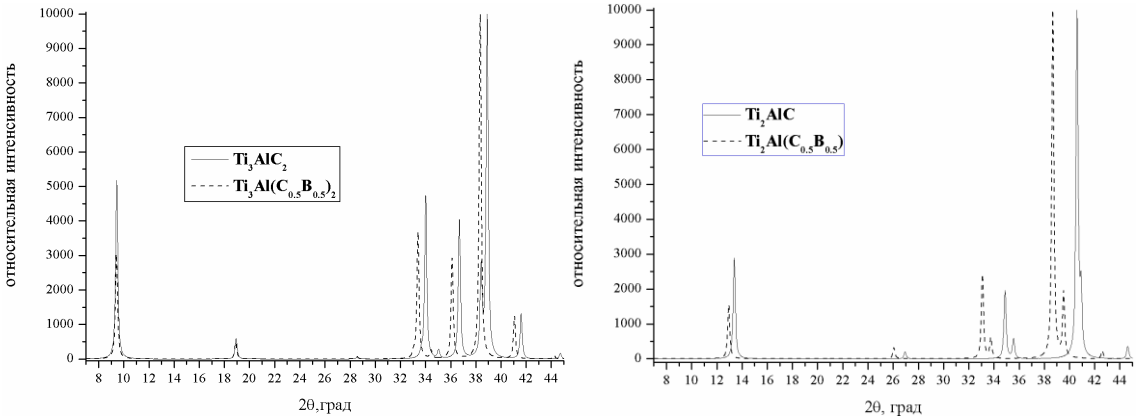

(a) (b)

Fig. 2 - Modeled XRD patterns of (a) Ti_3AlC_2 and $Ti_3Al(C_{0.5}B_{0.5})_2$ and (b) Ti_2AlC and $Ti_2Al(C_{0.5}B_{0.5})$.

Using program package MERCURY [6], we modeled the diffraction patterns of $Ti_3Al(C_{0.5}B_{0.5})_2$ and $Ti_2Al(C_{0.5}B_{0.5})$. The results are presented in Fig. 2. No new reflexes within the range $7 \leq 2\theta \leq 45°$ were found. But the intensities of 002 reflections ($2\theta \approx 9.6°$ for the 312 phase and $2\theta \approx 13.1°$ for the 211 phase) are slightly different. Nevertheless, this observation cannotbe regarded as serious evidence for the insertion of B atoms into the multiatomic systems under investigation.

No doubt, the feasibility of synthesizing $Ti_3Al(C,B)_2$ and $Ti_2Al(C,B)$ compounds from Ti–Al–C–B blends deserves further investigation.

This work was financially supported by the Russian Foundation for Basic Research (project no. 15-08-02331).

REFERENCES

[1] Barsoum M.W., MAX phases: Properties of machinable ternary carbides and nitrides, Wiley–VCH, 2013.

[2] R.M. Atikur, R.M. Zahidur, Am. J. Mod. Phys., 4, (2015) 75-91.

[3] Halim J., Chartier P., Basyuk T., Prikhna T., Caspi El'ad N., Barsoum M.W., Cabioch Th., J. Eur. Ceram. Soc., 37, (2017) 15–21.

[4] A.G. Merzhanov, I.P. Borovinskaya, V.I. Ponomarev, I.Shch. Khomenko, Yu.V. Zanevsky, S.P. Chernenko, L.P. Smykov, G.A. Cheremukhina, Dokl. Ross. Akad. Nauk, 328, 1993, pp. 72-74.

[5] A. Bouhemadow, R. Khenata, M. Chegaar, Eur. Phys. J. B, 56, (2007) 209-215.

[6] Macrae C. F., Bruno I. J., Chisholm J. A., Edgington P. R., McCabe P., Pidcock E., Rodriguez-Monge L., Taylor R., van de Streek, J., Wood P. A., J. Appl. Crystallogr., 41, (2008) 466-470.

MAX COMPOUNDS BY SHS IN Ti–Al–C–B SYSTEM

E.A. Amosov[1], E.I. Latukhin[1], D.Yu. Kovalev[2], , S.V. Konovalikhin*[2], A.E. Sytschev[2]

[1]Samara State Technical University, Samara, Russia
[2] Institute of Structural Macrokinetics and Materials Science, Russian Academy of Sciences, Chernogolovka, Moscow, 142432 Russia
*ksv17@ism.ac.ru

Due to unique combination o their properties, MAX compounds $M_{n+1}AX_n$—where M is a trabsition metal, A a group IIIA or IVA element, and X = C, N—are thought to be very promising for numerous applications [1–3]. In this communication, we report on the SHS of a MAX phase with X = B from 3Ti + 2Al +2[(1 – *x*)C + *x*B] green powder compacts (*x* = 0.0, 0.15, 0.25, 0.50, 0.75, see Table 1). Combustion reaction was monitored by time resolved X-ray diffraction [4] and its products were characterized by conventional XRD (DRON-3M) with Rietveld refining.

Table 1 - Phase composition of the final product as function of boron content, at.%.

% at. B	Ti_2AlC	Ti_3AlC_2	TiC	TiB_2	$TiAl_3$	C	TiAl
0	28.5	46.3	5.6	-	19.6	-	-
15	10.6	41.1	7.9	6	34.5	>0	-
25	19.6	44.9	1.3	6.2	19.9	8.1	-
50	33.5	10.48	2	10.3	-	5.5	38.2
75	28.8	-	-	20.5	-	11.8	38.9

For $x < 50\%$, the diffraction patterns of products are nearly the same (Fig. 1a) and become different for $x \geq 50\%$ (Fig. 1b). The lattice parameters of Ti_3AlC_2 and Ti_2AlC varied within the limits of experimental spread (Table 2).

According to TRXRD results, combustion of 3Ti–2Al–2C occurs in several stages. At the first stage, predominant is the reaction yielding TiC crystals in the Ti–Al melt. In 5 s behind the wave, TiC dissolves in the melt thus giving rise ti formation of the MAX phases.

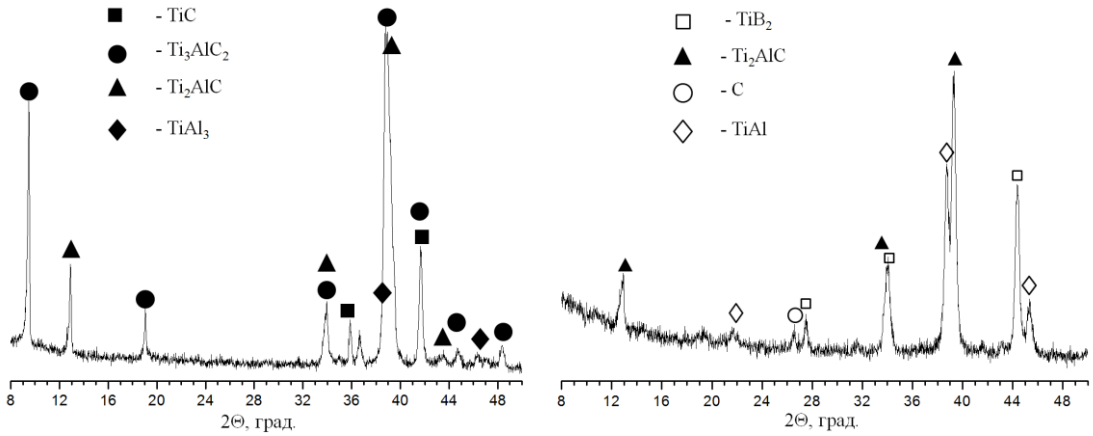

Fig. 1 - XRD patterns of products derived from 3Ti–2Al–2C (a) and 3Ti–2Al–2(0.25C–0.75B) green compacts (b).

Table 2 - Lattice parameters (*a*) of Ti_2AlC and Ti_3AlC_2 as a function of *x*.

x	Ti_3AlC_2	Ti_2AlC
0	3.08(3) 18.6(1)	3.06(4) 13.7(4)
15	3.08(3) 18.6(1)	3.05(8) 13.9(7)
25	3.07(3) 18.5(5)	3.06(6) 13.7(1)
50	3.07(4) 18.5(5)	3.05(7) 13.6(5)
75	– –	3.05(9) 13.7(2)
PDF2 000-52-0875 010-78-3753	3.069 18.501	3.06743 13.6988

We have assumed that the replacement of C atoms by larger B atoms is accompanied by an increase in lattice parameter [5]. Total amount of MAX phases attained a value of 75% while that of TiC, below 6%. An increase in *x* was accompanied by a decrease in the TiC content and appearance of free carbon in products.

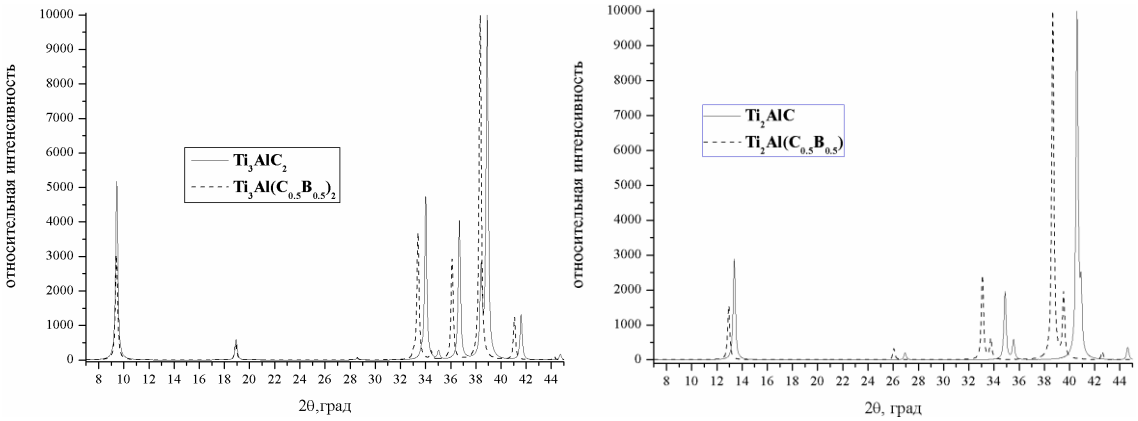

(a) (b)

Fig. 2 - Modeled XRD patterns of (a) Ti_3AlC_2 and $Ti_3Al(C_{0.5}B_{0.5})_2$ and (b) Ti_2AlC and $Ti_2Al(C_{0.5}B_{0.5})$.

Using program package MERCURY [6], we modeled the diffraction patterns of $Ti_3Al(C_{0.5}B_{0.5})_2$ and $Ti_2Al(C_{0.5}B_{0.5})$. The results are presented in Fig. 2. No new reflexes within the range $7 \leq 2\theta \leq 45°$ were found. But the intensities of 002 reflections ($2\theta \approx 9.6°$ for the 312 phase and $2\theta \approx 13.1°$ for the 211 phase) are slightly different. Nevertheless, this observation cannotbe regarded as serious evidence for the insertion of B atoms into the multiatomic systems under investigation.

No doubt, the feasibility of synthesizing $Ti_3Al(C,B)_2$ and $Ti_2Al(C,B)$ compounds from Ti–Al–C–B blends deserves further investigation.

This work was financially supported by the Russian Foundation for Basic Research (project no. 15-08-02331).

REFERENCES

[1] Barsoum M.W., MAX phases: Properties of machinable ternary carbides and nitrides, Wiley–VCH, 2013.

[2] R.M. Atikur, R.M. Zahidur, Am. J. Mod. Phys., 4, (2015) 75-91.

[3] Halim J., Chartier P., Basyuk T., Prikhna T., Caspi El'ad N., Barsoum M.W., Cabioch Th., J. Eur. Ceram. Soc., 37, (2017) 15–21.

[4] A.G. Merzhanov, I.P. Borovinskaya, V.I. Ponomarev, I.Shch. Khomenko, Yu.V. Zanevsky, S.P. Chernenko, L.P. Smykov, G.A. Cheremukhina, Dokl. Ross. Akad. Nauk, 328, 1993, pp. 72-74.

[5] A. Bouhemadow, R. Khenata, M. Chegaar, Eur. Phys. J. B, 56, (2007) 209-215.

[6] Macrae C. F., Bruno I. J., Chisholm J. A., Edgington P. R., McCabe P., Pidcock E., Rodriguez-Monge L., Taylor R., van de Streek, J., Wood P. A., J. Appl. Crystallogr., 41, (2008) 466-470.

POLYFUNCTIONAL POWDER SHS-MATERIALS BASED ON OXIDE BRONZES

M.K. Kotvanova*, S.S. Pavlova, N.N. Blinova, P.Yu. Gulyaev

Yugra State University, Khanty-Mansiysk, Chekhova, 16, Russia
* M_Kotvanova@ugrasu.ru

Alkaline oxide bronzes of transition metals are advanced materials of modern technology, because they have a unique combination of physical and chemical properties: electrical conductivity, thermal conductivity, chemical and thermal stability, corrosion resistance. Recently it was shown [1] that nanoparticles of tinaniun and tungsten oxide bronzes give high photothermal effect in laser heating of frozen biotissues, so they can be used as biofunctional materials.

Synthesis and physicochemical properties of oxide bronzes of titanium, molybdenum, tungsten are the subject of study by many authors. SH-synthesis of oxide bronzes was first proposed in our work [2]. Later, this method was used to produce molybdenum and tungsten bronzes with various compositions. Oxides of transition metals were chosen as precursors because of the similarity of their crystal structures Atoms of alkali metal in the process of bronze formation intercalate into the oxide lattice, occupying advantageous crystallographic positions (fig. 1). For titanium and tungsten frame structures with different types of octahedra connections form. For molybdenum bronze, as a rule, layered structure of MoO_3 is retained.

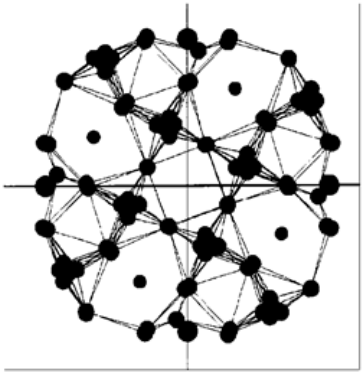

Fig.1. The projection of the tetrahedral bronze structure $Na_{0.33}WO_3$ on the X-Y plane

The possibility of obtaining oxide bronzes in the SHS-mode is determined by the thermodynamic characteristics of the chemical agents. In the absence of exothermic additives, the intercalation of potassium or another electropositive metal into the structure of the d-metal oxide is not justified thermodynamically. We proposed an effective exothermic mixture (CuO + d-metal), which led to the successful production of various SH-products of the oxide bronzes type. Reactions proceeded according to the schemes given below (as an example potassium-titanium bronze):

$$2\ CuO + Ti \rightarrow 2\ Cu + TiO_2 \qquad (1)$$

$$TiO_2 + 0{,}12\ KI \rightarrow K_{0,12}TiO_2 + 0{,}06\ I_2 \qquad (2)$$

We have shown that varying the quantitative ratios of the regents and the amount of the exothermic mixture can obtain bronze oxides of various compositions with different physical properties.

Using the system of optical control parameters SHS with automated analysis of thermal data [3], we estimated the combustion temperatures and velocity in a process of synthesis (fig. 2).

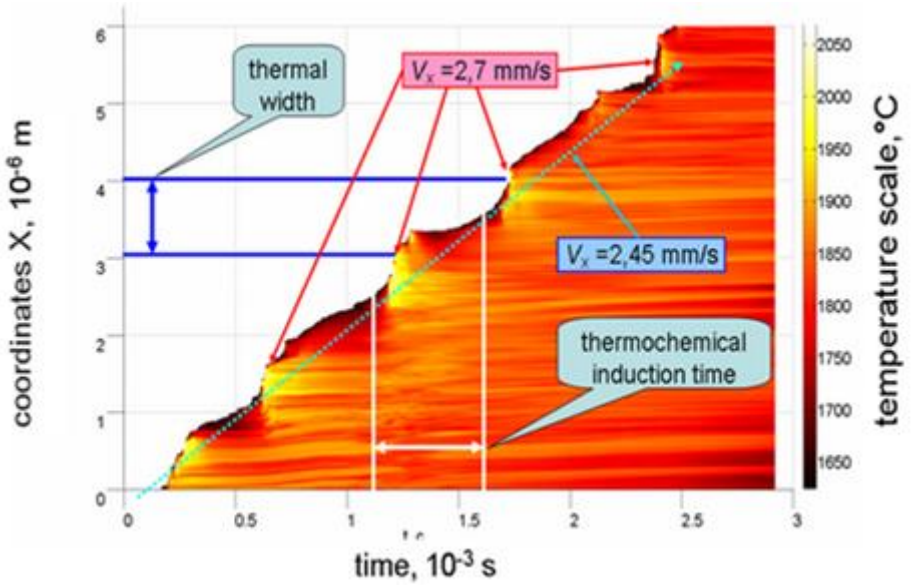

Fig. 2 - Thermogram for synthesis of K_xTiO_2

The obtained results are correlated with the thermodynamic characteristics and physicochemical properties of the initial oxides of titanium, molybdenum and tungsten (table). The most important factors are the enthalpies of formation, as well as the melting point of the initial oxides.

Table - Physicochemical characteristics of the initial oxides

Formula	$\Delta H^0_{f,\ 298}$, kJ/mol	Melting point,°C	Boiling point, °C	Combustion temperature for K_xMO_y, °C
TiO_2	– 943,9	1843	2500	2050
MoO_3	– 745,2	795	1257	No interaction
WO_3	– 842,7	1473	1667	800

This work was supported by the Russian Foundation for Basic Research (project No. 15-42-00106).

REFERENCES

[1] P.Yu. Gulyaev, M.K. Kotvanova, S.S. Pavlova, E.N. Sobol, A.I. Omel'chenko. Nanotechnologies in Russia, 7, 3-4, 2012, pp. 127-131.

[2] M.K. Kotvanova, S.S. Pavlova, N. N.Efremova. Proceedings of the Russian Universities: Chemistry and Chemical Technology, 9, 2013, pp. 88-91.

[3] M. Kotvanova, N. Blinova, P. Gulyaev, A. Dolmatov, S. Pavlova**.** Abstract Book of XIII International Symposium on SHS, Antalya, Turkey, 2015, p.160.

TIME RESOLVED X-RAY DIFFRACTION FOR DIAGNOSTICS OF SHS

D.Yu. Kovalev*, V.I. Ponomarev

Institute of Structural Macrokinetics and Materials Science, Russian Academy of Sciences,
142432 Chernogolovka, Moscow Region, Russia
* kovalev@ism.ac.ru

Study of the structure- and phase formation of materials during chemical reactions requires effective diagnostic methods that allow understanding the materials transformation. Creating of a sensitive high-speed X-ray detector is a fundamental step in developing of diffraction methods for dynamics of fast transformations in materials during chemical reactions. Time resolved X-ray diffraction (TRXRD) is a unique experimental method for study the evolution of the crystal structure during the process of phase transitions. The idea of the method consists in the registration sequence patterns with minimum time exposure from material in the process of its transformation, i.e. "diffraction cinema». The method allows to receive in controllable conditions of experiment with complete information not only about changes in phase composition, presence of intermediate products in high-temperature combustion front and in in a prehearing zone, but also to study influence of separate parameters (pressure, temperature, impurity) on the combustion process. This study presents the latest results obtained in ISMAN using the TRXRD.

TRXRD Study of Thermochemical Conversion of Iron Oxide [1]

Thermochemical conversion of transition metals compounds with forming of high-porous composite material, comprising nanosized particles of these metals can occur in the flameless combustion wave of energy-rich materials with the polymeric systems ballast. We investigated the phase formation in mixture of iron oxide (III) - hexogen in a nitrogen atmosphere. TRXRD method shown, that the process of reduction of iron oxide (III) in the wave of flameless combustion occurs in stage by stage manner (fig.1). The lines of the initial components disappeared when the combustion front reaches the detection area. We may observe the appearance of line of (200) FeO. Lines of the phase FeO are visible during 15 seconds and then disappear. At the same time the nucleation and growth of the intensity of the Fe_3O_4 phase lines (220) (311) (400) is observed. The analysis of the diffraction patterns reveals that the formation of the final product occurs through the intermediate phase FeO to the final Fe_3O_4 phase. The process occurs entirely in the solid phase, without amorphization of structure. Size of the coherent scattering area of Fe_3O_4 is 5-7 nm.

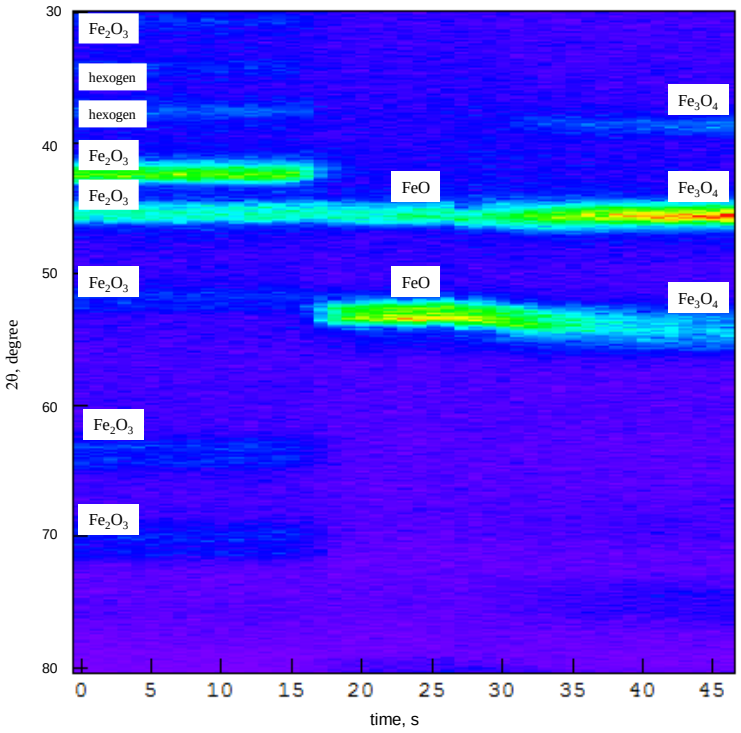

Fig. 1 - The diffraction pattern of the combustion process of mixture Fe_2O_3 – hexogen

TRXRD Study of Magnesium Diboride Obtained by SHS [2]

TRXRD was used to study the dynamics of phase formation in magnesium diboride during self-propagating high temperature synthesis (SHS) in the thermal explosion mode (fig.2). The MgB_2 phase was emerged without the formation of intermediate compounds. The effect of the heating rate on the formation mechanism of the MgB_2 phase was established. The presence of oxygen impurities has a significant impact on the kinetics and formation mechanism of MgB_2. If the heating rate exceeds 150 deg/min, the oxide coating is not formed around the magnesium particles, which results in the solid-phase reaction of $Mg+2B=MgB_2$ through a reactive diffusion mechanism. Moreover, the self-ignition temperature of the mixture is lower than the melting point for magnesium. Mechanical activation of the mixture leads to variations in the kinetics of MgB_2 formation, significantly increases the period of simultaneous existence of Mg and MgB_2, and reduces the temperature at which the reaction occurs.

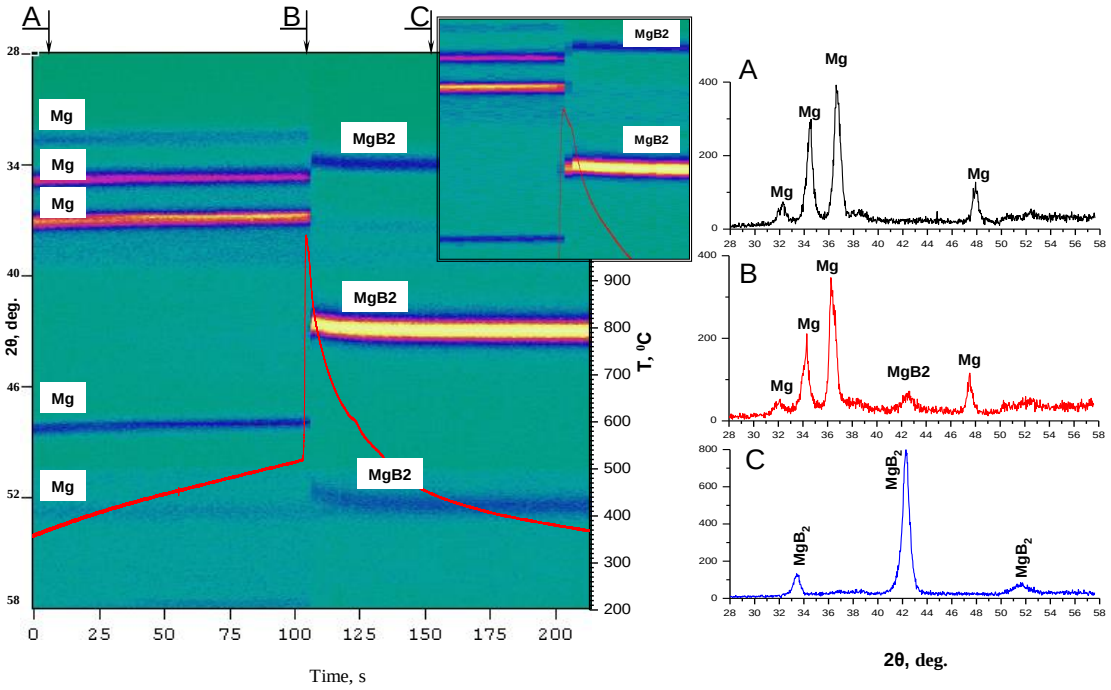

Fig. 2 - Diffraction pattern and thermogram of the Mg + 2B mixture

TRXRD Study of the Transition of an Amorphous TiCu Alloy to the Crystalline State [3]

An analysis of the diffraction pattern has shown that the crystallization of the amorphous TiCu alloy upon heating occurs for a short time (no longer than 0.5 s). A sharp transition is observed at the instant of crystallization, at which the intensity of the total diffraction pattern background decreases and diffraction lines of the crystalline phase γ-TiCu arise (fig.3). No intermediate crystalline phases are observed. The change in the alloy structure is accompanied by the exothermic thermal effect. The kinetics of the change in the total intensity of the diffraction spectrum in the period preceding the crystallization is non monotonic. The integrated spectral intensity decreases in a 10 sec before the occurrence of diffraction lines of the γ-TiCu phase at 300° C. The effect observed is related to the relaxation processes in the amorphous state and the onset of formation of long-range structural order.

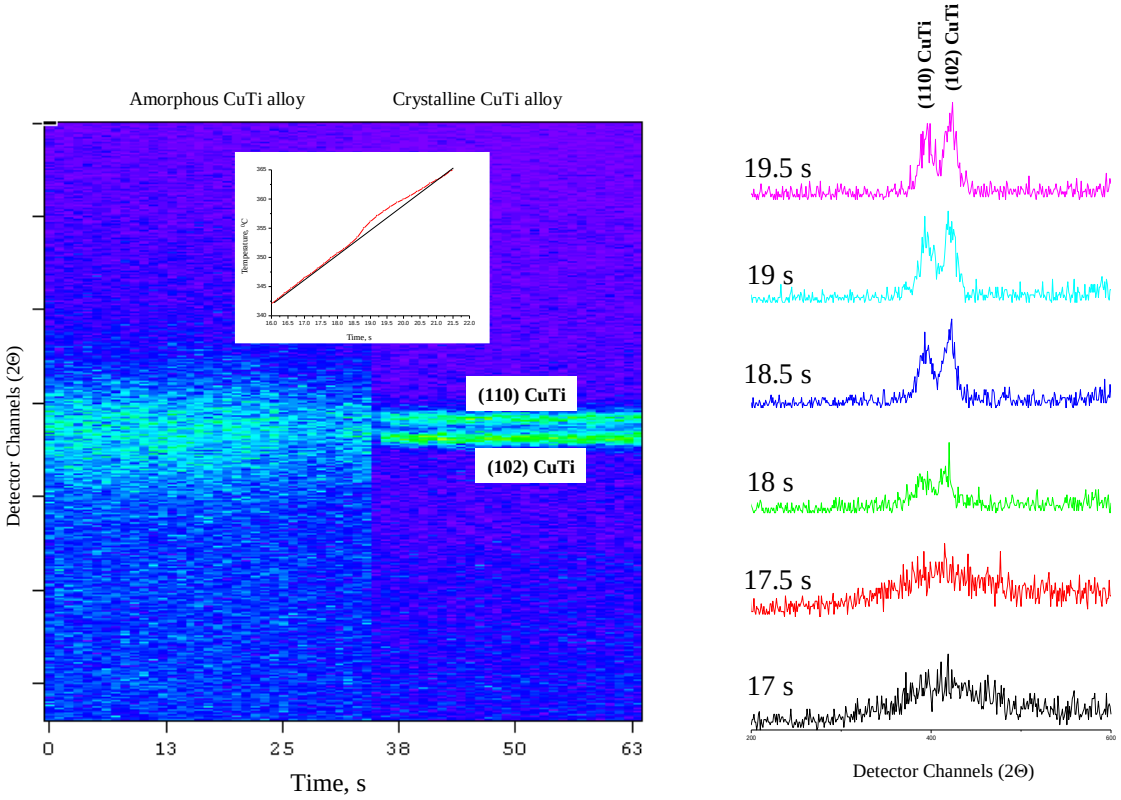

Fig.3 - Diffraction pattern and heating thermogram of the amorphous TiCu alloy.

Exothermic Self-Sustained Waves with Amorphous Nickel [4]

We investigated the self-propagating exothermic waves associated with crystallization of Ni from the amorphous precursor. TRXRD data indicates that amorphous nickel crystallizes in the temperature range 170° to 210°C. The results (fig.4a) show that, at v=120 K/min, long range order begins to develop at a temperature of 170°C. Figures 4b and c show several XRD patterns acquired at different stages of crystallization and kinetics of intensity for Ni (111) diffraction peak. The results of TRXRD analysis allow suggesting that the exothermic crystallization of α-Ni takes place between ~170° to 210°C during external heating conditions, with characteristic time scale on the order of few seconds. Self-diffusion of Ni atoms is the rate-limiting stage for crystallization.

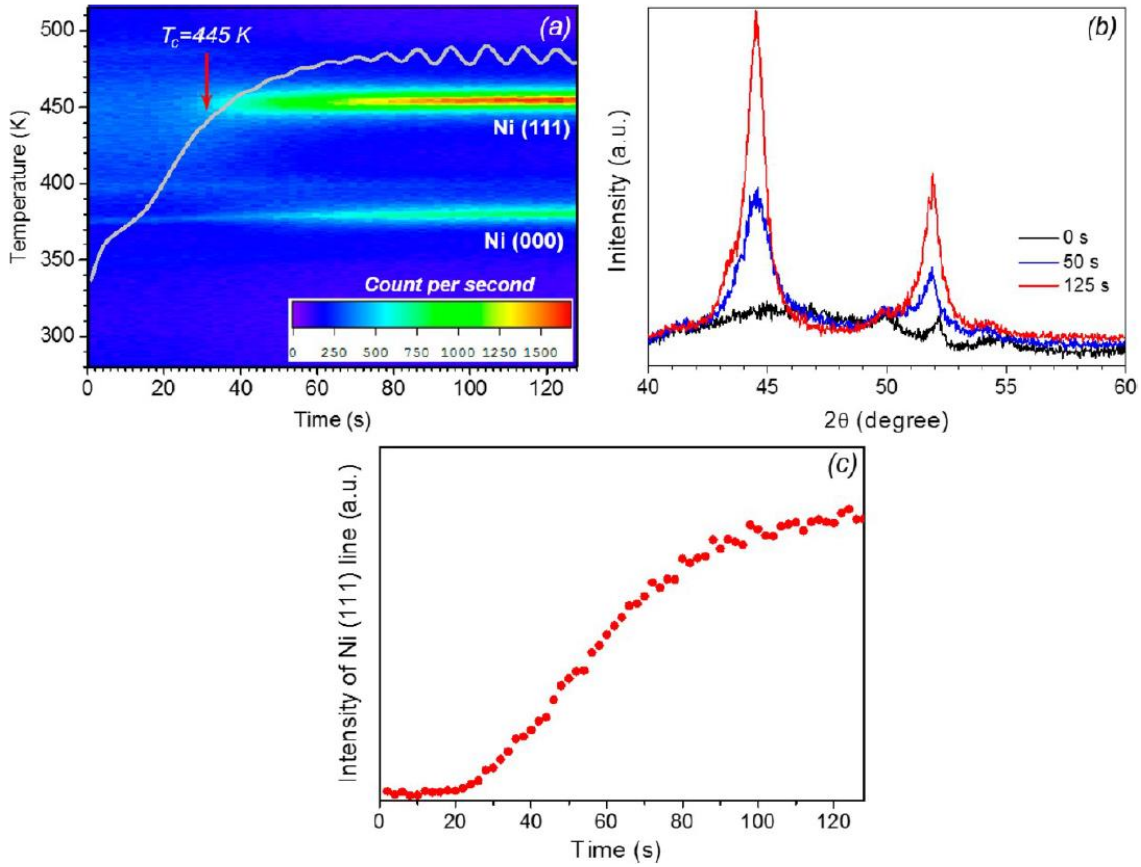

Fig.4 - TRXRD during crystallization of Ni from the amorphous precursor: dynamic of crystallization (a), selected diffraction patterns (b), and kinetics of crystallization (c).

Completed to date, TRXRD studies have shown high informative value method to determine the mechanism of structural and chemical transformations.

REFERENCES

[1] Yu.M. Mikhailov, V.V. Aleshin, D.Yu. Kovalev, XX Mendeleev Congress on general and applied chemistry. Vol. 2a: abstracts. – Ekaterinburg: Ural Branch of the Russian Academy of Sciences, 2016. – 464 p.

[2] D.Yu. Kovalev, A.Yu. Potanin, E.A. Levashov, N.F. Shkodich, Ceramics International, Vol.42, I.2, Part B, (2016) 2951-2959.

[3] D. Yu. Kovalev, S. G. Vadchenko, A.S. Rogachev, A.S. Aronin, M.I. Alymov, Doklady Physics, 2017, Vol. 62, No. 3, pp. 111–114.

[4] K.V. Manukyan, C.E. Shuck, M.J. Cherukara, S. Rouvimov, D.Yu. Kovalev, A. Strachan, A.S. Mukasyan, J. Phys. Chem. C, 2016, 120 (10), pp. 5827–5838.

NEW HORIZON TO PRODUCTION OF NARROW-FRACTION POWDERS AND GRANULES OF INTERMETALLIDES

V.V. Kurbatkina*[1], E.I. Patsera, A.G. Bodyan, E.A. Levashov

[1] National University of Science and Technology "MISIS", 4, Leninsky prospect, Moscow,119049, Russia
* vvkurb@mail.ru

NiAl and TiAl intermetallides are notable for their high scale resistance and heat resistance and are a basis of some structural materials for aerospace, gas turbine and atomic machinery. These alloys have valuable physicochemical and mechanical properties as well as better treatability in comparison to ceramic materials; and they are corrosion-resistant. In connection with development of additive 3d technologies for making geometrically complicated articles, there is a problem of obtainment of close-cut-fraction spherical powders with a regulated graininess. This work aims at obtaining close-cut-fraction powders based on NiAl and TiAl.

The particles of powders based on NiAl and TiAl obtained through various methods are typically sized at 40–60 μm. Such powders are difficult to crumble up, and plastic Ti_3Al phase present in TiAl-based alloys aggravates the situation.

In order to increase the porosity of the synthesis products and to reduce the particle size, the authors proposed to introduce gas-emitting and/or modifying functional additives into the reaction mixture. Peculiarities of the SHS process in Ni-Al and Ti-Al mixtures with the functional additives were studied. The structures and phase compositions of the products, including those tempered in a copper wedge, were researched using optical and electronic microscopy, X-ray spectral, X-ray structural and dynamic X-ray structural analysis. As a result of the research, sodium chloride was chosen as the functional additive. Influence of the NaCl concentration on the Ni – Al mixture combustion parameters was researched. It was demonstrated that the phase compositions of the synthesis products depend on the NaCl content, and the volatile sodium and aluminum chlorides play an active role in forming the synthesis products' structures. Formation of nickel aluminide starts in the warm-up zone as a result of the volatile chlorides' filtering from the combustion zone, then comes to its active stage in the combustion zone, and finishes in the postcombustion zone.

The SHS products from 90%(Ni-31,5%Al)+10% NaCl and 90%(Ti-36%Al)+10% NaCl mixtures are characterized by the NiAl and TiAl grain size of less than 20 μm, which is 2–3 times less than in the samples where to sodium chloride was not added. This is conditioned by crystallization of NaCl along the boundaries of the NiAl or TiAl grains, which impedes recrystallization of the grains and facilitates formation of the fine-grained structure. Optimal modes of conducting the synthesis and the NaCl concentration at which the SHS product will be easily crumbled up were determined. As a result, submicron powders based on NiAl and TiAl with a particle size of 5 μm and a nanoblock size of 30–70 nm (Fig. 1) were obtained.

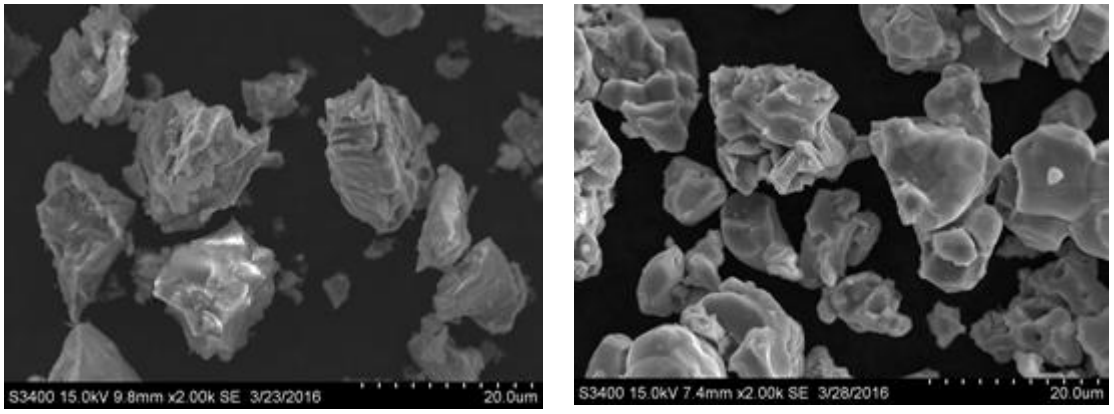

(a) (b)

Figure 1 - The microstructures of the SHS powders based on NiAl (a) and TiAl (b)

Through hot pressing and spark plasmatic sintering, the submicron powders were converted to compact metallomatrix composites based on NiAl and TiAl with a homogenous structure and a residual porosity of less than 0.1 %. The physico-mechanical properties and scale resistance of the sintered samples were studied. It was demonstrated that these composites have a higher level of physico-mechanical qualities as compared to materials of similar compositions prepared through alternative methods.

The submicron powders were used as precursors in the plasmatic spheroidization technology. Using this technology, spherical nonporous granules with a graininess of 10–20 μm (Fig. 2) have been obtained from the 20–50 μm fraction.

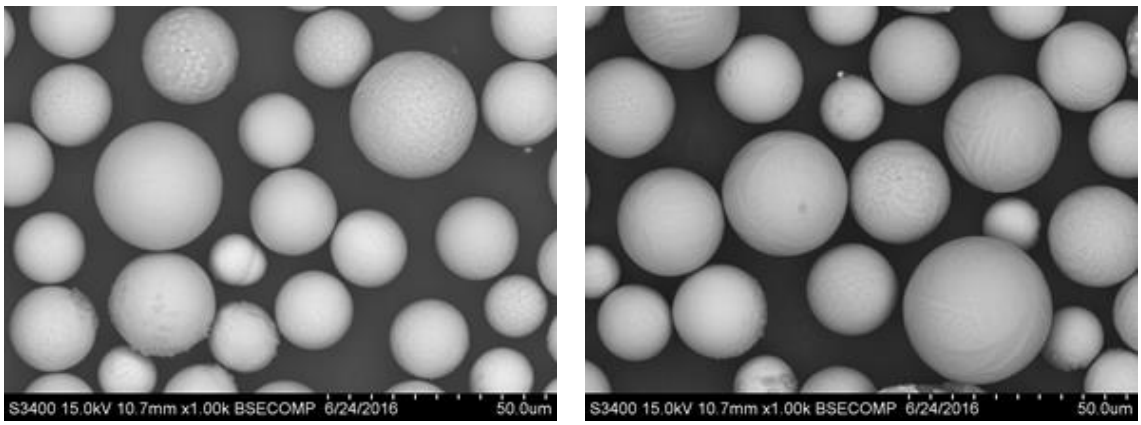

(a) (b)

Figure 2 - The microstructures of the NiAl (a) and TiAl (b) spherical powders

SYNTHESIS OF NANOSTRUCTURED COMPOSITE MATERIALS BASED ON ZIRCONIUM BORIDES

S.N.Kydyrbekova[1,2], A.Zh.Seidualiyeva[2], R.G.Abdulkarimova[1,2]

[1-] al-Farabi Kazakh National University, Almaty, Kazakhstan;
[2-] Institute of Combustion Problems, Almaty, Kazakhstan
symbat.kydyrbekova@mail.ru

Abstract: The aim of this work is synthesis of composite materials based on zirconium borides by self-propagating high temperature synthesis (SHS) method. The macrokinetic characteristics of SHS composite materials are determined depending on the composition of the initial charge. The SHS products were determined by X-ray phase analysis, which showed the high-temperature phases of zirconium borides and magnesium oxide. The influence of preliminary mechanochemical activation on the combustion temperature and on the strength characteristics of the samples was studied. Using scanning electron microscopy (SEM), the microstructure of the obtained materials was studied.

INTRODUCTION

Ceramics having high density made of zirconium compounds are used in packing thermocouples as melt filter and in induction furnaces (heated up to 2000℃) as a heating element. Zirconium diboride has a high melting point (over 3000 ° C), high hardness and strength, good thermal conductivity and electrical conductivity, high thermal stability. These qualities allow zirconium diboride to be a good material for high-temperature applications [1]. Composites based on zirconium diboride are used as crucibles, cutting tools, rocket engines. Zirconium diboride also has excellent resistance to oxidation. This indicates the fact stability of ZrO_2 was formed at high temperatures in an oxidizing atmosphere [2]. Composite materials based on ZrB_2-MgO are resistant to high temperatures and aggressive environment, they possess durability, also they are ecologically safe [3].

Synthesis must take place at a very high temperature for obtaining the refractory materials of high strength. At present, it is difficult to find the equipment with the ability to heat these materials. Moreover, simultaneous oxidation of two compounds is a very complex process. The most convenient method of obtaining these products is the method of self-propagating high temperature synthesis [4].

To increase the product yield, it is efficient to use the preliminary mechanical activated charge mixture (MA). It favorably influences the chemical reaction. In the process of mechanical activation due to complex mechanical influence (blow, an attrition) the ideal structure of substance changes and there appear various defects in the lattice. Preliminary mechanical activation increases the reactivity of SHS components [5].

EXPERIMENTAL

The process of SHS was carried out for the following system $ZrSiO_4$ + Mg + H_3BO_3. The process in this system mainly proceeds according to the reaction:

$$ZrSiO_4 + 2H_3BO_3 + 5Mg = ZrB_2 + 5MgO + 3H_2O + SiO_2$$

The SHS of the prepared samples was carried out in a muffle furnace at a temperature of 800℃, initiating combustion by magnesium. Temperatures of these samples were measured by heat-radiation pyrometer (optical pyrometer). The X-ray phase analysis of synthesis products was performed on a "DRON-4M" diffractometer with the use of cobalt K_a-radiation in 2θ = 10° -70° interval. The morphology of the obtained samples was studied by the scanning electron microscopy (QUANTA 3D 200i, FEI, USA).

RESULTS AND DISCUSSION

Regularities of combustion in the system $ZrSiO_4 + Mg + H_3BO_3$.

An important parameter of SHS-systems influencing the quality of the synthesized products is combustion temperature. It is at the maximal temperature developed in SHS-systems there occurs phase- and structure formation of the material.

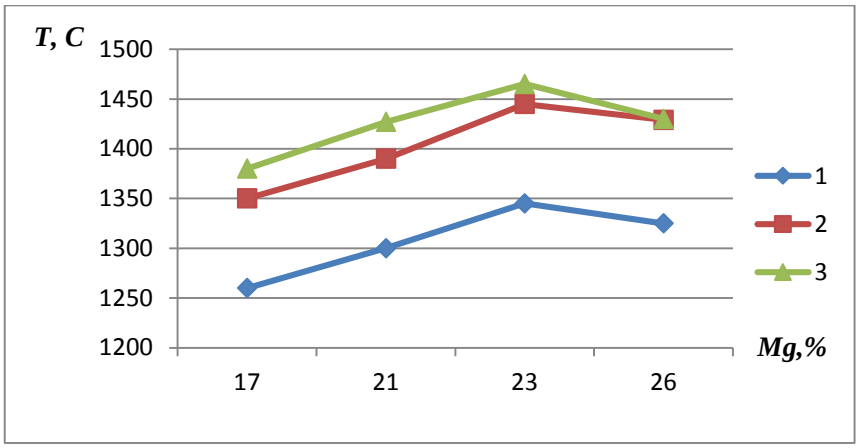

1-inactivated system; 2- 5 min of MA; 3- 10 min of MA

Figure 1 - The dependency of combustion temperature in $ZrSiO_4 + H_3BO_3 + Mg$ system on the content of magnesium (T_0 = 800℃)

Maximum combustion temperature was 1470℃. Preliminary activation time of the charge mixture also influences combustion temperature, the more the activation time, the higher the combustion temperature, therefore, reactions take place in a combustion wave more fully.

The qualitative and semiquantitative X-ray phase analysis (RFA) of SHS products structure for the $ZrSiO_4 + H_3BO_3 + Mg$ system is carried out. The obtained results are presented in Table 1.

Table 1 - X-ray phase analysis of the system $ZrSiO_4 + H_3BO_3 + Mg$ (T_0 = 800℃)

$ZrSiO_4 + H_3BO_3 + Mg$	(Mg %)	MA time, min	SHS products,%								
			Mg$_2$Si O$_4$	(B O$_2$)	ZrSiO$_4$	Zr O$_2$	O$_2$ mo	O$_2$t etra	Zr O$_2$ cub	Mg O	Zr B$_2$
	17	-	36.9	-	-	14.2	-	-	-	-	18.4
	21	-	49.9	13.0	1.2	-	6.7	5.4	-	-	19.6
	23	-	51.2	-	3.5	7.3	-	-	-	4.9	26.1
	17	10	38.8	12.6	7.2	-	18.5	1.2	-	-	20.9
	21	10	58.2	5.6	-	-	9.2	-	5.0	-	21.9
	23	10	58.4	4.5	-	-	8.6	-	4.5	2.8	21.2

Mechanochemical activation influences strength characteristics. At SH-synthesis, considerable formation of such substances as ZrB_2, MgO significantly increasing strength is observed the mechanical activated systems.

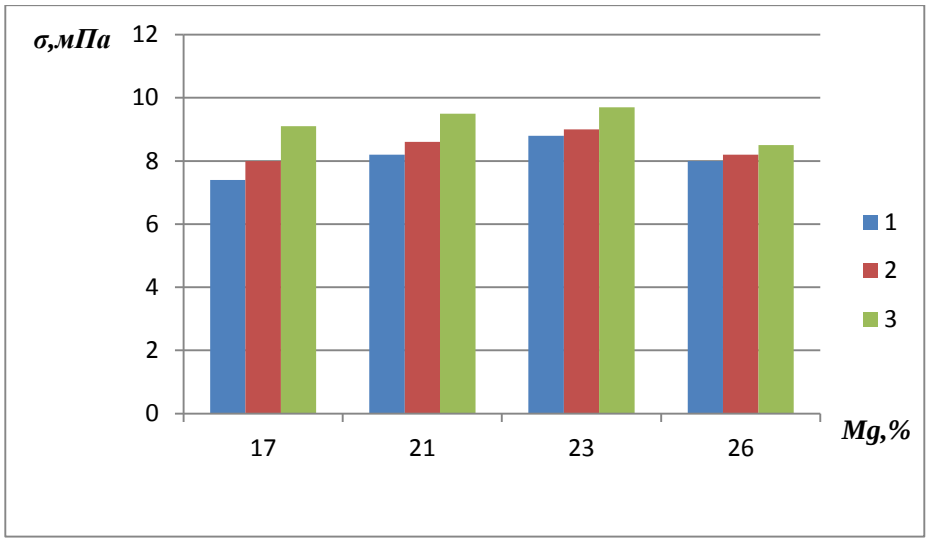

1-inactivated system; 2- 5 min of MA; 3- 10 min of MA

Figure 3-The dependency of compression strength on the content of magnesium and the time of MA in $ZrSiO_4 + H_3BO_3 + Mg$ system (T_0 = 800℃)

From Figure 4 it is possible to draw a conclusion that preliminary mechanochemical activation influences not only the content of ZrB_2 in the obtained composite material, but also on particle sizes: particle sizes of ZrB_2 were 160-200 nm. A complex use of MA and SHS gives the chance to obtaining ultradisperse material, when using available raw materials and the perspective SHS method.

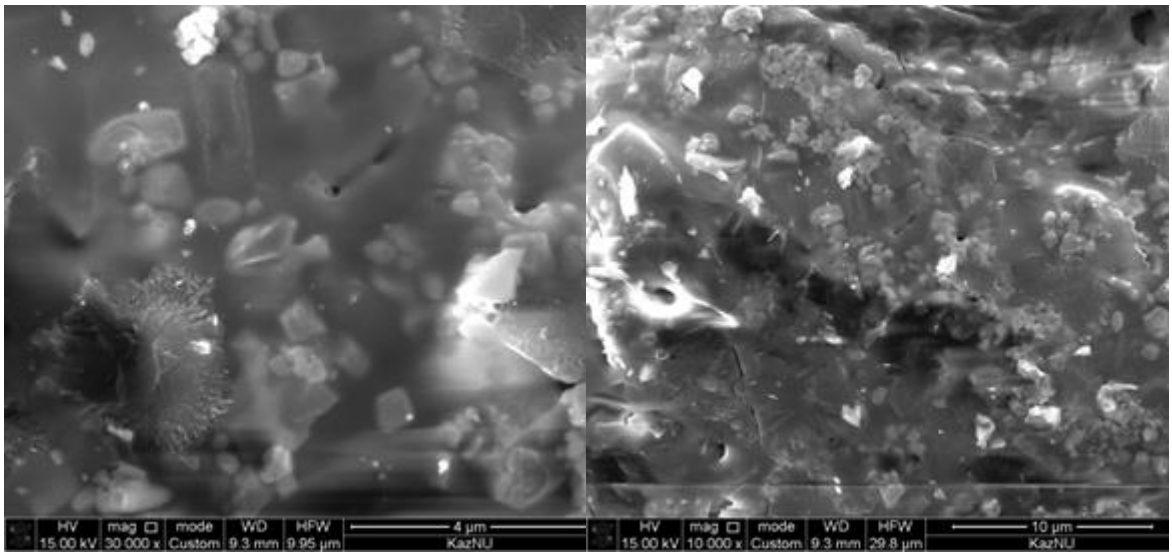

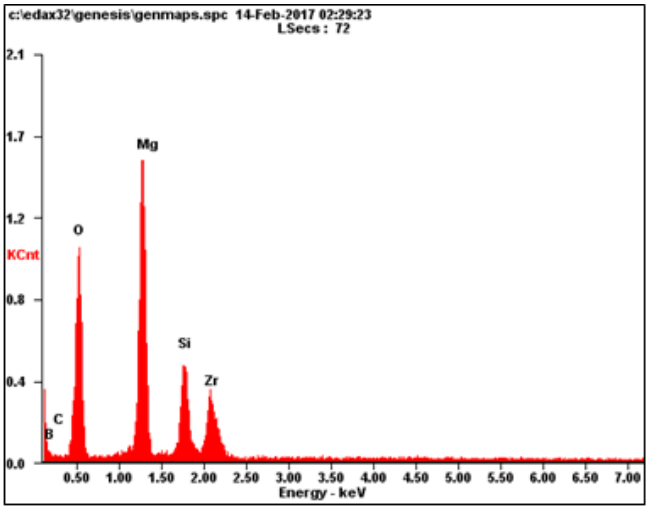

Element	Wt%	At%
BK	29.56	45.66
CK	1.44	2.00
OK	31.71	33.10
MgK	19.01	13.06
SiK	6.88	4.09
ZrL	11.40	2.09
Matrix	Correction	ZAF

Figure 4 - The microstructure of SHS products and elemental analysis SEM of the $ZrSiO_4$ + H_3BO_3 + Mg system

Thus, the possibility of obtaining nanodimensional zirconium diboride in the system of $ZrSiO_4$ + H_3BO_3 + Mg after SHS is shown. The influence of MA on a product yield and on particle sizes of zirconium diboride is stated.

REFERENCES

[1] M.Jalaly, M.Sh.Bafghi, M.Tamizifar, Mechanosynthesis of nanocrystalline ZrB_2-based powders by mechanically induced self-sustaining reaction method. // Advances in Applied Ceramics. Vol.112. №7. 2013. P.383-388.

[2] W.G.Fahrenholtz, G.E.Hilmas, I.G.Talmy, J.Zaykoski, Refractory diborides of zirconium and hafnium // Journal of the American Ceramic Society. Vol.90. №5. 2007. P.1347–1364.

[3] H.J.Yang, Y.T.Zhao, G.Chen, S.L.Zhang, D.B. Chen, Preparation and microstructure of in-situ (ZrB_2 + Al_2O_3 + Al_3Zr) composite synthesized by melt direct reaction // Trans.Nonferrous Met. Soc. China. 2012. P. 571-576.

[4] A.G.Merzhanov, The chemistry of self-propagating high-temperature synthesis // Journal of Materials Chemistry. №14. 2004. P.1779–1786.

[5] Boldyrev V.V. Mechanochemistry and mechanical activation of solid substances // Succsses of chemistry. – 2006. – V.75, №3. – P. 203-216. (in Russ)

HYBRID SHS-BASED TECHNOLOGIES FOR DESIGN OF HIGH-TEMPERATURE MATERIALS

E.A. Levashov*, V.V. Kurbatkina, E.I. Patsera, Yu.S. Pogozhev, I.V. Iatsyuk, A.A. Zaitsev, Yu.Yu. Kaplanskii

National University of Science and Technology "MISIS", Leninsky prospect, 4, Moscow, 119049, Russia
* levashov@shs.msis.ru

Efficient methods for fabrication of promising hard and refractory materials based on HfC (T_{melt}=3900°C), TaC (3800°C), HfB_2 (3380°C), ZrB_2 (3200°C), TaB_2 (3200°C), NbB_2 (3050°C) are currently being sought. High mechanical properties (strength, hardness, and Young's modulus) are essential requirements for these materials. Solid solutions of these compounds have a higher melting temperature. In particular, the melting temperature of binary carbide (Ta,Hf)C with 20% HfC content is ~3950°C. In addition to the rise in melting temperature, such parameters as specific resistance, hardness, the coefficient of thermal expansion (CTE), and thermal diffusivity are also characterized by an extremal dependence on composition of solid solution.

The combination of high thermal conductivity and low CTE defines the high thermal shock resistance of a material. The CTEs of transition-metal carbides and borides are almost identical: $(6–7)\cdot10^{-6}$ °C^{-1}. TaB_2 is an exception, since its CTE is noticeably higher than that of TaC ($8.2\cdot10^{-6}$°C^{-1} and $6.3\cdot10^{-6}$ °C^{-1}, respectively). Silicon-containing compounds, such as SiC, $MoSi_2$, and $ZrSi_2$, are added to borides to prevent decomposition of the barrier layer formed during oxidation. A borosilicate glass layer is formed in the presence of silicon and ensures the stability and protective properties.

The hybrid *off-line* technologies SHS + HP (hot pressing), SHS + SPS (spark plasma sintering) and *online* technologies such as reaction SPS (RSPS) or reaction HP (RHP) are used for synthesizing refractory solid-solution carbide and boride compounds.

The kinetics and the mechanism of combustion process and structure formation in systems Ta-Zr-C, Ta-Hf-C, Zr-Ta-B, Hf-Ta-B, Mo-Si-B, Zr-B-Si, Zr-B-Si-C have been studied [1-7]. It was found that mechanical activation (MA) of reaction mixtures and searching for the optimal operational conditions of fabrication of compacted materials play a crucial role in combustion synthesis of the most refractory solid solutions (Ta,Hf)C, (Ta,Zr)C, (Zr,Ta)B_2, and (Hf,Ta)B_2. When mechanical activation is carried out in air, the SHS product is the virtually single-phase carbide (Ta,Hf)C with the lattice parameter a = 0.4487 nm, which corresponds to 18 at. % of dissolved HfC and HfO_2 content is less than 1.0 %. The SHS product is a porous sinter cake with carbide grain size less than 10 μm, which can be easily refined in a ball mill to reach the grain size of 2–3 μm. SHS carbide and boride powders are the excellent raw materials for HP adn SPS. Hence, (Ta,Hf)C samples with density of 95–98%, hardness of 24.0–27.4 Gpa, Young's modulus of 423.6–484.4 GPa, and elastic recovery of 44.3–46.1 have been produced. Samples with density up to 98% have been produced by SPS.

The RSPS process has been performed to produce compacted samples of nanostructured SiC with density up to 97% [8]. A comparison of two approaches, SHS + SPS and RSPS, for production of HfB_2, TaB_2, ZrB_2-SiC, HfB_2-SiC, TaB_2-SiC, TiN–TiB_2, B_4C–TiB_2, WSi_2–SiC ceramics revealed several important conclusions [9-14]. First, it was found that the kinetic

mechanisms governing the reactions for the RSPS of the single-phase (HfB_2, TaB_2) and composite (ZrB_2-SiC, HfB_2-SiC, TaB_2-SiC) systems are different, i.e. combustion-type and gradual solid state diffusion, respectively. Second, when the combustion reaction takes place, a beneficial effect is obtained if a two-step mechanical pressure cycle is implemented during the RSPS process, i.e. the applied load is increased immediately after the reaction occurrence. Third, the RSPS method is preferable for the preparation of highly dense single-phase systems. In contrast, the opposite outcome is found when considering binary composites, where relatively mild sintering conditions are required to obtain fully dense materials when starting from SHS powders.

Two hybrid technological routes are also developing for synthesis of advanced powders based on NiAl and TiAl for additive techniques. First route includes three stages: 1- centrifugal SHS casting of a semi-product using oxide raw material; 2- vacuum induction remelting (VIR) of semi-product with structure modification and electrode molding; 3 - plasma rotation electrode process (PREP) and further classification of powders to the specified grain size. Second route includes two stages: 1 - elemental SHS of required composition; 2 – particles treatment in discharge plasma for spherical morphology obtaining.

Advanced NiAl-CrCoHf alloy with the allowable impurity content, high strength with partial plastic deformation at the room temperature was developed [15-17]. Content of alloying and functional additives, crystallization conditions were optimized in order to achieve hierarchical SHS-alloy CompoNiAl-M5 with 4 levels structure: *1st level* - large sized grains consist of colonies of NiAl dendrites separated from each other by 1-2 μm layers of Cr-base solid solution and Hf (~1 μm) particles; *2nd level* is a single NiAl dendrite with central part containing Co, Cr and Cr-rich periphery; *3rd level* – 50-150 nm Cr-based spherical core-shell inclusions inside NiAl matrix; *4th level* – 3-4 nm precipitations of Cr in the body of NiAl matrix appeared after annealing through Guinier – Preston zone formation. The *4th level* nanocrystal grows up from 3-4 nm to 40 nm after 30 min annealing at 700^0C. Moreover, it was in situ observed the annealing resulting in the fragmentation of 3rd level Cr-based inclusions from size 250-300 nm to 20-30 nm. Cr content in a core (about 50 nm thick) decrease from center to periphery that is demonstrates diffusion mechanism of precipitation's formation. Such 4 level structures were observed in alloys with relation Cr/Co~1- 3. It was shown that the coherent structure of interphase between NiAl phase and Cr- inclusions forms in case of its size less than 80 nm. Compressive strength of SHS- alloy samples at T_{room} achieve to 2260±210 MPa.

Evolution of the microstructure of the VIR alloy $Ni_{41}Al_{41}Cr_{12}Co_6$ isothermally exposed to 20, 350, 550, 750, 850 °C has been studied by in-situ HR TEM. Recrystallization becomes visible after 700 °C in SHS alloy and 550 ^{0}C in case of VIR alloy. After annealing, the VIR alloy exhibited strength of 1720 MPa at room temperature. Strength of the alloy after VIR decreased because of the increasing size of dendrites, inclusions, and precipitates. High-temperature strength and creep resistance of new alloys were investigated. Interesting that heritage of hierarchical 4 level structures has been observed even in ingot after VIR, in granules produced by PREP, and in dense materials manufacturing with SLS, SEBS and HIP technologies.

This work was carried out with financial support from the Ministry of Education and Science of the Russian Federation in the framework of Increase Competitiveness Program of NUST «MISiS» (No.K2-2016-073).

REFERENCES

[1] E.A. Levashov, A.S. Mukasyan, A.S. Rogachev, D.V. Shtansky, Inter. Materials Reviews, 62, 4, (2017) 203-239.

[2] E.A. Levashov, Yu.S. Pogozhev, A.Yu. Potanin, N.A. Kochetov, D.Yu. Kovalev, N.V. Shvyndina, T.A. Sviridova, Ceramics International, 40, (2014) 6541–6552.

[3] A.Yu. Potanin, Yu.S. Pogozhev, E.A. Levashov, D.Yu. Kovalev, A.V. Novikov, Eurasian Chemico-Technological Journal, 16, (2014) 53-58.

[4] Yu.S. Pogozhev, A.Yu. Potanin, E.A. Levashov, A.V. Novikov, T.A. Sviridova, N.A. Kochetov, Russian Journal of Non-Ferrous Metals, 55, 6, (2014) 632–638.

[5] E.I. Patsera, E.A. Levashov, V.V. Kurbatkina, D.Yu. Kovalev, Ceramics International, 41, 7, (2015) 8885–8893.

[6] E.I. Patsera, V.V. Kurbatkina, S.A. Vorotylo, E.A. Levashov, A.N. Timofeev, Ceramics International, 42, (2016) 16491-16498.

[7] Y.S. Pogozhev, I.V. Iatsyuk, E.A. Levashov, A.V. Novikov, N.A. Kochetov, D.Y. Kovalev Ceramics International, 42, (2016) 16758–16765.

[8] D.O. Moskovskikh, Y-C Lin, P.J. McGinn, A.S. Mukasyan, Journal Eur. Ceram. Soc., 35, 2, (2015) 477–486.

[9] R. Orrù, G. Cao, Materials, 6, (2013) 1566–1583.

[10] I.J. Shon, J.H. Park, I.Y. Ko, et al. Ceramics International, 37, (2011) 1549–1555.

[11 L. Nikzad, R. Orrù, R. Licheri, et al., Journal Am. Ceram. Soc., 95, 11, (2012) 3463–3471.

[12] C. Musa, R. Orrù, R. Licheri, et al., Mater Lett., 65, (2011) 3080–3082.

[13] R. Licheri, C. Musa, R. Orrù, Journal of Alloys and Compounds, 663, (2016) 351–359.

[14] Yang Z., Liu Z., Quyang J., et al., Int Journal Refract Metals Hard Alloys, 41,(2013)54–59.

[15] Yu. S. Pogozhev, V.N. Sanin, Ikornikov D.M., D.E. Andreev, V.I. Yukhvid, E.A. Levashov, Zh.A. Sentyurina, A.I. Logacheva, A.N. Timofeev, Inter. Journal of SHS, 25, 3, (2016) 186–199.

[16] A.A. Zaitsev, Zh.A. Sentyurina, E.A. Levashov, Yu.S. Pogozhev, V.N. Sanin, P.A. Loginov, M.I. Petrzhik, Materials Science & Engineering A, 690, (2017) 463-472.

[17] A.A. Zaitsev, Zh.A. Sentyurina, E.A. Levashov, Yu.S. Pogozhev, V.N. Sanin, D.A. Sidorenko, Materials Science & Engineering A, 690, (2017) 473-481.

STRUCTURE FORMATION AT CONSECUTIVE LAYER-BY-LAYER PACKING OF MONODISPERSED GRANULES

M. A. Ponomarev*, V. E. Loryan

Institute of Structural Macrokinetics and Materials Science, Russian Academy of Sciences, Chernogolovka, Moscow region, 142432, Russia
*map@ism.ac.ru

One of the main tasks within SHS processes is definite macro- or microstructure formation in the synthesis product [1,2]. Density uniformity and ordered arrangement of components in the volume of preliminarily structured powder heterogeneous systems have an effect on the combustion process, structure of pore space and density distribution in the synthesis product [3]. Besides it is reasonable to use model systems with regular arrangement of components and corresponding reaction cells in the volume, e.g. as tetrahedral or cubic packing, for reliable comparison of theoretical calculation and experimental results when studying combustion in heterogeneous systems [4]. This work continues studying structure formation in thin separate layers of the model systems [5, 7]. The aim of our investigation is to study the peculiarities of multilayer structured billet formation at consecutive portion packing of monodispersed granules. The investigation results are actual for obtaining composite materials by SHS from bidispersed mixtures with spherical components or those containing clad or mechanically activated composite granules [3].

The regularities of consecutive portion packing of granule loading into the moulds of various geometry (a circle (D=4, 10, 15 mm), hexahedron (L=15 mm) and square (L=14 mm)) were studied. The density of the packed granule system was counted as the ratio of the total load mass to the volume occupied by the granules between the upper and bottom punches in the mould independently on the filling degree of separate monolayers in the sample. It allows comparing the peculiarities of structure formation in the model systems with those in ordinary powder multicomponent SHS mixtures.

The fills of monodispersed steel granules (d=1000 μm), spherical titanium granules Ti (s) of a narrow fraction (d_1~290 μm), aluminum powder ACD-4 with spherical particles d_1~1-10 μm, and Ti(s)+Al mixture were used. The packing process in matrixes with a smooth base and in those with the fixed monolayer of balls formed as tetrahedral or octahedral packing (for initiation of the certain package formation in the system) was investigated. The peculiarities of multilayer billets formation were studied at consecutive portion packing of thin layers with the masses (or a number of granules in a single filling portion (δN_o)) varying in the experiments. Fig.1 and 2 show packing density of granules (d=1000 μm) in the hexagonal mould and a change in the upper monolayer structure with an increase in the billet height.

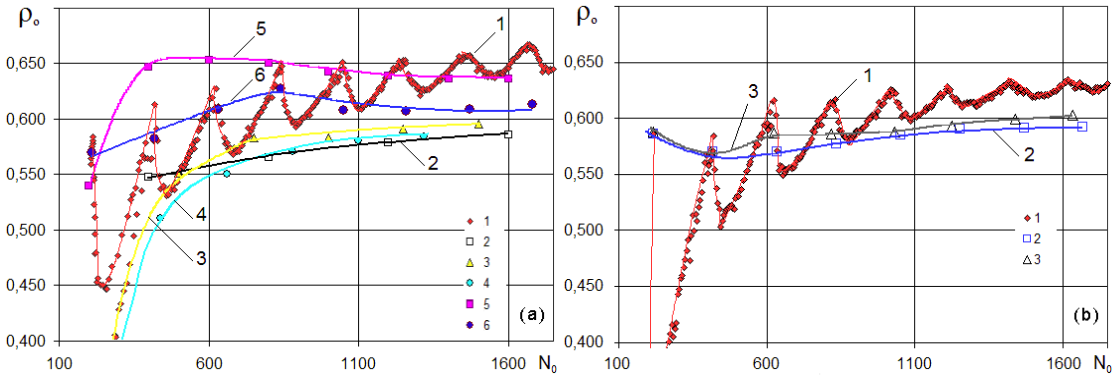

Fig.1 - Packing density of granules (d=1000 μm) (hexagonal mould): (a) – consecutive pressing, smooth base: 1 – δN_o=5; 2 - δN_o=400; 3 - δN_o=250; 4 - δN_o=220; 5 - δN_o=200; 6 - δN_o=210; (b) – the first monolayer (tetrahedral packing) is fixed: 1 – consecutive pressing (δN_o=5); 2, 3 – ordinary pressing (a step close to extremes period, ρ_o): 2 - δN_o=200; 3 - δN_o=197.

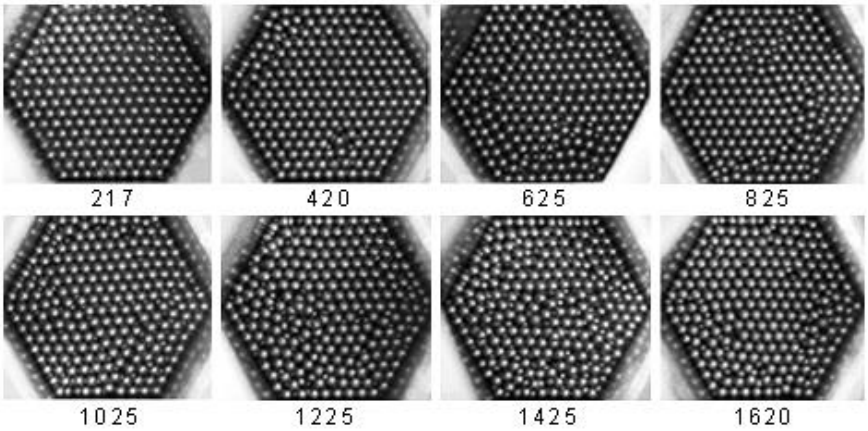

Fig.2 - The upper monolayer (the first layer is fixed, δN_o=5, N_o=217, 420, 625, etc.).

The packing density of granules (d=1000 μm) in the square mould is shown in Fig.3. According to the comparison of the experimental data of billets densities achieved at the consecutive layer-by-layer portion packing in the moulds of various cross sections, the packing density of granules (in N_o interval under study) in the hexagonal matrix is 0.67; it is significantly higher than the analogous value obtained in the case of the square mould (~0.575) and cylindrical matrix (~0.55). The dependences of ρ_o=ρ_o(N_o) in all the moulds under study at consecutive portion packing of small portions of granules have distinct extremes – density maximums and minimums which are analogous to those which were observed earlier at packing of thin layers of SHS green mixtures and spherical particles [5, 6]. Density maximums correspond to tetrahedral regular dense packing of ideal balls. Analogous dependences are also observed at consecutive portion packing of thin layers of Ti(s)+Al green mixture and its coarse component (Fig.3). The obtained results are rather actual and useful for SHS, especially for producing long pressed billets with significant uniformity.

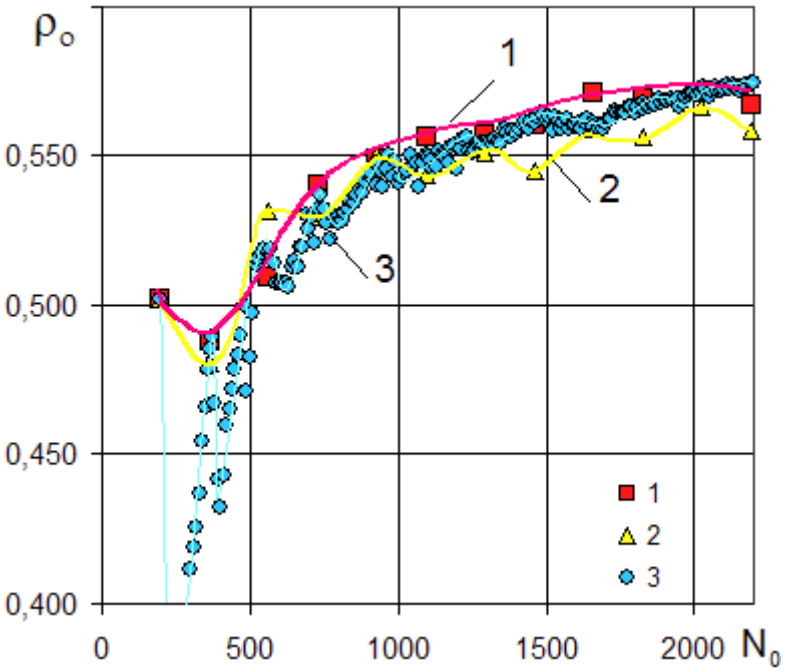

Fig.3 - Packing density of granules (d=1000 μm) (a square mould, the first monolayer is fixed (octahedral packing)): 1 – ordinary pressing (alternation of δN_o=196 and δN_o=169 portions); 2, 3 – consecutive pressing: 2 - alternation of δN_o=196 and δN_o=169 portions; 3 - δN_o=5.

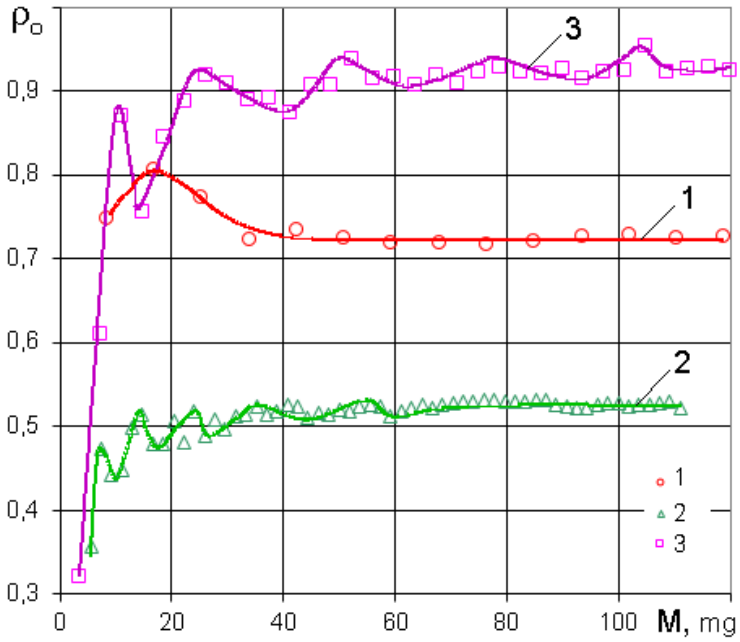

Fig.4 - Sample density (consecutive pressing, a round mould, D=4 mm): 1 – Al (δM=8.5 mg); 2 – Ti(s) (δM=1.85 mg); 3 - Ti(s)+Al (δM=3.75 mg).

REFERENCES

[1] Amosov, A.P., Makarenko, A.G., Samboruk, A.R. et al. Granulation in the powder technology of self-propagating high-temperature synthesis. Russ. J. Non-ferrous Metals. May 2013, Volume 54, no. 3, pp. 267–273. DOI:10.3103/S1067821213030024.

[2] Galakhov, A., Powder compact structure, 2: Methods for increasing particle packing uniformity, *Refract. Ind. Ceram.*, 2014, vol. 55, no. 3, pp. 209–217;

[3] M. A. Ponomarev, V. E. Loryan, A. S. Shchukin, and A. G. Merzhanov SHS in Preliminary Structured Compacts: II. Ti–2B and Ti–Al Blends, *Int. J. Self_Prop.High_Temp. Synth*, 2013, vol. 22, no. 4, pp. 202–209. DOI: 10.3103/S1061386213040055.

[4] Kochetov, N.A., Rogachev, A.S., Emel'yanov, A.N. et al. Microstructure of Heterogeneous Mixtures for Gasless Combustion. Combust Explos Shock Waves. 2004, vol. 40, no. 5, pp. 564–570. DOI: 10.1023/B:CESW.0000041408.95421.d2.

[5] M.A. Ponomarev, V.E. Loryan, A.G. Merzhanov Uniaxial Compression of Ti, B, and T–B Powders: Structurization in Case of Spherical Ti Particles,*Intl.J.SHS*,2012,vol.21.no.1,pp.51.

[6] M.A.Ponomarev, V.E. Loryan Self-ordering of balls in compressed thin layers, *Int. J. Self_Prop. High_Temp. Synth*. 2016, vol. 25, no. 1, pp 43–49.

[7] M.A. Ponomarev, V.E. Loryan, I.P. Borovinskaya, SHS of Ti-Al-B system from Ti+2B mixture with aluminum-clad titanium spherical particles // XIII International Symposium on Self-Propagating High-Temperature Synthesis, October 12 – 15, 2015, Antalya - TURKEY, Book of Abstracts, P.180-181.

SHS IN Ti-B AND Ti-Al-B STRUCTURED SYSTEMS AT PRELIMINARY WARMING-UP

M. A. Ponomarev*, Loryan V. E.

Institute of Structural Macrokinetics and Materials Science, Russian Academy of Sciences, Chernogolovka, Moscow region, 142432, Russia
* map@ism.ac.ru

The peculiarities of SHS of composite materials from Ti-B and Ti-Al-B powder mixtures with preliminary warming-up of structured samples obtained by the method of layer-by-layer compression [1] were studied. The initial mixtures of Ti-B system contained black amorphous boron (< 10 μm) and titanium of two types – coarse spherical granules (Ti(s)) (~290 μm) and dendrite particles (Ti(di)) of the types PTS (d1~120 μm) and PTM (narrow fractions d2<40 μm and d3~100 μm). The initial mixtures of Ti-Al-B system of (Ti+2B)+(Ti+Al) composition contained coarse spherical titanium granules (~290 μm) cladded with aluminum layer (20-30 μm) – (Ti(s)+Al) and powder mixtures of black amorphous boron and titanium with dendrite particles. The mixture of boron and titanium with dendrite particles played the role of "a chemical furnace" and provided warming-up and joining of coarse titanium granules to the reaction. The components of titanium (PTS and PTM)-boron mixtures were degasified at vacuum annealing (during 40 min at 620ºC at residual pressure of 10^{-4} torr). The following reactive mixtures were formed from the powders: a(Ti(s)+Al)+(1-a)(Ti(d1)+2B)) and a(Ti(s)+2B)+(1-a)(Ti(di)+2B)) with the variation interval a=0-0.8. The mixtures were pressed into quartz containers (internal diameter D~4 mm, length ~43 mm) by consecutive layer-by-layer portion compression [2]. The influence of the mixture composition, components dispersion, preliminary gas removal from the components at vacuum annealing, initial warming-up temperature (T_o=20-500º C) on the product structure was studied. SHS was carried out in the combustion mode at argon atmosphere. When the billets were warmed up to T_o<200º C, the combustion temperature profiles of Ti-B system demonstrated two and more temperature micropeaks (Fig.1-a); they proved the existence of several stages of the synthesis - at first, boride matrix was formed in the reaction Ti(di)+2B and then titanium Ti(s) particles melted and the melt joined the reaction with the matrix material. At higher initial temperatures T_o>200º C (a<0.4), the matrix frame material was formed faster at interaction of titanium with dendrite particles with boron. As a result, spherical particles of titanium from one layer (a cross layer to the sample axis) melted and joined the reaction faster, and the only temperature maximum was observed in the temperature profiles (Fig.1-b). In this case the maximum temperature T_b in the combustion wave was growing (by ~400ºC) and a significant increase in the average combustion rate (u) was observed – 3-4 times (e.g., from 2.7 cm/s at T_o=20º C up to 7.6 cm/s at T_o=470º C – for a(Ti(s)+2B)+(1-a)(Ti(d2)+2B) at a=0.4). The initial temperature increase to 470º C resulted in more than 3 times growth of the product compression strength – up to 70 MPa. The use of titanium dendrite particles of fine fraction (<40 μm) allowed increasing the material compression strength 1.5-3 times in comparison with the initial mixtures containing coarse titanium powder (~125 μm). After the preliminary annealing the content of hydrogen admixture in the components was 2-3 times lower; it resulted in a decrease in the impurity gas pressure in the combustion front and an increase in the combustion rate (up to 30 %), and reduced the influence of impurity gases on porous structure formation in the synthesized material.

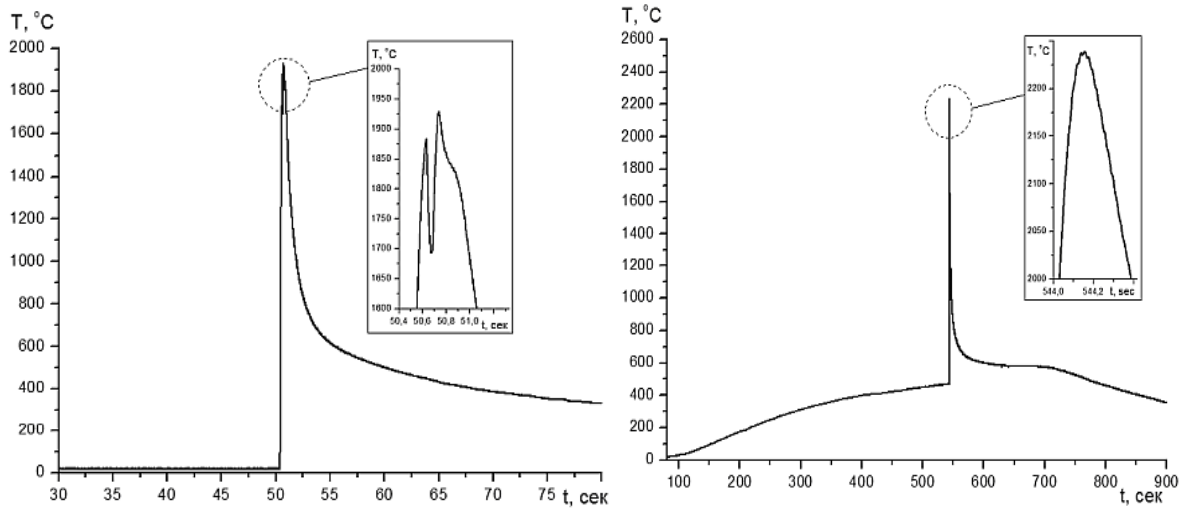

Fig.1 - Combustion wave temperature profile for *a*(Ti(s)+2B)+(1-*a*)(Ti(d2)+2B), *a*=0.4: a) T_o=20° C; b) T_o=470° C.

The synthesis product obtained at T_o=20-500° C contains pores of four main types [2]. The fine pores of titanium diboride matrix round the spherical macropores are filled with the material of melted Ti(s) particles after the reaction with the matrix (Fig.2). The matrix fragments round the spherical macropores look like hollow granules (the wall thickness – from tens to hundred microns) and appear to be a part of the matrix. The granule walls have a composite structure. The pore sphericity is higher at higher temperatures, T_0.

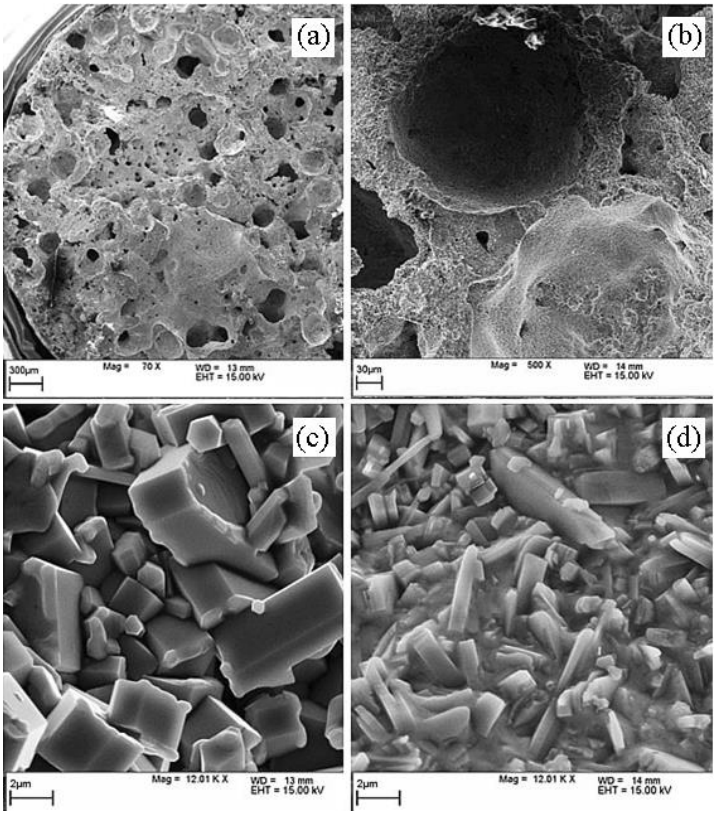

Fig.2 - SHS product micro- and microstructure (fracture surface) (*a*(Ti(s)+2B)+(1-*a*)(Ti(d1)+2B); *a*=0.6; T_o=445° C): a) cross fracture; b) granule fracture with macropore; c) TiB_2 crystals on on the surface of middle-sized pores in matrix; d) macropore surface after Ti(s) melt penetration into the matrix porous frame.

The synthesized product has a composite structure. The boride frame of the matrix is formed by crystallites. They are close to the macropores and have a large laminated shape. They look like long rectangulars. The elemental composition of the matrix nearby the macropore corresponds to the phases TiB_2 and TiB, at a distance - TiB_2. The light areas round the boride phase are close in their elemental composition to that of Ti(s) initial granules (titanium alloyed by aluminum and vanadium) and correspond to Ti, Ti_3Al phases. The matrix microstructure between the macropores has a fine-grain structure, its pores are uniformly saturated by titanium (the light area). According to the information of X-ray Diffraction (XRD), with T_0 growth the portion of TiB_2 phase in the synthesis product grows.

When the SHS product was obtained from the mixture of titanium granules cladded with aluminum and fine titanium with boron, an increase in T_0 up to 450°C resulted in the

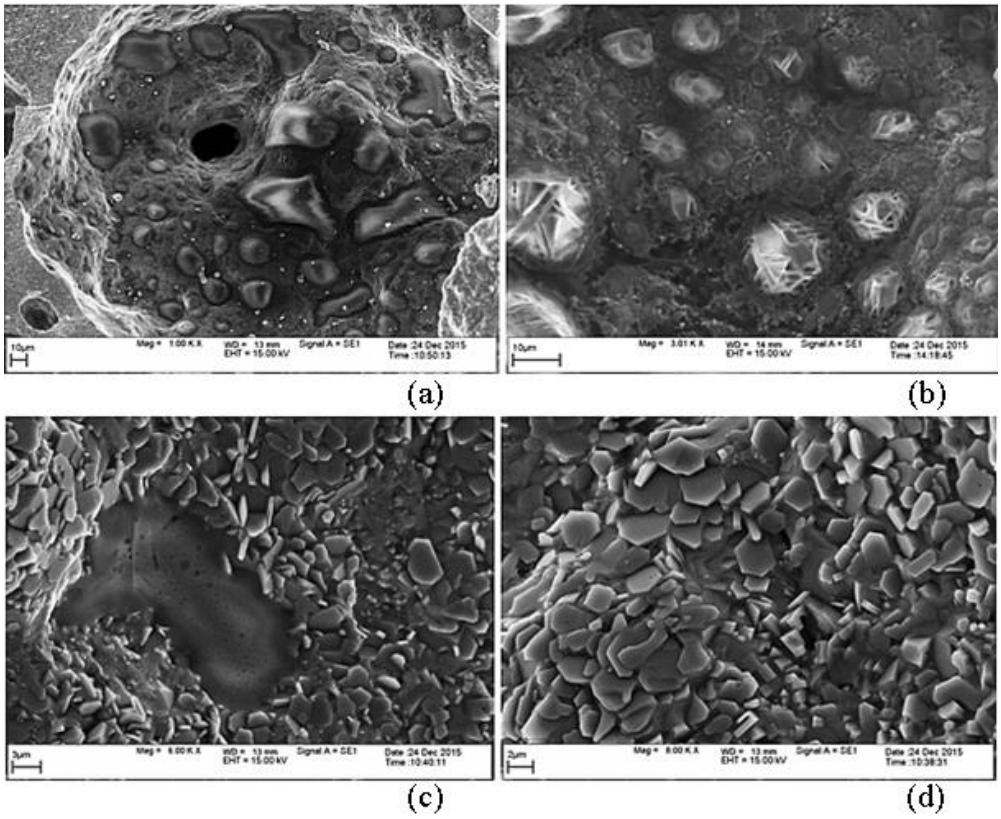

Fig.3 - Fracture structure and surface of macropores (a, b, d) and middle-sized pores (c) in the SHS product (a(Ti(s)+Al)+(1-a)(Ti(d1)+2B); a=0.4; T_o=450°C (a, c, d); T_o=240°C (b).

growth of the maximum temperature T_b in the combustion wave and significant growth of the average combustion rate – 3.5 times (e.g., from 2.4 cm/s at T_o=20° C up to 8.7 cm/s at T_o=450° C – for the mixture a(Ti(s)+Al)+(1-a)(Ti(d2)+2B) at a=0.4). The material compression strength (at synthesis at T_o=450° C) was 2.5 times higher – up to 77 MPa. The structure of the composite material and macro- and middle-sized pore surfaces are shown in Fig.3. The phase composition of the material includes TiB_2, TiAl, Ti_3Al, Ti.

REFERENCES

[1] M.A. Ponomarev, V.E. Loryan, A.G. Merzhanov Uniaxial Compression of Ti, B, and T–B Powders:Structurization in Case of Spherical Ti Particles,*Intl.J.SHS*,2012,vol.21.no.1,pp.51.

[2] M. A. Ponomarev, V. E. Loryan, A. S. Shchukin, and A. G. Merzhanov SHS in Preliminary Structured Compacts: II. Ti–2B and Ti–Al Blends, *Int. J. Self_Prop.High_Temp. Synth*, 2013, vol. 22, no. 4, pp. 202–209. DOI: 10.3103/S1061386213040055.

SHS PROCESSING OF COPPER WASTE INTO COPPER POWDER

H.A. Mahmoudi[*1,3], L.S. Abovyan[2], S.L. Kharatyan[1,2]

[1] Yerevan State University, 1, A. Manukyan str., Yerevan, AM-0025, Armenia
[2] A.B. Nalbandyan Institute of Chemical Physics NAS RA, 5/2, P. Sevak str., Yerevan, AM-0014, Armenia
[3] National Iranian Copper Industries Company (NICICO), Kerman, Iran
* mahmoody.h@gmail.com

In the work the possibility of processing of copper waste of wiring industry (Iran) under the combustion mode and preparation of copper powder have been studied. The copper waste used in this study represents mainly copper (I) oxide with small amount of metallic copper and having plate-like form of particles with linear size up to 2.5 mm (0.4-1.0 mm - 70 wt.%). At that the content of metallic copper is comparatively higher in the fraction less than 0.1 mm. After drying at 100°C and 7 hours ball milling the particle size became practically less than 1 mm (0.1-0.25 mm - 70 wt.%).

The possibility of copper (II) oxide reduction under the combustion mode has been shown for the first time in [1] by using polystyrene (PS) as a reducer (as well as other organic compounds). The same approach was used in [2] for preparation of copper powder from the mixtures of CuO/Cu_2O and CuO/Cu. It should be emphasized that because of low exothermicity of Cu_2O-PS reaction, the reduction of pure copper (I) oxide by polystyrene in combustion mode is impossible (maximum value of T_{ad}=460°C at PS/Cu_2O=0.05-0.06). By this reason combustion limit exist for $CuO-Cu_2O$-PS system at 40 wt.% content of Cu_2O [2].

In this work for increasing the exothermic effect of Cu_2O-PS reaction and reduction of copper waste (hereinafter Cu_2O) to metallic Cu in combustion mode the reactions thermal coupling approach [3] was applied. Namely, the weakly exothermic (Cu_2O-PS) reaction was coupled with high exothermic NH_4NO_3-PS (hereinafter Nt-PS) one.

Determination of optimal conditions of the process was based on the results of preliminary thermodynamic calculations for the above-mentioned system. Particularly, it was calculated and shown, that the mixture (Nt+αPS) have maximum enthalpy and adiabatic temperature at α=0.05-0.06. At that T_{ad}=2000°C.

In the experiments cylindrical pellets 20 mm in diameter and 45-50 mm height were prepared from different initial mixtures (Cu_2O+0.06PS)+x(Nt+0.06PS). Main variables are x value and particle size of the waste. Thermocouple technique was used to measure the main combustion parameters: temperature (T_c) and velocity (U_c). After passing the combustion front and cooling-down the burned samples were examined by XRD analysis and scanning electron microscopy.

As a result the dependences for T_c and U_c vs. x value were obtained, microstructure and phase composition of final products were determined (fig.1, 2). It was revealed that combustion limit is observed with a significant decrease in the high caloric additive content, namely at x=0.15 (for milled waste with particle size ≤0.4 mm).

According to XRD analysis results, at x>0.2 complete reduction of copper takes place. At x=0.2 final product contains also traces of Cu_2O. The results obtained showed the possibility of using polystyrene with high caloric (Nt-PS) mixture for reducing copper waste to metallic copper

under the combustion mode. Optimum conditions for obtaining powdered copper with certain microstructure were found out.

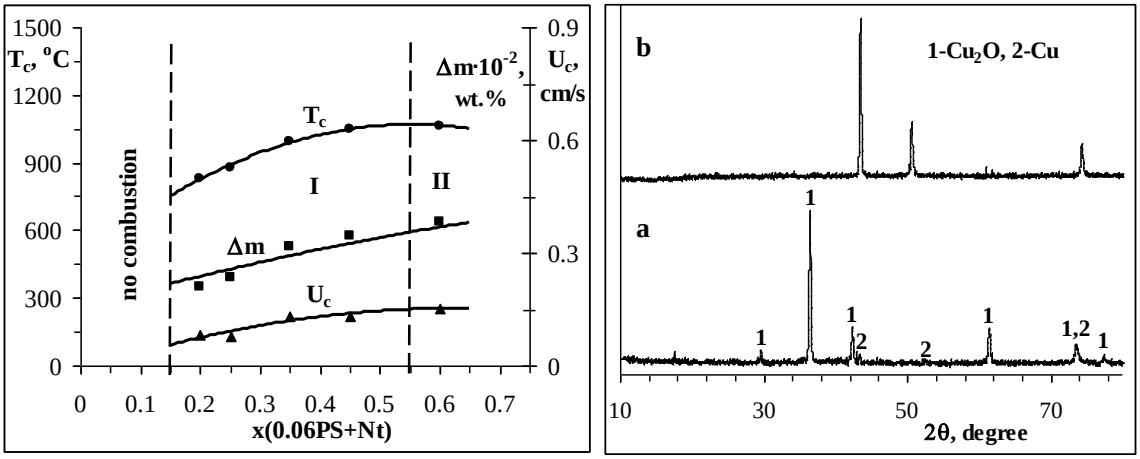

Fig.1 - Combustion temperature (T_c), velocity (U_c) and mass loss (Δm) *vs.* x for the Cu_2O+0.06PS - x(0.06PS+Nt) system. I– formation of Cu powder, II– formation of liquid Cu

Fig.2 - XRD patterns of the initial copper waste (a) and combustion product (b) of the (Cu_2O+0.06PS) + 0.35(0.06PS+Nt) mixture

A series experiments were performed also using carbon as reducer. The results showed that despite the realization of combustion reaction and even high enough combustion temperature (T_c=780-1080°C), only partially reduced copper is obtained with high content of free carbon. This result shows how important is to use a gasifying organic reducing agent instead of solid carbon.

REFERENCES

[1] M.H. Yamukyan, Kh.V. Manukyan, S.L. Kharatyan, Chemical Engineering Journal, 137, (2008) 636-642.

[2] L.S. Abovyan, S.L. Kharatyan, Chem. J. Armenia [in Russian], 63, No.4, (2010) 431-442.

[3] S.L. Kharatyan, A.G. Merzhanov. Int J SHS, 21, No.1, (2012) 59-73.

PECULIARITIES OF ALUMINOTHERMIC COMBUSTION OF OXIDE SYSTEMS UNDER HIGH NITROGEN PRESSURE

Mansurov Z.A., Fomenko S.M.

The Institute of Combustion Problems

ABSTRACT

In this work there has been studied some processes of aluminothermic reduction of some oxide systems in solid-state combustion mode, in nitrogen environment, in high-pressure reactor in order to obtain the nitride containing composites. The properties of synthesis products that obtained at various nitrogen pressures were determined.

Key words: self-propagating high-temperature synthesis (SHS), high pressure, oxide systems, nitrides, composites.

INTRODUCTION

Nitride-containing ceramic powders that obtained by combustion of metal nanopowder mixtures in air are the promising materials for applications. Under certain conditions, during combustion of aluminum nanopowders in air the aluminum nitride phase (more than 80% by weight) [1,2] is stabilized in final products. Nitrides— are compounds of refractory metals with nitrogen, many of which have high fire resistance, unique semiconducting and dielectric properties, high chemical stability and deserve special attention [3, 4]. Actual task for producing of high-temperature nitride ceramic at high pressures of reacting nitrogen is not only compound synthesis, but also the formation of material structure, its geometric form [5]. Previously, we have been studied some combustion regularities of oxide systems under high nitrogen pressure conditions [6]. For improvement of structural characteristics in investigated systems there was used stronger oxidant - chrome oxide (III) [7].

EXPERIMENTAL PART

SH – synthesis was carried out in high-pressure reactor. The basic unit of research setup is a reactor vessel with a capacity of 45 liters, is made from heavy-walled metal, provided with top and bottom cover. For thermocouple outputs and electrical supply the current fittings were installed in bottom cover. Supply and gas outlet is conducted through flexible cables of high pressure, equipped with quick disconnect fittings, are installed at top cover. To increase the concentration limits for realization of SHS synthesis, a tubular heating furnace that heating the tested sample up to 1000◦C was placed inside the reactor. For control of temperature data of SH- synthesis processes, a computer temperature recording system was used. By direct measuring method, the thermocouple signal that installed inside the reactor was transmitted through the current-carrying connections of bottom cover via shielding wires to crate system LTR-U-1. Combustion products were subjected to X-ray diffraction analysis using diffractometer DRON-3M. Topography and microstructure of surface samples, as well as qualitative and quantitative analysis of the composition in pointed regions were carried out using multifunctional scanning electron microscope Quanta 3D 200i with integrated systems of focused ion beam and energy-dispersive spectrometer at the National Nanotechnology Laboratory of the al-Farabi Kazakh National University.

For realization of experimental works the following components were used: PA-4 aluminum powder (99.0%), zincconcentrate concentrate of Obukhovsky GOK (Kazakhstan, ZrSiO4 content - 98.1%), silicon and zirconium powders, silicon and chromium oxides, natural quartzite (the content SiO_2 – 97,0 %), silica sol of the DeguDent GmbH company (Germany), nitrogen gas of increased purity in cylinders (nitrogen content not less than 99.9%, vol.). Dispersion of initial components was no less than 90 μm.

For determination of thermophysical and strength characteristics, the samples were prepared in the form of cylinders with a diameter of 20 mm and with height of 40 mm, the cylinders were made by pressing method in press mold at a pressure of 70 MPa. The dried samples were placed into tube furnace, is located inside the reactor of high-pressure (HPR), where in nitrogen environment, at a temperature of 1100-1150 K the spontaneous combustion of the samples was occurred , and self-propagating high-temperature synthesis of nitride-containing composites was carried out. Initial pressure of nitrogen in reactor was varied from 0.5 to 2.0 MPa. Compositions of experimental samples are given in Tables 1-2.

Table 1 - Compositions of initial experimental samples in a system AI – $ZrSiO_4$ –C

Component	Content, % mass.			
Al	25	30	25	30
$ZrSiO_4$	65	60	70	65
Zr	5	5	5	5
C	5	5	0	0

Table 2 - Compositions of initial experimental samples in system Al – $ZrSiO_4$– Cr_2O_3 и Al – SiO_2 – Cr_2O_3

Component	Content, % mass.			
Al	10	13	13	15
$ZrSiO_4$	38	35	-	-
Cr_2O_3	50	50	50	50
SiO_2	-	-	37	35
CaF_2	2	2	-	-

RESULTS AND DISCUSSIONS

Allegedly the mechanism of molecular transformations in system Al – MeO – N_2 is as follows:

$MeO + Al \rightarrow Al_2O_3 + Me$ (1) where $MeO = Cr_2O_3, SiO_2, ZrSiO_4$

$2Me + N_2 \rightarrow 2MeN$ (2)

For obtaining of carbonitride composites, a small amount of carbon in the form of graphite was introduced into some prototypes. Introduction of graphite lead to a slight increase of combustion temperature, which was 1670 K and nitrogen pressure which was 0.5 MPa and aluminum content of 30%. However, under the conditions of preliminary heating of a system, the formation of gaseous carbon nitride reaction is occurred.

Carbide phases in end synthesis product were not detected.

The energy capacity of aluminothermal systems based on zircon and silicon oxide is low, and as a consequence the reaction temperatures are low, and therefore the synthesized samples showed insufficient strength. To increase the synthesis temperature and giving to composites enhanced mechanical properties, a stronger oxidant - chromium oxide (III) was introduced into the system. Below there is a proposed mechanism of chemical transformations in the system

$Al - ZrSiO_4 - Cr_2O_3 - N_2$:

$$Cr_2O_3 + Al \rightarrow Al_2O_3 + Cr \quad (4)$$

$$ZrSiO_4 + Al \rightarrow Al_2O_3 + Zr + Si \quad (5)$$

$$Cr + N_2 \rightarrow Cr_2N \quad (6)$$

$$Zr + N_2 \rightarrow ZrN \quad (7)$$

$$3Si + 2N_2 \rightarrow Si_3N_4 \quad (8)$$

Thus, in our opinion, a multistage process of nitride-containing composite formation is realized, when the main heat emission is occurred in the first stage of aluminothermic reduction of metal oxide, and the nitration process of the reduced metal is carried out at the final stages of the synthesis.

The addition of chromium oxide into the systems Al–ZrSiO4 and Al–SiO2 is significantly increase the combustion temperatures (see Fig. 5), which reaches 1770 K in a system of Al–SiO2 with an aluminum content of 15% and nitrogen pressure of 0.5 MPa.

With an increasing of nitrogen pressure, the combustion temperature is decreased monotonically. This is due to the fact that heat emission of exothermic compounds is caused by aluminothermic reduction of metal oxide. And with an increase of nitrogen pressure, the heat output of the samples is increased; this fact leads to an increase of heat losses and a decrease of combustion temperature in the system. Structural characteristics of synthesized nitride-containing composites are determined. Synthesized samples were determined for ultimate compressive strength. With an increasing of nitrogen pressure and aluminum content for all samples, the compressive strength is increased. The introduction of graphite leads to a reduction of strength due to formation of gaseous compounds of carbon that lead to an increase of porosity and composite softening.

Figure 1 shows the dependence of ultimate compressive strength on nitrogen pressure in reactor in the systems Al-ZrSiO4-Cr2O3 and Al-SiO2-Cr2O3 at various aluminum contents. With an increasing of nitrogen pressure and aluminum content in investigated system the compression strength of composite is increased monotonically and reaches 100 MPa. Ultimate compressive strength for zircon-containing system reaches 120 MPa at nitrogen pressure of 1.5 MPa, which is more than in twice increases the tensile strength of samples which not containing chromium oxide.

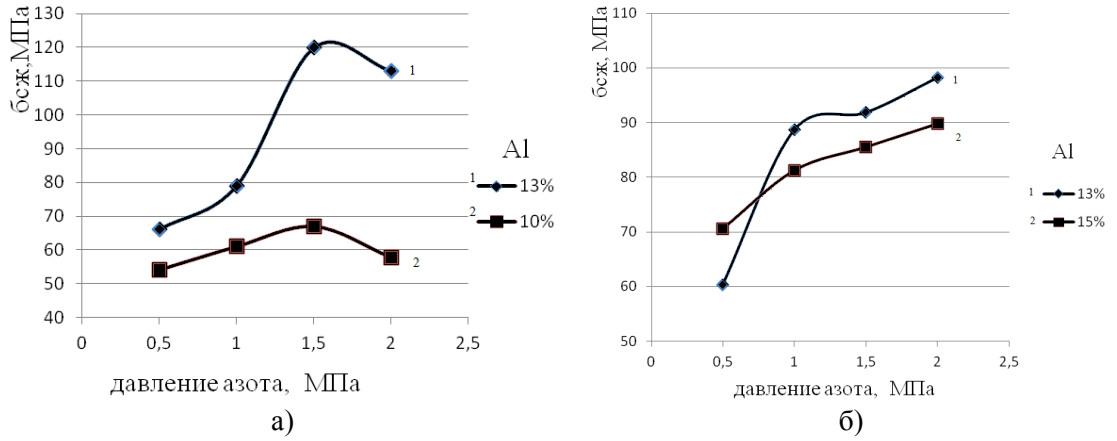

Figure 1 - The dependence of synthesized sample strength on nitrogen pressure in reactor: a – Al – $ZrSiO_4$ – Cr_2O_3; б – Al – SiO_2 – Cr_2O_3

Some investigations of morphology and microstructure of composite have been performed depending on experimental conditions and the ratio of initial components. The study of microstructures on chips of investigated samples in system Al-ZrSiO4 (figure 2) showed some morphological difference of composite structure with graphite and without it.

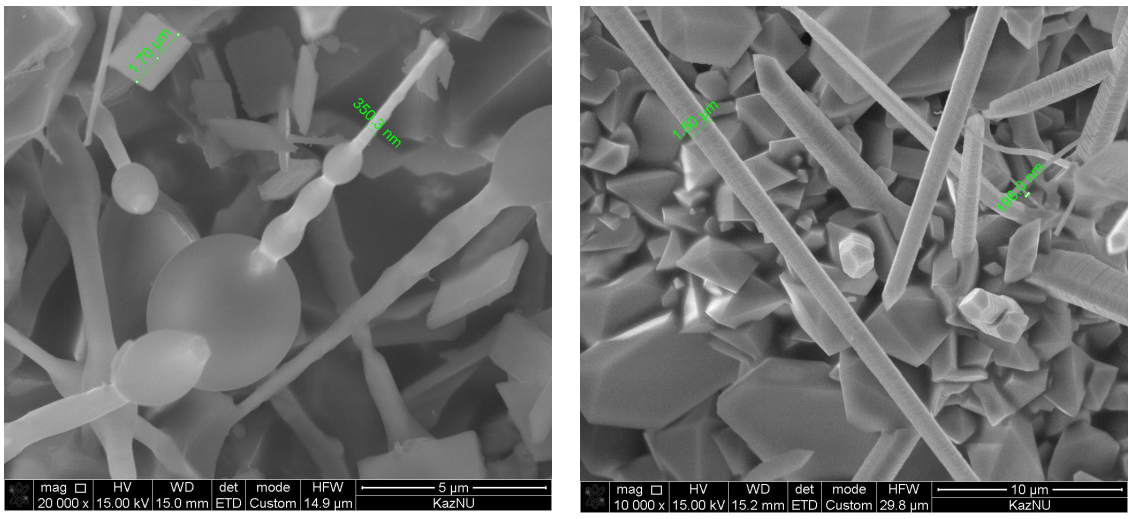

а) б)

Figure 2 - Microstructure and external appearance of synthesized sample chips in systems: а) Al – $ZrSiO_4$ – Zr –C , б) Al – $ZrSiO_4$ – Zr

Investigation of samples microstructure in system Al – $ZrSiO_4$ – Cr_2O_3 have shown the presence of filamentary whiskers in composite structure. In samples that containing chromium nitride (Figure 3a), there are observed filamentary twisted spirals, at the ends of which there are spherical formations. Precisely this form of whiskers gives strength to composite. In system Al – SiO_2 – Cr_2O_3 the crystals of irregular shape from chromium-aluminum spinel serve as the matrix of composite (Fig. 3b).

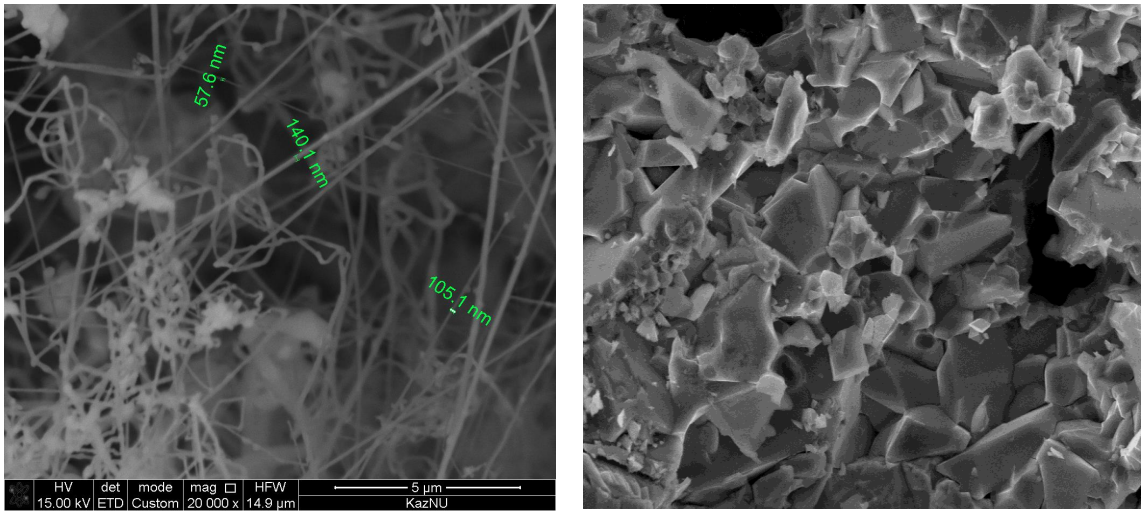

а) б)

Figure 3 - Microstructure, external appearance and characteristic crystal sizes of synthesized composite in systems: a – Al – $ZrSiO_4$ – Cr_2O_3; b – Al – SiO_2 – Cr_2O_3

CONCLUSION

X-ray diffraction phase analysis and structural characteristics of SHS products, a large number of samples based on zircon, silicon chromium oxides are determined depending on the content of active components and nitrogen pressure in reaction vessel. It has been established that along with metal nitrides and aluminum oxide, the composition of composite contains appreciable amounts of silicides and oxynitrides.

Electron-microscopic studies of SHS products with energy-dispersive elemental analysis was carried out, which unequivocally point to the reinforcing and strengthening role of rod-like and filamentary structures of nitrides and metal oxynitrides in oxide matrix of composite.

Research results shows that SHS processes in multicomponent systems in nitrogen environment under high pressure make it possible to obtain nitride-containing composite materials, possessing not only high refractoriness and metal resistance, but also high strength characteristics.

REFERENCE

[1] Ilyin A.P., Tolbanova L.O. Synthesis of nitrides by combustion of aluminium and wolframite nanopowder in air // Physics and chemistry of material processing. – 2013. – № 8. – P 80–85.

[2] Gromov A.A., Habas T.A., Ilyin A.P. and others. Combustion of metal nanopowders. – Tomssk: Deltaplan, 2011. – 282 p.

[3] Inna P. Borovinskaya, Vazgen E. Loryan, and Vladimir V. Zakorzhevsky. Combustion Synthesis of Nitrides for Development of Ceramic Materials of New Generation. Nitride Ceramics: Combustion Synthesis, Properties, and Applications, First Edition. Edited by Alexander Gromov and Liudmila Chukhlomina. .Published 2014 byWiley-VCH Verlag GmbH & Co. KGaA.

[4] Borovinskaya I.P. Synthesis peculiarities of SHS-ceramics at high gas pressures. In collection Self-propagating high –temperature synthesis: theory and practice, 2001, Chernogolovka, P.236-251.

[5] Mukasyan A.S., Stepanov B.V., Galchenko Yu.A., Borovinskaya I.P. About structure formation mechanism of silicon nitride during combustion of silicon in nitrogen. Combustion, Explosion, and Shock Waves №1. P.45-52. 1990.

[6] Fomenko S.M., Mansurov Z.A., Bekzhanova M.T., Korkembay Zh., Alipbayev A.N. Aluminothermal combustion in systems = Al – $ZrSiO_4$ – N_2 and Al – SiO_2 – N_2 under conditions of nitrogen high pressure. Proceedings of VII International symposium «Combustion and plasmachemistry». – Almaty, 2013. – P.51-55.

[7] A.C. 87006, application. 29609. Obtaining method of ceramics. Fomenko S.M., Mansurov Z.A., Alipbayev A.N.,Abdulkarimova R. G., 14.05.2014.

[8] Fomenko S.M., Mansurov Z.A., Alipbayeva A.N Korkembay Zh., Abdulkarimova R. G. Obtaining of nitride-containing composites based on zircon and silicon oxide in high-pressure plant by SHS method . VIII International symposium « Physics and chemistry of carbon materials». - Almaty 2014 . – P.210-214.

PARTICLE SIZE DEPENDENT PRESSURE DISCHARGE PROPERTIES OF AL-BI(OH)$_3$ NANO-ENERGETIC GAS GENERATORS

S. A. Yolchinyan, M. A. Hobosyan, and K. S. Martirosyan

[1] The University of Texas at Rio Grande Valley, Brownsville, TX 78520, USA
*karen.martirosyan@utrgv.edu

Nano-energetic gas generators (NGGs) are energetic formulations comprised of metallic fuel and metallic or non-metal oxide particles [1]. Recently, we have demonstrated that hydroxides can play the role of oxidizers in nano-energetic formulations [2]. Specifically, for Al-Bi(OH)$_3$ system, the thermodynamic calculations show that the reaction between aluminum and bismuth hydroxide is highly exothermic. The interaction between Al and Bi(OH)$_3$ follows the reaction:

$$2Al + 2Bi(OH)_3 = Al_2O_3 + 2Bi + 3H_2O + \Delta H\ (-1.92\ kJ/g) \qquad (1)$$

According to HSC-7 calculations, the energetic capacity for the system (1) is 1.92 kJ/g. Compared to well-known Al-Bi$_2$O$_3$ system, the gas generation in system (1) is twice higher, reaching 0.0087 mol/g for Al-Bi(OH)$_3$ formulation [2]. This opens great perspective for using this material in applications where the generation of large amounts of gaseous products is critical, such as microthrusters [3,4].

Figure 1 shows the dependence of the adiabatic temperature and equilibrium concentration of condensed and gaseous phases during the exothermic reaction in system (1). Interesting to note that the energetic density calculated for unit volume for the system (1) is 8.83 kJ/cc. When the molar ratio Al/Bi(OH)$_3$ increases from 0.5 to 1 mostly all the bismuth product converts to the gaseous phase. Additionally, when the ratio increases above 1, the temperature increases to more than 2000 K, resulting to gradual decomposition of water into hydrogen and the released oxygen is consumed for excess aluminum oxidation. At molar ratio 2 the highest adiabatic temperature was calculated to be 2970 K, where the products are about 1 mol solid Al$_2$O$_3$, 1 mol gaseous Bi, and ~1.6 moles of gaseous mixture of molecular H$_2$ and atomic hydrogen. At this point, the reaction pathway becomes

$$2Al + Bi(OH)_3 = Al_2O_3 + Bi(g) + 1.4H_2(g) + 0.2H(g) \qquad (2)$$

The further increase of fuel to oxidizer molar ratio results some partial decomposition of solid Al$_2$O$_3$ into Al$_2$O gaseous and Al gaseous, however the amount of atomic hydrogen is quickly decreasing due to reduction of adiabatic temperature. Thus, in our experiments we used molar ratio for Al and bismuth hydroxide to be 2 according to reaction (2). We also took into account the extra oxide shell mass on aluminum nanoparticles. In addition, we investigated the pressure discharge dependence on non-stoichiometric fuel to oxidizer ratio, for comparison with thermodynamic calculations.

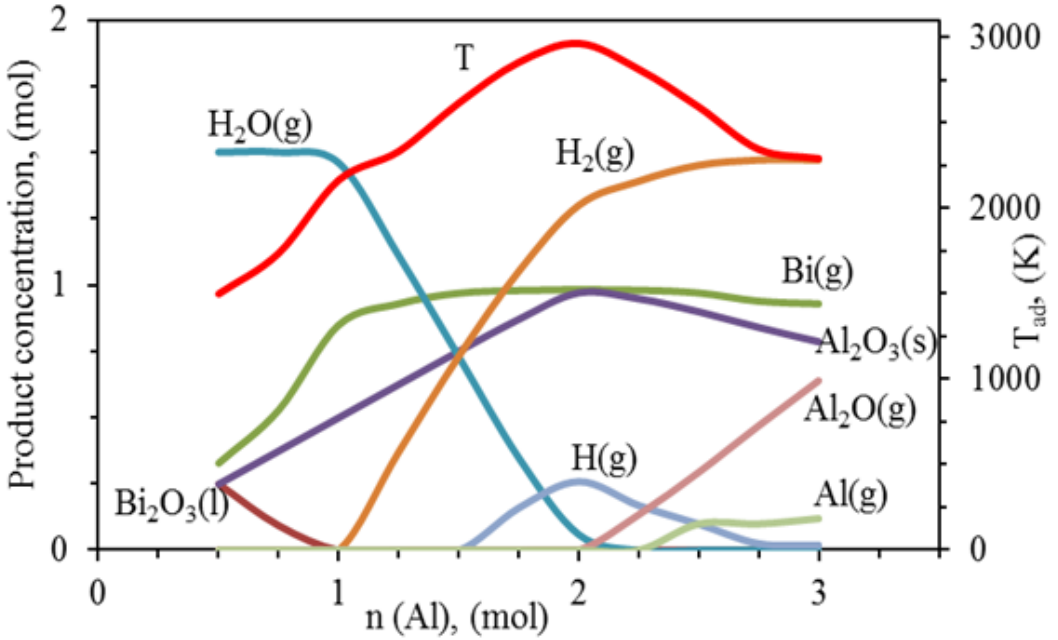

Figure 1 - Dependence of the adiabatic temperature and equilibrium concentration of condensed and gaseous phases on fuel concentration during the exothermic reaction in system Al-$Bi(OH)_3$: (red line is adiabatic combustion temperature).

The commercial bismuth hydroxide particles (Sigma Aldrich) have broad size distribution, ranging from few micrometers to 100 micrometers and above (Figure 2a). Thus, it was necessary to homogenize the commercial bismuth hydroxide particles in high energy ball mill, to control the effect of the mechanical activation on particle size reduction, decomposition energy of bismuth hydroxide, and oxidizing activity in the nanostructured system Al-$Bi(OH)_3$. The milling energy applied during the mechanical activation decreases the particle size of bismuth hydroxide particles to sub-micrometer and nano-metric size domain (Figure 2b). Thus, if the homogenization time is in order of 15 minutes, the micro-sized particles are mostly in sub-micrometer size. The thermogravimetric analysis shows that the decomposition of bismuth hydroxide starts at around 390 ºC with 28.8 J/g degradation energy (Figure 2c). The second mass loss starts at around 502 ºC, and the decomposition is essentially completed at around 590 ºC. The energy required for all steps of decomposition was around 107 J/g. For the particles milled for 15 min, the first step consumes 23.8 J/g energy, the second endotherm energy decreases to 41.5 J/g (Figure 2d) and the energy for last step increases to 11 J/g. The overall decomposition energy is about 76 J/g, 30 % less than that for as-received powder.

Figure 2e represents the pressure vs time plot for Al-$Bi(OH)_3$ thermites prepared with as received and mechanically milled $Bi(OH)_3$ powder up to 10 and 15 min with different weight percentages of Al.

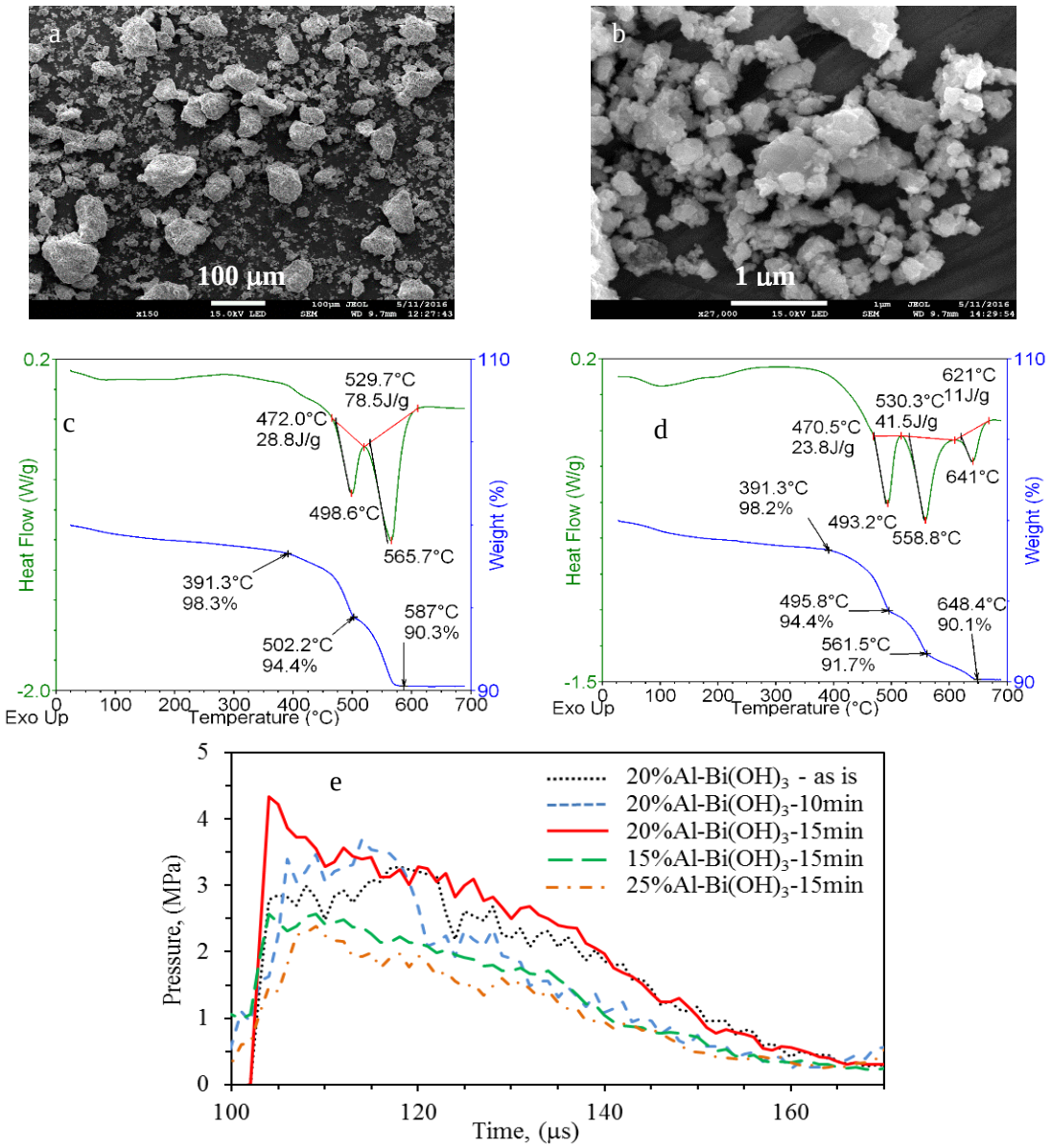

Figure 2 - SEM images for (a) as received $Bi(OH)_3$; (b)15 minutes milled $Bi(OH)_3$, (c) heat flow and weight change dependence on the temperature for (c) as received $Bi(OH)_3$; (d) 15 minutes milled $Bi(OH)_3$, (e) discharge pressure dependence on time for Al-$Bi(OH)_3$ thermites prepared with as received, 10 and 15 min mechanical treated $Bi(OH)_3$, with 20 wt. %Al, and thermite prepared with 15 min treated $Bi(OH)_3$ and different weight percentages of Al. The charge mass in all cases is 0.2 g, and the reactor volume is 0.342 L.

The highest pressure for thermite prepared with as-received $Bi(OH)_3$ was 3.33 MPa for 0.2 g thermite, while for 15 min treated $Bi(OH)_3$ is 4.34MPa (30 % pressure rise).

Thus, the nano-energetic mixture prepared with sub-micrometer and nano-sized bismuth hydroxide is highly reactive and powerful, and is comparable to strongest known nano-energetic formulations. The best mass ratio for generating highest pressure discharge value was 2:8 fuel to oxidizer. Thus, metal hydroxides are promising components for nano-thermites which may

generate vigorous amount of gaseous products and have extreme pressure discharge abilities, which are useful for applications such as microthrusers.

ACKNOWLEDGMENTS

We would like to acknowledge the financial support of this research in part of the Army Research Office (grant No. 66389-CH-REP) and NSF PREM (award DMR-1523577: UTRGV-UMN Partnership for Fostering Innovation by Bridging Excellence in Research and Student Success).

REFERENCES

[1] Martirosyan K. S., "Nanoenergetic gas generators, principle and applications," J. Materials Chemistry, vol. 21, pp. 9400-9405, 2011.

[2] Hobosyan, Mkhitar A., Srbuhi A. Yolchinyan, and Karen S. Martirosyan. "A novel nano-energetic system based on bismuth hydroxide." RSC Advances 6, no. 71 (2016): 66564-66570.

[3] Martirosyan, Karen S., Mkhitar Hobosyan, and Sergey E. Lyshevski. "Enabling nanoenergetic materials with integrated microelectronics and MEMS platforms." In Nanotechnology (IEEE-NANO), 2012 12th IEEE Conference on, pp. 1-5. IEEE, 2012.

[4] I. Puchades, L.F. Fuller, S. E. Lyshevski, M. Hobosyan, L. Ting, K.S. Martirosyan, MEMS and 3D-Printing Microthrusters Technology Integrated With Hydroxide-Based Nanoenergetic Propellants, ELNANO, IEEE Xplore, (in print), 2017.

SELECTIVE LASER MELTING OF COMBUSTION SYNTHESIZED 2Mo-Cu AND 3Cu-Mo COMPOSITES

T.T. Minasyan[*1,3], S.V. Aydinyan[1,3], S.L. Kharatyan[1,2]

[1]A.B. Nalbandyan Institute of Chemical Physics NAS RA, P.Sevak 5/2, 0014, Yerevan, Armenia
[2]Yerevan State University, A. Manukyan 1, 0025, Yerevan, Armenia
[3]Tallinn University of Technology, Ehitajate tee 5, 19166, Tallinn, Estonia
*tatminas@gmail.com

The increasing scientific interest in Mo-Cu alloys (with various content of Mo) is conditioned by the fact, that they form a pseudo-alloy and depending on the Mo/Cu ratio, constituent elements may be either matrix or dispersing component. The Mo-Cu materials combine the properties of both metals and can emerge improved or new properties even leading to the optimization of alloy properties, such as high thermal and electrical conductivity, low and alterable thermal expansion coefficient, low weight, nonmagnetic and well high-temperature behavior [1-2]. In view of these features they find their main applications as micro electrical equipment, welding electrodes**,** microwave carriers, optical and power packages, heat sinks, micro electrical packages/hybrids and butterfly packages for telecom systems.

In this work it was proposed to synthesize Mo-Cu composite powders with molar ratio of constituent metals Mo:Cu=2:1 and Mo:Cu=1:3 from oxide precursors in combustion mode by applying reaction's coupling approach [3,4] using Mg+C combined reducers and further densification by selective laser melting (SLM) technique. It is assumed that it may became a promising combination of cost and energy-efficient combustion synthesis with fast developing and waste-free manufacturing technique of selective laser melting (SLM) [5].

Before the experimental investigations thermodynamic calculations were performed to reveal the possibility of combustion in the CuO-$2MoO_3$-yMg-xC and $3CuO$-MoO_3-yMg-xC systems. Optimum areas for the complete reduction of metals were found out according to reducer's ratio and ambient gas pressure for both the systems. Thus, 2.2 and 1.7 mole amounts of magnesium were chosen as optimal for the CuO-$2MoO_3$-xMg-yC and $3CuO$-MoO_3-xMg-yCsystems respectively. The optimum composition of mixtures was found by changing the amount of carbon in the initial mixture. The combustion peculiarities of the CuO-$2MoO_3$-$2.2Mg$-xC and $3CuO$-MoO_3-$1.7Mg$-xC systems were investigated in the wide range of carbon amount from 0 to 4 (4.5) moles. As a result $CuO+2MoO_3+2.2Mg+3.7C$ and $3CuO+MoO_3+1.7Mg+3.4C$ mixtures were found as target mixtures for complete reduction of both the metals. Following the synthesis acid leaching was performed to get rid of byproduct magnesia and 2Mo-Cu and 3Cu-Mo composites were obtained.

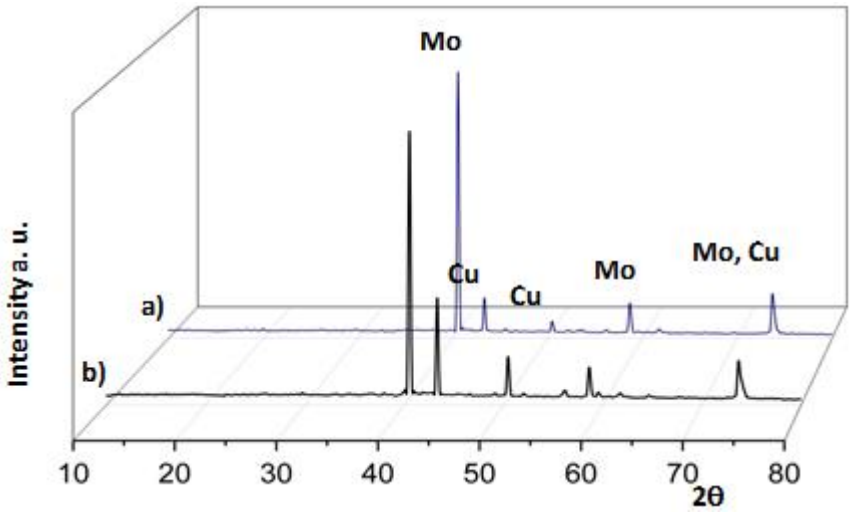

Fig.1 - XRD patterns of the leached powder obtained at combustion of a) $CuO+2MoO_3+2.2Mg+3.7C$ and b) $3CuO+MoO_3+1.7Mg+3.4C$ mixtures

To obtain dense and both functionally and geometrically complex structured Mo-Cu shapes with good dimensional tollerance, the synthesized powders were treated by SLM, as there are now numerous examples of the successful implementation of metal SLM. The experiment parameters, such as layer thickness, laser current, exposure time and point distance were studied and optimized.

It is expected that the suggested approach is able to expand the application fields of both SHS and SLM, find scientific interest and industrial usage.

REFERENCES

[1] X.Wang, L.Hu, H.Wang, E.Wang, Rare Metal Mat. Eng., 40, 5, (2011) p. 902.
[2] G. Chen, G. Wu, L.Jiang, Zhu, D. Sun, Key Eng. Mater., 353, (2007) p. 2883.
[3] A.G. Merzhanov, Int. J. SHS, 20, 1, (2011) p. 61.
[4] S.L. Kharatyan, A.G. Merzhanov. Int. J. SHS, 21, (2012) p. 59.
[5] E. Juste, F. Petit, V. Lardot, F. Cambier, J. Mater. Res., 29, 17, (2014) p. 2086.

CONSOLIDATION/SYNTHESIS OF CERAMIC MATERIALS BY SPARK PLASMA SINTERING

D.O. Moskovskikh*[1], A.S. Mukasyan[2]

[1] National University of Science and Technology MISiS, Moscow, Leninskiy prospekt 4,119049, Russia
[2]University of Notre Dame, Notre Dame, IN 46556, USA.
* mos@misis.ru

Self-propagatinghigh temperature synthesis (SHS), is an energy saving and attractive method for production of a variety of advanced micron- and nano-scale materials with properties that are superior to those manufactured by conventional methods [1]. In turn, spark plasma sintering (SPS), also known as the field-assisted sintering technique (FAST) is a novel sintering technique [2]. During SPS, a strong-pulsed current is directly passed through the electrically conducting pressure die and the sample. The unique features of the SPS process is the possibilities to apply extremely high heating rates, up to several hundred degrees per minute, and subsequently to achieve full densification within minutes. Combination of SHS and SPS in one-step method to produce pore free ceramics is a new promising technique for fabrication of advanced materials [3].

In this work bulk silicon (SiC) and boron (B_4C) carbides were fabricated from mixtures of elements (silica, boron and carbon) by use this one-step, so-called, reactive spark plasma sintering (RSPS) approach. It was demonstrated that preliminary high-energy ball milling (HEBM) of the Si+C and B+C powder mixtures leads to the formation of composite particles with enhanced reactivity. Using these reactive composites in RSPS permits tuning of the microstructure for the synthesized ceramics and thus produced materials with desired properties. Optimization of HEBM + RSPS conditions allows rapid (less than 30 min of SPS) fabrication of ceramics with porosity less than 1%, high hardness (SiC~24 GPa and B_4C~35 GPa), and good fracture toughness of ~ 5 $MPa \cdot m^{1/2}$ [4,5].

The authors gratefully acknowledge the financial support of the Ministry of Education and Science of the Russian Federation in the framework of Increase Competitiveness Program of NUST «MISiS» (№ К2-2016-065), implemented by a governmental decree dated 16th of March 2013, N 211.

REFERENCES

[1] A.G. Merzhanov The chemistry of self-propagating high-temperature synthesis J. Mat. Chem., 14 (12), 2004, pp. 1779-1786.

[2] Z.A. Munir, U Anselmi-Tamburini, M. Ohyanagi, The effect of electric fieldand pressure on the synthesis and consolidation of materials: a review of the spark plasma sintering method. J Mater Sci, 41, 2006, pp. 763–77.5.

[3] R. Orru, G. Cao, Comparison of Reactive and Non-Reactive Spark Plasma Sintering Routes for the Fabrication of Monolithic and Composite Ultra High Temperature Ceramics (UHTC) Materials, Materials, 6 (5) 2013, pp. 1566-1583

[4] D.O. Moskovskikh, Y. Song, S. Rouvimov, A.S. Rogachev, A.S. Mukasyan, Silicon carbide ceramics: Mechanical activation, combustion and spark plasma sintering, Ceramics International, 42 (11), 2016, pp. 12686-12693.

[5] D.O. Moskovskikh, K.A. Paramonov, A.A. Nepapushev, N.F. Shkodich, A.S. Mukasyan, Bulk boron carbide nanostructured ceramics by reactive spark plasma sintering, Ceramics International, 43 (11), 2017, pp. 8190-8194.

FIFTY YEARS OF DISCOVERY: HISTORY AND FUTURE

I.P. Borovinskaya[1], A.S. Mukasyan*[2]

[1] Institute of Structural Macrokinetics and Materials Science, RAS, Chernogolovka 142432, Russia
[2] Department of Chemical & Biomolecular Engineering, and §Nuclear Science Laboratory, Department of Physics, University of Notre, Dame, Notre Dame, Indiana 46556, United States
* amoukasi@nd.edu

In the 1960s, a group of researchers from the Institute of Chemical Physics USSR Academy of Sciences (Figure 1), leaded by the young head of the laboratory Alexander G. Merzhanov, searched for combustion systems, which would be burned without producing a gas flame [1]. This was necessary in order to understand the role of reactions in the condensed phase during combustion of gunpowder and solid rocket propellants. During this work the scientists unexpectedly discovered a new phenomenon of "wave localization for self - retarding solid state reactions" [2], or in modern terms the *solid flame* [3, 4]. The essence of the invention was formulated as follows [2]: "Experiments established the previously unknown phenomenon of wave localization for self-retarded solid-state reactions, consisting in the fact that the chemical interaction between the solid dispersed components occurs without melting and gasification of the reactants and products, after thermal initiation is localized in a zone moving spontaneously in the space of the reagent in the form of a combustion wave''.

Figure 1 - Inventors: A.G. Merzhanov, I.P. Borovinskaya, V.M. Shkiro.

From the standpoint of conventional combustion, a solid flame is enigmatic, because it is hard to believe that solely solid-state diffusion may define the self-sustaining nature of the combustion process. It is a prevalent opinion that self-propagating combustion processes, such as metallothermic reactions, exist due to relatively fast mass transport in the liquid phase (diffusion and convection), therefore, melting of at least one component in the system is considered as a necessary condition for combustion. However, it was unequivocally shown that Mother Nature indeed "allows" the solid flame phenomenon [5, 6].

It is even more important that based on this fundamental phenomenon a novel technological approach for fabrication of variety of materials, i.e. self-propagating high-temperature synthesis

(SHS), has been developed [7]. History of the using of the self-sustained reactions for material's preparation is discussed in variety of publications [1, 8-11]. No doubt that, while having predecessors including works by N.N. Beketov and H. Goldschmidt, only after thorough fundamental research initiated by A.G. Merzhanov and co-workers, SHS became the widely recognized technology for synthesis of almost any type of advanced inorganic materials (Figure 2).

Figure 2 - Materials and net-shape articles produced by SHS

Following A.G. Merzhanov [1] we may outline three stages for the development of SHS field. First stage (1967-1972) was related to the works primarily accomplished in Institute of Chemical Physics in Chernogolovka. This stage was dedicated to establishing the initial knowledge on the solid flame phenomenon. Year 1972 can be outlined as an "initiation" of the second stage, i.e. "self-propagating" of SHS ideas along the different Institutions in Former Soviet Union. Starting from this time several scientific SHS centers have been established, including in Armenia (in the Institute of Chemical Physics Armenian Academy of Sciences), Ukraine (in the Institute of the Material Sciences, Ukraine Academy of Sciences), Uzbekistan (in Institute of Nuclear Physics, Uzbekistan Academy of Sciences), Kazakhstan (Institute of Combustion Problems), Georgia (in F. Tavadze Institute of Metallurgy and Materials Science). Three SHS Centers were developed in Russia, i.e. in Tomsk (in Tomsk State University), Samara (in Samara State Technical University) and Moscow (in National University Science and Technology, MISIS). Many of these Centers worked together in the Multidisciplinary Scientific Technical Complex (MSTC) "Thermo-synthesis" established in 1987.

Finally, in 1980th the SHS started getting a worldwide recognition first in USA and Japan, followed by China and many other countries. Recent analysis of published literature (Web of Science) shows that scientists in 117 countries are involved in the research in SHS and combustion synthesis fields. Number of publication increases almost exponentially (Figure 3). New directions, where self-sustained reactions are used for fabrication of advanced materials and coatings, have been established. Among them solution combustion synthesis, originated by Indian scientists attracted most attention (see recent review [12]). Another currently popular filed is combustion synthesis of ceramics [13, 14], especially by combination of SHS and spark plasma sintering [15], where contribution of scientists for US, Italy and Japan is difficult to overestimate.

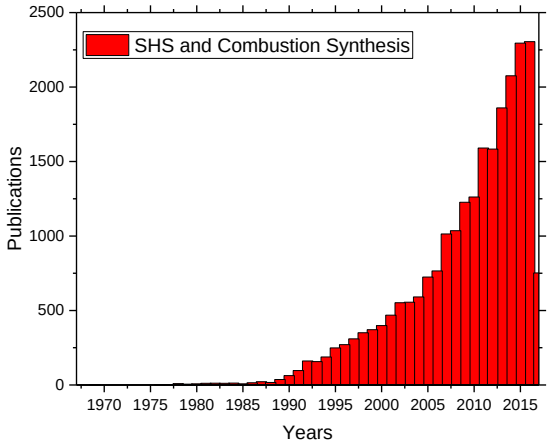

Figure 3 - Number of publications per year in the field of SHS and Combustion Synthesis

Combustion of nano-structured reactive foils, developed in US is another current hot spot in the field of rapid gasless reactions [17, 18]. Also a variety of nano materials including 0, 1 and 2 dimensional structures were produced by different combustion synthesis approaches (recent review [12, 18]). In this direction, one can find many exciting publications of the researchers specifically from China and South Korea. Combination of mechanical activation (MA) and SHS, so-called MASHS, initiated by scientists from Russia and France now found worldwide attraction ([19, 20]). Among theoretical approaches, we want to outline a rapid development of molecular dynamic simulation (MDS) methods to analyze SHS processes [21].

In this lecture, we will overview, discuss and analyze all above and other issues related to the history, status and prospective of this exiting multidisciplinary branch of science, which stared with the discovery of solid flame 50th years ago.

REFERENCES

[1] A.G. Merzhanov A.G., 40 years of SHS: A Lucky Star of Scientific Discovery (story-presentation with elements of a scientific paper), Bentham Science Publisher, Brussel, Belgium, 2012, 104 p., doi**:** 10.2174/97816080512811120101.

[2] A.G. Merzhanov, V.M. Shkiro V.M., Borovinskaya I.P., "Phenomenon of wave localization for self - retarding solid state reactions", Diploma № 287, filed 05.07.1967; Vestnik of USSR Academy of Science, № 10, 1984 (in Russian).

[3] A.G. Merzhanov, Solid flame: Discovery, concepts, and horizons of cognition, Cmb. Sci. Technol., 1994, Vol. 98, Nos. 4–6, pp. 307–336.

[4] A.G. Merzhanov, A.S. Mukasyan, Solid-Flame Combustion (Tverdoplamennoe Gorenie), Moscow: Torus Press, 2007, p. 336 (in Russian).

[5] V.M. Shkiro, G.A. Nersisian, I.P. Borovinskaya, Combust. Explos. Shock Waves, 14(4) 1978, pp. 455–460.

[6] C. E. Shuck, K.V. Manukyan, S. Rouvimov, A. S. Rogachev, A.S. Mukasyan, Comb. & Flame, 163, 2016, pp. 487-493.

[7] A.G. Merzhanov, I.P. Borovinskaya, Self-spreading high-temperature synthesis of refractory compounds, Dokl. Chem., 1972, 204(2), pp. 429–431.

[8] A.G. Merzhanov A.G. Self-propagating high-temperature synthesis: Twenty years of search and findings. In: Combustion and Plasma Synthesis of High-Temperature Materials, Munir Z., Holt J.B., Eds., New York: VCH, 1990, pp. 1–53.
[9] V. Hlavacek, Combustion synthesis: A historical perspective, Amer. Ceram. Soc. Bull., 1991, 70(2), pp. 240–243.
[10] A.G. Merzhanov, History and Recent Development in SHS, Ceramics International, 21(5), 1995 pp.371-379
[11] A.S. Rogachev, A.S. Mukasyan, Combustion for Material Synthesis, CRC Press, Taylor and Francis, 2015, 398 p.
[12] A. Varma, A.S. Mukasyan, A.S. Rogachev. K. Manukyan *Chemical Review*, 116, 2016, pp.14493-14586.
[13] Book: Nitride Ceramics: Combustion Synthesis and Applications, Editors: AA. Gromov, L. Chukhlomina, Wiley, VCH, 2014, pp.234.
[14] E.A. Levashov, A.S. Mukasyan, AS. Rogachev and DV. Shtansky, *International Materials Reviews* 62(4), 2017, pp 203-239.
[15] R. Orrù R, G. Cao G., *Materials*, 6, 2013 pp. 1566–1583.
[16] T.P. Weihs , Fabrication and characterization of reactive multilayer films and foils, in: K. Barmak, K.R. Coffey (Eds.), Metallic Films for Electronic, Magnetic, Optical and Thermal Applications: Structure, Processing and Properties, Wood- head Publishing, Swaston, UK, 2014, pp. 160–243. Chapter 6 .
[17] A.S. Rogachev, Russ. Chem. Rev. 77, 2008, pp. 21–37.
[18] A. S. Mukasyan, K. Manukyan, Current Opin.in Chem. Eng., 2015, 7, pp. 16–22.
[19] E.L. Dreizin, Progress in Energy and Combustion Science, 35, 2009, pp. 141–167
[20] A .S. Rogachev, A .S. Mukasyan, Comp. Expl. Shock Waves 46 (2010) 243–266.
[21] V. Turlo, O. Politano, F. Baras Acta Materialia, 120, (2016) pp.189-204

SYNTHESIS OF INORGANIC RADICALS

G.I. Ksandopulo, A.N. Baideldinova, L.V. Mukhina, E.A. Ponomareva

Institute of Combustion Problems, Almaty, Bogenbai Batyr str., 172, Kazakhstan
milabrega@yandex.ru

For the first time the synthesis of solid-phase radicals was considered in works of V.V. Voyevodskiy [1] using tetrafluorethylene and ionizing radiation influence on it. At the same time, in reactions of their recombination, anomalous values of the activation energies and compensating effect were observed. The assembly of observing factors was used as the basis of assumption, in a certain range of temperatures there are occurred phase changes in crystalline structure of the sample. In this case, the effective activation energy of recombination reactions decreases with increasing temperature.

The compensating effect is a property of crystalline structure of substance, rather than the reacting particles. Accordingly, if the energy of the interatomic bonds higher, so the compensating effect is more significant in inorganic radicals (HP) can be expected. Thanks to HP, it would be possible to have a specific effect on the mechanism of a wide range of inorganic processes.

The problem of synthesis and condensed products of SHS containing HP is considered. The practical importance of HP is conditioned by their free valence, to the possibility of influencing high-temperature chemical processes as agents that have a modifying effect on the kinetics of the crystallization of melts of various metals, causing a change in their crystalline structure, as well polymerization processes of inorganic and organic systems. The free valence of HP is also capable to realize the function of catalysts.

In works [2-4] there are presented fundamentals of SHS oxide systems theory with mass transfer is conditioned by the rotational forces action to the propagating combustion wave. The preparation of metal-melt clusters and the method of forming the momentum of their flow were first considered as a shock agent for attacking a reaction mixture of a selected composition.

The size of the metal particles Me at the time of their formation within the front of SHS wave is 2-3 · 10-6 m [5]. If the reaction of metal reduction from its oxide proceeds under resting conditions, so these particles coalesce unimpeded, forming firstly enlarged aggregates and further ingot. In the conditions of the action of rotation forces, there is a transfer of products from the combustion front zone (Figure 1). Their trajectory is directed towards the fresh mixture, correspondingly to the resultant vector of the acting forces - centrifugal F_n and Coriolis $F_к$;

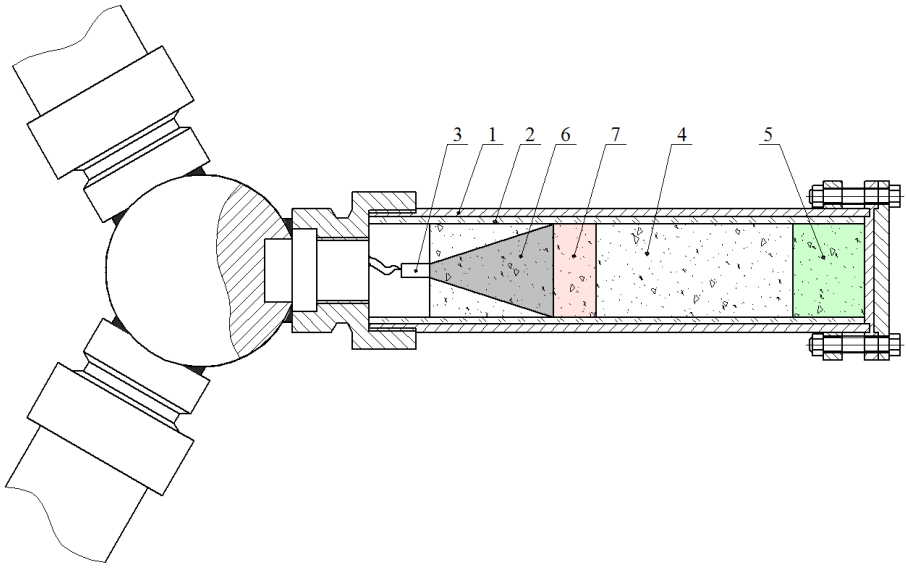

1 - steel case, 2 - transparent tube-insert, 3 - incendiary cartridge, 4 - high-calorie, attacking stream, 5 - receiver layer, attack medium, 6 - primary direction of development of the combustion wave front, 7- transition zone to superadiabatic regime

Figure 1 - Scheme of the rotary reactor and the main processes

The sample with a length L and diameter D from the metal oxide mixture and aluminum was placed in a cylindrical reactor is fixed perpendicularly to the rotation axis. After combustion initiation, the melt of reaction products (Al_2O_3 together with metal drops Me), as noted above, is thrown into the layer of fresh combustible mixture of SHS wave. Possessing by high temperature and kinetic energy of motion, each component of melts penetrates to varying degrees, during the reaction time τ into the pores of the boundary fresh layer · by a depth ε, giving away the thermal energy and zeroing the kinetic energy at the moment of impact.

The kinetic and thermal energies of drifting particles that appeared in last layer are preserved, because there is no more impact on the surface of the reaction layer. Thus, the energy of cluster flow is conditioned by the linear dimension of burning sample, the concentration of the metal in it, and the number of revolutions n.

As described above and in works [4-8], the mixtures γ-Al_2O_3 и B_2O_3 + Al were selected as attacked. The synthesis was carried out by clusters of tungsten, molybdenum, and copper reduced in the course of SHS. The composition of the products revealed the presence of nontrivial crystalline phases number identified by XRF spectra. As an example, we can mention $Al_{20}B_4O_{36}$, $Al_{7,7}Mo_{30}Si_{3,3}$, B_2Mo_5Si. The obtained product of compositions indicates the formation of intermediate phase and nonequilibrium products. The transformation time of 10-3 s is essentially the relaxation time of a nonequilibrium state in a certain temperature range with a maximum exceeding of melting point of tungsten. The observed uniform distribution of products in the attacked layer indicates to significant predominance of impact energy over the surface and viscous forces of the cluster.

The studies carried out on the EPR spectrometer it indicate a high degree of disequilibrium achieved at the time of the attack. The spectra indicate signals corresponding to the formed inorganic radicals.

Thus, an extensive opportunity opens up to synthesize new materials and create chemical processes where the Arrhenius barrier reaches 1 mJ. Creation of successively attacked layers in reactor and an increase in the rotational speed of up to 10,000 rpm, it is possible to replace the attacking clusters of heavy metals On attacking clusters of light metals.

REFERENCES

[1] B.B. Voevodsky. Physics and chemistry of elementary chemical processes.– M.: «Science». – 1969. – P. 250.

[2] Ksandopulo, G. I. SHS in Conditions of Rotation: Thermal and Concentration Combustion Limits for Oxide Systems Taken as an Example // International Journal Of Self-Propagating High-Temperature Synthesis. – 2011. –Vol. 20.– P. 220-223.

[3] Ksandopulo, G. I. Non-chain autoacceleration of SHS wave in conditions of rotation // International Journal Of Self-Propagating High-Temperature Synthesis. – 2015. – Vol. 24. – P. 8-13.

[4] Baideldonova A, Ksandopulo G, Mukhina L. Initiation of the adiabatic wave of combustion for obtaining the substances with the free valence // 3rd International Conference on Competitive Materials and Technology Processes (IC-CMTP3) IOP Publishing IOP Conf. Series: Materials Science and Engineering. – 2016. – Vol. 123

[5] Kirdyaashkin A.I., V.D. Kitaye, V.G. Salamatov, R.A. Yusupov Peculiarities of structural dynamic of high-temperature metal-thermal processes as exemplified by the system FeO–Al–Al_2O_3. // Combustion and explosion physics. – 2008.– T. 44, № 1, – P. 80-84.

[6] Ksandopulo G. I., Baydeldinova A.HN, Muhina L.V., Ponamareva E.A., Azizov Z.M. Nanocarbon structures and other nontrivial substances in SHDS products during centrifugal acceleration // International symposium «Physics and chemistry of carbon materials / Nanoengineering» International conference «Nanoenergetic materials and nanoenergy ». – Almaty. – 2016. – P. 3-7.

[7] Ainabaev A.M., Arkhipov M.P., Baydeldinova A.N., Omarova K.I., Ksandopulo G.I. Out of Furnace Synthesis of High-Temperature Ceramic Materials in the Revolving Reactor // 2nd International Conference on Competitive Materials and Technology Processes. – Micds – Lillafured, Hungary. – 2012. – P. 139.

[8] Ksandopulo G.I., Baideldinova A.N., Shevchenko V.N., Ksandopulo G.G. High-Temperature Centrifuge / RoK Patent No 68316 as of 26.05.2010. Innovative RoK Patent No 23988 as of 26.05.2010.

[9] Ksandopulo G.I., Baideldinova A.N., Ainabaev A.M., Arkhipov M.P., Omarova K.I. Macrokinetics of SHS-process Under the Effect of Centrifugal Force. // Eurasian Chemical-Technological Journal. – 2011, № 3-4. – Vol. 13.

REGULARITIES AND MECHANISM OF FORMATION OF ALUMINIDES IN TiH_2-ZrH_2-AL SYSTEM

S.K. Dolukhanyan, G.N. Muradyan, A.G. Aleksanyan, O.P.Ter-Galstyan, N.L.Mnatsakanyan and A.G.Hakobyan

Nalbandyan Institute of Chemical Physics, NAS 5/2 P. Sevak Str., Yerevan, 0014, Armenia,
seda@ichph.sci.am

This work presents the studies on the formation of titanium and zirconium aluminides by Hydride Cycle (HC) method. Aluminum based alloys have a number of characteristics making them attractive in modern technology. Because of the stable passivating oxide layer, they are very resistant to oxidation and have many other useful characteristics, including low density, high elasticity, high melting points, etc. Therefore, interest in aluminum-based alloys is associated with a broad perspective of practical application as design materials: in atomic and hydrogen energy, in the defense, aerospace, shipbuilding, chemical, automobile industries, etc. The alloying with Group IV transition metals (Ti, Zr and Hf) is used for making better the mechanical, physical and chemical properties (hardness, wear and corrosion resistance, etc.) of aluminides.

Traditional melting (induction, electric arc) is the most-known method for production of metal aluminides. Its realization needs high-temperature induction or arc furnace. The formation of aluminides by this method is a long, multi-stage process, requiring creation of deep vacuum and inert medium at high temperature (800-2500°C). In the powder metallurgy, the sintered samples must be subjected to heat treatment at T=850-900°C during 30-40 hours or more. The mechanical alloying method demands 10-40 hours or more. During mixing, the batch components adhere to the drum wall, changing their ratio. Besides, the batch is contaminated by the materials of balls and drum. The differences in the densities, melting and evaporation temperatures of the components complicate the current technologies. Dense oxide film on the particle surface of metal powders hinders the mutual diffusion of components. In recent decades, the method of self-propagating high-temperature synthesis (SHS) has been used for the synthesis of aluminides. But for its implementation, additional activation of the initial batch is often required.

Thus, the possibilities of the traditional technologies are mostly exhausted, and the search for more efficient, industrially reliable, cheap methods for the synthesis of high-quality aluminides of a given composition and structure is an actual task of modern materials science.

We propose the "Hydride cycle" method (HC), developed at the Institute of Chemical Physics of Armenian National Academy of Sciences, as a new method for the synthesis of refractory alloys and intermetallides. The essence of HC consists in taking the mixture of transition metal hydrides (or one metal hydride with another metal) as starting materials. When this mixture is compacted and heated, at temperature slightly above the dissociation temperatures of the hydrides, hydrogen is removed and a strong, nonporous alloy formed. More than 100 alloys were produced in the Ti-Zr, Ti-Hf, Zr-Hf, Ti-Nb, Ti-Zr-Hf, Zr-Ni, etc. systems. This method was successfully used for the synthesis of titanium and zirconium aluminides and of their hydrides. The demanded for HC transition metal hydrides were produced by SHS.

The task of the present work was to define the basic regularities and the mechanism of formation of aluminide phases in TiH_2-ZrH_2-Al system by HC. In the experiments, 99.9% purity zirconium (PCRK brand), PTM-1 titanium and 99.7% aluminum powder were used. Preliminarily, the titanium and zirconium hydrides (H_2 content of 4.01 and 2 wt. %, respectively) were synthesized by SHS method. The hydrides were crushed to fractions <50 μm, thoroughly mixed with aluminum and pressed in collate molds to cylindrical pellets with diameter of 22-25 mm and height of 8-10 mm at pressure of 20000-45000 KgF. The experiments were carried out in a hermetic unit consisting of a quartz reactor, oven, devices for monitoring the vacuum and temperature. The samples were placed in the reactor, evacuated and heated to the temperature of 600-1000ºC. The obtained samples were identified by chemical, differential-thermal (DTA, derivatograph Q-1500) and X-ray phase (XRF, diffractometer DRON-0.5) methods.

In Table 1 the results obtained for the system $(0.75\text{-}x)TiH_2$-$xZrH_2$-0.25Al (Ti_3Al - Zr_3Al) are shown. The effects of titanium and zirconium hydrides' ratio, of compaction pressure, temperature and heating rate at dehydrogenation and sintering on the characteristics (phase composition, density, absorption properties, etc.) of the resulting aluminides were studied. In HC, the titanium and zirconium aluminides are formed in accordance with the reaction:

$$(0.75\text{-}x)TiH_2 + xZrH_2 + 0.25Al \rightarrow Ti_{0.75\text{-}x}Al_{0.25}Zr_x \text{ aluminide} + H_2\uparrow \quad (0 \leq x \leq 0.75)$$

During heating of the initial charge $(0.75\text{-}x)TiH_2 + xZrH_2 + 0.25$ Al, the exothermic peaks at 650-670°C were registered on the HC thermograms. They indicate on the interaction of titanium and zirconium hydrides with aluminum (Table 1).

The thermal effects occurring at heating the batch were defined by thermal analysis. Fig. 1 shows the thermogram of $Ti_{0.55}Al_{0.25}Zr_{0.2}$ aluminide formation in HC and the DTA curves for heating of the initial $(0.55TiH_2 + 0.20ZrH_2 + 0.25Al)$ batch.

The formed compact titanium and zirconium based aluminides without crushing interacted with hydrogen in combustion mode (P_H=5-10 atm, T_{comb}=500-650°C), forming hydrides (Table 1). According to DTA, these hydrides decompose at 540-560°C. Fig. 2 shows the diffraction patterns of $Ti_{0.55}Al_{0.25}Zr_{0.2}$ aluminide and its hydride $Ti_{0.55}Al_{0.25}Zr_{0.2}H_{0.67}$.

Table 1 - Characteristics of the aluminides synthesized by HC

Initial reagents, at. %			DTA /HC exo effects, °C	Phase composition, parameters of crystal lattice, Å	Calculated formula	$T_{comb.}$, °C	H_2 cont., wt. %	Aluminum hydride formula, and type of crystal lattice
TiH_2	Al	ZrH_2						
0	25	75	630 /670	sol.sol. Al in HCP Zr + X phase a= 3.242; c=5.176	$Zr_{0.75}Al_{0.25}$	540	1.47	$Zr_{0.75}Al_{0.25}H_{1.07}$; ОЦТ +X phase
15	25	60	650 /680	sol.sol.Al and Ti in Zr + B_2 phase a=3.234; c=5.178	$Ti_{0.15}Al_{0.25}Zr_{0.6}$	430	1.3	$Ti_{0.15}Al_{0.25}Zr_{0.6}H_{0.89}$
25	25	50	650 /660	sol.sol. Al and Ti in Zr+ B_2 phase a =3.243; c=5.175	$Ti_{0.25}Al_{0.25}Zr_{0.5}$	430	1.3	$Ti_{0.25}Al_{0.25}Zr_{0.5}H_{0.83}$
35	25	40	660 /650	B_2 phase; a=3.384 +sol.sol. Al in Ti and Zr	$Ti_{0.35}Al_{0.25}Zr_{0.4}$	360	1.32	$Ti_{0.35}Al_{0.25}Zr_{0.4}H_{0.79}$
45	25	30	660 /670	B_2 phase;a=3.348 + (α_2) DO_{19}	$Ti_{0.45}Al_{0.25}Zr_{0.3}$	330	1.57	$Ti_{0.45}Al_{0.25}Zr_{0.3}H_{0.87}$
55	25	20	660 /640	B_2 phase; a=3.318 + (α_2) DO_{19}	$Ti_{0.55}Al_{0.25}Zr_{0.2}$	310	1.32	$Ti_{0.55}Al_{0.25}Zr_{0.2}H_{0.67}$
65	25	10	660 /690	DO_{19}; a =5.894; c = 4.629 + B_2 phase; a=3.307	$Ti_{0.65}Al_{0.25}Zr_{0.1}$	300	1.28	$Ti_{0.6}Al_{0.3}Zr_{0.1}H_{0.59}$
75	25	0	670 /660	α2-Ti_3Al; (DO_{19}) *a* =5.83, *c* = 4.647	$Ti_{0.75}Al_{0.25}$	500	2.27	$Ti_{0.7}Al_{0.3}H_{1.0}$ FCC

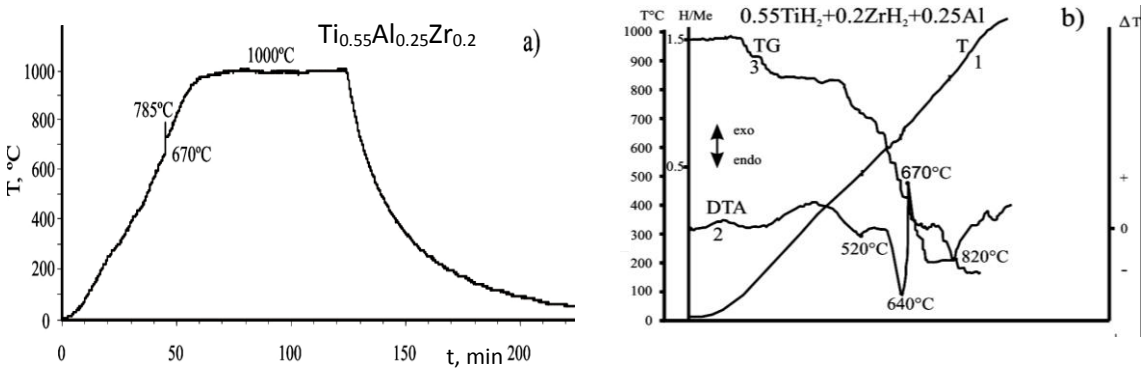

Fig.1 - Thermogram of aluminide formation in HC (a) $Ti_{0.55}Al_{0.25}Zr_{0.2}$; (b) DTA curves for heating of the initial batch, $0.55TiH_2 + 0.20ZrH_2 + 0.25Al$

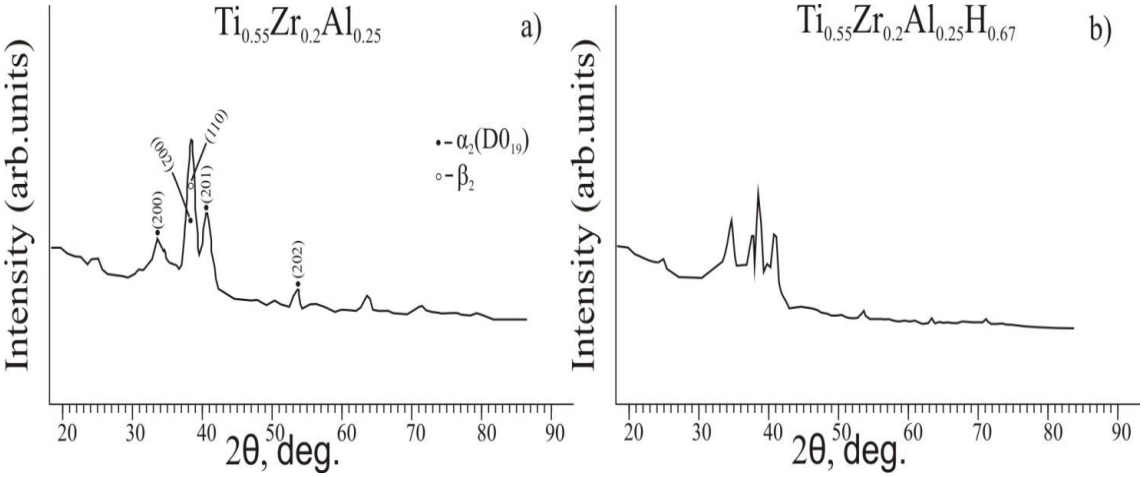

Fig.2 - Diffraction patterns of: a) $Ti_{0.55}Al_{0.25}Zr_{0.2}$ aluminide; b) its $Ti_{0.55}Al_{0.25}Zr_{0.2}H_{0.67}$ hydride

CONCLUSIONS

1. Titanium and zirconium based aluminides were synthesized: $Ti_{0.25}Al_{0.25}Zr_{0.5}$; $Ti_{0.35}Al_{0.25}Zr_{0.4;}$ $Ti_{0.55}Al_{0.25}Zr_{0.2}$; $Ti_{0.65}Al_{0.25}Zr_{0.1}$ et al.
2. The formation in HC of titanium and zirconium aluminides is significantly affected by the ratio of the components, temperature and heating rate of the initial charge.
3. At HC, the metals are strongly activated due to splitting of Me-H links and the oxide film is removed from their surfaces. The "open links" and cleaned surfaces promote solid state inter-diffusion of aluminum, titanium and zirconium. Nanoscale size crystallites in powders of titanium and zirconium hydrides (20-80 nm) also promote the rapid formation of aluminides at relatively low temperatures. All these phenomena create favorable conditions for solid phase diffusion mechanisms of three-aluminides formation in HC.
4. The noteworthy advantages of synthesis of three-aluminides in HC as compared to the existing methods are: relatively low temperature (800-1000ºC) and short time (30-60min) of processing; formation of single-phase three-aluminides at one technological step.

ACKNOWLEDGMENT

The work is implemented at the financial support of the Ministry of Education and Science of the Republic of Armenia

MODELING OF THERMAL FIELD DURING SHS-ELECTRIC ROLLING

T.Namicheishvili, L. Antashvili, G. Oniashvili, G. Tavadze, Z.Melashvili, A. Tutberidze, G.Zakharov, Z. Aslamazashvili

LEPL - Ferdinand Tavadze Metallurgy And Materials Science Institute

It is known, that during Self-Propagating High-Temperature Synthesis (SHS), when giving thermal pulse, the exothermic chemical reaction is initiated and the combustion wave front is displaced in the mixture of reagents with distinct speed [1,2,3]. As a result of the synthesis of reagents, participating in the reaction, the solid product is obtained. Recently, the increased interest is dedicated to the materials obtained by the mentioned method, in particular synthetic hard armor materials with metastable structure, high chemical purity, perfect mono crystalline grains and high physical and mechanical properties [6].

The SHS process itself is quite fast and the duration of the combustion phase is in the range 0.5-15 s[3], which significantly limits the compaction hot pressure processing ranges of the material. Truly the temperature regime of pressure processing determines the hardness and strength characteristics of materials. As a result of combustion there is significant temperature gradient between sample temperature and neighborhood, which provokes the intensive heat loses, especially with the direct contact of cold tool during the hot pressure compaction, which itself significantly makes influence on the structure.

The temperature loses which takes place during the interaction with cold rolls, which is hard to compensate from the deep layers due to the fast ($t_{rol} \approx 5s$) process, creates anisotropic temperature field in the cross section and the deformation of surface layers develops at relatively low temperatures. The described process stipulates not uniform mechanical properties in the cross section of the product and in some cases due to the thermal stresses there are micro crack formation. Therefore for the ensuring the uniform properties of the product during the compaction, it is necessary to ensure isothermal regime during the hot pressure processing. The realization of the process in nonstop regime can be achieved by proposed combined technological processes of SHS and electric rolling [16,17].

The working principle of the method is following: container, which is loaded with pre-compacted chasm, is delivered to the rolls of specific rolling equipment. Electric energy is delivered in the heart of deformation area with the use of electric contact, placed between container and rolls and the heat, generated in the initial section of deformation heart, initiates the SHS process. Before the entering of material in the rolls, the displacement of combustion front creates the particular zone of chasm combustion (planned section), the rolls are switched on and the electric rolling process starts and the hot, viscous-plastic compacted chasms are delivered to the rolls in nonstop regime (Fig 1).

For the realization of uninterrupted deformation it is necessary that the speed of rolling and combustion front displacement to be equal and the other important condition is the compensation of heat loses, which is possible by uninterrupted supplying of heating current in deformation zone during the rolling. The demolishing of SHS process (demolishing of speed synchronization), either the process is out of the deformation zone section, or the combustion zone is shifted on the left so, that the product gets cool and the compaction is practically impossible.

While discussing the thermal problems in SHS processes, the convection movement of reagents is insignificant. In addition, as diffusion coefficients are much less than temperature conductivity coefficient, we can ignore their influence on thermal processes [5]. Herewith, as the SHS process is fast process, we may discuss the whole process as adiabatic.

Fig.1 - Scheme of SHS-electric rolling

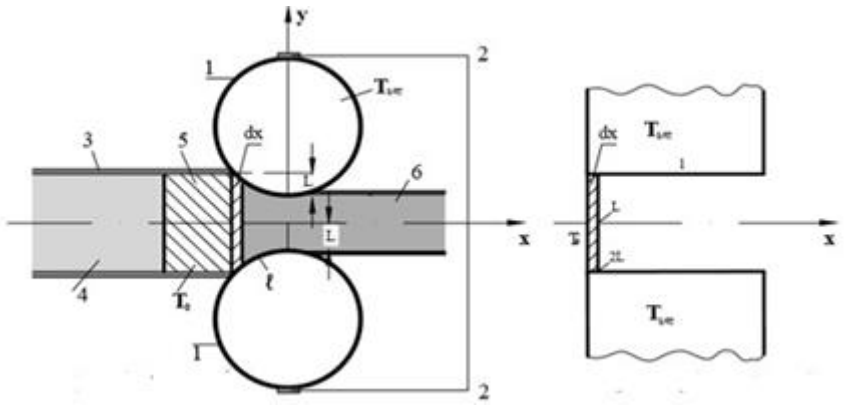

a) Scheme of SHS – Electric Rolling b) Scheme of thermal-physical problem

1. Rolls; 2. Electrical contacts; 3. Container; 4. SHS chasm; 5. Combustion Zone; 6.Final product

Hereafter we can discuss the adiabatic process of combustion and problem of full transformation of reagents. For the main condition we use the equation of enthalpy at the start T_0 temperature of reagents and final T_{ad} temperature of product[2,6].

$$\sum_{i=1}^{m}[H(T_0)]_i = \sum_{j}^{n}[T_{ad})]; \qquad (1)$$

At the adiabatic temperature of combustion the enthalpy of product can be written as follow:

$$\sum_{j=1}^{n}[H(T_{ad})]_j = \sum_{j=1}^{n}[H(T_0)]_j + \int_{T_0}^{T_{ad}} \sum_{j=1}^{n} C_j dT \qquad (2)$$

where C_j is the thermal capacity of j product, which is the function of temperature [$C_j=f_j(T)$];

According to (1) and (2) equations the heat released by exothermic reaction is totally spent on the heating of combustion product from initial T_o to the final temperature $T_{ad.}$

The special algorithm of free energy minimization gives relevantly precious results by analyzing the temperatures and balanced compounds of products. This method is used in the software "ISMAN-TNERMO" for the calculating of different parameters of SHS processes. The software is created for multi component heterogeneous systems to calculate thermodynamic balance and is effectively used for the decision of problems connected to the synthesis possibilities and adiabatic temperatures of combustion of inorganic products for SHS processes.

According to number of experimental investigations [1,6] it is established, that the temperature of initiation of SHS for metal-ceramic reagent chasms is in the ranges 800-850^{0}C.

The electric characteristics of electric-contact heating equipment is manly depended on the electric resistivity of workpiece that have to be heated, which varies/changes during the heating process according to the temperature variations.

The total energy consumed by the electric-contact equipment is calculated by the following formula [7]:

$$W=\frac{cG(T_2-T_1)}{\eta_0 \tau cos\varphi} \quad (3)$$

Where, c- is the heat capacity of the material; G-mass of the material; T_1 and T_2 initial and final temperatures of material correspondingly; η_0-coefficient of efficiency; τ- time of heating; $cos\varphi$ –power coefficient of the equipment. The current, necessary for the heating of the workpiece from T_0 to T_1 temperature in time interval τ, is calculated according to the following formula[7]:

$$I = \sqrt{\frac{GC(T_1-T_0)}{\tau \eta_t R}} \quad (4)$$

Where: η_t – is heat coefficient of efficiency in the particular moment of time, R- average actual electric resistivity of the workpiece in the presented range of heating. The parameters C,η_t and R in the formula (4) are nonlinear functions of temperature. For the simplicity of calculations in the set interval $\Delta T=T_1-T_0$ we use the average values. Accordingly, formula (4) calculates the average value of heating current which is necessary for warming up the workpiece to T_1 temperature in time.

The heat-physical problem progressing in deformation zone

In the stationary regime of SHS-electric rolling, the combustion process of chasm is progressing just nearby the deformation zone (Fig.1). As a result the workpiece is warmed up to T_2 temperature and is delivered to the rolls in hot condition. In this case there is the process of contact heat transfer to the neighborhood and to the cold rolls from hot workpiece.

SHS combustion zone is located just next to the deformation area, the workpiece in in contact with the neighborhood for a short period of time, accordingly the heat loses by convection and heat transfer is too small and can be ignored.

Proceeding from the fast-acting process of deformation and high temperature of chasm, due to the heat transfer by convection displacement of mass, also by the plastic deformation and work of surface friction forces, it is practically possible to ignore the heat component influences. During the hot rolling the heat transfer coefficient α between workpiece and rolls, can be calculated theoretically[8,11]. Besides, the experimental dates for defining the mentioned coefficient also exists [12,13,14]. According to the experimental data the value of α coefficient varies from $5\cdot10^3$-10^4 W/m$^{2\cdot}$ ^{0}C.

Heat quantity, transferred from hot product to 1 m^2 roll in time interval τ [11,15]

$$Q= \propto (T_0 - Trol\ )\ \tau f \quad (5)$$

Where, is α is a coefficient of heat transfer between the product to the rolls; T0 is the initial temperature of the product; T_{rol} temperature, which could be established in case of absence of heat resistance between contacting surfaces; τ is a time of contact.

$$f =\frac{2}{\sqrt{h-a\tau}} - \frac{1}{h^2 at}(1-\exp(h^2 at)\operatorname{erfch}\sqrt{at}) \quad (6)$$

Where: h - relative coefficient of heat transfer and h=$\frac{\propto}{\lambda}$; c - comparative mass heat capacity; ρ - hardness; **a** - coefficient of heat conductivity.

Therefore, inside the deformed volume the **Fourier** expression for one dimensional occasion for non stationary temperature regime, will be written as follow:

$$\frac{\partial T}{\partial \tau}=\alpha\frac{\partial^2 T}{\partial x^2} \qquad \frac{\partial T}{\partial \tau}-\alpha\frac{\partial^2 T}{\partial x^2}=0 \qquad (7)$$

The problem can be formulated as follow: unbounded plate (stripe) with the Width 2L, which have the similar temperatures T_0 in the whole volume, during the time interval $0\leq\tau\leq\tau_1$ suffers contact based heat exchange with the rolls, which itself have constant T_{rol} temperature. Consider, that the heat exchange process between stripe and rolls are according to Newton low. We can define the value of heat loses and and temperature field of the stripe, which equals $\tau_1=\frac{\sqrt{R\Delta h}}{V_{rol}}$

Where: R - radius of rolls; Δh-is absolute stretch; V_{rol}- speed of rolling.

The problem that has to be discussed schematically is presented on Fig.1-b.

In terms of heat transfer, the problem is symmetric for axis Y, therefore it is possible to be discussed either one-roll system, or two-roll system:

For first occasion will be written $\frac{\partial T}{\partial \tau}-\alpha\frac{\partial^2 T}{\partial x^2}=0 \quad 0<x<2L\,,\ \tau>0$

Initial condition T(0,x)=T_0=const;

Boundary condition T(τ,0)=0 da T(τ,2L)=0

The solutions in this case will be following: T(x, τ)=$\frac{4T_0}{\pi}\sum_{n=1}^{\infty}\frac{e^{-2n^2a\tau}}{2n-1}\sin(2nx)$, 2n=$\frac{\pi}{L}(n-\frac{1}{2})$

And second $\frac{\partial T}{\partial \tau}-\alpha\frac{\partial^2 T}{\partial x^2}=0 \quad 0<x<2L\,,\ \tau>0$

Initial condition: T(o,x)=T_0=const ; Boundary conditions T(τ,0)=0 and $\frac{\partial T}{\partial x}|_{x=L}=0$

The solution can be found as follow:

$$T(x,\tau)=\frac{4T_0}{\pi}\sum_{n=0}^{\infty}\frac{e^{-2n^2a\tau}}{2n-1}\sin(2nx), \quad 2n=\frac{\pi}{L}(n+\frac{1}{2})$$

It is clear that both solutions are the same [0,L] interval. Indeed, if in the second solution we make transformation of summing index as n=m-1, we will get the first solution. The same problem can be overcomed by using the numerical methods, private difference or method of finite elements.

As far as the time of contact with rolls τ_1 and temperature function T(x, τ) are known, we can calculate temperature gradient

$$\Delta T=T(x,0)-T(x,\tau)$$

This corresponds to the lost heat quantity during the contact of product and rolls in deformation zone(5).

For creation isothermal character of the process, it is necessary to compensate heat loses. This can be achieved by providing heat quantity, generated by applying electrical current in

deformation zone during the rolling process. The necessary value of current is determined by expression (4).

ACKNOWLEDGEMENT

This work was supported by Shota Rustaveli National Science Foundation (SRNSF) [grant # 216972. “Research of Producing Special-Purpose Composite by SHS – Electric Rolling”.

REFERENCES

[1] A.R.Merzhanov – "Processes of burning and synthesis of materials", Chernogolovka, prod.-e of ISMAE, 1999, 512 pages.
[2] E.A.Levashov, A. S. Rogachyov, V. V. Kurbatkina, Yu. M. Maximov, V. I. Yukhvid – "Perspective materials and technologies of the self-extending high-temperature synthesis", M. 2011, p. 378.
[3] A. S. Rogachyov, A. S. Mukasyan – "Burning for synthesis of materials", M. 2012, p. 398.
[4] D.S.Dvoretsky, S.I.Dvoretsky, L. S. Stelmakh, A.M.Stolin – "The system analysis and optimization of processes of SVS-formation of hard-alloy materials", the TGTU Bulletin, 2015, volume 21, No. 2, page 344-359.
[5] The self-extending high-temperature synthesis: theory and practice. Chernogolovka, publishing house of Teritoriya, page 435.
[6] E.A.Levashov, A. S. Rogachyov, V. I. Yukhvid, I. P. Borovitskaya – "Physical and chemical and technological bases of the self-extending high-temperature synthesis", M.1999.
[7] D. I. Romanov – "Electrocontact heating of metals", 1981, page 165.
[8] N. I. Yalova, M. A. Tylkin, P.I.Polukhin, D. I. Vasilyev – "Thermal processes at to processing of metals and alloys pressure", M. "Higher school", 1973, page 631.
[9] M. A. Mikheyev – heat transfer Bases. Gosenergoizdat. 1966.
[10] V.P.Isachenko, V. A. Osipov, A. S. Sukomel - "Heat transfer", M. "Energy", 1975, page 488.
[11] G.P.Ivantsov – the Magazine of technical physics. 1937,T.III, issue 10.
[12] M. Ya. Brovman, Yu.S.Dodin – Inzhenerno the physical magazine, 1964, No. 11.
[13] V. I. Shilov, G. V. Morzeeva – Works of institute of metallurgy, the issue 12, Sverdlovsk, 1965, page 123-134.
[14] A. I. Chernogolov, V. I. Shilov - Works of institute of metallurgy, the issue 13, Sverdlovsk, 1965.
[15] N.Yu.Tayts, etc., News of higher education institutions, 4M,1964, No. 7.
[16] T.Namicheishvili, A. Nozadze –“Electrical system of electric-contact equipment”Sientific publications of GTU, #7(400).
[17] T.Namicheishvili, J.Lortkifanidze – Specific equipment for isothermal rolling and aspects for selection the rolls. Journal of NAS Georgia “Moambe”, Vol.168, #2, 2003,pp.286-288.

NANOSIZED MOLYBDENUM CARBIDE SYNTHESIZED BY SOLUTION COMBUSTION SYNTHESIS WITH SUBSEQUENT THERMAL TREATMENT

Khachik Nazaretyan[1], Hasmik Kirakosyan[1,2], Sofiya Aydinyan[1,2]*, Suren Kharatyan[1,2]

[1] A.B. Nalbandyan Institute of Chemical Physics NAS RA, 0014, 5/2, P.Sevak str., Yerevan, Armenia
[2]Yerevan State University, 0025, 1, A. Manukyan str., Yerevan, Armenia
* sofiya.aydinyan25@gmail.com

Molybdenum carbide have long since attracted considerable interest for technological application because of its high melting point, chemical stability, extremely high hardness, high strength, and excellent resistance against mechanic and corrosive wear. In addition, molybdenum carbide showed catalytic properties similar to those of noble metals, which led to an explosion of interest in the use of molybdenum carbide as catalysts for a wide range of reactions.

In this work we present a novel route to the synthesis of nanosize molybdenum carbide by the solution combustion synthesis (SCS) [1] with subsequent heat treatment at 1100°C performed by using a high speed temperature scanner (HSTS) [2].

SCS involves self-sustained reactions in a solution of metal containing oxidizers (typically metal nitrates) and a fuel, e.g., water-soluble organic amines, acids, amino-acids, etc. In our work, for the preparation of nanosize molybdenum carbide we used ammonium heptamolybdate (AHM), and glucose as an organic reducer. For the increasing of reaction enthalpy NH_4NO_3 was utilized as an auxiliary oxidant. In the study, the above initial materials were dissolved into deionized water, and then stirred to obtain a homogeneous solution which was heated to react. Evolution of substantive gas during the combustion reaction leads to porous morphology and high specific surface area for products. After much of the water has been evaporated, a viscous liquid forms (sol, then gel) which is autoignited and forms molybdenum (IV) oxide fine powder. Temperature profiles at SCS were registered by thermocouple technique. As can be seen from the thermogram, the T_{max} is about 550°C (Fig. 1a), and XRD pattern of the quenched sample contains only characteristic peaks of MoO_2 (Fig. 1b).

The corresponding reaction between AHM and glucose and ammonium nitrate for the formation of molybdenum oxide can be written as follows:

$$(NH_4)_6Mo_7O_{24}*4H_2O + \varphi_1C_6H_{12}O_6 + \varphi_2NH_4NO_3 \rightarrow MoO_2 + CO/CO_2 + H_2O + N_2$$

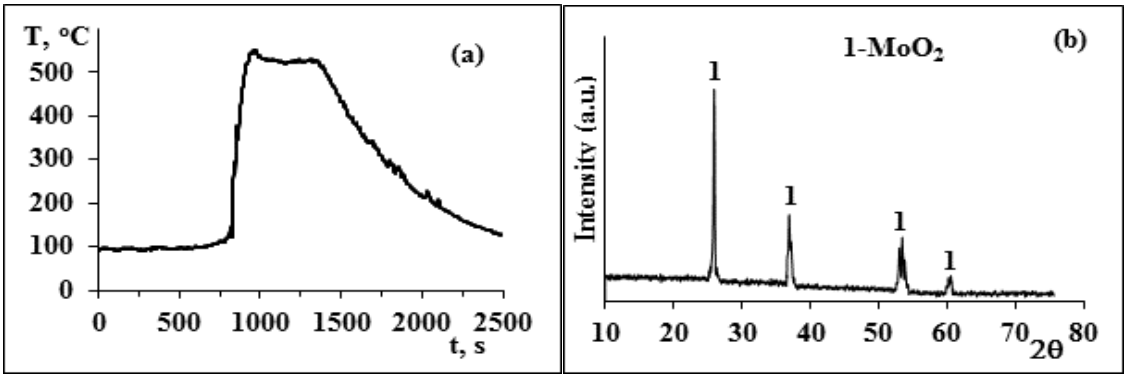

Fig. 1 - SCS thermogram of the AHM-$C_6H_{12}O_6$-NH_4NO_3 mixture (a), and XRD patterns of SCS product (b)

Then, the obtained product was impregnated by the suitable amount of a saturated solution of glucose and heated by HSTS-1 setup with 100°/min rate up to 1100°C and held for 3 minutes (Fig. 2a). As a result, it completely converted to molybdenum carbide (Fig 2b). The reaction can be represented by the following equation:

$$MoO_2 + C_6H_{12}O_6 \rightarrow Mo_2C + CO/CO_2 + H_2O + N_2$$

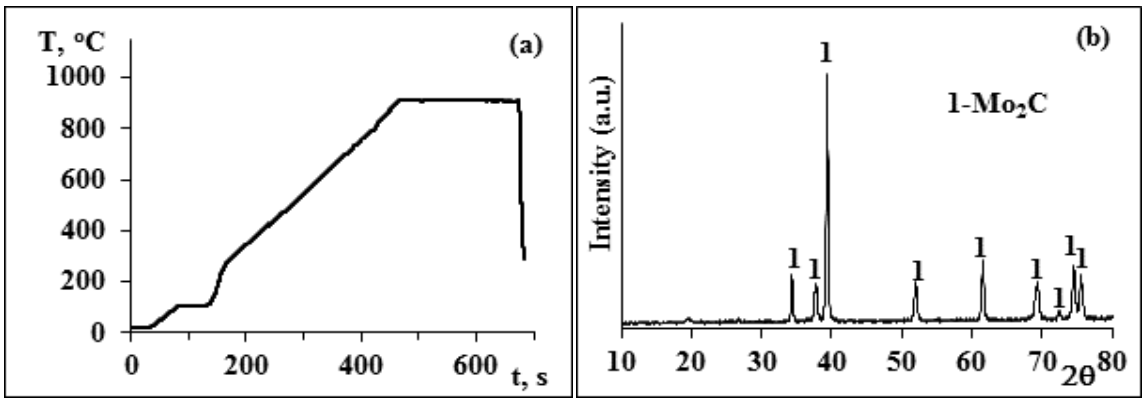

Fig. 2 - Heating thermogram of the MoO_2(SCS)+$C_6H_{12}O_6$ mixture (a) and XRD pattern of the cooled sample (b)

According to SEM examination, combustion product represents particles with submicron size.

REFERENCES

[1] S.L. González-Cortés, F.E. Imbert. Appl. Catal. A: General, 452, 2013, pp. 117-131.

[2] A.A. Nepapushev, K.G. Kirakosyan, D.O. Moskovskikh, S.L. Kharatyan, A.S. Rogachev, and A.S. Mukasyan. Int. J. SHS, 24, 2015, pp. 21-28.

HIGH TEMPERATURE KINETICS IN MECHANICALLY ACTIVATED SYSTEMS: ELECTRO-THERMAL ANALYSIS AND HIGH SPEED TEMPERATURE SCANNING

A. A. Nepapushev[a], K. G. Kirakosyan[b], D. O. Moskovskikh[a], S. L. Kharatyan[b], A. S. Rogachev[a,c], and A. S. Mukasyan[d]

[a]Center of Functional Nanoceramics, National University of Science and Technology, Russia
[b]Institute of Chemical Physics, National Academy of Sciences, Armenia
[c]Institute of Structural Macrokinetics and Materials Science, Russian Academy of Sciences, Russia
[d]Department of Chemical and Biomolecular Engineering, University of Notre Dame, USA
anepapushev@gmail.com

One of the most rapidly developing direction in the field of combustion synthesis is a high-energy ball milling (HEBM) of SHS reactive mixtures. HEBM found its application as a method to enhance self-propagating reactions for low exothermic mixtures [1-3]. It was also shown in literature that HEBM allows to expand combustion limits leading to a more complete reaction [4,5]. During such mechanical treatment it is possible to obtain nanostructure composites with the size of structural components in the range 10 - 100 nm. Moreover, the contact area between reactants also significantly increases. It is also important that new contact surfaces formed during HEBM in inert atmosphere are clean from the oxide films. All above leads to a high reactivity of the fabricated combustible mixture, i.e. reduces the ignition temperature, extends combustion limits, facilitates more complete combustion and in some cases increase the propagation velocity of a combustion wave. Obviously, HEBM affects the reaction kinetics in heterogeneous powder mixtures, but the mechanism of this effect is still not fully understood.

There are several hypothesis in literature, describing influence of HEBM on reactivity in such systems [6]. They can be divided on two groups: 1) based on the assumption that after HEBM reactants "store" energy; 2) based on the microstructure changes during HEBM. Energy-based mechanism implies that internal energy of the system increases due to increase of the surface and volume defects concentration caused by particles deformation. Energy accumulated by the crystal lattice after mechanical treatment results in the enhanced reactivity of powder mixtures during combustion synthesis. However, values of stored enthalpy in treated materials usually does not exceed several kJ/mole [7] which is much lower than the enthalpy of formation from the elements (e.g. 5Ti+3Si=Ti5Si3, ΔH=585 kJ/mole). Thus, we can conclude that energy "stored" by the crystal lattice cannot lead to the significant increase in the reactivity of powder mixtures after HEBM.

In recent publication [8] we showed that acceleration of the combustion reaction in Ni-Al system after short-term HEBM occurs due to a decrease in the reagent size and an increase in the contact surface area between the reactants. High-resolution TEM analysis reveals that the Ni + Al mixture after mechanical treatment contains nanocrystalline intermediate phases and these phases can serve as nano-precursors of heterogeneous exothermic reaction, enhancing the reactivity of the system and decreasing its activation energy (E_a).

However, there are no direct experimental data on the reaction kinetics of the mechanically treated mixtures. Kinetic studies on standard differential scanning calorimetry (DSC) does not provide the necessary data, since the heating rate in the standard DSC too small (1 - 100 °C per minute), whereby a further heating step is "annealed" nanostructured active reaction centers, and the resulting data does not match the actual kinetics in the rapid heating.

Here is reported the study of the kinetics of heterogeneous reactions in mechanically activated nanostructured composite materials (Ni+Al and Ti+0.6Si) by rapid heating. For determination of the E_a we used two approaches allowing to achieve fast heating rates, i.e. high-speed scanning electrotomography and electro-thermal analysis. Both methods are based on the heating of the investigated sample by passing current through it and registration of temperature-time profiles. Processing of the obtained temperature profiles allows us to determine the effective activation energy in considered systems. Thus, we obtained data on the dependence of the activation energy on the HEBM time in the Ni-Al and Ti+0.6Si recative mixtures. The reasons for the changing of effective activation energy are also discussed.

AKNOWLEGEMENT

The work was carried out with financial support from the Ministry of Education and Science of the Russian Federation in the framework of Increase Competitiveness Program of NUST «MISiS» (№ К2-2016-002), *implemented by a governmental decree dated 16th of March 2013, N 211.*

REFERENCES

[1] L. Takacs, Progress in Materials Science 47 (2002) 355–414.
[2] E.L. Dreizin, Progress in Energy and Combustion Science 35 (2009) 141–167.
[3] F. Bernard, E. Gaffet, International Journal of Self-Propagating High-Temperature Synthesis 10 (2001) 109–132.
[4] M.A. Korchagin, T.F.Grigorieva, A.P.Barinova, Int. J. of SHS. 9 (2000) 307–320.
[5] A.S. Rogachev, A.S. Mukasyan, Comb., Expl.and Shock Waves 4 (2010) 243–266.
[6] A. S. Mukasyan, B. Khina, R. Reeves, S. Son, Chem. Eng. J., 174 (2011) 677– 686
[7] C.C. Koch, Nanostructured Mater. 9 (1997) 13–22.
[8] A.S. Rogachev, N.F. Shkodich, S.G. Vadchenko et.al, J. Alloys Compd. 577 (2013) 600-605.

COMPLEX HIERARCHICAL NANO- AND MICROCRYSTALS OF AlN GROWN IN THE COMBUSTION WAVE: MICROSTRUCTURAL CHARACTERISATION AND GROWTH MECHANISM

H.H. Nersisyan[1, *], J.H. Lee[1,2], S.H. Lee[2], J.H. Choi[2]

[1]RASOM, Chungnam National University, 99 Daehak-ro, Yuseong-gu, Daejeon 305-764, Republic of Korea
[2]Graduate school of Department of Advanced Materials Engineering, 99 Daehak-ro, Yuseong-gu, Daejeon 305-764, Republic of Korea
* haykrasom@hotmail.com

ABSTRACT

An effective solid-state combustion route for fabricating a new type of AlN hierarchical microstructures is developed. These hierarchical structures were consisting of cylindrical or hexagonal central axis decorated with AlN dendritic microcrystals. Depending on the shape and mutual arrangement of the microcrystals, tower-like, feather-like, flower-like and pine tree-like hierarchical structures of AlN were obtained. The chemistry of combustion reaction and the formation mechanism of hierarchical structures is discussed in regard to analysis results. The discussion of growth mechanism leads to the conclusion that the growth rate can vary from crystal to crystal as a function of the combustion conditions, including the reaction temperature and the concentration of aluminum in liquid and gas phases.

TEXT

In recent years, the controllable synthesis of nanomaterials with unique morphologies and sizes has attracted increasing interest because of the shape-dependent properties of nanomaterials. The self-assembly of one-dimensional nanostructures into hierarchical nanoarchitectures is of particular importance and is fascinating because the nanoarchitectures are promising building blocks for nanoscale electronic and photonic structures [1-3]. Among the structural ceramic materials, a huge attention has been paid to the AlN for its unique properties such as a direct wide band gap (6.2 eV), high thermal conductivity (140-200 W/m·K), superior compressive strength (280-400 MPa), a high piezoelectric response, small or even negative electron affinity.

In this article, we report the combustion synthesis of new morphology 3-D hierarchical nanostructures of AlN. By regulating the reaction parameters, the structures of AlN could evolve from a wildflower patterned crystals to multilayer hierarchical structures. These 3-D AlN hierarchical structures were grown by the combustion of Al-AlF_3-ZnF_2-NH_4Cl reaction mixture under nitrogen gas pressure.

In the lengthwise cross-section of the combusted sample, three zones could be distinguished: surface (1), intermediate (2) and central (3) (Figure 1a). The surface consisted of nanowires and nanoparticles, and this was the largest zone in the sample. Molten Al decorated with AlN fragments of differing morphology was typical for the intermediate zone. The central zone resembles a large void, which is full of AlN fragments of differing morphology. This is the most interesting region, from which we could harvest the most interesing and formerly unknown hierarchical structures of AlN. Figure 1b is an image captured from the central zone and shows the presence of AlN 3-D structures, including such as, feathers, stellar dendrites, 6-fold symmetry crystals, and multi-story micro towers. The XRD peaks of micro and nano crystals

crystals collected from the central zone perfectly match single-phase AlN (Figure 1c). The highest peak intensities ($2\theta = 33.3°$ and $37.9°$) indicate that the growth of AlN crystals is fastest in the $(10\bar{1}0)$ and $(10\bar{1}1)$ planar directions.

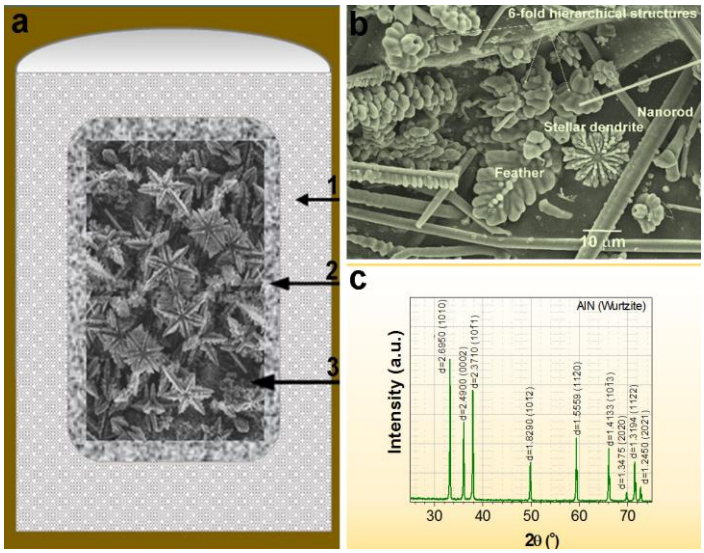

Figure. 1- (a) Lengthwise cross-sectional view of as-combusted sample; (b) Central zone morphology, (c) XRD patterns of the reaction product collected from the central zone.

FESEM observations revealed at least two routes for the formation of the hierarchical structures: (1) dissolution of nitrogen gas into Al melt and subsequent dendritic crystallization of melt into hierarchical structures, and (2) formation of central axis (rod- or arrow-type) and subsequent decoration by newly formed AlN crystals. The first route of hierarchical crystallization is shown in Figure. 2a.

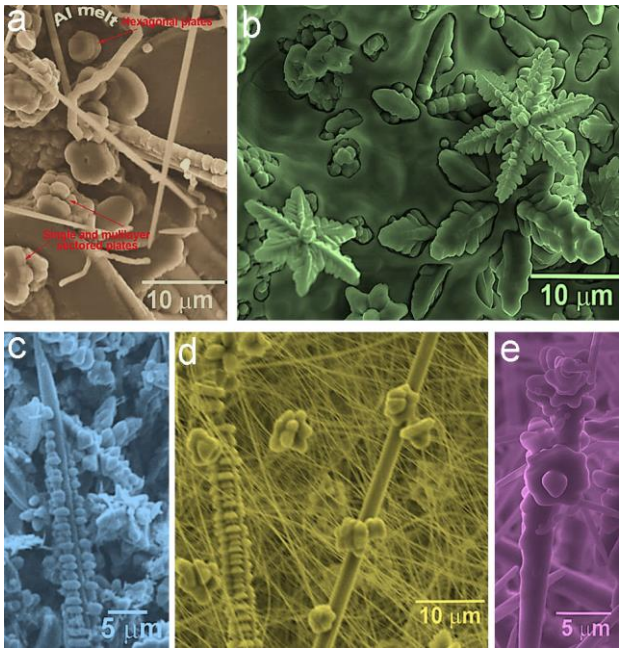

Figure 2 - (a, b) SEM fragments of hexagonal and sectoral plates of AlN; (c-e) The "blooming" process of AlN microrods.

The plate-type crystals that formed after partial crystallization of the Al melt were preserved and can be seen clearly. Assembled hexagonal plates of AlN are seen in the upper part of the micrograph. In the left bottom part, we can see a half-grown structure that resembles multilayer sectored plates. Additional microstructural fragments with dendritic growth of AlN micro crystals are shown in Figure 2b. Typically, the growth process of several crystals was already completed resulting in 6-fold morphological fragments, but the growth process of some of the crystals was still in progress. We can see a number of dendritic branches half-protruding from the molten mass. EDS analysis conducted on the different dendritic fragments led to the conclusion that their composition always corresponds to the AlN phase. The fragments on Figure 2c-e demonstrate the second route of crystallization, where the central axis is formed first, and then is decorated by AlN crystals. Figure 2c shows arrow-type micro rode covered partially with AlN crystals. The growth process was not completed and empty zones on the central axis remained. Figure 2d shows the "blooming" process of an AlN micro rod: several flower-like sprouts can be seen on this micro rod. The sprouts more likely were formed due to interaction between AlF_3 (or lower fluoride) and N_2 on the micro rod surface. The "blooming" of the micro rod and its transformation into a multilayer structure can also be seen ion Figure 2e.

Normally, based on the experimental findings, we might suggest that in the combustion process, a dendritic growth mechanism of AlN hierarchical structures was realized. Calculated surface energies for different facets of AlN indicated that $(10\bar{1}1)$, $(01\bar{1}1)$, and $(10\bar{1}0)$ facets have the highest surface energy (5.6, 5.59, and 5.3 $J \cdot m^{-2}$, respectively) and are thermodynamically the most unstable. Therefore, they are the most probable locations from which the dendritic branching will be initiated [4]. This data is in good agreement with the XRD data shown in Figure 1c.

ACKNOWLEDGEMENTS

This research was supported by the Basic Science Research Program through the National Research Foundation of Korea (NRF), and was funded by the Ministry of Education (NRF-2016R1D1A1B03936187).

REFERENCES

[1] L. W. Yin, Y. Bando, Y. C. Zhu, M. S. Li, Y. B. Li and D. Golberg, Adv. Mater. 17,2005, pp. 110-114.

[2] J. R. Heath, P.J. Kuekes, G.S. Snider and R.S. Williams, Science 280, 1998, pp. 1716-1721.

[3] Y. Huang, X.F. Duan, Q.Q. Wei and C.M. Lieber, Science 291, 2001, pp. 630-633.

[4] H.H. Hersisyan, D.Y. Kim, W. Kang, B. Han and J.H. Lee, Cryst. Growth Des. 16, 2016, pp. 5305-5311.

INVESTIGATION OF NiB MASTER ALLOY PRODUCTION VIA SHS METHOD

O.Odabas*[1], M.Bugdayci[1,2], S.Kan[1], O.Yucel[1]

[1]Metallurgical and Materials Engineering Department, Faculty of Chemical and Metallurgical Engineering, Istanbul Technical University, 34469, Maslak, Istanbul, Turkey
[2]Chemical and Process Engineering Department, Faculty of Engineering, Yalova University, 77100, Yalova, Turkey
* odabas15@itu.edu.tr

Self-propagating high temperature synthesis (SHS) is one of the important methods to synthesize advanced materials such as ceramics (e.g. TiB_2, B_4C, Si_3N_4); abrasives, cutting tools and polishing powders (e.g. TiC, cemented carbides); resistive heating elements (e.g. $MoSi_2$), shape-memory alloys (e.g. TiNi); high-temperature structural alloys (e.g. nickel aluminides); master alloys (e.g. AlTiB); neutron attenuators (e.g. refractory metal hydrides) as well as conventional metals and their alloys [1, 2]. Although the discovery of metallothermic reactions (Beketov 1865; Goldschmidt 1895) is earlier, combining with flame propagation theories and the first gasless metallothermic combustion experiments were conducted by Merzhanov et al. in the middle of 1960s [3]. SHS reactions are highly exothermic. Thus, the propagation of reactions and the yield of reaction products continue in self-sustaining mode without requiring additional heat [4, 5]

The aim of this study is to produce NiB master alloy via SHS method instead its two current industrial production methods, carbothermic and aluminothermic reduction, in an electric arc furnace. With the increased environmental concerns, primarily on carbon emissions and energy saving, the SHS process with its lower energy costs and lower environmental impact may become a favourable / preferable production method of NiB.

Thermochemical evaluations were made to estimate the adiabatic temperatures and possible product compositions in the final product by using FactSage 6.4 thermochemical software. The aluminothermic reduction process was performed in ceramic crucibles which were pre-heated in a furnace at 500ºC for 30 min. before powder mixture were poured in it. Under normal gravity and atmospheric conditions, oxides of metals (NiO, B_2O_3) and fluorspar (CaF_2) as flux for good slag metal separation and Al as a metallic reductant were used. To obtain optimum flux ratio for the best slag metal separation 5 different experiment organized (1%wt. - 2.5%wt. - 5%wt. - 7.5%wt. -10 %wt. CaF_2) and optimum result obtained from 5 %wt. CaF_2 value with 89 % metallic recovery. By changing the parameters such as reductant aluminum content and molar ratios of other initial components, we expected to change the yield of target product. Also, NiB master alloy should typically contain 15-20% B, 80-85% Ni and the balance of permissible contaminants. We obtained NiB contains 12%wt. B.

REFERENCES

[1] Z. A. Munir, U. Anselmi-Tamburini, Materials Science Reports, 3 (1989) 277 – 365.
[2] O. Yücel, F. Ç. Şahin, High Temperature Materials and Processes, 20 (2) (2011) 137 – 142.
[3] A. G. Merzhanov, Ceramics International, 21 (1995) 371 – 379.
[4] A. Varma, J. P. Lebrat, Chemical Engineering Science, 47 (1992) 2179 – 2194
[5] A. Turan, M. Bugdayci, O. Yucel, High Temp Mater Proc, 34 (2) (2015) 185-193.

SHS AND RELATED TECHNOLOGIES APPLIED TO DEVELOPMENTS IN UNDERWATER ENVRONMENT

O. Odawara*

PROSAP, Inc., #706 Fujita Bldg., 3-5-2 Shimomeguro, Meguro-ku, Tokyo 153-0064, Japan.
(*: Emeritus Professor, Tokyo Institute of Technology)
odawara@justsap-me.org

Self-propagating high-temperature synthesis (SHS) reactions propagate self-sustainingly without any oxygen supply and form high-temperature field at the back of the reaction zone. The technological merits of SHS have been revealed in versatile areas with the additional techniques on such a joining method as “stereo fabrication of large-sized matters with hollow ceramic units assembling” and a capsule formation as “large-sized light and tough aggregate fabrication with metal and/or ceramic hollow spheres”. The SHS and related technologies have been successfully applied to R&D studies under microgravity environments from 1980s [1], which have nowadays broadened their goals toward human space access in space exploration beyond low-earth orbit (LEO) to the Moon, Mars and others. One of the key challenges in the development is to achieve “extended stays of humans in space” by establishing advanced technologies in the fields of robotics, micro-machines, space solar energy and multiple resource utilizations with loss minimization of energy and mass. Material resources will be strongly restricted and almost impossible to be resupplied from the earth for distant and long-term missions performance; none would be enough to develop technologies with resources only from the earth, so it should be required to utilize resources on other places with different nature of the earth, i.e., *in-situ* resource utilizations (ISRU) [2].

According to the NEEMO (NASA Extreme Environment Mission Operations) project, the aquanauts are able to simulate living on a spacecraft and test spacewalk techniques for future space missions, which means that the underwater environment has the additional benefit of allowing NASA to "weight" the aquanauts to simulate different environments. When considering the recent challenging goal in space exploration, our targets can expand not only in space exploration but also in underwater environment, i. e., toward extending human-stays in both of “extreme environments”, where the SHS and related technologies can work practically in fulfilling efficient for the goal of the technological success. The technologies of survival system formations including the availability of renewable and/or self-sustaining energy also play a critical role, specially, in the prime of

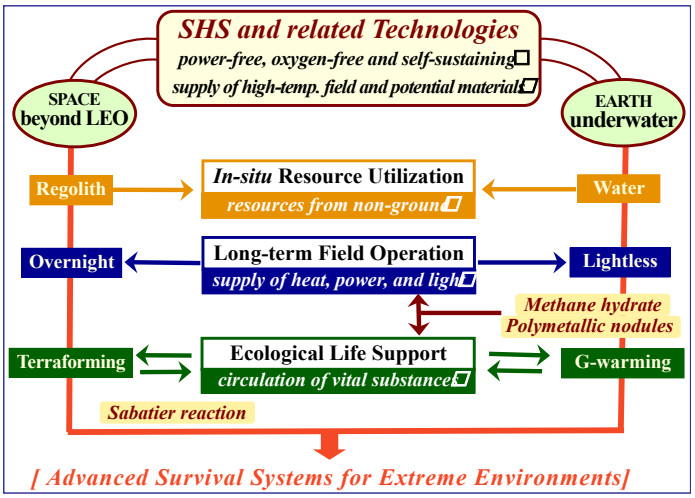

Fig. 1 - Guidelines of the SHS and related technologies for the environments of underwater and beyond LEO

extreme environment utilizations. The present paper mainly concerns "long-term field operation" and "ecological life support" as well as the ISRU as shown in Fig. 1. For example, the former refers to sustainable lunar-night (overnight) survival [3], and the latter to CO_2-reduction and H_2-extraction for essential life support system establishment.

There are a number of reaction parameters which affect SHS and related reactions, e.g. reactant particle size, stoichiometry (including the use of diluents or inert reactants), green density, thermal conductivity, ignition temperature, heat loss and, therefore, maximum temperature, heating and cooling rates and physical conditions of reactants (solid, liquid, gas). Differences between space and underwater environments are in the existence of regolith and water as resources, respectively. As shown in Fig. 1, water can play a key role for the processes of CO_2-reduction and H_2-extraction as well as others in life support systems.

Long-term field operation with supply system development of heat, power and light

The geothermal R&D on "natural volcanic occurrence of hydrogen: fuel production from magma [4] is also considered to make SHS and related technologies advanced in underwater environment utilization, especially in the fields of undersea resources such as submarine hydrothermal polymetallic ore and methane hydrate [5]. The magma reaction with hydrogen extraction principally proceed on the reducing action of basaltic magma on injected water under high-pressure condition, which chemical interaction causes the oxidation of ferrous components in the basalt and the production of hydrogen (Eq. (1));

$$2FeO\ (magma) + H_2O\ (fluid) \rightarrow Fe_2O_3\ (magma) + H_2\ (fluid) \quad \cdots\cdots\cdots\cdots\ (1).$$

Fresh basaltic lava contains on the order of 10wt% ferrous oxide (FeO) and 1 to 2wt% ferric oxide (Fe_2O_3). These components are present as dissolved constituents within the silicate melt and in minerals (e.g., olivine, pyroxene, magnetite) suspended in the magma. The predominance of ferrous over ferric oxide in basaltic magma is in large part responsible for the reported concentrations of hydrogen and carbon monoxide observed in the above volcanic gas collections.

The related reactions can be evaluated with such as Al-H_2O and Al-CaO-H_2O systems by focusing on the reduction of water resulting in hydrogen extraction as follows;

$$2Al\ (s) + 3H_2O\ (l) \rightarrow 2Al_2O_3\ (s) + 3H_2\ (g) \quad \cdots\cdots\cdots\cdots\cdots\cdots\ (2)\ \text{and}$$
$$2Al\ (s) + CaO\ (s) + 4H_2O\ (l) \rightarrow CaO \cdot Al_2O_3\ (s) + 3H_2\ (g) \quad \cdots\cdots\cdots\ (3).$$

R&D on ecological-life-support system establishment

As the technologies applied to life-support technologies for a Japanese moon base concentrating on air and water recycling, the Closed Ecology Experimental Facilities has already been established and set on the International Space Station [6] for performing extraction of hydrogen and carbon dioxide reduction mainly with Sabatier reaction, which can lead various "spin-off" R&D approaches in marine and undersea environment utilization. The atmospheric revitalization process is shown in Fig. 2 as a part of the self-contained full-circulated life support system. Carbon dioxide in the atmosphere exhaled by crew is separated and concentrated with zeolite. Then, the carbon dioxide is mixed with hydrogen in the presence of a

ruthenium catalyst around 300°C and the mixture reacts to produce water and methane by the Sabatier reaction (Eq. (4)).

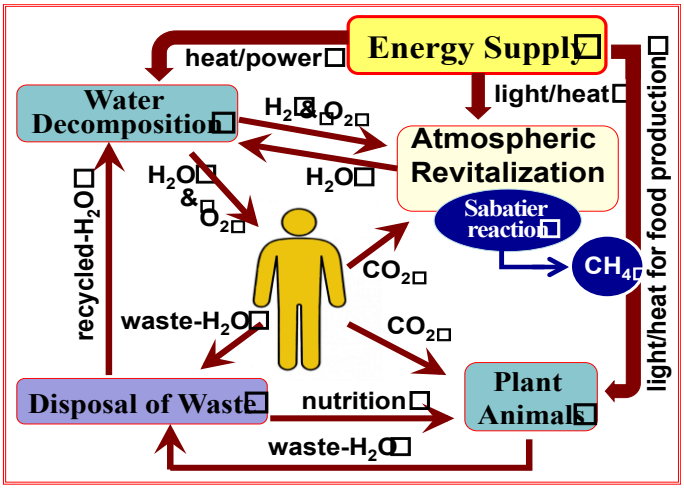

Fig. 2 - Schematic design of self-contained full-circulated life support system

$$CO_2 + 4H_2 = CH_4 + 2H_2O, \quad \triangle H = -165 \text{ kJ/mol} \qquad \ldots\ldots \quad (4).$$

The obtained water is electrolysed to obtain oxygen and hydrogen. The crew then breathe the oxygen and exhale CO_2, and the process repeats. The processes of concentrating CO_2, well-known technologies of Sabatier reaction and water electrolysis are used.

In the present work, the potential of SHS and related technologies in underwater environment is outlined as well as that in space exploration. With the nature in underwater environment, the both influences from high-temperature and high-pressure on water are also much interested to study on further SHS and related technologies with supercritical water. Supercritical water can be found around hydrothermal vents at deep-undersea, which might be effective for forming long-lasting nano-emulsions. These technological concepts shown in the present work for both space and underwater environments would be also useful as spin-off technologies in other extreme environmental fields. These R&Ds on ISRU, overnight and life-support achieved with the aid of SHS and related technologies would make further steps of the challenging missions advance forward.

REFERENCES

[1] O. Odawara, Ceramics Int'l., 3, 1997, pp. 273-278.

[2] G. B. Sanders and W. E. Larson, Adv. in Space Res., 47, 2011, pp. 20–29.

[3] Y. Konno, T. Fujii, A. Sato, K. Akamine, M. Naiki, Y. Masuda, K. Yamamoto and J. Nagao, Energy Fuels, 31, 2017, pp. 2607–2616.

[4] C.J.M. Northrup, Jr., T.M. Gerlach, P.J. Modreski and J.K. Galt, SAND77-0509, 1977.

[5] O. Okishio, H. Nagano and H. Ogawa, Appl. Therm. Eng., 91, 2015, pp. 1176-1186.

[6] A. Shima, M. Sakurai, Y. Sone, M. Ohnishi, A. Yoneda and T. Abe, Int'l. J. Microgravity Sci. Appl., 30, 2013, pp. 86–93.

STUDY OF THE EFFECT OF DISPERSION POWDERS OF NICKEL AND TITANIUM CARBIDE ON THE STRUCTURE AND PROPERTIES OF DIAMOND TOOLS

Oglezneva S.A.*[1], Saenkov K.L.[1]

[1] Perm national research polytechnic university, Russia, Perm, 614990, Komsomolsky Av. 29,
*director@pm.pstu.ac.ru

Introduction. Cutting and grinding tools with metal bond, is the most sought after tools for processing non-metallic materials (natural stone, building materials), as it has high thermal conductivity, wear resistance, provides high speed grinding [1]. One of the effective methods of manufacturing the composite powder of diamond tools is powder metallurgy. The improved properties of the composite material can be achieved through the use of nanodispersed metal powders [2] and the formation of the structure of metastable austenite [3], which is in the process of the work hardened due to the formation of deformation martensite [4] that as a result improves the fixation of the diamond grains increases the strength of the ligaments and cutting properties of the tool [5]. However, the consolidation of nanosized powders typically require sintering with the application of pressure, such as plasma-spark sintering [6, 7].

The work purpose is research of structure and properties of powder systems, "Fe – Ni – TiC – C (diamond)" on the basis of the fine iron powder and micro - and nanodispersed powders of Nickel and titanium carbide with the sintering and spark plasma sintering (SPS).

Methods. Samples were made from powder mixtures that contain 6-18 wt. % Nickel, 8 wt. percent titanium carbide, 7, 5 wt. % of diamond grains, the rest is iron. It have been used as the basis of carbonyl iron powder brand Navy with an average size of 11 microns; the titanium carbide powders: the first, made by the carbothermically with an average size of 5 microns, and the second, obtained by the method of the explosive mechanochemical synthesis in a planetary mill from titanium and graphite. It has been added powders of nickel carbonyl PNK – UT3 with sizes of 3-5 μm or nanosized with the size 50-80 nm, restored salt, as well as synthetic diamond powder AC 32 400/315. Mixture of powders was mixed in a mixer for 8 hours. Then the powders were pressed at a pressure of 400 MPa and were annealed for removing internal stresses in hydrogen for 2 hours at a temperature of 600 C, the samples were then re-extruded to reduce porosity at a pressure of 600 MPa and sintered finally in hydrogen for 5 hours at a temperature of 900-950 ^{0}C. Diffusion couples "iron-nickel" extruded at a pressure of 600 MPa. Sintering was conducted at temperatures of 800, 900 and 1100 °C, using thermo-mechanical analyzer (dilatometer) Setaram (France) in argon atmosphere under a load of 0.07 MPa, and the installation of the spark plasma sintering Dr. Synter SPS-1050b in argon atmosphere at temperatures of 800-900 °C and a pressure of 30 MPa, exposure 5 min. diffusion Coefficients were calculated by the method of Matano-Boltzmann. The concentration of elements was determined using an analytical field emission scanning electron microscope ULTRA 55/60 Carl Zaiss with an energy dispersive analyzer.

Sintered samples were tested on density and calculated porosity, the HRC hardness, microhardness, strength in three-point bending specimens without cracks according to standard procedures on 3 samples per point, and measurement error was 10 %. The study of microstructure was performed on thin sections, etched in nital, using the metallographic microscope Carl Zeiss Axiovert 40MAT by increasing 100-200. X-ray phase analysis was performed using the Shimadzu XRD – 6000 in the Kα radiation of Cu c Ni filter.

Tribological tests were carried out on the friction machine SMTS – 2 at a frequency of 300 rpm. Steels and diamond tools were tested on the wear by friction on the counterbody of corundum, we calculated the relative wear as a ratio of loss of mass of the sample and the counterbody.

The results and discussion. The diffusion coefficient (*D*) in the "Fe – Ni" as with micro-dispersed and nano-dispersed powder of nckel, at a temperature near the phase transformation in iron (900 ^{0}C) was higher than that at 1100 ^{0}C. In systems with nano-sized particles of nikel powder *D* at temperatures of 900 and 1100 ^{0}C were 2-3 times higher than in the system with the ultrafine powder. SPS provides increase in *D* by an order of magnitude in comparison with the free sintering at more lower temperatures and the 5-minute time. When the temperature SPS was increased from 800 to 900 ^{0}C, the diffusion coefficient increased about 2 times. The calculated coefficients of the equation of kinetics of sintering of Evensen. The addition of nanosized Nickel powder to micron-sized powder of iron lowers the activation energy several times, with 45 to 7 *kJ/mol*. The use of SPSS for the system powders "iron-nikel" significantly lowers the activation energy of sintering by maintaining a high concentration of structural defects to the beginning of isothermal sintering at high heating rate and the application of pressure in the process of consolidation (of 5.2 and 3.6 *kJ/mol* for the system with the ultrafine powder of Nickel and nano-dispersed, respectively). The values of the coefficients of the equation of kinetics of sintering confirm that intense shrinkage occurs already during heating; and sintering under pressure during isothermal exposure is much more intense. When you add the powder titanium carbide to the system of powders of iron and Nickel activation energy of sintering increases by 10 times when the free sintering due to the reduction of area of metallic contact is 85 *kJ/mol*, while at SPS is only 2 times (up to 11 *kJ/mol*).

Grain size in the sintering composition materials, contain nanodispersed powders of nikel and titanium carbide was 4 μm, with the ultrafine additives - 8 μm. In the process of SPS, as with the free sintering, in system "iron-nickel-titanium carbide" is formed by ferrite-austenitic structure, in which, after the friction on the abrasive is the transformation of metastable austenite to martensite deformation. The volume of transformation in materials with nanosized alloying additions was 30 %, and was 10 % in material with micro powders; thus, the greater was the amount of transformation, the higher was the hardness, microhardness and wear resistance. The coefficient of grinding in the corundum by the diamond tool with ultrafine additives was 0.6, and with nanodispersed was 4.0.

Conclusions. The use of nanodispersed powders of Nickel and titanium carbide for the manufacture of a matrix of diamond tools leads to improved physical-mechanical, tribological and cutting properties of the material due to the increased volume of the phase transformation of metastable austenite to deformation martensite.

Acknowledgments. The work is executed at support of RFBR grant No. 16-48-590224.

REFERENCES

[1] Composite diamond-containing materials and coatings, V. A. Vereshchagin, V. V. Zhuravlev, “Science and techno”, Minsk, 1991, p. 208.

[2] A. A. Zaytsev, V. V. Kurbatkina, E. A. Levashev, Izv. Universities. Nonferrous metallurgy, 2, 2008, pp. 57-59.

[3] Steel with metastable austenite. M. A. Filippov, V. S. Litvinov, and R. M.: Nemirovskii, “Metallurgy”, Moscow, 1988. p. 256.

[4] V. N. Antsiferov, M. G. Latypov, A. A. Shatsov, MITOM, 8, 1997, pp. 15-19.
[5] S. A. Oglezneva, Friction and wear, Vol. 32, 4, 2011, pp. 409 – 414.
[6] Powder metallurgy of nanocrystalline materials, M. I. Alymov, "Nauka", Moscow, 2007, p. 169.
[7] A. A. Anisimov, V. I. Mali, Journal FGV, vol. 46, 2, 2010, pp. 135-138.

PECULIARITIES OF SYNTHESIZING SINGLE-PHASE SOLID SOLUTIONS BASED ON TANTALUM CARBIDE

V.V. Kurbatkina[1], E.I. Patsera[1], S.A. Vorotilo[1], N.A. Kochetov[2], E.A. Levashov[1]

[1] National University of Science and Technology "MISIS", Leninsky Prospect, 4, Moscow, 119049, Russia

[2] Institute of Structural Macrokinetics and Materials Science, Russian Academy of Sciences, 8, Academician Osipyan st., Chernogolovka town, Moscow oblast, 142432

HfC, TaC and ZrC carbides have high values of the melting temperature, corrosion resistance, hardness and resistance to evaporation when exposed to radiation. As a rule, solid solutions have higher values of hardness and thermal stability as compared to the elements they are formed of. However, the extremely high melting temperatures of these materials impede obtaining them through traditional powder metallurgy technologies. That is why this work researches into the possibility of obtaining the solid solutions through the self-propagating high-temperature synthesis (SHS). It demonstrates the influence of mechanical activation modes on the phase compositions and structures of both the initial reagents and the synthesis products in Ta-Zr-C and Ta-Hf-C systems.

The mechanical activation was carried out in АИР-0.015 and Activator 2S planetary mills. Influence of the conditions of treating the mixtures was researched: time, ratio of the balls' mass to the material's one, rotational speed of the drums, sequence of charging the components, activation environment. The combustion heat of the activated charge mixture was determined with a fast-acting combustion calorimeter. The carbide powders were obtained by crumbling the product up in a rotating ball mill. The phase compositions were researched through X-ray phase analysis. The microstructures and chemical compositions of the samples were studied using the SEM and EDS methods.

When mechanically activated, the Ta particles are deformed into scales, and smaller C and Zr particles are embedded into them, after which agglomerated granules sized at 200–300 μm form. If the MA time increases, microdeformation of the tantalum lattice rises and its coherent-scattering region reduces, which evidences the increase of the amount of the energy stored. The research into effect of the MA environment (air, argon, vacuum) demonstrated that the SHS product is single-phase (Ta,Zr)C carbide with the content of admixtures amounting to less than 3%. When synthesized from the reaction mixtures obtained in oxygen-free atmosphere, three phases — TaC, ZrC and (Ta,Zr)C — form. The SHS MA modes have been determined that ensure obtaining 100 % single-phase (Ta,Zr)C solid solution with a lattice parameter of a= 0.4488 nm, which corresponds to 15 at.% ZrC in the double carbide without ZrO_2 traces.

The Ta-Hf-C reaction mixtures were mechanically activated in centrifugal planetary mills with various rotational speeds of the drums. When the drum's rotational speed was increased 3.5 times, the coherent-scattering region decreased by an order of magnitude, and the lattice microdeformation degree rose 1.5–2 times. It was experimentally established that at T_0 less than 550 K it is impossible to initialize the SHS reaction in the MA mixture activated at 678 rpm. Only after MA at the maximal rotational speed, the combustion process was successfully realized. A separate activation increases the proportion of admixture oxides. As a result, practically single-phase carbide with a lattice parameter of a = 0,4487 nm, which corresponds to

18.0 at.% of dissolved HfC, has been obtained. The hafnium oxide admixture content has not exceeded 1 %.

The work has been done with financial support from the Ministry of Education and Science of the Russian Federation within the framework of the project part of State Assignment No. 11.233.2014/K.

METATHETICAL REACTION MECHANISMS IN THE Ti-B-N SYSTEM

J.M. Pauls*[1], A.S. Mukasyan[1]

[1] Department of Chemical & Biomolecular Engineering, Univerisity of Notre Dame, Notre Dame, 117 Cushing Hall, 46556, USA
* jpauls@nd.edu

Since their initial discovery, self-propagating high temperature exothermic reactions [1, 2] have enabled the development of a plethora of material production techniques along with the synthesis of a wide range of novel materials with many applications. In addition to conventional thermal means of reaction initiation via localized or volume pre-heating, mechanically-induced and shock-induced reaction synthesis [3, 4] have also been developed.

Here we report on mechanisms of phase transformation that occur within the unassisted exothermic propagating reactions of the Ti-B-N ternary system [5, 6, 7]. Reactive nanocomposites of TiN/3B and 3Ti/2BN were prepared using high-energy ball milling (HEBM) of initial reactant powders. Unassisted propagating reaction of TiN/3B has not been previously reported.

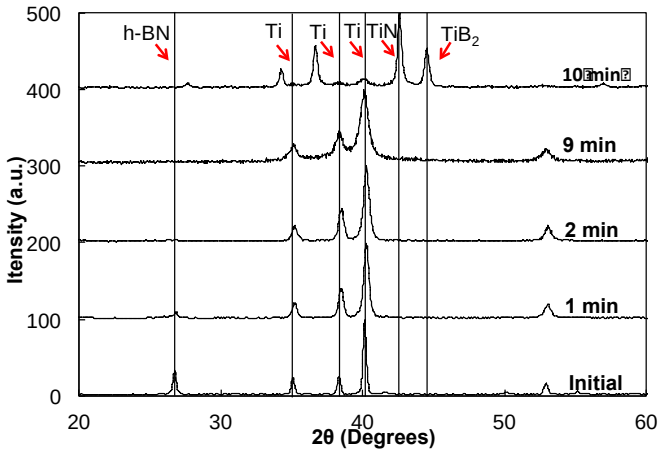

Figure 1- Powder X-ray diffraction patterns of 3Ti/2BN prepared for different durations of high-energy ball milling.

Thermodynamic calculations indicate that for both systems reaction initiation temperatures are well below the melting points of any reactants or products. For TiN/3B, the adiabatic combustion temperature is well below the melting or dissociation points of any reactants, intermediates, or products indicating that this is a solid flame-type system [8] where mass transfer occurs via a solid-state mechanism. This reaction proceeds according to the exothermic reaction (1)

$$3B + TiN \rightarrow BN + TiB_2 + Q \qquad (1)$$

Comparative study is made of the metathetical reaction:

$$3Ti + 2BN \rightarrow 2TiN + TiB_2 + Q \qquad (2)$$

which is also exothermic, despite the reactant nitride functioning as an “oxidizing agent” in both reactions and simultaneously appearing as a product of “oxidation” in the opposite reaction. In

the above-mentioned circumstances, i.e. absence of ternary phases in Ti-B-N system it is fundamentally interesting to determine the route for the "reverse" (as compared to reaction 1) reduction of BN by Ti in reaction 2.

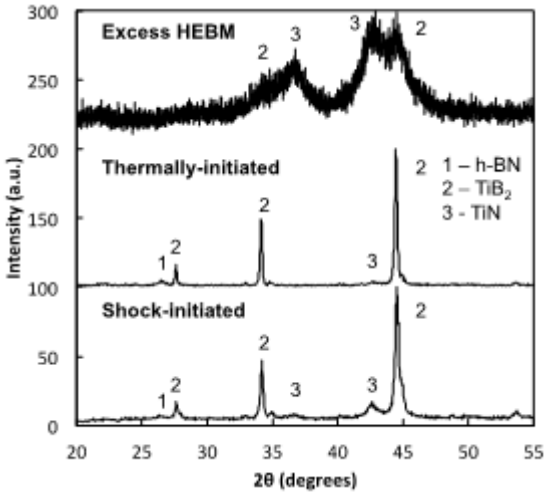

Figure 2 - Powder X-ray diffraction patterns of reaction products from TiN/3B: thermally initiated, shock-initiated, mechanically-induced during high-energy ball milling.

Electron microscopy investigation of the composite products of the TiN-3B reaction initiated under different temperature and pressure conditions provides insight into the reaction mechanism. Specifically, the reaction products produced via three methods of initiation (thermal, shock, and mechanically-induced during HEBM) along with the initial composite material were studied via transmission electron microscopy. The mechanically induced reaction during HEBM was incomplete and will therefore be referred to as quenched. The distribution of product phases compared to the initial composite material and the observed degree of conversion provide several clues regarding the process of reaction.

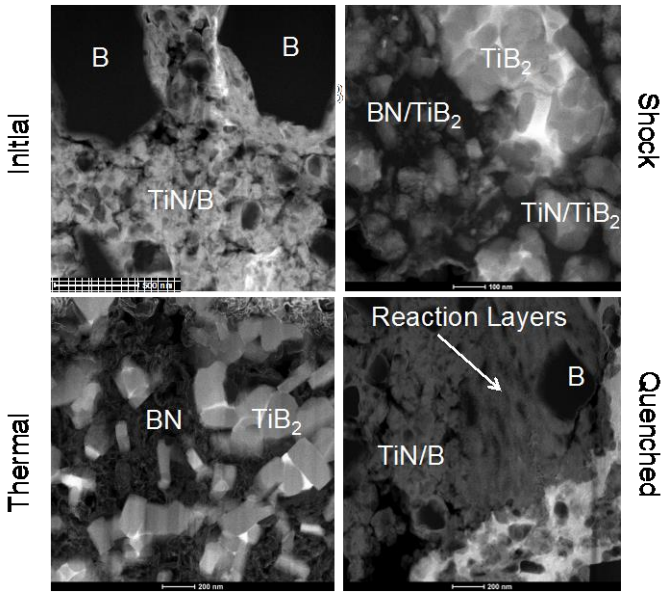

Figure 3 - STEM images of TiN/3B-based composites

The initial composite material consists of widely dispersed size distribution (5 nm – 1 μm) of boron crystals situated in a field of fine (5 nm – 20 nm) titanium nitride crystallites. Scherrer analysis of the reaction products reveals that the average product crystallite size decreases from thermal initiation to shock initiation and from shock-initiation to mechanically-induced initiation during HEBM. This decreased size is likely due to a decreased characteristic time of heating which is too short to permit the diffusion of boron to reaction sites except in those regions that initially contained boron nano-crystallites.

TEM analysis of quenched TiN/B particles revealed nucleation sites of TiB_2 distributed throughout the regions of finely mixed TiN and B whereas no BN was observed. This observation requires further confirmation to determine whether there is a decrease in nitrogen content between the initial and quenched material.

Conclusions from TEM analysis address the mechanisms of phase transformations that occur within the time scales of the propagating high temperature reaction front. Further studies utilizing x-ray and electron microscopy techniques are in progress to better our understanding of the reaction mechanism and diffusion behavior occurring in the reactions of the Ti-B-N ternary system.

REFERENCES

[1] A.G. Merzhanov and A.S. Rogachev, Pure and Appl. Chem., 64, 1992, pp. 941-953.

[2] Combustion for Materials Synthesis, ed.by A.S. Rogachev and A.S. Mukasyan, CRC Press, Boca Raton, FL, 2014.

[3] D.L. Gurev, Y.A. Gordopolov, S.S. Batsanov, A.G. Merzhanov, V.E. Fortov, App. Phys. Letters, 88, 2006, 024102.

[4] N.N. Thadhani, J. Appl. Phys., 76, 1994, pp. 2129-2138.

[5] E. Faran, I. Gotman, E.Y. Gutmanas, Materials Letters, 43, 2000, pp. 192-196.

[6] M.A. Korchagin and B.B Bokhonov, Comb. Expl. And Shock Waves, 46, 2010, pp. 170-177.

[7] T.S. Bilyan, K.V. Manukyan, S.L. Kharatyan, J.A. Puszynski, Inter. Journal of SHS, 15, 2006, pp. 235-245.

[8] C.E. Shuck, K.V. Manukyan, S. Rouvimov, A.S. Rogachev, A.S Mukasyan, Comb. and Flame, 163, 2016, pp. 487-493.

SHOCK-ASSISTED LIQUID-PHASE CONSOLIDATION OF SHS-PROCESSED TA-AL BASED COMPOSITES

[1,2]Akaki Peikrishvili, [2]Laszlo Kecskes, [1]Giorgi Tavadze, [3]Bagrat Godibadze

[1]F. Tavadze Institute of Metallurgy and Materials Science, Tbilisi, 0186, Georgia
[2]Weapons and Materials Research Directorate US Army Research Laboratory, Maryland, USA
[3]Tsulukidze Mining Institute, Tbilisi, 0186, Georgia
apeikrishvili@yahoo.com

The novelty of proposed nonconventional approach relies on the fact that the consolidation of the samples from coarse (around 5 μ) Ta-Al and Ta-Al-B4C blend powders was performed in two stages. First-the explosive predensification of the powders was performed at room temperature. In all cases, the second stage was done by the hot explosive compaction (HEC) but at temperatures under 1000ºC with intensity of loading around 5 GPa. Cylindrical compaction geometry was used in all of the HEC experiments (Figure 1a).

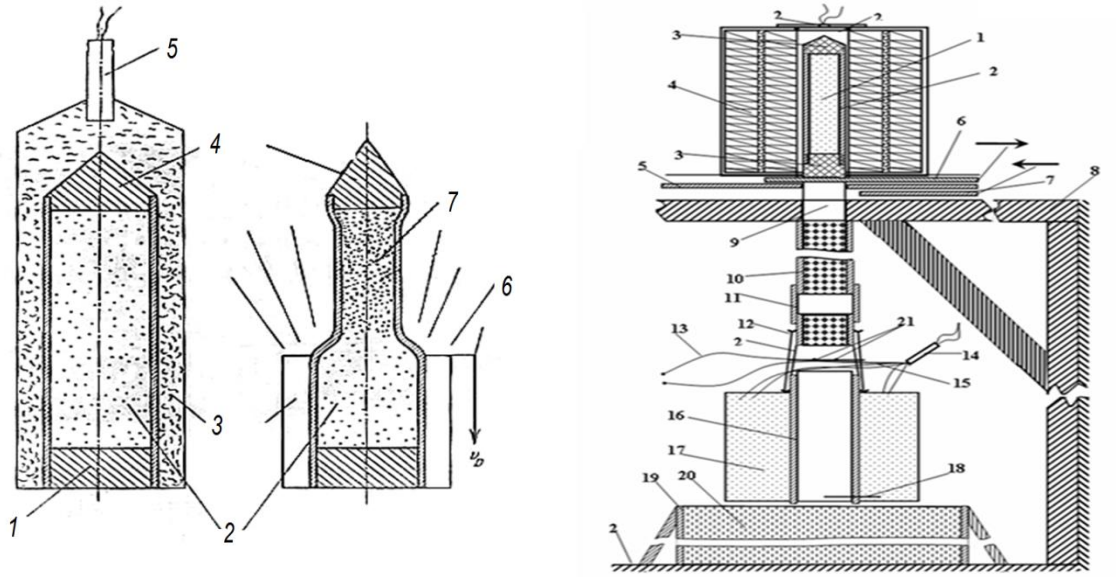

Figure 1 - The arrangement of two stage fabrication of powders.

a) Predensification by shock waves at room temperature: 1-Bottom plug of steel tube; 2. Precursor powders; 3. Explosive powder; 4. Upper plug of steel tube; 5. Electric detonator; 6. Products of detonation; 7. Consolidated powders.

b) HEC device : 1. consolidating powder material; 2. Cylindrical Steel container, 3. Plugs of steel container, 4. Heating wires of furnace, 5. Opening and closing movement of furnace, 6. Opening sheet of furnace, 7. Closing sheet of furnace, 8. Basic construction of HEC device, 9. Feeding steel tube for samples. 10. Movement tube for heated container, 11. Connecting tube from rub, 12. Accessory for fixing explosive charge, 13. Circle fixing passing of steel container. 14. El. Detonator, 15. Detonating cord, 16. Flying tube for HEC, 17. Explosive charge, 18. Lowest level of steel container, 19.Bottom fixing and stopping steel container, 20. Sand.

The key operational component of the planning experiments HEC with vertical configuration of explosive charge that allows to consolidate coarse and nanoscale precursors at elevated temperatures is presented on Fig. 1b. Application of vertical configuration of the explosive charge allows to increase without limitation their sizes.. As a result the pulse duration during the compression (loading) will increases too resulting of obtaining samples with higher densities. From the other hand increasing of pulse duration will allows to decrease consolidating temperature and as a result to reduce the cost of obtained billets too.

The preliminary predensified cylindrical billet (1) was located in central hole of heating furnace (4). The heating billet is fixed in furnace by the opening and closing movement mechanism (6). After heating of billet up to necessary temperature the opening (6) sheet will opens furnace and billet moves through the feeding cylindrical system (9-11) to the set-up of explosive charge (17).

After receiving signal that billet passed feeding system and is located in final position (13) the detonation through the detonators and detonation cords there takes place.

The Fig. 2 represents the view of HEC billets at 940°C with intensity of loading under 10GPa.

a) b) c)

Figure 2 - The view of HEC billets based on Ta-Al precursors consolidated with intensity of loading under 10 GPa. a) Heating of predensifyed Ta-3Al billets above 950°C with further SHS reaction; b) HEC of Ta-3Al billet at 940°C, c) HEC of Ta-3Al-10% B4C billet at 940°C

As it was established in order to prevent starting of SHS reaction before shock wave loading and to maintain billets without cracks it's necessary to heat samples under 940°C temperature. The increasing of temperature above the mentioned value leads to starting of SHS reaction. The extraction of gases inside of consolidated billets starts, the geometry of billets changes and as a result further transportation of sample towards of charge becomes impossible (fig.2a). The loading of Ta-3Al billets under 940°C temperature results starting of SHS reaction on the shock wave frond that provides sharp jumping of residual temperature behind of shock wave front and as a result melting of steel containers wall and even guide steel tubes jacket melting there takes place (fig.2b). The application of B4C passive additive and consolidation of Ta-3Al-10%B4C precursors provides reduction of residual temperature behind of shock wave front and as a result no melting process there occur (fig. 2c).

The figures. 3 & 4 shows the microstructures and analyses of HEC Ta-3Al-10%B4C and Ta-Al precursors obtained at 940°C and 900°C temperatures with intensity of loading under 10GPa.

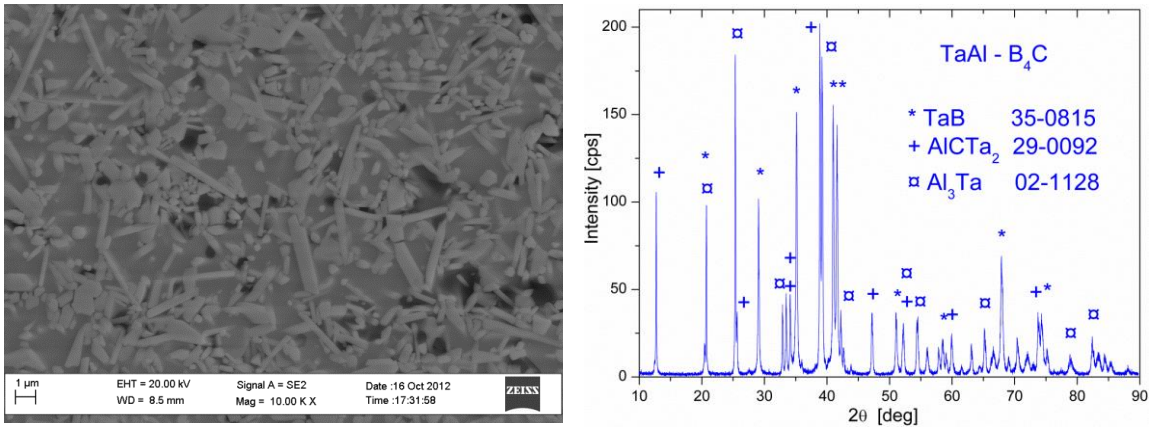

a) b)

Figure 3 - The microstructure and diffraction picture of HEC Ta-3Al-10%B4C composite after two stage consolidation at 940°C with intensity of loading under 10GPa. a) microstructure; b) Phase analyse.

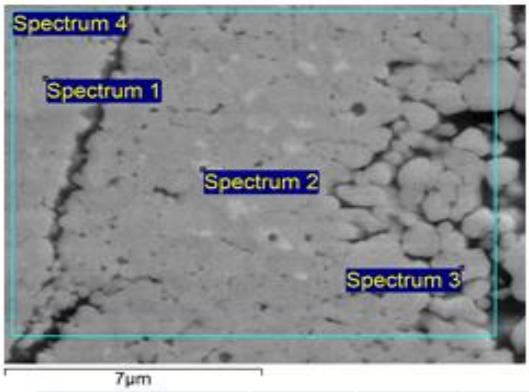

TaAl, T-900C°.

All results in weight%

Spectrum	In stats.	Al	Ta	Total
Spectrum 1		27.67	72.33	100
Spectrum 2		23.57	76.43	100
Spectrum 3		29.85	70.15	100
Spectrum 4		30.69	69.31	100

Element	Line	App. Conc	k ratio	Intensity corr.	Weight%	Weight% sigma	Atomic%	Standard
Al	K_SERIES	65.67	0.4557	1.4553	30.69	0.51	74.81	Al2O3
Ta	M_SERIES	77.73	0.7773	0.7522	69.31	0.51	25.19	Ta
Totals					100			

Figure 4 - The microstructure and elemental analyses of HEC Ta-Al precursors consolidated at 900°C with intensity of loading under 10GPa.

As it's seen from microstructure and correspondent diffraction picture (Fig 3b) and elemental analyses (fig 4) in both cases almost full syntheses and formation of Tantalum aluminates there takes place. The investigation of microstructure of HEC Ta-3Al-B4C composites and analyses of diffraction picture shows that at high temperature, under shock wave loading there took please full dissolution of boron carbide with further redistribution of B and C atoms. As a result the formation of tantalum diborides -TaB_2 and tantalum aluminates -Ta3Al /T_2AlC. (fig. 3b) behind of shock wave front there takes place. The needle like particles on microstructure

(figure 3a) as it was confirmed by micro X-ray spectral analyses belongs to mentioned TaB2 phase.

The figure #5 represents the microstructures of HEC TaAl intermetallic compound obtained at 900 °C with intensity of loading under 10GPa.

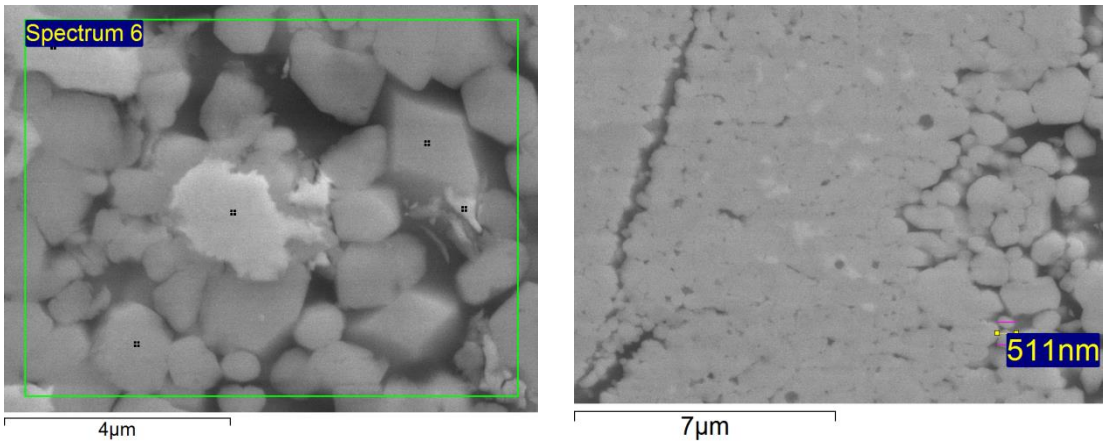

a) b)

Figure 5 - The microstructure of HEC TaAl intermetallic compound obtained at 900 °C. a) reminder unreacted Ta phase; b) formation of microcrystalline structure;

As it was established the low consolidation temperature and low quality of blending of Ta-Al powders leads to partial SHS reaction behind of shock wave front and unreacted reminder tantalum (Ta) phases in whole volume of HEC billets may be observed (fig.5a).

The investigation of grain sizes of HEC tantalum aluminates (TaAl), showed that the dimensions of particle size for synthesized aluminates changes between the 200-900nm depending on HEC temperature and starting phase content.

In whole comparing previous results connected with HEC of Ni-Al and Ti-Al composites (including clad precursors) with current investigation shows that Ta-Al based precursors are much more promising from the standpoint of features of explosive consolidation processes and formation of intermetallic compounds. This is due to high density of Ta powder (16.4 g/cm^3) and the high reactivity of Ta-Al system. Application of HEC technology may be solved previously fixed problems, based on developed of high intensity of compression (loading) and high consolidation needed for initiation of SHS processes during heating.

INVESTIGATION OF COATING FROM POWDER PARTICLES RECEIVED AFTER HIGH-SPEED IMPACT

E.V. Petrov*, V.S. Trofimov

Institute of Structural Macrokinetics and Materials Science RAS, Chernogolovka, Academician Osipyan str., 8, 142432 Russia
*petrow-ewgeni@mail.ru

Dynamic methods associated with the use of explosion energy occupy a special place among the various methods of processing materials. The main attention is paid to the near-surface zone, where the main processes occur, when studying materials treated with a high-speed particle flow. The impact of a flow of particles with a steel obstacle leads to the stopping of most of them in the near-surface zone and the formation of the coating from the stopped particles on the surface of sample.

As a steel obstacle samples were selected from steel St.3 with a diameter of 20 mm and a height of 30 mm. Tungsten powder, with a particle size of 5-20 μm (66%), and a nickel powder with a particle size of 6-16 μm (68%) were used in the experiments.

During the experiment, the sample was placed in a guiding channel, on top of which was located a ring with powder material in a bulk density with a mass of 3 g. A charge of an explosive with a detonator was mounted on the ring. There was a clearance between the particles of the powder and the charge of explosive. The role of the clearance was to a decrease in the peak pressure acting on the powder particles. The clearance also ensures a continuous loading of the powder particles, during which the necessary impulse of a shock wave of a rectangular profile is communicated to it. Shock wave generated by the charge of explosive and the stream of detonation products went through the powder and together with powder impacted on the sample [1].

Investigation of the surface of steel samples showed that after the impact of a flow particles of tungsten and nickel on the surfaces leads to formation a coating with a thickness varying between 10 and 30 μm and the formation of a transition zone occur.

An SEM survey of the near-surface zone of samples treated with a high-speed flow of nickel particles revealed phase changes in the structure of the steel and the region of distribution of nickel in the near-surface zone (Fig. 1).

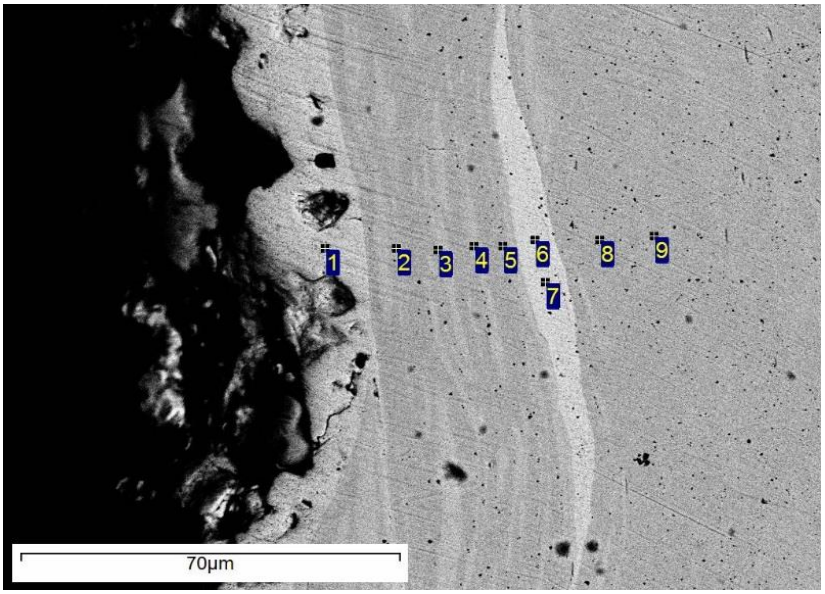

Spectrum	1	2	3	4	5	6	7	8	9
C	37.6	30.7	30.8	29.5	28.0	29.4	28.6	25.9	23.8
Fe	9.5	69.3	69.2	70.5	71.9	3.6	3.8	74.1	76.2
Ni	52.9	---	---	---	---	66.9	67.5	---	---

All results in wt. %

Fig. 1 - SEM image of the sample surface after treatment with a flow of nickel particles and EDS data for the surface layer

The a surface layer of tungsten particles is formed as a result of the impact of a high-speed flow of tungsten particles with the surface of the steel sample. This coating consists of tungsten, iron and their intermetallic compound. Globular particles at the interface of the tungsten and iron which surround the tungsten particles are formed in the near-surface layer of samples [2]. This indicates a reaction diffusion at the interphase boundary with the formation of intermetallic compounds on the basis of the initial components. This structure is characterized by of carbide "fringe" from globular particles of tungsten carbide.

This work was financially supported by the Russian Foundation for Basic Research (project no. 15-08-00571a).

REFERENCES

[1] V.S. Trofimov, E.V. Petrov and M.I. Alymov, Inter. Journal of SHS, 25(2), 2016, pp. 125-128.

[2] E.V. Petrov, V.S. Trofimov and A.S. Shchukin, Tambov University Reports. Series: Natural and Technical Sciences, 21(3), 2016, pp. 784-786.

MA SHS OF ADVANCED BIOCOMPATIBLE AND BIOACTIVE MATERIALS IN Ti-C-Co/Fe-$Ca_3(PO_4)_2$-Ag-Mg SYSTEM

Yu.S. Pogozhev*, A.Yu. Potanin, A.V. Novikov, N.V. Shvindina, E.A. Levashov

National University of Science and Technology "MISIS", Leninsky prospect, 4, Moscow 119049, Russia
* vspogozhev@mail.ru

A promising direction in modern medical technology is surface functionalization of metallic implants by creating composite coatings with sufficient levels of mechanical characteristics, biocompatibility, bioactivity and antibacterial properties [1].

Such coatings can be obtained by pulsed electrospark deposition (PED) – a promising method in the field of surface engineering. The technology enables formation of an adhesively strong layer, resulting from fusing both the molten electrode and the molten substrate materials within the pulsed arc discharge. However, this method requires the use of composite multicomponent electrodes for deposition of coatings. Fabrication of the electrodes with homogeneously distributed metallic and non-metallic components is necessary to obtain a coating with excellent properties, to simplify the deposition process, and to increase their reproducibility and productivity.

The capabilities of pulsed electrospark deposition can be substantially extended by using of composite electrodes based on ceramics produced by self-propagating high-temperature synthesis (SHS) [2]. SHS provides a highly dense, homogeneous structure with the necessary mechanical, thermal, and electrical properties of electrode materials for PED. SHS method also allows to homogeneously distribute the functional nanosized dopants introduced in small amounts (<5 %). Significant antibacterial and sterilizing effect while preserving the bioactive properties of PED coatings has been achieved with electrodes containing nanosized antibacterial additives [3].

Ceramic electrodes for PED of bioactive coatings in the Ti–C−$Ca_3(PO_4)_2$–Co/Fe–Mg–Ag system with different content of metallic Co/Fe binder were fabricated by forced SHS pressing [4-6]. Preliminary mechanical activation (MA) of the initial mixture makes it possible to reduce an average size of structural components and increase the homogeneity of their distribution in green mixture, and consequently in the compact synthesized products. As a result of intensive plastic deformation during MA process composite particles (granules) with a lamellar structure are formed. The layers in these granules consist of different mixture components. Granules in MA mixture presents alternating elongated layers of Ti and Co/Fe with a thickness of 2-3 μm, between there basic layers there is a uniformly distributed layers with a thickness of less than 500 nm consists of $Ca_3(PO_4)_2$, Ag and Mg powders. It was found that an addition of Co or Fe as a binder elements in to green mixture leads to refinement of the electrode materials structure. This improved the mass transfer of the material from the electrode to the substrate, which leads to increase Ca, P, and Ag content in PED coatings. Co/Fe-free SHS materials consist of a TiC_x rigid frame with the $Ti_3PO_{(x)}$ phase homogeneously distributed along the TiC_x grain boundaries and local precipitations of CaO phase. In the case of the Co-added SHS electrodes complex phosphide CoTiP and TiCo intermetallic compound occur in the electrodes composition. The TiFe intermetallic compound and FeTiP phosphide were formed by the addition of Fe in to green mixture. The introduction of antibacterial additives in the form of silver and magnesium led to the formation of a $AgMg_x$ solid solution, with x = 0.12 - 0.14. PED coatings contain the

Ag-based 20–200 nm inclusions uniformly distributed both on the surface and within the coating.

The authors gratefully acknowledge support from the Ministry of Education and Science of the Russian Federation in the framework of the Increase Competitiveness Program of NUST "MISiS" (No. K2-2016-011) and from the Russian Foundation for Basic Research (project no. 16-08-00525).

REFERENCES

[1] Biomaterials Science: an introduction to materials in medicine, ed.by B.D. Ratner, A.S. Hofman, Elsevier Academic Press, London, 2004, p.520.
[2] E.A. Levashov, A.G.Merzhanov, D.V. Shtansky, Galvanotechnik, 9, (2009) 2102-2114.
[3] D.V. Shtansky, I.V. Batenina, P.V. Kiryukhantsev-Korneev, et al., Appl. Surf. Sci., 285, (2013) 331-343.
[4] A.Y. Potanin, E.A. Levashov, Y.S. Pogozhev, et al., Ceram. Int., 41, (2015) 8177-8185.
[5] A.N. Sheveyko, O.S. Manakova, E.I. Zamulaeva, et al., Surf. Coatings Technol., 302, (2016) 327-335.
[6] N.V. Litovchenko, A.Yu. Potanin, E.I. Zamulaeva, et al., Surf. Coatings Technol., 309, (2017) 75-85.

THE FEATURES OF MgB_2 THERMAL EXPLOSION SYNTHESIS AND INFLUENCE OF DOPING AGENTS

A.Yu. Potanin[1]*, Yu.S. Pogozhev[1]**, E.A. Levashov[1], D.Yu. Kovalev[2], N.Yu. Khomenko[2]

[1] National University of Science and Technology "MISIS", Leninsky prospect, 4, Moscow 119049, Russia
[2] Institute of Structural Macrokinetics and Materials Science, Russian Academy of Sciences, Academica Osipyana, 8, Chernogolovka, Moscow Region 142432, Russia
* a.potanin@inbox.ru ; ** yspogozhev@mail.ru ;

Nanostructured ceramics based on magnesium diboride MgB_2, with the effect of superconductivity, is promising for cryoelectronic devices at liquid hydrogen and neon temperatures. In particular, the superconductors can be used to produce electric motors, cryopumps, support-free vehicles, magnetic bearings, current limiters, and intense magnetic fields [1]. Absence of phase transitions in this material, low specific weight, relatively low cost, ease of production in comparison with the metal oxide ceramics and strength characteristics allow its application in a wide range of technical solutions [2].

Development of an effective ceramics production technology based on MgB_2 is an urgent task [3]. One of such technologies is a self-propagating high-temperatures synthesis (SHS), which allows to produce of various compounds without high energy consumption and ensures the chemical purity of the final products due to the self-purification effect in the combustion wave. There are a lot of parameters of SHS process which gives a great influence on phase composition, structure and properties of final synthesis product, like initial and combustion temperatures and rate, initial mixture heating rate, characteristics of raw materials, specific density and etc [4].

In this research we used the time-resolved X-ray diffraction (TRXRD) method to study the effect of Mg + 2B mixture heating rate on the dynamics of phase formation during thermal explosion in helium environment. It was shown that MgB_2 phase occurs with no intermediate compounds. The presence of oxygen impurity in initial mixture is a significant factor affecting MgB_2 formation kinetics. When heating rate of the initial mixture Mg + 2B is high ~ 150–200 °C/min an oxide film is not formed on the surface of magnesium particles, since there is not enough time for this. Thus reaction $Mg + 2B \rightarrow MgB_2$ proceeds by a mechanism of reaction diffusion immediately upon magnesium melts at 650 °C. Synthesis products are mostly consists of nanosized MgB_2 particles and small amount of MgO less then 5 %. When the heating rate is 30-50 °C/min, a relatively thick oxide layer grows on the surface of magnesium particles. This layer inhibits melt spreading and the temperature of thermal explosion increases up to 1100 °C. In this case synthesis products also contain nanosized MgB_2 particles and an increased amount of oxide MgO ~ 15 %. So, there is an inverse dependence between heating rate and the starting temperature of thermal explosion [5].

Preliminary mechanical activation (MA) of the initial mixtures using planetary ball mill leads to changes in combustion kinetics at MgB_2 formation, significantly increases the period of simultaneous existence of Mg and MgB_2, and reduces the starting temperature of thermal explosion at which the chemical reaction occur.

Doping of initial mixture Mg + 2B by Cu, Zn and Ag leads to formation of intermediate intermetallic compounds based on Mg like Cu_2Mg, $CuMg_2$, Zn_2Mg, $Zn_{20}Mg_{51}$ and AgMg during

synthesis. In turn, this leads to a lack of magnesium, prevents the formation of MgB_2, and leads to the formation of MgB_4 during combustion in thermal explosion mode. Introduction of Al additive in the amount of 0.05-0.3 % in to initial mixture allows to obtain a single-phase product consists of solid solution based on magnesium diboride.

The authors gratefully acknowledge support from the Russian Foundation for Basic Research and the Moscow Government (project no. 15-38-70013 «mol_a_mos»).

REFERENCES

[1] A.L. Ivanovskii, Phys. Solid State, 45, (2003) 1829-1859.
[2] A.I. Golovashkin, Sov. Phys. Usp., 30, (1987) 659-670.
[3] I. Zlotnikov, I. Gotman, E.Y. Gutmanas, J. Eur. Ceram. Soc., 25, (2005) 3517-3522.
[4] Combustion for Material Synthesis, A.S. Rogachev, A.S. Mukasyan, Taylor & Francis Group, 2015, p. 424.
[5] D.Yu. Kovalev, A.Yu. Potanin, E.A. Levashov, et al., Ceram. Soc., 42, (2016) 2951-2959.

SHS OF MULTICOMPONENT TARGETS AND THEIR APPLICATION IN MAGNETRON SPUTTERING OF FUNCTIONAL COATINGS

Yu.S. Pogozhev*, E.A. Levashov, D.V. Shtansky, E.I. Patsera, V.V. Kurbatkina, A.Yu. Potanin, A.V. Novikov, F.V. Kiryuhantsev-Korneev

National University of Science and Technology "MISIS", Leninsky prospect, 4, Moscow, 119049, Russia
* pogozhev@rambler.ru

A wide range of composite targets (cathodes) based on ceramics, metalloceramics and intermetallide compounds for magnetron sputtering of functional multicomponent nanostructural coatings (MNCs) can be obtained via forced SHS pressing technology. Such kind of composite SHS- targets possess a high relative density up to 99.5 %, homogeneous or gradient structures and high chemical purity along with necessary mechanical properties, thermal and electrical conductivities. During the magnetron sputtering with using of multicomponent composite SHS- targets, the substance is transferred with a homogenous flow of metallic (Ti, Ta, Cr, Mo, Al, Zr, etc.) and non-metallic (Si, C, O, N, P) atoms and ions, since a target contains all the elements required for the formation of the coating. SHS- pressing technology allows to obtain disk and planar-extended segmented targets (Figure 1) which can be used in both laboratory scale and industrial magnetron installations.

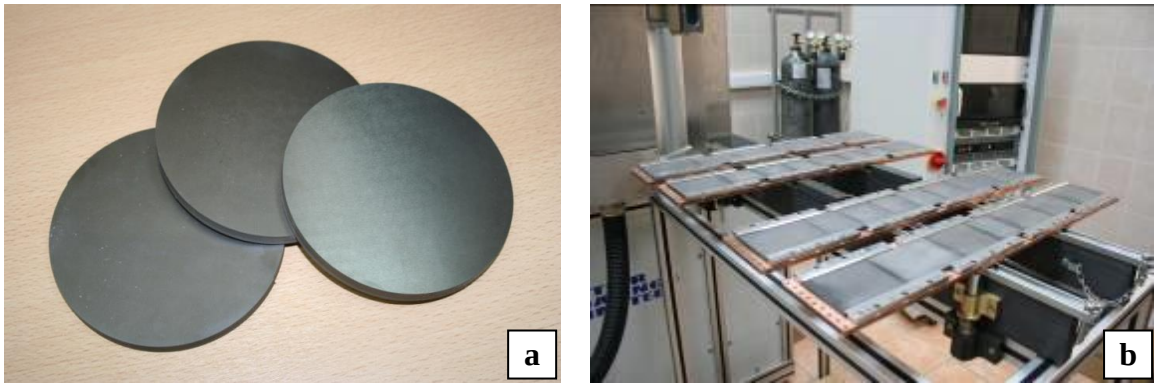

Figure 1- Composite disk (a) and planar-extended segmented (b) ceramic-based targets obtained via forced SHS pressing.

Many compositions of SHS-targets, intended for the physical vapor deposition (PVD) of functional coatings for cutting tools, parts of aircraft and rocket engines, internal-combustion engines, medical devices and etc., have been developed. Multi-component SHS-targets in the TiB_2-Ti_5Si_3, TiC_xN_y-Ti_5Si_3-$TiAl_3$, CrB_x-Cr_5Si_3-Cr_4Al_{11}, $MoSi_2$-MoB, Mo_5SiB_2, ZrB_2-$ZrSi_2$, SiC-B_4C, and etc. systems have been synthesized [1-5]. These SHS-targets have been successfully applied for the magnetron sputtering of heat-resistant MeSiBN (Me: Mo, Zr, Cr, Al, Ti) coatings with an enhanced thermal stability [6-9]. The metal (Cr-, Ni-, and Mo-alloys, WC-Co) and non-metal materials (Si, Al_2O_3) were used as the substrates. TiSiBN coatings demonstrated hardness up to 30 GPa, good long-time oxidation resistance at 900 ^oC, but exhibited a poor resistance to the metal atoms diffusion from the metal substrates. TiAlSiBN had extremely low crystallite size less then 3 nm and good oxidation resistance at 1000 ^oC. CrAlSiBN, MoSiBN, and ZrSiBN coatings showed hardness 30-40 GPa, and good oxidation resistance at 1200-1400 ^oC. CrAlSiBN revealed the best wear resistance in terms of cyclic impact loadings and in sliding

conditions at room temperature. On the other hand MoSiBN showed the low wear rate and low friction coefficient at T≥500 ºC due to formation of MoO_3 which is solid lubricant. Moreover MoSiBN successfully resisted to the diffusion of metal atoms from the substrate up to 1000 ºC.

SHS-targets made of $TiC_{0.5}$-CaO, TiC_xN_y-Si_3N_4-CaO, $TiC_{0.5}$-Ti_3PO_x-CaO and (Ti,Ta)C_x-Ti_3PO_x-CaO compositions [10,11] have found an application for the deposition of multifunctional bioactive nanostructured films (MuBiNaFs) onto orthopedic and dental implants, as well as implants for cranio-maxillo-facial surgery, fixation of the cervical and lumbar spine and etc. MuBiNaFs exhibit reduced Young's modulus – 230-350 GPa, high-resistance to longtime elastic strain to failure as an indicator of coating durability and wear resistance, high elastic recovery up to 75 %, high adhesion strength up to 50 N, low friction coefficient of 0.12-0.22, high hardness in the range of 25-40 GPa, also they have a good biocompatibility and are non-toxic [12].

The SHS process combined with preliminary mechanical activation (MA) of the reactionary mixture is successfully applied for obtaining $M_{1-n}AX_n$- phase targets based on: Ti_3AlC_2 [13], Ti_2AlC, Ti_3SiC_2, Cr_2AlC and $Ti_{1-x}Cr_xAlC$ [14]. They are applied for magnetron sputtering of protective corrosion- and heat-resistant coatings. TiAlCN coatings [15] possess high hardness 32–35 GPa, low friction coefficient below 0.25, high thermal stability up to 1200 °C, and superior performance in dry milling tests against high Cr steel. Coatings with high Cr content [15] demonstrated improved oxidation resistance up to 1000 °C and superior electrochemical behavior, but their mechanical and tribological properties were deteriorated. In addition, MA SHS made it possible to obtain targets on the basis of CrB_x and MoB borides, as well as of Ti_2CrB_2 and Cr_4Ti_9B [16] ternary compounds for deposition of hard wear-resistant coatings.

Resistance of the ceramic based SHS-targets to thermal cycling is increased due to applying functionally-gradient materials (FGMs) [17], when a ceramic sputtering layer, for example, $TiC_{0.5}$-Ti_3PO_x-CaO, is fastened to a load-bearing layer, which has a high thermal and electrical conductivity, for example, the one made from titanium. Besides, the difference between thermal expansion coefficients of the ceramic and metallic layers is smoothed due to the intermediate gradient layers. The working life of such FGM targets is limited by the thickness of the sputtered layer. The second way to improve the thermal stability of SHS-targets is to reinforce the material with a refractory component (Ta, W, Mo, etc.), for example, with the use of continuous fibers or meshes, which are put into the reactionary mixture at the stage of the briquette obtaining before performing the SHS process.

Development of the ceramic based SHS- targets requires the prior conduct of the whole complex of researches in the field of structural macrokinetics including experimental studies of the kinetics and the mechanisms of combustion process, possible routs of the chemical reactions during combustion synthesis, peculiarities of phase- and structure formation of the final products in dependence of the synthesis conditions and etc. All of these studies were carried out for above mentioned compositions. Obtained results allowed to find optimal conditions of the synthesis and fabricate SHS-targets for application in different installations for ion-plasma sputtering: in direct-current magnetron systems, high-frequency and pulse magnetron systems, magnetron systems with additional inductively coupled plasma, arc evaporators and etc.

This work was carried out with partial financial support from the Russian Science Foundation (project № 14-19-00273).

REFERENCES

[1] E.A. Levashov, Yu.S. Pogozhev, A.Yu. Potanin, N.A. Kochetov, D.Yu. Kovalev, N.V. Shvyndina, T.A. Sviridova. Ceramics International 40, (2014) 6541–6552.

[2] Yu.S. Pogozhev, E.A. Levashov, E.I. Zamulaeva, A.Yu. Potanin, A.Yu. Vlasova, A.V. Novikov, N.A. Kochetov. *Galvanotechnik*, 2 (2015) 371-376.

[3] Yu.S. Pogozhev, I.V. Iatsyuk, E.A. Levashov, A.V. Novikov, N.A. Kochetov, D.Y. Kovalev. Ceramics International, 42 (2016) 16758–16765.

[4] E.A. Levashov, Yu.S. Pogozhev, A.S. Rogachev, N.A. Kochetov, D.V. Shtanskiy. Russian Journal of Non-Ferrous Metals, 53, 1 (2012) 77–84.

[5] A.F. Fedotov, A.P. Amosov, A.A. Ermoshkin, V.N. Lavro, S.I. Altukhov, E.I. Latukhin, D.M. Davydov. Russian Journal of Non-Ferrous Metals, 55 (2014) 477-484;

[6] Ph.V. Kiryukhantsev-Korneev, D.V. Shtansky, M.I. Petrzhik, E.A. Levashov, B.N. Mavrin. Surface and Coatings Technology, 201, 13 (2007) 6143-6147.

[7] Ph.V. Kiryukhantsev-Korneev, J.F. Pierson, K.A. Kuptsov, D.V. Shtansky. Applied Surface Science, 314 (2014) 104-111.

[8] Ph.V. Kiryukhantsev-Korneev, J.F. Pierson, K.A. Kuptsov, D.V. Shtansky, Applied Surface Science 314 (2014) 104.

[9] Ph.V. Kiryukhantsev-Korneev, A.V. Bondarev, D.V. Shtansky, E.A. Levashov. Protection of Metals and Physical Chemistry of Surfaces, 51, 5 (2015) 794–802.

[10] A.Yu. Potanin, E.A.Levashov, Yu.S. Pogozhev, N.V. Shvindina, D.Yu. Kovalev. Ceramics International, 41, (2015) 8177–8185.

[11] E.A. Levashov, A.S. Rogachev, Yu.K. Epishko, N.A. Kochetov. Russian Journal of Non-Ferrous Metalls 48 (2007) 496-506.

[12] D.V. Shtansky, N.A. Gloushankova, I.A. Bashkova, M.A. Kharitonova, T.G. Moizhess, A.N. Sheveiko, Ph.V. Kiryukhantsev-Korneev, A. Osaka, B.N. Mavrin, E.A. Levashov. Surface and Coatings Technology, 202 (2008) 3615–3624

[13] A.Yu. Potanin, P.A. Loginov, E.A. Levashov, Yu.S. Pogozhev, E.I. Patsera, N.A. Kochetov. Eurasian Chemico-Technological Journal 17 (2015) 233-242.

[14] E.A. Levashov, Yu.S. Pogozhev, D.V. Shtansky, M.I. Petrzhik. Russian Journal of Non-Ferrous Metals, 50, 2 (2009) 151-160.

[15] D.V. Shtansky, Ph.V. Kiryukhantsev-Korneev, A.N. Sheveyko, B.N. Mavrin, C. Rojas, A. Fernandez, E.A. Levashov. Surface and Coatings Technology, 203 (2009) 3595–3609.

[16] E.A. Levashov, Yu.S. Pogozhev, V.V. Kurbatkina, et. al. Advances in ceramic - synthesis and characterization, processing and specific applications. C. Sikalidis (Eds), InTech Open Access Publisher, (2011) 3-48.

[17] E.A. Levashov, D.V. Larikhin, D.V. Shtansky, A.S. Rogachev, A.E. Grigoryan, J.J. Moore. The Physics of Metals and Metallography, 94, 5 (2002) 473-483.

CAPILLARY MELT FLOW AND SPIN REGIMES OF GASLESS SYSTEMS

V.G. Prokof'ev*[1], V.K. Smolyakov[2]

[1] Tomsk State University, Tomsk, 36, Lenin Ave., 634050, Russia
[2] Department for Structural Macrokinetics, Tomsk Scientific Center of SB RAS, 10/3 Akademichesky Ave., Tomsk, 634021,Russia.
* pvg@ftf.tsu.ru

Unstable three-dimensional combustion regimes of gasless systems are one of the most interesting problems in the combustion theory. Numerical studies [1-3] revealed a large number of regimes characterized by a diverse propagation of high-temperature reactions and their interaction within the framework of a three-dimensional solid-phase model. The results have shown that the so-called spin combustion (propagation of reactions along a spiral trajectory) is one of the special cases of unstable combustion. It should be noted that unstable gasless combustion regimes were found and investigated in the systems which contained a low-melting component in porous samples in experiments [4, 5].

The simulation of gasless combustion, considering the melting of one of the mixture components, found the new regimes of unstable combustion [6, 7]. The parameters of the phase transition were shown to influence on the stability of combustion. The study found the conditions for the formation of «strong spin waves», the regimes of which differed in the rate of reactions in the axial and tangential directions. The melt flow in pores, which determined convective heat transfer, revealed new regimes for the formation of composite materials [8]. For a solid-flame combustion model, the stability boundary is determined by the quantity $\alpha_{st}=9.1\mathrm{Td}-2.5\mathrm{Ar}=1$ [9], where, $\mathrm{Td}=\frac{cRT_*^2}{QE}$, $\mathrm{Ar}=\frac{RT_*}{E}$, E is the activation energy; R is the gas constant; T_* is the combustion temperature; c is the heat capacity; Q is the thermal effect of a reaction. The combustion regime is stationary for $\alpha_{st}> 1$. When one of the mixture components starts melting and spreading, the boundary of stable regimes is shifted to a region of lower α_{st}. The melt is assumed can be filtrated only at a temperature that is above the melting temperature. This study presents a 3D numerical solution for the gasless combustion of a cylindrical sample with allowance for the convective flow of a melt. The combustion modes are found and described for small values of the stability parameter $\alpha_{st}\approx 0.5$.

When a convective flow rate is higher or approximately equal to the mean axial rate of the reaction front propagation, combustion is stabilized, the reaction front becomes flat, and the combustion regime becomes stationary, regardless of the sample radius, which is connected with additional convective heat transfer from the product zone to the chemical reaction zone. The decrease in the melting point leads to the fact that combustion is stabilized earlier due to the convective flow of the melt as compared with the high-temperature phase transition, since the depth of melt into the heating zone is increased. In the strong instability region of the combustion wave, new spin combustion regimes are found, which are characterized by a high tangential rate of combustion U_φ in comparison with the axial component of the rate U_z. The combustion front is presented by a pulsating loop in the perpendicular cross section of a cylindrical sample for $\alpha_{st} = 0.68$ (Fig.1) and has a spiral shape that varies periodically in time, $\alpha_{st} = 0.51$ (Fig.2) and $\alpha_{st} = 0.045$ (Fig.3).

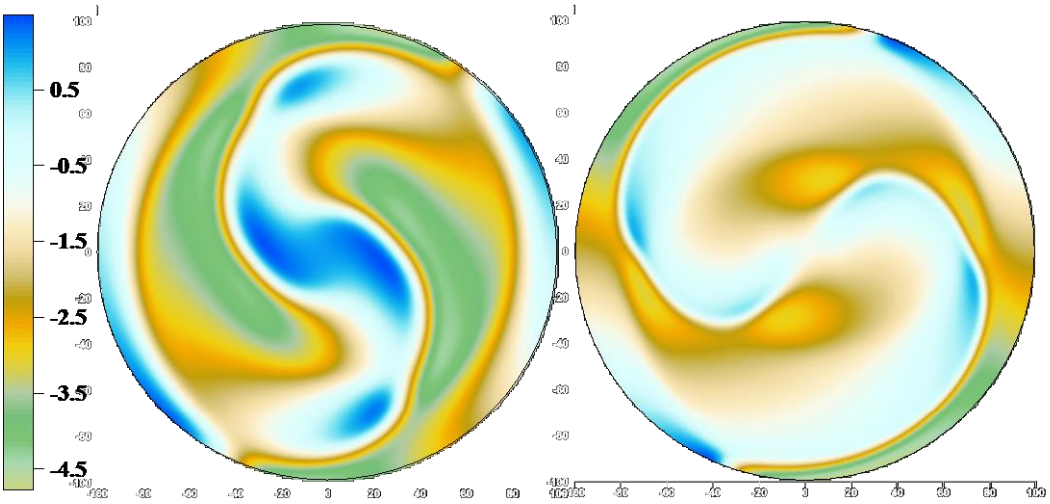

Fig. 1 - Temperature distribution in the cross section perpendicular to the cylinder axis during passage through the front point on the cylinder axis: the sample radius R=100, α_{st}=0.68

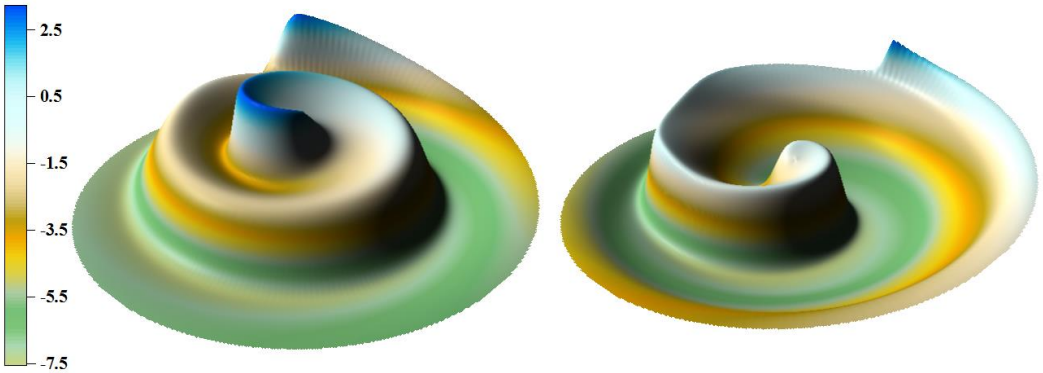

Fig. 2 - Temperature distribution in the cross section perpendicular to the cylinder axis during passage through the front point on the cylinder axis: the sample radius R=100, α_{st}=0.51

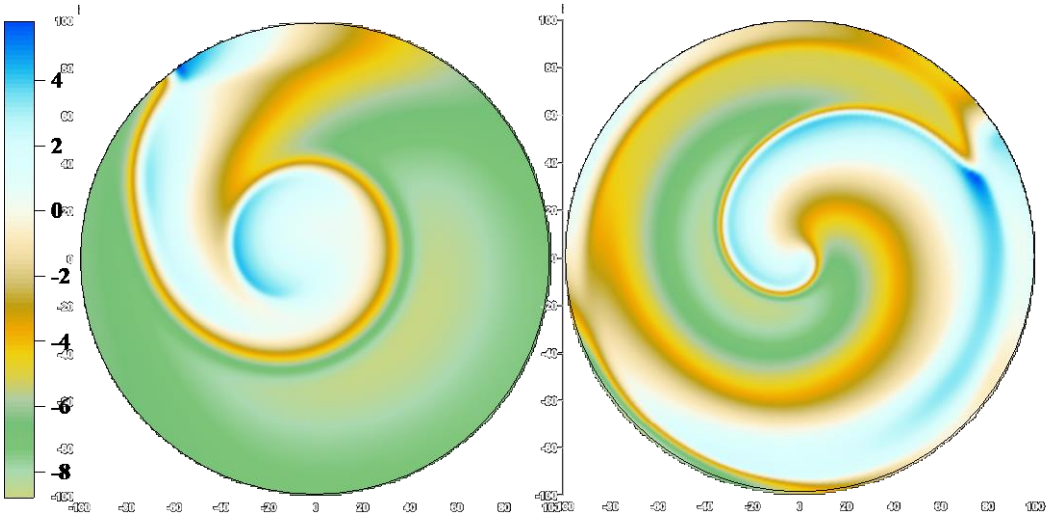

Fig. 3 - Temperature distribution in the cross section perpendicular to the cylinder axis and passage through the front point on the cylinder axis: the sample radius R=100, α_{st}=0.45

The conducted computations showed the qualitative influence of convective heat transfer on the characteristics of combustion.

This work was funded by the Competitiveness Enhancement Programme of Tomsk State University for 2013-2020.

REFERENCES

[1] T. P. Ivleva and A. G. Merzhanov, Mathematical Modeling of Three-Dimensional Spin Modes of Gasless Combustion Waves, Dokl. Ross. Akad. Nauk, 369 (2), 1999, pp. 186–191.

[2] T. P. Ivleva and A. G. Merzhanov, Three-Dimensional Spin Modes of Gasless Combustion Waves, Dokl. Ross. Akad. Nauk, 371 (6), 2000, pp. 753–758.

[3] T. P. Ivleva and A. G. Merzhanov, Mathematical Simulation of Three-Dimensional Spin Regimes of Gasless Combustion, Combust., Expl., Shock Waves, 38 (1), 2002, pp. 41–48.

[4] Yu. M. Maksimov, A. G. Merzhanov, A. T. Pak, and M. N. Kuchkin, Unstable Combustion Modes of Gasless Systems, Combust., Expl., Shock Waves, 17 (4), 1981, pp. 393–400.

[5] Yu. M. Maksimov, A. T. Pak, G. B. Lavrenchuk, Yu. S. Naiborodenko, and A. G. Merzhanov, Spin Combustionof Gasless Systems, Combust., Expl., Shock Waves, 15 (3), 1979, pp. 415–418.

[6] V.G. Prokof'ev and V.K. Smolyakov, Effect of the Phase Transition on Three-Dimensional Unstable Regimes of Gasless Combustion, Combust., Expl., Shock Waves, 52 (3), 2016, pp. 313–319.

[7] V.G. Prokof'ev and V.K. Smolyakov, Spinning Combustion Regimes in Gasless Systems Containing One Melting Component, Russian Journal of Physical Chemistry B, 10(6), 2016, pp. 997-1000.

[8] V.G. Prokof'ev and V.K. Smolyakov, Gasless Combustion in Two-Layer Structures: A Theoretical Model, Inter. Journal of SHS, 22, 2013, pp. 5-10.

[9] K. G. Shkadinskii, B. I. Khaikin, and A. G. Merzhanov, Propagation of a Pulsating Exothermic Reaction Front in the Condensed Phase, Combust., Expl., Shock Waves, 7 (1), 1971, pp. 15–22.

A COMPREHENSIVE OVERVIEW OF THE RECENT ADVANCEMENTS AND THE MOST PROMISING PERSPECTIVES OF MICROWAVE ENERGY APPLICATIONS TO COMBUSTION SYNTHESIS

R. Rosa*, L. Trombi, P. Veronesi, C. Leonelli

Department of Engineering Enzo Ferrari, University of Modena and Reggio Emilia, via P. Vivarelli 10, 41125 Modena, Italy
* roberto.rosa@unimore.it

Microwave heating fundamentally differs from other heating techniques as the consequence of its unique characteristic of being based on the electromagnetic energy transfer from the microwaves source to the interacting material, which according to its electric, dielectric, and magnetic properties can convert the absorbed energy into heat. This peculiar heating mechanism is at the basis of a plenty of unquestionable advantages that were reported during the last three decades in most of the different branches of chemistry as well as materials science, thus including also combustion synthesis. After a brief overview of the microwave heating fundamentals as well as of the different components constituting the scientific microwave applicators, all the most significant and recent advancements in the use of microwaves as energy source in both solid state as well as solution combustion synthesis processes will be comprehensively reviewed, highlighting the unique opportunities arising from the coupling of these two energy efficient techniques. Moreover the possible employment of less conventional frequencies as well as the use of new-generation solid state generators will be critically discussed also in the framework of scaling-up and microwave reactor design considerations.

REFERENCES

[1] R. Rosa, L. Trombi, P. Veronesi, C. Leonelli, Inter. Journal of SHS, submitted.

SELF-PROPAGATING THERMAL WAVES IN THIN FILMS: NEW KINDS OF SHS PROCESSES

A.S.Rogachev

Institute of Structural Macrokinetics and Materials Science Russian Academy of Sciences (ISMAN), Chernogolovka Moscow region, acad. Osipyana str. 8, 142432 Russia
* rogachev@ism.ac.ru

Several kinds of self-propagating heat waves in thin films (coatings or free-standing foils) were discovered up-to-now. First, self-propagating waves of explosive crystallization were observed in amorphous antimony [1]. This phenomenon was found also in other vacuum-deposited amorphous metallic (Yb, Bi, V, Sb, etc.) or semiconducting (Si, Ge) thin films [2–6]. This process achieved widespread use in production of nanocrystalline films for solar cells [7]. Second, exothermic self-sustained waves were discovered, is reactive multilayer foils [8]. Driving forces are quite different for waves of crystallization and waves of reaction. Mechanisms of the reactive waves in thin multilayer foils were widely discussed (see, for example, reviews [9, 10]). Quenching of the reaction wave allowed us to shed some light on reactive mechanism in the Ni/Al multilayer foils [11-13]. Apart from vacuum deposition, alternative method for producing amorphous metallic foils is a quick quenching of melts. Materials produced by this method are commonly named metallic glasses; they found application for powerful magnets and transformers, while bulk metallic glasses represent promising engineering materials [14]. The self-propagating thermal waves in metallic glasses were unknown until recently such phenomenon was detected in CuTi glassy metal tapes [15].

In this work, overview of new resultsis on macroscopic behavior, phase/structure transformations and evolution of some properties induced by self-sustained exothermic waves in these three mentioned above classes of the materials are presented. It is shown that, despite of different composition and production methods of thin films, the self-propagating waves in all cases have thermal nature.

In order to compere the three main classes of thermal waves, let us consider films of amorphous Sb, CuTi and nano-lamellate Ni/Al. Propagating velocities (U) and maximum temperatures (T_m) of the self-sustained waves differ significantly among various types of the films. Evidently, these characteristics depend directly on the heat released during the process. Thus, heat evolution of the reaction Ni+Al=NiAl is 1400 J/g, while heat of amorphous-crystalline transformation, measures by DSC method, has been found to be much less: 87 ± 20 J/g for Sb and 148 ± 7 J/g for CuTi. The relatively large dispersion of specific heat release for Sb can be explained by presence of Cu-substrate, which complicates precise measurement of the mass of pure antimony film in the samples studied by DSC. Expectably, higher heat release results to higher T_m and much higher U of the reactive waves in multilayer Ni/Al foils in comparison with the waves of crystallization. It worth noting that values of T_m for Sb and CuTi films are lower than melting points of Sb (904 K) and bulk intermetallic phase CuTi (1158 K), as well as eutectic point (1143 K for Cu_3Ti_2 – Cu_4Ti eutectic). Despite the difference in T_m values, normalized temperature - time profiles of the thermal waves have some similarity, as shown in Figure 1.

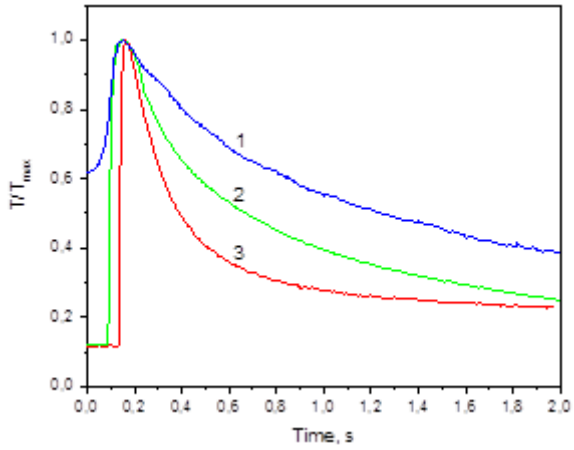

Figure 1 - Temperature–time dependences in the middle point of the films normalized by maximum temperature: $Cu_{50}Ti_{50}$ (1), Ni/Al (2) and Sb (3). Measured by thermal imaging camera.

All three systems exhibit relatively short exothermal self-heating with duration of the temperature rise stage about 150 ms for CuTi, 35 ms for Sb, and a few ms or less for Ni/Al. A stage of cooling down (right slope of the temperature peaks in Fig. 1) are several times longer than the self-heating stage. A higher cooling-down rate in case of Sb can be associated with the presence of Cu substrate. The global characteristics of the wave propagation process depends on phase and structure transformations taking place in each system. A conclusion can be made that in all considered systems the self-propagating waves have thermal nature and propagate due to exothermic effect of physical (amorphous-to-crystalline transformation) or chemical (heterogeneous reaction) processes.

REFERENCES

[1] G. Gore, The London, Edinburg, and Dublin Philosophical Magazine and Journal of Science 9, 1855, pp. 73–74.
[2] L.N. Aleksandrov, F.L. Edelman, Phys. Stat. Sol. (a) 76, 1983, pp. 409-427.
[3] V.A. Shklovskii, V.M. Kuzmenko, Sov. Phys. Usp. 32(2), 1989, pp. 163–180.
[4] K. Ohdaira, T. Fujiwara, Y. Endo, S. Nishizaki, H. Matsumura, J. Appl. Phys., 106, 2009, pp. 044907 (1-8).
[5] K.Ohdaira, H.Matsumura, Thin Solid Films, 524, 2012, pp. 161–165.
[6] H.J.Leamy, W.L.Brown, G.K.Celler, G.Foti, G.H.Gilmer, Appl. Phys. Lett. 38(3), 1981, pp. 137.
[7] R.E.I. Schropp, R. Carius, G. Beaucarne, MRS Bull., 32, 2007, pp. 219–224.
[8] Metallic Films for Electronic, Magnetic, Optical and Thermal Applications: Structure, Processing and Properties, ed. by Barmak, K. and Coffey, K.R., Woodhead Publishing, 2014, T.P.Weihs, Ch. 6, pp. 160–243.
[9] D.P.Adams, Thin Solid Films, 576, 2015, pp. 98–128.
[10] A.S.Rogachev, Russ. Chem. Rev., 77, 2008, pp. 22–38.
[11] Rogachev, A.S., Vadchenko, S.G., and Mukasyan, A.S., Appl. Phys. Lett., 101, 2012, pp. 063119.
[12] A.S.Rogachev, S.G.Vadchenko, F.Baras, O.Politano, S.Rouvimov, N.V.Sachkova, A.S.Mukasyan, Acta Mater., 66, 2014, pp. 86–96.

[13] A.S.Rogachev, S.G.Vadchenko, F.Baras, O.Politano, S.Rouvimov, N.V.Sachkova, M.D.Grapes, T.P.Weihs, A.S.Mukasyan, Combust. Flame, 166, 2016, pp. 158–169.
[14] W.L. Johnson, Current Opinion in Solid State & Materials Science, 1, 1996, pp. 383-386.
[15] A.S. Rogachev, S.G. Vadchenko, A.S. Shchukin, I.D. Kovalev, A.S. Aronin, JETP Letters 104, 2016, pp. 726–729.

NEW PHASES BY SOLUTION COMBUSTION SYNTHESIS

S.I. Roslyakov *[1], A.S. Mukasyan[2,1]

[1] National University of Science and Technology «MISIS», 119049, Moscow, Russia
[2] University of Notre Dame, Department Chemical and Biomolecular Engineering, 46556, Notre Dame, IN, USA
* nanoceram_misis_ros@misis.ru

Solution combustion synthesis (SCS) method that involves self-sustained reactions in a solution of metal containing oxidizers and fuels, e.g. water-soluble linear and cyclic organic amines, acids and amino acids, currently attracts attention of scientists all over the world. This form of combustion synthesis is well-known, extremely versatile, simple, rapid, energy saving and green technology offers some unique conditions for effective production of nanomaterials. The characteristic synthesis time is about seconds, with maximum temperatures as high as 1500 ^{o}C, without using any external heat source. The short process duration allows to fabricate super-nano (less than 10 nm) scaled powders and high temperatures facilitate the formation of desired crystalline structure without additional calcination. Typically SCS yields various types of nanosized oxides from simple binary compositions (e.g., iron oxides) to complex doped phases (e.g., perovskites), with different physical and chemical properties, which include luminescent nanophosphors, semiconductors, high surface area supported catalysts, and bioceramics [1-3].

During the last three years, the SCS field has experienced an explosion of interest with more than hundreds articles published and number of citations exceeding 12,000. The published papers are related to different science and engineering disciplines, including synthetic inorganic chemistry and electrochemistry, chemical and electrical engineering, bio- and materials science. Such rapid success in a variety of applications became possible due to recent breakthroughs in understanding of fundamental mechanism of structure and phase formation during SCS that allowed to synthesize several transition metals (Ni, Cu, Co) and alloys (CuNi, NiCo). It is shown that the combustion of nickel (and/or copper) nitrate and glycine mixture at near-stoichiometric and fuel-lean conditions indeed produces fine oxide powders. However, excessive quantities of fuel lead to the formation of pure metal or alloy. It is also shown that the combustion front propagates because of the reaction between N_2O and NH_3, which are the products of decomposition of the oxidizer and fuel. The excess of NH_3 gas produced in fuel-rich conditions rapidly reduces nickel oxide to pure metal in the reaction front [4,5]. A new class of metal-based materials produced by SCS opens vast opportunities for this flexible method to synthesize a wide range of compounds with tailored nanostructures and properties. Indeed, the $Ni(NO_3)_2$−glycine reactive mixtures impregnated onto fumed silica were used to prepare supported Ni/SiO_2 catalysts via the SCS method, varying the fuel to oxidizer ratio as well as the atmosphere (air, argon, helium) in the reaction chamber. It was shown that highly dispersed nickel nanoparticles (5 nm) formed in the reaction front possesses high activity during the ethanol decomposition toward hydrogen at low temperatures (200 °C) and excellent stability toward deactivation with essentially no change of catalyst activity over 100 h of operation [6].

In the present work, we report about new phases such as bimetallic ($FeNi_3$), nitrides (Ni_4N and/or $CuCoN_{0.6}$, $FeNi_3N$) and high entropy alloys obtained during solution combustion process under different synthesis atmosphere (Figure 1).

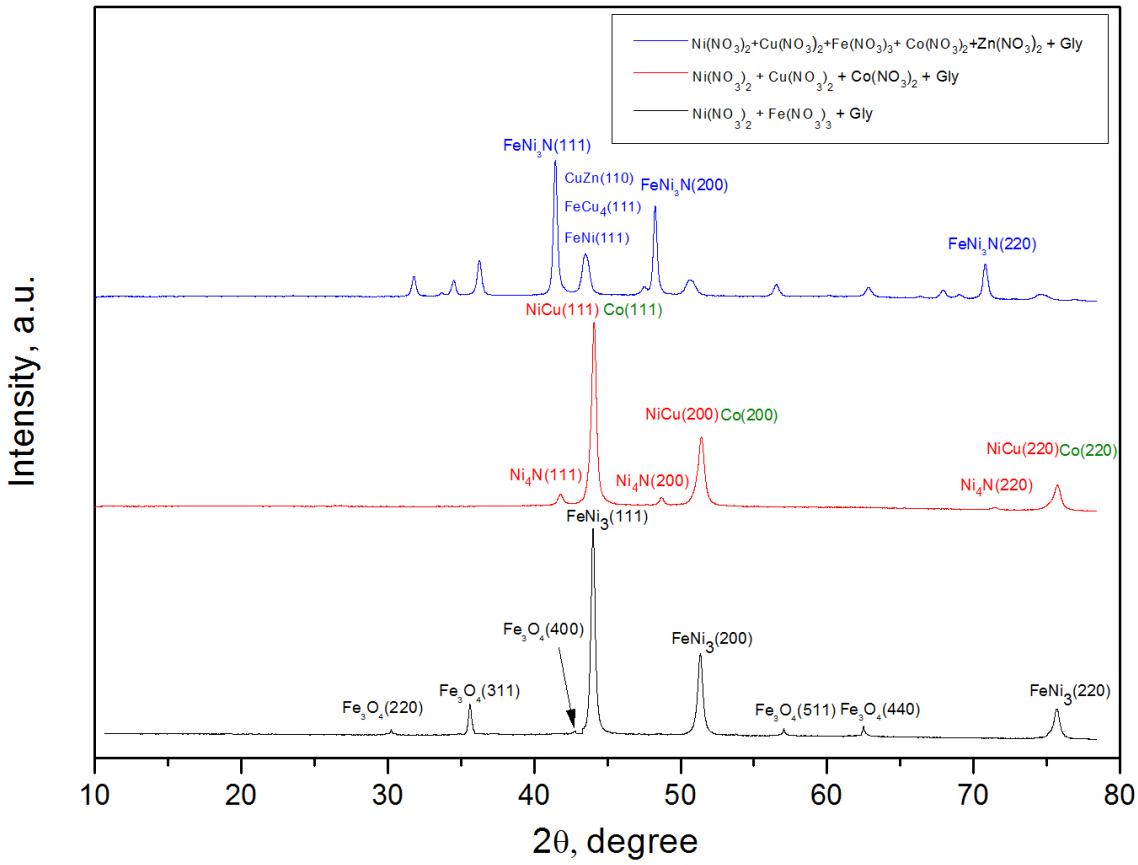

Figure 1 - XRD patterns of combustion synthesized products of different solution-based systems

The authors gratefully acknowledge the financial support of the Ministry of Education and Science of the Russian Federation in the framework of Increase Competitiveness Program of NUST «MISiS» (№ К2-2016-002), implemented by a governmental decree dated 16th of March 2013, N 211.

REFERENCES

[1] A. Varma, A.S. Mukasyan, A.S. Rogachev, K. Manukyan, Chemical Review, 116, 2016 pp. 14493-14586.

[2] Chemistry of Nanocrystalline Oxide Materials: Combustion Synthesis, Properties and Applications, K.C. Patil, M.S. Hegde, T. Rattan, S.T. Aruna, World Scientific Pbulishing Co. Pte. Ltd, Singapore, 2008.

[3] S.T. Aruna, A.S. Mukasyan, Curr. opinion in solid state materials science, 12, 2008, pp. 44-50.

[4] K.V. Manukyan, A. Cross, S.I. Roslyakov, et al., J. Phys. Chem. C, 117, 2013, pp. 24417-24427.

[5] A. Kumar, E.E. Wolf, A.S. Mukasyan, AIChE J., 57, 2011, pp. 3473−3479.

[6] A. Cross, S.I. Roslyakov, K.V. Manukyan, et al., J. Phys. Chem. C, 118, 2014, pp. 26191-26198.

SHOCK-WAVE COMPACTION OF METAL/FLUOROPOLYMER POWDER MIXTURES

I. V. Saikov*, M. I. Alymov, S. G. Vadchenko, and I. D. Kovalev

[1] Institute of Structural Macrokinetics and Materials Science, Russian Academy of Sciences, Chernogolovka, Moscow, 142432 Russia
* revan.84@mail.ru

The article is devoted to the investigation of the interaction of metals with a polymer matrix (polytetrafluoroethylene) with the throwing a flat impactor on them, and also under conditions of shock wave consolidation in cylindrical recovery fixtures (Fig. 1). The kinetics and thermal effects of these interactions are of scientific and practical interest for materials science in obtaining new structural and functional materials [1]. Study the principal possibility of synthesis in the compositions liable to exothermic reactions by shock-wave action and the influence of the synthesis initiation method on the structure and properties of final products are actual tasks [2].

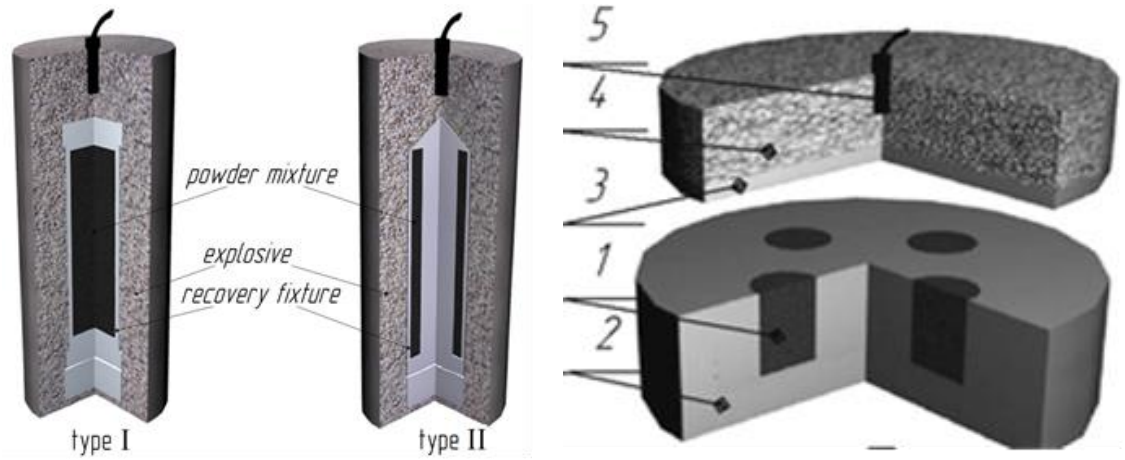

A B

Fig. 1 - Geometries of shock compaction; A - in cylindrical recovery fixtures; B - throwing a flat impactor (1 - powder mixture, 2 - matrix, 3 - impactor, 4 - BB, 5 - detonator)

The essential role of the activating additives (Al, Ti, B) to initiate, pass a chemical reaction in the powder mixture and the final phase formation is experimentally shown. Under similar conditions, a two-phase mixture of Me + fluoropolymer did not react.

Reaction is most intensively initiated in the lower part of cylindrical recovery fixtures fig. 1a. In this zone, a passing shock wave is reflected from as a compression wave and a sharp increase in pressure is observed. This is accompanied by an increase in the rate of chemical transformations.

In the presence of boron in the parent powder, the reaction of the metal with boron is seen to be superior to that of the metal and carbon. A greater amount of carbon from the fluoropolymer goes to the formation of TiC in the presence of titanium in the initial charge. For example, reaction of Ti+C has advantage over reaction of W+C. Fluorine from fluoropolymer is spent for formation of AlF_3 [3].

Powder mixtures based of mix (Ni-Al) and also Ti and Hf with additives of boron are easier initiated and most fully react (without the rest of initial metal) at the impactor's throwing according to the scheme fig. 1b

The reported study was funded by RFBR according to the research project № 16-03-00777 a.

REFERENCES

[1] Explosive treatment of metal-polymeric compositions, N.A. Adamenko, A.V. Fetisov, A.V. Kazurov, VolGTU Publ., Volgograd, 2007, p.251.

[2] M.I. Alymov, L.B. Pervukhin, A. S. Rogachev, O.L. Pervukhina, I.V. Saikov I, Letters on Materials, 4, 2014, pp. 153-158

[3] M. I. Alymov, S. G. Vadchenko, I. V. Saikov, and I. D. Kovalev, Inorganic Materials: Applied Research, 2, 2017, pp. 340–343.

MORPHOLOGICAL AND METALLOGRAPHIC ANALYSIS OF METALLIC POWDERS PRODUCED BY THE METHOD OF HYDRO-VACUUM DISPERSION OF MELTS

D. Sakhvadze[1*], G. Jandieri[2], I. Bolqvadze[3], A. Shteinberg[4], T. Tsirekidze[5]

[1] G-Metall LLC, Tbilisi, Georgia
[2] Metallurgical Engineering and Consulting LTD, Tbilisi, Georgia
[3] G-Metall LLC, Tbilisi, Georgia
[4] ALOFT, Chem. Eng. and Mater. Sci. Consulting Inc., Berkeley, California, USA,
[5] Iteda LTD, Tbilisi, Georgia
* david.sakhvadze@yahoo.com

Among numerous techniques for melt dispersion, the method of hydro-vacuum suction of a molten metal using an apparatus for producing metallic powders from a melt [1] deserves special attention. In this apparatus, water moving in the closed loop channels generates vacuum, which is used to disperse the melt. The product in the form of metal powder is removed from the active zone with the same water [2]. In this case, the particle structure formation occurs under the conditions of rapid quenching which requires attaining a certain degree of supercooling below the temperature, at which the free energies of the homogenous liquid phase and the oversaturated liquid phase are equal [3].

The supercooling degree should be such as the latent heat of crystallization released during the formation of a new phase propagates with the rate lower than that of the cooling of the melt film, which prevents heating of the solid and liquid phases. In this case, a metastable structure forms in the thin layer of the crystallizing metal while the solid metastable phases do not disintegrate [4].

The shape, size and structure of powder particles are the main characteristics determining the technological properties of metallic powders. Formation of particles of certain size and dispersity from melts depends on numerous parameters. The most important of them is the gravity acting on the drops of melt produced by the action of a high-pressure water jet on a liquid metal flow.

The mechanism of melt dispersion by the method of hydro-vacuum suction of molten metal is principally different from the mechanism of melt dispersion by a high-pressure water jet. For the dispersion, such properties of the meal as its viscosity, surface tension and density are the most important. Viscosity is generally determined by the strength of the atomic bonding and the density of atomic packing, while surface tension characterizes the work of formation of the physical surface of phases per surface unit. At the initial stage of formation during dispersion, the drops are generally of irregular shape and tend to be spherically shaped due to the action of the surface tension force. However this tendency may not be realized if they quickly harden. Therefore, if the drop balling time is less than the time of its hardening, the drop will be spherically shaped; otherwise solid particles of irregular shape will form [5].

At the hydro-vacuum suction, from the moment the melt flow gets into the inlet box, where it is surrounded by a circular high-pressure water flow, intensive vaporization takes place due to a significant difference in the temperatures of the melt and water. The produced vapor is removed from the working area with the rate of the supplied water flow. The water pressure is 12 kg/cm^2, while the vacuum amount at the entrance of the inlet part of the sucker is 0.9 kg/cm^2. The

intensive vapor suction conditions creates a difference in the relative rates between the vapor and surface of the sucked melt, which causes the destruction of the jet surrounded by the high-pressure water flow. It is very important that under these conditions, the forming drops of melt are in the state close to weightlessness. Before getting into the cooling medium, the jet of melt goes up due to the force of vacuum and no gravitational force affects the particles at the moment of crystallization. This is proved by a special morphology of the particles and a high specific surface area of the produced powders (Fig. 1). Fig. 1 shows the view of powder particles produced by the method of high-vacuum suction of melts. As can be seen, regardless of the material type the powder particles have a developed surface and low thickness. It should be noted that the shapes of the particles for different disperse compositions of the powders are almost identical.

1 2 3 4

Fig. 1. Morphology of metallic powders produced by the vacuum-suction method
1-aluminium and 2-iron, dispersity 1000-630 μm;
3-aluminium and 4- iron, dispersity 315-250 μm.

Some results of the metallographic characterization of the iron powder produced by the method of hydro-vacuum suction of molten cast iron are presented (Fig 2). The cast iron was melted in an induction furnace and fed to the sucker at melt temperature of 1480 ^{o}C. The chemical composition of the powder is $Fe_{tot.}$-93.14% (Fe_{comb}-89.27%), C-3.5%, Si-1.97%, Mn-0.72%, P-0.11%, S-0.09%, Cr-0.16%.

The analysis of the microstructure shows that even in the same powder batch the particles differ by structural and phase status. This phenomenon can be explained by a difference in the conditions of crystallization, mostly – essentially different temperature gradient and particles' cooling rate, a part of which is crystallized under conditions of direct thermodynamic action of water, another part being hardened in the water steam jacket.

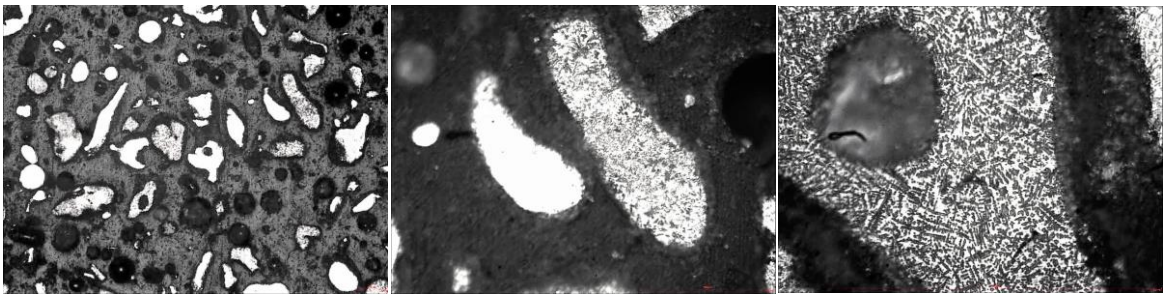

1 2 3

Fig. 2 - Microstructure of produced metallic powders at different magnification
1. x100; 2. x400; 3. x1000.

The experiments performed using aluminum powder under conditions of iron aluminothermy and copper cementation from solutions have proved the high reactivity of powders produced by the method of hydro-vacuum suction.

REFERENCES

[1] Patent GE P20156384 (B), B22F9/08. Device for producing metallic powder from melt // Sakhvadze D., Jandieri G., Tsirekidze T., Gorbenko I. Published 2015.10.12.

[2] Device of molten granulation for obtaining the powder materials for SHS. Sakhvadze D., Gorbenko I., Tsirekidze T., Jandieri G., Steinberg A. International symposium on self-propagating high-temperature synthesis. 10.10. 2015 Antalya, Turkey.

[3] Sally I.V. Crystallization at very high cooling rates. Kyiv, Naukova Dumka, 1972. -136 p.

[4] Kovalevskaya Z.G., Kovalevskiy E.A. Instigation of the structure of alloys based on iron produced at quenching from the melt. International Journal of Applied and Fundamental Research No. 11, 2014. - pp. 345-349.

[5] Kiparisov S.S, Libenson G.A. Powder Metallurgy. Metallurgy. Moscow, 1991 – 59 p.

70Cu–30Fe ALLOY BY SHS METALLYRGY AND THERMOMECHANICAL PROCESSING

V. V. Sanin*[1], M. R. Filonov[1], Yu. A. Anikin[1], D. M. Ikornikov[2], V. I. Yukhvid[2]

[1] National University of Science and Technology MISiS, Leninsky pr. 4, Moscow, 119049 Russia
[2] Institute of Structural Macrokinetics and Materials Science, Russian Academy of Sciences, Chernogolovka, Moscow, 142432 Russia
*sanin@misis.ru

Alloys with limited solibility in solids and liquids—such as Cu–Fe alloys—are difficult to fabricate by conventional methods [1]. These are normally produced by melting in microgravity, melting in crossed electromagnetic fields, mechanical intermixing of melts, mechanical alloying, and other techniques that are unprofitable and yield largely inhomogeneous products.
In this work, we fabricated 70Cu–30Fe alloys in a two-stage process involving: (**a**) metallothermic SHS of cast ingots under artifcial gravity and (**b**) subsequent pull-type forging at 850°C followed by cold drawing. The alloy under consideration may find its application in designing magnetically hard materials [2].

Combustion synthesis (stage **a**) was conducted in the centrifugal machine desribed elsewhere [3] for $n = a/g = 2 –50$, where a is the centrigugal acceleration and g the accelerationofgravity. The main process parameters as a function of a/g are presented in Fig. 1.

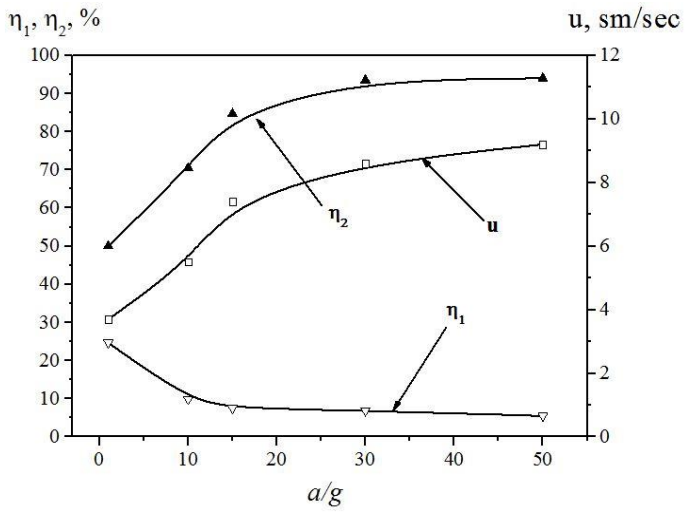

Fig. 1 - Burning velocity u, material loss η_1, and yield of cast alloy η_2 as a function of a/g.

As follows from Fig. 2, the SHS-produced alloy exhibits an heirarchical three-level structure. The first level (Figs. 2a, a') can be characterized by uniform distribution of Fe grains (10–30 μm in size) over the entire ingot volume. At the second level (Figs. 2b, b', b'') we can discern the Cu particulates (0.5–4 μm) uniformly distributed within the Fe grains.

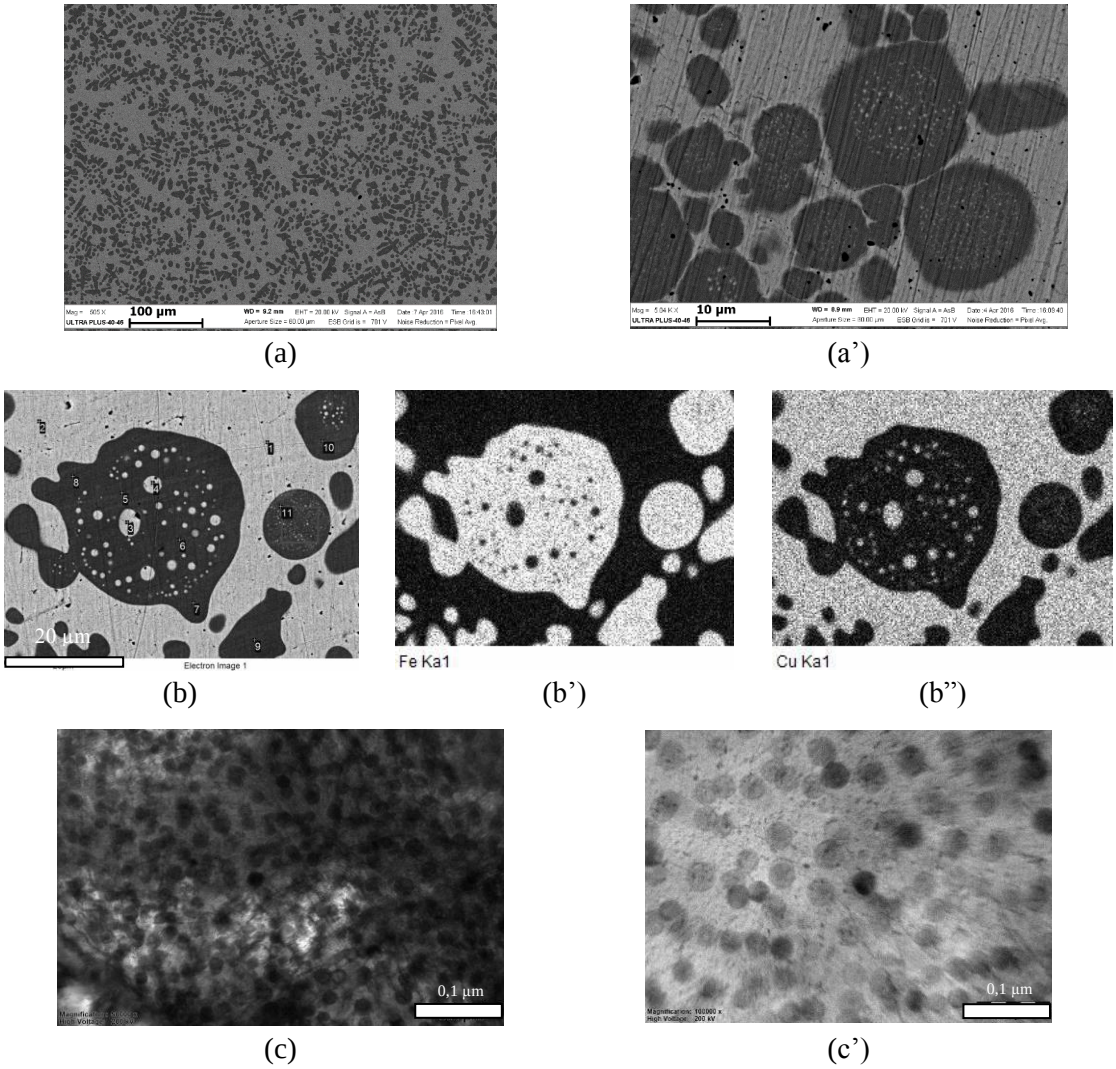

Fig. 2 - TEM/EDS results for SHS-produced 70Cu–30Fe alloy.

At still larger magnification (Figs. 2c, c'), we can discern the third structural level, that is, the submicron Fe particles (20–25 nm) uniformly distributed within a Cu matrix. Such a structure can be explained by specific conditions of SHS metallurgy. A high combustion temperature (above 2500 K) ensures the elevated solubility of Cu in Fe. Then, at the stage of crystallization, ever decreasing temperature facilitates the precipitation of Cu in the form of fine particles.

At stage **b**, SHS-produced ingots were warmed in furnace up to 850°C and subjected to pull-type forging to obtain 10-mm rods (their structure is shown in Fig. 3a) and then to cold drawing (v = 4.5 m/s, separation between draw plates 0.2 mm) to obtain a wire with a diameter of 4.5 mm (ε = 67%, Fig. 3b) or 3 mm (ε = 86%, Fig. 3c).

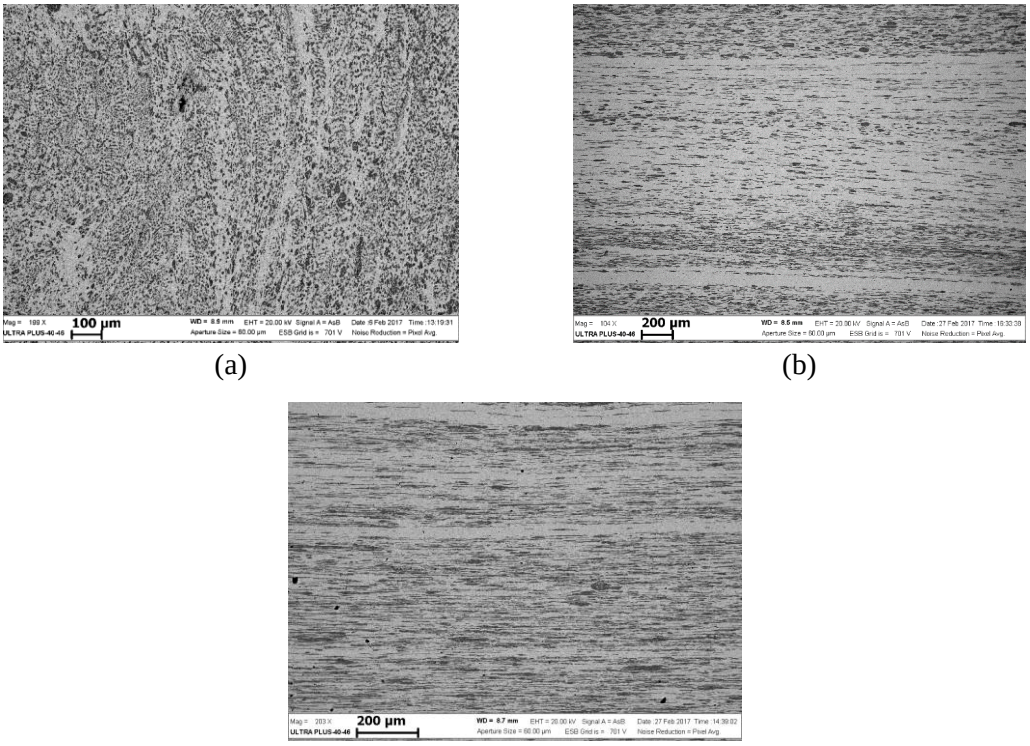

(a) (b)

(c)

Fig. 3 - Microstructure of material cross section after pull-type forging (a) and cold drawing to ε = 67 (b) and 86% (c).

Thermomechanical processing of SHS-produced Cu–Fe alloys can be readily used to regulate their structure and to fabricate bulk materials with longitudinally oriented structural constituents, which opens up new horizons for designing magnetic materials based on the systems with limited solubility.

REFERENCES

[1] Yu.S. Avraamov and A.D. Shalyapiun, Alloys with limited solubility in the liquid phase, Interkontakt Nauka, Moscow, 2002 (in Russ.).

[2] M.El. Ghannami, C. Gómez-Polo, G. Rivero, and A. Hernando, Europhys. Lett., 26, (1994) 701-706.

[3] V.N. Sanin, D.M. Ikornikov, D.E. Andreev, and V.I. Yukhvid, Russ. J. Non-Ferr. Met., 55, (2014) 613-619.

SHS OF CAST REFRACTORY ALLOYS FOR REPROCESSING INTO MICRO GRANULES USED IN 3D ADDITIVE TECHNOLOGIES

V.N. Sanin*[1], V.I. Yukhvid[1], D.E. Andreev[1], D.M. Ikornikov[1],
E.A. Levashov[2], Yu.S. Pogozhev[2]

[1] Institute of Structural Macrokinetics and Materials Science, Russian Academy of Sciences, Chernogolovka, Moscow, 142432 Russia
[2] National University of Science and Technology MISIS, Leninskii pr. 4, Moscow, 119049 Russia
* svn@ism.ac.ru

The necessity of improving the service parameters of modern materials for aerospace applications, power engineering, and chemical industry has given strong impetus to designing novel materials [1, 2], such as intermetallic alloys (IAs) [3, 4], metal-matrix eutectic composites (MMCs) based on refractory metals [5], and new multicomponent alloys termed high-entropy alloys (HEAs) [6–8]. A main difficulty in designing the above materials is high sensitivity of their phase composition to the presence of alloying agents, impurities, process parameters, structural imperfections (e.g. liquation phenomena), sinterability, and ductility. The fabrication of complicated items by conventional methods, including casting, machining, spark erosion, thermo-mechanical treatment etc., is a labor and material consuming process. A challenge here can be the so-called additive technology (AT). The most promising kind of AT is selective laser smelting whicht requires that starting materials be in the form of spherical granules (micro granules) with strictly defined size and morphology.

In this communication, we present some recent results on fabrication of micro granules by combined use of SHS metallurgy [9] and subsequent treatment including electrovacuum remelting into electrodes for centrifugal plasma sputtering (Fig. 1) or classification of SHS-produced composite powders and their spheritization (short-term plasma treatment) (Fig. 2).
In this communication, special emphasis will be made on the formation of micro granules during the combustion of thermite mixtures as reported previously for Ni–Al mixtures [10]. The preparation of HEA-based granules will be reported for the first time.

Process parameters for preparation of NiAl–(Cr, Co, Hf), TiAl–(Nb, Cr), Nb–NbC, Nb–NbSi, and HE alloys have been worked out and optimized, including (a) the roadmap for basic technological stages of SHS process, (b) formation of micro granular precursors and (c) comparative analysis of raw materials and micro granules. Typical results are exemplified in Figs. 1 and 2. The details will be discussed at presentation.

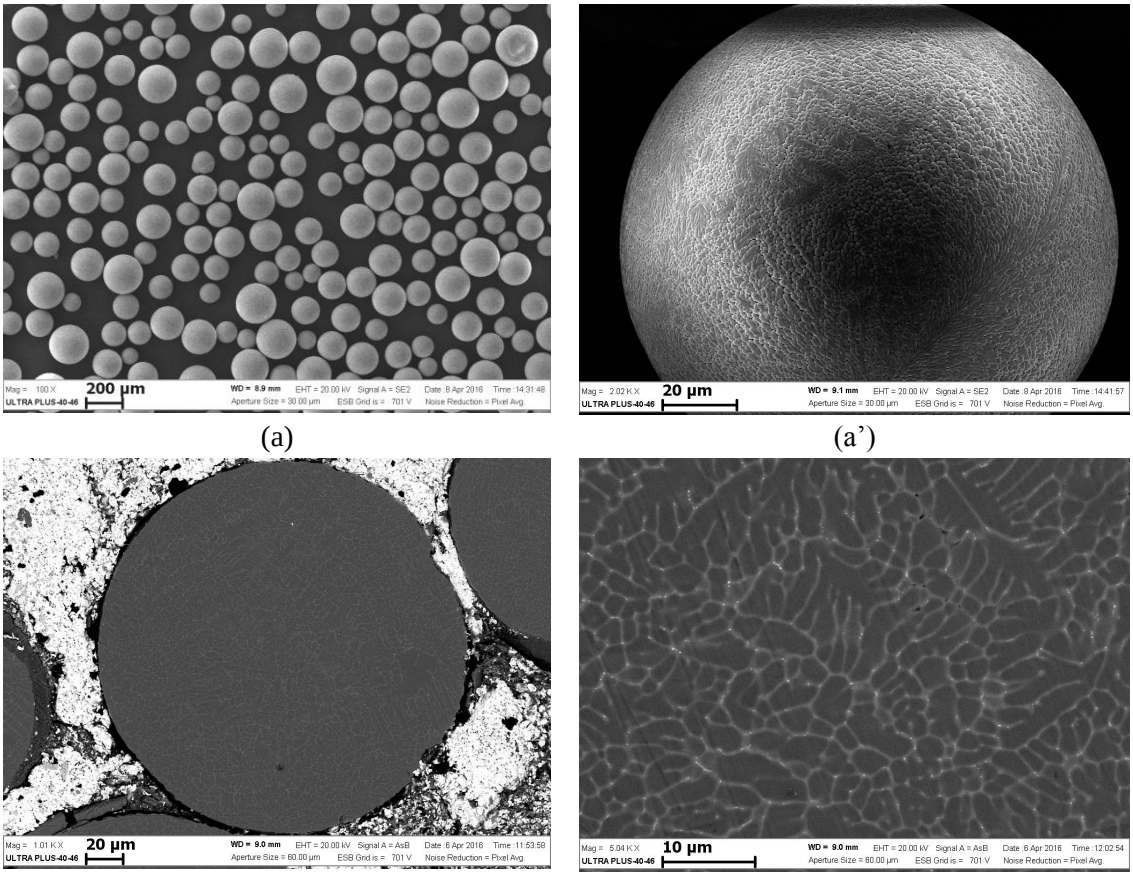

(a) (a’)

(b) (b’)

Fig. 1 - The overall view (a, a’) and microstructure (b, b’) of SHS-produced microgranular NiAl–(Cr–Co–Hf) precursors.

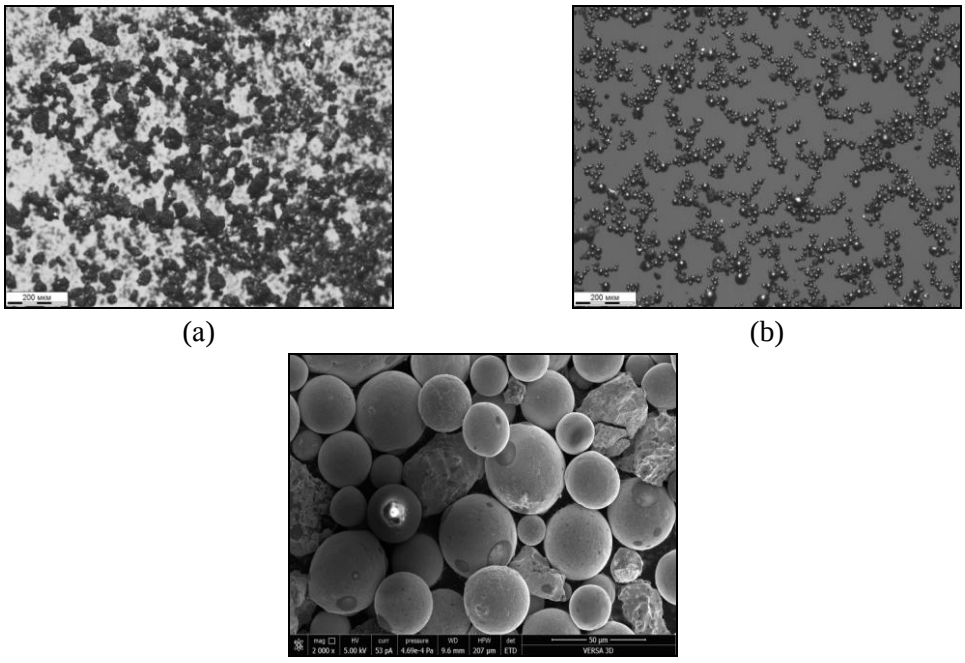

(a) (b)

(c)

Fig. 2 - The overall view SHS-produced Nb–NbC composite powders (a) and the powders after spheritization by short-term plasma treatment (b, c).

Thus the cast refractory alloys can be readily fabricated by centrifugal SHS. The process can be recommended for practical implementation in production of micro granules for AT. The present results can be expected to make a background for industrial-scale manufacturing of new micro granules by integrated technologies with valued service parameters.

This work was partially supported by the Russian Foundation for Basic Research (project no. 16-08-00398).

REFERENCES

[1] R. C. Reed, The Superalloys: Fundamentals and Applications, Cambridge University Press, Cambridge–New York, 2006.

[2] Askeland, D.R. and Phule, P.P., The Science and Engineering of Materials, Brooks & Cole Publ., Cengage Learning (USA), 2005.

[3] P. Jóźwik, W. Polkowski, Z. Bojar, Materials, 8, (2015) 2537–2568. doi 10.3390/ma8052537 .

[4] L.Y. Sheng, J.T. Guo, and H.Q. Ye, Mater. Design, 30, (2009) 964–969.

[5] R.J. Grylls, B.P. Bewlay, H.A. Lipsitt, and H.L. Fraser, Philos. Mag. A, 81, (2001) 1967–1978.

[6] D. Miracle, J. Miller, O. Senkov, C. Woodward, M. Uchic, and J. Tiley, Entropy, 16, (2014) 494–525. doi 10.3390/e16010494 .

[7] O.N. Senkov, G.B. Wilks, D.B. Miracle, C.P. Chuang, and P.K. Liaw, Intermetallics, 18, (2010) 1758–1765.

[8] F. Otto, A. Dlouhý, C. Somsen, H. Bei, G. Eggeler, and E.P. George, Acta Mater., 61, (2013) 5743–5755. https://doi.org/10.1016/j.actamat.2013.06.018

[9] V.N. Sanin, D.M. Ikornikov, D.E. Andreev, and V.I. Yukhvid, Russ. J. Non-Ferr. Met., 55, (2014) 613–619.

[10] D.M. Ikornikov, D.E. Andreev, V.N. Sanin, and V.I. Yukhvid, Int. J. Self-Propag. High-Temp. Synth., 20, (2011) 15–19.

COLD ROLLING OF SHS-PRODUCED CAST HIGH-ENTROPY ALLOYS Co–Cr–Fe–N–Mn–Al–C: EVOLUTION IN MICROSTRUCTURE AND MECHANICAL PROPERTIES

V.N. Sanin[1], D.M. Ikornikov[1], D.E. Andreev[1], V.I. Yukhvid[1],
N.D. Stepanov[2], S.V. Zherebtsov[2], G.A. Salishchev[2]

[1]Institute of Structural Macrokinetics and Materials Science, Russian Academy of Sciences, Chernogolovka, Moscow, 142432 Russia
[2]Belgorod State University, Belgorod, 308015 Russia

Multicomponent high-entropy alloys (HEAs) [1] attract the attention of researchers because of their novelty [2,3] and unique properties [2–4]. So the *fcc* Co–Cr–Fe–Ni–Mn alloy [5] exhibited high ductility at room and cryogenic temperatures [6] and record breaking fracture toughness at cryogenic temperatures [7]; but the yield strength of the alloy was rather low.

There have been many efforts to improve the properties of the CoCrFeNiMn alloy. It was found than the highest strength can be attained in the alloys with a fcc matrix strengthened with the particles of some another compound [8]. However, the design of precipitation-strengthened HEAs with optimal properties requires additional efforts.

One of possible candidates for precipitation strengthening is carbon whose presence can be expected to result in precipitation of carbide particles [9]. Many carbon-containing Co–Cr–Fe–Ni–Mn HEAs have already showed encouraging mechanical properties by combining high strength with good ductility. However, the effect of Al on deformation of the alloys has not been explored so far. Although similar studies on carbon effect are available, their results are highly controversial. Mechanisms of deformation and strengthening can be revealed by studying the evolution in microstructure and mechanical properties during cold working [25, 29].

In this work, we explored changes in the structure/properties of high entropy alloy $Al_{3.4}C_{0.7}Co_{22.3}Cr_{19.7}Fe_{22.9}Ni_{22.4}Mn_{8.6}$ during its cold rolling. The cast alloy was fabricated by metallothermic SHS from powder mixture of oxides (NiO, Cr_2O_3, Co_3O_4, Fe_2O_3, MnO_2) and Al as a reducing agent as described elsewhere [10]. Thus produced ingots were then used to prepare 10 × 10 mm bars for subsequent rolling at varied conditions. The chemical composition of the as-cast alloy is given in Table 1.

Table 1 - Chemical composition of $Al_{3.4}C_{0.7}Co_{22.3}Cr_{19.7}Fe_{22.9}Ni_{22.4}Mn_{8.6}$ alloy.

	Al	C	Co	Cr	Fe	Ni	Mn
At. %	3.37	0.69	22.35	19.67	22.85	22.44	8.62
Wt %	1.65	0.15	23.92	18.57	23.17	23.92	8.64

Some mechanical properties of rolled $Al_{3.4}C_{0.7}Co_{22.35}Cr_{19.7}Fe_{22.9}Ni_{22.4}Mn_{8.6}$ alloy—yield strength ($\sigma_{0.2}$), ultimate tensile strength (σ_{UTS}), uniform elongation (ε_u), and elongation to fracture (ε_f)—are characterized in Table 2.

Table 2 - Tensile properties of $Al_{3.4}C_{0.7}Co_{22.35}Cr_{19.7}Fe_{22.9}Ni_{22.4}Mn_{8.6}$ alloy at different stages of cold rolling.

	$\sigma_{0.2}$, MPa	σ_{UTS}, MPa	ε_u, %	ε_f, %			$\sigma_{0.2}$, MPa	σ_{UTS}, MPa	ε_u, %	ε_f, %
As-cast	210	455	74	80		Annealing at 700°C	870	1060	13	24
20% rolling	545	650	18	25		Annealing at 800°C	610	925	25	38
40% rolling	945	980	3.7	7	80% rolling	Annealing at 900°C	530	875	27	41
60% rolling	965	1140	2.3	5.4		Annealing at 1000°C	435	820	36	44
80% rolling	1310	1500	1.3	6.5		Annealing at 1100°C	320	760	40	47

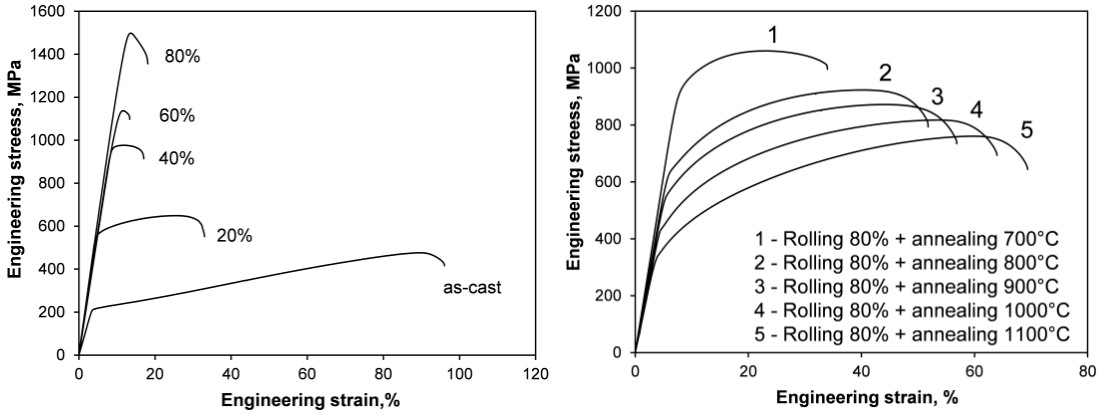

(a) (b)

Fig. 1 - Tensile stress–strain curves of $Al_{3.4}C_{0.7}Co_{22.35}Cr_{19.7}Fe_{22.9}Ni_{22.4}Mn_{8.6}$ after: (a) cold rolling with different thickness reductions and (b) after subsequent annealing at 700–1100°C for 1 h.

The stress–strain curves of the annealed $Al_{3.4}C_{0.7}Co_{22.35}Cr_{19.7}Fe_{22.9}Ni_{22.4}Mn_{8.6}$ alloy demonstrate (Fig. 1) that mechanical properties of the alloy can be further tailored by annealing treatment. Apparently, the alloy becomes softer and more ductile with increasing annealing temperature. For example, after annealing at 700°C the alloy still retains high strength: the yield strength and ultimate tensile strength have the values of 870 and 1060 MPa, respectively, at a reasonable ductility of 13 and 25%. An increase in the annealing temperature up to 900°C decreases the material strength, especially the yield strength (530 MPa).

It follows that the cast $Al_{3.4}C_{0.7}Co_{22.35}Cr_{19.7}Fe_{22.9}Ni_{22.4}Mn_{8.6}$ alloy can be readily fabricated by centrifugal SHS metallurgy in optimized conditions. The present results can be expected to make a background for industrial-scale manufacturing of new micro granules for use in integrated technologies.

The work partially was supported by the Russian Foundation for Basic Research (project no. 16-08-00398).

REFERENCES

[1] J.-W. Yeh, S.-K. Chen, S.-J. Lin, J.-Y. Gan, T.-S. Chin, T.-T. Shun, C.-H. Tsau, S.-Y. Chang, Adv. Eng. Mater. 6 (2004) 299–303. doi:10.1002/adem.200300567

[2] O.N. Senkov, G.B. Wilks, D.B. Miracle, C.P. Chuang, P.K. Liaw, Intermetallics 18 (9), 1758–1765.

[3] D.B. Miracle, J.D. Miller, O.N. Senkov, C. Woodward, M.D. Uchic, J. Tiley, Entropy, 16, 2014) 494–525 (25. doi:10.3390/e16010494

[4] O.N. Senkov, C. Woodward, D.B. Miracle, JOM, 66, (2014) 2030–2042. doi 10.1007/s11837-014-1066-0

[5] B. Cantor, I.T.H. Chang, P. Knight, A.J.B. Vincent, Mater. Sci. Eng. A, 375, (2004) 213–218. doi:10.1016/j.msea.2003.10.257

[6] F. Otto, A. Dlouhý, C. Somsen, H. Bei, G. Eggeler, E.P. George, Acta Mater., 61, (2013) 5743–5755. https://doi.org/10.1016/j.actamat.2013.06.018

[7] B. Gludovatz, A. Hohenwarter, D. Catoor, E.H. Chang, E.P. George, R.O. Ritchie, Science, 345, (2014) 1153–1158. doi 10.1126/science.1254581

[8] J.Y.Y. He, H. Wang, H.L.L. Huang, X.D.D. Xu, M.W.W. Chen, Y. Wu, X.J.J. Liu, T.G.G. Nieh, K. An, Z.P.P. Lu, Acta Mater., 102, (2016) 187–196. doi 10.1016/j.actamat.2015.08.076

[9] N.D. Stepanov, N.Y. Yurchenko, M.A. Tikhonovsky, G.A. Salishchev, J. Alloys Comp., 687, (2016) 59–71. doi 10.1016/j.jallcom.2016.06.103

[10] V.N. Sanin, D.M. Ikornikov, D.E. Andreev, and V.I. Yukhvid, Russ. J. Non-Ferr. Met., 55, (2014) 613–619.

SHS-PRODUCED CAST Ni–Cr–W ALLOY: STRUCTURAL CHARACTERIZATION AND MECHANICAL PROPERTIES

Yu.R. Kolobov[1,2], S.S. Manokhin[1,2], Yu.E. Kudymova[1,2], D.N. Klimenko[1,2], V.N. Sanin*[,3], D.M. Ikornikov[3], D.E. Andreev[3]

[1] State Research University, Belgorod, Russia
[2] Institute for Problems in Chemical Physics, Russian Academy of Sciences, Chernogolovka, Russia
[3] Institute of Structural Macrokinetics and Materials Science, Russian Academy of Sciences, Chernogolovka, Russia
*svn@ism.ac.ru

Due to wide use of heat-resistant Ni–Cr–W alloys in power engineering, aerospace industry, and related areas, there is the everlasting search of new methods for their production, including the technique of SHS metallurgy, also known as metallothermic SHS [1].

This work aimed at comparative analysis of commercial Ni–Cr–W alloy (VZh98 brand, see Table 1) with similar SHS-produced alloys.

Table 1 - Elemental composition of VZh98 alloy (GOST 5632-72).

Ni	Cr	W	Fe	Ti	Al	Mn	C	Si
Base	23.5–26.5	13–16	<4	0.3–0.7	<0.5	<0.5	<0.1	<0.8

Our Ni–Cr–W alloy was prepared from the mixture of commercially available nickel, chromium, tungsten oxides (mean particle size below 100 μm) in the absence/presence of added carbon black. Combustion was carried out in a centrifugal machine as described elsewhere [1, 2].

The SEM images in Fig. 1 suggest that our alloy represents a Ni-based solid solution. No contamination with carbon from a graphite cartridge was observed, as well as any change in the phase composition of resultant alloy. Also, we did not detect any precipitates based on W and Cr.

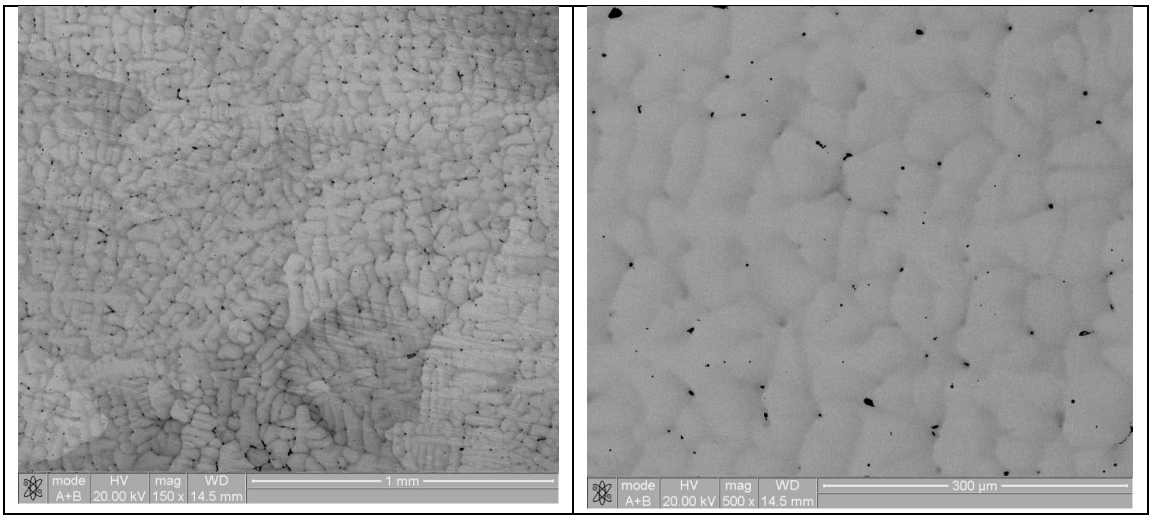

Fig. 1 - The outer surface of SHS-produced alloy.

Figure 2 illustrates the effect of carbon black added in an amount of 0.1 wt %. Within the grid, we detected elevated concentrations of W and Cr. The precipitates are seen to be uniformly distributed over the entire sample volume. The mechanical properties of the alloys under study are chacterized in Table. 1.

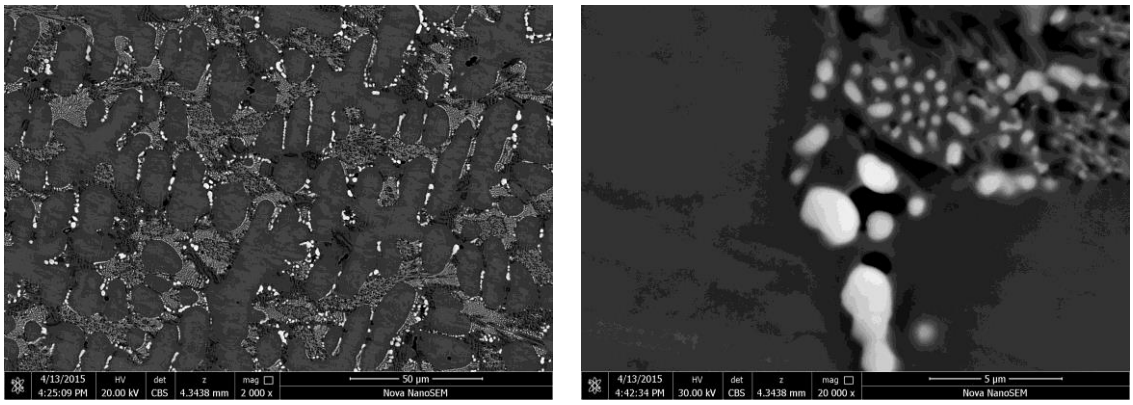

Fig. 2 - SEM images of SHS product alloyed with 0.1 wt % C.

Table 2 -Mechanical properties of the alloys.

	H_v at 20°C	Loading ($10\ s^{-1}$) at 1000°C	
		$\sigma_{0.2}$, MPa	σ_{cr}, MPa
Commercial alloy (VZh98)	200	20	50
SHS product not alloyed with C	190	90	120
SHS product alloyed with 0.1 wt % C	260	120	145

As follows from Table 2, the SHS product alloyed with 0.1 wt % C takes advantage over the commercial alloy in its strength characteristics. The effect of strengthening can be assigned to the presence of the carbide phase that hampers the motion of dislocations and the process of grain boundary sliding. The resistance to deformation increases due to the formation of the dendrite phase in SHS-produced alloy (Fig. 1).

Thus the fabrication of heat-resistant alloys by metallothermic SHS can be regarded as rather promising.

The work partially was supported by the Russian Foundation for Basic Research (project no. 16-08-00398).

REFERENCES

[1] V.N. Sanin, D.M. Ikornikov, D.E. Andreev, and V.I. Yukhvid, Russ. J. Non-Ferr. Met., 55, (2014) 613–619.

[2] V.N. Sanin, D.M. Ikornikov, N.V. Sachkova, V.I. Yukhvid, Complex boride metal-matrix composites by SHS under high gravity, Int. J. Self-Propag. High-Temp. Synth., 23, (2014) 151-160. doi 10.3103/S1061386214030091

EXPERIENCE IN TESTING OF HIGH-TEMPERATURE MATERIALS FOR VARIOUS COMPONENTS OF METALLURGICAL UNITS AT ENTERPRISES OF KAZAKHSTAN

Doctor of Technical Sciences Satbayev B.N., Doctor of Technical Sciences Koketayev A.I., Shalabayev N.T., Satbayev A.B.

Astana branch of the Republican State Enterprise "National Center on Complex Processing of Mineral Raw Materials of the Republic of Kazakhstan" over the past few years, with the support of the largest in Kazakhstan metallurgical plant of "ArcelorMittal Temirtau" JSC, carried out works to develop and implement the developed refractory materials based on SHS technology.

The principal difference between these refractories is the content of the active chemical mixture in their composition, which, when heated, interacts with the remaining components of the charge in the self-baking regime. In this case, the refractory body is synthesized with the formation of refractory oxides, which leads to an improvement in the quality of the material.

It should be noted that materials prepared for testing are unshaped refractory masses and are created on the basis of self-baking high temperature technology (SHS) and are used for lining highly aggressive zones of metallurgical aggregates of ferrous and non-ferrous metallurgy, cement kilns, energy boilers and chemical industry.

During the pilot-industrial tests, high-temperature materials for the following units of metallurgical aggregates were investigated:

1. Exothermic mixture for warming of the cast iron mirror of cast iron ladles;
2. High-alumina gutter mass for the main gutters of blast-furnace production;
3. High-alumina concrete mixture for lining the shelters (covers) of the aspiration system of the main troughs of blast furnaces;
4. The airborne anhydrous mass based on quartzite and silicon carbide, designed to close the blast hole of the blast furnace.

At "ArcelorMittal Temirtau" JSC there was a problem of overgrowing cast-iron ladles with the formation in the neck of the "roof", which complicated the discharge of cast iron in the mixer compartment of the converter shop, both in the mixer and in the cast iron ladle. This problem is especially aggravated in the winter period and in cases of unstable iron removal by the converter shop. Tare-bucket due to "skull formation" is growing, capacity is decreasing. We have to cut off the "roofs", burn holes for casting and draining cast iron. The sprinkling of a cast iron mirror in the ladle with a fine coke, vermiculite did not solve the cardinally existing problem.

To solve this problem, we developed an exothermic mixture for warming the cast iron mirror in cast iron ladles in order to reduce heat losses during the transportation of pig iron to the converter shop.

In addition, "ArcelorMittal Temirtau" JSC offered high alumina grooved masses for lining the main blast furnace. Experimental-industrial tests showed that the tested mass is not inferior in its characteristics to the masses supplied by the world's leading companies, and exceeds the duration of work by at least 10%. At the same time, the cost of mass is lower than that purchased by the metallurgical plant.

At the request of the employees of the Blast Furnace Shop of "ArcelorMittal Temirtau" JSC, a "High-alumina concrete mixture for the lining of shelters (covers) of the aspiration system of the main blast furnaces of blast furnaces" was proposed.

So, previously used mass for gutter covers, purchased from foreign companies, served from 10 to 30 days. Because of sudden temperature changes, the refractory material was destroyed, the mass disintegrated and the lid came into disrepair, which required re-lining it.

The use of the high-alumina concrete mixture prepared on the basis of corundum with the use of silicon carbide (the mass share of SiC in the finished product is within 7-10%) and the hydraulic bond, as well as with the mass fraction of Al_2O_3 of not less than 80%, allowed us to increase the resistance on medium covers without repair up to 60 days, the durability of the manipulator cover was 30 days.

At many metallurgical enterprises, there is a problem associated with the opening and closing of the air hole, from where the metal is discharged from the furnace. A similar problem exists at "ArcelorMittal Temirtau" JSC.

For these purposes, an airless anhydrous mass based on quartzite and silicon carbide was developed to close the blast hole of the blast furnace. Tests of the proposed flyweight showed a decrease in the consumption of borax and oxygen tubes, the length of the canal channel remained constant, with the release of the smelting products, the jet flowed smoothly, without splashing, the cast iron and slag were dispensed in full.

In general, conducted pilot-industrial tests of refractories developed in the AF RGP "NCMDS RK" showed good production and technical properties at "ArcelorMittal Temirtau" JSC. The results of these tests make it possible to draw a conclusion about the correctness of the chosen research direction, to develop other compositions of refractory materials for various types of thermal aggregates of ferrous and non-ferrous metallurgy, cement-kiln furnaces, energy boilers, chemical industry, etc.

QUASI-PERIODIC MATERIALS – A PARADIGM SHIFT IN CRYSTALLOGRAPHY

D. Shechtman

Technion, Haifa, Israel and
ISU, Ames, Iowa, USA

Crystallography has been one of the mature sciences. Over the years, the modern science of crystallography that started by experimenting with x-ray diffraction from crystals in 1912, has developed a major paradigm – that all crystals are ordered and periodic. Indeed, this was the basis for the definition of "crystal" in textbooks of crystallography and x-ray diffraction. Based upon a vast number of experimental data, constantly improving research tools, and deepening theoretical understanding of the structure of crystalline materials no revolution was anticipated in our understanding the atomic order of solids.

However, such revolution did happen with the discovery of the Icosahedral phase, the first quasi-periodic crystal (QC) in 1982, and its announcement in 1984. QCs are ordered materials, but their atomic order is quasiperiodic rather than periodic, enabling formation of crystal symmetries, such as icosahedral symmetry, which cannot exist in periodic materials. The discovery created deep cracks in this paradigm, but the acceptance by the crystallographers' community of the new class of ordered crystals did not happen in one day. In fact it took almost a decade for QC order to be accepted by most crystallographers. The official stamp of approval came in a form of a new definition of "Crystal" by the International Union of Crystallographers. The paradigm that all crystals are periodic has thus been changed. It is clear now that although most crystals are ordered and periodic, a good number of them are ordered and quasi-periodic.

While believers and nonbelievers were debating, a large volume of experimental and theoretical studies was published, a result of a relentless effort of many groups around the world. Quasi-periodic materials have developed into an exciting interdisciplinary science.

This talk will outline the discovery of QCs and describe the important role of electron microscopy as an enabling discovery tool.

METALLIC GLASSES $Cu_{50}Ti_{50}$ BY MECHANICAL ALLOYING AND THEIR HEAT-INDUCED STRUCTURAL TRANSFORMATIONS

N.F. Shkodich*[1,2], A.S. Rogachev[1,2], S.G. Vadchenko[1], D.Yu. Kovalev[1], A.A. Nepapushev[2], I.D. Kovalev[1]

[1]Institute of Structural Macrokinetics and Materials Science, Russian Academy of Sciences, Chernogolovka, Russia
[2]National University of Science and Technology MISiS, Moscow, Russia
* N.F.Shkodich@mail.ru

Amorphous alloys, or metallic glasses, are a relatively new class of materials with a specific combination of technologically interesting properties. These materials are characterized by the absence of a regular crystal structure (short-range ordering). Such a structural configuration ensures a unique combination of properties that cannot be attained in crystalline materials, such as high mechanical strength, corrosion/radiation resistance, and specific electric/magnetic properties [1]. It explains ever growing interest in studies on the formation of amorphous structures and their crystallization and on industrial-scale implementation of amorphous materials. Metallic glasses can be produced in several routes such as solid-state reaction, mechanical alloying (MA), fast quenching, etc. [2–4]. Compared to other conventional techniques, MA has an advantage that (a) amorphous alloys can be obtained at temperatures much below the crystallization temperature of its constituents and (b) structural changes may happen during the amorphization reaction.

In this work, we explored the formation of amorphous Cu–Ti alloy during high-energy ball milling (HEBM, τ = 1–30 min) and subsequent crystallization. Powder mixtures with a composition of $Cu_{50}Ti_{50}$ were prepared using the elemental powders of Cu (PMS-B brand, d < 45 μm, 99.5% pure) and Ti (PM brand, d = 2.0–4.5 μm, 99.95% pure). Starting and milled powder mixtures were characterized by XRD, electron diffraction, high-resolution SEM/EDS, and high-resolution TEM. Thermal stability and the amorphous–crystalline transition in Cu–Ti metallic glasses were analyzed by differential scanning calorimetry (DSC) and time-resolved X-ray diffraction (TRXRD).

During HEBM processing, the structure of the initial powder mixture undergoes a substantial evolution. According to the SEM data, a set of randomly distributed particles of starting Cu–Ti powder mixture was found to form a layered structure during first minutes of mechanical treatment. With increasing milling time, the layer thickness decreases. After 20 min of mechanical treatment, the formation of a relatively uniform amorphous Cu–Ti structure was observed. While unprocessed Cu–Ti mixtures exhibited strong and narrow diffraction peaks of Cu and Ti, the HEBM resulted in gradual broadening of the diffraction peaks accompanied by a decrease in their intensity. Solid-state amorphization of $Cu_{50}Ti_{50}$ alloy powder was achieved at τ = 20 min (~93% of amorphous phase). HR TEM images of amorphous Cu–Ti powders suggest that the material consists of amorphous matrix with a small admixture of nanocrystalline (2–8 nm) inclusions. The DSC results for mechanically amorphized $Cu_{50}Ti_{50}$ alloys have revealed the occurrence of heat evolution from the amorphous–crystalline phase transformation, up to 80 J/g (8.9 kJ/mol) in the temperature range 336–369°C.

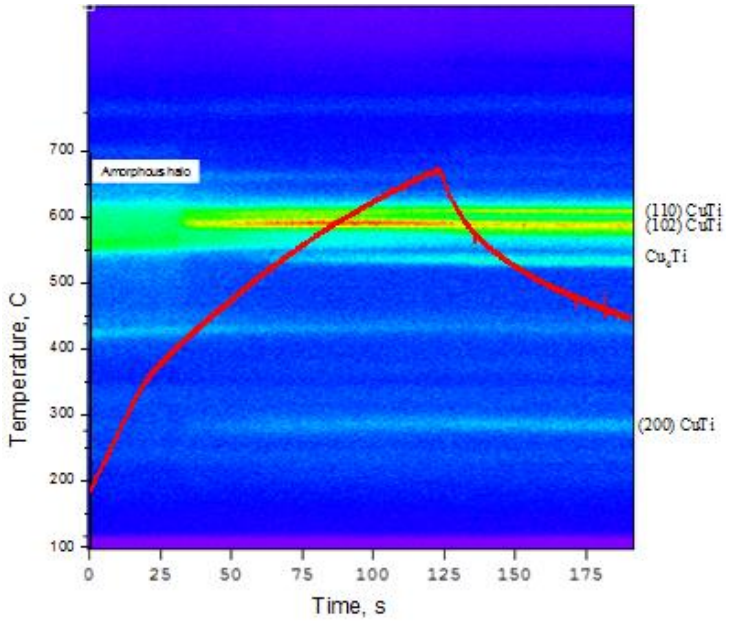

Fig.1 - Time-resolved XRD patterns for mechanically amorphized $Cu_{50}Ti_{50}$ alloy.

TRXRD results for the amorphous to crystalline phase transformation during heating under helium have shown (Fig. 1) that the crystallization of the HEBM $Cu_{50}Ti_{50}$ alloy gets started around 400°C, i.e. much below the temperature of the eutectic formation in the Cu–Ti system (875°C) and accomplished in 10–15 min without melting.

The diffraction pattern of the initial alloy exhibited a wide halo and high background level. The amorphous-crystalline transition during heating occurred gradually: the background noise decreased, whereas three diffraction peaks corresponding to (110), (102), and (200) lines of the γ-CuTi phase (tetragonal, *P*4/*nmm*) gradually appeared. At 500°C, a diffraction peak of the Cu_4Ti phase was observed, thus indicating an incomplete amorphization of Cu–Ti powder mixture during HEBM. Based on the duration of the γ-TiCu diffraction peaks formation, we can assume a diffusion mechanism for the amorphous–crystalline transition HEBM-produced Cu–Ti alloy.

Our results may turn useful for some technological applications and in designing amorphous bulk materials with unique properties.

This work was financially supported by the Russian Science Foundation (project no. 16-13-10431: Self-sustaining thermal waves in amorphous media).

REFERENCES

[1] M. Davidson, S. Roberts, G. Castro, R.P. Dillon, A. Kunz, H. Kozachkov, M.D. Demetriou, W.L. Johnson, S. Nutt, D.C. Hofmann, Adv. Eng. Mater., 15, (2013) 27-33.

[2] N.F. Shkodich, A.S. Rogachev, S.G. Vadchenko, D.O. Moskovskikh, N.V. Sachkova, S. Rouvimov, A.S. Mukasyan, J. Alloys Comp., 617, (2014) 39-46.

[3] E. Pineda, P. Bruna, B. Ruta, M. Gonzalez Silveira, D. Crespo, Acta Mater., 61, (2013) 3002–3011.

[4] K. Brunelli, M. Dabala, R. Frattini, G. Sandona, I. Calliari, J. Alloys Comp., 317-318, (2001) 595-602.

SHS IN SURFACE ENGINEERING

D.V. Shtansky, E.A. Levashov, Ph.V. Kiryukhantsev-Korneev, K.A. Kuptsov, A.N. Sheveyko

National University of Science and Technology "MISIS", Moscow 119049, Russia
shtansky@shs.misis.ru

Utilization of SHS in surface engineering is rapidly growing field. The heat released during SHS is useful in terms of providing high adhesion strength between coating and substrate. The surface treatment process which combines SHS and coating deposition is referred as **SHS coating**. The process can be subdivided according to the method of coating deposition, type of precursor materials, type of external heat source to initiate combustion reaction, as well as the densification method used for synthesized products [1].

In the field of surface engineering, SHS is frequently combined with other methods such as centrifugation, microwave and induction heating, laser cladding, sol–gel, concentrated solar energy treatment, high velocity oxy-fuel thermal spraying, reactive and atmospheric plasma spraying, plasma transferred arc overlay welding, and electroless plating. Various metallic, ceramics, metal matrix composite, steel matrix composite, and ceramic matrix composite coatings were fabricated. There are two main routes of coating deposition which may be classified as SHS: (i) a mixture of exothermically reactive powders or a cold pressed product is applied to the substrate surface as a precursor and then ignited by an external energy source and (ii) SHS-derived powders, targets or electrodes were fabricated separately and then used in coating deposition technologies such as plasma spraying, magnetron and ion sputtering, electro-spark deposition, and electroless plating. The first route is often referred to as an in situ or single step process because both processes, namely SHS and coating deposition, occur simultaneously.

The possibilities of various physical vapor deposition (PVD) technologies can be extended through the application of SHS targets and electrodes. Coatings with an improved combination of properties can also be produced through non-vacuum methods, for example by pulsed electrospark deposition (PED), using electrodes fabricated by SHS. The method utilizes an exothermic reaction initiated by an electric discharge within an inter-electrode space.

Recently, newly designed deposition equipment which combines PED and PVD techniques was employed. The PVD part of the deposition unit has two modules: magnetron sputtering and cathodic arc evaporation. The bottom layer, which is expected to provide superior adhesion strength and high mechanical properties, can be fabricated by means of computer controlled PED in air, argon atmosphere (1 atm), or vacuum (10 Pa). The top layer with high tribological properties can be deposited using either magnetron sputtering or cathodic arc evaporation. Using the deposition facility described above, TiNbCN and TiCNiAl coatings were fabricated and studied. The two-layered PED-PVD TiNbCN coatings showed higher dynamic impact resistance at a maximum applied load of 1000 N and better tribological properties (lower friction coefficient and wear rate) compared with the single layer PED TiNbC-binder counterparts. The two-layered PED-PVD TiCNiAl coatings were compared with single layer PED and PVD references coatings. Although the PED TiCNiAl coatings demonstrated high wear resistance during sliding and abrasion, they had relatively high friction coefficient, low hardness and poor corrosion resistance. In contrast, the single-layer PVD TiCNiAl coatings showed low friction coefficient, good mechanical properties, and high corrosion resistance, but

low wear resistance. In the two-layered PED-PVD TiCNiAl coatings, the PED sublayer acts as mechanical support, whereas the top PVD layer provided antifriction and anticorrosion characteristics (Fig. 1).

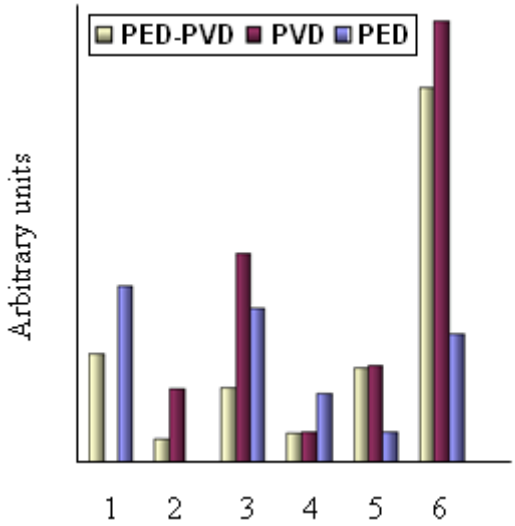

Fig. 1 - Coating characteristics. 1 - Corrosion current; 2 - abrasive wear, 3 - impact wear, 4 - friction coefficient, 5 - elastic recovery, 6 - hardness.

Finally, applications of SHS targets and electrodes to produce multifunctional coatings on the surface of various biomaterials are considered.

ACKNOWLEDGEMENTS

The authors gratefully acknowledge the financial support from the Russian Scientific Foundation (Agreement No.15-19-00203)

REFERENCES

[1] E.A. Levashov, A.S. Mukasyan, A.S. Rogachev, D.V. Shtansky, Int. Mater. Rev. 62(4) (2017) 203-239.

QUANTITATIVE 3-D RECONSTRUCTION OF REACTIVE NANOCOMPOSITES: EFFECT OF NANOSTRUCTURE ON ACTIVATION ENERGY

C. E. Shuck*[1], A. S. Mukasyan[1]

[1] University of Notre Dame, Notre Dame, IN 46556, United States of America
*cshuck@nd.edu

Reactive nanocomposites (RNCs) are a class of high energy density systems that are safe and can be rapidly converted into usable forms of energy. They are fully dense materials that contain all necessary reactants within individual chemical cells and can be utilized in any environment, including in vacuum or underwater. RNCs have been proposed for use as solid fuels, for energy storage, among numerous other energetic applications [1-3]. Additionally, RNCs are used for synthesis of many advanced and refractory materials through combustion synthesis (CS) approaches. CS has been shown to be a versatile material synthesis method, allowing for production of metals, ceramics, biological materials, and countless other advanced and functional materials [4].

Through use of High-Energy Ball Milling (HEBM), specifically Arrested Reactive Milling (ARM), oxygen free Ni/Al composite particles were prepared with a variety of HEBM times (See Figure 1). As the milling time is increased, up until the critical time, it is known that the internal nanostructure of the particles becomes more intermixed in thin tortuous lamellar structures. These structures have increased surface area contact and lower reactant diffusive distances [5]. It is well known that solid-phase reactivity is related to the surface area contact between the reactants [6]. However, to date, there has not been a statistically valid quantitative study on the relationship between the nanostructure, including diffusive distances and surface area contact, and the observed chemical kinetics. The goal of this work is to provide statistically proven quantitative data on the nanostructural characteristics of the HEBM-induced high energy density materials (HEDM), utilizing 3D reconstruction of the complete sample volume (Figure 2). Correlations of these nano-features with statistical, experimentally proven values of the HEDM chemical kinetics in the Ni-Al system are also investigated.

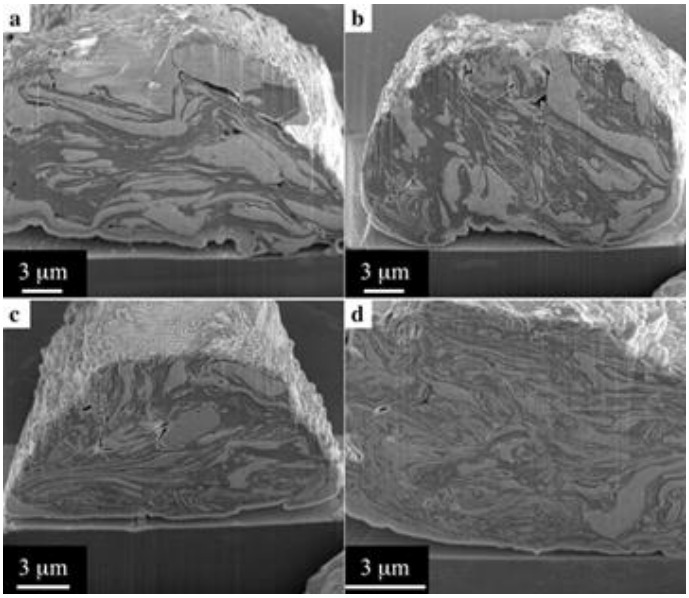

Figure 1 - HEBM-produced Ni/Al nanocomposite materials with a) 10, b) 20, c) 30, and d) 40-min milling times.

Experimental datasets from Ni/Al composite particles of each investigated HEBM time are collected using FIB-SEM ion beam milling, consisting of thousands of images for each analyzed particle, until statistical convergence is reached. Each dataset is digitized using 3D reconstruction software and analyzed using distance-ordered thinning algorithms, diffusive distance maps, and surface texture mapping. Using the 3D reconstructions, accurate analysis relating to diffusive layer thickness of both Ni and Al, surface area contact between reactants, along with a multitude of other nanostructural features can be determined [7].

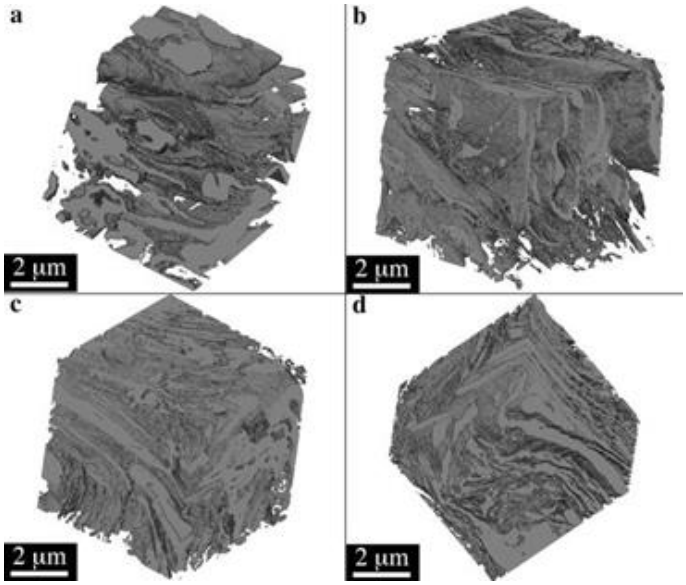

Figure 2 - Complete sample volume 3D reconstructions of the Ni/Al nanocomposite materials for the a) 10, b) 20, c) 30, and d) 40-min milling times.

To study the reaction kinetics, the electrothermal explosion method (ETE) was used to study the reaction kinetics. This technique utilizes rapid Joule-preheating until ignition. The resulting time-temperature profile is analyzed, allowing for the activation energy (E_a) and pre-exponential factor (k_0) to be extracted. Combining the quantitative nanostructural data, an accurate relationship was determined that relates E_a to the surface area contact (Figure 3). This, for the first time, shows that the reaction kinetics can be directly controlled through mechanical processing steps. Additionally, it gives insights into the fact that this is not a truly intrinsic activation energy, but is instead an effective activation energy (E_{ef}).

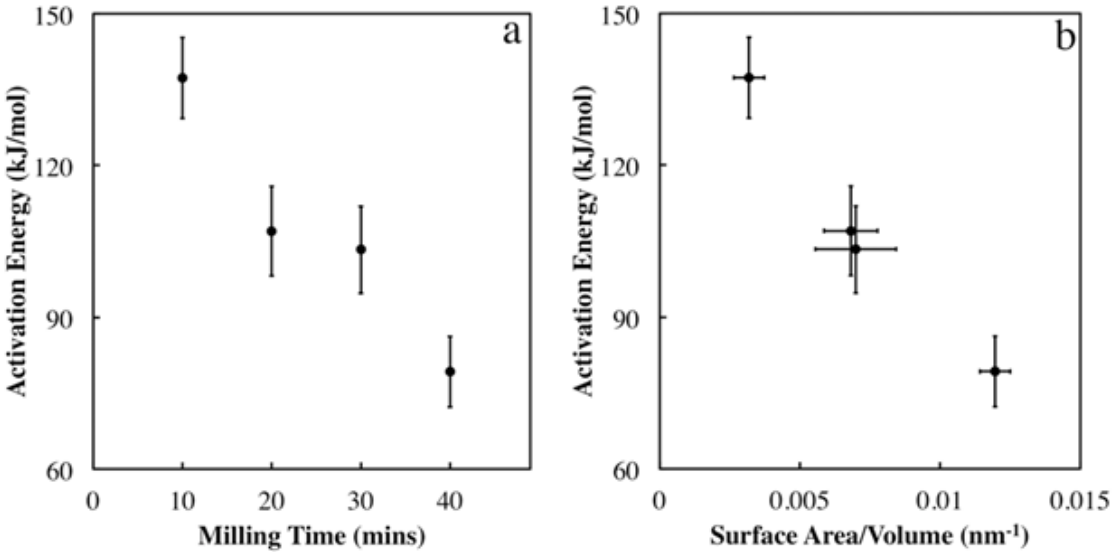

Figure 3 - Dependence of effective activation energy of the reaction as a function of milling time a) and specific contact surface area b) between Ni and Al phases.

Using this experimental correlation, it is possible to more fundamentally understand the reaction kinetics and the processes that contribute to them. Considering that in solid state reactions, namely all SHS reactions, there are two possible limiting steps for the reaction. The first is the diffusion rate and the second is the reaction rate. Using the extracted kinetic parameters, E_{ef} and k_0, in conjunction with the structural parameters, it is possible to understand the trends that are observed. Furthermore, this work highlights the importance of determining structural kinetics in relation to the observed kinetics, without proper understanding of the structure, correct interpretation of the data is impossible.

To further understand the chemical reaction process, a limiting case was examined. Using low-temperature in-situ TEM studies, the diffusive rate can be directly measured (Figure 4). By measuring the diffusive rate, without the influence of chemical reactions, the upper bound of possible E_{ef} can be determined in conjunction with the diffusive pre-exponential factor. This gives valuable insight into a process that is limited by two physical processes; by fully characterizing one of the limiting cases, a greater understanding of the relationship between E_{ef}, the intrinsic chemical reactivity, and the diffusion process. Additionally, this gives additional insight of the role temperature and nanostructure have on these processes. This greater understanding allows for complete characterization of the single-step approximation to chemical kinetics within SHS systems, which further provides the ability to determine the mechanisms that drive the chemical reactions.

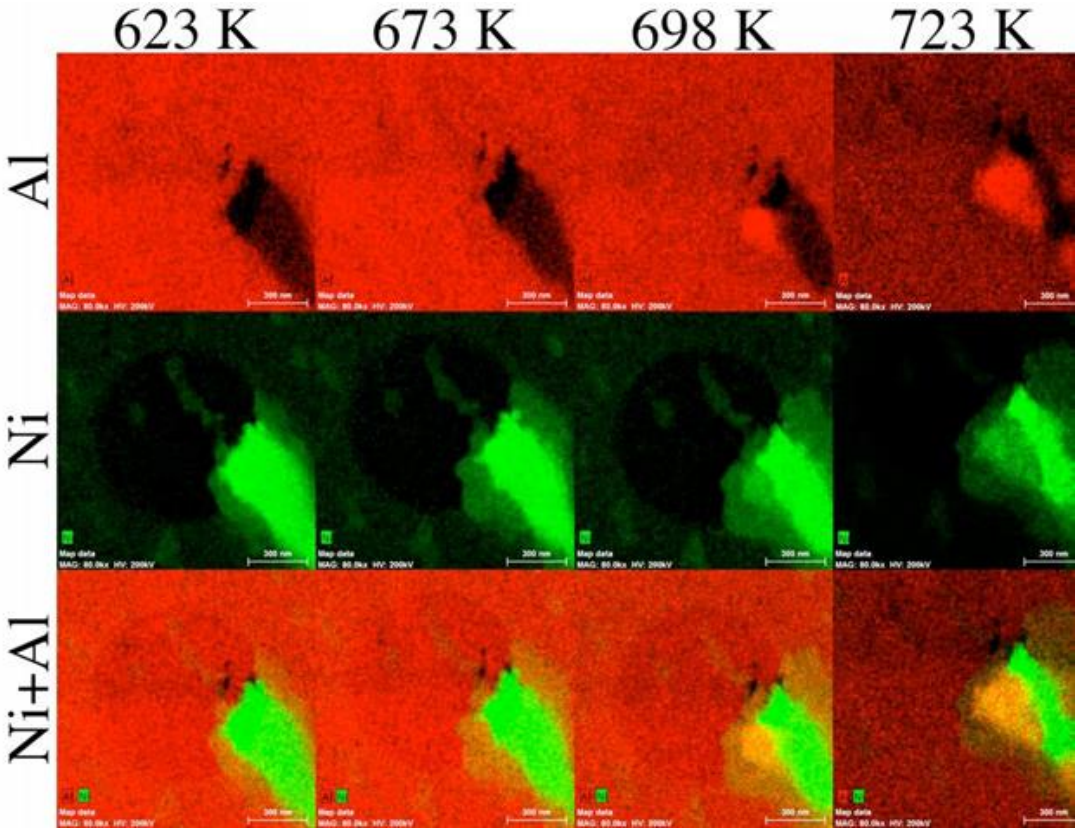

Figure 4 - Low-temperature in-situ TEM diffusion studies into the Ni/Al system.

REFERENCES

[1] E. L. Dreizin, Prog. Energy Combust. Sci., 35, (2009) 141−167.
[2] W. Choi, S. H. Hong, J. T. Abrahamson, et al., Nat. Mater., 9, (2010) 423−429.
[3] J. Baxter, Z. Bian, D. Danielson, et al., Energy Environ. Sci., 2, (2009) 559−588.
[4] S. T. Aruna and A. S. Mukasyan, Curr. Opin. Solid State Mater. Sci., 12, (2008) 44−50.
[5] C. E. Shuck, J. M. Pauls, and A. S. Mukasyan, J. Phys. Chem. C 120, (2016) 27066−27078.
[6] C. E. Shuck and A. S. Mukasyan, J. Phys. Chem. A 121, (2017) 1175-1181.
[7] C. E. Shuck, M. Frazee, A. Gillman, et al., J. Synchrotron Radiat., 23, (2016) 990−996.

SOLUTION COMBUSTION SYNTHESIS OF VANADIUM OXIDE BY GLISIN AND CITRIC ACID

E. Yilmaz*, B. Derin, O. Yucel, M. S. Sonmez

Department of Metallurgical and Materials Engineering, Istanbul Technical University, Sarıyer, 34469, Istanbul, Turkey
*esma.yilmaz@itu.edu.tr

Vanadium can take more than one valence and thus can form different oxide compounds. These oxides have different properties due to their different compositions. For example, VO_2 and $H_2VO_3O_8$ are used as an optical, electrical, electrochemical, thermochromic and thermal switch material. VO_2 has also different polymorphic forms, which can reveal stable and metastable phases. For instance, VO_2, which is a monoclinic metastable phase, is used as a cathode material especially in lithium ion batteries. Thin films of vanadium oxide (V_2O_5) are used in electrochromic and thermochromic devices, uncooled bolometric detectors, laser protection, solar cell windows, high-capacity lithium battery electrodes, electrical and optical switching devices, light modulators [1-2].

In this study, vanadium oxide nanoparticles were synthesised by solution combustion method. Glicyne ($C_2H_5NO_2$), citric acid ($C_6H_8O_7.H_2O$) and mixture of these two reactants were used as a fuel material during solution combustion synthesis (SCS), while ammonium meta-vanadate (NH_4VO_3) was used as an oxidant. The structure, morphology and chemical composition of the samples were characterized by using XRD and SEM & EDS methods. Surface area of synthesised particles were determined by BET analysis. The effect of different fuel materials on synthesised products were investigated.

REFERENCES

[1] Jagadeesh, A., Rattan, T. M., Muralikrishna, M., Venkataramaniah, K. 2014. ‘‘Instant one step synthesis of crystalline nano V_2O_5 by solution combustion method showing enhanced negative temperature coefficient of resistance’’, 121, 133-136.

[2] Kaid, M. A. 2006. ‘‘Characterization of electrochromic vanadium pentoxide thin films prepared by spray pyrolysis’’, J. Solids, 29, 273-291.

SOLUTION COMBUSTION SYNTHESIS OF TUNGSTEN TRIOXIDE

S.S. Kaplan, B. Derin, O. Yucel – M. S. Sonmez

Department of Metallurgical and Materials Engineering, Istanbul Technical University, Sarıyer, 34469, Istanbul, Turkey
* kaplans16@itu.edu.tr

Tungsten trioxide is used in wide range of applications. Due to its high coloration efficiency and high cyclic stability, it is a good candidate for thermochromic applications such as smart windows, antiglare mirrors, high contrast displays, and active camouflage. In these applications, WO3 is generally preferred to be amorphous because of higher electrochromic performance than crystalline phase. However, amorphous phase is not robust as crystalline phase, and causing to some problems in applications [1, 2].

In this study, WO3 synthesis by solution combustion method were experimentally investigated by using citric acid and ammonium tungsten oxide hydrate as fuel and oxidative material, respectively. The effect of solution combustion synthesis parameters such as fuel type, fuel oxidizer ratio, homogenization on final product were studied. XRD, SEM, and BET analysis were conducted to determine powder properties.

REFERENCES

[1] Ma D., Wang H., Zhangb Q., Li Y., Self-weaving WO3 nanoflake films with greatly enhanced electrochromic performance, J. Mater. Chem., 2012, 22, 16633.

[2] Rajagopal S., Nataraj D., Mangalaraj D., Djaoued Y., Robichaud J., Khyzhun O.Y., Controlled Growth of WO3 Nanostructures with Three Different Morphologies and Their Structural, Optical, and Photodecomposition Studies, Nanoscale Res Lett (2009) 4:1335–1342.

SHS JOINING OF W WITH NiAl: TRANSITION ZONE STRUCTURE

A.S. Shchukin, A.E. Sytschev*

Institute of Structural Macrokinetics and Materials Science, Russian Academy of Sciences,
Chernogolovka, Moscow, 142432, Russia
* sytschev@ism.ac.ru

As is known, high heat resistance and mechanical strength of Ni–Al alloys and related materials can be markedly improved by dispersion-strengthening using submicron and nanosized carbides, nitrides, and other refractory compounds or rare-earth metals [1, 2]. As for the Ni–Al–W system [3], eutectic NiAl–W alloys are being used to fabricate porous foils, nanofiber matrices and wires [4, 5], turbine blades and similar machine parts [6]. The feasibility of preparing NiAl intermetallics containing above 10% W by hot isostatic pressing was demonstrated in [7] along with the positive influence (up to 700°C) of newly formed finely dispersed phases containing Mo and W. Ni–W and NiAl–W systems belong to the class of so-called systems with unipolar solubility: Ni is insoluble in W, while W is moderately soluble in Ni (up to 17 at. % near the Ni melting temperature). But within a thin (1 nm) layer at the grain boundary, the solubility may be higher by an order of magnitude [2]. It is known that alloying of Mo–W blends with Ni strongly accelerates the sintering process (activated sintering). The diffusion of Ni over the grain boundaries was also found to strongly facilitate superplastic flow at elevated temperatures.

In this communication, we report on SHS reaction in the Ni–Al–W system with special emphasis on subtle details of SHS joining between NiAl and W substrate as a function of green composition and amount of NiO added as a heat-generating agent (booster). Combustion products were characterized by SEM (Zeiss Ultra Plus microscope based on an Ultra 55 apparatus) equipped with an EDS facility (INCA Energy 350 XT, Oxford Instruments).

The structure of the weld seam is presented in Fig. 1 and Fig. 2c. In the (Ni–Al)/W transition layer, one can discern the dendrites of α–W (Fig. 2d), pseudo-binary eutectics of β–NiAl (with precipitates of W-containing phase below 50 nm in size), acicular inclusions of γ'–Ni_3Al, and nanostructured (α + γ + γ') eutectics with a grid structure (Fig. 1c, d) formed by solid solution and Ni_3Al grains with the size about 100 nm. After etching, we also observed the presence of branching bundles of W fibers up to 10 μm long and 50 nm in diameter (Fig. 2a, b).

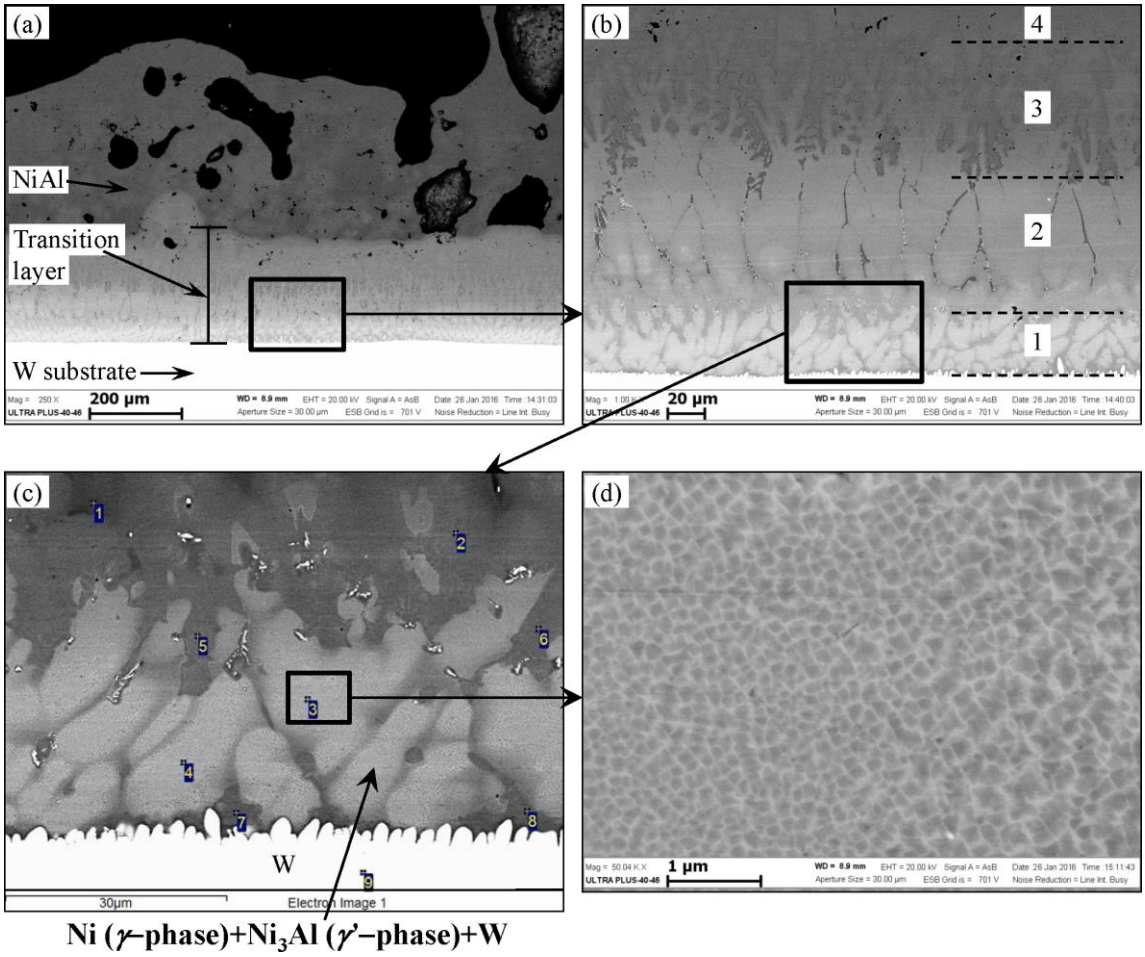

Fig. 1 - SEM images of the NiAl–W weld (a, c) and nanostructured (α + γ + γ') eutectics with a grid structure.

SHS reaction resulted in modification of the W surface with formation of dendrites (Fig. 2e) and globular precipitates (Fig. 2f) [8]. All this facilitates strong joining of W substrate with NiAl coating.

The W content of green (Ni + Al) + (1–5) at. % W mixtures had no influence on the amount of dissolved W (0.4 at. %). Upon addition of NiO to (Ni + Al) + 5 at. % W + *x*NiO mixtures (*x* = 1–5 at.%), the amount of dissolved W attained a value of 0.6 at. % at *x* = 5 at.%. In this case, no formation of globular precipitate was observed (Fig. 3). An increase in *x* was accompanied by a decrease in the amount of NiAl–W eutectics and an increase in that of W-containing dendrites.

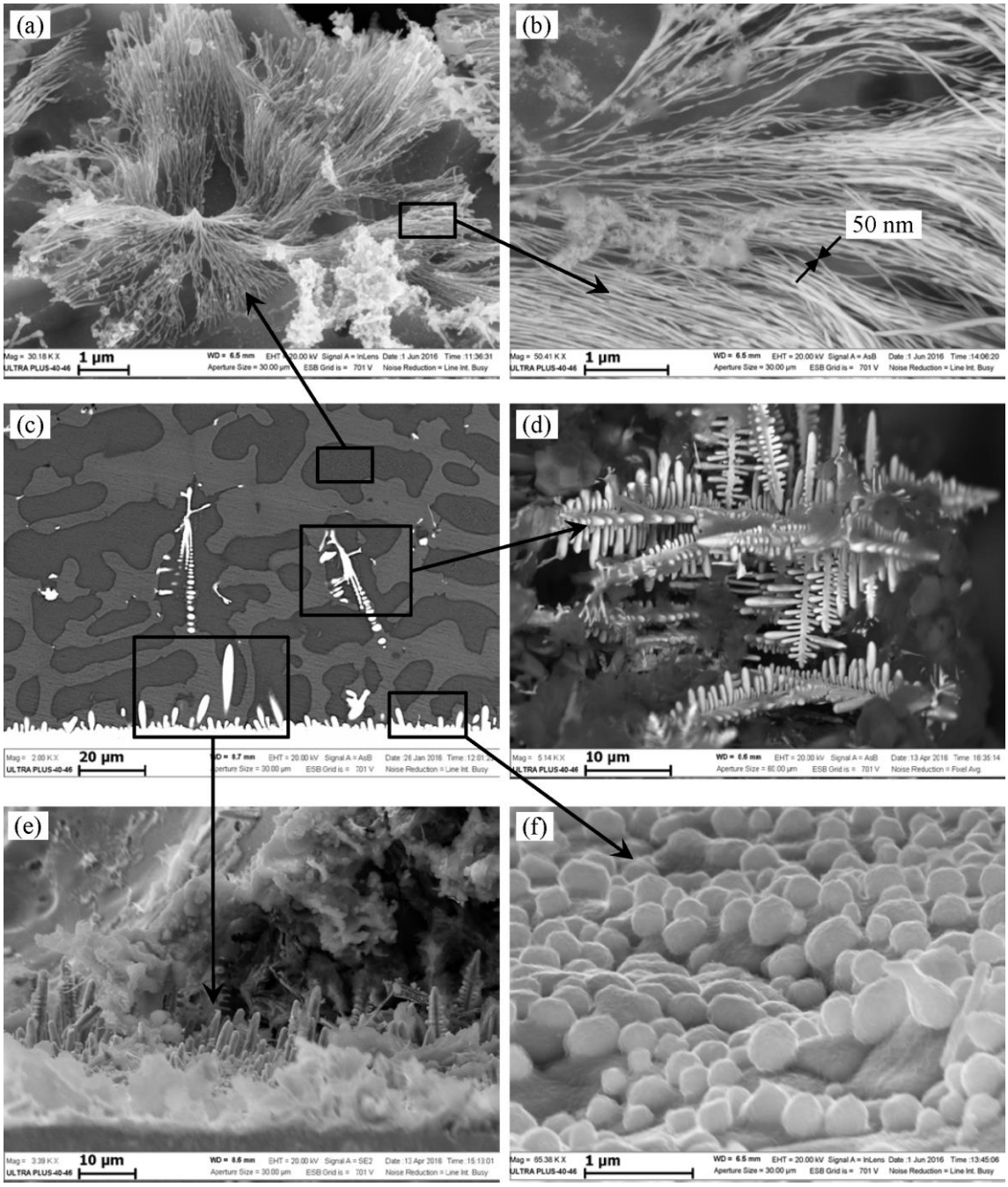

Fig. 2 - SEM images of the bundles of fibers etched from NiAl-W eutectic (a, b); joint section between W foil and NiAl intermetallide before etching (c); dendrites in the transition layer after etching (d) and globular and dendritic-like formations on the W surface of the foil after etching (e, f).

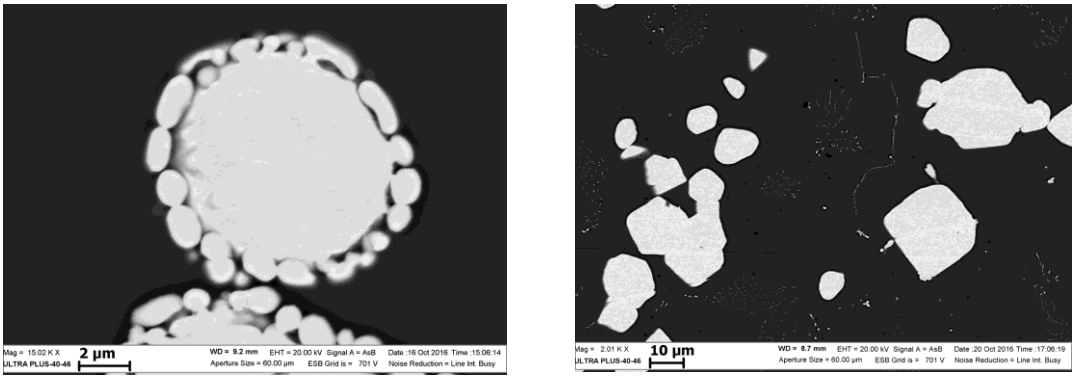

(a) (b)

Fig. 3 - SEM images of SHS-produced NiAl–W composite: (a) (Ni+Al) + 3 at. % W and (b) (Ni+Al) + 5 at. % W + 1 at. % NiO.

REFERENCES

[1] Matveeva N.M. and Kozlov E.V. Uporyadochennye fazy v metallicheskikh sistemakh (Ordered Phases in Metallic Systems). Moscow: Nauka, 1989.

[2] Kolobov Yu.R. Diffuzionno-kontrolruemye protsessy na granitsakh zeren i plastichnost' metallicheskikh polikrustallov (Diffusion-Controlled Processes at Grain Boundaries and Ductility of Metallic Polycrystals). Novosibirsk: Nauka. 1998.

[3] Popovič J., Brož P., Buršík J. Microstructure and phase equilibria in the Ni–Al–W system. Intermetallics. 2008. Vol. 16. No. 7. P. 884–888.

[4] Hassel A.W., Smith A.J., Milenkovic S. Nanostructures from directionally solidified NiAl-W eutectic alloys. Electrochimica Acta. 2006. Vol. 52. No. 4. P. 1799–1804.

[5] Milenkovic S., Drensler S., Hassel A.W. A novel concept for the preparation of alloy nanowires. Phys. Status Solidi A. 2011. Vol. 208. No. 6. P. 1259–1264.

[6] Brož P., Buršík J., Stará Z. Phase Equilibria in the Ni–Al–W System at 900°C. Monatshefte für Chemie. 2005. Vol. 136. No. 11. P. 1915–1920.

[7] Takahashi T. and Dunand D.C. Nickel aluminide containing refractory metal dispersoids: Microstructure and properties. Mater. Sci. Eng. A. 1995. Vols. 192–193. P. 195–203.

[8] Sytschev A.E., Vrel D., Kolobov Yu.R., Kovalev D.Yu., Golosov E.V., Shchukin A.S., Vadchenko S.G. Combustion synthesis in the Ni-Al-W system: Some structural features. Int. J. Self-Propag. High-Temp. Synth., 2013. Vol. 22. No. 2. P. 110–113.

SELF-PROPAGATING HIGH-TEMPERATURE SYNTHESIS IN THE Ni–Al–Nb TERNARY SYSTEM

A.E. Sytschev, D.Yu.Kovalev, D. Vrel[a], and S.G. Vadchenko

Institute of Structural Macrokinetics and Materials Science, Russian Academy of Sciences, Chernogolovka, Moscow, 142432 Russia
[a] Université Paris 13, Sorbonne Paris Cité, LSPM, CNRS - UPR3407, 99 av. J.-B. Clément, 93430 Villetaneuse, France
sytschev@ism.ac.ru

Due to a combination of high-temperature strength, heat resistance, high thermal conductivity, and good corrosion resistance, Al–Ni intermetallics are widely used in the automotive industry, aerospace engineering, and power plants [1]. Since these materials are also known for their low ductility and proneness to brittle failure [2], alloying elements are usually added to improve their mechanical behavior [3]. Following this approach, Nb has been tried as a high-temperature strengthening agent for polycrystalline NiAl with at least marginal success [4]. When IV–V Group metals (Me=Ti, Zr, Hf, V, Nb, Ta) are added to nickel aluminide, the dominant phase is in equilibrium with Laves (NiMeAl) and Geissler (Ni_2MeAl) phases. Upon dissolution, these metals (Ti, Zr, Hf, V, Nb and Ta) occupy predominantly aluminum sublattice positions within nickel aluminide [5]. A novel ternary eutectic in the Nb–Al–Ni system with a directed lamellar structure and improved thermophysical parameters was found, with the $Al_{54.4}Ni_{12.3}Nb_{33.3}$ [6]. Arc melting of Ni–Al–Nb mixture also leads to formation of the B2 NiAl and the NiAlNb Laves phase. It was found that a eutectic between these two compositions occurs close to 16.0 at % Nb with a eutectic transformation temperature of 1487°C [7].

In this study we investigated the process of structure formation during combustion synthesis in the thermal explosion mode in the Ni–Al–Nb system using Time-Resolved X-Ray Diffraction (TRXRD), enabling real-time recording phase composition evolution of the reactive mixture during combustion synthesis.

According to XRD analysis of the synthesized samples the following phases were detected: ~65 wt % NiAl, ~35 wt % NbNiAl (Laves phase), and traces of Nb_5Ni. The lattice parameters of NbNiAl (a = 0.4963 nm, c = 0.7991 nm) are smaller than the tabulated ones (a = 0.50 nm, c = 0.8093 nm). Figure 1 presents typical time-resolved diffraction patterns on the sample surface. Just after initiation, reaction between Al and Ni starts with the melting of the reagents. As a result, we observe a sharp drop in the intensity of Ni and Al peaks down to zero, accompanied with the emergence of the peaks of the NiAl phase. Decreasing intensity of Nb peaks indicates the beginning of its dissolution in the Ni–Al melt. Niobium peaks are detected all along the experiment (Fig.1), because the probing beam penetrates only to a 30-40 μm depth, smaller than the average particle size of niobium (mean size: 50 μm). Indeed, due to the fast cooling at the surface, Nb can completely dissolve only when completely surrounded by Ni–Al melt. Within 6–7s after thermal explosion, the emergence of the NbNiAl phase is observed (Fig. 1). Figure 2 represents the time evolution of the intensity of the main diffraction peak for each crystalline phase, representing the kinetics of the phase formation (NiAl, NiAlNb) and transformation (Ni, Al and Nb consumption), starting from the initiation of the reaction.

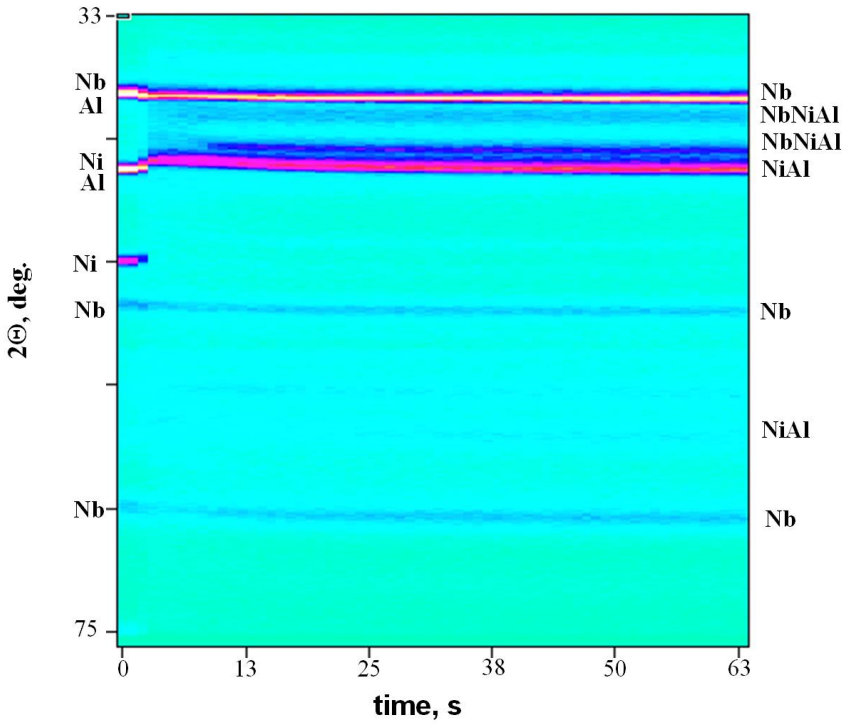

Fig.1 - Time-resolved diffraction patterns on the 40Ni-40Al-20Nb (at. %) sample surface.

The decrease in the intensity of the Nb diffraction peaks (Fig.2) results from the transformation of Nb to the NiAlNb ternary intermetallic by interdiffusion. Niobium dissolution in Ni–Al melt leads to the subsequent formation of NiAlNb which crystallizes from the melt. Since strong heat release from the surface prevents complete dissolution of Nb particles, especially considering the large mean size of Nb particles (<50μm), we observe the presence of Nb peaks on the surface diffraction pattern obtained during time-resolved XRD.

SEM images in Fig. 3 illustrate the eutectic, fractal-like dendritic microstructure of the synthesized alloys. Constituent components of synthesized material involve NiAl grains (d = 20–30 μm) and fine colonies of the NiAl phase (d < 1 μm). This can be explained by the rather fast cooling down that prevents the homogenization of resulting material. According to EDS data, the composition of dark areas is close to NiAl while that of bright areas, to NbNiAl, the contrast resulting from the fact that Nb is an heavier element. The NiAlNb Laves phase forms at the boundaries of NiAl grains and hence form a continuous phase.

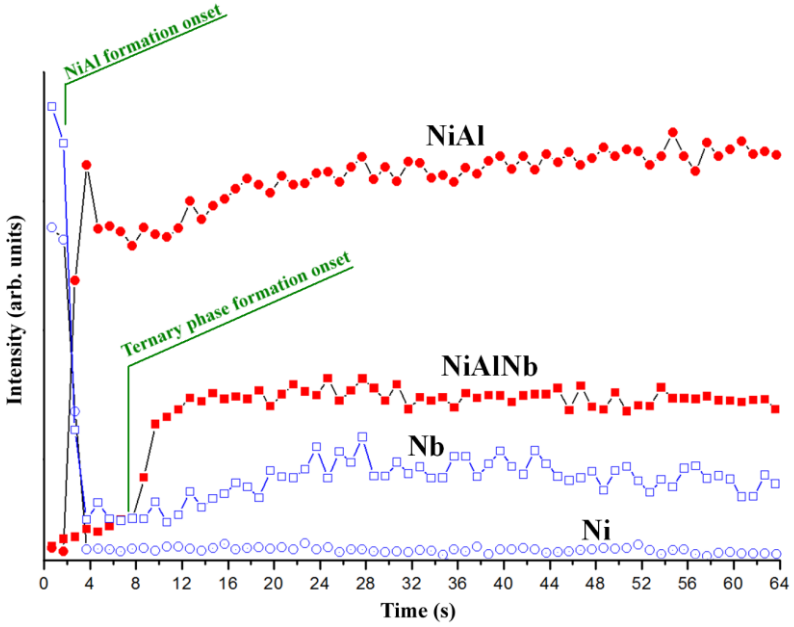

Fig.2 - Kinetics of phase transformations during combustion synthesis in the 40Ni–40Al–20Nb system (at %).

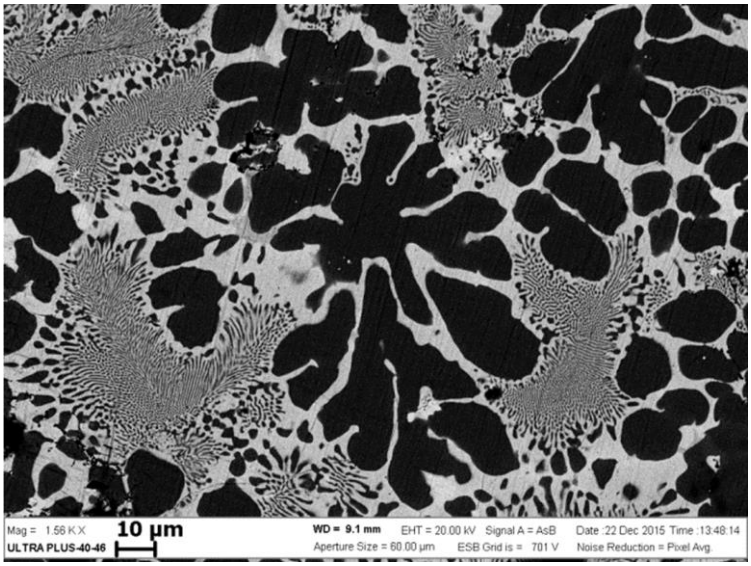

Fig.3 - 40Ni-40Al-20Nb (at%) alloy microstructures synthesized by combustion synthesis.

According to EDS analysis, the material is seen to contain, in addition to NiAl and NbNiAl, Nb and Nb_2NiAl phases. The sample presents a dendritic microstructure similar to the one observed within the volume, with two phases as previously, NiAl on the one hand and NiAlNb, with an average composition close to $Ni_{40}Al_{40}Nb_{20}$, slightly depleted in Nb, as compared to the initial mixture composition.

Indeed, Nb reacts only partially near the surface of the sample due to a partial quenching of the dissolution process. As a result, some residual Nb large grains are visible on the SEM micrograph and a thin layer with a composition close to $Ni_{25}Al_{25}Nb_{50}$ is observed around the Nb grains.

Due to the fast reaction rate of the combustion synthesis process and the fast cooling rate of the sample, specifically near the surface, it must be pointed out that these results are far from equilibrium. Nevertheless, all the detected phases on this micrograph might be attributed to existing phases in the phase diagram: points 3 and 4 correspond to Nb, point 5 to the NbNi phase, points 6 and 7 to the T_2 Laves phase, points 8 and 9 to the NiAl B2 phase, and finally, points 10 and 11 to the T_1 Geissler phase, even though this composition is out of the pseudo-binary NiAl-Nb phase diagram.

REFERENCES

[1] Bochenek, K., Basista, M., Advances in processing of NiAl intermetallic alloys and composites for high temperature aerospace applications, Progress in Aerospace Sciences, 79 (2015) 136–146.

[2] Liu, C.T., Ma, J., Sun, X.F., and Zhao, P.C., Mechanism of the oxidation and degradation of aluminide coating on the nickel-base single-crystal superalloy DD32M, Surface Coat. Technol., 204 (2010), 21–22, 3641–3646.

[3] Hou, P.Y. and McCarty, K.F., Surface and interface segregation in β-NiAl with and without Pt addition, Scr. Mater., 54 (2006), 5, 937–941.

[4] Whittenberger, J., Westfall, L., and Nathal, M., Compressive strength of a B2 matrix NiAl-Nb intermetallic at 1200 and 1300 K. Scripta Metall. 23 (1989), 12, 2127-2130.

[5] Druzhkov, A.P., Perminov, D.A., Stepanova, N.N. Positron Annihilation Study of the Influence of Doping on the 3d Electron States in the Ni_3Al Intermetallic Compound, Phys. Solid State, 52 (2010), 10, 2005-2011.

[6] Rios, C.T., Milenkovic, S., Caram, R., A novel ternary eutectic in the Nb–Al–Ni system. Scripta Materialia, 48 (2003), 10, 1495-1500.

[7] Ferrandini, P.L., Araujo, F.L.G.U., Batista, W.W., Caram, R. Growth and characterization of the NiAl–NiAlNb eutectic structure, Journal of Crystal Growth, 275 (2005), e147-e152.

INTERACTION OF Ta WITH Ni–Al INTERMETALLICS IN A SELF-PROPAGATING HIGH-TEMPERATURE SYNTHESIS

A.S. Shchukin[1]*, D. Vrel[2], and A.E. Sytschev[1]

[1]Institute of Structural Macrokinetics and Materials Science, Russian Academy of Sciences, Chernogolovka, Moscow, 142432 Russia

[2] Université Paris 13, Sorbonne Paris Cité, LSPM, CNRS - UPR3407, 99 av. J.-B. Clément, 93430 Villetaneuse, France

*shchukin@ism.ac.ru

The NiAl intermetallic compounds have attracted attention as potential high temperature light-weight materials with an exceptional combination of high strength and low specific weight, thermal stability, good oxidation/corrosion resistance, high thermal conductivity, and strength at high temperature [1]. Formation of intermetallics in the Ni–Al system can be explored for sintering, spark plasma sintering, diffusion soldering, and gas detonation deposition of coatings. As it is well known, NiAl intermetallics can be prepared by self-propagating high-temperature synthesis (SHS) [2]. On the other hand, SHS reactions can also be used as a tool for joining similar and dissimilar materials and coating processing [3]. Meanwhile, no reliable technological processes for SHS joining and coating have been proposed so far. The reactive compacts can act as local heat source for joining many materials. Since heating is localized to the interface during joining, temperature sensitive components or materials can be joined without thermal damage, and the thermally affected zone may be controlled and limited by adjusting process parameters.

In this work, we explored the interaction between SHS produced Ni–Al intermetallics using mechanoactivated Ni-Al mixture deposition on Ta substrates resulting in the formation of interpenetrating junctions. The intermetallic nickel aluminides may be formed by NiAl and/or Ni_3Al, wherein the ternary Laves phases based on Ni, Al and Ta may be formed. In particular, the formation of ternary Laves phases in the form of NiAlTa may occur in the tantalum NiAl (Ta) blend. The ternary phase based on Ni, Al and Ta, provide by the presence of the corresponding grain boundaries of the NiAl - crystallites and/or Ni_3Al - crystallites for a corresponding increase in the strength and the creep resistance of the material. Such ternary Laves phases can be in the form of hexagonal C14 structure while NiAl in the B2-structure is present. SHS-assisted deposition of intermetallic coating onto a refractory Ta substrate can be expected to open up new approach for producing materials with improved structure and properties.

In our study, commercial powders of Al (particle size d < 44 μm), and Ni (d=3÷7 μm) were used as starting materials. Composition of initial reacting mixture was Ni-Al = 1:1. Initial mixtures were prepared in a Turbula mixer. Cold-worked Ta substrates (6.35 mm in diameter 6.35 high) shown in Fig. 1 were processed in a planetary mill Fritsch Pulverizette-7 together with Ni–Al powder mixture. Mechanical treatment resulted in removal of the oxide layer from the Ta surface, its roughening, and deposition of activated Ni–Al mixture. X-ray analysis of the Ta substrate coated by (Ni+Al) initial mixture did not show the formation of new phases after mechanical activation (Fig.2).

(1) (2)

Fig.1 - The view of the initial (1) and MA treated (2) Ta substrate.

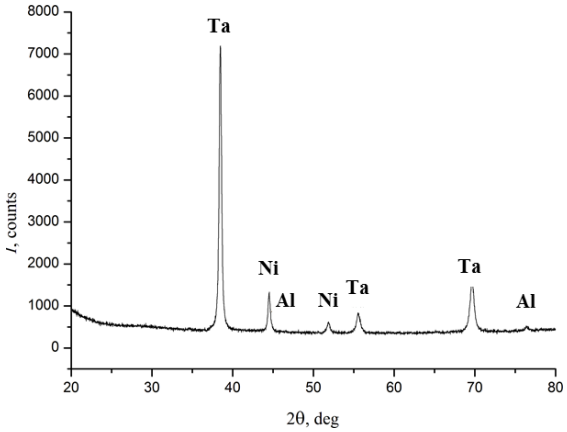

Fig.2 - X-Ray data of the Ta substrate coated by (Ni+Al) initial mixture.

After MA, the processed Ta substrates were immersed into raw Ni–Al mixture, compressed into 20 mm diameter and 10 mm height samples (Fig. 1) and ignited under the thermal explosion mode. The adiabatic combustion temperature of the Ni-Al mixture is ~ 1630°C, which is below the maximum solubility temperature of Ni in Ta (20 at.% at 1788°C) and Al in Ta (12 at.% at ~ 2000°C), but above the solubility temperature of Ta in Ni (14 at.% at 1360°C) [4]. According to the phase diagram, Ni_3Ta, Ni_2Ta, NiTa, Ni_8Ta, Al_3Ta, Al_3Ta_2 binary intermetallics and six ternary compounds TaNiAl, $TaNi_2Al$, $Ta_{0.5}Ni_3Al_{0.5}$, $Ta_5Ni_2Al_3$, and $TaNiAl_2$ may form at temperatures below 1630°C [5, 6]. It was found that as a result of the interaction of the NiAl with the Ta substrate, a multilayer transition zone with a thickness of 2 to 20 μm was formed. Fig. 3 shows a structure of the transition zone formed between Ta and SHS-produced Ni–Al intermetallics along with corresponding EDS results. The transition zone exhibits the presence of most of the intermetallics predicted by the constitution diagram of the Ta–Ni–Al system. The layer nearest to the substrate (points 3 and 4, in Figure 4) has a uniform composition and a thickness of 0.25 to 0.6 μm. The next layer (points 5 and 6 in Figure 4) has a more developed structure in the form of dendritic eutectic structures and a thickness of up to 30 μm.

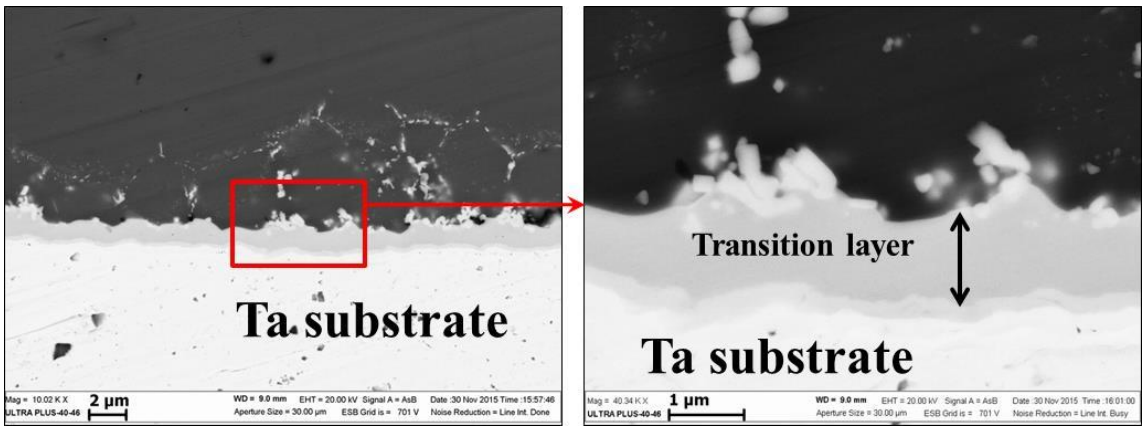

Fig. 3 - Microstructure of the transition layer.

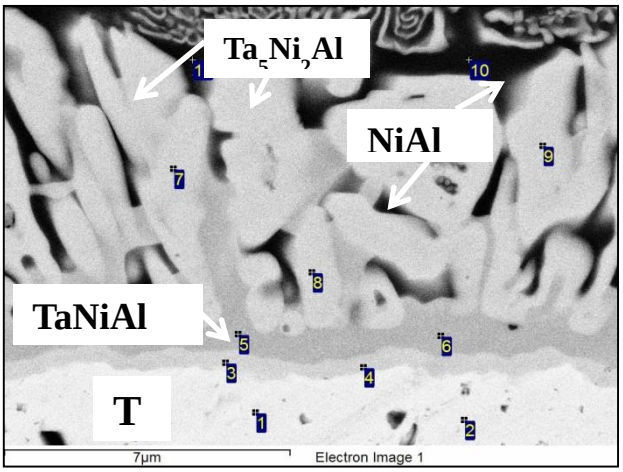

Spectrum	Al	Ni	Ta
1	-	-	100,0
2	-	-	100,0
3	21,5	21,0	57,5
4	21,6	22,2	56,2
5	33,6	28,2	38,2
6	34,1	28,2	37,7
7	27,9	23,1	48,0
8	31,6	19,0	49,4
9	29,3	21,3	49,4
10	46,4	48,1	5,5
11	46,2	46,4	7,4

Fig.4 - Microstructure and EDS data of the transition layer, (at%).

According to the EDS data (points 5 and 6 in Fig.4), the composition of this layer is close to the ternary compound TaNiAl (Laves Phase), which has a wide range of Ni homogeneity. On the side of the deposited NiAl layer, another phase (points 7, 8 and 9 in Figure 4) is formed in the transition zone in the form of elongated particles up to 3-5 μm in size. The composition of this phase is close to the $Ta_5Ni_2Al_3$. $Ta_5Ni_2Al_3$ formed the diffusion zone of all the specimens, which was approximately 6 μm in extent (Fig.4), and consisted of a number of grains with a β-phase matrix and Ta-rich precipitates, which grew perpendicular to the Ta substrate with a rod shape and bright contrast. As a result of grain-boundary diffusion in the fused Ni–Al layer, grains of globular form on the basis of $Ta_xNi_yAl_z$ up to 0.5 μm in size were formed on the NiAl grain boundaries, presumably on the basis of the ternary phase of $Ta_xNi_yAl_z$. The possible mechanism of phase formation at combustion temperature is as following:

(1) melting of (Ni+Al) reactive reagents resulting to the NiAl (β) formation;

(2) Ta dissolution in Ni-Al melt resulting to the TaNiAl (τ_1) formation:

$$(Ni\text{-}Al)\ L \leftrightarrow NiAl\ (\beta) + TaNiAl\ (\tau_1);$$

(3)ternary peritectic reaction at T=1000^0C:

$$NiAl(\beta) + TaNiAl(\tau_1) + (Ni\text{-}Al)\ L \leftrightarrow TaNi_2Al\ (\tau_2).$$

Various Ta-containing NiAl-base alloys show a strengthening with the TaNiAl Laves phase, with Cl4 structure [7]. Such behavior of mechanical properties is a result of both solid-solution strengthening and second-phase strengthening. Indeed, materials based on the intermetallic compound NiAl strengthened with the Laves phase NiAlTa or the Heusler phase Ni_2AlTa have shown promise for use in some high-temperature structural applications [8]. Therefore, mechanoactivated SHS in a mode of thermal explosion can be recommended as a method for strong joining of Ta substrate with Ni–Al intermetallic coating with a tailored composition.

REFERENCES

[1] G.K. Dey. Physical metallurgy of nickel aluminides. Sadhana, February (2003), Volume 28, Issue 1, pp. 247-262.

[2] A. Biswas, S.K. Roy, K.R. Gurumurthy, N. Prabhu, S. Banerjee. A study of self-propagating high-temperature synthesis of NiAl in thermal explosion mode, Acta Mater., (2002), vol. 50, no. 4, pp. 757-773.

[3] A.E. Sytschev, S.G. Vadchenko, O.D. Boyarchenko, D. Vrel, N.V. Sachkova. SHS joining of intermetallics with metallic substrates. Int. J. SHS, (2011), Vol. 20, No. 3, pp. 185-190.

[4] Diagrammy sostoyaniya dvoinykh metallicheslikh system, ed. by N.P. Lyakishev, Mashinistroenie, Moscow, 1996, p. 992.

[5] A. Zakharov. Aluminium-Nickel-Tantalum, in MSIT Ternary Evaluation Program, MSIT Workplace, G. Effenberg (Ed.), MSI, Materials Science International Services GmbH, Stuttgart; Document ID: 10.14883.1.20 (1993) (Crys. Structure, Equi. Diagram, Ass., 28).

[6] V. Raghavan, J. Phase Equil. Diff., 27, 4, (2006) 405-407.

[7] B. Zeumert, G. Sauthof. Intermetallic NiAl-Ta alloys with strengthening Laves phase for high-temperature applications. I. Basic properties. Intermerallics, 5 (1997) 563-577.

[8] D.R. Johnson, B.F. Oliver. Ternary peritectic solidification in the NiAl-Ni_2AlTa-NiAlTa system. Materials letters, (1994), vol. 20, n 3-4, pp. 129-133.

SUCCESSES AND WAYS OF DEVELOPMENT OF SHS IN GEORGIA

G.F. Tavadze

LEPL - Ferdinand Tavadze Metallurgy And Materials Science Institute

Today the famous experts in the field of SHS from all over the world have gathered in this hall, and, it is probably logical that I want to acquaint the audience with the work of our Institute in this direction and, more generally, with some works on inorganic materials science.

I will begin with a very general statement that today's technological progress depends to a large extent on the production and processing of new materials with special properties. It is for this reason that the problems of material science are mentioned at the beginning of the priority scientific directions of all civilized countries. It is generally accepted that materials science, along with the problems of ecology and biomedicine, determines the path of human development in the 21st century [1].

The name of our Institute indicates that in Georgia it determines the development of this important scientific direction. The foundations of the Institute were laid 72 years ago by Academician Ferdinand Nestorovich Tavadze, which is reflected in the name of the Institute. Many innovations are connected with his name: the study of the diagrams of the state of multi-component systems, in particular, the iron-chromium-manganese-nickel system, the production of stainless, cryogenic-resistant, wear-resistant, heat-resistant steels, corrosion problems, boron problems and much more.

Now the main thing is about our some works in the field of inorganic materials science and SHS (self-propagating high-temperature synthesis).

Our Institute fruitfully cooperates with the relevant scientific centers of Ukraine, Russia, the USA, Israel, Turkey and therefore, I think, many of the guests who are present here are familiar with our problems and will confirm that a number of the scientific and technological results received by us is accompanied by the international resonance.

Now about the main thing - about some of our works in the field of inorganic materials science.

It is known that the properties of material are primarily due to its chemical composition. Of the elements that create the greatest diversity of our world, majority are made of metals. Of their combinations are obtained most of inorganic materials. However, in addition to the chemical composition, the properties of materials determine its structure. For example, depending on the structure in which carbon is represented, it can be in the form of graphite, ash or diamond; steel, which is an alloy of iron and carbon, is microscopically represented by different structural components, the ratio of which depends on the rate of cooling. The cooling rate determines the process of martensitic, bainitic, cane, sorbitol and pearlitic transformations and, as a result, the operational properties of the product.

During the rapid cooling of the melt, the viscosity increases catastrophically. Atoms lose mobility characteristic of the liquid state, the material "freezes" in the amorphous state and hereditarily preserves the structural elements of the liquid. Consequently, in the conditions of cooling molten metal at ultrahigh rates, it is possible to expect the production of supersaturated solid solutions, completely new structures characteristic of the liquid state, a significant increase in the inter-resolvability of the components in the solid phase, fixation of the amorphous state,

etc. Hence, the structure, i.e. the spatial distribution of particles significantly determines the properties of matter and can be controlled by the cooling rate, i.e. the degree of deviation from the equilibrium state.

Obviously, from the point of view of structural diversity, the process of cooling the melt with ultra-high speed has an inexhaustible reserve. And it was in this direction that Ferdinand Nesterovich Tavadze instructed us to conduct a study 50 years ago - to me as a student and, at that time, my supervisor, Jumber Varlamovich Khantadze, who today heads the Scientific Council of our Institute.

As a result of obtaining such a task, a problem appeared that required research in other areas, namely, modeling of molten metal as a structurally disordered object.

If we look at the structural aspect of the inorganic world that exists around us, we easily find that matter in nature basically exists either in the form of a crystalline, ordered, regular lattice (various minerals, metals, alloys, etc.) or in the form of a disorder irregular substance (liquids, amorphous substances, friable materials, etc.). At the same time, the atomistic model of the structure of matter, according to which atoms are regarded as rigid spheres, are equally applicable to regular and irregular, disordered structures.

The chaotic, structural model with irregular packing, which is based on the results of a systematic study of the irregular filling of space by steel balls (approximation to hard spheres) and the mathematical theory of packing , is developed at the Institute by Doctor of Chemical Sciences, Professor Jumber Varlamovich Khantadze. The goal of mechanical modeling is the creation of a geometric image of a random structure and the establishment of a statistical pattern of its construction. It makes it possible to represent the spatial distribution of particles in an unordered structure, similar to the model represented by balls of an ideal crystal, which shows the regularity of the spatial distribution of particles and determines the distance between the particles and the Wigner-Seitz cell, and limits the volume per particle.

The structural model of a disordered, irregular system describes: the concentration-fractional dependence of the packing density coefficient, the structural motifs - the variety of geometric-statistical Voronoi polyhedra, the microscopic characteristics - the coordination number, the number of heterogeneous contacts, their concentration-fractional dependence etc. The results obtained are successfully used for the general characterization of granular structures [2,3] and, in particular, for the characterization of powders used in SHS [4,5], which we will discuss below, and also on this topic will be the report of Prof. J.V. Khantadze.

As it was said above. in conditions of rapid cooling of the melt, when the cooling rate reaches one million degrees per second, the boundaries of inter-solubility increase, supersaturated solid solutions are obtained, new intermediate compounds are formed, an amorphous state is often fixed, and completely new structures appear.

The study of the processes of supercooling of the melt with ultrahigh speeds requires a very complex and skilful experimental investigation, all the more so because we chose such refractory and aggressive objects as boron and its alloys with elements of group IV A, V A of the periodic system and 3d transition metals. This choice was due to the general interest to them both from the theoretical point of view, as well as the prospects of their application in practice. It is known that as a result of the interaction of boron with transition metals, we obtain more solid borides. In addition, the light isotope B^{10} is one of the most active neutron absorbers, and

B^{11}, on the contrary, is the best neutron-transparent material. Therefore, boron is widely used as a neutron-absorbing or neutron-transparent material in the manufacture of converters, counters and other equipment. Boron is often used in the form of thin-walled products of different configurations. Therefore, naturally, the interest in boron and its compounds is so high until today.

Boron is an anisotropic material, characterized by low thermal conductivity and high brittleness. To receive from crystal boron the perfect product without defect is too complex challenge. On slide 1. Fig. 1 shows the general view (a) and the schematic diagram (b) of the electron beam device, specially designed and built by us for melting and cooling with high velocities of refractory inorganic materials. In this setup, we first obtained films of elemental boron and its compounds with a thickness of 40 ÷ 200 microns. under cooling conditions at a rate of ~ 10^6grad / sec.

For quenching from liquid state three different schemes of cooling were applied. Slide 2, Fig. 2.

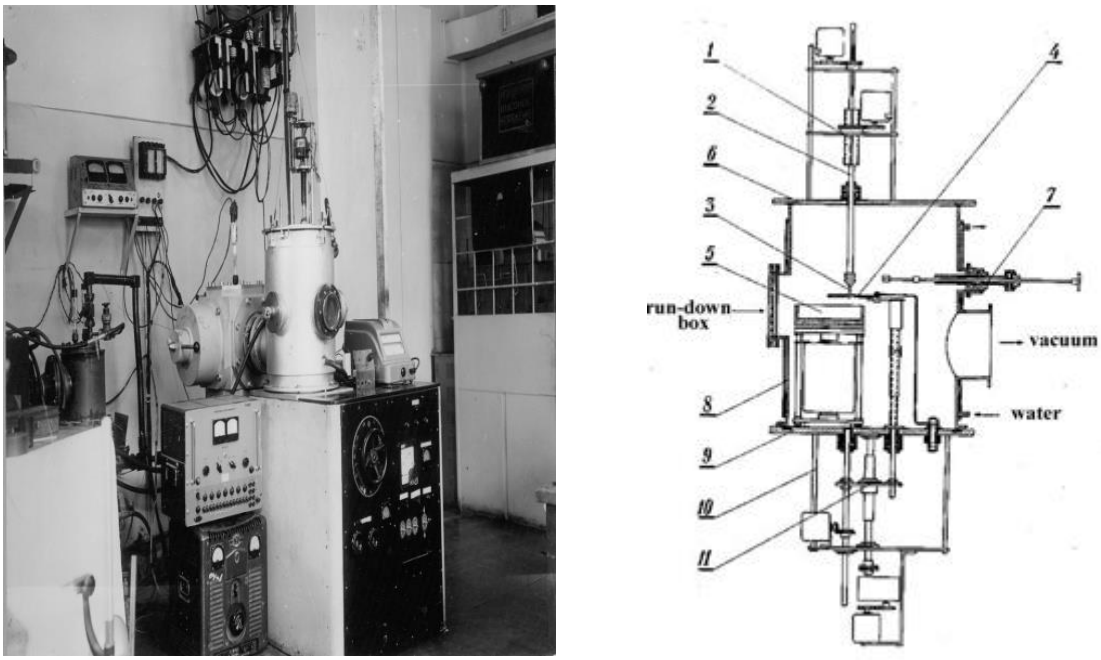

Slide 1. Fig. 1. Installation for electron-beam melting and cooling with ultrahigh speeds of refractory inorganic materials

a) General view and b) Schematic diagram

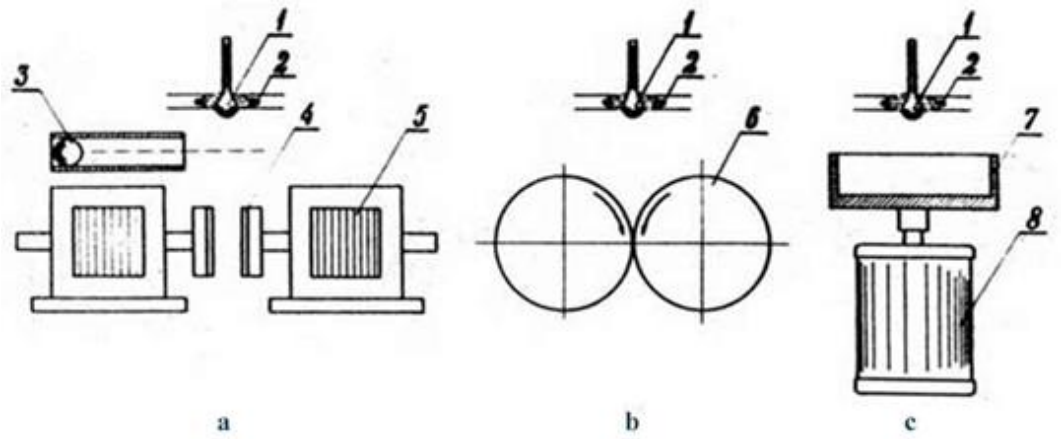

Slide 2. Fig. 2. Cooling with ultrahigh speed in conditions of a) compression, b) rolling and c) centrifugation

Studies have shown that the borides of the metals under investigation (Fe, Co, Ni, Zr, Hf) under conditions of ultrahigh-speed cooling crystallize as **quasieutectic**, i.e. supersaturated solid solutions with a finely dispersed structure. Please draw your attention to the term " **quasieutectic** ". This term was introduced by us in 1980. By this term, we stressed the perfect eccentricity, even the uniqueness of the structure of the preparation we received. In this context, we must mention the work of Professor Dan Schechtman, who in 1984, in rapidly cooled alloys Al-Mn discovered crystallographic elements with symmetry of the fifth order. Such a symmetry is acceptable for disordered systems, but based on the postulates of solid state physics, it is inadmissible for metal objects. To denote this feature, Professor Dan Shechtman called his crystal "**quasicrystal**". Afterwards, by Professor Schechtman virtuosic technology of electronic diffraction were studied double Ca-Cd, Yb-Cd, triple Fe-Cu-Al, and a set of other systems and in 2012, for the discovery of "quasicrystals", Professor of the Haifa University "Technion" (Israel) Dan Schechtman was awarded the Nobel Prize.

This case deserves special attention, as it demonstrates that scientific achievements in modern materials science are determined by the perfection of two factors - the technological process and the method of investigation. As a result of the improvement of the technological process developed by us, it became possible to produce from boron and its alloys various products, among them cylindrical and spherical containers. **Slide 3. Fig. 3**. Later, this technology was introduced in the Kharkov Institute of Physics and Technology as a method of manufacturing special containers.

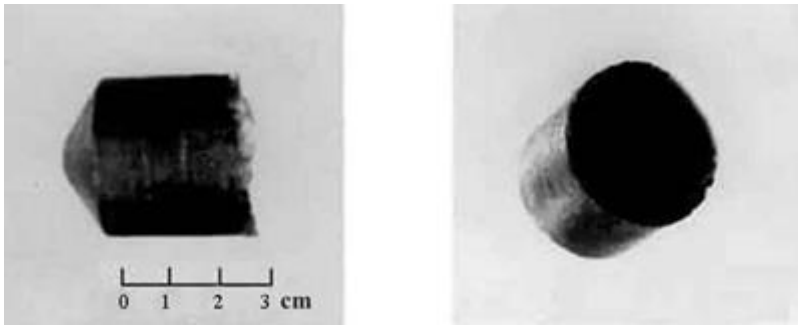

Slide 3. Fig. 3. A laboratory sample of a cylindrical container of crystalline boron obtained by centrifugal casting

The experience gained in the process of studying the effect of ultrahigh cooling rates on the process of crystallization of inorganic materials and phase transformations has been successfully applied in the technology of self-propagating high-temperature synthesis (SHS).

The product obtained in the conditions of melt cooling at ultrahigh rates and the material synthesized by the SHS method are characterized by a different degree of deviation from the equilibrium conditions, which is associated with the transience of the processes and makes it possible to obtain materials and products from them with different properties. As a result of the works carried out in these areas, we have created scientific and technological foundations for the production of inorganic materials with special properties using high-temperature fast processes. It is about them that I want to tell you.

Works on SHS in our Institute began in the late 70s of the last century and they are connected with two well-known scientists and personalities: with the author of the discovery and the founder of the SHS-direction, Academician A.G. Merzhanov and supporting this scientific direction and the main initiator of the introduction of SHS in our Institute, Academician F.N. Tavadze.

As is known, this technology is based on a scientific discovery, which was discovered as a result of research into solid rocket fuel combustion processes in the late 60s of the last century. It turned out that the self-braking reactions propagated in the form of a combustion wave, its propagation velocity was of the order of 10 cm per second, and the temperature reached ~ 40000C. Early this phenomenon was not known, therefore the explanations of the mechanism and the regularities of burning with a solid flame aroused great interest and disagreement.

This discovery immediately attracted the attention of our Institute, as it became evident that this method provided the solution to many of the earlier unresolved problems. The Institute immediately established scientific contacts with Professor Merzhanov. While physicists and chemists were discussing the details of this process, the two institutions began collaborating in the field of materials science. And this cooperation certainly had a huge impact on the development of self-propagating high-temperature synthesis.

It should be noted that SHS can be successfully applied to produce such new materials, the synthesis of which is either impossible with traditional methods or is associated with great difficulties. The Institute has three varieties of self-propagating high-temperature synthesis:
- SHS - with a restorative stage;

- SHS - pressing;

- SHS - casting / metallurgy

and the corresponding scientific and technological bases were developed.

The Institute has developed SHS technology to produce elemental boron, boron carbide and boron nitride from boron oxide (B_2O_3) and potassium tetraborate (KBF_4) by magnesium and aluminum reduction, slide 4, Table 1

Slide 4
Table 1

SHS - with a recovery stage

$4B+C \rightarrow B_4C+9,3kkal/mol$	(Reaction 1)
$2B_2O_3+6Mg+C=B_4C+6MgO+269$ kkal/mol	(Reaction 2)
Systems were studied**:** **KBF_4-Mg; KBF_4-Al;**	(Reaction 3)
KBF_4-Mg-C; KBF_4-Al-C;	(Reaction 4)
KBF_4-Mg-N_2; KBF_4-Al-N_2	(Reaction 5)

By SHS- with a reducing stage with the participation of potassium tetraborate was obtained:

- elemental boron with purity **99%,** with outpot of final product **~95-97%;**
- boron carbide with purity **99%,** with outpot of final product **~96-97%.**

From potassium tetraborate fluorate enriched with isotopic boron we obtain: **B^{10}, B^{11}** with their successive enrichment.

As a result of the thermodynamic analysis, it was established [6] that, from the energy point of view, the magnesium-thermal reduction of tetraborate is more preferable. This process is also advantageous from a technological point of view, since the volatile combustion products (KF, MgF_2) are easily removed from the reaction zone, unlike the refractory oxides MgO and Al_2O_3 formed in the case of reduction of B_2O_3.

By SHS - with the recovery stage with the participation of potassium tetraborate it was obtained [2,3]: elementary boron and boron carbide of 99% purity, with the yield of the final product ~ 95-97%, and when enriching potassium tetraborate with isotopic boron, the corresponding products containing isotopic boron - **B^{11}**.

It should be noted that with the help of SHS - with a recovery stage, compounds are synthesized that can not be obtained directly from the reacting elements due to the weak exothermicity of the process. For example, reaction 1, slide 4

$4B+C \rightarrow B_4C+9,3$ kkal/mol (1)

is not feasible in the SHS mode because of the small thermal effect of the reaction (**9.3 kkal / mol**). However, **B_4C** is synthesized as a result of reaction 2, slide 4

$2B_2O_3+6Mg+C=B_4C+6MgO+269$ kkal/mol, (2)

which is rapidly developing due to the large amount of heat released - the thermal effect of the reaction.

SHS - with a recovery stage is used in the preparation of multicomponent composite ceramic and metal-ceramic materials. These include functional gradient materials. In this field, for the first time, we used together the methods of SHS - with the recovery stage and SHS - pressing. This direction is one of the leading directions in today's scientific subject of our institute.

From the point of view of practical application, composite ceramic materials that represent a mixture of carbides, borides, nitrides and oxides of transition metals are very interesting.

On the basis of the conducted studies, the goal was to obtain a ceramic armor material that would be characterized by low weight, high physical and mechanical properties, high ballistic stability, manufacturability and low price, which would significantly distinguish it from metal armor and from known ceramic armor materials.

By combining the SHS- recovery stage and the SHS-compacting, which as we said above, was used for the first time, a composite ceramic armor material with the phase composition $B_4C \cdot TiB_2 \cdot Al_2O_3$ code-named "Tory" was produced. This work was later awarded with the state award of Georgia.

Armor plates received by the SHS-compaction method are advantageously distinguished by physical-mechanical characteristics from hot-pressed products - boron carbide, aluminum oxide, etc. Slide 5, table 2.

Slide 5
Table 2

SHS Composition ceramic	Young's modulus E, gpa	Coefficient of fracture intensity $K_{1C,}$ mpa-$m^{0,5}$	Hardness HV, kg/mm^2	Density ρ, gr/cm^3	Crushing strength σ_{mc} gpa,	Porosity %
B_4C. TiB_2.Al_2O_3 (2:1:7)	410 GP 400	13,2 GP 9,8	2670 GP 2650	3, 45 GP 3,54	4,7 GP 3,2	3-6 GP 4-5
B_4C. TiB_2.Al_2O_3 (3:2:5)	425 GP411	13,7 GP10,6	2850 GP 2800	3,48 GP 3,40	5,2 GP 3,8	3-6 GP 3-5

Some physical and mechanical characteristics of armored plates obtained by the SHS-pressing method

When investigating the fracture toughness of composite ceramics, it was found that during the action of a diamond pyramid on a composite material, cracks propagate not in a straight line but in a branching in fine-grained regions of the material by numerous microcracks. Thus, practically stopping the main cracks in the phase components of the compositions, slide 6 of Fig. 4.

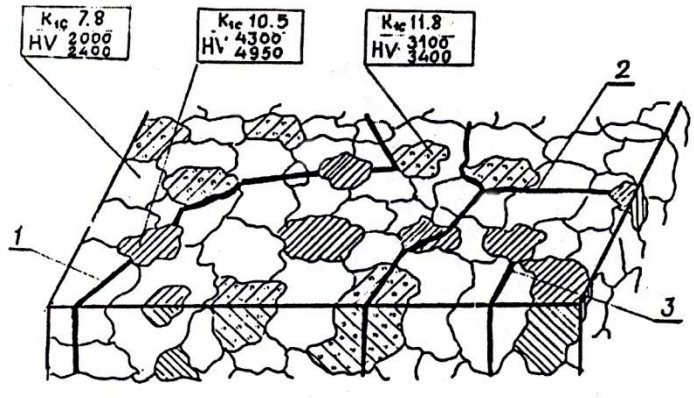

Slide 6, Fig.4. Schematic representation of the propagation of cracks in the composition 1 - curvature of the trajectory of cracks; 2 - branching of cracks; 3 - stop (fastening braking) of cracks stitching.

The voltage intensity factor in the K_{1C} composition is 10-13 mp $m^{0,5}$. This value is several times higher than the voltage intensity factors of the individual B_4C, TiB_2; Al_2O_3 phases.

On (slide 6) in Fig. 5. A raster micrograph of a ceramic composite armored material B_4C; TiB_2; Al_2O_3 (2: 1: 7) is shown on which a picture of phase distribution is visible.

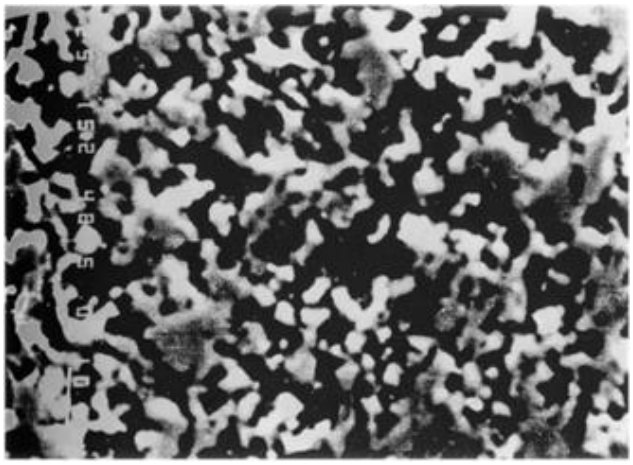

Slide 6, Fig. 5. Raster micrograph of the structure of the ceramic composite with the phase composition of the armored element **$B_4C \cdot TiB_2 \cdot Al_2O_3$**

Based on the studies carried out, a gradient two-layer ceramic- metal ceramics material was obtained. The full-scale test of the developed metal-ceramic armored plate was carried out in accordance with the NIJ IV and STANAG 3+ standards and showed that they could be successfully applied to protect the equipment from an armor-piercing bullet of caliber 12.7X99, with an energy of 18000-20000 Joule with a large ballistic resource. slide 7 video.

With the use of SHS technology, the Institute has synthesized metal superconducting compounds of A-15 class, based on vanadium [7], niobium [8-10] and also high-temperature superconducting material (HTSC) based on erbium: **$ErBa_2Cu_3O_{6,69}$** [11,12].

Based on the conducted studies and obtained superconducting materials, using the energy of the explosion, the technology of obtaining superconducting products was developed. Ин вeveloped technology, our institute together with Kurchatov Institute of Atomic Energy began to manufacture models of superconducting magnetic windings intended for an international project known as the "Tokomak".

The Institute is working on the development of a new energy-efficient technology for the synthesis of materials, which combines self-propagating high-temperature synthesis with electroresonant irradiation [13]. The innovation consists in the following: for the initiation of the process, the microwave electroresonance effect on the charge was first applied. As a result, during the "incubation" when the initial charge is heated, gases are released, intensive self-cleaning takes place, and at the last stage volumetric combustion occurs. At the same time, the burning rate increases by no less than an order of magnitude, the resulting synthesis product is homogeneous, uniformly heated, and much more liable to the compaction process.

With this technology it is possible to obtain powder materials in the form of nano and micropowders, as well as compositions in the SHS-compacting mode. The consumption per unit of thermal energy is 25-50 times less than in comparison with similar characteristics of other high-temperature units (laser, plasma). As a result, by practically zero energy costs are produced expensive products in the form of structural ceramics, hard alloys, armor materials, etc.

The application of this heating method in the SHS process leads to the possibility of synthesizing materials to an entirely new level. As a result of the analysis, it has been established that by this method of initialization it is possible to synthesize such low-energy materials, which usually do not burn.

The second problem, which is being solved at present, is based on the original rolling technology developed at the Institute [14]. In the process of electric rolling, the heating mode is localized directly in the deformation zone by supplying electric power to the rolls and deformation occurs under conditions of a stationary thermal regime.

We developed a combined innovative technological process for self-propagating high-temperature synthesis and electric rolling [14], which ensures the production of high-quality materials (including gradient materials).

We continue to study fast-flowing high-temperature processes and their use in order to create new functional materials, including in the nano state. I am sure that SHS, as a scientific and technological direction, has a great prospect for the development of inorganic materials science for the entire twenty-first century.

This is the scientific and technological direction on which the research described above is based and which is being intensively and successfully developed in our institute.

I hope that the symposium participants in their reports, messages and discussions will demonstrate the success, importance and significance of the results obtained and the perspectivity of SHS as a scientific and technological direction.

Good luck, dear colleagues!

REFERENCES

[1] Опыт Евросоюза и передовая международная политика относительно науки. Проект Евросоюза. Тбилиси, 2007, 284 с. (На грузинском языке).

[2] Тавадзе Г.Ф., Штейнберг А.С. Получение специальных материалов методами самораспростряющегося высокотемпературного синтеза. Тбилиси, Изд-во Меридиани, 2011, 206 с.

[3] Giorgi F. Tavadze, Alexayder C. Shteinberg. Production of Advanced Materials by Methods of Self-Propagating High - Temperature Synthesis.Springer, 2013, p.156.

[4] Тавадзе Г.Ф., Хантадзе Д.В. Термохимическое обоснование влияния дисперсности компонентов шихты на процесс СВС. Georgian Engineering News.#3 ,2010, 86-89.

[5] Tavadze G., Khantadze J. The Impact of Fractional Difference of Components on the Properties of Hard Alloys Produced by the SHS Method. Bull. Georg. Natl. Acad. Sci. 2010, 4, #3, 70-73.

[6] Tavadze G., Nadiradze A., K. Ukleba K. Thermodynamic Probability of obtaining Boron, Carbide and Boron Nitride from Potassium Tetrafluoboron and Boron Oxide at Self-Propagating High-Temperature Synthesis. Bull. Georgian National Academy of Sciences, 2010, vol. 4. no.2. 74-81.

[7] Бежитадзе Д.Т., Юхвид В.И., Тавадзе Г.Ф. и др. Влияние инертной добавки на закономерности горения в системах V2O5-Al-Si и V2O5-Al-SiO2 при атмосферном давлении Сообщения АН ГССР, 123, №2, 1986, 349-352.

[8] Бежитадзе Д.Т., Юхвид В.И., Тавадзе Г.Ф. и др. Закономерности горения системы Nb2O5-Al при атмосферном давлении. Сообщения АН ГССР, 125, №1, 1987, 98-100.

[9] Нацвлишвили Т.Н., Бежитадзе Д.Т., Тавадзе Г.Ф. и др. Закономерности горения системы Nb2O5-Al-Sn при атмосферном давлении. Сообщения АН ГССР, 133, №1, 1989, 117-120.

[10] Нацвлишвили Т.Н., Бежитадзе Д.Т., Тавадзе Г.Ф. и др. Способ получения станида ниобия. Авторское свидетельство СССР. №1453928.

[11] Тавадзе Г.Ф., Бежитадзе Д.Т., Нацвлишвили Т.Н. и др. Удельное электросопротивление и магнитная восприимчивость сверхпроводящего соединения ErBa2Cu3O6,69 синтезированного в режиме горения. Сообщения АН ГССР, 131, №1, 1988, с.98-100.

[12] Кутелия Э.Р., Асатиани Д.Ш., Цивцивадзе Д.Т., Тавадзе Г.Ф. и др. Морфологические особенности сверхпроводящего соединения ErBa2Cu3O6,69 полученного методом СВС. Сообщения АН ГССР, 133, №1, 1989, 125-127.

[13] M.Poladashvili, G.Tavadze, G.Oniashvili, A.Khvadagiani, Z.Aslamazashvili, G.Zakharov. Innovation combined nanotechnology ERI/SHS and the system ER-2S. Book of Abstracts, УДК 534.222.2536.469544.45T29 ISBN 978-5-9903212-3-6, 2016.

[14] G.Tavadze, T.Namicheishvili, G.Oniashvili. Method of receiving inorganic materials manufactures from powder exothermic charges. Patent of Georgia p 6541.

NUMERICAL MODELLING OF FLAME TEMPERATURE OF GEL SOLUTION COMBUSTION SYNTHESIS OF NANOCRYSTALLINE NICKEL-BASED CATALYST AND COMPARISON WITH EXPERIMENTAL DATA

O. Thoda,[1,2] G. Xanthopoulou,[1,2] V.Prokof'ev,[3] G. Vekinis,[1] A. Chroneos,[2,4]

[1]Institute of Nanoscience and Nanotechnology, NCSR "Demokritos", Agia Paraskevi Attikis, 15310, Greece
[2]Faculty of Engineering, Environment and Computing, Coventry University, Priory Street, CV1 5FB, UK
[3]Tomsk State University, 36, Lenin Ave, Tomsk,634050, Russia
[4]Centre for Manufacturing and Materials Engineering, Coventry University, Priory Street, CV1 5FB, UK
g.xanthopoulou@inn.demokritos.gr

Nickel, an important hydrogenation catalyst, was successfully synthesized by Gel Solution Combustion Synthesis (G-SCS) from a gel containing nickel nitrate (66.7%) and glycine (33.35%) at 500, 600, 650 and 700ºC. The combustion temperature of solution combustion reaction plays a significant role in phase formation and physical characteristics of the products and depends on various process parameters. XRD results of the resulting Ni/NiO catalysts are presented in Figure 1 synthesised at various temperatures.

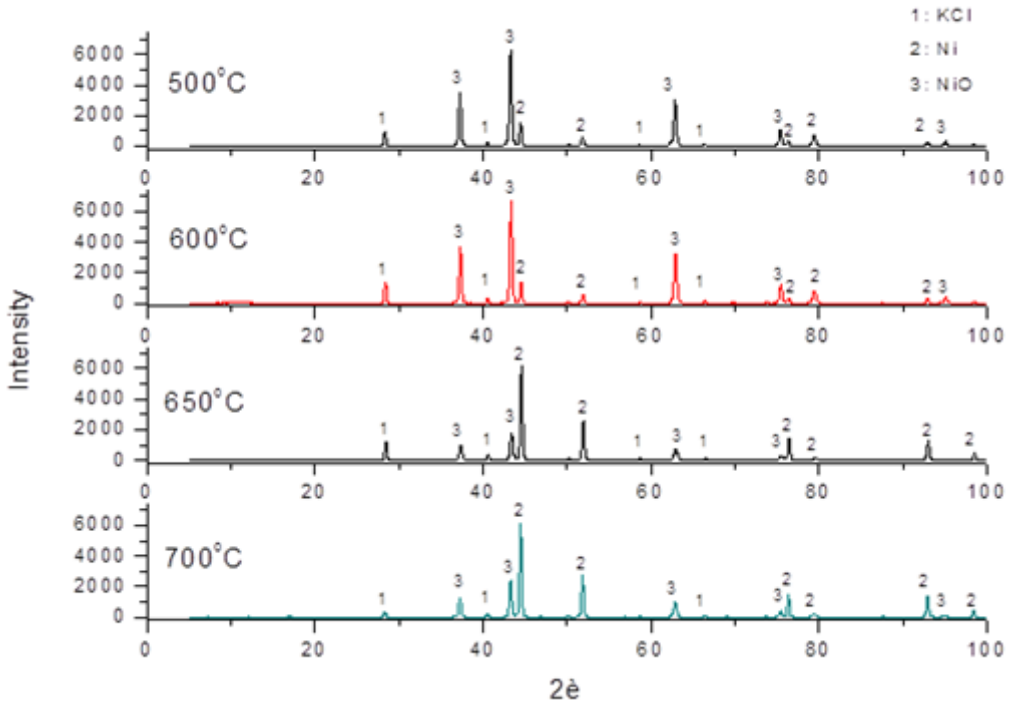

Figure 1 - XRD spectra of Ni-NiO SCS catalysts produced at different temperatures

Formation of Ni and NiO during G-SCS can be explained by a multi-branch reaction cascade, based on the general equation: $2Ni(NO_3)_2 \cdot 6H_2O + C_2H_5NO_2 \rightarrow Ni + NiO + NO_2 + 2NO + N_2 + 2CO_2 + 29/2\ H_2O + 5/2O_2$

The influence of the furnace's preheating temperature on the catalysts' composition is shown in Figure 2 which indicates that increasing the preheating temperature results in increased nickel concentration in the final G-SCS product.

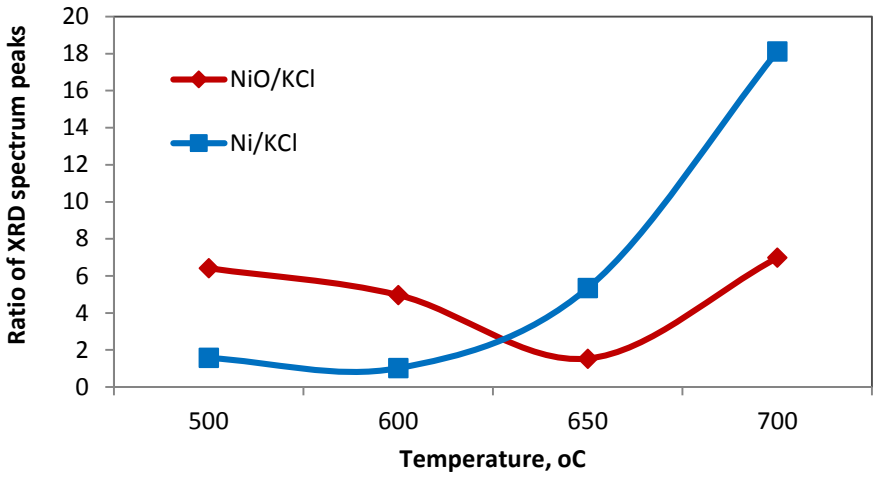

Figure 2 - Influence of preheating temperature on the composition of G-SCS catalysts.

Following these observations, an attempt has been made to analytically model (using the Semenov method) and evaluate the influence of preheating temperature on the flame temperature as well as on the physico-chemical characteristics of the products. During modelling the following assumptions are made:

1. The SCS mixture (nickel nitrate + glycine) is homogeneous and its temperature depends only on time, which corresponds to zero-dimensional formulation of the problem.

2. Any relative movements of the different phases are neglected.

3. The formation and release of gaseous products are solely determined by the change in mass of the solution.

The simplest model to describe this behaviour is that developed by Semenov [1]. In accordance with accepted assumptions, the model includes:

Equation of heat balance

$$c_{eff}(T)m(\eta)\frac{dT}{dt} = S\alpha(T_{fur} - T) + Qm(\eta)(1-\eta)k_0 \exp(-E/RT); \quad (1)$$

Effective heat capacity function

$$c_{eff}(T) = c_0 + Q_{vap}\delta(T - T_{vap}), \quad (2)$$

where the c_{eff} formulation allows the heat consumed to be utilised by the phase transition as described for melting in [2]);

Equation for evolution of condensed mass

$$m = m_0 - (m_0 - m_s)\eta; \quad (3)$$

Chemical kinetics equation

$$\frac{d\eta}{dt} = (1-\eta)k_0 \exp(-E/RT). \quad (4)$$

with the initial conditions: $T(0)=T_0$, $\eta(0)=0$, $m(0)=m_0$ (5)

where: δ(T) is the Dirac delta function, K^{-1}; Q_{vap} is the latent heat of phase transition, $kJkg^{-1}$; T_{vap} is the temperature of phase transition, K; c_0 is condensed-phase heat capacity without phase transition, $kJkg^{-1}K^{-1}$; η is the depth of conversion; S is the area of the bottom of the container, m^2; α is the heat transfer coefficient, $Wm^{-2}K^{-1}$; T_{fur} is the furnace pre-heating temperature, K; Q is the heat of reaction, $kJkg^{-1}$; E is the activation energy, $kJmol^{-1}$; R is the universal gas constant, $Jmol^{-1}K^{-1}$; k_0 is the pre-exponential factor, s^{-1}; m_0 is the initial mass of the mixture, kg and m_s is the mass of the solid products (Ni+NiO), kg.

The formulated equations (1) - (5) can only be solved numerically. By numerical optimisation the parameters were found to be: c_0=2.64; φ=0.19; Q_{vap}=2260; T_{vap}=430; c_0=2.64; S=0.006; α=200; T=773÷973; Q=1050; E=150; $k_0=10^{11}$; m_0=0.014; m_s=0.0032. The calculation results according to the system of equations (1) - (5) are presented in Fig. 3.

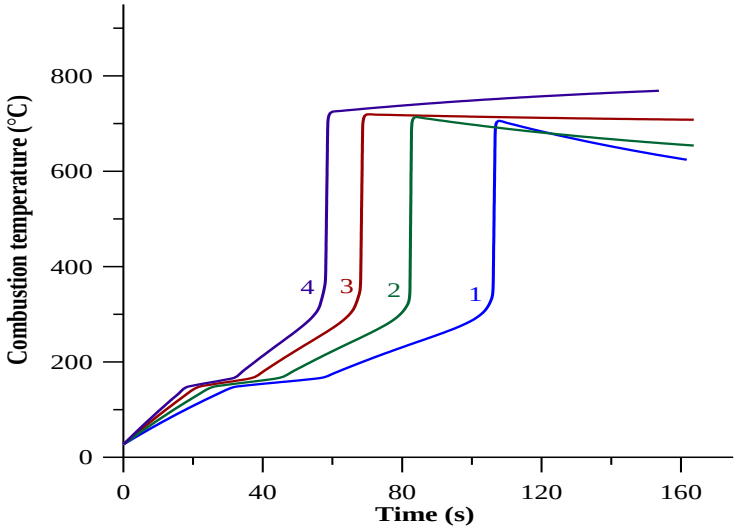

Fig.3 - SCS combustion temperature in the glycine - $Ni(NO_3)_2$ system as a function of time for four furnace temperatures: 1: T_{fur}=500 °C; 2: T_{fur}=600 C; 3: T_{fur}=700 °C and 4: T_{fur}=800 °C

A characteristic feature of the change in temperature with time is the isothermal region corresponding to the phase transition temperature T_{vap}. The short duration of this region is a potential barrier for the main synthesis reaction. The temperature of the furnace T_{fur} determines the heating rate of the mixture and, due to the nonlinear behaviour of the system, the time for complete conversion to η = 1 sharply decreases with increasing furnace temperature, as shown in Figure 4 in comparison with experimental results. This means that the combustion temperature of the system depends little on T_{fur}, in contrast to the classical version of SHS where the combustion temperature depends on the initial temperature [3].

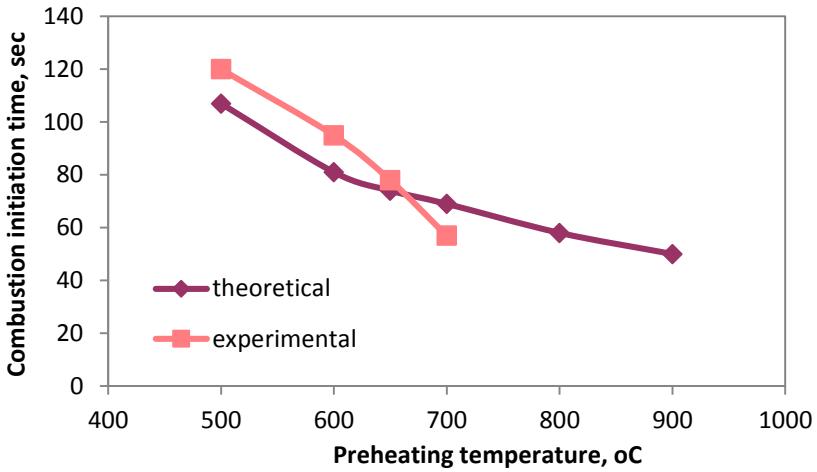

Fig.4 - Influence of preheating temperature on the time of combustion initiation.

The adequacy of the above model was checked by experimental data which are presented on Figure 5.

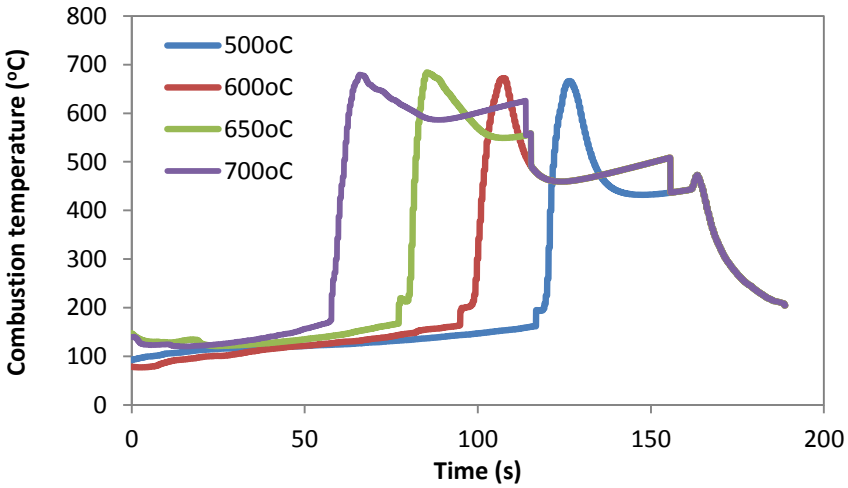

Fig.5 - Influence of preheating temperature on the combustion temperature.

The numerical modelling showed that the system's combustion temperature (both calculated and experimental) is only slightly influenced by T_{fur}, (Fig.3 & 5), in contrast to the classical version of SHS [3], where the combustion temperature depends strongly upon the initial pre-heating temperature.

REFERENCES

[1] N. N. Semenov, Some Problems in Chemical Kinetics and Reactivity. Parts 1 and 2, Pergamon Press, London [1959].

[2] V. G. Prokof'ev, V. K. Smolyakov, Non-stationary combustion regimes in gasless systems with a low-melting inert component, Combust. Explosion Shock Waves, 38, (2002), 143.

[3] A. G. Merzhanov, B. I. Khaikin, Theory of combustion waves inhomogeneous, Prog Energy Combust Sci, 14, (1988), 1–98 .

DEVELOPMENT OF SOLUTION COMBUSTION SYNTHESIS TECHNOLOGY FOR NICKEL-BASED HYDROGENATION CATALYSTS

O. Thoda,[1,2] G. Xanthopoulou,[1,2] G. Vekinis,[1] A. Chroneos,[2,3]

[1]Institute of Nanoscience and Nanotechnology, NCSR "Demokritos", Agia Paraskevi Attikis, 15310, Greece
[2]Faculty of Engineering, Environment and Computing,Coventry University, Priory Street, CV1 5FB, Coventry, UK
[3]Centre for Manufacturing and Materials Engineering, Coventry University, Priory Street, CV1 5FB, UK
g.xanthopoulou@inn.demokritos.gr

Solution Combustion Synthesis is a versatile method for the production of various materials directly in the nanoscale. The main source of heat comes for the exothermic combustion reactions that take place once the water in the solution has evaporated, so it is a self-sustaining thermal synthesis process [1]. It is already widely used to prepare catalysts for laboratory and industrial purposes, due to the advantages it offers. On the other hand, SCS is a very sensitive synthesis method and in this work an effort was made to investigate the main parameters that influence the final products' composition and properties.

Nickel nitrate hexahydrate ($Ni(NO_3)_2 \cdot 6H_2O$) and aluminium nitrate nonahydrate ($Al(NO_3)_3 \cdot 9H_2O$) were used as oxidizers and glycine as the reducer. In most cases distilled water was added to the initial gel mixture to facilitate mixing prior to SCS. The parameters that were investigated during this work were:

- water quantity in the initial SCS mixture,
- pre-treatment of water used in the initial SCS mixture,
- duration of heated stirring as a pre-treatment for SCS initial solution,
- fuel (reducer) to oxidizer ratio and total fuel concentration in the initial SCS mixture
- preheating temperature,
- heating mode during SCS, and
- time in furnace after SCS was completed.

All produced catalysts were tested for catalytic liquid-phase hydrogenation of unsaturated hydrocarbons in order to investigate the effect of the synthesis parameters on the catalysts' catalytic behaviour. It was concluded that all the parameters above influence the SCS process and subsequently the final products' composition and activity in the hydrogenation process, as shown in Figure 1.

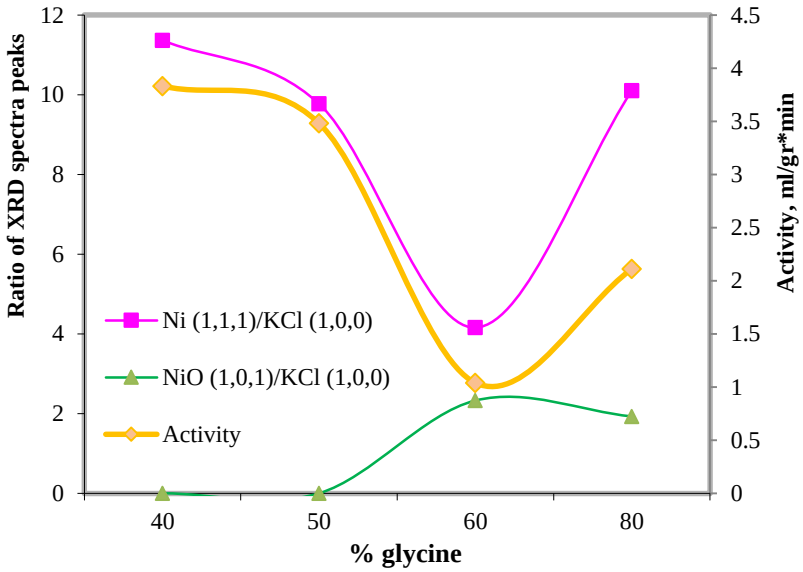

Figure 1 - Dependence of the catalysts' composition and catalytic activity on amount of glycine in an initial SCS mixture of $Ni(NO_3)_2$, glycine in 75ml H_2O.

The structural properties of the products such as crystallite size and crystal lattice spacing were also influenced by the synthesis parameters. Typical examples of structural changes and varying catalytic activity of the SCS catalysts produced shown in Figures 2 and 3.

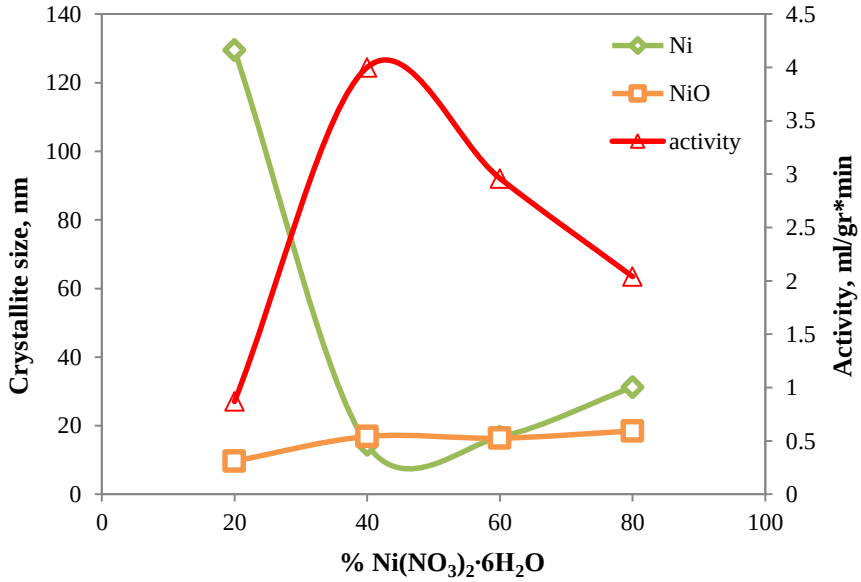

Figure 2 - Influence of $Ni(NO_3)_2 \cdot 6H_2O$ concentration in the initial SCS mixture ($Ni(NO_3)_2$ + $Al(NO_3)_3$, 40% glycine, 75ml H_2O) on the Ni & NiO crystallite size and catalytic activity in liquid-phase hydrogenation.

Furthermore, the specific surface area - is a critical parameter for nanomaterials and especially catalysts –was also studied. The influence of glycine concentration in the initial SCS mixture and the heating mode (directly in a pre-heated furnace at 500°C or placed in the

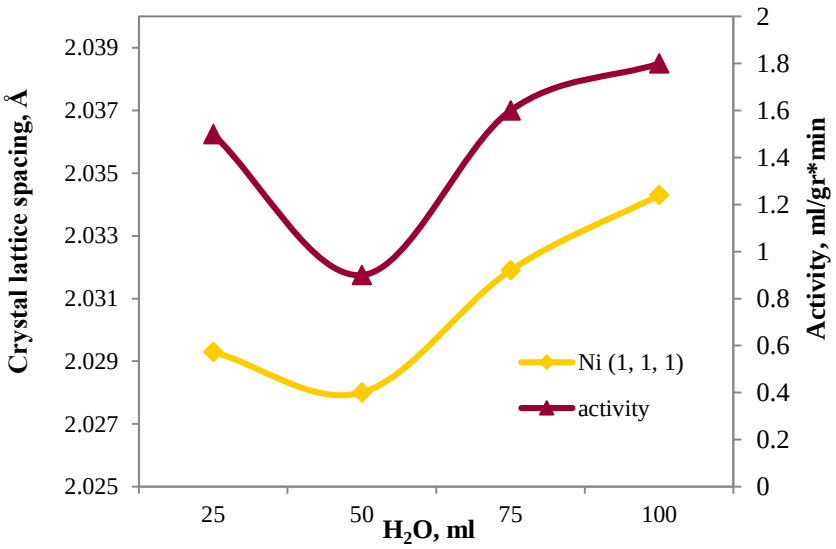

Figure 3 - Influence of water quantity in SCS mixture (66,7% $Ni(NO_3)_2$*$6H_2O$, 33,3% glycine, water) on crystal lattice spacing and activity

furnace at room temperature and heating up to 500°C with approximately 7-7.5°C/min heating rate) of the initial solution of $Ni(NO_3)_2$, glycine in 75 ml distilled water on the catalysts' specific surface area and activity in liquid-phase hydrogenation is presented in Figure 4.

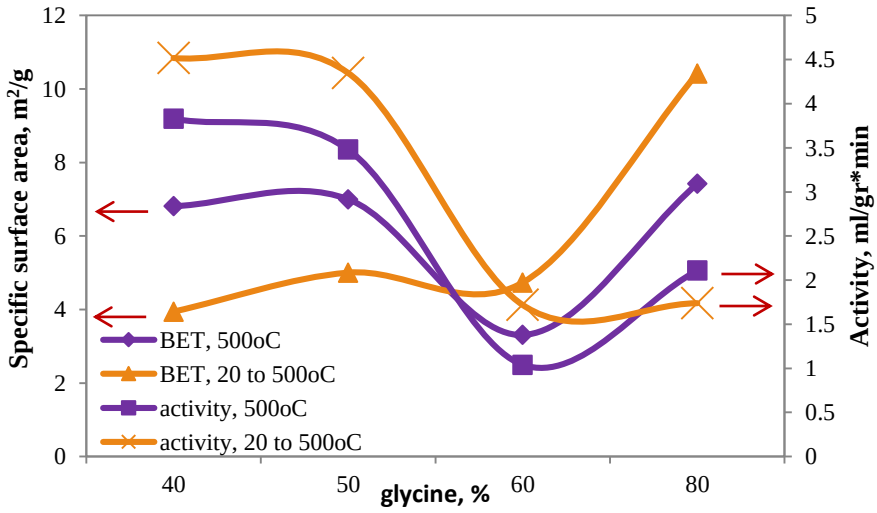

Figure 4 - Influence of glycine concentration in the initial SCS solution and heating mode on the catalysts' surface area and activity

As shown on Figure 5, changes in the fuel/oxidizer ratio have a large effect on the BJH adsorption pore size distribution (Harkins – Jura calculation) and the total porosity of the materials. In Figure 5 the lowest and the highest ratios only are included, in order to point out the significant differences between those cases.

Figure 6 depicts the time-variation of the probability density function, $\varphi(\varepsilon;t)$, of the local adsorption energy, ε, and the points where a local minimum in each graph $\varphi(\varepsilon;t)=\varphi(t)$ is found which are the points distinguishing the different types of each catalyst's active sites.

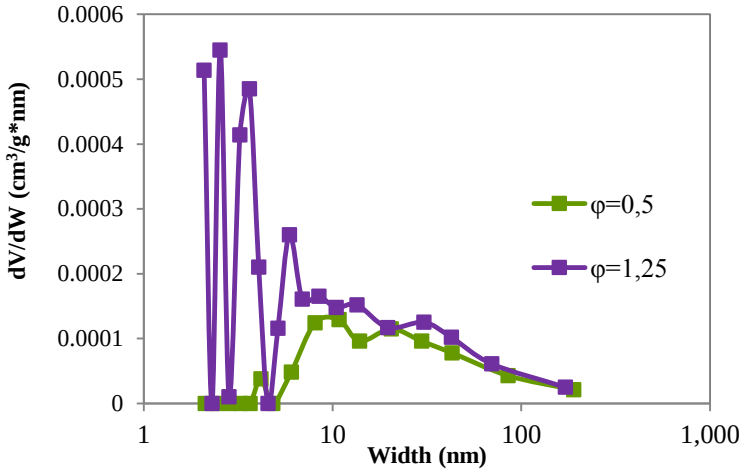

Figure 5 - Influence of fuel to oxidizer ratio on Ni catalysts' BJH adsorption pore distribution

Analysis of these results show that up to four different kinds of active sites (A, B, C, D) are fully activated and clearly distinguishable for each of the catalysts made with 100 ml, 25ml and 75 ml water [2].

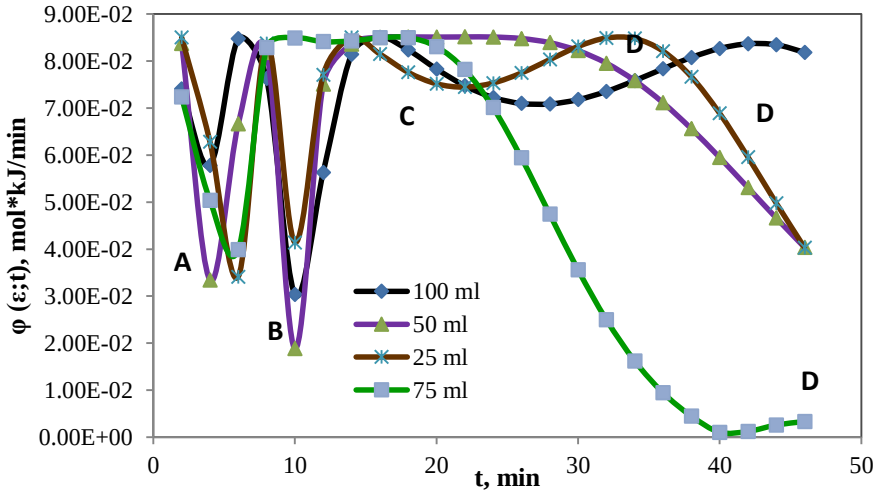

Figure 6 - Surface topography of catalytic active sites for SCS catalysts prepared with four different water quantities in their initial solution, at 80°C

As a general conclusion of this on-going work, SCS has been shown to be a very effective method to synthesize catalysts for the hydrogenation process. On the other hand, it is very sensitive to many synthesis parameters which have a major influence on the properties of the final products in a very complex way.

REFERENCES

[1] A. Varma, A. S. Mukasyan, A. S. Rogachev, K. V. Manukyan, Solution Combustion Synthesis of Nanoscale materials, Chem. Rev. , 116, 23, (2016) , 14493–14586.

[2] G. Xanthopoulou, O. Thoda, E. D. Metaxa, G. Vekinis, A. Chroneos, Influence of atomic structure on the nano- nickel-based catalysts activity produced by Solution Combustion Synthesis in the hydrogenation of maleic acid, J. Catal., 348, (2017), 9-21.

ON THE VERSATILITY OF MICROWAVES IGNITION IN SOLUTION COMBUSTION SYNTHESIS: THE CASE OF NICKEL NITRATE – GLYCINE SYSTEM

L. Trombi*, R. Rosa, P. Veronesi, C. Leonelli

[1] Dipartimento di Ingegneria Enzo Ferrari, Università degli Studi di Modena e Reggio Emilia, via P. Vivarelli 10, 41125 Modena, Italy
* lorenzo.trombi@unimore.it

In recent years many researches focused on Solution Combustion Synthesis (SCS) of nano-sized ceramic (e.g. oxides and perovskites) and metallic powders (in the form of elemental or alloyed metals). The SCS technique consists in a number of self-sustained reactions occurring typically in a water solution. This solution is composed by an oxidizer, usually a metal nitrate and a fuel, like a water-soluble linear or cyclic organic amine, acid and/or amino-acid [1]. This allows a combustion reaction particularly efficient to occur in a homogenous and extremely rapid way, which can be easily exploited on an industrial scale, in order to obtain nano-structured powders at a significant lower cost compared to other synthetic routes.

The aim of this study is to deeply investigate the peculiar ignition mechanism represented by the use of microwave energy on a well known and well conventionally studied [1] system, i.e. the reactive mixture composed by nickel nitrate oxidizer and glycine fuel.

Indeed, starting from the measurement of the dielectric properties of the different starting reactive mixtures as a function of fuel to oxidizer ratio, all of the different possibilities offered by the use of scientific single-mode microwave applicators will be investigated.

Particularly the effect of the incident frequency, the disposition of the load inside the applicator, the exploitation of pulsed electromagnetic energy, the continuation in irradiating the sample after the ignition, the use of a coaxial cable to realize a real SHS, on the combustion synthesis parameters and consequently on the products structure and composition will be presented.

REFERENCES

[1] K. V. Manukyan, A. Cross, S. Roslyakov, S. Rouvimov, A. S. Rogachev, E. E. Wolf and A. S. Mukasyan, J. Phys. Chem. C, 117, 2013, pp. 24417−24427.

A NOVEL PREPARATION TECHNIQUE OF METAL AND METAL OXIDE HOLLOW MICROSPHERES BY SPRAY SOLUTION COMBUSTION SYNTHESIS

Trusov G.V. *[1,3], Tarasov A.B.[2,3], Roslyakov S.I.[3], Rogachev A.S.[1,3], Mukasyan A.S.[3,4]

[1] Institute of Structural Macrokinetics, Russian Academy of Sciences RAS, Chernogolovka, Russia;
[2]Lomonosov Moscow State University, Moscow, Russia;
[3]National University of Science and Technology "MISIS", Moscow, Russia;
[4]University of Notre Dame, USA
* german.v.trusov@gmail.com

Pure metal and metal oxide nanoparticles are most demanded materials for scientific and industrial applications. They are widely used also in different forms and modifications as pigments, conducting paints, catalysts, magnetic recording media, for medical purposes in magnetothermia etc [1]. Although many different approaches are developed to obtain such nanoparticles with required properties, any new technique allowing a direct synthesis of single-phase nanomaterials still attracts a significant attention.

As it has been shown, a "solution combustion" technique (SCS) is one of the most promising candidate for different magnetic pure metal and oxide materials production with controllable properties, like iron oxides [2] or pure nickel. The method is based on the usage of highly exothermic self-sustained redox reactions between metal nitrates and organic "fuels", which are mixed on a molecular level in aqueous solution. Heating of reaction solution leads to water evaporation and formation of a homogeneous reactive mixture, followed by reaction initiation with rapid heat release. The intensive adiabatic self-heating of the environment and appearance of a great amount of gaseous products facilitates the formation of oxide or even pure metal nanocrystalline aggregates. The further development of the method requires to overcome aggregation of the resulted nanoparticles.

In this work we propose a hybrid technique for the synthesis of oxides and metals based on the method of the aerosols pyrolysis and solutions combustion synthesis (Figure 1), using inexpensive starting reagents and allowing to affect on the specific surface area, the crystallinity of the samples, and also introduce alloying additives to produce composites.

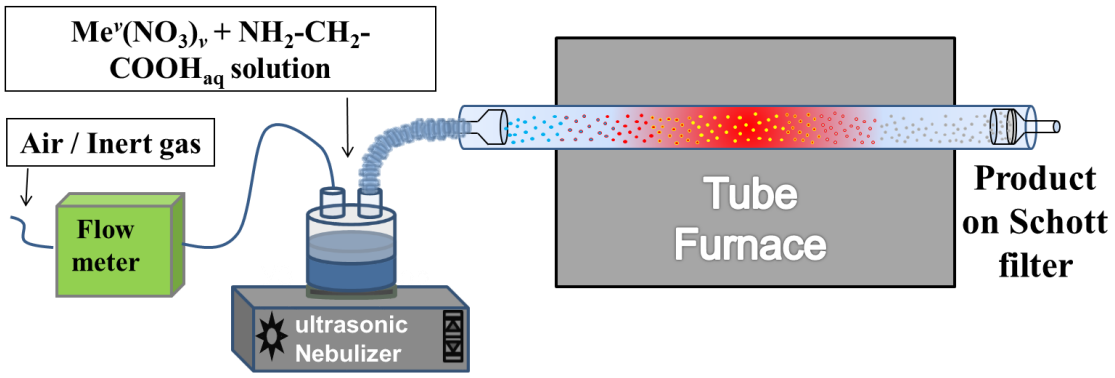

Figure 1 - Scheme of the installation of synthesis of microspheroidal particles

The classical method of the aerosols pyrolysis implies the spraying of the initial reagents and the subsequent thermal decomposition in various hardware design of the installation. Spray

reagents are commercially available or pre-synthesized in the laboratory. A feature of the proposed procedure is the presence of the fuel in the initial reaction mixture. As a result of the mixture passage through a tube furnace an exothermic reaction occurs on the droplets of the water aerosols leading to the formation of the oxides or metals and crystallization of the product.

A new modification of the SCS method was proposed: spray solution combustion synthesis for the obtaining nanostructured metal hollow microspheres. The furnace temperature, the composition of the reaction solution, the carrier gas and its flow rate are critical parameters, which determines the phase composition of the resulting microspheres. By changing these parameters, it is possible to obtain pure Ni and Cu metals (Fig. 2), pure oxides (NiO, Cu_2O) or a mixture of these phases.

We have developed the solution combustion reaction in the individual micron-size droplets of ultrasounic - generated aerosols using an oxidizer and fuel, namely iron, nickel and copper nitrates and glycine. An aqueous reaction solutions were nebulized in a preheated to 400-800^{o}C quartz tube furnace using ambient air or argon as a carrier gas to produce well dispersed powders with magnetic properties. Phase composition, morphology and optical properties of resulted powders were studied by XRD, SEM, TEM and BET techniques. All powders were found to contain metal or metal oxide phases depending on synthetic conditions and consisted of non-aggregated hollow micron - sized spheres with a complex internal structure. All oxide products demonstrated high values of specific surface area. Based on the obtained results, the possible reaction mechanism was proposed what could help to develop the synthetic conditions for a direct synthesis of another metal and oxide materials.

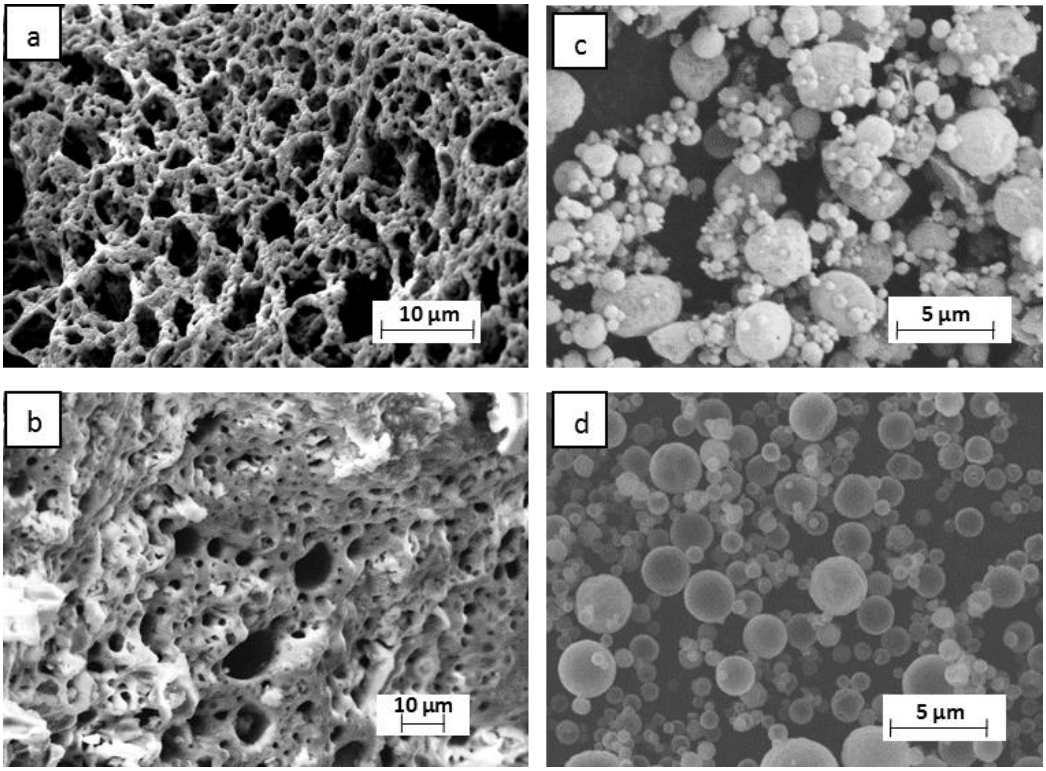

Figure 2 - SEM images of the pure nickel (a and c), copper oxide (b and d) obtained via convention SCS (a, b) and Solution Combustion in Aqueous Aerosols (c, d) techniques.

It was shown that the outer diameter of the sphere is primarily determined by the diameter of the initial droplets formed by the ultrasonic nebulizer. The observed thickness of the microsphere wall varies in the range of 20-50 nm. The developed method is rather universal and allows synthesizing various hollow microspheres, including pure metals such as Cu, Ni, Co, and metal alloys (NiCu, NiFe, CoCu, etc.), as well as almost all known oxides.

The authors gratefully acknowledge the financial support of the Ministry of Education and Science of the Russian Federation in the framework of Increase Competitiveness Program of NUST «MISiS» (№ К2-2016-065), implemented by a governmental decree dated 16th of March 2013, N 211.

REFERENCES

[1] Metal Nanoparticles: Synthesis, Characterization, and Applications, L.F. Daniel, A.F. Colby, CRC Press, 2001, p. 352.

[2] K. Deshpanda, A. Mukasyan, A. Varma, Direct Synthesis of Iron Oxide Nanopowders by the Combustion Approach: Reaction Mechanism and Properties, Chem. Mater., 16, 2004, p. 4896.

PREPARATION OF HIGHLY POROUS METAL MATERIAL BASED ON NICKEL HOLLOW MICROSPHERES BY SPARK PLASMA SINTERING

Trusov G.V. *[1,3], Tarasov A.B.[2], Moskovskih D.O.[3], Rogachev A.S.[1,3], Mukasyan A.S.[4]

[1] Institute of Structural Macrokinetics, Russian Academy of Sciences RAS, Chernogolovka, Russia;
[2]Lomonosov Moscow State University, Moscow, Russia;
[3]National University of Science and Technology "MISIS", Moscow, Russia;
[4]University of Notre Dame, USA
* german.v.trusov@gmail.com

Nickel are most demanded oxide materials for scientific and industrial applications. They are widely used in different forms and modifications as catalysts, magnetic materials, for medical purposes [1]. Although many different approaches are developed to obtain nickel with required properties, any new technique allowing a direct synthesis of single-phase materials still attracts a big attention.

As it has been shown recently, a "solution combustion" technique is one of the most promising candidate for nickel production with controllable properties [2]. The method is based on the usage of highly exothermic self-sustained redox reactions between metal nitrates and organic "fuels", which are mixed on a molecular level in aqueous solution. Heating of reaction solution leads to water evaporation and formation of a homogeneous reactive mixture, followed by reaction initiation with rapid heat release. The intensive adiabatic self-heating of the environment and appearance of a great amount of gaseous products facilitates the formation of oxide nanocrystalline aggregates. The further development of the method requires to overcome aggregation of resulted nanoparticles.

In present work, we have developed the solution combustion reaction in the individual micron-size droplets of ultrasounic - generated aerosols using an oxidizer and fuel, namely nickel nitrate and glycine. An aqueous reaction solution was nebulized in a preheated to 800^{o}C quartz tube furnace to produce gray powder depending on preparation temperature and aerosol flow velocity. Phase composition, morphology and optical properties of resulted powders were studied by XRD, SEM, TEM and BET techniques. The magnetic powder obtained at high temperatures or low flow velocity was found to be a well crystalline single-phase nickel. Powder consisted of non-aggregated hollow micron - sized spheres with a complex internal structure. All oxide products demonstrated high values of specific surface area.

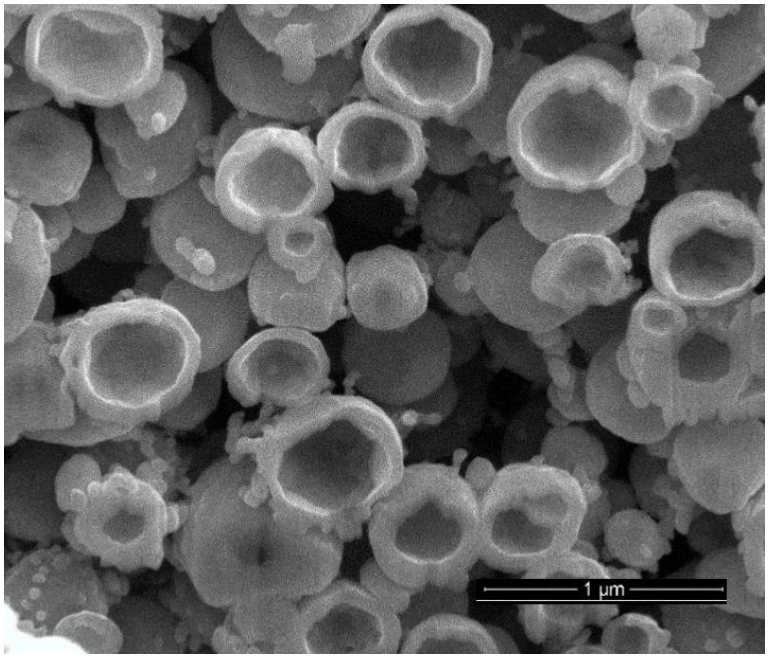

Fig. 1 - SEM images of the sintered nickel microspheres by spark plasma sintering (SPS) without pressure.

Metallic porous materials on the basis of fine nickel powders are used as an insulating material in the thermal protection systems (TPS) on reusable carrier rocket. Outer cover of the carrier rocket made from such porous materials increases it thermal protection system from the aerodynamic surface heating to the temperatures up to 1000 °C.

To obtain such a new material, synthesized nickel powder sinters to create a cellular structure (fig.1) of metal microspheres in which instead of intercrystalline volumetric macropore perform internal cavity of the microspheres, the shell of which are connected by a necks due to the sintering process. Thermal conductivity measurement results shows that metal the samples sintered from the nanothin-walled nickel microspheres have an extremely low thermal conductivity, which proves their use as materials for thermal protection.

The authors gratefully acknowledge the financial support of the Ministry of Education and Science of the Russian Federation in the framework of Increase Competitiveness Program of NUST «MISiS» (№ К2-2016-065), implemented by a governmental decree dated 16th of March 2013, N 211.

REFERENCES

[1] S.T. Aruna, A.S. Mukasyan, Combustion synthesis and nanomaterials, Current Opinion in Solid State and Materials Science, 12 (3), 2008, pp. 44-50.

[2] K. Manukyan, Allison Cross, S. Roslyakov, S. Rouvimov, A. Rogachev, Eduardo E. Wolf, and A. Mukasyan, Solution Combustion Synthesis of Nano-Crystalline Metallic Materials: Mechanistic Studies, J. Phys. Chem. C, 117 (46), 2013, pp. 24417–24427.

COMPOSITE MATERIALS PREPARED BY SELF-PROPAGATING COMBUSTION SYNTHESIS FOR CATALYTIC METHANE REFORMING

G. Xanthopoulou[1], S.A. Tungatarova*[2], K. Karanasios[1], T.S. Baizhumanova[2], Z.T. Zheksenbaeva[2], M. Zhumabek[2], G.N. Kaumenova[3]

[1]Institute of Nanoscience and Nanotechnology, NCSR Demokritos, Aghia Paraskevi,15310 Athens, Greece
[2]D.V. Sokolsky Institute of Fuel, Catalysis and Electrochemistry, 142 Kunaev str, 050010 Almaty, Kazakhstan
[3]al-Farabi Kazakh National University, Almaty, Kazakhstan
* tungatarova58@mail.ru

The SHS catalysts on the base of NiO-Al-α-Al_2O_3 were prepared from powder mixtures consisting of nitrates, metals, and oxides for catalytic methane reforming. The second series of catalysts was prepared by traditional method: samples were prepared by the incipient wetness impregnation of dispersed α-Al_2O_3. The resulting catalysts were characterized by XRD and SEM methods. Surface area of the samples was determined by BET method. During the SHS experiments the combustion velocity was measured.

SHS catalysts on the base of initial batch Al-NiO-Al_2O_3 but different ratio of components have a similar qualitative composition, but there are differences in the phase ratio. The proportion between the phases determined from the relative intensities of the X-ray diffraction peaks are shown in Fig. 1 and Fig. 2. At 52-53% Al and 26-27% NiO observed maximum yield of the reaction products: NiAl, $NiAl_2O_4$.

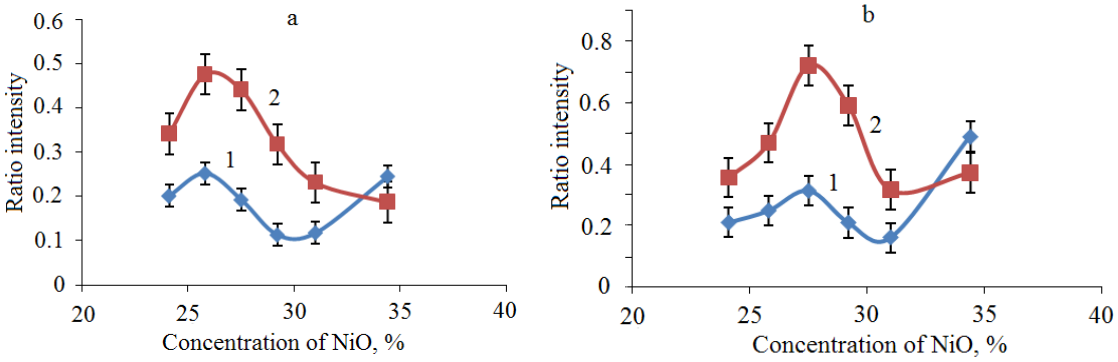

Fig. 1 - Dependence of concentrations ratio of different phases in SHS catalysts at change of NiO content in composition of initial batch NiO-Al-Al_2O_3. a: 1 – AlNi/Al, 2 – AlNi/NiO; b: 1 – $NiAl_2O_4$/Al, 2 – $NiAl_2O_4$/NiO

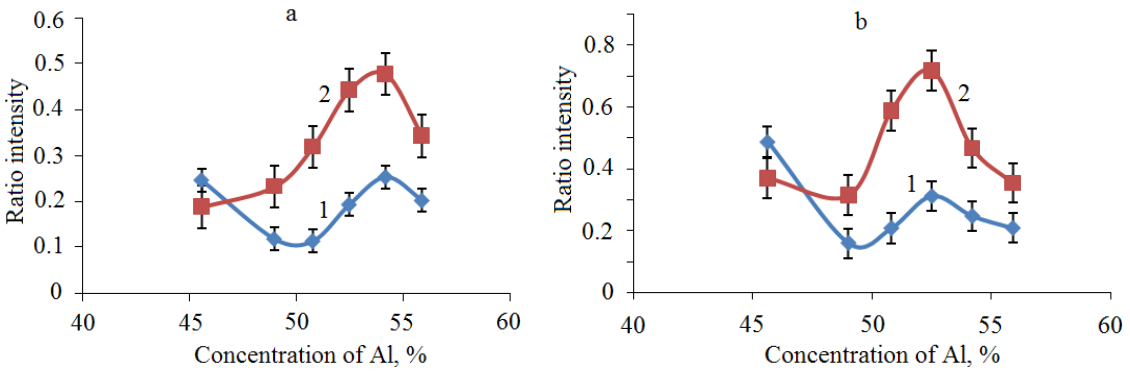

Fig. 2 - Dependence of concentrations ratio of different phases in SHS catalysts at change of Al content in composition of initial batch NiO-Al-Al_2O_3. a: 1 – AlNi/Al, 2 – AlNi/NiO; b: 1 – $NiAl_2O_4$/Al, 2 – $NiAl_2O_4$/NiO

Thus, changes in the composition of the initial batch results in a change in the phase ratio in SHS reaction products (Fig. 1 and Fig. 2).

Dependence of the combustion velocity from the initial batch composition was investigated. The increase of NiO concentration and decrease of the Al concentration in the initial charge increases combustion velocity. It is connected with approach the stoichiometric composition, and therefore a greater heat generation affects the increase in the reaction rate.

The maximum yield of products is not observed at the highest temperatures due to the fact that at higher temperatures there is a rapid oxidation of the metal and thus decreases the output of intermetallics. High temperatures (when there is more than 27% of nickel oxide and lower than 55% aluminum in the initial batch) affect the stabilization of the crystal lattice.

The study of SHS catalysts structure was carried out using a scanning electron microscope (catalysts with NiO: 24.1 and 34.4 wt% concentration in the initial batch). It was found that the phase analysis by method of chemical analysis is corresponding to the data of XRD analysis: Al, α-Al_2O_3, Al-Ni, Ni, NiO, $NiAl_2O_4$. Fig. 3 demonstrates analysis data for catalyst with initial batch composition: 24.1% NiO + 55.9% Al + 20% Al_2O_3. Chemical analysis was conducted for indicated in the photographs regions. Nickel, aluminum and oxygen ratio varies in different areas of catalyst. A high content of nickel, aluminum and oxygen corresponds to the spinel phase. The virtual absence of oxygen at a high content of nickel and aluminum corresponds to NiAl.

Thus, catalysts were synthesized on the base of the initial batch NiO-Al-α-Al_2O_3 and combustion characteristics, composition and structure of the obtained catalysts were studied.

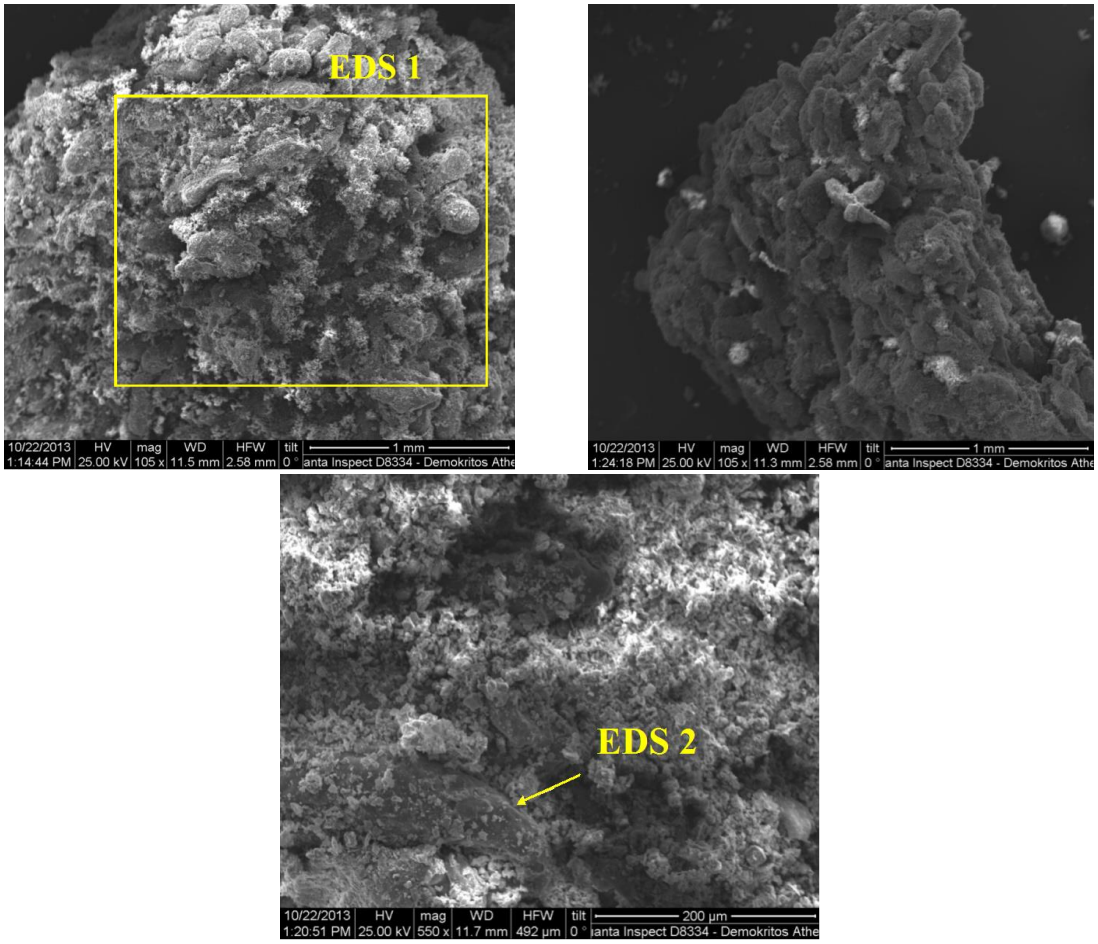

Fig. 3 - SEM catalyst photos on the base of initial batch: 24.1% NiO + 55.9% Al + 20% Al_2O_3 (furnace temperature T = 900°C)

Obtained SHS catalysts tested for catalytic activity in the carbon dioxide dry reforming of CH_4 at 750-900°C. The best results for SHS catalysts based on systems NiO-Al-Al_2O_3 are: 93% CH_4 conversion, 100% conversion of CO_2, product yield reaches 92% H_2 and 99% CO. H_2/CO ratio in the reaction product varies in the range of 0.7-1.35. Increasing the reaction temperature, in most cases, increases the ratio of H_2/CO due to the amplification of dehydrogenation reaction. Results for CO_2 and CH_4 conversion, H_2/CO ratio in the reaction products as well as H_2 and CO yields were studied for catalyst on the base of systems NiO-Al-Al_2O_3-MoO_3, Al-NiO-H_3BO_3, Al-Mg-NiO-Al_2O_3-MgO_2. It was shown that additives to NiO–Al-Al_2O_3 system did not lead to positive results.

Effect of catalyst composition on the conversion of CH_4, CO_2 and the ratio of H_2/CO seen in relation to the concentration of aluminum in the starting material. To maximize the yield of CH_4 the optimum aluminum content in the initial batch is 51% and for CO_2 – 51-56% of Al in the initial batch. Such effect also seen in relation to nickel oxide, because from nickel oxide concentration depends content of nickel spinel - active catalyst component. Comparing these data with those in Fig. 1 and Fig. 2, it can be concluded that the catalyst with 29% nickel oxide and 51% aluminum in the starting material, after the SHS reaction contains a maximal concentration of NiAl, $NiAl_2O_4$ active phases into carbon dioxide reforming of CH_4.

Effect of structural deformation and the composition of catalysts on the conversion of CH_4, CO_2 and H_2/CO (at 900°C) shown in Fig. 4.

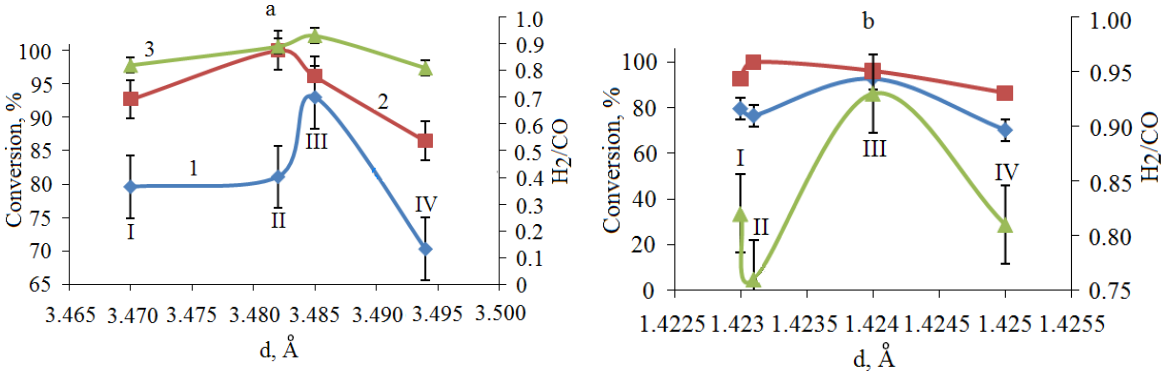

Fig. 4 - Effect of structural deformation and composition of catalysts on the conversion of CH_4, CO_2 and H_2/CO. a – Al_2O_3: I – 24.1% NiO, II – 25.8% NiO, III – 29.2% NiO, IV – 34.4% NiO; b – $NiAl_2O_4$, I – 24.1% NiO, II – 27.5% NiO, III – 29.2% NiO, IV – 34.4% NiO. 1 – conversion of CH_4, %, 2 – conversion of CO_2, %, 3 – H_2/CO. T = 900°C

Fig. 4 data indicate a clear structural dependence of the catalyst activity. The optimal lattice parameter for maximum conversion of CO_2 and CH_4 are 3.48 - 3.485 Å for aluminum oxide, which plays the role of a catalyst carrier and 1.42 Å - for $NiAl_2O_4$ playing the role of catalyst.

The study of catalysts of similar composition but prepared by the traditional method of wetness impregnation and further their comparison with SHS catalysts is very interesting. A series of catalysts was prepared by impregnation method: 24.1% NiO + 55% Al + 20% Al_2O_3, 25.7% NiO + 54.2% Al + 20% Al_2O_3, 27.5% NiO + 52.5% Al + 20% Al_2O_3, 29.2% NiO + 50.8% Al + 20% Al_2O_3. Investigation of catalysts was carried out under the following conditions: CH_4 : CO_2 : Ar = 1 : 1 : 1, GHSV - 860 h^{-1}. Analysis of the data shows that the conversion of feedstock has similar values both on SHS catalysts, and on traditional supported samples. However, target products yield is significantly higher for SHS catalysts: hydrogen yield is about 48-51% on the supported catalysts, and ~ 80% on SHS catalysts; CO yield is about 40-42% on supported catalysts, while about 90% on SHS catalysts. These data indicate a significant advantage of the new composite materials produced by combustion synthesis process. The obtained target products on above-mentioned catalysts are cleaner, which do not require additional treatment. SHS catalysts show higher activity in CH_4 partial oxidation, H_2 yields (52.0-67.0%) are higher compared with supported samples (53.9-57.2), and for CO - (21.0-27.1) instead of (21.9-24.2).

DENSITY FUNCTIONAL THEORY (DFT) MODELING AND EXPERIMENTAL INVESTIGATION OF THE PROPERTIES OF SHS-MATERIALS: THE CASE OF SOLID SOLUTIONS IN Ta-Zr-C SYSTEM

S.Vorotilo*, K.P. Sidnov, V.V. Kurbatkina, E.I. Patsera, E.A. Levashov

NUST MISIS, Leninsky Prospect str., 4, Moscow, Russia.
*s.vorotilo@misis.ru

Density Functional Theory (DFT) allows calculating of various properties of solids, including solid solutions. Aforementioned properties include crystal lattice parameters under various pressures, some mechanical properties (bulk modulus, shear modulus), optic properties, conductive properties, sound velocity, etc. The ability to calculate the properties of the desirable phase and then synthesize it will greatly enhance the effectiveness of development of new materials.

However, DFT(as well as all other models) has its restrictions. All calculations are made for 0 K temperature, micro- and nanostructure of the material is not taken into consideration, generated crystal units usually are not bigger than 100 atoms, These factors can cause major discrepancies between the calculated properties and real ones. Therefore, it is pivotal to assess the applicability of the DFT modeling for every class of materials of interest by comparing the calculated results with experimental ones.

In this work, solid solutions of refractory carbides in the Ta-Zr-C systems were chosen for the validation of DFT modeling approach. These solid solutions are perspective for use as ultra-high temperature ceramics (UHTC) due to their exceptional thermal and mechanical properties. Currently, there is no available modeling data for the solid solutions in the Ta-Zr-C system; in general, modeling data on the solid solutions is precious little. Predominant majority of modeling is dedicated to stoichiometric compounds, whereas in real materials solid solutions are ubiquitous. Therefore, validation of DFT for carbide solid solutions has a theoretical as well as practical value.

(Ta, Zr)C solid solution with 80 at.% TaC - 20% at.% ZrC were synthesized by the SHS because the SHS allows the production of solid solutions with the very homogeneous distribution of elements. Also, the calculation of enthalpy of formation of TaC, ZrC and (Ta, Zr)C may allow a better understanding of the phase transformation mechanisms during the SHS in Ta-Zr-C system.

The goal of this work was to calculate the enthalpy of formation, bulk modulus and crystal lattice parameter of 80 at.% TaC – 20 at.% ZrC solid solution and to compare the calculated results with the experimental ones.

Two equations were used to calculate the properties of 80%TaC-20%ZrC solid solution: Vinet's exponential equation and Birch-Murnaghan isothermic equation. 48 atoms cell was used for calculations (Fig. 1) with 6x6x6 K-points grid and Monkhorst-Pack integration scheme.

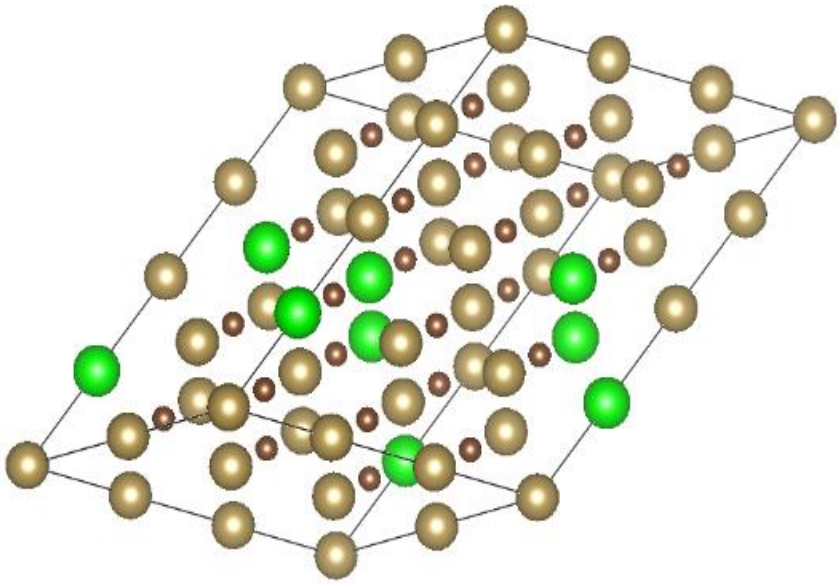

Figure 1 - 48 atoms FCC unit, used for calculations. Brown spheres represent tantalum, green spheres represent zirconium, dark spheres represent carbon.

We calculated the volume modulus B0, crystal lattice parameter and its dependence on external pressure, enthalpy of formation of TaC, ZrC as well as (Ta, Zr)C (table 1). Calculated results for TaC and ZrC were compared to available data. Crystal lattice parameter and bulk modulus for (Ta, Zr)C were compared to our experimental measurements, described in [1].

Table 1 - Calculated and experimental parameters for TaC, ZrC and 80%TaC-20%ZrC solid solution

Energy of formation					
Phase	Vinet equation, eV		Birch-Murnaghan equation, eV		Theoretical data from other sources, eV
TaC	-11,12		-11,12		11,12 [2]
ZrC	-9,73		-9,73		9,69 [2]
TaC-20%ZrC	-10,43		-10,43		-
Solid solution formation energy	eV	kJ/mol	eV	kJ/mol	-
	-0,01085	-0,00105	-0,01090	-0,00105	

Bulk moduli				
Phase	Vinet equation, GPa	Birch-Murnaghan equation, GPa	Theoretical data from other sources, GPa	Experimental data, GPa
TaC	321,75	323,98	323,94 [2]	329 [3]
ZrC	212,03	213,27	221,25 [2]	187-243 [3]
TaC-20%ZrC	271,93	274,27	-	272

Crystal lattice parameters				
Phase	Vinet equation, nm	Birch-Murnaghan equation, nm	Experimental data from other sources	Our experimental data
TaC	0,4478	0.4492	0,4482 [4]	0,4454
ZrC	0,4721	0,4737	0.4724 [4]	0,4686
TaC-20%ZrC	0,4491	0,4590	-	0,4493

Admixing enthalpy of 80%TaC-20%ZrC solid solution is equal to -1 J/mol, suggesting that solid solution formation is a very low-exothermic process. During the SHS, the formation of the solid solution must occur only after the formation of TaC and ZrC, due to the release of heat during the highly exothermic reactions of tantalum and zirconium with the carbon. This hypothesis is corroborated by the study of stopped combustion fronts in Ta-Zr-C system as well as dynamic XRD data [5]

Also, we can assume that 80%TaC-20%ZrC solid solution remains stable after the formation and does not undergo any phase transformations, albeit in Ta-Zr system there is a monotectoid transformation at 1073 K [6]

Conclusions: Modeling of properties of TaC, ZrC and 80%TaC-20%ZrC solid solution and comparison of modeling and experimental data shows the validity of DFT method for modeling of properties of solid solutions of carbides of refractory metals. Also, modeling data provides an insight into phase formation mechanisms during the SHS.

This work was carried out with partial financial support from the Ministry of Education and Science of the Russian Federation in the framework of state assignment No.11.1207.2017/ПЧ .

REFERENCES

[1] Kurbatkina V.V. et al. Conditions for Fabricating Single-Phase (Ta,Zr)C Carbide by SHS from Mechanically Activated Reaction Mixtures // Ceram. Int. Elsevier, 2016.

[2] Jain A. et al. The Materials Project: A materials genome approach to accelerating materials innovation // APL Mater. 2013. Vol. 1, № 1. P. 11002.

[3] Ultra-High Temperature Ceramics: Materials for Extreme Environment Applications // John Wiley & Sons/ed. William G. Fahrenholtz, Eric J. Wuchina,William E. Lee Y.Z. John Wiley & Sons, 2014. 441 p.

[4] Nakamura K., Yashima M. Crystal structure of (NaCl)-type transition metal monocarbides M C (M =V, Ti, Nb, Ta, Hf, Zr), a neutron powder diffraction study // Mater. Sci. Eng. B. 2008. Vol. 148. P. 69–72.

[5] Patsera E.I. et al. Production of ultra-high temperature carbide (Ta,Zr)C by self-propagating high-temperature synthesis of mechanically activated mixtures // Ceram. Int. Elsevier, 2015. Vol. 41, № 7. P. 8885–8893.

[6] B. Predel (auth.), O.Madelung. (ed). Pu-Re – Zn-Zr. 1st ed. Springer-Verlag Berlin Heidelberg, 1998.

SYNTHESIS OF TUNGSTEN AND TUNGSTEN ALLOYS NANOPARTICLES FOR TOKAMAKS

S. Dine[1], C. Grisolia[2], G. Peiters[3], B. Rousseau[3], N. Herlin[4], D. Vrel[1,*]

[1] LSPM, Université Paris 13, CNRS UPR 3407, 99 avenue Jean-Baptiste Clément, 93430 Villetaneuse, France
[2] CEA Cadarache, IRFM/SI2P/GCFPM, 13108 Saint-Paul-lez-Durance cedex, France.
[3] CEA Saclay, SCBM, iBiTec-S, Tritium Labelling Laboratory, Building 547, PC n°108, 91191 Gif-sur-Yvette, France
[4] CEA, IRAMIS-NIMBE, Laboratoire Francis Perrin (CEA CNRS URA 2453) et OMNT, Bat 522, CEA Saclay, 91191 Gif-sur-Yvette Cedex, France
* dominique.vrel@lspm.cnrs.fr

INTRODUCTION

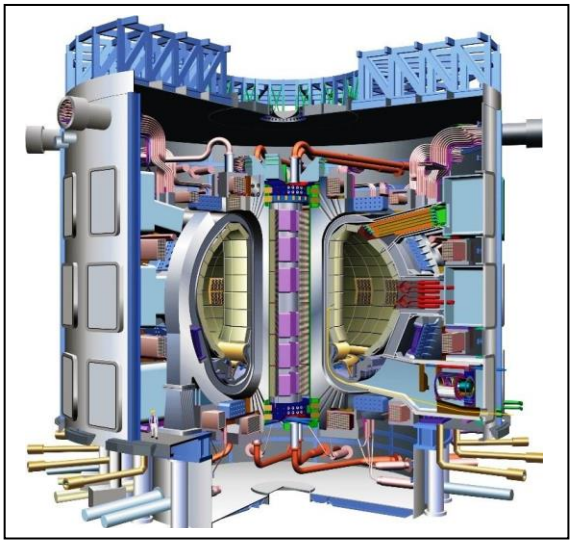

The ITER (meaning "the way" in Latin, at first an acronym for "International Thermonuclear Experimental Reactor") Reactor, which is still under construction in the south of France, will be the largest Tokamak to study the fusion reactions using magnetic confinement, according to the following mechanism:

$$^{3}_{1}T + ^{2}_{1}D \rightarrow ^{4}_{2}He + n + 17.6MeV$$

The bottom part of the reactor, which plays a key role in the magnetic confinement, is called the divertor. This part is the place where most of the particle bombardment will take place, and, as a result, the material chosen to build it must be highly resistant to sputtering. Moreover, because sputtering will occur anyway, it must have a small influence on the plasma stability, must not be subjected to hydride formation which would trap a significant amount of injected fuel, have a good thermal conductivity, a good thermal resistance, be insensitive to neutrons, etc. For these reasons, tungsten has been chosen as being the best compromise.

In a first series of experiments, we have been synthesizing tungsten nanoparticles by milling, mechanically activated SHS, and SHS, in order to understand their behavior [1]. Indeed, as sputtering will occur, it is dramatically important to control the amount of nanoparticles present within the reactor, as highly detrimental events could follow an accidental Loss Of Vacuum Accident (LOVA): particles might be set in suspension in the air, have an explosive behavior due to static electricity, or present fast, SHS-like oxidation due to the high temperatures. Periodical cleanups are therefore scheduled, and toxicological studies on these particles have been performed as human operators might get in contact with these particles [2]. In addition, we also studied the tritium retention of these particles [3].

Our studies focus today on the elaboration of tungsten and tungsten alloys in order to actually produce the plates which will be used within the reactor. It has been shown recently that tungsten could have a much lower Ductile-to-Brittle-Transition-Temperature (DBTT) if under

the form of nanoparticles, where a particle size of 700 nm would be small enough to lower this temperature to room temperature. Naturally, the addition of alloying elements could also improve this ductility enhancement. Rhenium is well known for such an improvement, however its price remains prohibitive. We will therefore choose other elements within the refractory metals family, Vanadium as a first step, but also Chromium for the enhancement this material may brings in the corrosion resistance of the resulting alloy.

TUNGSTEN SYNTHESIS

Tungsten powders were synthesized through thermite reactions from tungsten trioxide using magnesium as the reducer in the propagating mode of SHS, with the following reaction scheme:

$$WO_3 + 3Mg \rightarrow W + 3MgO$$

As our reactions happen at high temperature, far above magnesium boiling temperature, magnesium has to be used in excess to ensure the reaction completeness. The magnesium amount will then be referred to using its excess amount from the stoichiometry.

Adiabatic temperature is used as one of the parameters of our reactions. It is calculated from the database of the THERMO© program, using the reaction enthalpy and the heat capacities of the products. In addition, the heat capacities of the magnesium in excess and of a diluent used in our mixtures (NaCl) are considered. We therefore are adapting our mixtures to set these two parameters: (i) the excess magnesium and (ii) the adiabatic temperature.

Reaction is then started using a Joule heated tungsten coil either in air or under confinement. After reaction and cooling down of the sample, the diluent, excess magnesium and magnesia are completely removed by lixiviation in 2M HCl at 50°C for 2h, then filtered and rinsed with de-ionized water, and finally dried.

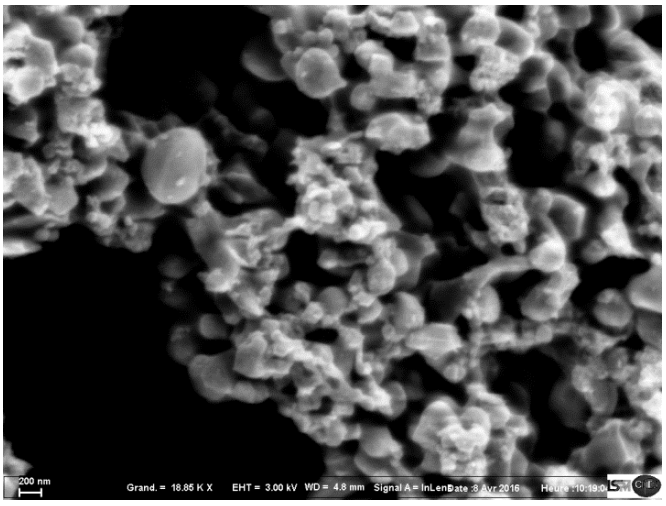

W powder, +100%Mg, T_{ad}=1800°C

We started with small sample yielding 2 grams of metal, for which it was necessary to add huge amounts of excess magnesium to get a good purity. Indeed, the surface/volume ratio for such a sample is large and magnesium could escape from the reaction zone too easily. For larger samples, 20 grams in air, then 20g under confinement and finally 50g under confinement, the needed amount of excess magnesium to provide pure W would decrease dramatically, below 25% (all masses are the final W masses, not including MgO, excess Mg nor NaCl). Both the increase of sample volume and confinement are thus favorable to yielding high purity powders, as shown on the XRD pattern below.

The morphologies of the resulting powders are presented in the micrograph below. Although the size of the resulting powder may vary with the experimental conditions, we may see on this figure that the final particles are in the nanometric range.

TUNGSTEN ALLOYS SYNTHESIS

Tungsten alloys were synthesized also through thermite reactions in the propagating mode of SHS, using, in addition to WO_3, Cr_2O_3 and V_2O_5, and adjusting the magnesium and NaCl amounts accordingly to control Mg excess and adiabatic temperature, following the reactions:

$$Cr_2O_3 + 3Mg \rightarrow 2Cr + 3MgO$$

$$V_2O_5 + 5Mg \rightarrow 2V + 5MgO$$

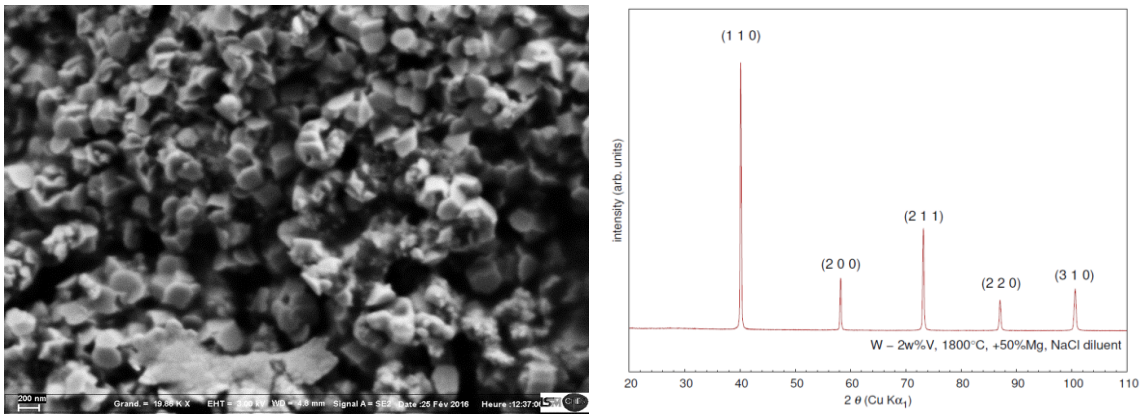

W-V2w% powder, +50%Mg, T_{ad}=1800°C

XRD results, figure below, reveal a homogeneous diffraction pattern. Although the peaks width might be due not only the small grain sizes but also composition gradients, no detectable intermetallic phase was found.

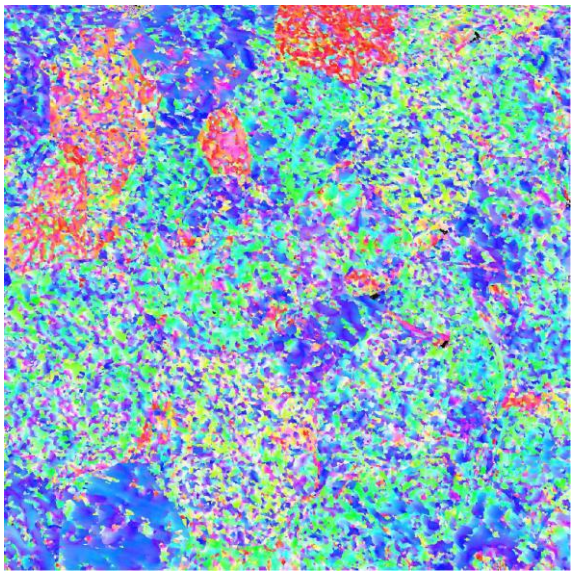

EBSD orientation map on a 60µm x 60µm square, showing apparent large grains with a fine nanometric substructure. Sample W-V4w% sintered for 5 minutes, 2000°C,

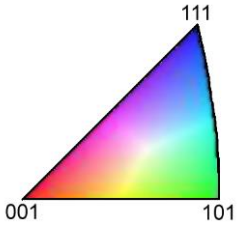

DENSIFICATION

Powders were then densified using SPS. This technique was chosen amongst others for its short duration time, allowing a limited grain growth. The densified samples were then characterized using XRD, SEM, EDS mapping and EBSD, which reveals an apparent large grained structure with a very fine nanostructure.

CONCLUSION

A complete set of results will be presented concerning tungsten and all the alloys mentioned as a function of their synthesis mode; moreover, preliminary results concerning mechanical properties on dense bulk materials will be shown.

REFERENCES

[1] S. Dine, S. Aïd, K. Ouaras, V. Malard, M. Odorico, N. Herlin-Boime, A. Habert, A.Gerbil-Margueron, C. Grisolia, J. Chêne, G. Pieters, B. Rousseau, D. Vrel, Advanced Powder Technology, 26 (2015) 1300-1305.

[2] A. El Kharbachi, J. Chêne, S. Garcia-Argote, L. Marchetti, F. Martin, F. Miserque, D. Vrel, M. Redolfi, V. Malard, C. Grisolia, B. Rousseau, International Journal of Hydrogen Energy, 39 (2014), p. 10525-10536.

Ni-BASED CATALYTIC COATINGS SYNTHESIZED BY IN-FLIGHT SCS DURING FLAME SPRAYING

A. Marinou, O. Thoda, G. Xanthopoulou*, G. Vekinis

Institute of Nanoscience and Nanotechnology, National Center for Scientific Research "Demokritos", Aghia Paraskevi Attikis, 15310, Greece
*g.xanthopoulou@inn.demokritos.gr

Solution Combustion Synthesis (SCS) is one of the most efficient techniques used to synthesize high selectivity catalysts directly in the nano-scale [1], including Ni-based catalysts which are widely used in various catalytic processes. Combustion-assisted flame spraying ("CAFSY") was recently developed to produce catalytically active nickel aluminide coatings on ceramic substrates [2]. The CAFSY process showed [3] that combustion synthesis occurs both in-flight as well as on the substrate. In this work we report on Ni-based catalysts produced by in-flight SCS during flame spraying, a novel method which combines conventional flame spraying and solution combustion synthesis into a single step. A fine spray of the aqueous SCS solution is inserted into the flame wherein the water is evaporated and the SCS catalyst is synthesized rapidly in the flame. The fine particles of nano-structured catalysts are then applied as coating on the Mg-Al-O carrier and penetrate very efficiently into all the surface pores. Figure 1 shows the schematic diagram of the in-flight SCS during flame spraying and presents the main parts of the novel arrangement.

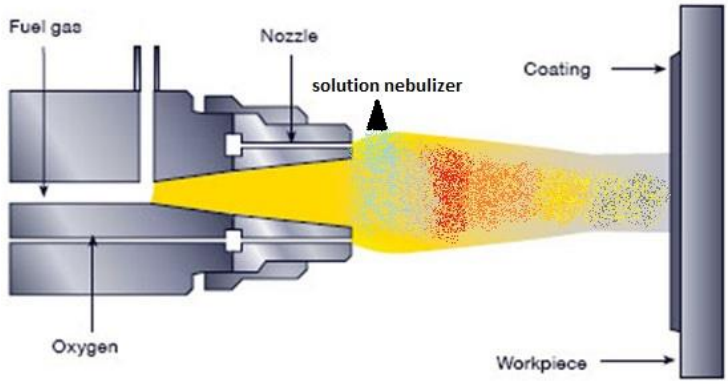

Fig.1 - Schematic diagram of in-flight SCS during flame spraying

The solution nebuliser inserts fine droplets directly into the hot zone of the flame, which is the main difference with the CAFSY method where powder mixtures are inserted in the flame. The fine spray droplets are evaporated immediately and the SCS-synthesised catalytic nano-powders are accelerated until they impact and penetrate into the spinel carrier. The oxyacetylene flame raises the temperature of the solution significantly almost instantaneously which triggers the exothermic SC process within the time available. This is significantly different from previously reported in-flight synthesis of catalysts using added methane gas to induce reaction [4].

In this work we report on nickel-based nano-catalysts synthesized by in flight Solution Combustion Synthesis (SCS) from starting solutions of nickel nitrate $Ni(NO_3)_2 \cdot 6H_2O$ with glycine as fuel in the ratio of 2:1. In order to facilitate the homogenization 100ml distilled water

was added to the initial SCS mixture. Flame spraying was carried out by a Sulzer's Metco Thermospray Gun (5P-II) and the solution was inserted into the flame using an adjustable nebuliser. The synthesized SCS nano-catalysts were deposited as thin coatings on a ceramic Mg-Al-O carrier previously made by SHS from an initial mixture of 7.41% Al + 8.33% Mg + 39.63% $Mg(NO_3)_2$ + 32.41% Al_2O_3+ 4.81% MgO + 7.41% H_2BO_3.

The nano-structured catalysts were characterised by SEM, EDAX, phase analysis (XRD) and measurement of their specific surface area using the BET method. The catalyst's performance was studied in liquid-phase hydrogenation of maleic acid (0.26g of maleic acid for 50ml H_2).

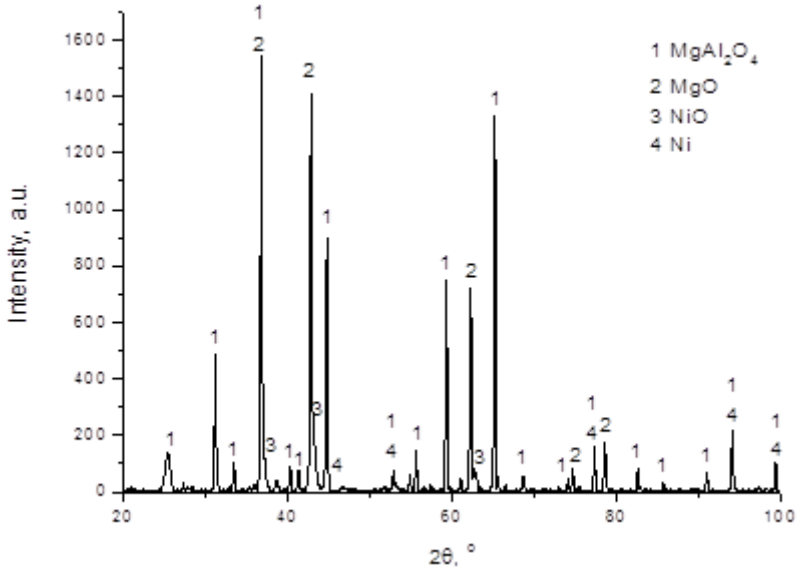

Fig.2 - XRD analysis of the nano-catalyst including the Mg-Al-O carrier

XRD analysis (Figure 2) shows that the coatings consist of Ni and NiO phases (the other phases shown are from the carrier) which indicates that SCS was completed in-flight. The following reactions take place by in-flight SCS in the flame over times of milliseconds:

$$Ni(NO_3)_2 \cdot 6H_2O + C_2H_5NO_2 \rightarrow Ni + NiO + NO_2 + 2NO + N_2 + 2CO_2 + \frac{29}{2}H_2O + \frac{5}{2}O_2 \quad \text{(i)}$$

$$Ni(NO_3)_2 \cdot 6H_2O \xrightarrow{54℃} Ni(NO_3)_2 \cdot 4H_2O \xrightarrow{85.4℃} Ni(NO_3)_2 \cdot 2H_2O \quad \text{(ii)}$$

$$Ni(NO_3)_2 \cdot 6H_2O \rightarrow 2NiO + NO_2 + NO + N_2 + 6H_2O + \frac{7}{2}O_2 \quad \text{(iii)}$$

$$NiO + H_2 \rightarrow Ni + H_2O \quad \text{(v)}$$

$$Ni + O_2 \rightarrow NiO + \frac{1}{2}O_2 \quad \text{(vi)}$$

$$2CH_2NH_2COOH + 6O_2 \rightarrow 4CO_2 + 5H_2O + NO + NO_2 \quad \text{(vii)}$$

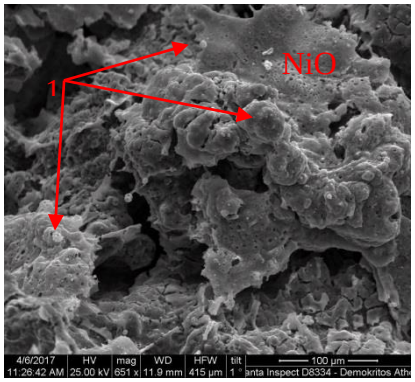

Element	Wt %	At %
O	0.18	0.67
Ni	99.82	99.33
Total	100.00	100.00

Fig.3 - SEM photo of the surface of the catalyst and EDX quantitative analysis of point 1

SEM microstructural examinations of the surface of the coating (Figure 3) confirmed the presence of NiO and Ni phases. The grey spherical phases are identified by EDX as Ni phase.

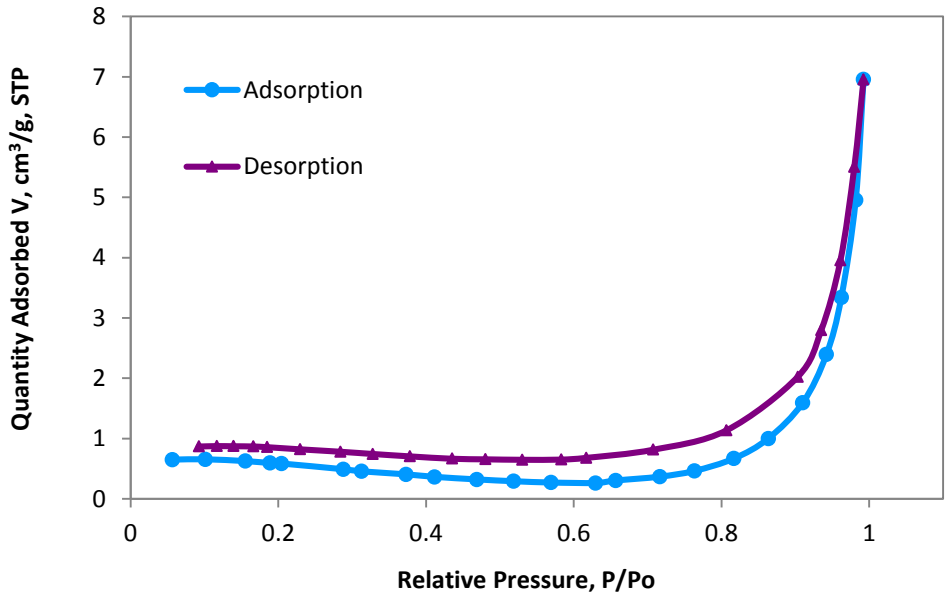

Fig.4 - Hysteresis curve of in-flight SCS Ni-based final product

The results of BET analysis using nitrogen as adsorbent are shown in Figure 4. The type V isotherm indicates uncontrolled formation of the multi-layer followed by capillary condensation [5]. Such structures results because lateral interactions between adsorbed molecules are stronger than those between the measured product and the adsorbate (nitrogen). A characteristic feature of type V isotherm is its hysteresis loop which is associated with capillary condensation taking place in mesopores. Based on the hysteresis loops classification, the obtained adsorption-desorption curves are ranked as type H3 [5]. This indicates that the final nano-structured product consists of aggregates of plate-like particles forming slit-like pores. BJH pore analysis was also carried out in the BET surface area analyzer (Gold App P2800) and is presented in Figure 5.

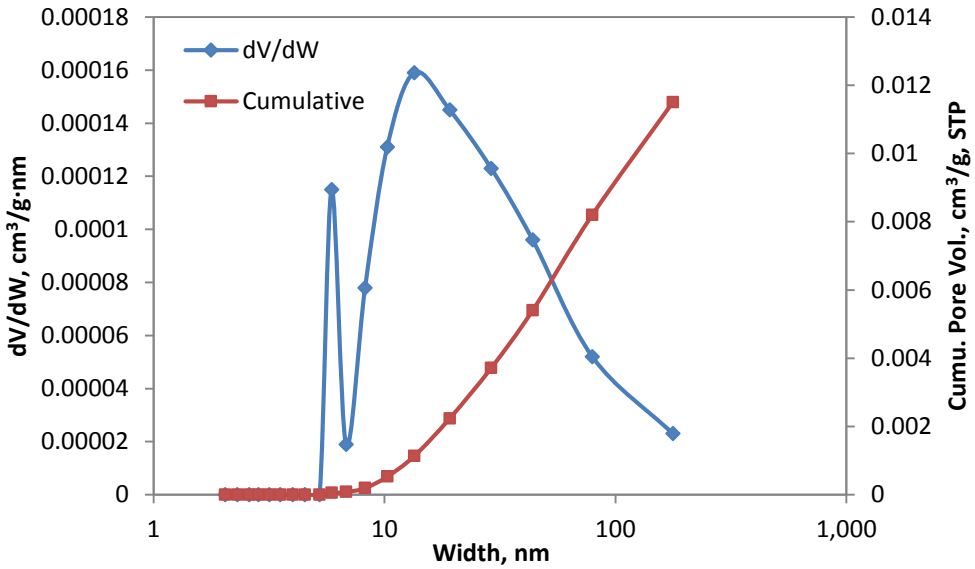

Fig.5 - BJH pore analysis of in-flight SCS Ni-based nano-catalysts

The BJH pore size analysis confirms the existence of nano-pores in the SCS Ni-based which resulted in a measured specific surface area of 2.47m^2/g.

REFERENCES

[1] G. Xanthopoulou, O. Thoda, E. D. Metaxa, G. Vekinis, A. Chroneos, Journal of Catalysis, 348, 2017, 9-21

[2] G. Xanthopoulou, A. Marinou, K. Karanasios and G. Vekinis, Coatings, 2017, *7*, 14

[3] A. Marinou, Synthesis of High Temperature Coatings by the New Method CAFSY, Ph.D.Thesis, University of Ioannina, Ioannina, Greece, 2015

[4] R. Koirala, S. Pratsinis, A. Baiker, Chem. Soc. Rev., 2013, 45, 3053

[5] Sing et al, Pure & Appl. Chem., 1985, 57, 603-619

SINGLE STEP PREPARATION OF Cu-Cr-O AND Ni-Cr-O NANO CATALYSTS FOR CO OXIDATION BY SOLUTION COMBUSTION SYNTHESIS

V. Novikov[1], G. Xanthopoulou*[1,2], Yu.Knysh[1]

[1]Department of Theory of Aircraft Engines, Samara State Aerospace University,
34 Moskovskoye shosse, 443086 Samara, Russia
[2]Institute of Nanoscience and Nanotechnology, NCSR "Demokritos",
Agia Paraskevi 15310 Athens, Greece
*g.xanthopoulou@inn.demokritos.gr

Solution Combustion Synthesis method provides a cheap oxide catalysts in the form of nano-sized powders, which have very high catalytic activity at low temperatures. Nanomaterials on the base of Cu-Cr-O system (including spinels $CuCr_2O_4$ and $CuCrO_2$) by SCS described in the following works [1-3]. As fuel was used glycine [1] and citric acid [2-3], Cu and Cr source in the synthesized compounds were nitrates of these metals. However, the synthesis in all described works takes place in several stages (including temperature annealing), which requires a lot of time [1-3]. catalysts The aim of this work is to investigate the possibility of $CuCr_2O_4$, $CuCrO_2$ and $NiCr_2O_4$ spinels synthesis by SCS without additional temperature treatment (in one stage) and study of those SCS catalysts activity in CO oxidation.

The following materials were used in the experiments as initial components: copper nitrate, nickel nitrate, chromium nitrate, urea - $CO(NH_2)_2$. Spinels produced by reaction of $CuO + Cr_2O_3 = CuCr_2O_4$, $2CuO+Cr_2O_3 \rightarrow 2CuCrO_2+ 1/2O_2$,$NiO +Cr_2O_3 \rightarrow NiCr_2O_4$ after oxides were originated from nitrates during heating. Concentration of chromium and nickel nitrate in mixture with the copper nitrate was changed from 0 to 100%. Ratio of the nitrates in the initial batch to urea in all experiments are : 32% urea and 68% of chromium nitrate and 42% urea and 58% of nickel nitrate, 50 ml of water also added. XRD, SEM-EDX, BET analysis were performed, temperature of combustion was measured. Catalytic properties of Cu-Cr-O spinel studied in the CO oxidation reaction at temperatures 150-550^oC and volume speed 2400 h^{-1}(l/l catalyst per hour) using gas mixture (99% air + 1% CO).

According to XRD analysis there are CuO, Cr_2O_3, $CuCr_2O_4$, $CuCrO_2$ and Cu in the final products of SCS. Copper exist in the final composition only in case of 16.7%-50% $Cr(NO_3)_3 * 9H_2O$ (or 83.3-50% $Cu(NO_3)_2$) concentration in the initial batch, this could be connected with much lower combustion temperature (fig.1) at this concentrations and less possibility of copper oxidation. Copper can originate due to following reactions:

$CuO+NO \rightarrow Cu+NO_2$

$CuO+CO \rightarrow Cu+CO_2$

$CuO + NH_3 \rightarrow Cu + N_2 + H_2O$

There is also possibility that mechanism of copper formation is connected with conditions of optimum ratio of HNO_3 formation during decomposition of nitrates and NH_3 produced during combustion of urine, then in the exothermic reaction HNO_3+NH_3 can be produced hydrogen, which reduce copper oxide:

$Cu+H_2 \rightarrow Cu +H_2O$.

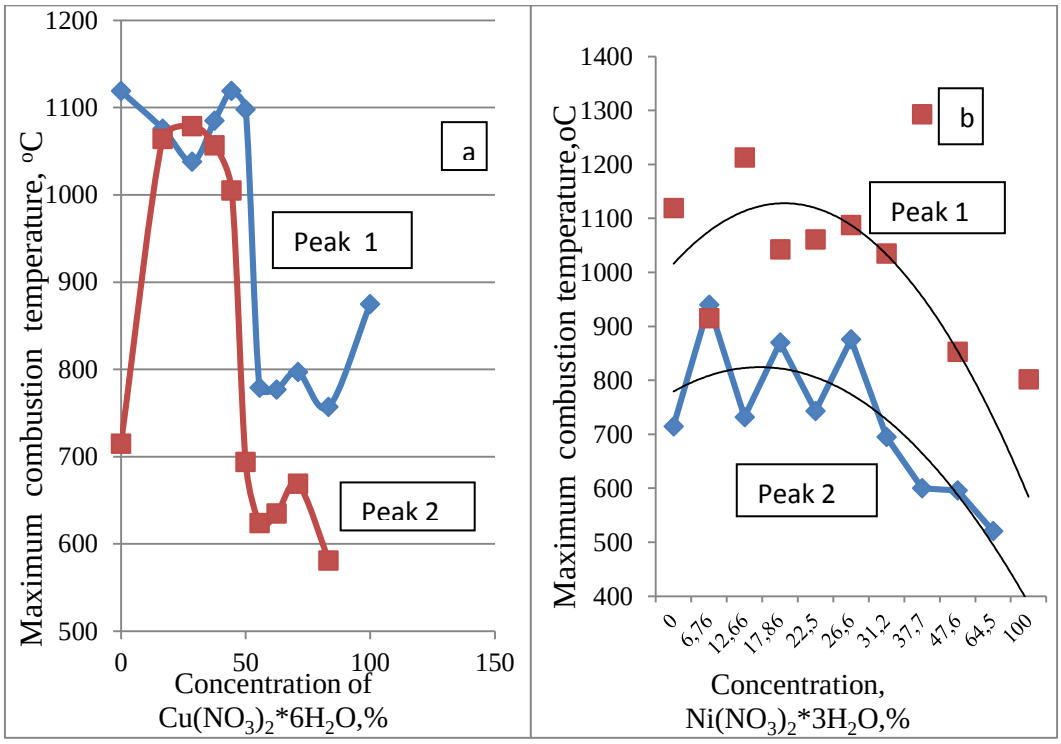

Fig.1 - Influence of copper (a) and nickel (b) nitrate concentration in the initial batch composition: Cr $(NO_3)_3$ * $9H_2O$, $Cu(NO_3)_2$*$6H_2O$ (or $Ni(NO)_2$*$3H_2O$) and urea (42%) on the combustion temperature (Peak1- combustion temperature at first peak; Peak2-combustion temperature at second peak).

Confirmation of such hypothesis can be fact that in all cases exist 2 peaks of maximum on the temperature curve (second peak connected with origination of copper), but XRD show copper metal only at 16.7%-50% Cr $(NO_3)_3$ * $9H_2O$ (or 83.3-50% $Cu(NO_3)_2$* $6H_2O$) concentrations in the initial batch. Existence of second peak on temperature curve (fig.1a) when there is no copper nitrate in the initial batch could be connected with chromium origination, but it was not determined by XRD, probably Cr was oxidized immediately after SCS. At the same time when copper metal is present in the catalyst there is increasing of the CuCrO2 spinel in ratio $CuCrO_2/CuCr_2O_4$ (ratio calculated from XRD results) (fig.2).

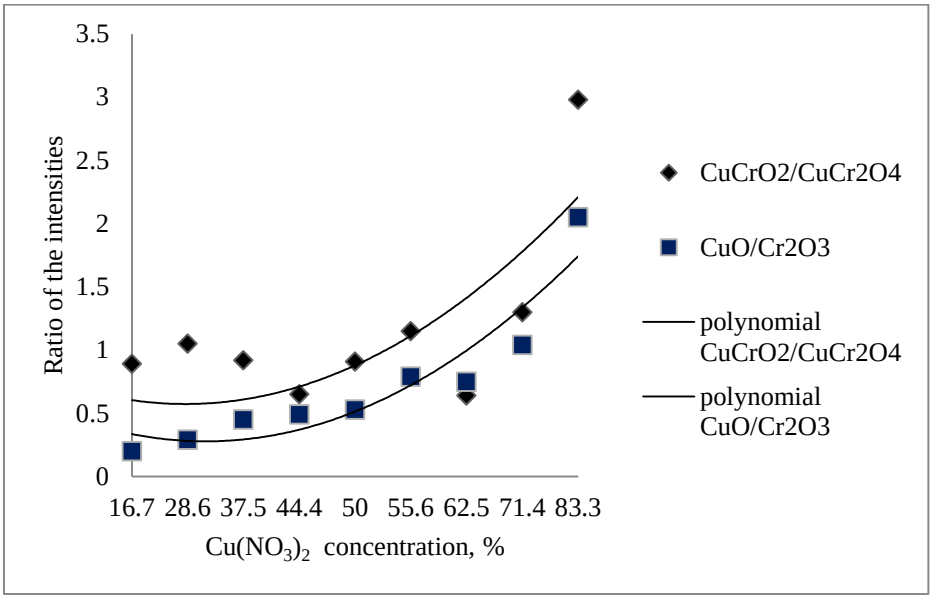

Fig. 2 - Semi-quantitive analysis of SCS products (oxides and spinels) concentration in the Cu-Cr-O system. Influence of initial batch composition on the catalyst composition.

Analysis of XRD results show that at low concentration of chromium nitrate in the initial batch there is $CuCrO_2$ spinel due to reaction :

$2CuO + Cr_2O_3 \rightarrow 2CuCrO_2 + ½\ O_2$

Increasing of concentration of chromium nitrate leads to increasing of $CuCr_2O_4$ in the product due to reaction:

$CuO + Cr_2O_3 = CuCr_2O_4$

$Cr_2O_3 + 2CuCrO_2 + 1/2O_2 = 2CuCr_2O_4$

Copper, CuCrxOy and $NiCr_2O_4$ spinels have catalytic activity in the CO oxidation process, this explains data fig.3 where at the concentration 55%-83.3% of $Cu(NO_3)_2*6H_2O$ CO conversion reach 90-99%.

Surface area depends from initial composition of batch and varies from 5 to 37 m^2/g. Large surface area has catalysts with high concentration of chromium nitrate in the initial batch. This regularity can be explained by higher (approximately 2 times) gas formation at the decomposition of $2Cr(NO_3)_3*9H_2O \rightarrow Cr_2O_3+2NO+4NO_2+5/2O_2+9H_2O$ than $Cu(NO_3)_2*6H_2O \rightarrow CuO+NO+NO_2+O_2+6H_2O$.

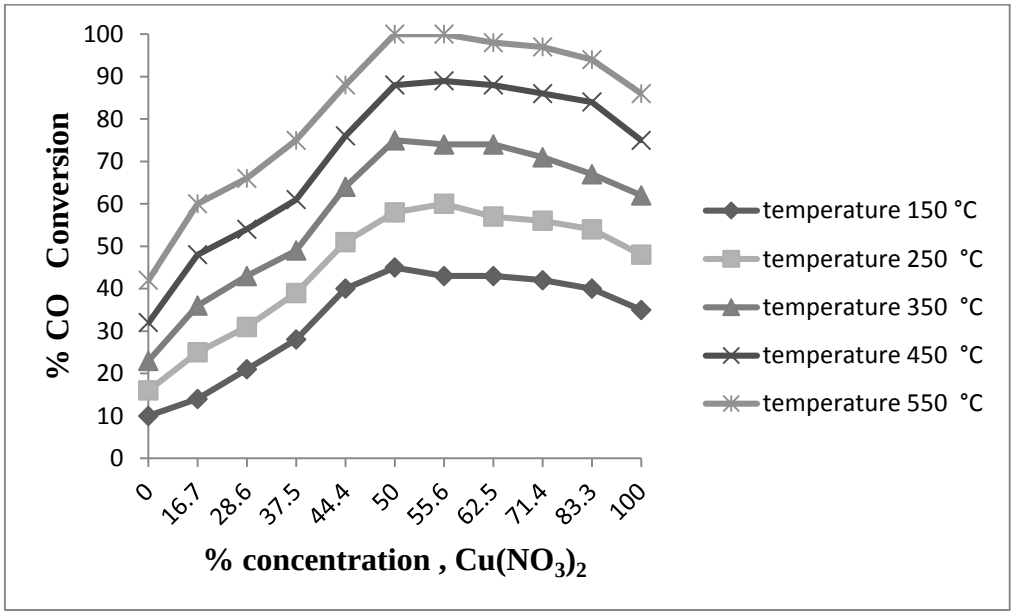

Fig. 3 - Dependence of CO conversion from copper nitrate concentration in the initial batch: $x\mathrm{Cu(NO_3)_2}+y\mathrm{Cr(NO_3)_3}+\mathrm{CO(NH_2)_2}$ at different reaction temperatures.

Thus**,** it was found that $CuCr_2O_4$, $CuCrO_2$ and $NiCr_2O_4$ can be produced when copper nitrate exceed stoichiomentric ratio in the mixture with chromium(or nitrate. Temperature of combustion influence copper concentration in the catalyst. The specific surface area of the catalysts is varied between 5 m^2 /g and 37 m^2 /g calculated from the BET adsorption equation. Surface area and composition (spinels and copper) of the catalysts influence activity of the SCS catalysts in CO conversion.

References

[1] Yung-Tang Nien, Mon-Ru Hu, Te-Wei Chiu, Jaw-Shiow Chu. Antibacterial property of $CuCrO_2$ nanopowders prepared by a self-combustion glycine nitrate process// Materials Chemistry and Physics 179 (2016) 182-188.

[2] Pengfei Wang, Peng Li, Ting-Feng Yi, Xiaoting Lin, Yan-Rong Zhu, Lianyi Shao, Miao Shui, Nengbing Long, Jie Shu. Fabrication and electrochemical properties of CuCrO2 anode obtained by a sol–gel method// Ceramics International 41 (2015) 6668–6675.

[3] Wei Li, Hua Cheng. Cu-Cr-O nanocomposites: Synthesis and characterization as catalysts for solid state propellants// Solid State Sciences 9 (2007) 750-755.

MULTIWAVE SCS REGIME IN THE SYSTEM Mn-Zn-Na-Si-O

E. Pavlou, G. Xanthopoulou*, G. Vekinis

[1]Institute of Nanoscience and Nanotechnology, NCSR "Demokritos", Agia Paraskevi Attikis, 15310, Greece
*g.xanthopoulou@inn.demokritos.gr

Solution combustion synthesis (SCS) in the Mn-Zn-Na-Si-O system has been studied at a pre-heating temperature of 600ºC with a mixture of $Zn(NO_3)_2$, Na_2SiO_3, $Mn(NO_3)_2$ and 60wt% Urea which supplies combustion fuel and also acts as the reduction agent. Such SCS mixtures are actually used to produce stable nano-structured pigments. The methodology of the experiments has been described previously [1]. The influence of the nitrate concentration on the final SCS composition and other properties has been investigated and reported. Interestingly, in this system 4 consecutive waves of combustion were found to occur and shown in the photos from the synthesis video and of the products after each wave in Figure1.

70 sec 75 sec 80sec 90sec 110sec 120sec 135sec 140sec

after 1st wave after 2nd wave after 3rd wave after 4th wave

Fig.1 - Four waves of combustion during SCS in the system: 50%$Zn(NO_3)_2$ + 50%Na_2SiO_3 + 60%Urea +2% $Mn(NO_3)_2$ preheated at 600ºC

A possible explanation for the occurence of a multiwave regime of combustion may be connected with the possibility of the conversion of manganese oxides [2] as follows:

$$3\ MnO_2 \rightarrow Mn_3O_4 + O_2 \quad (T=530^oC)$$

$$2\ MnO_2 \rightarrow Mn_2O_3 + 1/2\ O_2 \quad (T=530\text{-}940^oC)$$

$$3Mn_2O_3 \rightarrow 2Mn_3O_4 + 1/2\ O_2 \quad (T=940\text{-}1090^oC)$$

If hydrogen forms during combustion, which is possible during SCS due to the dissociation of water [3], then it is possible to obtain conversion of Mn_3O_4 to Mn_3O_4 at a temperature as low as 230°C and of Mn_3O_4 to MnO at 300°C.

Such conversions have been confirmed by X-ray diffraction (XRD) of the intermediate products and the results are shown in Figure 2 (only the peaks for manganese oxides are marked in the figure). XRD showed that there are also ZnO, $ZnMn_2O_4$, $ZnMnO_3$, SiO_2 in the final product. Some peaks are missing due to the defect structure of the products.

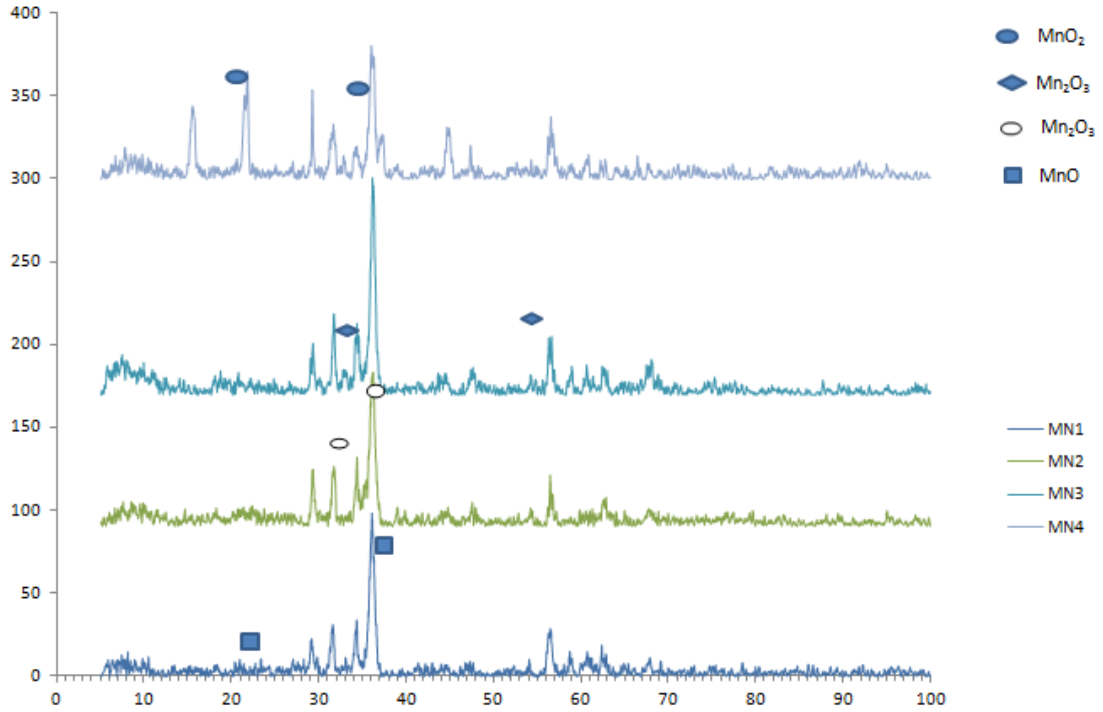

Fig.2 - X-ray diffraction patterns of the SCS products of an initial mixture of: 30%$Zn(NO_3)_2$ + 50%Na_2SiO_3 + 60%Urea +22% $Mn(NO_3)_2$, at a preheating temperature 600°C: MN1: 1st wave of combustion, MN2: 2nd wave of combustion, MN3: 3rd wave of combustion, MN4: 4th wave of combustion. Only manganese oxides are identified and marked.

Measurements of the combustion temperature during SCS in the systems which contain 2% and 22% of manganese nitrate were carried out by placing three type K thermocouples within the solution ("bottom"), close to the solution-air interface ("middle") and at about 2.5 cm above the solution ("top") and the results are shown in Figure 3. The bottom thermocouple registered only one clear peak which is probably because of increasing of the reaction mixture volume and the wave character of combustion. The results indicate that the maximum combustion temperature was about 700°C which is too low for the formation of MnO and Mn_3O_4. We therefore explain the synthesis of the identified Mn_3O_4 and MnO by the transient formation of hydrogen during SCS which reacts exothermically with manganese oxides.

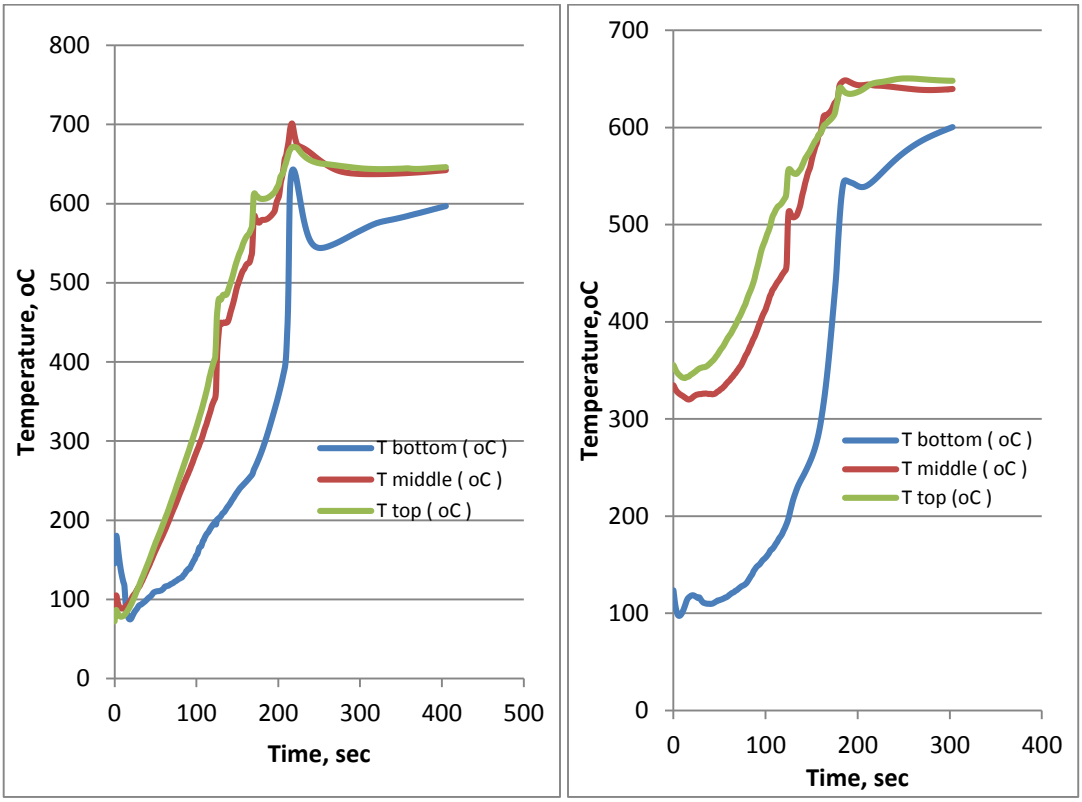

Fig.3 - Temperature curves for SCS of mixtures: 50%$Zn(NO_3)_2$+50%Na_2SiO_3+60%Urea+2% $Mn(NO_3)_2$ (left) and 30%$Zn(NO_3)_2$+50%Na_2SiO_3+60%Urea+22% $Mn(NO_3)_2$ (right).

The colour characteristics of the SCS products (pigments) are shown in Table 1. The colour of the pigments depends on the concentration of manganese nitrate in the initial mixtures and becomes darker with increasing nitrate concentration.

Table 1 - Color characteristics of SCS manganese pigments.

Sample name	Initial batch	Colour characterization CIE L*a*b* (D60/2)	Colour Of pigment
CC1	50% $Zn(NO_3)_2$ 50% Na_2SiO_3 60% Urea 0,1% $Mn(NO_3)_2$	L* 84,83 a* -1,02 b* 30,77	
CC2	50% $Zn(NO_3)_2$ 50% Na_2SiO_3 60% Urea 0,5% $Mn(NO_3)_2$	L* 80,25 a* 3,4 b* 44,8	
CC3	50% $Zn(NO_3)_2$ 50% Na_2SiO_3 60% Urea 1% $Mn(NO_3)_2$	L* 74,77 a* 5,87 b*45,21	

CC4	50% $Zn(NO_3)_2$ 50% Na_2SiO_3 60% Urea 2% $Mn(NO_3)_2$	L* 64,19 a* 6,26 b* 35,86	
CC6	50% $Zn(NO_3)_2$ 50% Na_2SiO_3 60% Urea 5% $Mn(NO_3)_2$	L* 50,91 a* 9,55 b* 36,18	
CC7	50% $Zn(NO_3)_2$ 50% Na_2SiO_3 60% Urea 10% $Mn(NO_3)_2$	L* 43,57 a* 4,55 b* 23,71	
CC8	50% $Zn(NO_3)_2$ 50% Na_2SiO_3 60% Urea 20% $Mn(NO_3)_2$	L* 39,57 a* 4,4 b* 18,58	

In summary, we observed 4 waves of combustion during SCS of manganese pigments due to the formation of manganese oxides of valences II-IV in the system Mn-Zn-Na-Si-O by exothermic reaction with transient hydrogen, as confirmed by temperature profiles, XRD and SEM.

REFERENCES

[1] E. Pavlou, G. Xanthopoulou, M. Tsigonias & G. Vekinis, Solution Combustion Synthesis of luminescent pigments based on the systems, Co-Al-Mg-Ba-O, Co-Al-B-O and Co-Ba-B-O for ink applications, International symposium SHS2015, 12-15October, Antalia, Turkey, p. 141-143.

[2] G. Remi, Course of Inorganic Chemistry, Leipzig, Akademische Verlagsgesellschaft Geest &Portig K.-G. v.2 , 1961.

[3] V. Arvind Varma, A. S. Mukasyan, A. S. Rogachev, and K. V. Manukyan, Solution Combustion Synthesis of Nanoscale Materials, American Chemical Society (ACS Publication), Chem. Rev., DOI: 10.1021/acs.chemrev.6b00279.

SOOT OXIDATION USING CHROMIUM-BASED SCS CATALYSTS APPLIED ON A MAGNESIA-SPINEL CARRIER BY FLAME SPRAYING

K. Papadopoulos[1,2], A. Marinou[1], G. Xanthopoulou[1]*, G. Vekinis[1], M.Karakasidis[2]

[1]Institute of Nanoscience and Nanotechnology, NCSR "Demokritos, Aghia Paraskevi, 15310 Athens, Greece
[2]Department of Material Science & Engineering, University of Ioannina, 45110, Greece
*g.xanthopoulou@inn.demokritos.gr

Spinel-type mixed oxides are of considerable interest due to their use in different fields including environmental protection and catalysis. Previous studies have shown that copper chromite spinels synthesised by SCS or SHS are very effective catalysts, due to the tetragonally-distorted spinel structure which acts as a burn rate modifier in solid propellants [1] and in CO oxidation [2]. Internal combustion engine exhausts consist of a complex mixture of gases (including soot, CO, NOx, HC, etc.) whose composition depends on a variety of factors such as the type of engine, vehicle speed, acceleration/deceleration rates, etc. Diesel soot oxidation and NOx in particular have a significant adverse impact on both global warming and public health. Copper chromite catalysts are some of the most efficient materials for many processes and have been used widely as catalysts for hydrogenation, dehydrogenation, hydrogenolysis, soot oxidation, alkylation, cyclization, etc [3]. It is therefore thought that they could be active as emission-control catalysts as well.

In the present work, chromium-based catalysts were synthesized by Solution Combustion Synthesis (SCS) from solutions of 40% $K_2Cr_2O_7$, 60% $Cu(NO_3)_2*3H_2O$ and 40% urea as fuel. In some experiments CrO_3 was used instead of $K_2Cr_2O_7$. The synthesized SCS catalyst was then deposited as a coating on a MgO-spinel carrier (previously prepared by SHS) by flame spraying. The effects of SCS solution concentration and preheating temperature as well as spraying distance and number of sprayed layers on the catalyst atomic structure, composition and its catalytic activity in soot oxidation were investigated. The structure of the catalysts was characterized by SEM, EDAX, XRD and their specific surface area and pore distribution were measured by the BET method with nitrogen gas.

The materials' catalytic performance was studied for oxidation of diesel soot. The catalyst was mixed with soot in the ratio 1:3 by weight in an alumina reactor and the combustion initiation and burning-out temperatures of the soot were determined in an in-house built apparatus at a heating rate of about 10^{o}C per minute. Figure 1a shows typical pore distribution curves for the SCS catalysts while Figure 1b shows the combustion initiation and burn-out temperatures against total specific surface area of the materials. The results indicate that, in spite of the presence of nanopores, the specific surface area is low at 0.68-1.07 m^2/g and there is no clear dependence of catalytic activity on surface area, probably because the surface area is similar for all catalysts.

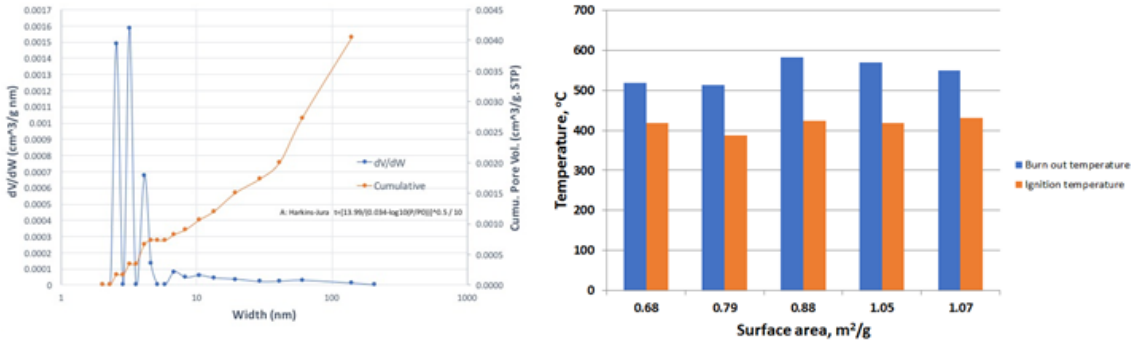

a b

Figure 1 - a) Adsorption and pore distribution of a Cu-Cr-O catalyst and b) influence of surface area on the catalytic properties of Cu-Cr-O system in diesel soot oxidation.

The influence of the total concentration of solids in water used for SCS and that of the preheating temperature during SCS on the activity of catalysts for diesel soot oxidation is shown in Figure 2.

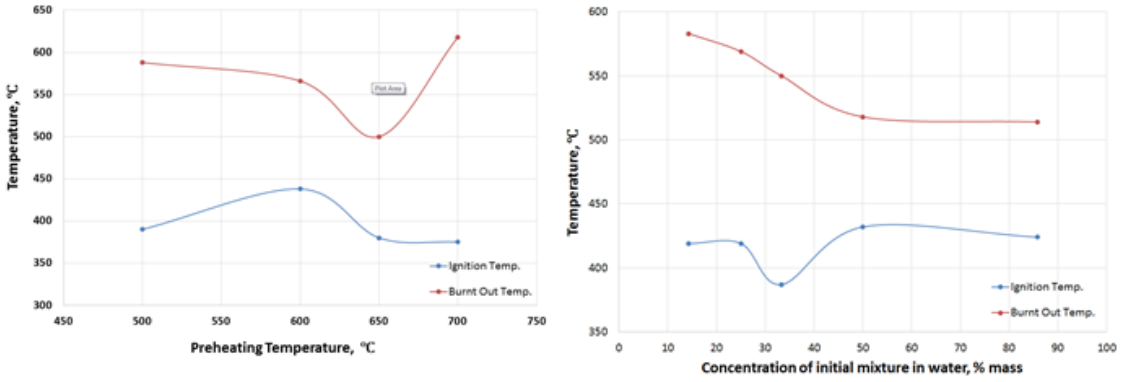

a b

Figure 2 - Influence of a) preheating temperature and b) total concentration of solids in water on the catalytic properties of Cu-Cr-O system in diesel soot oxidation.

The higher measured catalyst activity at a SCS preheating temperature of 650°C is probably connected with the higher activity of the spinels for soot oxidation, which is supported by the fact that the ignition temperature for soot combustion decreases. On the other hand, the increased burning out temperature when SCS was carried out at 700°C is probably connected with decreased surface area at high SCS preheating temperature.

Figure 3 shows the influence of the number of spraying passes (which is proportional to the amount of catalyst coating the carrier) and spraying distance on the catalytic properties of SCS Cu-Cr-O system for soot oxidation.

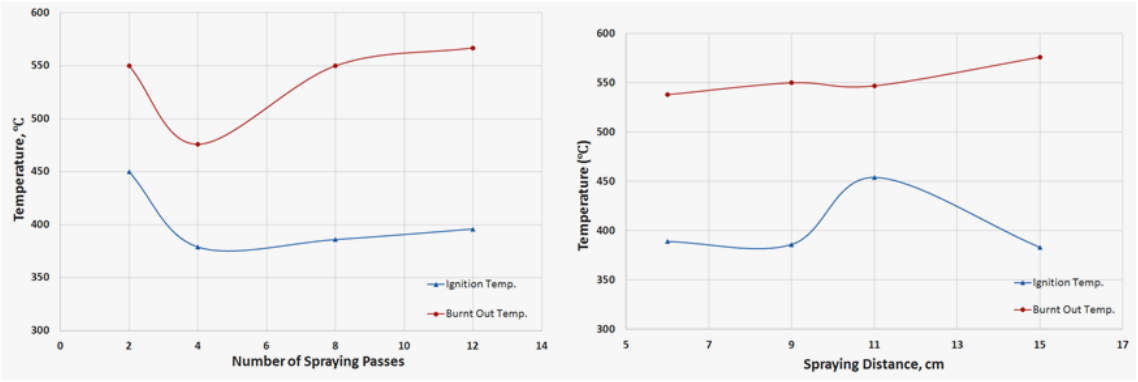

a b

Figure 3 - Influence of a) number of spraying passes and b) spraying distance on the catalytic properties of Cu-Cr-O system for oxidation of diesel soot.

The amount of catalyst sprayed on the carrier plays a major role in catalytic activity (Figure 3a). With just 2 spraying passes the carrier mass increases by 7.7wt% (all of it made up of catalyst) but with 4 passes the mass increase is 10.9wt% which gives a significant improvement in measured catalytic activity as evidenced by the burning-out temperature dropping by 80^0C. This is because the sprayed-on catalyst penetrates very deeply into the open surface pores and covers the whole surface. This is probably why further increasing of catalyst on carrier up to 16% of mass is not affected by increasing the ignition temperature. Considering the burn-out temperature, further increasing of catalyst amount on the carrier results in lower catalytic activity. Spraying distance (fig.3 b) influences catalyst activity in a complicated way: the greater the distance the more catalyst is applied on the carrier (from about 4 to 17.9% by total mass), while increasing the spraying distance decreases the temperature on the surface of carrier and this leads to changes in the surface area and composition of the catalyst, especially the ratio of $CuCr_2O_4$ to $CuCrO_2$ in the final composition of the coated catalysts.

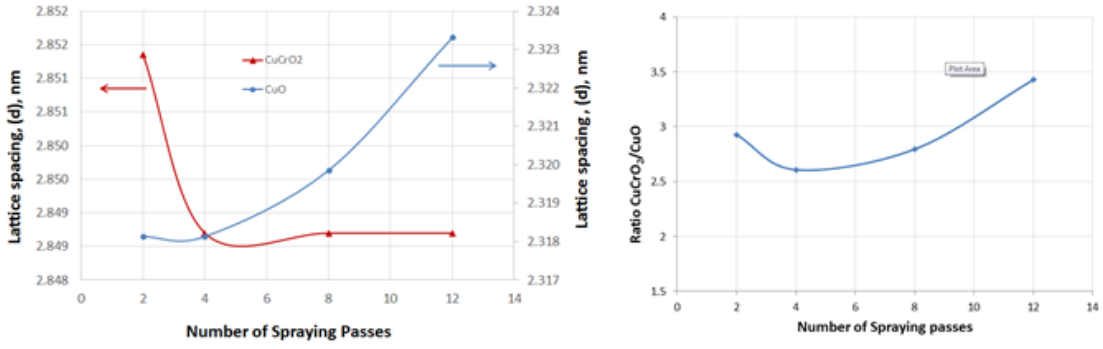

a b

Figure 4 - Influence of number of passes on a) lattice spacing of $CuCrO_2$ and CuO and b) ratio of $CuCrO_2$/CuO

Comparing Figures 3a and 4a indicates that ignition temperature of soot oxidation depends from crystal plane lattice parameters of $CuCrO_2$ with an optimum at 2.849Å. CuO also play role in catalysis, especially as it influences the products' desorption process. According to Figure 4a copper oxide parameters of crystal plane lattice increase with number of spraying passes which

could be the reason for the observed changes in catalyst activity (Figure 3a). Figure 4a shows that with increasing number of spraying passes the ratio $CuCrO_2$/CuO increases which can be explained by the increase in thermal treatment time with increasing number of spraying passes, a necessary condition for spinel formation from oxides.

In conclusion Cu-Cr-O SCS powder sprayed on carrier surface using flame spraying has catalytic activity which depends on initial mixture concentration in water, preheating temperature, powder composition and parameters of spraying: distance and number of passes.

REFERENCES

[1] P. S. Sathiskumar, C. R. Thomas, G. Madras, Ind. Eng. Chem. Res., 51(30), 2012, , pp 10108–10116.

[2] G. Xanthopoulou and G.Vekinis , Applied Catalysis B: Environmental, 19(1998), p.37-44.

[3] W. Shangguan, Y. Teraoka and S. Kagawa, Reports of the Faculty of Engineering, Nagasaki University, 25 (No. 45), 1995, pp. 241-248.

COMPARISON OF THE ACTIVITY OF SHS, SCS AND IMPREGNATED CATALYSTS IN THE REACTION OF CARBON DIOXIDE CONVERSION AND OXIDATIVE CONVERSION OF METHANE WITH CONNECTION TO COMBUSTION SYNTHESIS PARAMETERS

G. Xanthopoulou*[1], S.A. Tungatarova[2], K. Karanasios[1], T.S. Baizhumanova[2], M. Zhumabek[2]

[1]Institute of Nanoscience and Nanotechnology, NCSR Demokritos, Aghia Paraskevi, 15310 Athens, Greece,
[2]D.V. Sokolsky Institute of Fuel, Catalysis and Electrochemistry, D.Kunaev str.,050010 Almaty, Kazakhstan
* g.xanthopoulou@inn.demokritos.gr

Processing of natural gas into motor fuel has become one of the major problems of chemistry. Partial oxidation and carbon dioxide reforming of CH_4 attract a great attention in recent years. The catalysts prepared by three different methods were tested. Activity of SHS catalysts on the base of initial batch NiO-Al-α-Al_2O_3, and with additives (H_3BO_3, MgO_2, MoO_3) prepared by Self-propagating High-Temperature Synthesis (SHS) method, and by impregnation (IMP) (Ni/Al_2O_3 catalyst) were tested in the partial oxidation of CH_4 in following conditions: volume velocity - 2500 h^{-1} (l/l catalyst/hour), composition of gas mixture: 34% CH_4 + 17% O_2 + 50% Ar, table 1.

Table 1 - Oxidative conversion of methane on SHS catalysts (initial batch NiO-Al-α-Al_2O_3) and impregnated catalysts (Ni/Al_2O_3)

Composition of the initial batch	Conversion CH_4, %		Yield H_2, %		Yield CO, %		H_2/CO	
	SHS	IMP	SHS	IMP	SHS	IMP	SHS	IMP
24.1% NiO 55.9% Al 20% Al_2O_3	90.0	78.8	61.5	54.9	21.0	21.9	2.9	2.5
25.8% NiO 54.2% Al 20% Al_2O_3	84.2	66.9	62.0	57.2	26.4	22.4	2.3	2.6
27.5% NiO 52.5% Al 20% Al_2O_3	96.0	69.4	67.0	53.9	27.1	24.2	2.5	2.2
29.2% NiO 50.8% Al 20% Al_2O_3	81.7	73.7	52.0	55.7	25.9	22.8	2.0	2.4

SHS catalysts has more high activity in partial oxidation of CH_4: H_2 yield (52.0-67.0%) on SHS catalysts and (53.9-57.2%) on impregnated catalysts, CO yield – (21.0-27.1%) on SHS catalysts and (21.9-24.2%) on impregnated catalysts. For SHS catalysts received optimum ratio H_2/CO = 2 (29.2% NiO+50.8% Al+20% Al_2O_3), for impregnated catalyst ratio is 2.2-2.6. The SHS catalysts of the NiO-Al-α-Al_2O_3 series, were also tested with additives (H_3BO_3, MgO_2, MoO_3) in this process and they show a high activity in partial oxidation of CH_4, yields (52.0-67.0%)

and selectivity for H_2 (90.9-100%) exceed those of the other tested samples. The ratio of H_2/CO = 3.2-4.9. Catalysts on the base of Ni-Co-Zr-O, prepared by SHS, also were tested in dry reforming of CH_4, but results were much more low in comparison with described catalysts (table 1). The activity of catalysts based on the initial mixture of 47% $Ni(NO_3)_2$+2% $Co(NO_3)_2$+1% $Zr(NO_3)_2$+50% glycine+36.15% $Al(NO_3)_3$+13.85% $Mg(NO_3)_2$, obtained by Solution Combustion Synthesis (SCS) were also studied in the oxidative conversion of CH_4. A mixture of CH_4:O_2 = 2:1 (34% CH_4, 17% O_2) and 50% (Ar±H_2O), was used to study the oxidation of CH_4 into synthesis gas at 750-900°C. The results of the H_2 and CO yield as well as selectivity for the target products for these catalysts depending on the volume velocity (500-8500 h^{-1}) and temperatures (850-900°C) (figure 1).

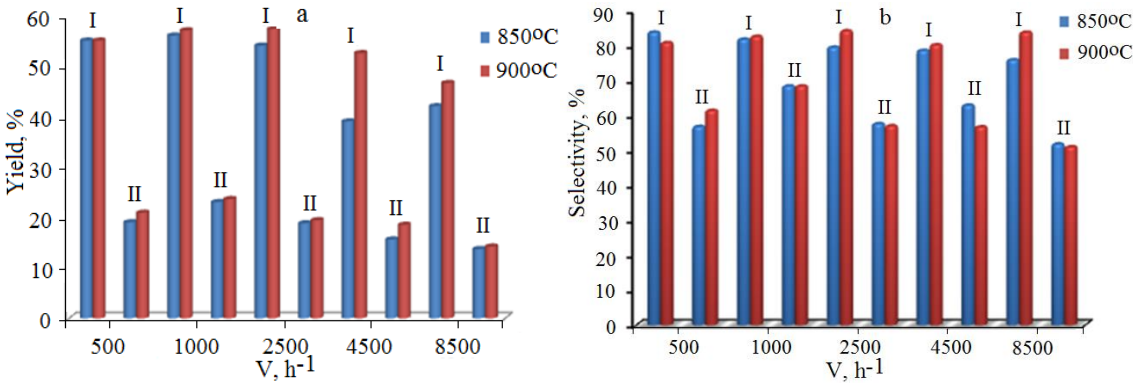

Fig. 1 - Influence of the volume velocity on the yield and selectivity for H_2 and CO at different temperatures on the SCS catalyst on the base of initial batch 47% $Ni(NO_3)_2$+2% $Co(NO_3)_2$+1% $Zr(NO_3)_2$+50% glycine+36.15% $Al(NO_3)_3$+13.85% $Mg(NO_3)_2$. a – yield: I –H_2, II – CO; b – selectivity: I – H_2, II – CO

On this catalyst, when the temperature and volume velocities varied from 500 to 8500 h^{-1}, the yields of H_2 and CO, their selectivity, and the H_2/CO ratio, which plays an important role for further syntheses of alcohols and hydrocarbons, were determined. It is shown that at volume velosity from 1000 to 2500 h^{-1}, it is possible to obtain the highest yield and selectivity for the target products. For example, at V = 2500 h^{-1}, up to 55-57.3% H_2, 19-19.4% CO with selectivity up to 84.2% in H_2 and 57% in CO, the ratio H_2/CO = 2.8-2.9. Similar results were obtained at a volume velocity of 1000 h^{-1}. It should be noted that the H_2/CO ratio is more optimal in this case and corresponds to a value of 2.3-2.4. A further increase in the space velocity, or a decrease, leads to a decrease in the process indices.

The activity of Ni-Co-Zr-O, Ni-Co-Zr-Al-O, Ni-Co-Zr-Al-Mg-O SCS catalysts were also tested (figure 2).

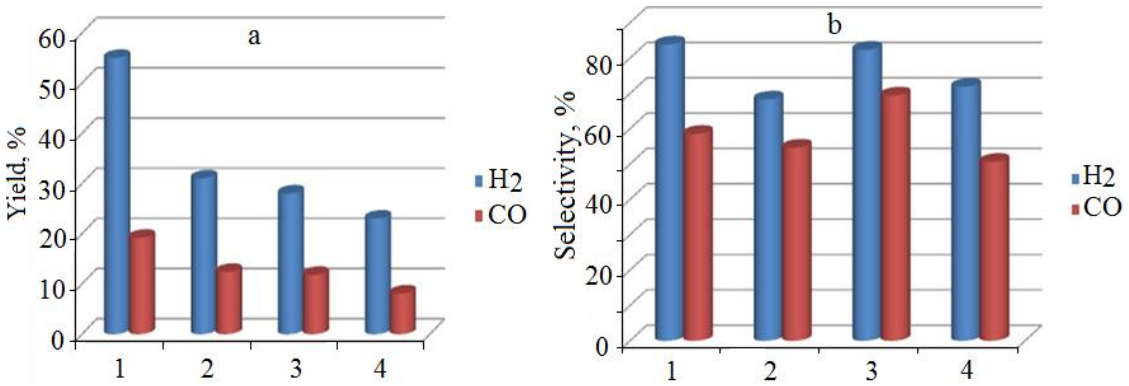

Fig. 2 - The effect of the composition of catalysts on the yield and selectivity of H_2 and CO: a - H_2 and CO yield, b-selectivity on H_2 and CO. 1 - 47% $Ni(NO_3)_2$+2% $Co(NO_3)_2$+1% $Zr(NO_3)_2$+50% glycine+36.15% $Al(NO_3)_3$+13.85% $Mg(NO_3)_2$, 2 - 35% $Ni(NO_3)_2$+10% $Co(NO_3)_2$+5% $Zr(NO_3)_2$+50% glycine+36.15% $Al(NO_3)_3$+13.85% $Mg(NO_3)_2$, 3 - 20% $Ni(NO_3)_2$+20% $Co(NO_3)_2$+10% $Zr(NO_3)_2$+50% glycine+36.15% $Al(NO_3)_3$+13.85% $Mg(NO_3)_2$, 4 – 16.7% $Ni(NO_3)_2$+16.7% $Co(NO_3)_2$+16.7% $Zr(NO_3)_2$+50% glycine+36.15% $Al(NO_3)_3$+13.85% $Mg(NO_3)_2$; V = 2500 h^{-1}.

It is shown that on the compositions with the highest Ni contents, the highest results for synthesis gas are obtained. Nevertheless, at 20% Ni content the selectivity catalyst for the desired products is rather high and the H_2/CO ratio is the most optimal in comparison with the rest of the samples (2.3 instead of 2.8-2.9). Comparison of the data on the oxidative conversion of CH_4 on catalysts of the composition 47% $Ni(NO_3)_2$+2% $Co(NO_3)_2$+1% $Zr(NO_3)_2$+50% glycine+36.15% $Al(NO_3)_3$+13.85% $Mg(NO_3)_2$, prepared by the SCS and impregnation method it is established that the values of the process parameters are close, however, in terms of commercial use, the catalyst prepared by the SHS method has a greater advantage due to lower energy costs. The process of impregnation, drying and calcination requires many hours of thermal procedures, which leads to an increase in the cost of the catalyst. SHS catalysts also tested for catalytic activity in the carbon dioxide dry reforming of CH_4 in the temperature range 750-900°C. CO_2 and CH_4 conversion, H_2/CO ratio in the reaction products as well as H_2 and CO yields for the studied SHS catalysts on the base of system NiO-Al-α-Al_2O_3 shown in figure 3. Fig. 3 shows that the best results for SHS catalysts based on systems NiO-Al-Al_2O_3 are: 93% CH_4 conversion, 100% conversion of CO_2, product yield reaches 92% H_2 and 99 % CO. Ratio H_2/CO in the reaction product varies in the range of 0.7-1.35. Increasing the reaction temperature, in most cases, increases the ratio of H_2/CO due to the amplification of dehydrogenation reaction.

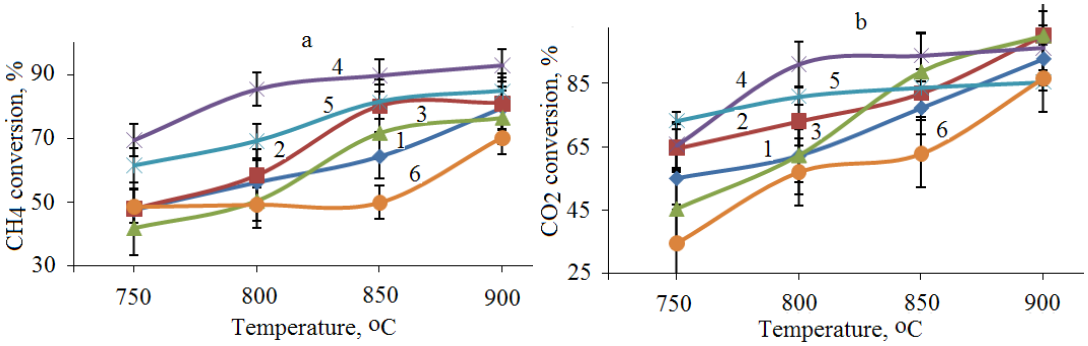

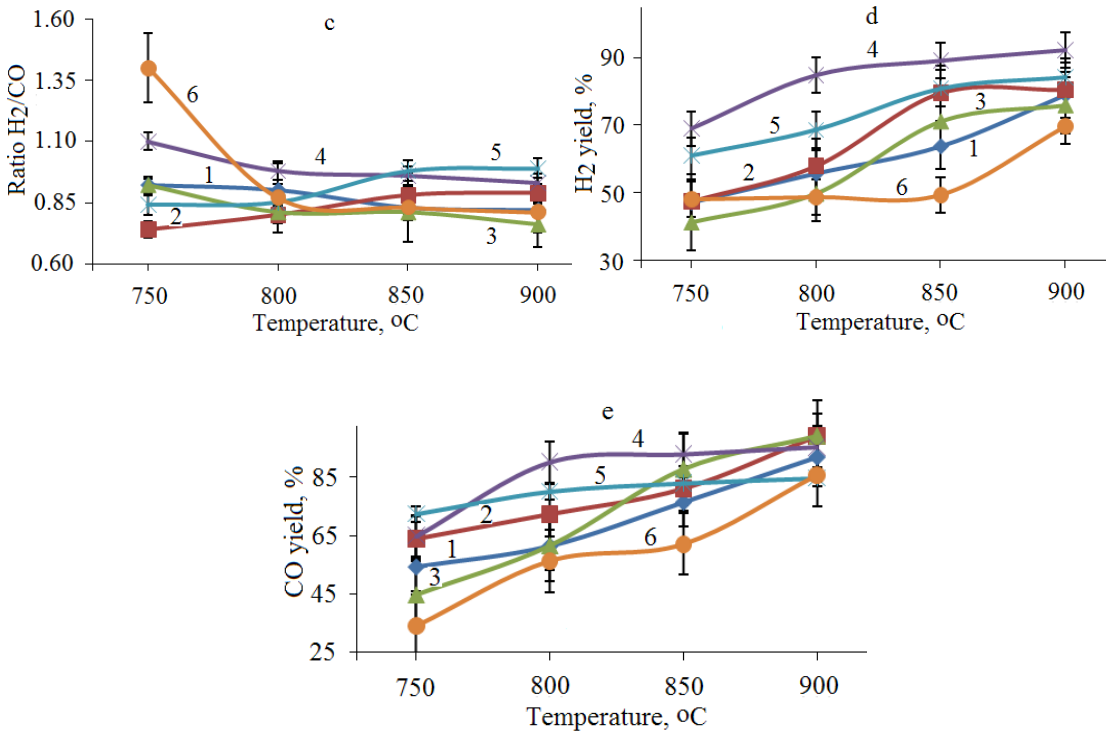

Fig. 3 - The indicators of carbon dioxide reforming of methane according to the reaction temperature for SHS catalysts on the base of system NiO-Al-Al_2O_3. 1 – 24.1% NiO + 55.9% Al + 20.0% Al_2O_3, 2 – 25.8% NiO + 54.2% Al + 20.0% Al_2O_3, 3 – 27.5% NiO + 52.5% Al + 20.0% Al_2O_3, 4 – 29.2% NiO + 50.8% Al + 20.0% Al_2O_3, 5 - 31% NiO + 49% Al + 20.0% Al_2O_3, 6 – 34.4% NiO + 45.6% Al + 20.0% Al_2O_3; V – 860 h^{-1}

Thus, series of catalysts were synthesized by SHS, SCS and impregnation, and their physicochemical properties and activity in the reaction of carbon dioxide conversion and oxidative conversion of methane were studied. The analysis of the obtained results show cause of the activity of the active catalysts.

METALLOTHERMIC PRODUCTION OF ANTIMONY

S.P. Basag[1], A. Turan[2], O.Yücel*[1]

[1]Metallurgical and Materials Engineering Department, Faculty of Chemical and Metallurgical Engineering, Istanbul Technical University, 34469, Maslak, Istanbul, Turkey
[2]Chemical and Process Engineering Department, Faculty of Engineering, Yalova University, 77200, Yalova, Turkey
*yucel@itu.edu.tr

The atomic number of antimony is 51 and, it is a metalloid in the 15th group of the periodic table. It is mainly found as a sulphide mineral stibnite (Sb_2S_3) in the nature and, has over 100 mineral species. Antimony has a melting point of 630 °C and a boiling point of 1587 °C. Its density is about 6.7 g/cm^3 at room temperature. Antimony is a lustrous grey metal that has a Mohs Scale Hardness of 3. This metalloid exists in two forms; metallic antimony is bright, silvery, hard and brittle, non-metallic form is a grey powder. Antimony has poor electric (417 nΩ·m at 20 °C) and heat conduction. It is not attacked by dilute acid or by alkalis and stable in dry air [1-4].

Gasification and reduction method, electrolyte method and the Niederschlag Process are among the mostly applied methods to produce metallic antimony [1, 5]. In the Niederschlag Process, antimony, which is presented in Sb_2S_3, can be directly reduced with the addition of metallic iron and a slight amount of carbon (to soften the bonds) in reverbetory type furnaces or in vertical furnaces. In the method antimony can be reduced in one step and, it is candidate to be the most economic and energy-efficient production method for antimony production if the process can be optimized to work with high metallization ratios. Sulphur, which is decomposed from stibnite, interacts with iron resulting in the formation of a slag-like-matte phase over reduced metallic antimony. The type and main reaction of the Niederschlag Process are given with Equation (1) and Equation (2) respectively [5].

$$Me_1X + Me_2 \rightarrow Me_1 + Me_2X \quad (1)$$

$$Sb_2S_3 + 3Fe \rightarrow 2Sb + 3FeS \quad (2)$$

The specific heat value of Equation (2) is 617.4 j/g. Although it is a metallothermic reduction equation, it is not in self-sustaining mode due to its specific heat value less than 2250 j/g. So, application of additional heat, like volume combustion processes, is a necessity. Another limitation on the process is that reduction reaction slows down over 950 °C whereas the charge fully melts at about 1100 °C (Figure 1).

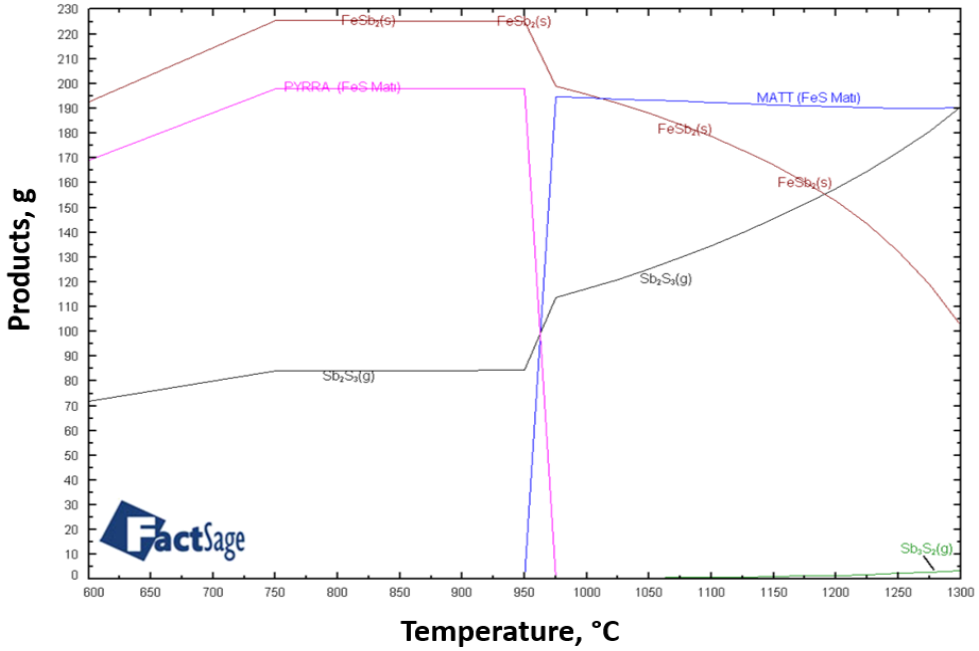

Figure 1 - Thermodynamical predictions on the possible products of the Niederschlag Process with increasing process temperature (plotted by using FactSage 6.4 database).

Various flux materials can be used for the process, such as silica (SiO_2), sodium borax decahydrate ($Na_2B_4O_7•10H_2O$), calcium carbonate ($CaCO_3$), glauber salt or $NaHCO_3$ to avoid metal lost [5].

In the present study, the parameters of metallic Sb production from Sb_2S_3 flotation concentrate (Table 1), which was mined in Etibakır A.Ş. Emirli Mine and concentrated in Halikoy Flotation Plant, were investigated by using the Niederschlag Process.

Table 1 - Chemical content of stibnite concentrate (wt. %).

Sb	S	Fe	Pb	Sn	Al	As	SiO_2
68.67	27.11	1.08	0.14	0.12	0.08	0.08	0.14

As-received dry concentrate was mixed with borax, sodium carbonate and SiO_2 as flux materials and iron as reductant. Used flux ratios were 10.5% for borax, 20.1% for sodium carbonate and 10.5% for SiO_2 (flux / Sb_2S_3 concentrate, %). Experiments were conducted with various iron reductant ratios and refractory acidity ratios. The all experiments were conducted in an electrical resistant furnace at 1100 °C for a process duration of 60 minutes. Duration and temperature were fixed for all experimental sets.

At the experiment which was conducted in the crucible having an acidity ratio of 3.2 and with the addition of 100% stoichiometric Fe had the highest metal recovery ratio was calculated as 79.25% (Figure 3 and Figure 6). It was determined that the lost amount of antimony was collected in the dust collector of furnace in the form of Sb_2O_3 during the experiments. The effect of acidic flux addition (borax and SiO_2, Figure 4) and the use of carbon to soften the bonds between Sb and S were also investigated during the experiments.

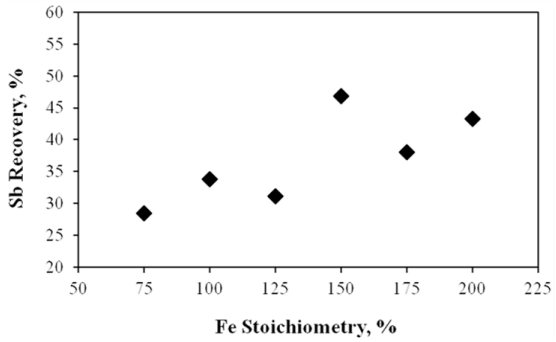

Figure 2 - Sb recovery ratios with increasing Fe stoichiometry for 1.4 crucible acidity ratio.

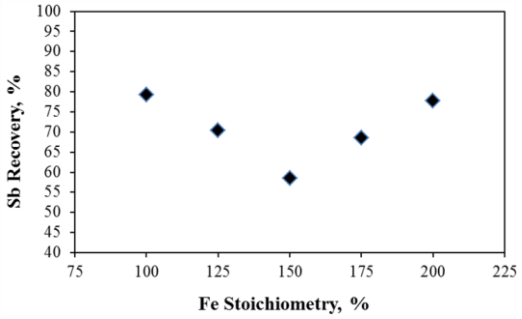

Figure 3 - Sb recovery ratios with increasing Fe stoichiometry for 3.2 crucible acidity ratio.

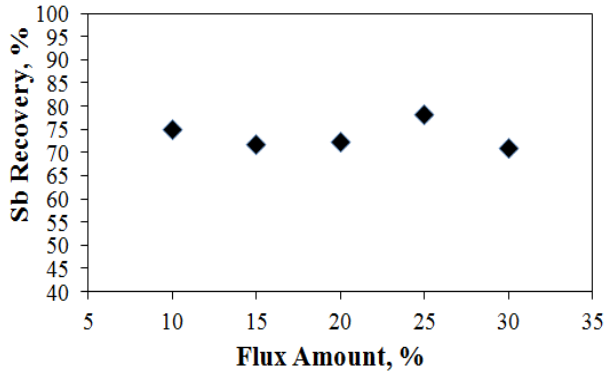

Figure 4 - Sb Recovery ratios with increasing acidic flux addition ratio (Flux/Sb_2S_3 wt.%).

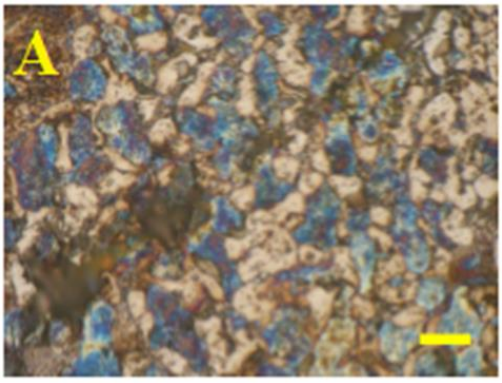

Figure 5 - Optical microscopy micrograph of metallic phase received with 100% Fe stoichiometry for 1.4 crucible acidity ratio.

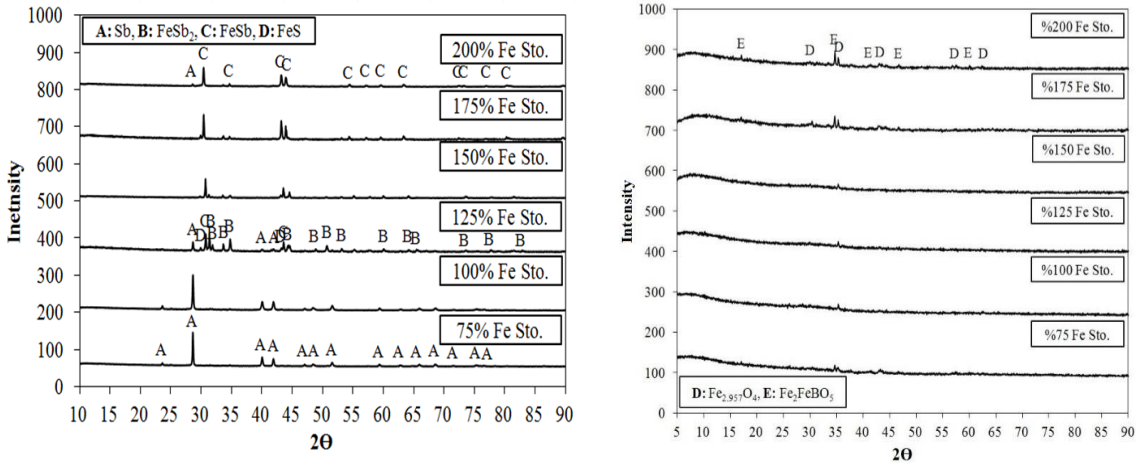

Figure 6 - XRD patterns of obtained metallic phases (left) and slag phases (right) with increasing Fe stoichiometry for 3.2 crucible acidity ratio.

REFERENCES

[1] K. Hanusch, K. A. Herbst, G. Rose, H. U. Wolf, Antimony, Ed. by F. Habashi, Handbook of Extractive Metallurgy: Volume: II, Wiley-VCH, Weinheim, Germany, 1997.

[2] C. G. Anderson, Chemie der Erde, 72, Issue: 4, 2012, pp. 3-8.

[3] S. C. Grund, K. Hanusch, H. J. Breuning, H. U. Wolf, Ullmann's Encyclopedia of Industrial Chemistry, Wiley-VCH, Weinheim, Germany, 2006.

[4] J. Emsley, Nature's Building Blocks, An A-Z Guide to the Elements, Oxford University Press, Oxford, United Kingdom, 2002.

[5] F. Y. Bor, Ekstraktif Metalurji Prensipleri: Volume II, İTÜ Matbaası, Istanbul, Turkey, 1989.

SHS METALLURGY OF COMPOSITE MATERIALS: BASIC PRINCIPLES AND MEANS OF CONTROL

V.I. Yukhvid*, D.E. Andreev, V.N. Sanin, V.A. Gorshkov

Institute of Structural Macrokinetics and Materials Science, Russian Academy of Sciences, Chernogolovka, Moscow, 142432 Russia
*yukh@ism.ac.ru

As is known, composite materials (CMs) can be subdivided in two groups: (a) hard alloys and heat resistant materials and (b) functionally graded and layered materials. CMs can be fabricated by the methods of conventional or powder metallurgy as well as by techniques of forced SHS compaction [1] and SHS joining [2]. This lecture will address the development of SHS metallurgy since the earlier 80s [2–6], with inclusion of some recent unpublished results.

A typical process of SHS metallurgy involves the following stages: (*i*) combustion of green mixture, (*ii*) gravity-assisted phase segregation, and (*iii*) cooling down and crystallization. In order to suppress material splashing, the process in carried out under elevated pressure or in centrifugal machines.

Thermit-like reactions yielding cast composites proceed by the following scheme:

$$MeO + Red + AA \rightarrow CCM + Ox \qquad (1)$$

where MeO stands for metal oxide (NiO, CoO, CrO_3, MoO_3, Nb_2O_5, etc.), Red is a reductant (Al, Ca, Mg, etc.), AA is alloying agent (C, B, Si, Hf, Ti, etc.), CCM is a target cast composite material (heat-resistant material, hard alloy, heterogeneous material), and Ox is metal oxide (Al_2O_3, CaO, MgO, etc.).

The extent of gravity-aided phase segregation (η) is defined by a ratio of characteristic cooling-down time for the melt to the time of motion of CM drops in the slag:

$$\eta \propto D^2 d^2 n g / \chi h \nu \leq 1 \qquad (2)$$

where D is the sample diameter, d the diameter of metal drops, n centrifugal overload, g the acceleration of gravity, χ thermal diffusivity of the two-phase melt, h height of burned sample, and ν the kinematic viscosity of the oxide melt.

In conditions of slow cooling-down and fast phase segregation, η becomes close to unity.

Conversely, the phase segregation is incomplete and the combustion product appears in the form of a heterogeneous structure representing an oxide matrix stuffed with CM particles.

Alloyed heat-resistant CMs and Reney catalyst. Scheme (1) was used to fabricate heat-resistant CMs based on Ni–Co, Ni–Al, Nb–Si pairs; and hard alloys based on Cr–C, Cr–Ti–C, Cr–Ti–Mo–C, Cr–B, Cr–Ti–B, Mo–C, WC, etc. A key point here was finding a proper balance between the amounts of alloying elements (AA) and Al in resultant CM. The problem was solved by using alloyed agents with reduced reactivity and upon spatial separation of the zone of oxides reduction with Al and that of AA dissolution in reduced metal. Convective motion of the melt (whose velocity grows with increasing n) facilitates the formation of uniform cast CM with fine structure.

For some important CMs, it is rather difficult to prepare ignitable green compositions. In order to activate combustion in such systems, we used the additives of heat generating compounds (boosters). In this way, we managed to fabricate Ti–Al, Ti–Al–Nb, etc. composites and a heterogeneous CM with Al_2O_3–CaO as a matrix with uniformly distributed Ti_2AlC particles.
Our technique followed by chemical activation was applied to obtain the Reney catalyst Ni–Co–Mn–Al. The active sites in this catalyst represent the Ni_3Al nucleus covered by a porous Ni–Co–Mn shell with a Reney structure.

Hard alloys. The mixtures of Cr, Ti, and Ni oxides with Al, C, and B were used to fabricate cast hard alloys based on Cr–C, Cr–B, Ti–C, Ti–B, Cr–Ti–C, and Cr–T–B with Ni as a binder. In these experiments, we disclosed the abnormal influence of carbon particle size d_C on burning velocity U and carbon content of hard alloys. With increasing d_C, U was found to increase, whereas the carbon content of hard alloys passed through a maximum. Microstructural analysis of Cr_3C_2–Ni and Cr_3C_2–TiC–Ni alloys derived from optimal green compositions with d_C = 400–500 μm shows that in this case the Ni matrix contains large platelets of chromium carbide, while Ti and C are localized on smaller TiC grains. Addition of Mo and combustion in conditions of artificial gravity facilitated the formation of finely grained alloys.

Functionally graded and layered CMs. Functionally graded materials (steel–ceramic, titanium–ceramic, and aluminum–ceramic) were obtained by using the technique of SHS surfacing. Combustion of Cr, Mo, Ti, and Ni oxides mixtures with Al, C, and B under pressure or in centrifugal machines was found to yield uniform coating of a cast hard-alloy strongly joined with steel, titanium or aluminum substrates. In this case, green mixture acted not only as a source of carbide of boride ceramics but also as a source of heat in the amounts sufficient for substrate melting.

Experiments with Fe–Al thermite in an axial centrifugal machine demonstrated the feasibility for deposition of corundum coatings on the inner surface of steel tubes and thus to fabricate layered materials and items. More complicate green mixtures were used to fabricate single-layer tubes with a heterogeneous (cermet) structure.

In cooperation with partners, pilot-scale processes for fabrication of alloyed CMs were patented; and pilot-scale batches of the composites were produced and tested on an industrial-scale level.

ACKNOWLEDGMENTS

This work was financially supported by the Russian Foundation for Basic Research (project no. 15-08-01442).

REFERENCES

[1] A.G. Merzhanov, Int. J. Self-Propag. High-Temp. Synth., 6, (1997) 119-163.
[2] V.I. Yukhvid, Pure Appl. Chem., 64, (1992) 977-988.
[3] A.G. Merzhanov, V.I. Yukhvid, I.P., and Borovinskaya, Dokl. Akad. Nauk SSSR, 255, (1980) 120-124.
[4] V.A. Gorshkov and V.I. Yukhvid, in: Proc. Int. Conf. on Modern Processes and Methods in Inorganic Materials Science, Tbilisi, 2012, pp. 66-73.
[5] V.I. Yukhvid, M.I. Alymov, V.N. Sanin, and D.E. Andreev, Key Eng. Mater., 684, (2016) 353–358.
[6] V.I. Yukhvid, Adv. Mater. Technol., no. 4, (2016) 23-34.

COMBUSTION SYNTHESIS OF Ni-W COMPOSITE NANOPOWDERS FROM OXIDE PRECURSORS

M.K. Zakaryan*[1,2], S.L. Kharatyan[1,2]

[1]A.B. Nalbandyan Institute of Chemical Physics NAS RA, P. Sevak 5/2, 0014, Yerevan, Armenia
[2]Yerevan State University, A. Manukyan 1, 0025, Yerevan, Armenia
*zakaryan526219@gmail.com

Interest in nickel-tungsten (Ni-W) alloys has expanded unusually rapidly in recent years due to their unique combination of tribological, magnetic, electrical and electro-erosion properties. They are also characterized by high tensile strength and premium hardness, as well as superior abrasion resistance, good resistance to strong oxidizing acids, and high melting temperature [1]. Current and possible future applications of Ni–W alloys include barrier layers or capping layers in copper metallization for ultra-large-scale integration (ULSI), electrodes accelerating hydrogen evolution from alkaline solutions, environmentally safe substitute for hard chromium plating in the aerospace industry, etc [2]. Ni-W alloys are usually electroplated from aqueous solutions containing $NiSO_4 \cdot 6H_2O$ and $Na_2WO_4 \cdot 2H_2O$ as the electroactive species, and organic acids as complexing [1].

In this work for the manufacturing of Ni-W composite powder the self-propagating high-temperature synthesis (SHS) method is applied [3] by using thermo-kinetic coupling approach [4]. Its essence consists in the coupling of low exothermic reduction reaction (MeO+C) with a high caloric (MeO+Mg) one with possible change of reaction pathway. Furthermore, using (Mg+C) combined reducer will allow to control the reaction temperature in a wide range at synthesis of Ni-W composite powders. Byproduct magnesia can be removed by acid leaching. First of all thermodynamic calculations were carried out for $NiO\text{-}WO_3\text{-}yMg\text{-}xC$ system to determine optimal conditions for joint and complete reduction of nickel and tungsten oxides, aimed at obtaining of Ni-W alloy. Based on the results of thermodynamic calculations magnesio-carbothermic co-reduction of nickel and tungsten oxides were performed with such amount of magnesium corresponding to low temperature area (y=1.7 mol). To find out the effect of carbon amount on the behavior of combustion perameters (temperature and velocity) a series of experiments were performed with changing carbon amount (fig. 1).

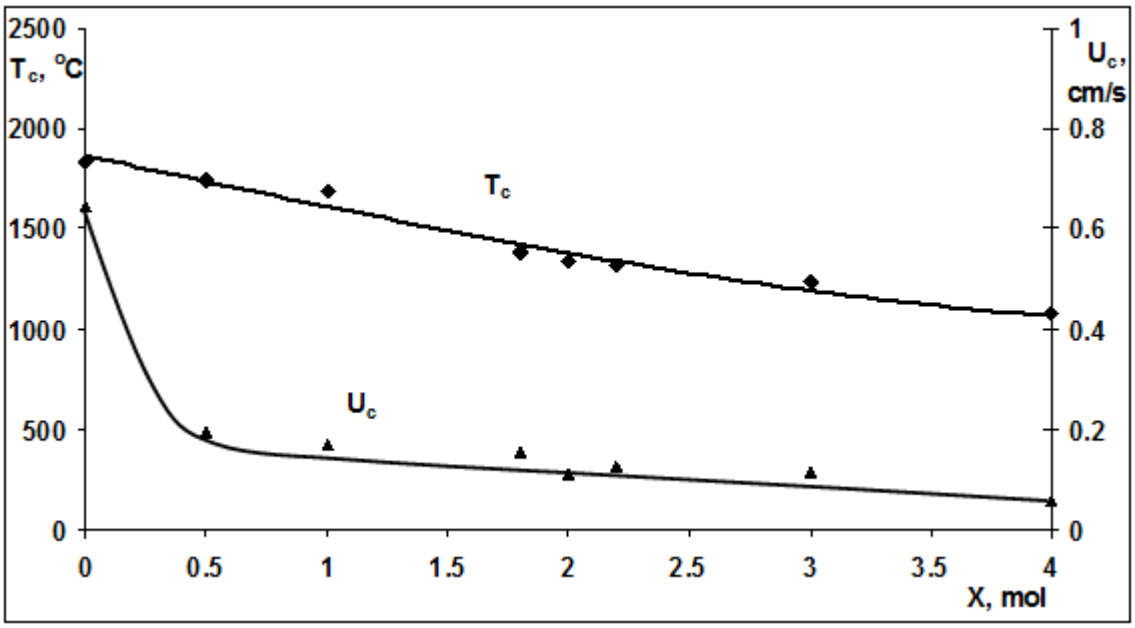

Fig. 1 - Combustion temperature and velocity vs carbon amount for the the $NiO\text{-}WO_3\text{-}1.7Mg\text{-}xC$ system, P=0.5 MPa

According to XRD analysis results, the variation of carbon amount makes possible to completely reduce precursors (at x=2.1-2.2) up to desired Ni and W metals. After acid leaching of completely reduced sample byproduct magnesia was removed and the products contain only fine-grained particles of target metals (fig. 2).

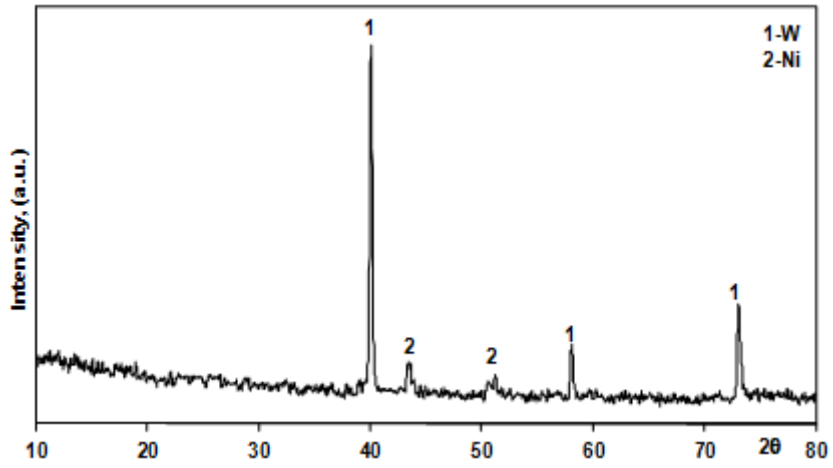

Fig. 2 - XRD pattern of combustion product after acid treatment

REFERENCES

[1] Kh.K. Khan, M. Mehmood, M. ul Hassan, J. Ahmad, Z. Iqbal, T. Muddasser. Met. Sci. Heat Treat., 53, 2011, pp. 87-90

[2] N. Eliaz, T.M. Sridhar, E. Gileadi. Electrochim. Acta, 50, 2005, pp. 2893–2904

[3] S.T. Aruna, A.S. Mukasyan. Curr. Opin. Solid State Mater. Sci., 12, 2008, pp. 44–50

[4] S.L. Kharatyan, A.G. Merzhanov. Int. J. SHS, 21, 2012, pp. 59-73.

SHS FERROBORON LIGATURE

G.Zakharov[1], G.Oniashvili[1], G.Tavadze[1], Z.Aslamazashvili[1], G.Mikaberidze[1], I.Bairamashvili[2], N.Djalabadze [3]

1 - LEPL - Ferdinand Tavadze Metallurgy And Materials Science Institute
2 - National Center of High Technologies
3 - Georgian Technical University

The combination of high hardness with plastic properties in borides, their high chemical inertness - represents an important class of inorganic compounds for creation of tools and structural steels of highly alloyed borides. One of the specific features of the structure of iron borides is that they hold particular place in compounds implantation. Conversely with compounds of metal with carbon, nitrogen, hydrogen, boride of metals can form covalent bonds between atoms of boron.

That is why their composition does not correspond to the usual degrees of oxidation of the elements. In addition, boron compounds have the ability to absorb neutrons intensively. This stipulates the using of boron compounds for the manufacture of control rods of reactors, as well as biological protection against neutron radiation.

Boron holds special position among reactor materials. It's uniqueness is stipulated by the simultaneous content of two stable isotopes – ^{10}B and ^{11}B. ^{10}B is characterized with the high section of absorption thermal and the fast neutrons, and ^{11}B is an effective mechanism to delay and reflect neutrons. In the nuclear equipment is widely applies materials, which include ^{10}B therefore on constructional boron steels became demanded alloys [1-3].Boron steels found wide application in the area of the Boiling nuclear reactors.

Besides, boron steels are widely used in production of containers for storage and transportation of radioactive wastes and reproduces nuclear fuel for absorption of secondary neutrons. Micro Additives of Ferro-boron ligature for obtaining boron steels make positive influence on physical-mechanical properties and radiation resistance of materials in the production of boron steels. Small amounts of atoms of boron form solid solutions of implants, which slower the development of porosity, which promotes segregation on structural defects of a crystal lattice and reduces diffusive mobility of the basic alloying elements in the course of radiation.
Ligatures, enriched with the ^{10}B isotope, can be used for micro-alloying of austenitic class steels, which is widely applied in nuclear equipment as construction materials, as far as the ^{10}B isotope excludes the formation of helium, which in general is accompanied by its formation in the nuclear reaction.

Carbothermic restoration and electrolysis from molten media are the most well-known industrial methods for obtaining Ferro boron ligatures [4,5].In particular, the carbothermal method of restoration is more complicated and long process, which takes place at a temperature of 2000^{o}C. The task can be successfully implemented using the SHS-metallurgy technologies. [6].
Realization of this task for obtaining Ferro boron ligature is possible by technology - SHS metallurgy, which is characterized by simple and small-sized equipment, high productivity and purity of the products obtained with environmental safety of the process [7-9].

The laboratory SHS centrifugal machine have been used as processing equipment for carrying out experimental works under the influence of centrifugal force at overloads at 1000 a/g.

Synthesis of final products was conducted in the graphite reaction cups, with an internal diameter of d=40 mm and a height of h=100 mm. Methodology of processing is standard [10].

The obtained products were investigated byX-ray diffraction and microspectrum analysis.To obtain final products are used a boron-containing material in the form of B_2O_3, iron oxides and as restoring metals were powders of aluminum, magnesium and magnesium-aluminum alloy.

In the experiments was studied influence of technological parameters (such as phase separation, the scattering of the reaction mass, the composition and dispersion of the components, the density of the initial mixture) on regularities of the synthesis of cast ligatures in the system Fe-B.

The influence of overloads on the regularities of the synthesis of cast ligatures and the mechanisms of structure formation of SHS products wasstudied.

As a result of investigations was established the defining technology factors influencing an exit and extraction of target elements of the Ferro boron ligatures. On the basis of the received results was established, that extraction of boron is more than 95%.

The analysis of the samples showed the presence of a high content of carbon in the casted ligatures. This can be explained by the fact, that the great affinity of iron to carbon, high synthesis temperature promotes the interaction of iron with carbon of the graphite reaction cup. The problem of the high content of carbon in the melt can be minimized with a technological way by creating a protective barrier between the reaction mixture and a graphite cup. It is important, because the content of carbon in boron steels the does not exceed 1,0% (wt).

The quantitative and elemental composition of the components of obtained ligatures alloy and slag were studied and established Fig. 1 and 2.Analysis of the structure and content of the alloys showed, that content of boron in the Ferro boron alloys doesn't exceed 22% .The analysis also showed that, there is no boron in the slag practically. Minimization of boron loss is an important circumstance, when receiving material enriched with an isotope boron^{10}B.

Based on conducted experimental results has been obtained Ferro boron ligature enriched with boron of natural isotope in the quantities sufficient for carrying out melting and receiving of boron steel.

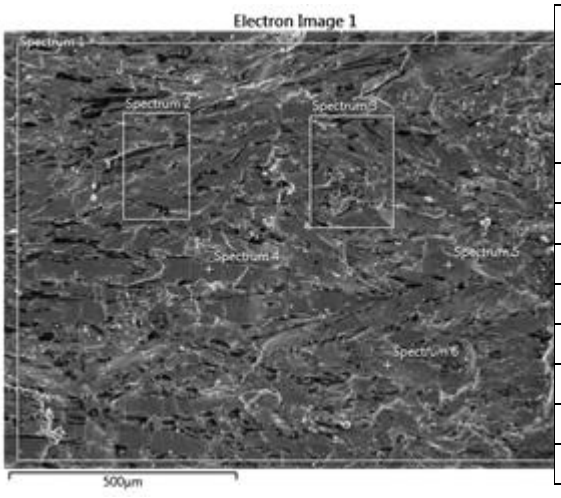

a

ResultType	Weight %		
SpectrumLabel	Spectrum 1	Spectrum 2	Spectrum 3
B	23.07	20.24	20.79
C	6.05	4.22	4.29
Al	4.90	4.88	4.64
Si	0.26	0.19	0.19
Ti	0.14	0.14	
Cr	0.34	0.27	0.31
Fe	65.24	70.06	69.78
Total	100.00	100.00	100.00

b

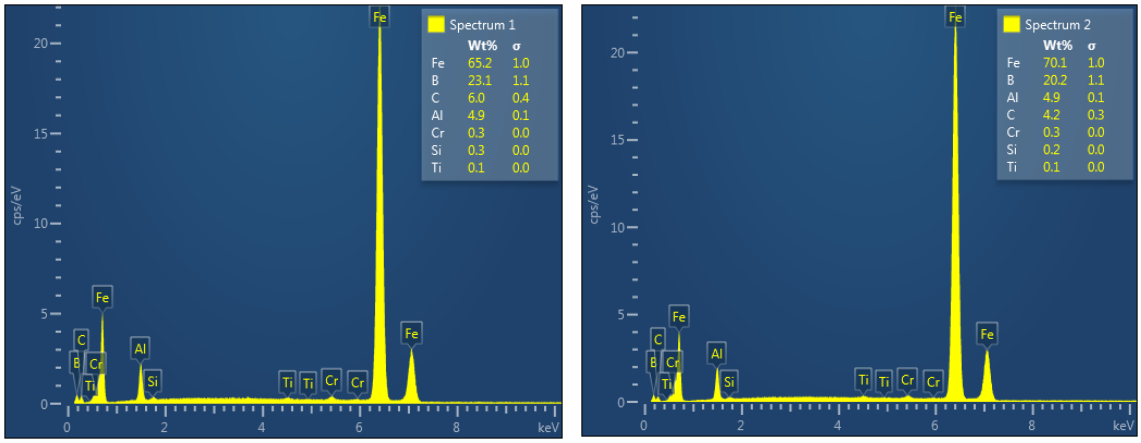

c d

Fig. 1 - Structure (a), composition (b) and distribution of elements (c, d) in the cast ferroboron

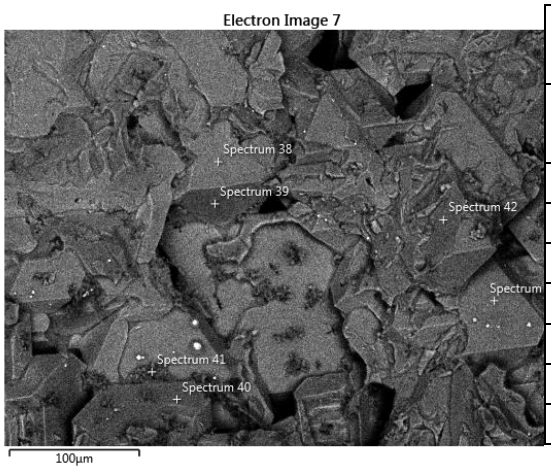

ResultType	Weight %		
SpectrumLabel	Spectrum 38	Spectrum 39	Spectrum 40
B			
N			
O	43.10	42.91	50.19
F	2.72	6.02	
Na	3.74	8.05	3.33
Al	50.44	43.02	46.48
Total	100.00	100.00	100.00

a b

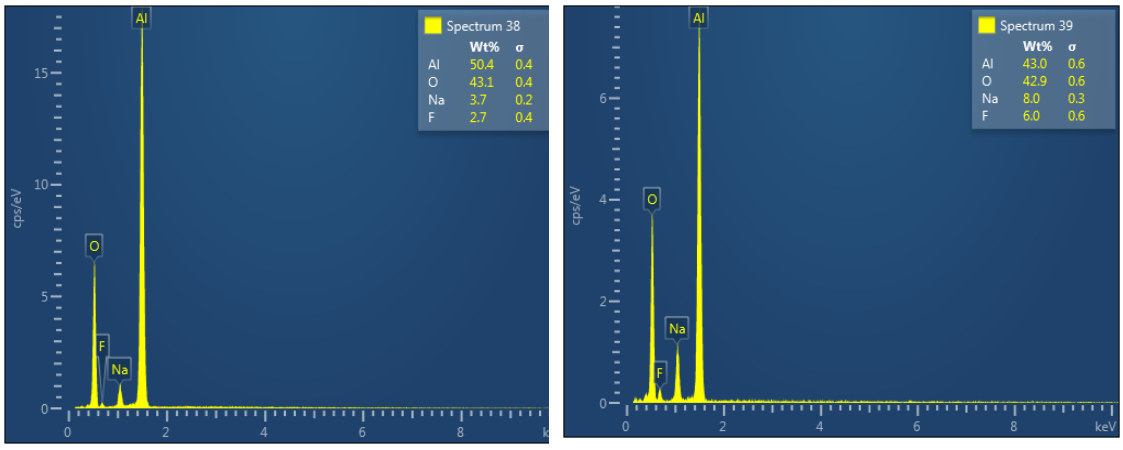

c d

Fig. 2 - Structure (a), composition (b) and distribution of elements (c, d) in Ferro boron slag

REFERENCES

[1] V.DRisovanyi, A.VZakharov, E.PKlochkov, V.BPonomarenko, E.MMuraleva, T.MGuseva. Absorbent materials for the control and protection rods of nuclear reactors. Ulyanovsk -pages 2012. 442.

[2] Samsonov G.V, Serebryakova T.I, Neronov V.A Borides. Atomizdat, 1975 pages 276-283.

[3] Khudyakov A.A, Ostrovsky Z.E, Rysovanny V.D et al. The state of the alloy of the SBI in the reactor after 31 years of operation VK-50 // Atomic Energy, 2002, T, 92, Issue 2 , pages114-118.

[4] Digonsky, S.V. Carbothermic reduction of oxide raw materials in nonequilibrium chemical systems. Digonsky // Technology of metals. - 2008. - No. 8.

[5] A.I Belyaev, E.A Zhemchuzhina, L.A Firsanova. Physical chemistry of molten salts, 1957A.G. Merzhanov, I.P. Borovinskaya, V.Shkiro. The phenomenon of wave Localization Self-inhibiting solid-phase reactions. State Register Discoveries № 287, 1984.

[6] Device for production hard alloys. Saqpatenti, P 5827, 2013. G. Zakharov, Z.Aslamazashvili, G. Oniashvili and all.

[7] Centrifugal SHS Surfacing of the refractory jnorganic materials. International Journal of Sejf-Propogating High-Temperature Synthesis Volume 3, Number 4, 1994. V.I. Yukhvid, A.R.Kachin,G.V.Zakharov.

[8] Центробежная СВС – наплавка на сталь. Журнал Литейное производство № 7, 2001. В.И.Юхвид, Г.Ш.Ониашвили, Г.В.Захаров.

[9] Dis. Cand. Tech. Sciences: Zakharov G.V. Production of materials in the Cr-Ti-Ni-C-Al2O3 system by centrifugal SHS technology, their structure and properties: Tbilisi - 1988.

DEVELOPMENT OF THE TECHNOLOGY SHS-METALLURGY IN GEORGIA

G.Zakharov, G.Oniashvili, G.Tavadze, Z.Aslamazashvili, G.Mikaberidze, M.Chikhradze, G. Urushadze

LEPL - Ferdinand Tavadze Metallurgy And Materials Science Institute

Knowledge of the SHS[1]process (self-propagating high-temperature synthesis) in combination with a scientifically substantiated and correctly established experiment allows us to have a clear idea of the essence of the processes taking place in the system under consideration. This allows us to identify factors and conditions that affect the course of the technological process.

On the basis of the theoretical and experimental investigations, the received results find practical application in manufacture for technological processing or in construction of the equipment.

- In order to solve scientific tasks is required:
- Preliminary researches and elaboration of conditions for the solution of tasks
- Improvement or elaboration for creating new processes and technical objects (Machines, equipment, etc);
- Elaboration of experimental design facilities;
- Assembly, adjustment of equipment and commissioning of the developed objects or processes.

Solving such problems at the Institute of Metallurgy and Materials Science Ferdinand Tavadze by the scientists of the SHS laboratory managed to make his contribution to the overall development of such a new scientific direction as SHS-metallurgy.

SHS – metallurgy is a new scientific direction. Use of advanced equipment and advanced processing methods make it possible to obtain refractory compounds and materials controlling explosion character of combustion type reaction at high temperatures.

The scientific and applied research studies have shown that the processes of phase separation and dispersion of the reaction mass, the formation phase and chemical composition of the micro-structure, as well as composition, density of the mixture, dispersion of the components, the field of mass forces, etc., have a major influence in the preparation of new materials and products from them[2-4].

The development of scientific achievements in the field of SHS-metallurgy also contributed to participation in international congresses, symposia, conferences, seminars, inventions, patents and project financing in various scientific and technical centers[5-9].

Over the period of the development of SHS – Metallurgy have been obtained heat resistance and high temperature strength, thermo-stable boron-containing composite materials and products with various porosity, under atmospheric conditions. In fig.1 is shown appearance of samples of various configurations in the form of bushings, cylinders, etc. It is possible to produce, from the same material, highly effective filters for cleaning the polluted water and air from industrial dust. Workability of the process and simplicity of the equipment allows to produce of products in the form of protective blocks that can be used for protection from radiation.

In the high pressure reactor have been obtained ultrafine powders of hard alloys, borides, carbides, nitrides, silicides and etc. The technologies have been developed for the production of

ferroaluminum, ferrovanadium, ferrochromium, nickel boron and ferromanganese. The patents and inventions are given to many developments [10-16].

The laboratory SHS centrifugal machine will be used as processing equipment for carrying out experimental works and receiving cast ligatures based on tungsten carbide under the influence of centrifugal force. The study carried out the research technological parameters was established of synthesis of casting materials for various configuration fig.2. In order to increase productivity, a multifunctional centrifugal machine (EMB) has been designed, with a horizontal axis of rotation in fig.4 [17]. The installation is capable to initiation in 12 reaction beakers in one technological cycle. The fact that during one stage of technological process possible is to receive material and product that is the essential advantage of this technology. In this case, in each reaction beaker can be placed up to four forming elements. This will allow us to receive up to 48 products simultaneously. In addition, replacing the round reaction equipment with a rectangular shape, will allow to receive up to 8 samples with dimensions of 70 x 70 mm.

SHS-process allows to obtain the entirely new compositions of master alloys and ferroalloys with a wide range of elemental composition in a very short time. This technology makes it possible to introduce simultaneously refractory and low-melting starting products in a wide range of compositions, which cannot be done by traditional technology. Thus, this technology gives us possibility to introduce refractory and low-melting starting products in a wide range of composition simultaneously, which cannot be done by traditional technology. The conventional methods is restricted by the longer smelting process and burning of fusible elements, due to different melting point. The ligatures with different composition were obtained from pretreated waste of manganese production, Fig. 4. On the basis of the received results of conducted experiments were established, that the technical solution can also be cost-effective.
In particular, the preliminary calculations showed that SHS-synthesized AlMn60 master alloy will be at least at 30% cheaper than the commonly produced alloy. To increase the productivity in the preparation of ligatures are developed working drawings of the experimental centrifugal machine (ECB), with a vertical axis of rotation fig. 3B [18].

After approbation and establishment of technical parameters of high-performance centrifugal machine is planned to develop an industrial plant. . It is assumed, that centrifugal machine is characterized by simple and relatively small-size (the occupied area of the industrial installation will not exceed 10м^2).At the same time productivity of ligature by using such installation will be at least 160 tons per year. The amount of the by-product, containing mainly of corundum, will be 250 tons / year. At the same time, the by-product is a raw material for production of abrasive materials and manufacturing of products from them. ECB gives us possibility to receive materials with different composition and purpose also, to obtain products that are limited only by the size of the reaction form.

According to the preliminary investigations silicon of technical purity have been produced from the Georgian natural raw materials under the influence of centrifugal force. In Fig. 5 shows the structure and composition of the alloy and slag of ferroboron ligature. The quantitative content of boron in ferroboron (FeB) compound is at least 22% by weight.

In this case, content of an isotope ^{10}B doesn't exist in the slag practically. This circumstance is important for obtaining of ferroboron material, which contain of a boron isotope ^{10}B. This special ligature is used for alloying boron steel, which is one of the best construction materials in the nuclear power industry.

The relationship between SHS - metallurgy and applied sciences everything is becoming more significant, that is reflected in the high level of research. New aspects for application of the obtained materials are observed. There are also connections with other technological directions. The search for new methods and a deeper study of their properties makes to draw conclusions about the continuation of scientific research in a wide variety of technological direction.

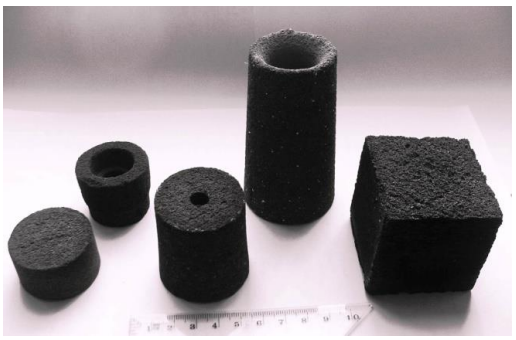

Fig. 1 - Examples of execution of products from boron containing materials under atmospheric conditions

Fig. 2 - Examples of cast hard alloys materials with different configuration obtained under the influence of centrifugal

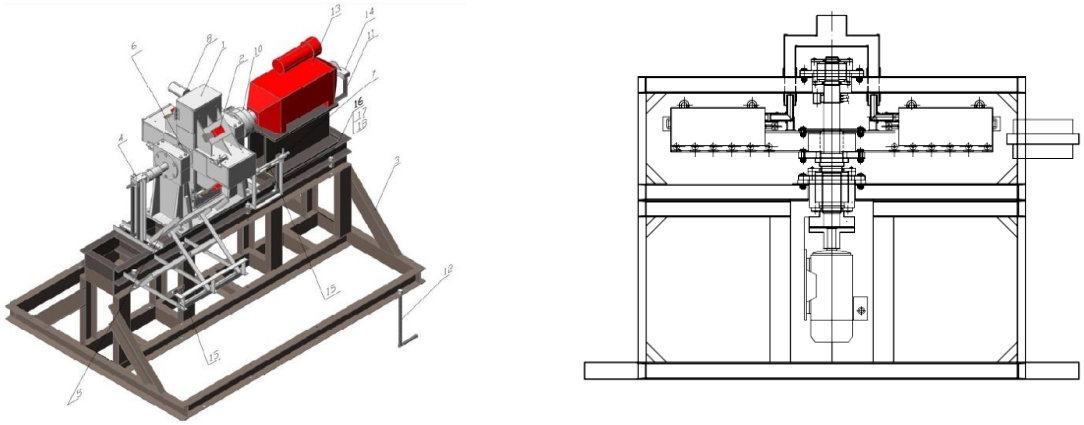

A B

Fig.3 - A - The experimental multifunctional centrifugal machine (ECB), with a horizontal axis of rotation

B - The experimental multifunctional centrifugal machine (ECB), with a horizontal axis of rotation

Fig 4 - Cast ligature with a different set of fusible andrefractory elements

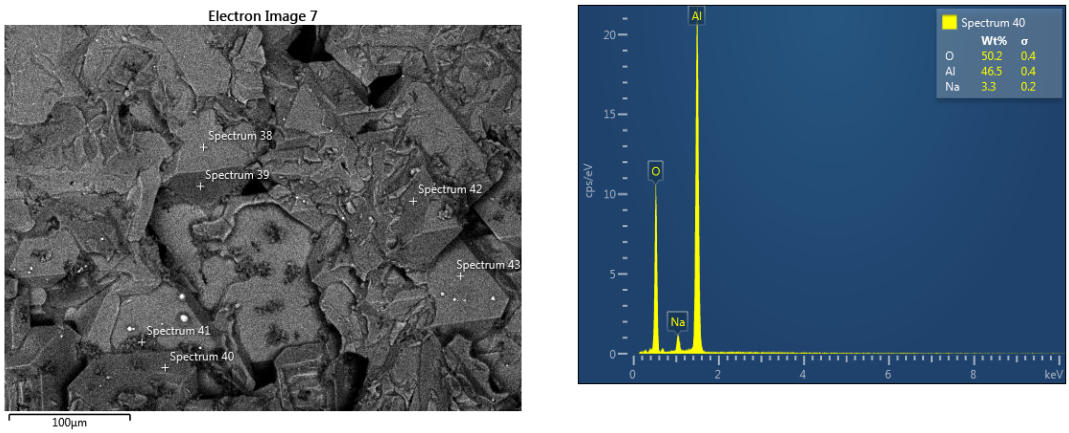

a

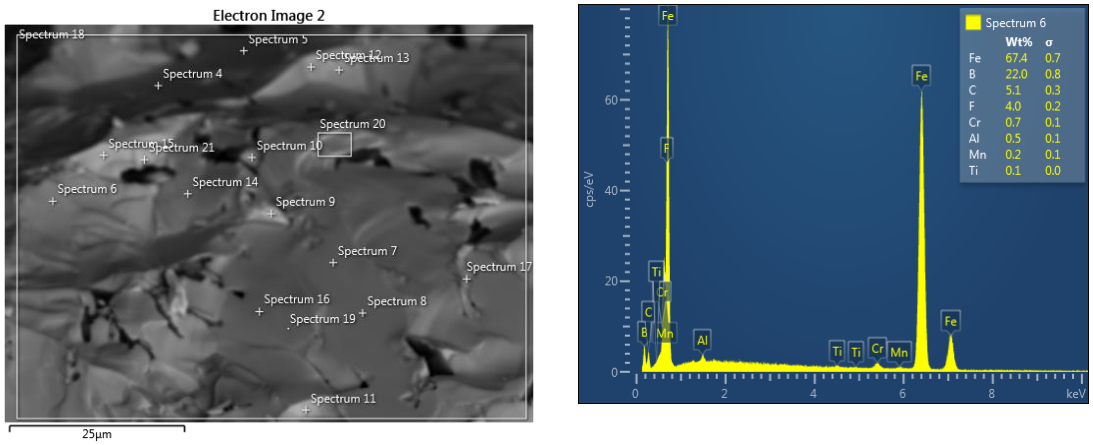

b

Fig. 5 - Cast ferroboron ligature obtained under the influence of centrifugal force. a - structure and composition of slag; b - structure and composition of ferroboron;

REFERERENCES

[1] A.G. Merzhanov, I.P. Borovinskaya, V.Shkiro. The phenomenon of wave Localization Self-inhibiting solid-phase reactions. State Register Discoveries № 287, 1984.

[2] Dis. Cand. Tech. Sciences: Zakharov G.V. Production of materials in the Cr-Ti-Ni-C-Al2O3 system by centrifugal SHS technology, their structure and properties: Tbilisi - 1988.
[3] V.I. Yukhvid, A.R.Kachin and G.V.Zakharov. Centrifugal SHS Surfacing of the Refractory Jnorganic Materials. International Journal of Sejf-Propogating High-Temperature Synthesis Volume 3, Number 4, 1994.
[4] Концепция развития самораспространяющегося высокотемпературного синтеза как области научно-технического прогресса. Изд-во «Территория» 2003.
[5] G.Sh. Oniashvili, V.I. Yukhvid and G.V.Zakharov. Centrifugal SHS - surfacing on steel. Magazine Foundry Production No. 7, 2001.
[6] Hard alloys obtaird by the method: SHS-Centrifugal cast. X11 International Simposium on SHS.Texas ,USA.pp. 291-292. 2013; G.Zakharov, Z.Aslamazashvili, G.Tavadze,M.Chikhradze.
[7] Production of special ferro-alloys by self-propagated high-temperature synthsis (SHS). The IST International Foundrymen and Material Scientists. Congress, 25-27 September 2006, Georgia. G. Zakharov, Z.Aslamazashvili and G. Oniashvili.
[8] Ecological Problems Related to Mining-Metallurgical Industries and Innovatory, Energy-Efficient Ways of Solving Them. Engineering, 2012, 4, 83-89, 2012. G. Jishkariani; G. Jandieri; D. Sakhvadze; G. Zakharov; G. Tavadze.
[9] Combined processing of waste organic polymers and manganese bearing waste/low grade ores into fuels and low-carbon manganese alloys. International Journal of Global Warming. Volume 10, Issue 1-3. pp. 242–262., 2016. A.Chirakadze, Z.Buachidze, G.Zakharov, G.Oniashvili, at all.
[10] Method of obtaining of ferro-aluminium. Georgian patent. № 691, 1996.
[11] Obtaining of ferro-alloys. Georgian patent P 6622, 2017.
[12] A method of making two-layer products.US 1589491,1987.
[13] Furnace charge for obtaining coatings on steel products.US1508528,1989.
[14] A method of producing without carbon ferromanganese. US1637345, 1990.
[15] The method of producing a composite material. US 1826470, 1992.
[16] Tonstick paint.Georgian patent№88, 1993.
[17] Method of obtaining product from exothermic powder chasms. Georgian patent.P6314, 2015.
[18] A method of producing a cast of splavov and device for their production. Georgian patent. file number №13796/01.Positive resolution 03.10.2016.

INFLUENCE OF OXYGEN IMPURITY ON α-PHASE CONTENT AT SHS OF SI_3N_4

V.V. Zakorzhevsky

Institute of Structural Macrokinetics and Materials Science, RAS Chernogolovka, Moscow region, 142432 Russia
zakvl@ism.ac.ru

In order to obtain silicon nitride ceramics with excellent characteristics silicon nitride powder with α-phase content $\geq$ 90 % should be used. When silicon nitride is synthesized by the furnace or diimide method, α-phase content is ~ 95 % since the synthesis process can be governed and occurs at the optimum temperature. However in the case of SHS it is rather difficult to achieve a high content of α-phase. The value of α- β transition of Si_3N_4 mainly depends on temperature, exposure time and existence of various admixtures and impurities [1,2]. Phase α→β transition starts at ~1450°C. Therefore the synthesis temperature should not be higher than 1500°C. Silicon melting point is 1419°C so it is rather difficult to synthesize α-phase of silicon nitride by combustion. For low-temperature mode of SHS of α-Si_3N_4 some gasifying additives or silicon powders with high specific surface area are used [3,4].

According to literature, oxygen impurity is known to have influence on phase-stability of α-Si_3N_4. If oxygen impurity content in α-Si_3N_4 is less than 0.1 mass %, α-Si_3N_4 is characterized by the same thermodynamic stability as β-Si_3N_4 [3]. Therefore if O_2 is a destabilizing factor for α-Si_3N_4, we can suppose that use of oxygen-free green mixture components will allow us to extend the temperature range of silicon nitride synthesis with retaining the high content of α-phase.

When the experiments in silicon nitride synthesis were carried out, the chemical composition of the products was not usually determined, and existence of impurities, including O_2, was not practically connected with α-phase content and synthesis temperature. The dependence of α-phase content on combustion temperature in SHS of Si_3N_4 for the powders with oxygen impurity in the range of 1.0-1.5 mass % is shown in [5].

This work demonstrates the results of investigation of synthesis temperature and oxygen impurity effect on the product phase composition at SHS of Si_3N_4.

For the experiments we used green mixture components with various contents of oxygen impurities. When the influence of high oxygen concentrations on phase formation of silicon nitride was studied, amorphous silicon dioxide was introduced into the green mixture. Some characteristics of the initial components are given in Table 1. In the case of low-temperature synthesis, ammonium chlorides and fluorides were added.

Table 1 - Green mixture initial components

Component	Impurity content, mass %			Specific surface area, m^2/g
	N_2	O_2	Fe	
Si	-	0.6	0.02	2.5
Si	-	2.2	0.1	10
Si_3N_4	38.9	0.5	0.05	2.5
Si_3N_4	38.3	2.0	0.09	7.5

The dry components were mixed in the ball mill during 1 hour. The initial nitrogen pressure was 60 atm. The green mixture mass was 3.0 kg. The experiments were carried out in the industrial SHS reactor of 30 l capacity.

The phase composition of the products was analyzed using "Dron2M" diffractometer. The combustion temperatures were measured by W/Re5-W/Re20 thermocouple.

Experimental study of phase composition dependence on synthesis temperature has proved the supposition on oxygen impurity effect on α-phase content at synthesis of silicon nitride. Fig.1 demonstrates the results of the temperature measurement in the cases when the green mixture contained various amounts of oxygen. When the green mixture contained a low amount of oxygen (0.5-0.7 mass %), the synthesis temperature range was 1400-1800°C. In the case of high content of oxygen impurity (2.0-2.5 mass %) the content of α-phase decreased from 1200-90 % to 95-65 % in the temperature range of 1400-1700 °C in comparison with the results obtained in [5].

X-ray phase analysis of Si_3N_4 samples obtained from the green mixture with a low content of oxygen impurity showed only two phases identified as α- and β-modifications of silicon nitride. The peak intensity of these phases changed depending on the synthesis temperature. Analysis of Si_3N_4 samples synthesized from the green mixture with a high content of oxygen impurity proved the existence of the additional phase of silicon oxynitride (Si_2N_2O). Due to our study we can conclude that the existence and intensity of the peaks of Si_2N_2O phase depend on the synthesis temperature. The comparison of high-temperature characteristics of silicon oxynitride and consequence of phase formation with a temperature increase allowed determining the role of oxygen impurity in the phase formation process. It was established that α→β transition at SHS of silicon nitride from the green mixture with high oxygen content occurs via the stage of silicon oxynitride formation and decomposition. Therefore the obtained results prove our supposition on the influence of oxygen impurity on α→β transition of silicon nitride.

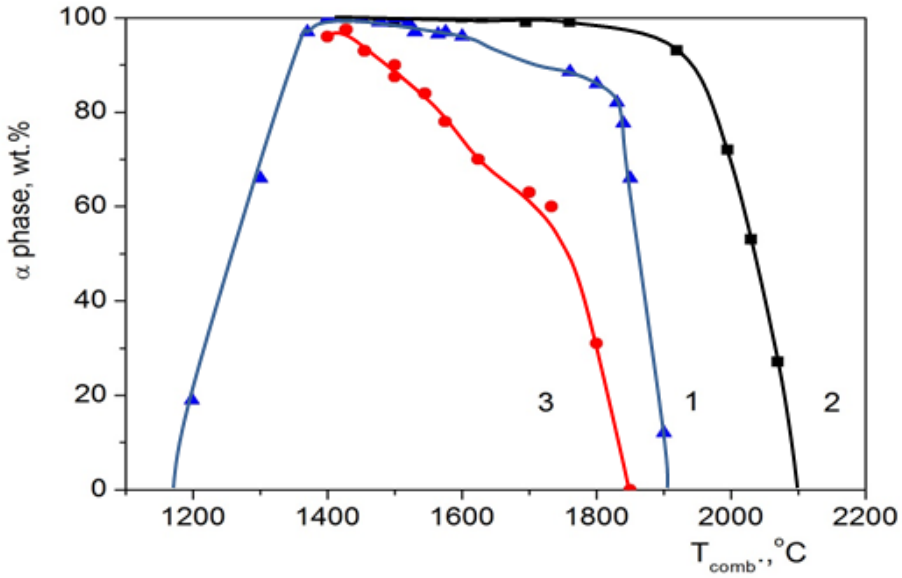

Fig.1 - Dependence of silicon nitride phase composition on synthesis temperature at the use of green mixture with various contents of oxygen impurity. O_2 content in synthesis product: 1 – 1.0-1.5 mass % [5]; 2 – 0.5-0.7 mass %; 3 – 2.0-2.5 mass %.

Low exposure time at the temperature of phase transition (higher than 1450°C) and low content of oxygen impurity in the green mixture components allow synthesizing silicon nitride with a high content of α-phase in a wide temperature range. The dependence of α-phase content on the synthesis temperature is determined by the specific times of the synthesis reaction and existence of oxygen impurity.

REFERENCES

[1] H. Suematsu, T.E. Mitchel, O. Fukunaga, and all., The α→β Transformation in Silicon Nitride Single Crystals. J. Am. Ceram. Soc. V.80. №3, 1997, pp. 615-620.

[2] Liwu Wang, Sukumar Roy, Wolfgang Sigmund and Fritz Aldinger, In situ Incorporation of Sintering Additives in Si_3N_4 powder by a Combustion Process. J. Europ. Ceram. Soc, V.19, 1999, pp. 61-65.

[3] A.G. Merzhanov, I.P. Borovinskaya, V.M. Martynenko. The method to obtain silicon nitride. Authors's certificate №1533215, 1983.

[4] V.V. Zakorzhevsky I.P. Borovinskaya, Combustion Synthesis of Silicon Nitride Using Ultrafine Silicon Powders. Powder Metallurgy and Metal Ceramics, Vol. 48, N. 7-8, 2009, pp. 375-380.

[5] V.V. Zakorzhevsky I.P. Borovinskaya. Some Regularities of α-Si_3N_4 Synthesis in a Commercial SHS Reactor. Int. J. SHS.V.9. №2. 2000, pp. 171-191.

საქართველოს მეცნიერებათა ეროვნული აკადემიის სტამბა
თბილისი – 2017
რუსთაველის გამზ. 52

Georgian National Academy Press
Tbilisi – 2017
52, Rustaveli Ave.